

This electronic thesis or dissertation has been downloaded from the King's Research Portal at <https://kclpure.kcl.ac.uk/portal/>



**Vascular Stem Cell Migration in Response to Dkk3 in Vascular Diseases
The emergence of a novel chemokine-like protein**

Bhaloo, Shirin Issa

Awarding institution:
King's College London

The copyright of this thesis rests with the author and no quotation from it or information derived from it may be published without proper acknowledgement.

END USER LICENCE AGREEMENT



Unless another licence is stated on the immediately following page this work is licensed

under a Creative Commons Attribution-NonCommercial-NoDerivatives 4.0 International

licence. <https://creativecommons.org/licenses/by-nc-nd/4.0/>

You are free to copy, distribute and transmit the work

Under the following conditions:

- Attribution: You must attribute the work in the manner specified by the author (but not in any way that suggests that they endorse you or your use of the work).
- Non Commercial: You may not use this work for commercial purposes.
- No Derivative Works - You may not alter, transform, or build upon this work.

Any of these conditions can be waived if you receive permission from the author. Your fair dealings and other rights are in no way affected by the above.

Take down policy

If you believe that this document breaches copyright please contact librarypure@kcl.ac.uk providing details, and we will remove access to the work immediately and investigate your claim.

Vascular Stem Cell Migration in Response to Dkk3 in Vascular Diseases

The emergence of a novel chemokine-like protein

By

Shirin Issa Bhaloo

A thesis submitted to King's College London for the
degree of Doctor of Philosophy

Cardiovascular Division

Faculty of Life Sciences & Medicine

King's College London

May 2017

In dedication to my Family

Acknowledgements

I wish to express my sincere gratitude to Professor Qingbo Xu for giving me the opportunity to pursue a PhD degree in his laboratory at King's College London. His support, trust, advice, motivation and encouragement throughout my PhD were invaluable and I will always take them with me.

I would like to specially thank Dr. Alexandra Le Bras for her daily supervision, for all the knowledge, expertise and time she shared, for the motivation and support she gave and for her precious advice, not only for my student life but also for my daily life.

I also wish to convey my appreciation to Dr. Yanhua Hu for her kind help and suggestions, particularly regarding animal work, and for her valuable support and encouragement during my PhD.

I would like to thank Ms. Sherrie King for her indispensable help in so many aspects of my PhD journey and for her daily smile and deeply cherished support and friendship.

Many thanks to Zhongyi Zhang for sharing his technical expertise and for his positivity and patience.

I also wish to thank my colleagues Ms. Wenduo Gu (Wendy), Mr. Yao Xie, Dr. Xuechong Hong (Stella), Dr. Ka Hou Lao (Raymond), Dr. Ana Moraga, Ms. Peiyi Luo, Mr. Zhichao Ni and Dr. Witold Nowak, for all the memorable moments we shared, including so many dinners, adventures and trips, which I hope they continue for a long and fun time.

Most importantly, I would like to thank my dear Parents and Sister, for always believing in me, supporting me and giving me so much love and courage.

Finally, I wish to express my appreciation to the Marie Curie Initial Training Network Research Fellowship Program and the British Heart Foundation for funding my PhD project.

Declaration

I, Shirin Issa Bhaloo, confirm that the work presented in this thesis is my own and I have been involved in the design, planning and conduct of all the experiments and the thesis writing.

Expert assistance was provided in some aspects of the project by the following colleagues from the Cardiovascular Division of King's College London.

Dr. Yanhua Hu isolated vascular progenitor cells and smooth muscle cells from murine aorta. For the *ex vivo* experiments, Dr. Hu also isolated murine aorta vessels.

The vector pShuttle-FLAG-HA was kindly provided by Dr. Lingfang Zeng.

Abstract

Stem/Progenitor cells, such as Sca-1+ cells, are abundant in the vascular adventitia and they can differentiate into SMCs and ECs. These cells participate in the vascular wall remodeling observed in atherosclerosis, injury-induced neointimal hyperplasia and vein graft atherosclerosis. The detailed mechanisms of progenitor cell migration towards the intima have not been fully investigated. We hypothesize that Dkk3 plays an important role in resident Sca-1+ vascular progenitor cell migration. In this work, mouse vascular progenitor cells were isolated from the adventitia and sorted for the Sca-1 marker. Using transwell and wound healing assays, we showed that Dkk3 induced adventitia-derived Sca-1+ vascular progenitor cell (Sca-1+ APCs) migration *in vitro*. Additionally, the aortic ring assay demonstrated that Dkk3 was also able to induce Sca-1+ cell migration *ex vivo*. Analysis of the signaling pathways revealed that MAPK kinase signalling cascade, PI3K/AKT pathway and Rho-GTPases family of proteins were involved in the regulation of Dkk3-induced Sca-1+ progenitor cell migration. Our experiments also identified similarities in the migratory response of Sca-1+ cells to Dkk3 and Sdf-1 α . Sdf-1 α receptors are well established and they include CXCR4 and CXCR7. In contrast, the receptor for Dkk3 has not been identified yet. The current study aimed at identifying the receptor(s) involved in Dkk3-driven migration of Sca-1+ cells. Co-IP analysis and Affinity Binding assay revealed that Dkk3 binds to CXCR7. The downregulation of CXCR7 by SiRNA transfection reduced Dkk3-mediated Sca-1+ APC migration and the activation of the downstream signalling pathways. Overexpression of CXCR7, on the contrary, enhanced cell migration. In order to perform an exhaustive analysis of the potential binding partners of Dkk3 and identify additional receptors, we performed a Yeast Two Hybrid experiment. The results showed that integrin α 5 (ITG α 5) and integrin β 1 (ITG β 1) interacted with Dkk3. Co-IP and Affinity Binding assays confirmed that Dkk3 bound to ITG α 5 and ITG β 1. Furthermore, downregulation of these integrins by SiRNA transfection suppressed the migration of Sca-1+ APCs triggered by Dkk3. Our work shows for the first time that Dkk3 acts as a chemokine-like protein able to induce the migration of resident Sca-1+ vascular progenitor cells. The pioneer identification of Dkk3 receptors and the elucidation of the signalling pathways involved in Sca-1+ APC migration could be of major interest for the development of novel drug-targeted therapies in vascular diseases.

Table of Contents

Abstract.....	4
Abbreviations.....	10
List of Figures.....	15
List of Tables.....	19
Chapter 1: Introduction.....	20
1.1 The Vascular System.....	21
1.1.1 The evolution on the knowledge of the arterial adventitia.....	22
1.2 Vascular progenitor cells.....	23
1.2.1 Circulating vascular progenitor cells.....	23
1.2.2 Resident vascular progenitor cells.....	25
1.2.3 Sca-1+ Vascular Progenitor Cells.....	30
1.3 Atherosclerosis.....	31
1.3.1 Pathogenesis of Atherosclerosis.....	31
1.3.2 Endothelial cells and Smooth muscle cells in atherosclerosis.....	33
1.3.3 The role of vascular progenitor cells in atherosclerosis.....	35
1.3.4 Treatment of atherosclerosis.....	38
1.3.5 Complications.....	39
1.4 Cytokines in atherosclerosis.....	41
1.4.1 The Chemokine – Chemokine receptor System.....	44
1.5 Cell migration.....	57
1.5.1 Signalling pathways involved in cell migration.....	61
1.5.2 The role of integrins in cell migration.....	69
1.6 The Dickkopf family of proteins.....	72
1.6.1 Receptors of Dickkopf proteins.....	73
1.6.2 Wnt signalling pathway.....	75
1.6.3 Dickkopf 3 protein in physiology and pathophysiology.....	78
1.7 Protein-protein interaction.....	79
1.7.1 Yeast Two Hybrid System.....	79
1.8 Ligand-Receptor binding.....	83
1.9 Hypothesis and Aims of Study.....	85
Chapter 2: Materials and Methods.....	87
2.1 Materials.....	88

2.1.1	List of cell culture reagents	88
2.1.2	List of chemicals and buffers.....	89
2.1.3	List of Proteins and Inhibitors	91
2.1.4	List of kits	92
2.1.5	List of Antibodies.....	93
2.1.6	List of Primers for RT-qPCR	94
2.2	Methods.....	97
2.2.1	Study Approval and Murine models	97
2.2.2	Cell culture of mouse Adventitial Progenitor Cells (APCs), mouse vascular Smooth Muscle Cells (SMCs) and mouse Endothelial Cells (mECs).....	97
2.2.3	Cell culture of Human Embryonic Kidney (HEK) 293T cells.....	98
2.2.4	Flow Cytometry.....	98
2.2.5	Total RNA extraction	99
2.2.6	Reverse transcription (RT) of RNA to obtain complementary DNA (cDNA).....	99
2.2.7	Quantitative Real-time Polymerase Chain Reaction (RT-QPCR)	100
2.2.8	Conventional Polymerase Chain Reaction (PCR)	100
2.2.9	Agarose gel electrophoresis.....	102
2.2.10	Treatment with recombinant proteins	102
2.2.11	Pharmacological inhibition of signalling pathways.....	102
2.2.12	Protein extraction	103
2.2.13	Western Immunoblotting	103
2.2.14	Co-Immunoprecipitation.....	104
2.2.15	Transwell migration assay.....	105
2.2.16	Wound Healing migration assay	106
2.2.17	BrdU Proliferation Assay	106
2.2.18	Aortic ring assay and immunofluorescence staining	107
2.2.19	Knock-Down of murine receptors with SiRNA	108
2.2.20	G-LISA Small GTPase Activation Assay	108
2.2.21	Cloning of Human receptors and plasmid amplification	109
2.2.22	Overexpression of receptors on HEK 293T Cells.....	114
2.2.23	Fusion of Dkk3 and Sdf1- α with Alkaline Phosphatase (AP)	115
2.2.24	Affinity Binding assay and Dissociation Constant (K_D) calculation.....	115
2.2.25	Yeast Two Hybrid Assay	116
2.2.26	Statistical Analysis of Data	124

Chapter 3: Results.....	125
3.1 Purity of Sca-1+ Adventitial Progenitor Cell population	126
3.2 Dkk3 induced the migration of Sca-1+ vascular progenitor cells, <i>in vitro and ex vivo</i>	128
3.2.1. Transwell migration assay of Sca-1+ progenitor cells towards Dkk3 and Sdf-1 α treatments	128
3.2.2 Wound healing migration assay of Sca-1+ progenitor cells in response to Dkk3 and Sdf-1 α treatments.....	130
3.2.3 Pdgf- β induced the migration of Sca-1+ APCs, <i>in vitro</i>	133
3.2.4 Dkk3 promoted the migration of Sca-1+ APCs, <i>ex vivo</i>	134
3.2.5 <i>In vitro</i> proliferation of Sca-1+ APCs only took place after 48 hours of Dkk3 treatment	144
3.2.6 Conclusion of part 1: Dkk3 induced the migration of Sca-1+ vascular progenitor cells, <i>in vitro and ex vivo</i>	146
3.3 CXCR7 is highly expressed in Sca-1+ APCs	147
3.3.1 Expression profile of chemokine receptors in Sca-1+ APCs.....	147
3.3.2 Expression profile of Dkk protein family related receptors, in Sca-1+ vascular progenitor cells	149
3.3.3 Conclusion of part 2: CXCR7 is highly expressed in Sca-1+ APCs.....	151
3.4 CXCR7 is involved in the migration of Sca-1+ APCs promoted by Dkk3 treatment	152
3.4.1 Downregulation of CXCR7 and Kremen1, by SiRNA transfection, decreased Sca-1+ APC migration driven by Dkk3 treatment	152
3.4.2 Overexpression of CXCR7 induced Dkk3-driven cell migration	162
3.4.3 Dkk3 binds to CXCR7	171
3.4.4 Conclusion of part 5: Dkk3 binds to CXCR7.....	174
3.5 Signalling pathways involved in the migration mechanism of Sca-1+ vascular progenitor cells induced by Dkk3 treatment	175
3.5.1 ERK activation is involved in Dkk3-driven migration mechanism of Sca-1+ APCs	175
3.5.2 Sdf-1 α mediated migration of Sca-1+ cells also involved ERK activation	177
3.5.3 PI3K/AKT signalling pathway is involved in Sca-1+ progenitor cell migration promoted by Dkk3	179
3.5.4 PI3K/AKT pathway is also involved in the migration of Sca-1+ cells upon Sdf-1 α stimulation	182
3.5.5 Activation of Rho GTPases is implicated in Sca-1+ APC migration mechanism induced by Dkk3	184
3.5.6 Conclusion of part 6: Signalling pathways involved in the migration mechanism of Sca-1+ APCs induced by Dkk3 treatment	193

3.5.7	The Wnt signalling pathway is not involved in Sca-1+ APCs migration mechanism stimulated by Dkk3 treatment.....	195
3.6	CXCR7 is upstream of Dkk3-driven migration mechanism of Sca-1+ APCs.....	199
3.6.1	CXCR7 downregulation repressed ERK phosphorylation in Sca-1+ APCs induced by Dkk3	199
3.6.2	CXCR7 knockdown by SiRNA transfection suppressed AKT phosphorylation in Sca-1+ APCs stimulated by Dkk3	200
3.6.3	Rac1 activation induced by Dkk3 is decreased in Sca-1+ cells transfected with CXCR7 SiRNA	201
3.6.4	Dkk3-driven RhoA activation in Sca-1+ cells was reduced upon CXCR7 downregulation	202
3.6.5	Conclusion of part 7: CXCR7 is upstream of Dkk3-driven migration mechanism of Sca-1+ APCs	203
3.7	Summary 1	203
3.8	Dkk3 binds to Integrins $\alpha 5$ and $\beta 1$, through which it induces the migration of Sca-1+ vascular progenitor cells	204
3.8.1	The Yeast-Two-Hybrid system revealed that Dkk3 interacted with Integrin $\alpha 5$ and Integrin $\beta 1$	204
3.8.2	Integrins $\alpha 5$ and $\beta 1$ expression in Sca-1+ vascular progenitor cells.....	224
3.8.3	Dkk3 binds to Integrins $\alpha 5$ and $\beta 1$ in Sca-1+ progenitor cells	225
3.8.4	Integrins $\alpha 5$ and $\beta 1$ are high affinity binding receptors for Dkk3.....	226
3.8.5	Downregulation of Integrins $\alpha 5$ and $\beta 1$ suppressed the migration of Sca-1+ APCs driven by Dkk3 stimulation	228
3.9	Summary 2	231
Chapter 4:	Discussion.....	232
4.1	Brief Overview and Summary of the Major Findings.....	233
4.2	The role of Dkk3 as a chemokine-like protein capable of inducing chemotaxis in Adventitia-derived Sca-1+ vascular Progenitor Cells.....	235
4.2.1	Dkk3 induces the migration of Sca-1+ vascular progenitor cells.....	236
4.2.2	Dkk3 binds with high affinity to CXCR7.....	243
4.2.3	Signalling pathways involved in the Dkk3-driven Sca-1+ vascular progenitor cell migration mechanism	252
4.2.4	CXCR7 is upstream of the Sca-1+ vascular progenitor cell migration mechanism stimulated by Dkk3	257
4.3	The Yeast Two Hybrid system reveals that Dkk3 interacts with Integrin $\alpha 5$ and Integrin $\beta 1$	259
4.3.1	Yeast Two Hybrid control tests	259

4.3.2	Screening of the Universal mouse normalized Library	260
4.4	Dkk3 binds with high affinity to Integrin α 5 and Integrin β 1.....	261
4.5	Integrin α 5 and Integrin β 1 are involved in the migration behaviour of Sca-1+ progenitor cells promoted by Dkk3	263
4.6	Schematic overview of Dkk3-mediated Sca-1+ APC migration mechanism	264
Chapter 5:	Conclusions	266
5.1	Conclusions	267
Chapter 6:	Future work.....	268
6.1	Future work and perspectives	269
Chapter 7:	Publications and Abstracts.....	273
7.1	Published.....	273
7.2	In Revision	273
7.3	In Peer Review	273
7.4	In Preparation	273
7.5	Abstracts presented in meetings	274
Chapter 8:	References	275

Abbreviations

3D	3 Dimensional
Ade	Adenine
AKT	Protein Kinase B
ANOVA	Analysis Of Variance
ApoE	Apolipoprotein E
ApoE KO	Apolipoprotein E Knock Out
ApoE^{-/-}	Apolipoprotein E deficiency / Apolipoprotein E Knock Out
CD133	Cluster of Differentiation 133 / Prominin-1
CD14	Cluster of Differentiation 14 / Monocyte differentiation antigen 14
CD144	Cluster of Differentiation 144 / VE-Cadherin
CD31	Cluster of Differentiation 31 / PECAM-1
CD34	Cluster of Differentiation 34 / CD34 Antigen
CD45	Cluster of Differentiation 45 / PTPRC
Cdc42	Cell division control protein 42
cDNA	Complementary Deoxyribonucleic acid
C-Kit	Proto-oncogene c-Kit / CD117 / Stem cell growth factor receptor
CMV	Cytomegalovirus
Co-IP	Co-Immunoprecipitation
CO₂	Carbon Dioxide
c-Src	Proto-oncogene Tyrosine-protein kinase Src
CXCL12	C-X-C Motif Chemokine Ligand 12 / Stromal cell-derived factor 1
CXCR2	C-X-C Motif Chemokine Receptor 2
CXCR4	C-X-C Motif Chemokine Receptor 4
CXCR7	C-X-C Motif Chemokine Receptor 7 / G protein-coupled receptor RDC1 Homolog / Atypical Chemokine Receptor 3
DAG	Diacylglycerol
DAPI	4', 6-Diamidino-2-Phenylindole
DDO	Minimal Media Double Dropouts

Dkk	Dickkopf
Dkk3	Dickkopf 3 protein
Dkks	Dickkopf proteins
DMEM	Dubelco Modified Eagle Medium
DMSO	Dimethylsulphoxide
dNTP	Deoxyribonucleotide Triphosphate
DVL	Dishevelled
ECM	Extra Cellular Matrix
ECs	Endothelial Cells
ELISA	Enzyme Linked Immunosorbent Assay
EMT	Epithelial-to-Mesenchymal Transition
EPCs	Endothelial Progenitor Cells
ERK	Extracellular signal-regulated kinases
ESCs	Embryonic Stem Cells
FAK	Focal Adhesion Kinase
FBS	Fetal Bovine Serum
Flk-1	Fetal Liver Kinase 1
GAL4	Galactose responsive transcription factor
GAL4 AD	GAL4 Activation Domain
GAL4 DNA-BD	GAL4 DNA-Binding Domain
GAPDH	Glyceraldehyde-3-Phosphate Dehydrogenase
G-CSF	Granulocyte-colony stimulating factor
GEF	Guanine nucleotide exchanging factor
GFP	Green fluorescent protein
Gli	GLI family zinc finger 1
GPCR	G Protein-coupled receptor
GTP	Guanosine Triphosphate
HEK	Human Embryonic Kidney
His	Histidine
HSCs	Hematopoietic Stem Cells

HUVEC	Human Umbilical Vein Endothelial Cell
ICAM-1	Intercellular Adhesion Molecule 1
IP3	Inositol Triphosphate
iPSCs	Induced Pluripotent Stem Cells
ITGα5	Integrin α 5
ITGβ1	Integrin β 1
JNK	c-Jun N-terminal kinase
K_D	Dissociation Constant
KDR	Kinase insert Domain Receptor
Klf4	Krüppel-like Family of Transcription Factor-4
LDL	Low Density Lipoprotein
Leu	Leucine
LIMK	LIM domain kinase 1
LRP5	Low-density lipoprotein receptor-related protein 5
LRP6	Low-density lipoprotein receptor-related protein 6
MAPK	Mitogen-activated Protein Kinase
M-CSF	Macrophage colony-stimulating factor
MEK	Mitogen-activated Protein Kinase Kinase
MLC	Myosin Light Chain
MLCP	Myosin Light Chain Phosphatase
MMP	Matrix Metalloproteinase
mRNA	Messenger Ribonucleic Acid
MSCs	Mesenchymal Stem Cell
O₂	Oxygen
PAK	P21-activated kinase
PCR	Polymerase Chain Reaction
Pdgf-β	Platelet Derived Growth Factor- β
PECAM-1	Platelet and endothelial cell adhesion molecule 1
PFA	Paraformaldehyde
PI3K	Phosphoinositide 3-kinase

PIP2	Phosphatidylinositol biphosphate
PIP3	Phosphatidylinositol 3,4,5 trisphosphate
PiPSCs	Partially induced Pluripotent Stem Cells
PKA	Protein Kinase A
PKB	Protein Kinase B / AKT
PKC	Protein Kinase C
PLC	Phospholipase C
PNPP	p-nitrophenyl phosphate
PPI	Protein-protein interaction
PTPRC	Protein Tyrosine Phosphatase, Rceptor Type C / CD45
QDO	Quadruple dropout medium
Rac-1	Ras-related C3 botulinum toxin substrate 1
REIC	Reduced expression in immortalised cells
RhoA	Ras homolog gene family, member A
RIPA	Radio Immunoprecipitation Assay
RNA	Ribonucleic Acid
ROCK	Rho-associated protein kinase
RT-PCR	Reverse transcription polymerase chain reaction
Sca-1	Stem cells antigen-1
Sca-1+ APCs	Adventitia-derived Sca-1+ vascular progenitor cells
SD	Single Dropout medium
Sdf-1α	Stromal cell-derived factor 1 α
Shh	Sonic hedgehog
SiRNA	Small interfering RNA
SM22α	Smooth Muscle Protein 22-alpha
SMCs	Smooth muscle cells
SM-MHC	Smooth Muscle Myosin Heavy Chain
SMPCs	Smooth muscle progenitor cells
TF	Transcription factor
Trp	Tryptophane

VCAM-1	Vascular Cell Adhesion Molecule-1
VEGFR2	Vascular Endothelial Growth Factor Receptor 2
VPCs	Vascular Progenitor Cells
VSMCs	Vascular Smooth muscle cells
vWf	Von Willebrand Factor
Y2H	Yeast Two Hybrid
α-SMA	α -Smooth Muscle Actin

List of Figures

List of figures	Page
Figure 1.1: Structure of blood vessels	21
Figure 1.1.1: Evolution on the knowledge of the arterial Adventitia	22
Figure 1.2.2: Distribution of Stem/Progenitor cells across the 3 layers of the vascular wall	29
Figure 1.3.1: Basic pathogenesis of atherosclerosis	32
Figure 1.3.2: Vascular smooth muscle cell contribution to plaque stability	34
Figure 1.4A: Inflammatory process in atherosclerosis regulated by cytokines	42
Figure 1.4B: Cytokines involved in atherogenesis	43
Figure 1.4.1.1: Classification of chemokines	45
Figure 1.4.1.2: Chemokine G protein-coupled receptor associated signalling pathways	48
Figure 1.4.1.3: The role of chemokines in atherogenesis	50
Figure 1.4.1.4A: The CXCL12/CXCR4 signalling pathway	54
Figure 1.4.1.4B: Structure and amino acid sequence of CXCR4 and CXCR7	55
Figure 1.5A: Steps involved in cell migration	58
Figure 1.5B: Cytoskeleton protein filaments	59
Figure 1.5C: Mechanism of protrusion formation by actin filaments	61
Figure 1.5.1.1A: Regulation of the cytoskeleton by Rho GTPases	63
Figure 1.5.1.1B: Downstream effectors of Rho GTPases	64
Figure 1.5.1.2: PI3K/AKT pathway and regulation of chemotaxis	66
Figure 1.5.1.3: Ras-Raf-MEK-ERK signalling pathway and regulation of chemotaxis	68
Figure 1.5.1.4: Signalling pathways regulated by β -arrestin	70
Figure 1.5.2: Integrins in focal adhesions	72
Figure 1.6: Structure of the Dickkopf family of proteins	73
Figure 1.6.1: Wnt signalling modulation by Dkk proteins	77
Figure 1.6.2: Wnt signalling pathways	78
Figure 1.7.1A: Yeast Two Hybrid system GAL4 transcription factor based	82
Figure 1.7.1B: Yeast mating strategy	83
Figure 1.7.1C: Reporter gene constructs in Y2HGold and Y187 yeast strains	84

List of figures	Page
Figure 1.8.1A: Ligand-receptor binding curve	86
Figure 2.2.15: Layout of fields in each transwell insert at 10X magnification	107
Figure 2.2.16: Layout of fields in each well of a 12-well plate, at 10X magnification	108
Figure 2.2.21A: Map of the vector pShuttle2-Flag-HA used for cloning	112
Figure 2.2.21B: Map of the vector pCMV3-HA	114
Figure 2.2.25.2A: Mating strategy for the control experiments	117
Figure 2.2.25.2B: pGBKT7-53 Plasmid Map	118
Figure 2.2.25.2C: pGADT7-T Plasmid Map	118
Figure 2.2.25.2D: pGBKT7-Lam Plasmid Map	119
Figure 2.2.25.3: Murine Dkk3 cDNA sequence and pGBKT7 plasmid Map	120
Figure 2.2.25.7: Co-transformation strategy for confirmation of positive interaction	124
Figure 3.1: Sca-1+ progenitor cell population purity analysis	127
Figure 3.2.1: Dkk3 and Sdf-1 α induced Sca-1+ APCs migration - Transwell migration assay	129
Figure 3.2.2: Dkk3 and Sdf-1 α induced Sca-1+ APCs migration - Wound healing assay	131
Figure 3.2.3: Pdgf- β induced the migration of Sca-1+ progenitor cells	133
Figure 3.2.4.1: Dkk3 induced cell outgrowth from the aortic rings	135
Figure 3.2.4.2: Dkk3 promoted Sca-1+ cell outgrowth from the aortic rings	140
Figure 3.2.5: <i>In vitro</i> proliferation of Sca-1+ progenitor cells in response to Dkk3	144
Figure 3.3.1: Expression profile of the chemokine receptors in ECs, Sca-1+ APCs and SMCs	148
Figure 3.3.2: Expression profile of Dkk protein family related receptors, in ECs, Sca-1+ APCs and SMCs	150
Figure 3.4.1.1: Sca-1+ APCs express low level of CXCR4	153
Figure 3.4.1.2: CXCR7 KD decreased Sca-1+ APC migration induced by Dkk3 or Sdf-1 α	155
Figure 3.4.1.3: Sca-1+ progenitor cell migration induced by Dkk3 is not decreased upon CXCR2 downregulation	157
Figure 3.4.1.4: Kremen1 Knockdown decreased Sca-1+ APC migration driven by Dkk3	158
Figure 3.4.1.5: Sca-1+ progenitor cells express low level of Kremen2	160
Figure 3.4.2.1: Sdf-1 α , but not Dkk3 stimulation, increased the migration of HEK 293T cells overexpressing CXCR4	162

List of figures	Page
Figure 3.4.2.2: Dkk3 and Sdf-1 α promoted the migration of CXCR7 overexpressing HEK 293T cells	164
Figure 3.4.2.3: Dkk3 and Sdf-1 α treatments had no effect on the migration level of CXCR2 overexpressing HEK 293T cells	166
Figure 3.4.2.4: Dkk3 stimulation had no effect on the migration of HEK 293T cells overexpressing either Kremen1 or Kremen2	168
Figure 3.4.3.1: Dkk3 co-immunoprecipitated with CXCR7 in Sca-1+ vascular progenitor cells	171
Figure 3.4.3.2: CXCR7 has high binding affinity for Dkk3	172
Figure 3.5.1: ERK activation is involved in Dkk3-driven migration mechanism of Sca-1+ vascular progenitor cells	176
Figure 3.5.2: Sdf-1 α -mediated migration of Sca-1+ cells also involved ERK activation	178
Figure 3.5.3: PI3K/AKT signalling pathway is involved in Sca-1+ progenitor cell migration promoted by Dkk3	180
Figure 3.5.4: PI3K/AKT pathway is involved in the migration of Sca-1+ progenitor cells upon Sdf-1 α stimulation	183
Figure 3.5.5.1: Rac1 activation is involved in Sca-1+ cell migration mechanism induced by Dkk3	185
Figure 3.5.5.2: RhoA signalling pathway is implicated in Sca-1+ progenitor cell migration mechanism stimulated by Dkk3 treatment	189
Figure 3.5.7.1: β -Catenin inhibition by FH535 had no effect in the Dkk3-mediated migration mechanism of Sca-1+ APCs	196
Figure 3.5.7.2: DVL inhibition by Peptide Pen-N3 had no effect in the Dkk3-driven migration mechanism of Sca-1+ APCs	197
Figure 3.6.1A: CXCR7 downregulation repressed ERK phosphorylation in Sca-1+ APCs induced by Dkk3	199
Figure 3.6.2A: CXCR7 knockdown by SiRNA transfection suppressed Dkk3-triggered AKT phosphorylation in Sca-1+ APCs	200
Figure 3.6.3A: Rac1 activation induced by Dkk3 was decreased in Sca-1+ cells transfected with CXCR7 SiRNA	201
Figure 3.6.4A: Dkk3-driven RhoA activation in Sca-1+ APCs was reduced upon CXCR7 downregulation	202
Figure 3.8.1.4: Co-transformation strategy for confirmation of positive interaction	221

List of figures	Page
Figure 3.8.2: ITG α 5 and ITG β 1 expression in Sca-1+ APCs, ECs and SMCs	224
Figure 3.8.3A: Dkk3 and ITG α 5 co-Immunoprecipitated with ITG β 1 in Sca-1+ progenitor cells	226
Figure 3.8.4: Integrins α 5 and β 1 are high affinity binding receptors for Dkk3	227
Figure 3.8.5: Downregulation of Integrins α 5 and β 1 suppressed Dkk3-driven Sca-1+ APC migration	229
Figure 4.2.2A: Sca-1+ expression on artificial vessel model	249
Figure 4.2.2B: Relation between Dkk3 plasmatic concentration and the risk of atherogenesis	250
Figure 4.6: Dkk3-driven Sca-1+ vascular progenitor cell migration mechanism	265

List of Tables

List of tables	Page
Table 1.2.2: Summary of publications on stem/progenitor cells resident in the vascular wall	26
Table 1.4.1: Chemokines and their corresponding chemokine receptors	46
Table 1.6.1: Receptors proposed for the Dkk proteins	75
Table 2.1.1 List of cell culture reagents	90
Table 2.1.2 List of chemicals and buffers	91
Table 2.1.3 List of Proteins and Inhibitors	93
Table 2.1.4 List of kits	94
Table 2.1.5 List of Antibodies	95
Table 2.1.6 List of Primers	96
Table 2.2.6 Reverse Transcription components	101
Table 2.2.8.1 List of reaction mix components	102
Table 2.2.8.2 Thermal cycling conditions for Pfu Polymerase-mediated PCR amplification	103
Table 2.2.8.3 Conventional PCR primer sequences and parameters	103
Table 2.2.11: List of pharmacological agents used to inhibit signalling pathways	104
Table 2.2.19: List of receptor SiRNA and respective control SiRNA	110
Table 2.2.21A: Reaction mixture for enzyme digestion of the vector	113
Table 2.2.21B: Reaction mixture for enzyme digestion of the insert	113
Table 2.2.21C: Reaction mixture for enzyme digestion of the vector	113
Table 2.2.25: List of items required for Yeast Two Hybrid experiment	116
Table 2.2.25.2: Yeast transformation strategy	119
Table 3.8.1.1A: Yeast transformation strategy	205
Table 3.8.1.1B: Positive and negative control results	206
Table 3.8.1.2: Test for Dkk3 auto-activation	211
Table 3.8.1.3A: Screening of the Universal mouse normalized Two-Hybrid Library	214
Table 3.8.1.3B: Identification of the library prey proteins that interacted with the bait Dkk3	217
Table 3.8.1.4: Results for the positive interaction confirmation test	222
Table 4.2.1: Comparison between Transwell and Wound healing migration assays	237

Chapter 1: Introduction

1.1 The Vascular System

The cardiovascular system consists of the heart and the blood vessels which distribute the blood in the body. The blood vessels comprise the arteries, arterioles, capillaries, venules and the veins. The capillaries are formed by a monolayer of endothelial cells underlying the basal lamina. Smooth muscle cells are absent but pericytes may envelope the capillaries. The arteries and the veins are composed of three tissue layers (Tunics) that surround the lumen of the vessel (Figure 1.1).

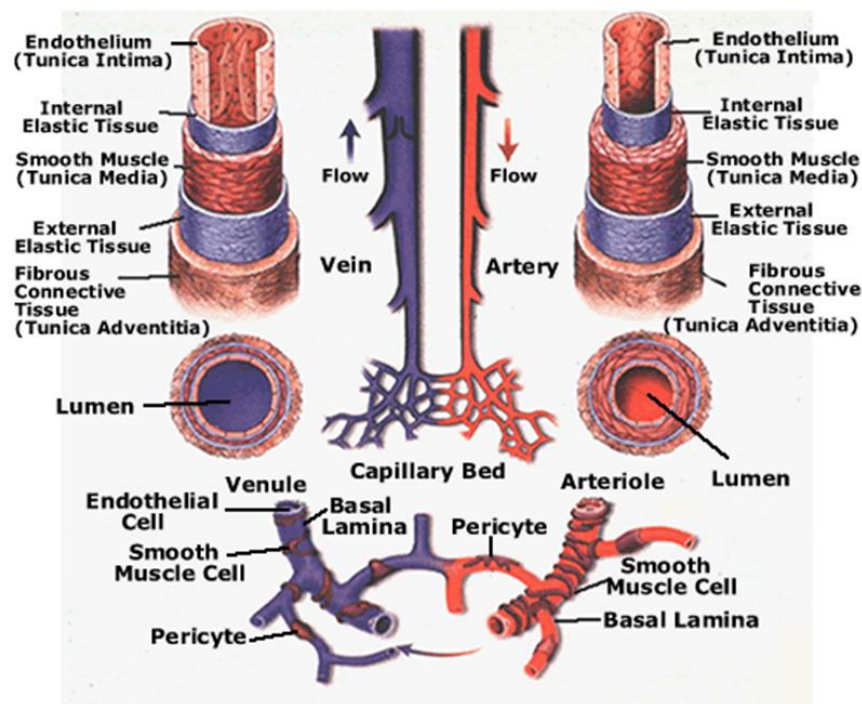


Figure 1.1: Structure of blood vessels. The arteries and the veins are composed of three tissue layers: the inner most layer (tunica intima), the media layer (tunica media) delimited by the internal elastic membrane and the external elastic membrane, and the external layer (tunica adventitia). (Source: <http://bme240.eng.uci.edu/students/08s/sshreim/bvd.htm>).

The tunica intima is the inner most layer of the blood vessel, which consists of a monolayer of endothelial cells (ECs) surrounded by a basal lamina and delimited by the internal elastic lamina. The middle layer of the vessel wall is the tunica media, comprising predominantly smooth muscle cells (SMCs) displayed circumferentially in sub-layers, which are supported by connective tissue (elastic and collagen fibers). The media is structurally supported by the external elastic lamina which separates it from the tunica adventitia. The adventitia is the external layer of the blood vessel and its outer limit is more difficult to define, as it blends with the perivascular connective tissue [1].

1.1.1 The evolution on the knowledge of the arterial adventitia

Until recently, the adventitia was considered a passive vessel wall layer comprising only fibro-elastic connective tissue. In larger vessels it was reported to also include the vasa vasorum, the lymphatic plexi and nerve fibers [2]. Today, the adventitia is considered a dynamic layer, in communication with the other vessel wall layers. It contributes to the growth and repair of the vessel wall and exhibits important roles in inflammation and vascular remodelling. Various cell types can be found in the adventitia, including fibroblasts, macrophages, adipocytes and pericytes (Figure 1.1.1) [3-5].

In 2004, Hu et al., were the first to reveal that the aortic adventitia contained resident vascular stem/progenitor cells expressing the markers Stem cell antigen-1 (Sca-1+), Stem cell factor receptor (CD117+; c-Kit+), Hematopoietic progenitor cell antigen CD34 (CD34+) and Fetal liver kinase-1 (Flk1+) [6]. Since then, a substantial number of studies has provided evidences regarding the stem cell niche properties presented by the adventitial layer. Passman et al., supported the finding of resident Sca-1+ cells by characterizing a sonic hedgehog (Shh) signaling domain restricted to the adventitial layer of the artery wall [7]. Campagnolo et al., reported that CD34+/CD31- cells, with a multilineage potential, could be found around the vasa vasorum in the adventitia of human saphenous veins [8]. Zengin et al., concluded that a population of CD34+ cells, capable of differentiating into endothelial or immune cells, was localized between the media and the adventitia of adult human blood vessels [9]. Psaltis et al., identified a macrophage progenitor cell population (Sca-1+/CD45+) in the adventitia of postnatal mouse vasculature [10]. Mesenchymal stem cells (MSCs) were also detected in human pulmonary artery adventitia, by Hoshino et al., [11]. Recently, Kramann et al., showed that the adventitial Gli+ MSC-like cells are progenitors of vascular smooth muscle cells [12].

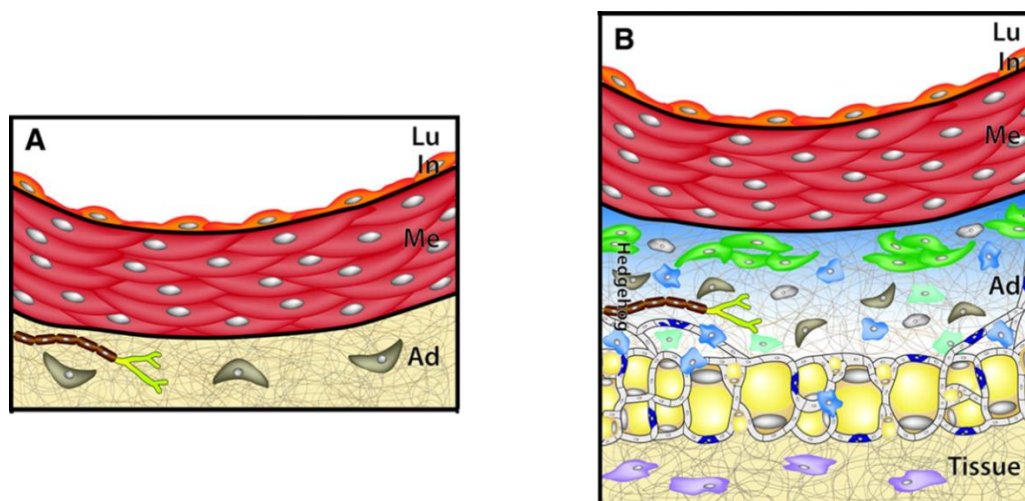


Figure 1.1.1: Evolution on the knowledge of the arterial Adventitia. A: Traditional adventitia layer: Collagen-rich extracellular matrix embedding fibroblasts (grey) and perivascular nerve. **B: Dynamic adventitia layer:** Complex adventitial layer comprising the collagen-rich extracellular matrix embedding not only fibroblasts and perivascular nerves, but also macrophages (blue), mast cells (pale green), CD34+/Sca1+ progenitor cells (dark green), T cells (grey), microvascular endothelial cells (light grey), pericytes (dark blue), and adipocytes (yellow)[5].

1.2 Vascular progenitor cells

Blood vessels are formed usually through two processes: Vasculogenesis and angiogenesis. Vasculogenesis refers to the creation of the primary vascular network, as observed during embryonic development, where the blood vessels are formed *de novo* from progenitor cells (angioblasts). Angiogenesis consists of the sprouting of new blood vessels from the pre-existing vascular networks and can occur at any time throughout an organism's life time. The vascular plasticity, either through vasculogenesis or angiogenesis, contributes to both vascular repair and vascular disease development.

Initially, the cells within the vasculature were thought to be terminally differentiated. Accumulating studies revealed that in fact, both vasculogenesis and angiogenesis comprise vascular progenitor cell homing or recruitment, proliferation and differentiation into smooth muscle cells (SMCs) and endothelial cells (ECs), amongst other cell types.

Vascular progenitor cells are adult stem cells that reside in specific sites of vascular tissues (stem cell niche site), including the bone marrow and the vessel wall. These cells are multipotent and commitment to specific cell lineages [13, 14].

Currently, two types of vascular progenitor cells are presented in the literature: circulating vascular progenitor cells and resident vascular progenitor cells.

1.2.1 Circulating vascular progenitor cells

Circulating vascular stem/progenitor cells correspond to the cells circulating in the blood flow from one tissue or organ to another. These cells, induced by signals released in response to certain stimulus, are mobilized to the vessel wall where they can differentiate into ECs or SMCs, amongst other types of cells.

The circulating stem/progenitor cells either belong to the hematopoietic-lineage (bone marrow-derived hematopoietic stem cells) or to the non-hematopoietic lineage. The origin of the latter group of cells is still unclear [15]. Accumulating studies have shown the detection of non-hematopoietic circulating stem cells. Aicher et al., revealed that liver-derived non-hematopoietic c-Kit+/CD45- progenitor cells can enter the circulation, following induction of hindlimb ischemia, and can contribute to postnatal vasculogenesis [16]. A study by Kuwana et al., concluded that circulating human CD14+ monocytes, precursor of macrophages and dendritic cells, possessed the potential to differentiate into mesenchymal lineage cells, such as adipocytes and osteoblasts [17]. Circulating mesenchymal stem cells (MSCs) were also mentioned in several studies. Wang et al., observed sequential fluctuations in the number of circulating mesenchymal stem cells CD45-/CD34- in patients who suffered a myocardial infarction [18]. Marketou et al., verified that patients with hypertrophic

cardiomyopathy exhibited an increase in the number of circulating MSCs (CD45-/CD34-/CD90+) compared to healthy individuals [19]. Finally, Zvaifler et al., found MSCs CD45-/CD34-/CD14- in the blood of normal individuals, and observed that these cells could differentiate into adipocytes or osteoblasts under appropriate conditions [20].

Interestingly, bone marrow-derived very small embryonic-like cells (VSELs) of non-hematopoietic lineage (CD45-/CD133+), displaying the phenotype of primitive pluripotent cells as they are enriched for early embryonic markers (Oct-4, Nanog, SSEA-4, Rex1, Dppa3 and Rif-1), were described to be mobilized to the peripheral blood, after acute myocardial infarction [21, 22].

The origin of circulating endothelial progenitor cells (EPCs) is attributed not only to a hematopoietic lineage, but also to a non-hematopoietic source, such as mesenchymal stem cells or even CD14+ monocytic cells [23, 24]. The most widely accepted phenotype for these cells is CD34+/KDR+/CD133+ and once they differentiate into mature ECs, the CD133+ marker is lost, while CD31+ and vWf, amongst other markers, start to be expressed [25-28]. EPCs are notoriously described in the literature and their function in cardiovascular diseases is rather controversial. If on one hand these cells are known to have a therapeutic potential due to their contribution to angiogenesis and endothelium repair [29-33], on the other hand studies have shown that EPCs have a role in the pathogenesis of vascular diseases [34-38].

Hematopoietic stem cells (HSCs) are multipotent self-renewing progenitor cells derived from the bone marrow. The transplantation of HSCs has become a standard therapeutic solution for patients suffering from disorders in their hematopoietic system or for cancer patients undergoing high dose chemotherapy [39, 40]. These stem cells can give rise to not only blood cells but also other cell types, including epithelial cells, hepatocytes, cardiomyocytes, SMCs and ECs [41]. Takakura et al., observed that HSCs participate in angiogenesis [42]. Contrastingly, Wang et al., concluded that HSCs directly contribute to arteriosclerosis [43]. Sata et al., demonstrated that HSCs (c-Kit+/Sca-1+/Lin-) from bone marrow give rise to SMCs and ECs that contribute to vascular remodelling [44].

The origin of EPCs and Smooth muscle progenitor cells (SMPCs) is still controversial. On one hand, some studies demonstrate that EPCs and SMPCs are bone marrow-derived cells [44-53]. Contrarily, other reports show that EPCs and SMPCs are not originated by bone marrow-derived cells. For example, Case et al., concluded that CD34+/CD133+/VEGFR-2+ are hematopoietic progenitor cells (HPCs) but not EPCs, as proposed by others, because these cells have never been isolated in order to give rise to EC progeny [54]. Timmermans et al., revealed that late EPCs (also known as endothelial outgrowth cells – EOCs) express CD34+, but they are not derived from CD133+ or CD45+ hematopoietic progenitor cells isolated from bone marrow or human cord blood [55]. Additionally, Yoder et al., demonstrated that endothelial cell colony-forming units (CFU-ECs), contrary to blood outgrowth endothelial cells (BOECs), are derived from HSCs and differentiate into phagocytic macrophages, instead of ECs [56]. Regarding the origin of SMPCs, Bentzon et al., argued that SMCs in atherosclerotic plaques of ApoE^{-/-} mice did not originate from bone marrow-derived circulating progenitor cells but rather from local vessel wall [57]. Interestingly, Daniel et al., verified that bone

marrow-derived SMPCs contribution to neointima was rare, whereas adventitial Sca-1+ and CD34+ cells were highly proliferative. The contribution of bone marrow-derived cells corresponded only to the inflammatory period in neointima formation [58]. Iwata et al., further supported this notion by showing that the few bone marrow-derived α -SMA+ (smooth muscle α -Actin) cells present in neointima lesion induced by Wire injury or in ApoE^{-/-} mice were SM-MHC (Smooth muscle myosin heavy chain) negative, but CD115+/CD11b+/F4/80+/Ly-6C+ (surface markers of inflammatory monocytes). Therefore, they demonstrated that bone marrow-derived cells contributed to vascular inflammation but not SMCs in neointima formation [59]. Hu et al., by using an artery allograft model and chimeric mice revealed that the SMCs in the atherosclerotic lesion predominantly originated from the local/recipient vessel and not from bone marrow cells [60]. Groenewegen et al., by using transgenic mice and aortic allograft model, also concluded that bone marrow-derived cells are not the source of SMCs in transplant arteriosclerosis and in-stent restenosis [61]. Collectively, these findings prompted research work in the exploration of other sources of EPCs and SMPCs, namely the vascular wall.

Circulating vascular progenitor cells seem to have a dual role in vascular diseases. They were shown to either promote vascular repair, thus being important for vascular regeneration, or to contribute to vascular lesions, such as atherosclerotic neointimal lesions [35, 36, 41, 62, 63].

1.2.2 Resident vascular progenitor cells

Until very recently, the existence of resident vascular progenitor cells was not known. Interestingly, in 2001, Alessandri et al., by performing the aortic ring assay with human embryonic aortas, showed for the first time *ex vivo* outgrowth of capillary-like structures. Moreover, the cells isolated from these outgrowths were CD34+/CD31- and differentiated *in vitro* into ECs [64]. This suggested that the circulating vascular progenitor cells were not the sole contributors for the new vessel formation and that the vessel wall itself could potentially contain resident vascular progenitor cells.

Later, in 2003, Majka et al., were able to isolate vascular progenitor cells resident in adult skeletal muscle. The cells comprised two distinct populations of cells. One corresponded to hematopoietic stem cells (denominated as side population – SP) and the other population of progenitor cells, although also derived from bone marrow, exhibited a more mesenchymal phenotype (non-SP), not being able to reconstitute blood. Once injected into injured muscle, the SP cells engrafted into the endothelium and the non-SP cell engrafted into smooth muscle [65]. In the same year, Tintut et al., also observed that the artery wall contains cells similar to MSCs, with *in vitro* multipotency ability [66]. In 2004, Messina et al., isolated and expanded cardiac stem cells capable of self-renewal and of differentiating into cardiomyocytes and vascular cells [67].

It was only in 2004, that the first evidence of non-bone marrow-derived resident vascular progenitor cells, present in the adventitia layer of the vessel wall, was provided. Hu et al., revealed that the

adventitia layer contained non-bone marrow-derived vascular progenitor cells expressing the markers Sca-1+, C-Kit+, CD34+ and Flk1+. Amongst these, the adventitial Sca-1+ cells were able to differentiate *in vivo* into SMCs and to participate in neointima formation [6].

Since then, numerous studies have been published proving the presence of vascular progenitor cells resident in the vessel wall, as a reservoir for multipotent stem/progenitor cells (Table 1.2.2). For instance, Ingram et al., showed that endothelial progenitor cells, resident in the *Intima* of umbilical vein and aortic vessel, could contribute to endothelial cell formation [68]. Mesenchymal stem cells were as well detected in the internal surface of human varicose saphenous vein. These cells were able to differentiate *in vitro* into osteoblasts, chondrocytes and adipocytes [69]. Also in human saphenous vein, Campagnolo et al., observed the localization of CD34+ cells around adventitial vasa vasorum, showing clonogenic and multilineage differentiation capacities [8]. Zengin et al., reported that endothelial progenitor cells CD34+/CD31-, capable of differentiating into mature endothelial cells, hematopoietic cells and macrophages, were displayed in a region contained between the *media* and the adventitia of adult human blood vessels [9]. Pasquinelli et al., demonstrated the presence of angiogenic mesenchymal stromal cells within the human thoracic aorta[70]. Still in the *media* layer, Sainz et al., isolated a side population of progenitor cells displaying a Sca-1+/C-Kit(-/low)/Lin-/CD34(-/low) profile, which generated cells with ECs and SMCs phenotype and vascular-like branching structures [71]. Furthermore, Torsney et al., identified within the neointima and adventitia of human atherosclerotic arteries, progenitor cells expressing Sca-1+, CD34+ and C-Kit+ markers, suggesting that these cells could be the source of SMCs, ECs and macrophages that form atherosclerotic lesions [72]. Pericytes, which are normally regarded as mural cells, have also been described to possess multipotent stem/progenitor cell properties, although controversy still exists regarding their distinction from MSCs [73, 74].

Table 1.2.2: Summary of publications on stem/progenitor cells resident in the vascular wall

Publication	Source of stem/progenitor cells	Stem/progenitor cells and markers	Differentiation potential
Alessandri et al., 2001	Human embryonic aorta rings	CD34+/CD31- cells	ECs
Tintut et al., 2003	Media of bovine aorta	Calcifying vascular cells – MSCs-like cells	Chondrogenic and leiomyogenic (SMCs) lineage cells
Hu et al., 2004	Adventitia of aortic roots	Adventitial Sca-1+ cells	SMCs
Covas et al., 2005	Internal surface of human saphenous vein	MSCs	Osteoblasts, chondrocytes, adipocytes
Ingram et al., 2005	HUVECs and HAECs (Intima)	EPCs	ECs

Publication	Source of stem/progenitor cells	Stem/progenitor cells and markers	Differentiation potential
Howson et al., 2005	Rat aorta	CD34+/Tie2+/CD31- cells	Pericytes
Sainz et al., 2006	Mouse aortic <i>media</i>	Sca-1+/C-kit(-/low)/Lin-/CD34(-/low) cells	ECs, SMCs
Zengin et al., 2006	Region between the <i>media</i> and the adventitia of human artery	EPCs	ECs, Hematopoietic cells, immune cells
Pasquinelli et al., 2007	<i>Media</i> -Adventitia of human thoracic aorta	CD34+ cells and C-kit+ cells	ECs
Torsney et al., 2007	Atherosclerotic lesion/Adventitia of human aorta and mammary arteries	CD34+, C-kit+ and Sca-1+ cells	NA
Invernici et al., 2007	Human fetal aorta	MSCs-like cells	ECs and mural cells
Passman et al., 2008	<i>Media</i> -Adventitia of mouse embryonic and adult arteries	Sca-1+ cells	SMCs
Hoshino et al., 2008	Adventitia of human pulmonary artery	MSCs	Osteogenic, adipogenic and myogenic lineage differentiation <i>in vitro</i>
Traktuev et al., 2008	Stromal-vascular fraction of human subcutaneous adipose tissues	CD34+ cells (pericyte-like cells)	NA
Crisan et al., 2008	Capillaries and microvessels of human fetal and adult tissues	Pericytes	Osteogenic, adipogenic and myogenic lineage cells
Barcelos et al., 2009	Human fetal aorta	CD133+ progenitor cells	NA
Liu et al., 2009	Human blood and intima of transplant atherosclerotic vessels	Myeloid/Progenitor cell lineage	ECs
Bearzi et al., 2009	Human coronary arteries and capillaries	C-kit+/KDR+ cells	ECs, SMCs, Cardiomyocytes
Pasquinelli et al., 2010	<i>Media</i> -Adventitia of human aortic and femoral arteries	Sca-1+, Notch-1+, Stro-1+ and Oct-4+ cells (Mesenchymal stromal cells)	Adipogenic, chondrogenic and leiomyogenic lineages
Campagnolo et al., 2010	Human saphenous vein	CD34+/vWF- and CD34+/CD31- cells	Pericytes/mesenchymal cells showing clonogenic and multilineage differentiation capacities
Zorzi et al., 2010	Rat aortic rings	Immature immunocytes	Macrophages and dendritic cells
Juchem et al., 2010	Venous <i>Intima</i> and atherosclerotic plaques	Pericytes	NA
Katare et al., 2011	Saphenous vein	Pericyte progenitor cells	NA

Publication	Source of stem/progenitor cells	Stem/progenitor cells and markers	Differentiation potential
Naito et al., 2011	<i>Intima</i> of mouse hindlimb vasculature and other tissues	EPCs	ECs
Klein et al., 2011	Human arterial adventitia	Multipotent stem cells	Pericytes and SMCs
Tsai et al., 2012	Neointimal lesion from a mouse model of restenosis by grafting a decellularized vessel to the carotid artery.	Sca-1+, CD34+ and C-kit+ cells	ECs, SMCs
Tang et al., 2012	<i>Media</i> of mouse, rat and human vessels	Multipotent vascular stem cells (Sox17+, Sox10+ and S100β+)	SMCs and chondrogenic cells
Psaltis et al., 2012	Adventitia of murine aorta	Sca-1+/CD45+ multipotent hematopoietic progenitor/stem cells (Macrophage precursors)	Inflammatory cells
Corselli et al., 2012	Adventitia - stromal vascular fraction of human white adipose tissue	MSCs	Clonogenic multipotent progenitors in culture
Montiel-Eulefi et al., 2012	Aorta ex-plants of Sprague-Dawley rat	Pericytes	Neural-like phenotype
Wong et al., 2013	Adventitial tissue of mouse aorta	Sca-1+ cells	SMCs
Chen et al., 2013	Adventitia of vein grafts	Sca-1+ cells	SMCs and adipogenic, osteogenic or chondrogenic lineages <i>in vitro</i>
Klein et al., 2013	Human arterial adventitia	CD44+ Multipotent stem cells	SMCs
Tigges et al., 2013	Mouse femoral artery adventitia	Pericyte-like cells, MSCs	NA
Yang et al., 2013	Human arteries, veins, small vessels and adipose tissue	Stromal cells (MSC-like cells CD105+); Vessel wall stromal cells CD34+/CD31-/CD105+	Multiple lineage cells
Psaltis et al., 2014	Adventitia of murine aorta	Sca-1+/CD45+ macrophage precursors	Macrophages
Klein et al., 2014	Murine aorta explants and angiogenic tumour blood vessels from human tumour samples	Nestin+ cells multipotent stem cells	SMCs and pericytes

Publication	Source of stem/progenitor cells	Stem/progenitor cells and markers	Differentiation potential
Zaniboni et al., 2014	Media of porcine aorta	MSCs	Adipogenic, osteogenic or chondrogenic lineages <i>in vitro</i>
Iacobazzi et al., 2014	Adventitia of vein remnants of coronary artery bypass	CD105+/CD45-/CD31- MSC-like cells	NA
Kramann et al., 2015	Microvasculature and adventitia of large arteries	Perivascular Gli1+ MSC-like cells	Myofibroblasts
Prandi et al., 2015	Human saphenous vein segments – Adventitia (<i>ex vivo</i> exposition to arterial-like pressure)	NG2+/CD44+/Sox-10+ cells	NA
Evans et al., 2015	Mouse aorta	MSCs	Adipogenic, osteogenic or chondrogenic lineages
Wu et al., 2015	Adventitia of rat arteries	CD34+ cells	SMCs
Shen et al., 2016	Rat carotid adventitia	CD34+ cells	SM22 α + cells

Even though there is enough evidence confirming the presence of resident progenitor cells in all the three layers of the vessel wall, the functional role of these cells is still not clear, leaving behind many unanswered questions [75-77]. Nevertheless, the vascular wall is now accepted to possess stem cell niche-like properties, particularly the adventitial layer, which can interact with the other vessel wall layers through its complex reservoir of progenitor cells (Figure 1.2.2).

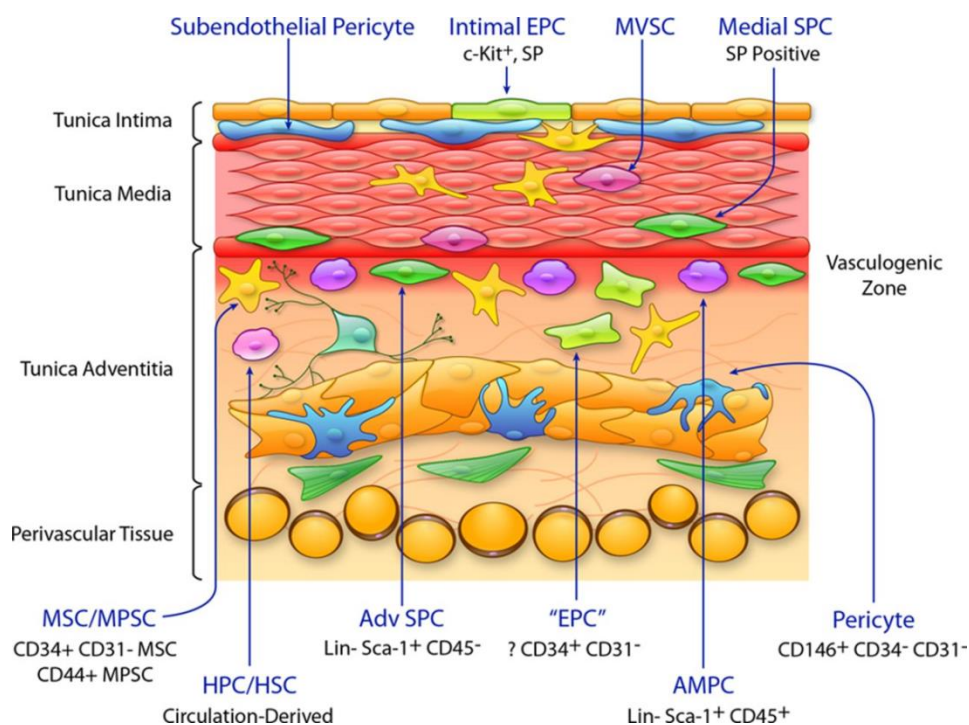


Figure 1.2.2: Distribution of Stem/Progenitor cells across the three layers of the vascular wall.

Stem/progenitor cells are present in all three layers of the vessel wall. The Intima may contain endothelial progenitor cells (EPCs), which may also be present in the vasculogenic zone between the media and the adventitia. Beneath the Intima pericytes with multipotency properties can be found. In the media, mesenchymal stem cells (MSCs) or multipotent stem cells (MPSCs) have been detected, together with side population of progenitor cells. The adventitia is notably rich in distinct populations of stem/progenitor cells, including Sca-1+ cells, adventitial macrophage precursors Sca-1+/CD45+ cells (AMPCs), CD34+/CD31- EPCs or MSCs, CD44+ multipotent stem cells and pericytes. Hematopoietic stem cells (HSCs) and hematopoietic progenitor cells (HPCs) may be recruited to the vasculature and thus be observed in the vessel wall. (Source: Psaltis et al.; Vascular wall progenitor cells in health and disease; Circulation Research; 2015)[77].

1.2.3 Sca-1+ Vascular Progenitor Cells

The Sca-1+ marker, also known as Ly-6A/E, was originally used to enrich adult murine hematopoietic stem cells (HSCs). Bone marrow cells expressing Sca-1+ marker demonstrated the potential to differentiate into ECs. Under homeostatic condition the endothelium of large arteries exhibits little Sca-1+ expression. However, in response to injury, the number of Sca-1+ cells in the endothelial layer of the aorta increases. Additionally, ApoE-deficient mice, which model arteriosclerosis, present elevated numbers of Sca-1 cells in the aortic endothelium.

Hu et al., demonstrated that adventitia-resident vascular progenitor cells expressed the Sca-1+ marker (Sca-1+ APCs) and that these cells contributed to atherosclerosis via migration and differentiation into SMCs [6]. Amongst other studies, the work of Yu et al., further supported the notion of the contribution of resident Sca-1+ cells to neointima formation [78]. Nevertheless, Sca-1+ APCs may possess a potential role in reparative and regenerative processes. The differentiation of Sca-1+ cells into SMCs or ECs may participate in vessel repair in atherosclerotic conditions, with endothelial layer regeneration and atherosclerotic plaque stability. Proliferation and migration of Sca-1+ APCs to the directed site to later lead to differentiation may precede the reparative process. Furthermore, these mechanisms could provide very useful application of Sca-1+ APCs in tissue engineering, such as artificial vessel generation.

1.3 Atherosclerosis

Atherosclerosis is a chronic pathological condition characterised by intense vascular remodelling and inflammatory processes. As a result, it usually leads to the development of important cardiovascular disorders, such as coronary artery disease, carotid artery disease, peripheral artery disease, myocardial infarction, stroke, amongst others. In 2012, cardiovascular diseases were considered one of the major causes of death worldwide, reason why so much research is focused on their pathogenesis and the discovery of therapeutic solutions for atherosclerosis [79].

1.3.1 Pathogenesis of Atherosclerosis

Genetic or environmental risk factors which may induce hypertension, hyperlipidemia, hyperglycemia, chronic inflammation, circulation of reactive oxygen species, amongst other disorders, can cause injury and dysfunction of the endothelial layer of the vessel wall. This constitutes the initiation step of atherogenesis and it includes the recruitment of blood cells, which adhere to the activated endothelium surface and infiltrate into the tunica *Intima* (Figure 1.3.1).

Lipoproteins from the plasma leak into the sub-endothelial areas through the impaired endothelium and are retained in the Intima. The white blood cells accumulate to uptake the toxic lipidic molecules, pathogens and dead cells. The fatty streak stage is hence achieved. Subsequently, upon the excessive load of lipoproteins, the macrophages get trapped in the arterial wall, forming foam cells and contributing to the bulge formation and the continuous inflammatory response [80-82].

The activated endothelial cells, the inflammatory cells and the platelets release cytokines and chemokines which signal SMCs and fibroblasts to migrate and proliferate from the other layers of the vessel to the Intima. The synthesis of extracellular matrix components including collagen, elastin and proteoglycans is therefore increased. Consequently, an atherosclerotic plaque is formed containing a necrotic core encompassing lipid deposition and debris of SMCs and macrophages. A fibrous cap, consisting of collagen, SMCs and fibroblasts, is formed to cover the growing plaque which narrows the vascular lumen of the artery with time. The atherosclerotic lesion is yet relatively stable, as the cap restricts the necrotic core inside the plaque.

However, the plaque can become unstable due to continuous accumulation of lipids and inflammatory molecules secreted by the inflammatory cells and the replacement of the SMCs in the cap by macrophages. At some point, the plaque is disrupted, platelets aggregate, the clotting cascade is activated and growth factors and chemokines are released, which recruit more cells. Consequently, the vessel lumen stenosis is increased which can culminate with a thrombotic occlusion. All conditions are gathered for an ischemic event to occur, such as myocardial infarction or stroke [82, 83].

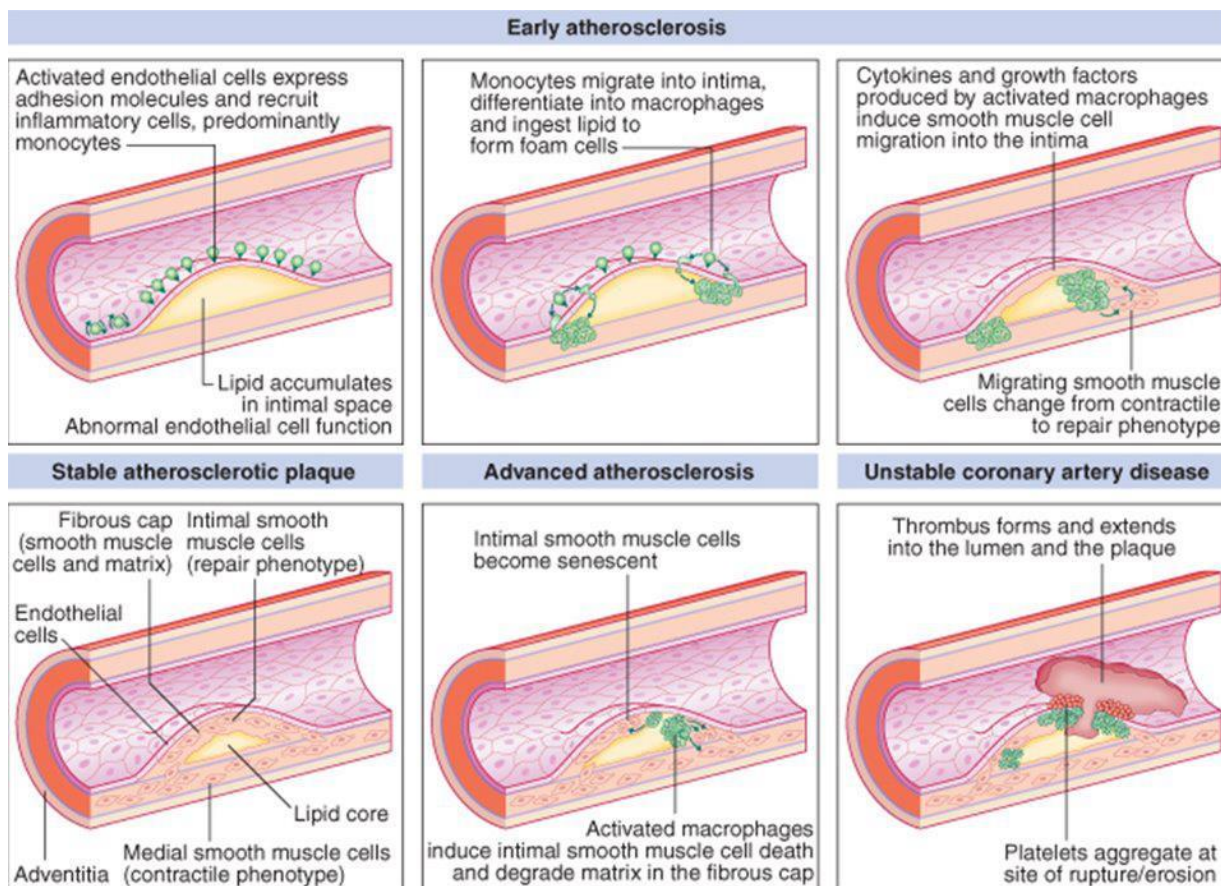


Figure 1.3.1: Basic pathogenesis of atherosclerosis. In response to physical or chemical injury, the endothelial layer becomes dysfunctional and endothelial cells are activated. Lipids in the blood accumulate in the intimal space and inflammatory cells, such as monocytes, are recruited to the site of lesion. The monocytes migrate into the intima and become macrophages to uptake the toxic lipids and the debris. The macrophages become foam cells and the bulge continues to grow. Cytokines and growth factors released by the inflammatory cells induce the recruitment of SMCs from the media to the intima to try to repair the lesion. Extracellular matrix components are released by the SMCs which form the fibrous cap of the atherosclerotic plaque, which contains the inner necrotic core. A stable atherosclerotic plaque is formed. With time, atherosclerosis lesion advances where the activated macrophages lead to cap SMCs death and degradation of the matrix of fibrous cap. The plaque becomes unstable, fissures appear and platelets aggregate at site of rupture. Thrombus forms with stenosis of the vessel lumen (Source: <http://healthtipsinsurance.com/stories/15261/Pathogenesis-Of-Atherosclerosis.html>).

In summary, an atherosclerotic lesion is characterized by lipid deposition, Intima thickening and narrowing of the lumen vessel. A neointima lesion is thus formed, with SMCs hyperplasia.

1.3.2 Endothelial cells and Smooth muscle cells in atherosclerosis

ECs and SMCs are both known to participate in atherogenesis. The initiating key event of atherosclerosis is the dysfunction of the endothelial layer, with increased permeability and impaired endothelium-mediated vasodilation. The activated ECs release chemokines to recruit SMCs, leukocytes and platelets and they express specific surface adhesion proteins which interact with the white blood cells and platelets, allowing their adhesion. In parallel, neighbouring ECs also migrate and proliferate to repair the injured endothelium. The regeneration of ECs represents a promising therapy in cardiovascular diseases [84-87].

An important feature of the SMCs is their phenotypic plasticity, which enables them to respond to the changes of the surrounding environment. During vascular development or in response to injury, the SMCs exhibit a synthetic, proliferative and migratory phenotype. On the other hand, mature SMCs are highly contractile with a low rate of synthesis of extracellular matrix (ECM) components. The SMCs are responsible for the regulation of the diameter and the tone of the blood vessels due to their contractility capacity [88-90].

Contractile SMCs can be identified by the markers Smooth muscle myosin heavy chain (SM-MHC), α -Smooth muscle actin (α -SMA), Calponin and Smooth muscle protein 22- α (SM22 α). In contrary, synthetic SMCs are characterised by the presence of abundant golgi and rough endoplasmic reticulum bodies, with a less elongated, more cobblestone-like morphology [89-91].

The normally quiescent SMCs, in response to the endothelial activation, the lipid accumulation and the undergoing inflammatory process, become activated during the development of atherosclerosis. Therefore, the SMCs undergo a modulation of their phenotype, from a contractile phenotype to a synthetic phenotype. As a result, the expression of the differentiation marker genes is down-regulated and the rate of SMC migration and proliferation abilities are increased, with an induction of the production of extracellular matrix, which all contribute to the formation of the neointima and the fibrous cap [92, 93].

The atherosclerotic neointima comprises SMCs hyperplasia. The SMCs content in atherosclerosis lesion is generally associated with increased plaque stability (Figure 1.3.2). Oppositely, plaque destabilization is linked with a decrease in the number of SMCs associated with an increase in macrophage content. Regardless of the controversy about the origin of the macrophages, since it is known that phenotypically modulated SMCs exhibit a downregulation in the SMC markers and may express macrophage markers, whereas macrophages turn on some SMC markers, atherosclerotic plaque stability is related to a higher ratio of SMCs to macrophages [93-95].

The mechanisms regulating the migration and proliferation of the SMCs to the neointima lesion are another crucial target highly explored in cardiovascular therapy.

Nevertheless, the pathogenesis of atherosclerosis is far more complex than the described above. Today, it is recognised that other key players have vital roles in vascular remodelling: the vascular stem/progenitor cells.

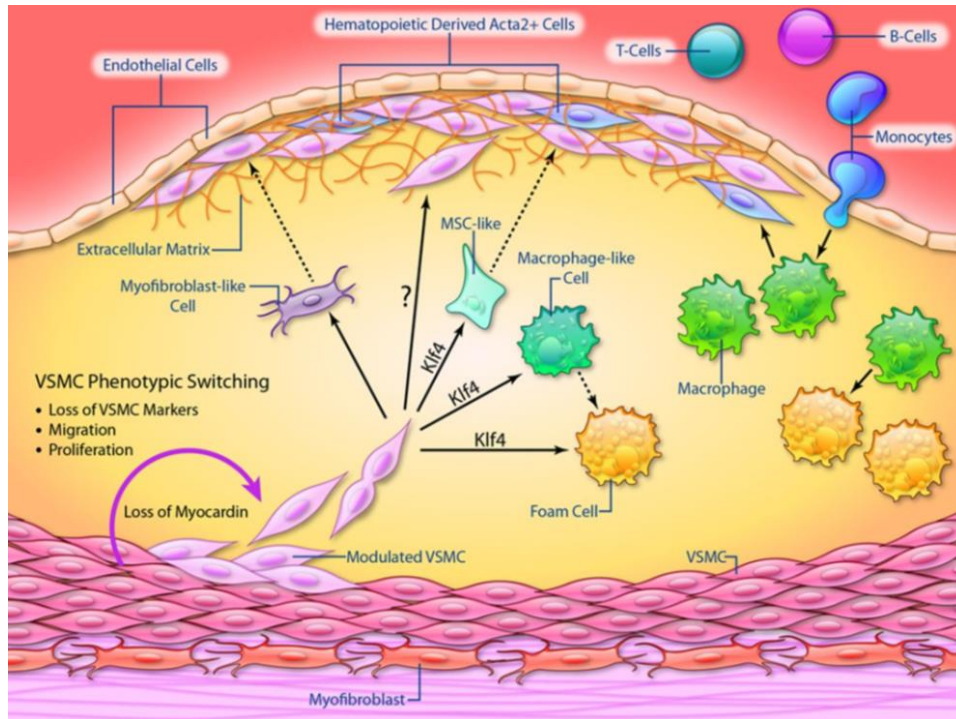


Figure 1.3.2: Vascular smooth muscle cell contribution to plaque stability. During atherogenesis, in response to stimuli, SMCs switch to a more migratory and proliferative phenotype, with the decrease of SMC-specific markers. SMCs synthesize ECM proteins and contribute to plaque stability and repair. Macrophage markers and properties can also be acquired by SMCs, which contrarily, contribute to plaque instability. The solid lines illustrate known pathways, whereas the dotted lines indicate pathways not yet directly validated. (Source: Bennet et al.; Vascular smooth muscle cells in atherosclerosis; 2016; Circulation research) [94].

1.3.3 The role of vascular progenitor cells in atherosclerosis

1.3.3.1 Circulating vascular progenitor cells in atherosclerosis

The adult bone marrow is a rich reservoir of tissue-specific stem/progenitor cells, including endothelial progenitor cells (EPCs) and smooth muscle progenitor cells (SMPCs). The progenitor cells are mobilized from the bone marrow in response to activator factors released under certain conditions such as endothelium dysfunction. In atherosclerosis, the secreted cytokines and growth factors induce the mobilization, recruitment and homing of the progenitor cells to the site of injury to repair the lesion.

In 1997 Asahara et al., was one of the first to report the participation of peripheral blood circulating stem/progenitor cells in neovascularization of ischemic tissues in mice [45]. Since then, many studies have described the role of circulating progenitor cells in vascular remodelling, namely in atherosclerosis. Xu et al., by using the vein grafts and transgenic mice carrying LacZ genes driven by an endothelial Tie2 promoter, showed that the recipient's circulating progenitor cells that derived from the bone marrow were able to regenerate the endothelium of the vein graft [29, 96]. Similarly, Takamiya et al., also revealed that the treatment with cytokine Granulocyte Colony-Stimulating Factor (G-CSF) mobilizes bone marrow C-Kit⁺/Flk-1⁺ progenitor cells to regenerate the endothelium and to inhibit neointimal formation after vascular injury [97]. However, reports also mention that several conditions characterised by increased inflammation and oxidative stress, as found in atherosclerosis, are associated with a decrease in EPCs availability [98]. Shimizu et al., reported that the SMC-like cells present in the intimal lesions formed during the graft arterial disease were derived from circulating bone marrow progenitor cells [49]. Sata et al., also concluded that the hematopoietic stem/progenitor cells, due to their ability to differentiate into SMCs, contribute to atherosclerosis patent in models of post-angioplasty restenosis, graft vasculopathy and hyperlipidemia-induced atherosclerosis [44].

1.3.3.2 Resident vascular progenitor cells in atherosclerosis

Despite the work published regarding the participation of circulating progenitor cells in the pathogenesis of atherosclerosis, an increasing number of studies began to demonstrate that there could be another source of vascular progenitor cells which could contribute to either the repair or the severity of the neointimal lesion.

For instance, Hagensen et al., by resorting to bone marrow cell transplantation of GFP-ApoE^{-/-} transgenic mice, claimed that the circulating endothelial progenitor cells do not contribute to the re-endothelization of the atherosclerotic plaque [85]. Hu et al., revealed that the origin of the SMCs in the neointimal lesion of vessel allografts was not the bone marrow progenitor cells, but instead the host cells [60]. This finding was further supported by the work of Bentzon et al., who also concluded

that there is a local vessel wall source of SMCs in atherosclerosis [57, 99] and by Nagai et al., who showed that the bone marrow cells contribute to vascular inflammation but they are not able to differentiate into SMCs [59].

Considering the body of work published in the literature and summarized in Table 1.2.2 regarding the presence of vascular progenitor cells in the vessel wall, it is possible to infer that these cells could be another potential source of ECs and SMCs in neointimal hyperplasia.

In 2004, Hu et al., revealed that abundant vascular progenitor cells were resident in the adventitia of ApoE^{-/-} mice aorta, expressing the markers Sca-1+, C-kit+, CD34+ and Flk-1+. Additionally, by applying Sca-1+ cells carrying the SM-LacZ gene to the adventitial side of the vein graft in ApoE^{-/-} mice, they found that the Sca-1+ cells were able to migrate to the neointima and differentiate into SMCs [6]. The role of the adventitial Sca-1+ cells as progenitor cells for SMCs was further supported by Passman et al., who characterized a sonic hedgehog (Shh) signalling domain restricted to the adventitial layer of the vessel wall. In Shh^{-/-} mice the number of adventitial Sca-1+ cells was drastically reduced and thus, the number of potential SMC progenitor cells was also decreased [100]. Xiao et al., attempted to elucidate the differentiation mechanism of Sca-1+ cells into SMCs, and found that it is mediated by collagen IV, integrins $\alpha 1$, $\alpha 5$ and $\beta 1$ and Pdgf- β receptor pathways [101].

The potential of Sca-1+ cells to differentiate into SMCs was also demonstrated by the work of Wong et al., in which an *ex vivo* bioreactor system model was used. The adventitial Sca-1+ cells were seeded on the outside of decellularized vessel and their migration towards the inner side of the vessel was increased in response to Sirolimus stimulation. Furthermore, the Sca-1+ cells formed neointima-like lesions and expressed elevated levels of SMC markers [102]. Another study by Chen et al., showed that the adventitia of vein grafts which underwent intense remodelling displayed a considerable number of Sca-1+ progenitor cells near the vasa vasorum area. These cells could differentiate *in vitro* into SMCs and had the potential to differentiate into adipogenic, osteogenic and chondrogenic lineages. Furthermore, *ex vivo* and *in vivo* experiments also demonstrated the migratory ability of the Sca-1+ cells to the inner side of the vessels, with a significant contribution in the content of neointimal SMCs [103]. In a different perspective, Toledo-Flores et al., recently published a work where they observed that the Sca-1+/CD45+ adventitial cells possess proangiogenic capacity and may be the source of the vasa vasorum expansion in atherosclerosis [104]. Contrastingly, Psaltis et al., identified the aortic adventitial Sca-1+/CD45+ cells as macrophage progenitor cells, which were upregulated in ApoE^{-/-} and LDL^{-/-} hyperlipidemic mice [10]. Interestingly, Torsney et al., investigated the expression of progenitor cell markers in human vessels. Although in small number, Sca-1+, CD34+, C-kit+ and VEGFR2+ markers were identified in the neointimal lesions and adventitia of the atherosclerotic vessels, and these markers were induced in comparison to their expression in the control human vessels [105]. Tsai et al., carried out a study which aimed at exploring the contribution of stem/progenitor cells to neointima formation in decellularized vessel grafts in a restenosis mouse model. A decellularized vessel was grafted in the mouse carotid artery and after 2 weeks a neointimal lesion was formed, which progressed to close the vessel lumen after 4 weeks. The lesion exhibited Sca-1+, C-kit+ and CD34+ cells, with multilineage differentiation

capacity. The isolated Sca-1+ cells were able to differentiate into SMCs or ECs according to the stimulation received [106].

Other vascular wall resident stem/progenitor cells were also proved to be a source of SMCs, or at least to exhibit a SMC-like cell phenotype, in atherosclerotic lesion. Amongst these mesenchymal stem cells, pericytes and macrophages are included [93, 107]. On the other hand, publications have emerged suggesting that SMCs, due to their phenotype plasticity, can actually de-differentiate or give rise to other cell types, such as macrophages and mesenchymal stem cells [93, 94, 108].

Vascular remodelling in atherosclerosis also comprises the paracrine effect exerted by the resident vascular progenitor cells (VPCs), which secrete paracrine factors to influence the behaviour of not only other progenitor cells but also SMCs, ECs and inflammatory cells. Migration and proliferation of these cells in response to cytokines, chemokines and growth factors released by the progenitor cells may contribute to repair, as is the case of endothelial regeneration. Neointima hyperplasia due to SMCs migration and proliferation is known to be as well a result from neighbouring paracrine effect, in which VPCs may have an important role.

1.3.3.3 *The dual role of vascular progenitor cells in atherosclerosis*

In regenerative medicine, the generation of EPCs constitutes a promising therapy for the endothelium regeneration and neovascularization. However, the number and the migratory ability of circulating EPCs is inversely correlated with risk factors for coronary artery disease [98, 109]. Furthermore, the transfer of EPCs may not always be beneficial, as ApoE^{-/-} mice which received bone marrow mononuclear cell transplantation not only presented increased neovascularization but also accelerated atherosclerotic lesion formation. When the mice were treated with EPCs the plaque instability increased [110, 111].

SMCs recruitment and consequent neointima hyperplasia is normally associated with plaque stability. Nevertheless, their high rate of migration and proliferation may expedite the lesion formation during restenosis. It is thus understandable that the same may apply to the vascular progenitor cells that migrate and differentiate into SMCs or inflammatory cells, as plaque destabilization may be triggered [62].

In view of this controversy, a great amount of research is required to further enlighten the role of the vascular progenitor cells in vascular diseases, especially regarding the mechanisms driving their migration, proliferation and differentiation in vascular remodelling. The elucidation of these mechanisms could provide vital information for the development of more efficient or novel therapies for vascular diseases.

1.3.4 Treatment of atherosclerosis

The most appropriate treatment for atherosclerosis includes changes in lifestyle, such as healthy diet and exercising. However, according to the severity and the cause of atherosclerosis, drugs and surgical procedures may be required.

The goals of the treatment comprise reducing the risk factors to slow down or halt the build-up of the atherosclerotic plaque, preventing atherosclerosis-related diseases, lowering the risk of blood clot formation, relieving the associated symptoms and widening or bypassing clogged arteries.

1.3.4.1 Drug treatment

One of the most important causes for the initiation and progression of atherosclerosis is the persistent increase in low-density lipoprotein (LDL) levels in the body. Sometimes, changes in life style alone are not enough to control the cholesterol levels. The most common pharmacotherapy used in this case are the statins which can slow or reverse the build-up of fatty deposits in the arteries and the chance of having a heart attack or stroke [112].

Another strategy used is to lower the blood pressure, which is very important in patients suffering from hypertension. In this case, angiotensin-converting enzyme (ACE), β -blockers, calcium channel blockers or diuretics can be prescribed.

Anti-platelet drugs, such as aspirin, can be used, which encompass the reduction of the probability of the platelets to aggregate and clump in the narrowed arteries, thus preventing the formation of blood clot and thrombosis. Alternatively, anticoagulant drugs may be applied, such as warfarin.

Because hyperglycemia constitutes a risk factor of atherosclerosis, especially in diabetic patients, drugs envisaging the control of glucose blood levels may be used.

Finally, as atherosclerosis is an inflammatory disease, the resource to anti-inflammatory drugs is many times indispensable [113].

When an artery is narrowed or blocked, the blood flow may be reduced or stopped, which can lead to myocardial infarction or stroke. In these severe cases of atherosclerosis, invasive techniques to open blockages or to go around them may be performed. Depending on which arteries are narrowed and how much they are blocked, different procedures are applied.

1.3.4.2 Percutaneous transluminal coronary angioplasty

An angioplasty is used to widen narrowed arteries. A catheter is inserted with a deflated balloon into the narrowed part of the artery. The balloon is inflated to widen the vessel and to improve the blood flow. Next, the balloon is deflated and the catheter is removed. The vessel is held open by means of a permanent stent. The stent is made of a wire mesh and it is usually coated with different drugs that can be released continuously into the lesion sites to prevent the vessel from re-narrowing [114].

1.3.4.3 Atherectomy

In cases where angioplasty or stenting cannot be performed, due to the location of the blockage, the hardness of the plaque and other factors, an atherectomy is typically performed. In fact, this procedure is more commonly used as a complement to angioplasty and stenting, by removal of significantly hardened blockages and thus allowing the insertion of the balloon and stent.

An atherectomy is normally used in patients with periphery or coronary artery disease and it consists of removing the plaque from an artery by means of tiny rotating blades or laser located at the end of a catheter. A collection system is also in place to enable the removal of the plaque from the vessel wall and the resulting debris. The removal of the plaque makes the artery wider and allows a better blood flow [115].

1.3.4.4 Coronary artery bypass grafting

In coronary artery bypass grafting, a healthy vessel from another part of the body or a tube made of synthetic fabric is used to create a graft to bypass or to go around the narrowed or blocked coronary artery. Normally, the grafting vessel is derived from the great saphenous vein or the internal mammary artery.

The healthy blood vessel or graft redirects the blood, hence improving or restoring the blood perfusion to the part of the myocardium which previously lacked the supply of blood flow because of the obstruction of the coronary artery.

1.3.5 Complications

After angioplasty or stent surgery, a re-narrowing of the artery or even blood clot may occur over time, which requires additional intervention.

1.3.5.1 Post-angioplasty restenosis

Vascular remodelling post-angioplasty or the in-stent restenosis can take place in the long term. Some of the risk factors of restenosis are the method used (presence or absence of stenting), the number and length of the stent, the existence of concomitant diseases such as diabetes, the location of the lesion and the severity of the occlusion.

Restenosis involves the aggregation of platelets, leukocytes and macrophages, which in turn result in the recruitment and proliferation of the SMCs and vascular progenitor cells. The initial step involves the injury of the endothelium or even the elastic lamina, which triggers an inflammatory reaction (early phase). With the release of cytokines and growth factors, cell migration and proliferation is followed with media and Intima hyperplasia (late phase). The resulting increase of extracellular matrix adds up to the bulk of the restenotic lesion, which may or not be stable. A neo-atherosclerosis process has taken place [116].

The surgical treatment for restenosis is either repeated angioplasty or open surgery. Additionally, the patient can undergo drug-eluting stenting, which decreases the occurrence of severe neointimal proliferation.

1.3.5.2 Late stent thrombosis after drug eluting stent application

The technology of drug-eluting stent (DES) was developed to attempt to reduce the excessive neointimal proliferation stimulated by the presence of the metallic structure of the stent. Therefore, a biocompatible or even biodegradable carrier polymer is added to the stent, which is coated with an anti-proliferative drug targeting the cell proliferation throughout the vessel wall. Application of DES enables the reduction of the incidence of post-angioplasty restenosis [117].

Nevertheless, late stent thrombosis and neo-atherosclerosis may still occur. For example, Wong et al., provided a possible mechanism for the reoccurrence of restenosis after sirolimus-eluting stent therapy. In their study, they show that sirolimus induces the migration of adventitial Sca-1+ vascular progenitor cells to the Intima of a decellularized vessel scaffold, where they form neo-intima like lesions and differentiate into SMCs [102].

Although there have been major improvements in the therapies for the prevention and treatment of restenosis, research is still required for optimization and aiming at reducing the incidence of restenosis.

1.4 Cytokines in atherosclerosis

Cytokines are a superfamily of proteins generally associated with inflammatory and immunological processes. They are involved in the signalling network between cells and in the regulation of many cell functions, such as migration, proliferation, differentiation, amongst others.

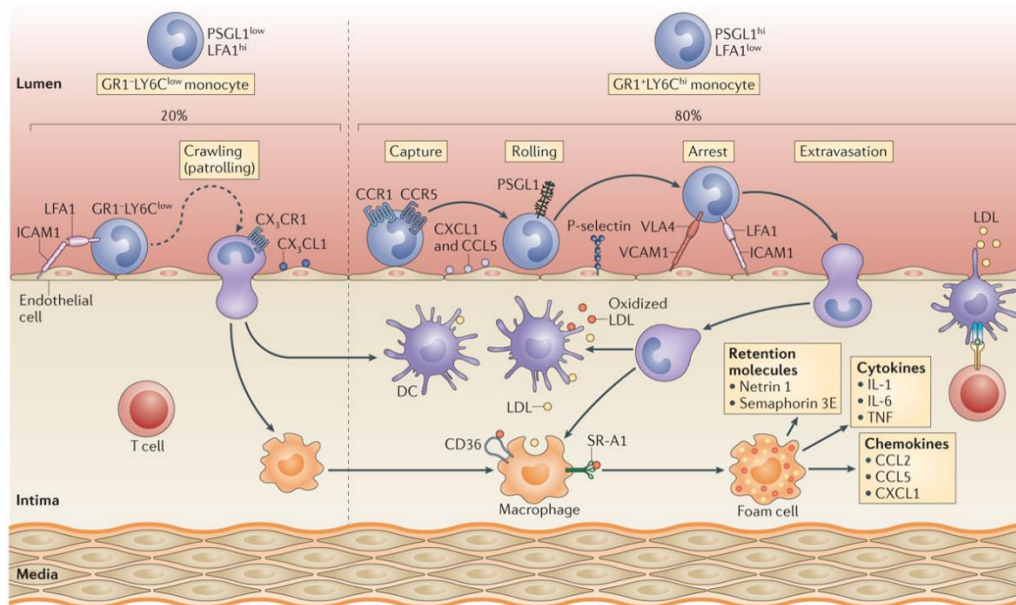
These molecules act by binding to specific receptors and they consist of a diverse group of glycoproteins comprising interleukins (IL), chemokines, colony stimulating factors (CSF), tumour necrosis factor (TNF), interferons (IFN) and transforming growth factors (TGF). Interleukins include IL-1 to IL-17; Colony stimulating factors include G-CSF, GM-CSF and M-CSF; Tumour necrosis factor include TNF- α and TNF- β ; Interferons include IFN- α , IFN- β and IFN γ ; Chemokines include CCL-1-CCL4, CCL4L1 and CCL4L2, CCL5-CCL28, CXCL1-CXCL17 and CXC3CL1 [118].

The cytokines are implicated in all stages of atherosclerosis and play distinct roles, being either pro-atherogenic (contribute to plaque development) or anti-atherogenic (contribute to either plaque formation attenuation or stabilization). The expression of many cytokines has been reported to be enhanced within human atherosclerotic lesions and co-localized with the increased expression of their corresponding receptors [119, 120].

The primary trigger of the atherosclerotic process is the level of circulating lipids, which can induce the production of cytokines by the monocytes and T lymphocytes. These cells secrete, respectively, TNF- α and INF- γ cytokines, which act upon the ECs by affecting their actin and tubulin cytoskeleton organization. The ECs cytoskeleton reorganization results in changes in their shape which enables the creation of gaps in the endothelium and hence an increase in the layer permeabilization. Consequently, LDL and immune cells enter the tunica intima where they accumulate. The oxidized LDL activates the ECs which begin to release various cytokines capable of attracting the circulating monocytes and other immune cells. Three chemokine-chemokine receptor pairs are relevant in the transmigration of the monocytes across the endothelium into the Intima: CCR2-CCL2, CX3CR1-CX3CL1 and CCR5-CCL5. These, together with CD31 and adhesion molecules (Ex.: VCAM1, ICAM1) expressed by the ECs, facilitate capture, rolling and transmigration of the monocytes (Figure 1.4A).

M-CSF is one of the major facilitators of the differentiation of monocytes into macrophages. Macrophages can either produce pro-inflammatory cytokines (IL-6, IL-12, TNF α) or anti-inflammatory cytokines (IL-10 and TGF- β), which work in concert to try to control the inflammatory process. T helper lymphocytes (Th lymphocytes) can modulate the macrophage function and hence influence the production of the macrophage-derived cytokines. For instance, IFN- γ and IL-1 β , secreted by the Th1 lymphocytes, promote the macrophage production of pro-inflammatory cytokines, whereas IL-4 and IL-14, produced by Th2 cells, stimulate the secretion of macrophage-derived anti-inflammatory cytokines. It is therefore notorious the role of the immune system in atherogenesis.

In the intima, cytokines are locally produced, which permanently activates the leukocytes and thus accelerates the transformation of macrophages into foam cells, by inducing the uptake and oxidation of lipids. TNF α , IFN- γ , IL-1 β and IL-2, which are pro-inflammatory cytokines, induce the apoptosis of the macrophages foam cells, with the release of their content into the Intima and lead to the enlargement of the lipid core. Together with the lipids, matrix metalloproteinases (MMPs) are also released. These, in synergy with several cytokines and growth factors, promote the remodelling of the extracellular matrix [121, 122].



Nature Reviews | Immunology

Figure 1.4A: Inflammatory process in atherosclerosis regulated by cytokines. Monocytes are recruited to the atherosclerotic site of lesion, due to the increased level of lipids and activation of the ECs. Various pairs of chemokine-chemokine receptors (CCR2-CCL2, CXC3CR1-CX3CL1 and CCR5-CCL5) are used by the monocytes to infiltrate the Intima. The infiltration process is facilitated by the adhesion molecules (ICAM1 and VCAM1) expressed on the ECs. The infiltrated monocytes differentiate into macrophages and engulf the atherogenic lipids, with the resulting formation of foam cells. Foam cells secrete pro-inflammatory cytokines, including IL-1, IL-6, TNF and chemokines such as CCL2, CCL5 and CXCL1. (Source: Moore et al.; Macrophages in atherosclerosis: a dynamic balance; 2016; Nature Reviews Immunology)[123].

Plaque destabilization results from the continuous inflammatory response via the action of the pro-inflammatory cytokines. On the other hand, TGF- β and IL-10, which constitute anti-atherogenic cytokines, contribute to plaque stabilization.

The SMCs, which have a vital role in atherogenesis, are also affected by the cytokines. The macrophages engulfing the lipoproteins produce cytokines which cause the recruitment of the SMCs to the site of the lesion. The activated ECs also secrete cytokines and growth factors (Platelet-

derived growth factor) which induce the migration of the SMCs from the media to the Intima. On the other hand, SMC apoptosis can be stimulated by pro-inflammatory cytokines, with inhibition of the production of ECM components by the SMCs, thus resulting in thinning of the fibrous cap.

Atherogenesis is the result of a complex network of cytokines and chemokines released by the different intervenient cell types (Figure 1.4B).

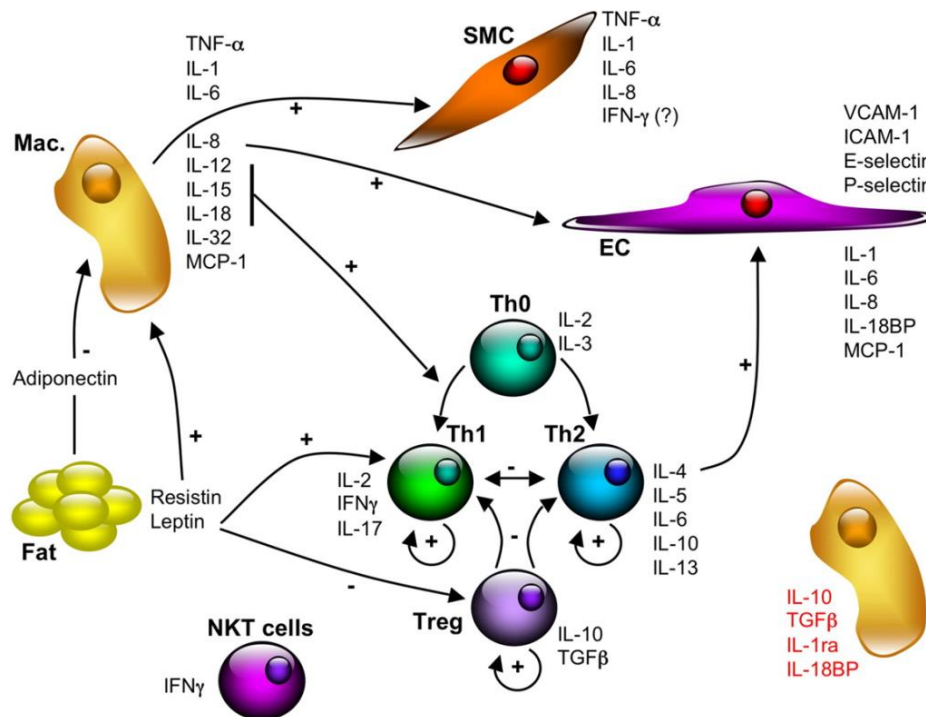


Figure 1.4B: Cytokines involved in atherogenesis. Different cell types produce cytokines. Macrophages produce IL-12 and IL-18 which induce the T cells to become pro-atherogenic. SMCs and ECs are also activated by the cytokines released by the macrophages. As a result, the activated cells secrete pro-inflammatory mediators. Macrophages also produce the anti-inflammatory cytokines IL-10 and TGF- β , which promote the differentiation of the anti-atherogenic T cells. Fat cells, such as adipocytes, produce both pro- and anti-inflammatory mediators. (Source: Tedgui et al.; Cytokines in atherosclerosis: Pathogenic and regulatory pathways; 2006; Physiological Reviews)[124].

Considering the key roles of the cytokines in the inflammatory process underlying atherosclerosis, therapeutic strategies include targeting the cytokines and their signaling pathways. For example, pro-inflammatory cytokines can be inhibited to reduce atherosclerosis. In contrast, anti-inflammatory cytokine induction may represent a valid approach to combat the inflammatory process.

In this work, an emphasis will be put on the chemokines, a sub-family of cytokines, whose key role is the induction of cell chemotaxis.

1.4.1 The Chemokine – Chemokine receptor System

Chemokines are known to be the chemotactic cytokines (induction of cell chemotaxis or recruitment) that mediate their activity by acting on seven transmembrane G protein-coupled receptors. The chemokine-chemokine receptor system is essential in regulating homeostasis, but it is also involved in the pathogenesis of many diseases.

1.4.1.1 Chemokine proteins

Chemokines are proteins that control the directional migration of cells across a concentration gradient (Chemotaxis). Initially, the chemotactic effect of the chemokines was shown to regulate immune cells movement in inflammatory processes. Today, chemotaxis is known to regulate many important processes, such as development, homeostasis, angiogenesis, vessel remodelling and fibrosis, amongst others [125].

Chemokines belong to a family of proteins structurally related, which are mainly divided into four groups, according to the number and position of the conserved amino terminal cysteine residues (Figure 1.4.1.1). In CXC chemokines one amino acid separates the first two cysteine residues (cysteine-X amino acid-cysteine); in CC chemokines the first two cysteine residues are adjacent to each other (cysteine-cysteine); in C chemokines the first and the third cysteine residues are lacking and so the second and fourth cysteine residues are linked by the only existing disulphide bond; in CX3C chemokines the first two cysteine residues are separated by three amino acids (cysteine-X-X-X-cysteine) and it is characterised by a transmembrane mucin-like domain.

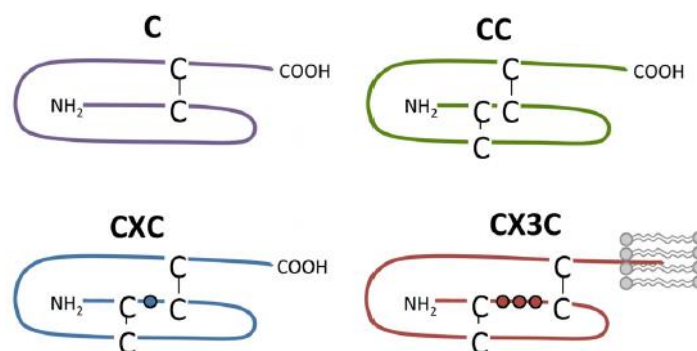


Figure 1.4.1.1: Classification of chemokines. Chemokines divided into 4 groups: C chemokines - the first and the third cysteine residues are lacking, the second and fourth cysteine residues are linked by a disulphide bond; CC chemokines - the first two cysteine residues are adjacent to each other; CXC chemokines - one amino acid separates the first two cysteine residues; CX3C chemokines - the first two cysteine residues are separated by three amino acids. Disulphide bonds depicted in black. (Source: Munnik et al.; Modulation of cellular signalling by herpesvirus-encoded G protein-coupled receptors; 2015; Frontiers in Pharmacology) [126].

Presently about 50 chemokines have been identified, having a size of 7-17 kDa. These proteins bind to chemokine receptors, which are seven transmembrane G protein-coupled receptors (GPCRs). The chemokine receptors have been categorized according to their corresponding ligands (CR, CCR, CXCR and CX3C).

The fact that more ligands exist than chemokine receptors indicates that the chemokine system exhibits a degree of redundancy, where chemokines may bind to more than one receptor with variable affinity [127] (Table 1.4.1).

Table 1.4.1: Chemokines and their corresponding chemokine receptors

		XCR1	CCR1	CCR2	CCR3	CCR4	CCR5	CCR6	CCR7	CCR8	CCR9	CCR10	CXCR1	CXCR2	CXCR3	CXCR4	CXCR5	CXCR6	CXCR8	ACKR1 / DARC	ACKR2 / D6	ACKR3 / CXCR7	ACKR4 / CCRL1	ACKR5	CX3CR1
Lymphotactin	XCL1	●																							
SCYC2	XCL2	●																							
TCA3	CCL1									●										●	●				
MCP-1	CCL2			●		●														●	●				
MIP-1 α	CCL3		●			●	●														●				
MIP-1 β	CCL4		●		●	●	●			●											●				
RANTES	CCL5		●	●	●	●	●								●					●	●			●	
MRP-1	CCL6																								
MCP-3	CCL7		●	●	●	●	●								●					●	●				
MCP-2	CCL8		●	●	●		●			●										●	●				
MIP-1 γ	CCL9														●										
MIP-1 δ	CCL10														●										
Eotaxin-1	CCL11				●		●								●					●	●				
MCP-5	CCL12			●																					
MCP-4	CCL13		●	●	●		●								●					●	●				
HCC-1	CCL14		●				●			●										●	●				
MIP-5	CCL15		●																						
HCC-4	CCL16		●	●			●													●					
TARC	CCL17					●				●										●	●				
PARC	CCL18									●										●					
MIP-3 β	CCL19								●						●								●	●	
Exodus-1	CCL20							●							●										

		XCR1	CCR1	CCR2	CCR3	CCR4	CCR5	CCR6	CCR7	CCR8	CCR9	CCR10	CXCR1	CXCR2	CXCR3	CXCR4	CXCR5	CXCR6	CXCR8	ACKR1 / DARC	ACKR2 / D6	ACKR3 / CXCR7	ACKR4 / CCRL1	ACKR5	CX3CR1	
SLC	CCL21							•	•																•	
MDC	CCL22					•																•				
MIP-3	CCL23		•																			•				
Eotaxin-2	CCL24				•																	•				
TECK	CCL25										•													•		
Eotaxin-3	CCL26				•																	•				•
CTAK	CCL27											•														
MEC	CCL28				•							•														
GRO- α	CXCL1												•	•							•					
GRO- β	CXCL2													•							•					
GRO- γ	CXCL3													•							•					
PF4	CXCL4													•							•					
ENA-78	CXCL5												•	•							•					
GCP-2	CXCL6												•	•							•					
NAP-2	CXCL7													•							•					
IL-8	CXCL8												•	•							•					
MIG	CXCL9				•										•											
IP-10	CXCL10				•										•						•					
ITAC	CXCL11				•										•						•		•			
Sdf-1	CXCL12														•	•							•			
BCA-1	CXCL13																•				•			•		
BRAK	CXCL14																									
Lungkine	CXCL15																									
SCYB16	CXCL16																	•								
DMC	CXCL17																	•	•							
Fractalkine	CX3CL1																								•	•

Note: The table was completed upon a thorough search in the literature [126, 128-136].

1.4.1.2 Chemokine receptors

The chemokine receptors GPCRs consist of approximately 350 amino acids and they are composed of seven transmembrane helices, connected by three extracellular loops and three intracellular loops. The acidic amino terminus (N-terminus) of the receptor is located at the extracellular site and the carboxyl terminus (C-terminus) is located intracellularly where it contains serine and threonine residues which are important for receptor regulation.

The heterotrimeric G proteins are coupled to the receptor through its C-terminus and they are responsible for regulating diverse signal transduction pathways involved in chemotaxis (Figure 1.4.1.2). The three subunits of the G protein are α , β and γ . Upon binding of the chemokine ligand, the GPCR undergoes a conformational change which leads to the activation of the G protein. This activation is achieved by the exchange of GDP for GTP, in the α subunit. As a consequence, the GTP- α subunit and the β/γ dimeric subunit dissociate from the GPCR and activate downstream effectors.

There are four classes of heterotrimeric G proteins, based on their α subunit: $G\alpha_s$, $G\alpha_i/G\alpha_o$, $G\alpha_q/G\alpha_{11}$, and $G\alpha_{12}/G\alpha_{13}$. Most of the chemokine GPCRs are known to be coupled to $G\alpha_i$ (Pertussis toxin sensitive) or $G\alpha_q$. $G\alpha_i$ inhibits the enzyme adenylyl cyclase which results in reduced levels of intracellular cyclic AMP, thus decreasing the activity of protein kinase A. On the other hand, $G\alpha_q$ transduces signals by inducing the activation of phospholipase C- β (PLC- β), which leads to the hydrolyses of PIP₂ (phosphatidylinositol 4,5-biphosphato) to produce IP₃ (inositol triphosphate) and DAG (diacylglycerol). Both of DAG and IP₃ can activate protein kinase C, either directly or indirectly via release of Ca^{2+} internally stored. The β/γ dimeric subunit activates phospholipase C- β , phosphoinositide-3-kinase (PI3K) and Rho GTPases. The latter family of proteins was reported to be also activated by the $G\alpha$ subunits. G protein is inactivated once GTP from $G\alpha$ is hydrolysed and the resulting $G\alpha$ -GDP recombines with the dimer β/γ [137].

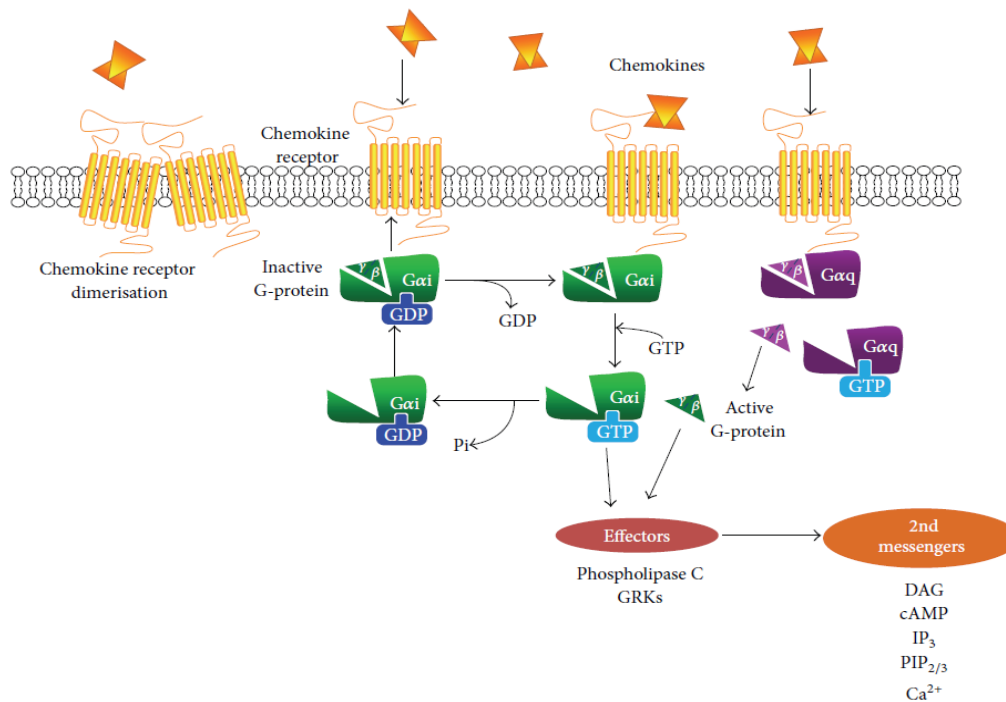


Figure 1.4.1.2: Chemokine G protein-coupled receptor associated signalling pathways. Chemokine binding to its receptor results in a conformational change of the GPCR and the exchange of GDP for GTP at the $G\alpha$ subunit. The heterotrimeric G protein dissociates into the $G\alpha$ subunit and the β/γ dimeric subunit, leading to the activation of the downstream signalling effectors. The chemokine GPCRs mostly comprise of $G\alpha_i$ (green) or $G\alpha_q$ (purple) subunits. Hydrolysis of GTP leads to the inactivation of the G protein, where GDP- $G\alpha$ re-associates with β/γ dimer. (Source: Patel et al.; The downstream regulation of chemokine receptor signalling: implications for atherosclerosis; 2013; Mediators of inflammation)[137].

One important feature of the chemokine receptors is that they can dimerize or even oligomerize, which influences for instance their interaction with the chemokines or with the G proteins, or their localization within the plasma membrane or even their internalization and recycling back to the membrane [136, 138].

The ligand-mediated activation of the chemokine receptors also triggers a signalling pathway that leads to the desensitization and internalization of the receptor. G protein receptor kinases (GRKs) phosphorylate the serine and threonine residues at the C-terminus of the receptor. As a result, β -arrestin and endocytosis-related molecules adaptin 2 (AP2) are recruited and form a complex with the receptor. Next, clathrin is attracted and the receptor is internalized into clathrin-coated vesicles. The internalized receptor-ligand complex moves along the endocytic pathway, until it is either dissociated, where the receptor is recycled back to the cell membrane, or it is transferred to late endosomes for lysosomal degradation. The latter process is associated with a slow desensitization process, with downregulation of the receptor. On the other hand, the recycling of the receptor back to the plasma surface induces receptor responsiveness, after desensitization [126, 133, 135, 139].

1.4.1.3 Chemokines in Atherosclerosis

Chemokines and their receptors actively participate in vascular remodelling, a characteristic process of atherosclerosis. These proteins can either be atherogenic or atheroprotective or even have a dual role depending on the cell type.

The modified lipids are the first drivers of chemokine induction by the various cell types, including macrophages, leukocytes, SMCs, ECs and vascular progenitor cells (Figure 1.4.1.3). Besides being chemoattractant, chemokines also regulate other cellular functions, such as proliferation, differentiation and apoptosis. They may activate platelets as well and induce their aggregation.

One vital role of chemokines is their involvement in plaque destabilization. The chemotaxis of leukocytes, the activation of ECs, the induction of monocyte infiltration into the Intima, the activation and recruitment of platelets, the induction of migration and proliferation of SMCs, the enhancement of the matrix degradation potential of the macrophages and the induction of apoptosis of foam cells, are all mechanisms promoted by the chemokines in atherosclerosis.

The above mentioned role of the chemokines is also verified in the pathogenesis of other vascular disorders. This is the case of restenosis and neointima formation in vascular grafts, which comprise arterial remodelling regulated by the chemokines [120].

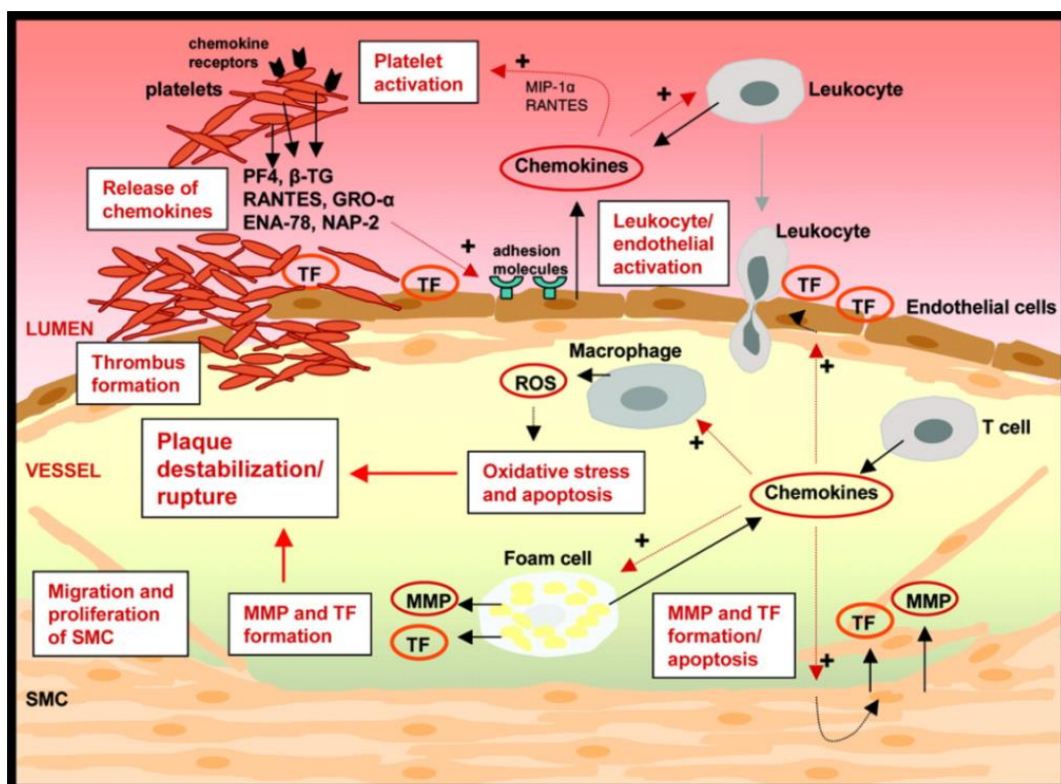


Figure 1.4.1.3: The role of chemokines in atherogenesis. Chemokines induce activation of ECs and of leukocytes. The leukocytes, in response to the chemokine stimuli infiltrate into the lesion site. Both T cells and macrophages/foam cells release further chemokines. As a result, SMCs migrate and proliferate, whereas the macrophages produce matrix degradation components, all contributing to plaque destabilization. Apoptosis of SMCs and ECs and increase in oxidative stress is promoted as well by the chemokines, further supporting plaque instability and rupture. Platelets are activated and recruited by chemokines and they can also mediate inflammation by releasing several chemokines, hence forming a pathogenic loop in plaque destabilization. (Source: Aukrust et al.; Chemokines and cardiovascular risk; 2008; Arteriosclerosis, Thrombosis, and Vascular Biology)[120].

The first chemokine-chemokine receptor pair to be implicated in the pathogenesis of atherosclerosis is the CCL2-CCR2 system. CCL2 is produced by monocytes, macrophages, ECs and SMCs, and it is an atherogenic chemokine. Upon deficiency of CCL2 or CCR2 the atherosclerotic lesion in mice is reduced.

CCL5-CCR5 system is another atherogenic pair. CCL5 is expressed by monocytes, macrophages, T cells and SMCs in atherosclerotic lesions and its deficiency is suggested to reduce the development of atherosclerosis in mice. CCL5 can also be released by platelets and activate ECs

Atherosclerotic plaques of mice aortas express CCR6 and its ligand CCL20. CCR6 deletion in ApoE^{-/-} mice decreases the atherosclerotic lesion and the content in macrophages. Controversially, CCR6 may also be atheroprotective via B cell regulation.

The CX3CL1 chemokine mediates cell adhesion and chemotaxis and it is produced by ECs. SMCs and foam cells express this chemokine as well. Its receptor CX3CR1 is found on monocytes, lymphocytes, platelets and SMCs. The deletion of both chemokine and respective receptor results in a reduction in the size of the atherosclerotic lesion and in the recruitment of macrophages. CX3CL1 induces the formation of platelet-monocyte complexes and the cross-talk between monocytes and SMCs [119, 140].

Finally, CXCR2 and its ligands CXCL1 and CXCL8 are detected in human and mouse atheroma. Upon activation of ECs, CXCL8 and CXCR2 expression is upregulated. The CXCL1-CXCR2 axis participates in the arrest of monocytes on the atherosclerotic endothelium, enabling their infiltration into the Intima.

Examples of atheroprotective chemokine system include the CCR1 receptor and its ligands CCL3 and CCL5. Deletion of CCR1 leads to an increase in the size of the aortic atherosclerotic lesion and it is proposed that CCR1 regulates T cell activation and its mobilization alongside the monocytes into the vessel wall.

The CXCL12-CXCR4 axis is as well regarded as a protective system in atherosclerosis. ECs and SMCs of human atherosclerotic plaques express both ligand and receptor. CXCL12 plasmatic levels in patients suffering from coronary artery disease and in ApoE^{-/-} mice are lower than in the respective controls. Additionally, CXCL12 (Sdf-1) induces platelet aggregation via its receptor CXCR4. In response to CXCL12, platelets migrate towards the lesion area [120, 140, 141]. This pair of chemokine and receptor will be explored in more detail in the next section.

In view of the implication of the chemokine-chemokine receptor systems in vascular remodelling and consequently in the pathogenesis of vascular diseases, including atherosclerosis, researchers have been attempting to develop drug therapies targeting the chemokines and their receptors.

Receptor antagonist design constitutes a very useful strategy. For example, plerixafor (AMD3100), is a competitive antagonist of CXCR4 and, although it was initially developed as an anti-HIV drug, currently it is used for stem cell mobilization from the bone marrow in tumour diseases. By inhibiting the binding of CXCL12 to CXCR4 expressed on the hematopoietic stem cells, these can be mobilized from their niche in the bone marrow to the blood flow and hence, these cells can be used for stem cell transplantation in patients suffering with for example non-Hodgkin's lymphoma or multiple myeloma.

Successful therapies may require strategies that target multiple chemokine and chemokine receptors, which reveals how vital it is to understand clearly the mechanisms leading to the chemokine-mediated cell response. Importantly, chemokines may also serve as biomarkers in cardiovascular diseases. For instance, the plasma levels of inflammatory markers represent a good predictor of the prognosis of some cardiovascular diseases. This represents another approach to be explored.

1.4.1.4 The chemokine CXCL12 (Sdf-1) and its receptors CXCR4 and CXCR7

CXCL12, also known as Stromal cell-derived factor 1 (Sdf-1), is a member of the CXC chemokine family and it consists of various isoforms: CXCL12- α , CXCL12- β , CXCL12 δ , CXCL12- ϵ and CXCL12- ϕ . The most well-known isoforms are CXCL12- α (Sdf-1 α) and CXCL12- β (Sdf-1 β), which are expressed throughout the body. Knockout of CXCL12 in mice reveals impaired hematopoiesis and defect in the heart and brain development, which results in embryonic lethality.

The receptors of CXCL12 are CXCR4 (CD184 or Fusin) and CXCR7 (RDC1). CXCR4 has been extensively studied, whereas the functions of CXCR7 still require further clarification.

The chemokine CXCL12 has been implicated in many diseases, including autoimmune diseases and cancer, where it regulates cell migration, proliferation and survival. It is also associated with tissue damage such as heart infarct, limb ischemia, toxic liver damage and other damages related to chemotherapy.

One key role of the CXCL12/CXCR4 axis is the homing of stem/progenitor cells in the bone marrow, where its expression is very high. Inhibition of the receptor CXCR4 enables the mobilization of the cells from the bone marrow to the peripheral blood, as CXCL12 can no longer bind to its receptor and thus retain them in the bone marrow. Moreover, intravenous injection of CXCL12 was shown to increase the number of circulating stem/progenitor cells in the blood flow.

In cardiovascular diseases, the mobilization of progenitor cells via CXCL12/CXCR4 has been extensively studied and this is particularly relevant for vascular injury models which comprise restenosis or neointima formation processes [142, 143]. Under physiological conditions, the number of circulating hematopoietic stem/progenitor cells (HSCs) is low, as the ECs from the bone-marrow sinusoids secrete CXCL12 which retains the HSCs in a stem cell-like niche in the bone marrow. This retention of CXCR4+ HSCs is further supported by CXCL12 secretion from the bone marrow stromal cells. In pathological conditions comprising stress or injury, the HSCs lose their anchorage properties and are mobilized to the circulation. An increased plasmatic level of CXCL12 seems to be involved in this process, where the CXCL12-induced migration of HSCs into the circulation is favoured over their retention in the bone marrow. Controversially, it is proposed that in the bone marrow, CXCL12 may downregulate the cell surface expression of CXCR4, which leads to a reduced level of retention of HSCs mediated by the CXCL12/CXCR4 axis.

Amongst the CXCL12-driven mobilized stem/progenitor cells are the smooth muscle progenitor cells (SMPCs), such as Sca-1+ SMPCs. Sca-1+ SMPCs mobilization by CXCL12 treatment increases the thickness of the fibrous cap. Therefore, research work has been carried out aiming at increasing the level of circulating SMPCs and thus promoting atherosclerotic lesion stabilization, to treat vulnerable lesions. In addition, direct injection of SMPCs in mice reveals to reduce atherosclerotic lesion development and improve plaque stability [144, 145].

In fact, in atherosclerosis of ApoE^{-/-} or LDLr^{-/-} mice, the CXCL12/CXCR4 axis seems to play an atheroprotective role, with contribution to the stabilization of the atherosclerotic lesions. However, it has also been associated with vascular injury-induced restenosis and neointima formation. CXCR4 blockade by AMD3100 reduces injury-induced neointimal size and SMC hyperplasia. Additionally, Sca-1+ cell mobilization is also reduced upon transplantation of CXCR4^{-/-} bone marrow, resulting in a decrease of the SMC content, since Sca-1+ cells were shown to differentiate into SMCs and to contribute to neointima formation.

CXCL12 has been also associated with endothelial barrier enhancement, with decrease in endothelial permeability. Additionally, ECs with CXCR4 deficiency contribute to neointima formation, with impaired reendothelization due to a decrease in ECs proliferation and migration. Overexpression of CXCR4 promotes endothelial recovery after vascular denudation. Thus, the beneficial effects of the CXCL12/CXCR4 axis have been explored in vascular regenerative medicine, with the use of endothelial progenitor cells (EPCs) to promote tissue reendothelization.

Still in this context, activated platelets are able to secrete CXCL12 which recruits circulating SMPCs and EPCs to the sites of arterial thrombi, to promote vascular remodelling. Conversely, CXCL12 is a potent chemotactic factor for platelets via CXCR4 and it induces their aggregation. This suggests a feedback loop for the CXCL12/CXCR4 axis in the regulation of the function of platelets in atherosclerosis [146].

Leukocytes or macrophages express as well CXCL12 and CXCR4 and this chemokine-chemokine receptor system is involved in accumulation of modified lipids and foam cells in atherosclerosis. CXCR4 blockade reduces the macrophage content and hence decreases neointimal lesion. Furthermore, the axis is also implicated in the release of neutrophils from the bone marrow and in the clearance of senescent neutrophils from the circulation.

The diverse roles played by the CXCL12/CXCR4 system shows that it is cell-specific and complex.

In human atherosclerotic lesions, compared to normal vessels, the expression of CXCL12 is increased, which indicates an association between CXCL12 and atherogenesis. On the other hand, angina patients showed a decreased plasmatic level of CXCL12 and a reduced surface expression of CXCR4 in peripheral blood mononuclear cells, compared to healthy controls. These findings indicate that the role of CXCL12 in atherogenesis is controversial and additional research is necessary to decipher the contradicting results observed [142, 144, 145, 147-149].

CXCL12 and CXCR4 are significantly expressed on cardiac myocytes and fibroblasts. Ischemic injury after myocardial infarction stimulates CXCL12 expression. This chemokine upregulation has a protective role by promoting myocardial repair, because CXCL12 exerts a survival effect on resident cardiomyocytes and recruits circulating progenitor cells, with increased neoangiogenesis. Thus, this chemokine also plays a role in tissue repair in response to ischemia [150].

The CXCR4 receptor is a GPCR and therefore, upon ligand binding, it acts via activation of the heterotrimeric G protein. In most of the cases, the CXCR4 $G\alpha$ subunit comprises the $G\alpha_i$ subunit, which upon activation, dissociates from the dimeric subunit $G\beta/\gamma$, and inhibits adenylyl cyclase, while activating the protein kinase c-Src (Figure 1.4.1.4A). The protein c-Src activates the Ras/Raf/ERK (MAPK kinases) signalling pathway which is involved in cell chemotaxis. The $G\beta/\gamma$ dimer activates directly the MAPK kinase signalling pathway.

$G\alpha_i$ acts as well via PLC- β to induce the hydrolysis of PIP2 into IP3 and DAG, which in turn increase the intracellular concentration of Ca^{2+} and activate PKC, thus promoting cell migration. Both $G\alpha_i$ and $G\beta/\gamma$ subunits can activate phosphoinositide-3 kinase (PI3K), which results in the phosphorylation of the serine/threonine kinase AKT, a protein that plays a role in cell migration, proliferation and survival. $G\alpha$ subunit can also activate the Rho GTPases family of proteins, which are crucially involved in cell migration. β -arrestin is involved in the endocytosis of GPCRs, and upon the binding of CXCL12 to CXCR4, it is recruited to induce receptor internalization and desensitization.

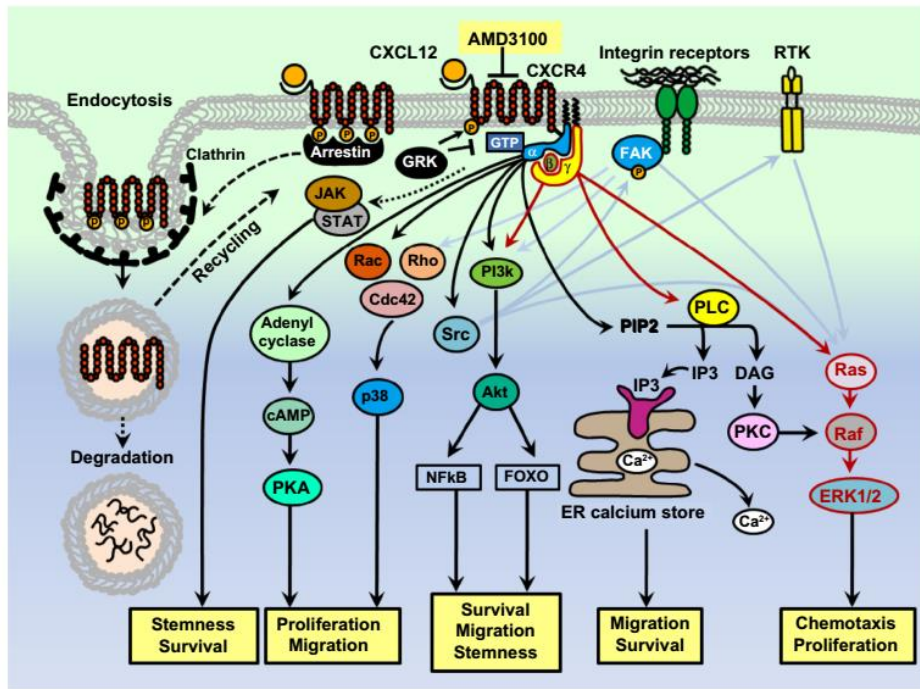


Figure 1.4.1.4A: The CXCL12/CXCR4 signalling pathway. CXCL12 binds to CXCR4 and leads to activation of the G protein coupled to the receptor. The G α subunit dissociates from the dimer G β/γ and inhibits adenylyl cyclase. Src is activated which in turn activates the Ras/Raf/ERK signalling pathway. This pathway is also directly induced by the dimer G β/γ , which activates as well PI3K, resulting in the induction of AKT mediated cell migration or survival. G α monomer activates PLC which hydrolyses PIP2 into IP3 and DAG. As a result, Ca²⁺ concentration is increased, hence inducing cell migration. Rho GTPases are a target of G α subunit and upon activation promote cell migration or proliferation. Upon CXCL12 binding to CXCR4 β -arrestin is recruited to induce receptor internalization and desensitization [151].

CXCR7 is another receptor of CXCL12. Initially, this receptor was considered a decoy receptor, as it does not act via activation of the G protein signalling, as observed with CXCR4. Therefore, CXCR7 was also regarded as a scavenger receptor, which sequesters CXCL12 to generate gradients of the chemokine and thus regulates CXCR4 signalling. However, since CXCL12 scavenging by CXCR7 prevents downregulation of CXCR4, there could also be a beneficial effect on the CXCL12/CXCR4 axis.

Studies of the structure of CXCR7 reveal that it has both similarities with chemokine receptors, but also unique features compared to GPCRs. CXCR7 is classified as a chemokine receptor due to its high binding affinity to the chemokines CXCL12 and CXCL11, due to its structural similarities with the other chemokine receptors, and due to its involvement in the regulation of cell migration, proliferation and differentiation. Classical chemokine receptors possess the canonical DRYLAIV (Asp-Arg-Tyr-Leu-Ala-Ile-Val) motif in their second intracellular loop (Figure 1.4.1.4B). CXCR7 contains instead the DRYLSIT (Asp-Arg-Tyr-Leu-Ser-Ile-Thr) motif, which is also found in other 7-transmembrane receptors, such as α 2 and β 1 adrenergic receptors, muscarinic acetylcholine

receptor, and serotonin receptor. This divergence of CXCR7 from the typical chemokine receptors led to its designation as an atypical chemokine receptor (ACKR3) [152-154].

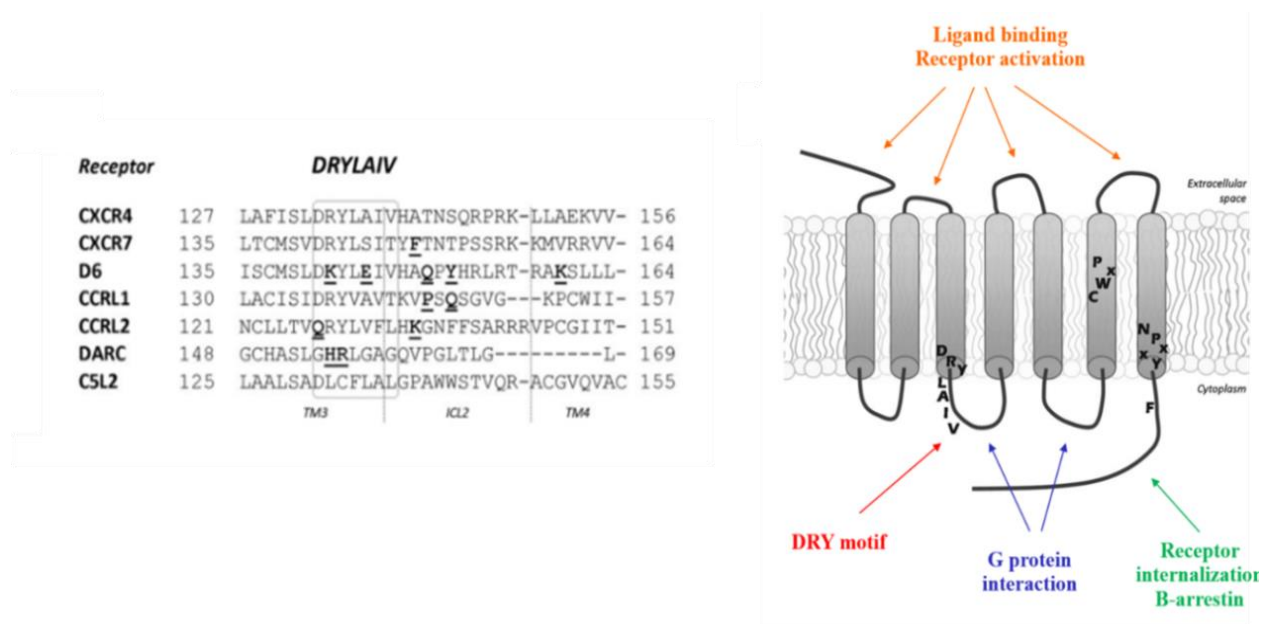


Figure 1.4.1.4B: Structure and amino acid sequence of CXCR4 and CXCR7. The chemokine receptor is a seven-transmembrane receptor with three intracellular and three extracellular loops. The ligand binds the extracellular site of the receptor and activates it. G proteins are coupled to the receptor through its second and third intracellular loop. Receptor internalization takes place with the recruitment of β -arrestin to the intracellular segment free of the receptor. The DRY motif, which is distinct between CXCR4 and CXCR7, is located in the second intracellular loop of the receptor. CXCR4 DRY motif comprises the amino acids Asp-Arg-Tyr-Leu-Ala-Ile-Val, whereas the CXCR7 DRY motif consists of the amino acids Asp-Arg-Tyr-Leu-Ser-Ile-Thr [154].

Since CXCR7 and CXCR4 can dimerize, the first was considered a co-receptor of the latter, leading to enhanced CXCL12 mediated signalling via G protein activation. CXCL12 has higher affinity for CXCR7 than for CXCR4 and homodimerization of CXCR7 is thus expected to bind to CXCL12 with greater affinity than homodimers or heterodimers of CXCR4 [153].

CXCR7 is known to interact with β -arrestin, resulting in either receptor internalization or MAPK kinase signalling pathway activation, through ERK1/2 or p38 phosphorylation [155]. More recently, other signalling pathways have been shown to be activated in response to CXCL12 binding to CXCR7. These include the PI3K/AKT and Rho GTPases pathways and they can induce cell migration, proliferation and survival [156]. These evidences have changed the view of CXCR7 as a mere decoy or scavenger receptor. Currently, CXCR7 is accepted as a fully chemokine signalling receptor but independent of G protein.

The cross-talk between CXCL12, CXCR4 and CXCR7 is a complex interaction that regulates important cellular responses, especially in cardiovascular diseases, in cancer diseases, in neovascularization and in neurogenesis.

Knockout of CXCR7 in mice results in defects in the heart, brain and kidney development [157]. In the bone marrow CXCR7 is expressed on lymphocytes and granulocytes, nevertheless, its expression in the immune system is tightly regulated and context specific. The binding of CXCL12 to CXCR7 in the bone marrow may decrease the availability of this chemokine, which can contribute to the regeneration of the bone marrow stem cell niche. Additionally, CXCR7 expression is important to direct the HSCs to their niche. Inhibition of CXCR7 causes increase of CXCL12 in the plasma. During inflammation, infection, ischemia and neoplasia, CXCR7 expression is highly induced and it is involved in the regulation of cell migration, proliferation and survival in these processes [158-160].

Similar to CXCR4, CXCR7 is expressed on vascular ECs and it participates in the regulation of stem cell trafficking and of immunological and inflammatory processes. During inflammatory the expression of CXCR7 is increased on leukocytes and endothelial cells [129, 159, 161]. In cancer diseases, ECs of tumour-associated vasculature significantly express CXCR7, which plays a pro-angiogenic role and contribute to tumour invasion. Accumulating studies further confirm that CXCR7 participates in endothelium repair and regeneration. An increased expression of this receptor on ECs is also implicated in the infiltration of inflammatory cells in autoimmune diseases, due to enhanced cell adhesion [161-163].

CXCR7 expression was also detected on vascular smooth muscle cells and it was reported that this receptor has a role in inducing the CXCL12-mediated proliferation of the SMCs in chronic allograft vasculopathy [161, 164]. Platelets also express CXCR7, which seems to be involved in their survival through anti-apoptotic effects. It is speculated that CXCR7-platelet expression is correlated with initial myocardial repair in patients with acute coronary syndrome. Research work has been developed to explore the regenerative capacity of platelets through CXCR7 [165]. More recently, CXCR7 was associated with differentiation of monocytes into macrophages, revealing that this receptor may play other crucial roles which have not been yet explored [153].

CXCR7 has been implicated in atherosclerosis, where it seems to lower hyperlipidemia by increasing the uptake of very-low-density lipoproteins (VLDLs) by the adipocytes, which enables regulation of the cholesterol level in the blood. CXCR7 deficiency increases serum cholesterol levels, which leads to monocytosis and macrophage accumulation, resulting in increased neointima lesion. Therefore, CXCR7 may have a key role in regulating lipidemia and inflammatory processes in atherosclerosis [166, 167].

Targeting the CXCL12/CXCR4/CXCR7 axis has been intensely explored to develop therapies for many diseases, particularly cardiovascular diseases.

1.5 Cell migration

Cell migration is the process by which cells move from one location to another, in response to stimuli, and it is essential for the development and maintenance of an organism, being also involved in pathological conditions.

Cell movement comprises essentially five steps (Figure 1.5A) and it is triggered by the sensing of a stimulatory signal, such as chemokines. The first step consists of the formation of a protrusion rich in actin polymers (lamellipodia and filopodia), which elongates the leading edge of the cell (extension step). Then, adhesion proteins enable the attachment of the protrusion to the substratum or extracellular matrix (attachment step). Next, a contraction step is followed, in which the cell body contracts via stress fibers formation to enable the retraction of the rear end of the cell and to pull the whole cell body forward due to the contractile forces generated. Consequently, the fourth step involves the release of the adhesion proteins at the rear end of the cell to allow progression of movement (rear release step). Finally, the recycling step encompasses the recycling of the cell migratory machinery to get the cell ready again for first step.

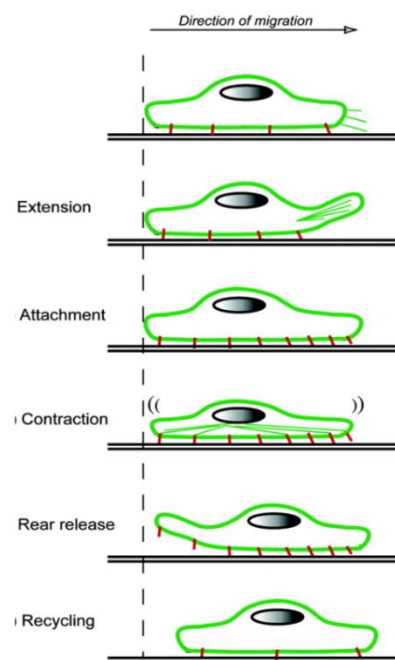


Figure 1.5A: Steps involved in cell migration. Cell movement comprises: Extension step: Formation of a protrusion rich in actin polymers (lamellipodia and filopodia); Attachment step: Adhesion proteins enable the attachment of the protrusion to the substratum or extracellular matrix; Contraction step: Cell body contracts via stress fibers formation to enable the retraction of the rear end of the cell and to pull the whole cell body forward; Rear release step: Release of the adhesion proteins at the rear end of the cell to allow progression of movement; Recycling step: Recycling of the cell migratory machinery to get the cell ready again for first step. (Image adapted from Lamalice et al.; Endothelial cell migration during angiogenesis; 2007; Circulation Research) [168].

The driving force of cell motility is the reorganization of the cell cytoskeleton proteins, which regulate the formation of the leading protrusions and the contraction of the cell body. There are three types of cytoskeleton proteins: Actin filaments, intermediate filaments and microtubules (Figure 1.5.B). These have a thin fibrous polymeric structure and have a variety of structural and functional roles.

Actin filaments, also known as microfilaments, consist of long polymerized intertwined chains in a helix of globular monomeric protein actin (G-actin). Actin is an ATPase and as such, it hydrolyses ATP to ADP upon polymerization. It is also the most abundant protein in the cell and it is contractile. The actin filaments are polar and hence they possess a plus end where the actin monomers are assembled for polymerization (barbed end) and a minus end in which the actin monomers are disassembled (pointed end). They can also organize into bundles to form the contractile stress fibers. Myosin motor proteins, which have the ability to convert chemical energy into movement, bind to the actin filaments and produce their movement to allow cell motility.

Microtubules consist of 13 filaments arranged in parallel to form a cylindrical structure. Each filament is composed of a series of α - and β -tubulin heterodimeric proteins. Each tubulin subunit binds to GTP and only the GTP of β -tubulin undergoes hydrolysis. The microtubule polymers are also polar with a plus end (fast growing end) and a minus end (slow growing end), which allows its assembly and disassembly. These cytoskeleton elements are important in determining the cell shape and they participate in the traffic of cell organelles and vesicles inside cell, as well as in separating the chromosomes during mitosis.

Intermediate filaments are formed of a bundle of extended subunit proteins. Four individual proteins assemble to form a tetrameric subunit. These, associate to form the unit length filament (ULF), which is composed of eight tetrameric subunits. ULFs can join end-to-end to other ULFs to grow longitudinally longer filaments. Nevertheless, the intermediate filaments are non-polar. One of the functions of these cytoskeleton proteins is to provide structural integrity to the cell [169].

The actin filaments and the microtubules have been recognized to have preponderant roles in cell motility. The protrusion of the lamellipodia at the leading edge of the cell results from the continuous growth of the actin filaments. The release of the contacting points of the actin filaments with the substratum, allows the retraction of the rear end of the cell and the progression of the movement in response to body contraction due to the formation of the stress fibers. Microtubules seem to also participate in the lamellipodial protrusion and adhesion in some cells.

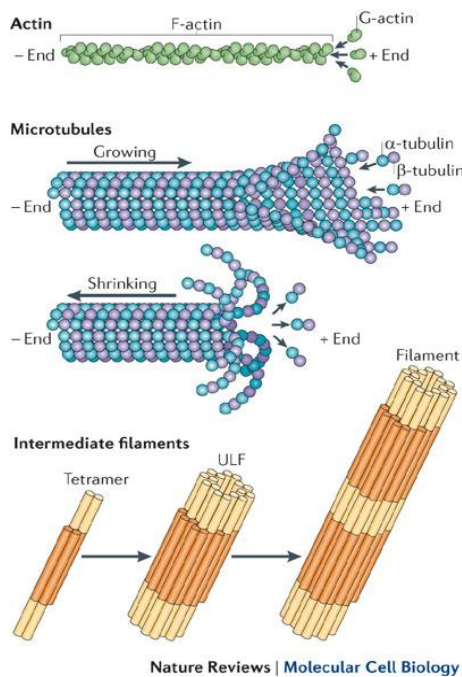


Figure 1.5B: Cytoskeleton protein filaments. Actin filaments: Actin filaments are long polymerized intertwined chains in helix of globular monomeric protein actin (G-actin). These filaments are polar and possess a plus end where the actin monomers are assembled for polymerization (barbed end) and a minus end in which the actin monomers are disassembled (pointed end). They organize into bundles to form the contractile stress fibers. Microtubules: Microtubules consist of 13 filaments arranged in parallel to form a cylindrical structure. Each filament is composed of a series of α - and β -tubulin heterodimeric proteins. The microtubule polymers are polar with a plus end (fast growing) and a minus end (slow growing), which allows its assembly and disassembly. Intermediate filaments: Intermediate filaments are formed of a bundle of extended subunit proteins. 4 individual proteins assemble to form a tetrameric subunit. These, associate to form the unit length filament (ULF), composed of eight tetrameric subunits. ULFs join end-to-end to other ULFs to grow longitudinally longer filaments. The intermediate filaments are non-polar. (Source: Mostowi et al.; Septins: the fourth component of the cytoskeleton; 2012; Nature Reviews Molecular Cell Biology) [169].

Unpolymerized actin monomers exist in the cell bound to profilin and other proteins (Figure 1.5C). Profilin exchanges the ADP for ATP on G-actin, making it competent and available for polymerization. In the presence of stimulatory signals, nucleation-promoter factors such as members of the WASP and the SCAR/WAVE families of proteins are activated. These in turn activate the Arp2/3 complex to nucleate actin filaments and thus induce branching, by attaching to the site of pre-existing actin filaments, which pushes the membrane forward. Formins such as mammalian Diaphanous formin 1 and 2 (mDia1 and mDia2) induce the progression of the actin polymerization by attaching themselves to the barbed ends of the filament formed previously by the Arp2/3 complex. The formins recruit actin monomers and use them to nucleate and elongate the filaments. Once new

filaments are formed and elongated, capping proteins, including gelsolin and CapZ, terminate growth and prevent depolymerization to conserve the actin filament. At the pointed ends, which are away from the fast growing ends associated with the protrusion elongation, actin subunits hydrolyse their bound ATP (related to actin aging) and dissociate γ -phosphate. This initiates debranching reactions in which cofilin depolymerizes the actin filament, with dissociation of ADP-actin subunits. Therefore, severing ends are formed and the free ends created can be used for re-initiation of actin filament polymerization. In addition, cofilin enables the recycling of the actin monomers. The turnover of the filament is slowed down by inactivation (phosphorylation) of cofilin. Profilin exchanges back the ADP for ATP in the actin monomers, hence contributing to the subunit pool which can be incorporated again back to the actin filament [170-173].

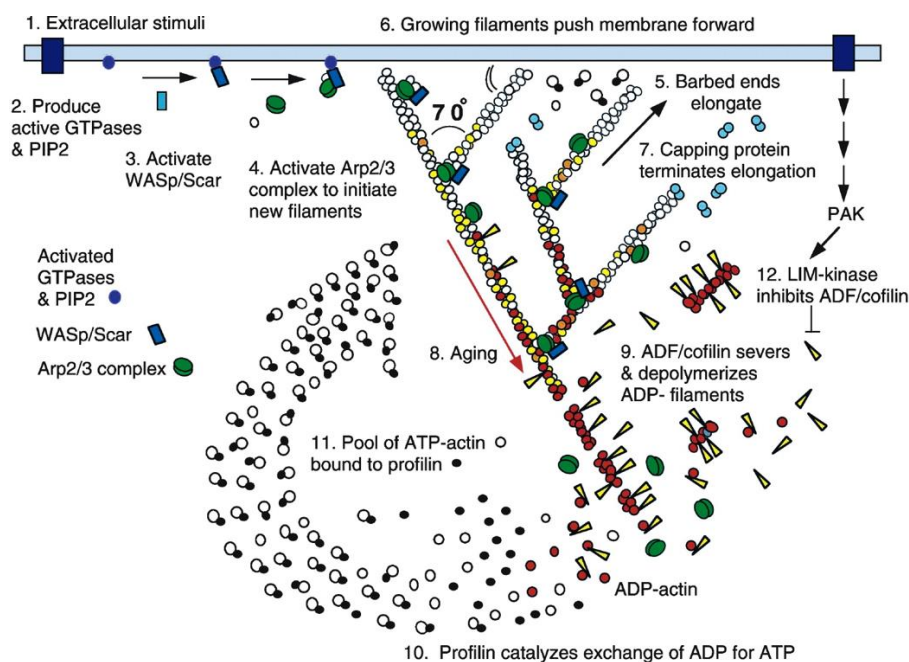


Figure 1.5C: Mechanism of protrusion formation by actin filaments. Actin filaments are responsible for cell protrusion growth in cell migration. Step 1: Extracellular signals activate receptors. Step 2: Signalling transduction pathways activate Rho GTPases and PIP2. Step 3: WASP and SCAR/WAVE family of proteins are activated. Step 4: WASP/SCAR proteins activate Arp2/3 complex which initiates actin nucleation. Step 5: New branches from the barbed ends grow and elongate. Step 6: Growing filaments push the membrane forward to form the protrusions. Step 7: Capping proteins terminate new branch growth. Step 8: Actin filaments age due to hydrolysis of ATP to give ADP on the actin subunits (white subunits turn yellow). Dissociation of γ -phosphate is followed (subunits turn red). Step 9: Cofilin severs ADP-actin filaments with dissociation of the actin subunit and thus depolymerization of the actin filaments. Step 10: Profilin catalyses exchange of ADP for ATP in the actin subunits (subunits turn white again) and returns the pool of ATP-actin. Step 11: The pool of ATP-actin bound to profilin is ready to incorporate again the actin filaments and elongate the barbed ends. Step 12: Cofilin is inactivated by LIM kinase and PAK, which were activated by Rho GTPases family proteins. (Source: Pollard et al.; Cellular motility driven by assembly and disassembly of actin filaments; 2003; Cell) [174].

Cell migration requires a coordinated rearrangement of the cytoskeleton machinery, as described above. This migration machinery is regulated by a complex and interconnecting signalling network that includes different signalling pathways. The next section will focus on the most relevant signalling pathways involved in cell migration.

1.5.1 Signalling pathways involved in cell migration

Cell migration begins with the interaction of an external signal that stimulates its corresponding receptor. This signal is transduced by several signalling pathway cascades which lead to the rearrangement of the cytoskeleton to allow the cell to move.

The most widely studied signalling pathways include the Rho GTPases family of proteins, the PI3K/AKT signalling pathway and the MAPK kinase signalling cascade.

1.5.1.1 *Rho GTPases family*

Rho GTPases belong to the Ras superfamily of proteins which comprises more than 130 members. The most well-known Rho family members are RhoA, Rac1 and Cdc42. A characteristic of these proteins is that they can cycle between an inactive state (bound to GDP) to an active state (bound to GTP). The switching between the two conformational states is tightly regulated by several molecules and it is in the active state that the Rho GTPases are able to interact with downstream effector to propagate the signalling transduction.

Guanine nucleotide exchanging factors (GEFs) promote the release of GDP to allow the binding of GTP, thus activating the GTPase proteins. The inactivation of these proteins is achieved by GTPase-activating proteins (GAPs) which stimulate the hydrolysis of GTP to yield GDP. The Rho-GDP bound proteins are sequestered in the cytosol by guanine nucleotide dissociation inhibitors (GDIs), which inhibit the dissociation of the guanine nucleotide and thus prevents the activation of the Rho GTPases.

RhoA, Rac1 and Cdc42 are mainly involved in cytoskeleton rearrangement and cell motility (Figure 1.5.1.1A). Rac1 is associated with lamellipodia protrusion and Cdc42 is involved in filopodia formation, which indicates that these proteins are active at the leading edge. RhoA stimulates the formation of contractile actomyosin fibers, which suggests that this protein is active in the body and rear of the cell. Accumulating studies have shown that RhoA is also active at the leading edge and that it may even be activated before Rac and Cdc42, revealing that localized RhoA orchestrates the initial membrane protrusion at the leading edge of the extension and this is rapidly followed by Rac and Cdc42 actions to reinforce the protrusion. Therefore, Rho GTPases activation is regulated in a strict spatiotemporal manner [175-177].

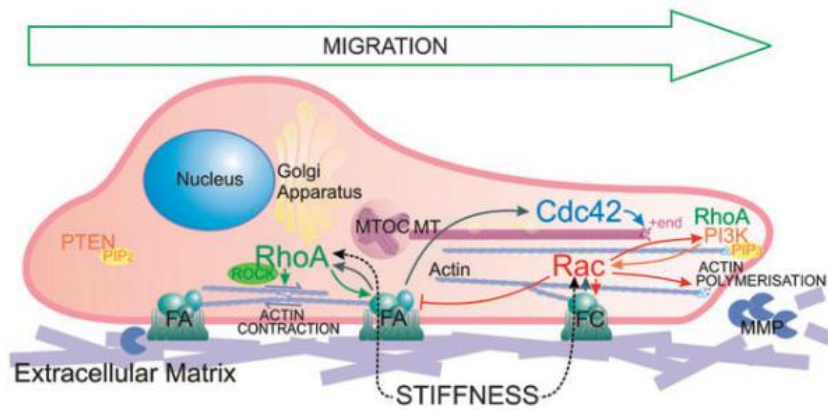


Figure 1.5.1.1A: Regulation of the cytoskeleton by Rho GTPases. Cell motility comprises the formation of a protrusion (lamellipodia) at the leading edge and body contraction with retraction of the rear end. Rac1 and Cdc42 are active at the leading edge of the cell and are involved in lamellipodia and filopodia formation, respectively. RhoA is also active at the leading edge and it is activated before Rac and Cdc42, to promote the initial membrane protrusion at the leading edge of the extension. Rac and Cdc42 activation rapidly follows to reinforce the protrusion. RhoA is active as well in the body and rear of the cell to stimulate the formation of contractile actomyosin fibers, which allow the progression of the movement forward. (Source: Binamé et al.; What makes cells move: requirements and obstacles for spontaneous cell motility; 2010; Molecular bioSystems) [178].

The downstream effectors of the Rho GTPases constitute a complex network of molecules that act on the cell cytoskeleton to induce cell migration (Figure 1.5.1.1B).

The activity of actin polymerization inducers such as formins, which include the molecule mDia, is regulated by the binding of Rho GTPases, leading to the relief of the head to tail autoinhibitory interactions in the formins. Consequently, mDia can then stimulate actin polymerization. The Arp2/3 actin nucleation complex is activated locally at the cell membrane by the WASP and SCAR/WAVE families of proteins. Rho GTPases activate the WASP (activated by Cdc42) and SCAR/WAVE (activated by Rac) proteins, which results in actin polymerization through Arp2/3 complex activation.

Actin filaments are organized in thick bundles by the action of myosin II that crosslinks antiparallel actin filaments and mediates contraction due to its ATPase-dependent motor domain. Myosin converts the energy of ATP hydrolysis into mechanical movement. Therefore, stress fiber formation and contraction are controlled by myosin II, whose activity is regulated by the phosphorylation of its light chain. RhoA regulates the kinases that phosphorylate myosin light chain (MLC). RhoA predominantly induces the phosphorylation of MLC (p-MLC) either directly or via its downstream effector Rho-associated serine/threonine kinase (ROCK). ROCK inhibits MLC phosphatase (MLCP) and can also phosphorylate MLC. As a result, cell contraction is achieved. In addition, LIM kinase (LIMK) is activated by ROCK, which results in phosphorylation of cofilin. When cofilin is phosphorylated, it is in

its inactive state and it cannot bind to actin, hence, depolymerization or turnover of the actin filament is prevented. Phosphorylation of MLC is enhanced at the sites of cell body contraction and in the region of trail retraction, but it is also enhanced at the lamellipodium region of the cells to stimulate protrusion. It has been shown that Rac and Cdc42 can as well induce phosphorylation of MLC at the leading edge.

P21 activated kinase (PAK) is activated by Rac1 and Cdc42, which results in the activation of LIMK by phosphorylation. As explained, LIMK inactivates cofilin. Therefore, Rac1 and Cdc42 are also involved in the regulation of actin turnover. PAK (p21-Activated kinase) is a serine/threonine kinase implicated in the rearrangement of the cytoskeleton and besides LIMK, it has other substrates, such as myosin II, whose activity is regulated by the phosphorylation of their regulatory light chains (serine or threonine sites) [175-177, 179, 180].

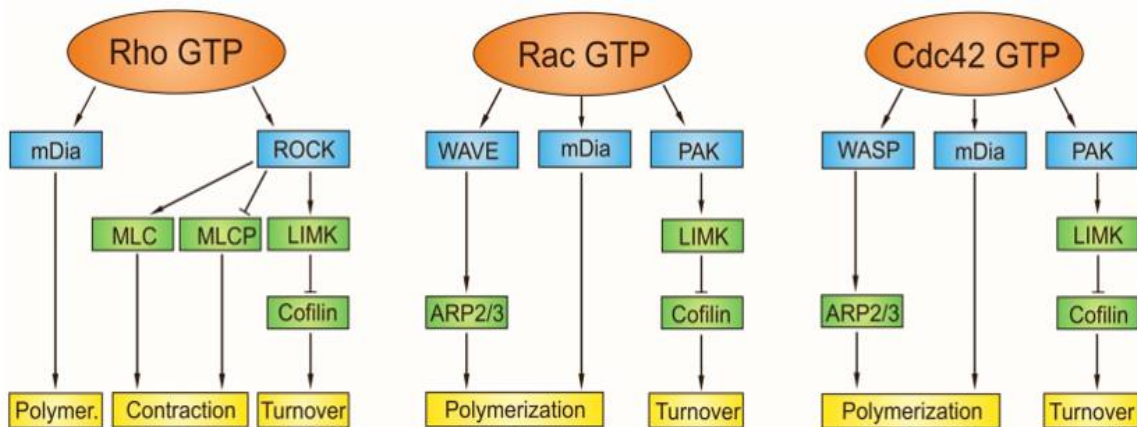


Figure 1.5.1.1B: Downstream effectors of Rho GTPases. The downstream targets of active Rho GTPases include the kinases such as p21-activated kinase (PAK) and Rho-associated coiled-coil kinase (ROCK), and the nucleation promoting factors such as mammalian Diaphanous formin (mDia), Wiskott-Aldrich syndrome protein (WASP), Wiskott-Aldrich syndrome protein-family verprolin homologous protein (WAVE). mDia-induced nucleation produces unbranched actin filaments and WASP and WAVE interact with Arp2/3 complex and generate branched microfilaments. PAK phosphorylates LIM-motif containing kinase (LIMK), which in turn phosphorylates and inhibits cofilin, thereby regulating the actin-filament turnover. RhoA stimulates actin filament growth and the interaction between actin and myosin through ROCK, which phosphorylates myosin II light chain (MLC), myosin light chain phosphatase (MLCP) and LIMK. Phosphorylation of MLC contributes to contractility [181].

Rho GTPases have a prominent role in cell migration and they regulate the actin polymerization machinery through a complex network of effectors. These proteins also interact with other relevant signalling pathways involved in cell migration mechanism.

1.5.1.2 The PI3K/AKT signalling pathway

Phosphoinositide 3-kinases (PI3Ks) are important regulators involved in a variety of cell functions, including migration, proliferation, differentiation and survival.

Upon binding of a chemokine to its GPCR receptor, the G protein is activated, with the dissociation of the $G\alpha$ -GTP subunit from the $G\beta/\gamma$ dimer subunit. The latter, at the plasma membrane, either directly binds to PI3K to activate it or induces Ras activation (inactive Ras-GDP switches to active Ras-GTP) which then activates PI3K (Figure 1.5.1.2). The $G\alpha$ monomeric subunit has been shown well in some studies to activate PI3K.

Activated PI3Ks phosphorylates the lipid molecules phosphatidylinositol (4,5)-biphosphate (PIP₂) to generate phosphatidylinositol (3,4,5)-triphosphate (PIP₃). The production of PIP₃ by PI3K occurs at the leading edge of migrating cells, whereas the degradation of the lipid takes place at the rear end of the cell, which explains the higher concentration of PIP₃ and PI3K at the site of actin polymerization at the front of the cell.

Protein kinase B (PKB), also known as AKT, lives in the cytosol in an inactive state. This signalling effector contains a PH domain which has a high affinity for PIP₃. Therefore, accumulated PIP₃ recruits AKT to the membrane and the resulting interaction leads to a conformational change of AKT with the exposition of its serine/threonine phosphorylation sites required for activation.

AKT is then activated by 3-phosphoinositide-dependent protein kinase 1 (PDK1) which prompts it to phosphorylate and regulate proteins involved in the remodelling of actin at the leading edge of the cell, including myosin II and PAK1. In addition, AKT also regulates the actin dynamics via its direct binding and phosphorylation. It is proposed that this interaction with actin is possible due to the PH domain of AKT.

Rho GTPases can regulate as well AKT activity by phosphorylation of its serine and threonine sites and targeting it to the actin cytoskeleton. Rho GEFs (Guanine nucleotide exchanging factor) contain a PH domain and thus they are downstream effectors of PI3K and PIP₂/PIP₃, which leads to the activation of the Rho GTPases and the consequent regulation of actin polymerization.

The inactivation of PIP₃ is performed by phosphatase and tensin homolog (PTEN) which is a negative regulator of the PI3K pathway [176, 182-185].

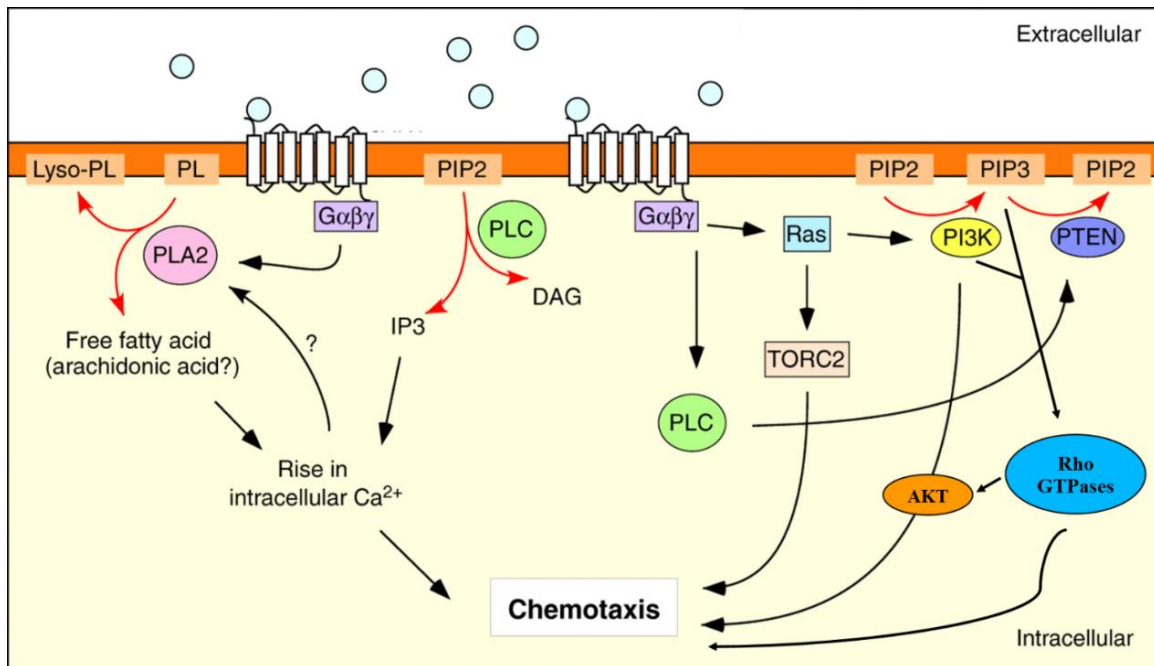


Figure 1.5.1.2: PI3K/AKT pathway and regulation of chemotaxis. Chemotaxis is regulated by the PI3K pathway. GPCRs are activated upon ligand binding. The G protein subunits activate PI3K either directly or through Ras activation. Activated PI3Ks phosphorylates phosphatidylinositol (4,5)-biphosphate (PIP2) to generate phosphatidylinositol (3,4,5)-triphosphate (PIP3). Accumulated PIP3 recruits AKT to the membrane which is activated by 3-phosphoinositide-dependent protein kinase 1 (PDK1) and Rho GTPases. Activated AKT phosphorylates and regulates myosin II and PAK1 and it also regulates the actin dynamics via its direct binding and phosphorylation. Rho GEFs (Guanine nucleotide exchanging factor) contain a PH domain and thus they are downstream effectors of PI3K and PIP2/PIP3, which leads to the activation of the Rho GTPases and the consequent regulation of actin polymerization. The inactivation of PIP3 is performed by phosphatase and tensin homolog (PTEN) which is a negative regulator of the PI3K pathway. Red arrows indicate enzymatic reactions. Black arrows indicate activation pathways. (Adapted from: Kölsch et al.; The regulation of cell motility and chemotaxis by phospholipid signalling; 2008; Journal of Cell Science) [183].

1.5.1.3 MAPK/ERK: Ras-Raf-MEK-ERK signalling pathway

Mitogen-activated protein kinases (MAPKs) are a family of related serine/threonine kinases that regulate a variety of cell functions, including migration, proliferation, differentiation, survival, amongst others. There are three well-known groups of kinases which diverge due to the differences of a motif present in their activation loops: Extracellular signal-regulated protein kinases 1 and 2 (ERK1/2) has a Thr-Glu-Tyr motif; p38 kinase has a Thr-Ala-Tyr motif; Jun N-terminus kinase (JNK) has a Thr-Pro-Tyr motif.

MAPKs are activated through a cascade of kinases (Figure 1.5.1.3). MAPKK kinases (MAPKKKs) are activated through phosphorylation or interaction with Ras/Rho GTPases. Next, they activate MAPKKs, which in turn activate MAPKs, through the phosphorylation of the threonine and tyrosine residues within the activation loop.

In line of the current project the MAPK/ERK pathway will be described in the context of chemotaxis. GPCR chemokine receptors are activated upon binding of a signal. As a result, the G protein is activated and G α subunit dissociates from G β/γ dimer subunit. Both subunits are involved in the activation of the Ras GTPase (Ras-GDP switches to Ras-GTP). Ras-GTP is implicated in the MAPK and PI3K signalling pathways.

Ras-GTP recruits MAPKKK Raf to the plasma membrane where it is activated. Activated Raf phosphorylates Ser/Thr MAPKK MEK1/2 (MAPK ERK kinase) and these in turn activate MAPKs ERK1/2 by phosphorylation of their threonine and tyrosine residues. ERK1 and ERK2 are two isoforms that share 85% of homology in their sequence and have very close protein size (ERK1 is 44kDa and ERK2 is 42kDa). In resting state, ERK1/2 is anchored in the cytoplasm. In response to stimulation they are activated and recruited either to the nucleus to activate transcription factors or to the cytosol to phosphorylate and activate substrates, such as cytoskeleton proteins.

ERK1/2 can phosphorylate Myosin light chain kinase (MLCK), which is a serine/threonine-specific protein kinase that phosphorylates the regulatory light chain of myosin II. Additionally, focal adhesion kinase (FAK) and paxillin are also phosphorylated by ERK1/2. FAK and paxillin are both expressed at focal adhesions and participate in the adhesion of the cell to the extracellular matrix. Therefore, ERK1/2 may regulate focal adhesion dynamics by modulating the FAK-paxillin interaction. ERK also phosphorylates calpain and hence, it can stimulate calpain's activity in the presence of low concentration of Ca²⁺, which is required for calpain's proteolytic activity. Calpain is involved in focal adhesion turnover and cell migration [186-189].

Protein kinase C (PKC) is a component of the GPCR-dependent signalling and it can activate ERK MAPK pathway. PKC is activated by DAG which is generated upon hydrolysis of PIP2 by PLC. Once PKC is activated, it can induce ERK phosphorylation through Raf activation. The hydrolysis of PIP2 into DAG and IP3 increases the intracellular Ca²⁺, and this in turn activates calcium and DAG dependent GEFs that can activate Raf and hence induce the ERK MAPK signalling cascade. Another

component of the G protein signalling is protein kinase A (PKA) and this serine/threonine kinase is more known for negatively regulate the ERK MAPK pathway. PKA is an effector of cAMP and thus it is activated upon increase of cAMP, which is regulated by the $G\alpha$ subunit. Once PKA is activated it can interact with Raf preventing its coupling with Ras to be activated. Furthermore, PKA can also activate phosphatases that can dephosphorylate ERK, hence inactivating it. Depending on the G protein signalling activated, the ERK MAPK pathway can either be positively or negatively regulated [190, 191].

Cooperation between ERK1/2 and Rho GTPases also has a key role in cell migration. As mentioned above, Ras GTPase can activate ERK1/2 MAPK pathway. Rac and Cdc42 are other two GTPases capable of activating MEK1/2 and ERK1/2. PAK, which is a downstream target of both Rac and Cdc42, can phosphorylate MEK, thus enabling the interaction of Raf with MEK and consequential activation of ERK. Studies also reveal an interaction between Rho and ERK, in which the first can activate the ERK pathway. Moreover, ERK can also regulate the activation of Rho GTPases, in a coordinated fashion, by either activating or inactivating Rho and Rac, to promote cell migration [192-195].

The cross-talk between ERK MAPK pathway and PI3K signalling pathway adds more complexity to the cell migration mechanism, and this cross-talk can either be positive or negative. For example, PI3K is an activator of Rac GTPase, which then activates PAK. As mentioned, PAK phosphorylates MEK which leads to ERK activation. Furthermore, Ras GTPase which activates PI3K is the upstream activator of the ERK MAPK cascade. Therefore, the effectors of one signalling pathway can affect the effectors of the other signalling pathway to generate a feedback loop of Ras GTPase. One example is the negative regulation of AKT, an effector of PI3K, on ERK activation through phosphorylation of the inhibitory site of Raf. Thus, if Raf is inhibited it cannot activate MEK and ERK [187, 192, 196].

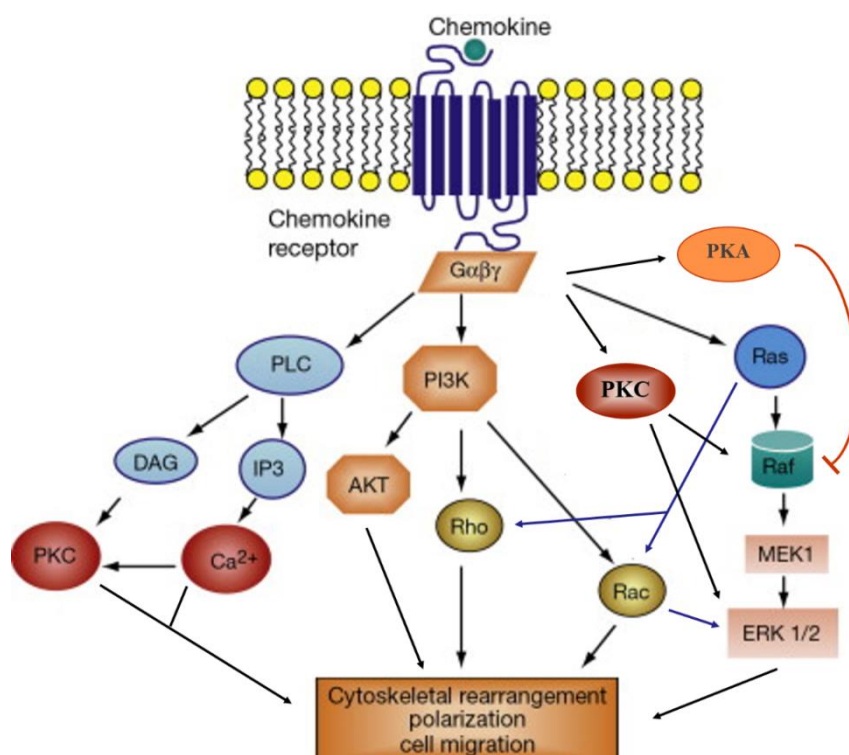


Figure 1.5.1.3: Ras-Raf-MEK-ERK signalling pathway and regulation of chemotaxis. The Ras-Raf-MEK-ERK signalling pathway is involved in cell migration induced by chemokine G protein-coupled receptor activation. Both $G\alpha$ subunit and $G\beta/\gamma$ dimer subunit are involved in the activation of the Ras GTPase which is implicated in the MAPK and PI3K signalling pathways. Ras-GTP activates MAPKKK Raf, which phosphorylates MEK1/2 and these in turn activate MAPKs ERK1/2. ERK1/2 can phosphorylate cytoskeleton and focal adhesion substrates to induce cell migration. Protein kinase C (PKC) induces ERK phosphorylation through Raf activation. PKA can interact with Raf preventing its coupling with Ras or it activates phosphatases that can dephosphorylate ERK, hence inactivating it. ERK1/2 and Rho GTPases interact with each other. ERK MAPK pathway and PI3K signalling pathway can regulate each other, which adds more complexity to the cell migration mechanism, and this cross-talk can either be positive or negative. PI3K is an activator of Rac GTPase, which then activates PAK. As mentioned, PAK phosphorylates MEK which leads to ERK activation. Furthermore, Ras GTPase which activates PI3K is the upstream activator of the ERK MAPK cascade. Therefore, the effectors of one signalling pathway can affect the effectors of the other signalling pathway to generate a feedback loop of Ras GTPase. (Adapted from: Sobolik-Delmaire et al.; Chemokine receptors; 2015; Encyclopedia of Biological Chemistry) [197].

1.5.1.4 β -arrestin mediated signalling pathways

The function of the GPCRs is mediated by three families of proteins: The heterotrimeric G proteins, the G protein-coupled receptor kinases (GRKs) and the β -arrestins. The G proteins are responsible for the signalling function of the GPCRs. More recently, GRKs and β -arrestins were shown to have more functions than just desensitizing the GPCRs. Accumulating studies demonstrate that β -arrestins besides regulating receptor endocytosis they can also induce signalling pathways in a complex network (Figure 1.5.1.4). Here, the most relevant for this project will be described.

β -arrestins can regulate the activation and the spatial distribution of MAPKs. ERK1/2 can either be directly activated by β -arrestin or by Src tyrosine kinase which is recruited first by β -arrestin. Additionally, specific MAPK components of the MAPK cascade can form a complex with β -arrestin. The scaffolding of Raf, MEK and ERK by β -arrestin facilitates the cell signalling to ERK and distributes activated ERK at the leading edge of the migrating cell. Therefore, actin dynamics through ERK pathway is regulated by β -arrestin. Other MAPK cascades, such as p38 and JNK can also be activated by β -arrestin.

The PI3K/AKT pathway is another signalling mechanism that is regulated by β -arrestin. PI3K activation and AKT phosphorylation are induced by β -arrestin, which can act as scaffold protein for these molecules as well. On the other hand, some studies show that β -arrestin can inhibit PI3K. Stimulation or inhibition of PI3K influences PIP2 which is known to regulate actin filament-related proteins. Furthermore, localized regulation of PI3K through β -arrestin scaffolding can affect the

activity of Rho GTPases. Direct regulation of AKT by β -arrestin constitutes another mechanism by which actin assembly is modulated, as AKT can activate myosin II through activation of PAK.

Finally, β -arrestin regulates actin assembly proteins. For example, this protein can activate RhoA and thus induce the formation of stress fibers. Moreover, cofilin, LIMK and MLC are all regulated as well by β -arrestin [156, 198, 199].

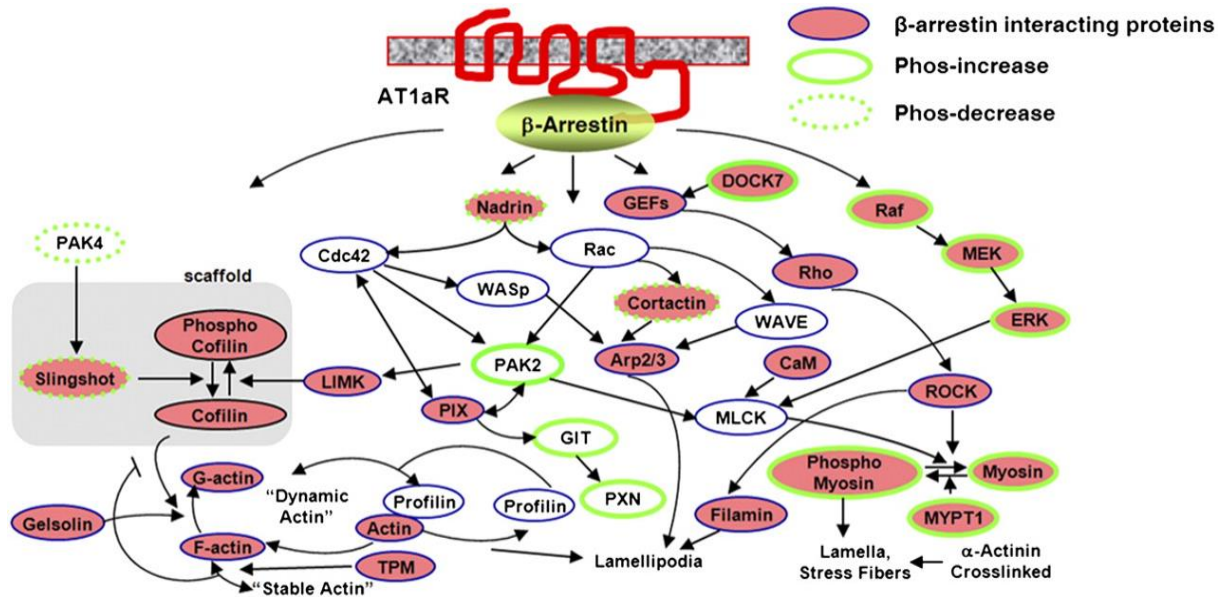


Figure 1.5.1.4: Signalling pathways regulated by β -arrestin. β -arrestins can regulate a complex network of signalling pathways. MAPKs spatial distribution and activation is regulated by β -arrestins. ERK1/2 is activated by β -arrestin. Additionally, specific MAPK components of the MAPK cascade form a complex with β -arrestin. The scaffolding of Raf, MEK and ERK by β -arrestin facilitates the cell signalling to ERK and distributes activated ERK at the leading edge of the migrating cell. Therefore, actin dynamics through ERK pathway is regulated by β -arrestin. Rho GTPases are activated by β -arrestin either directly or through effectors. Actin filament-related proteins, such as cofilin, LIMK and myosin are also regulated by β -arrestin [200].

1.5.2 The role of integrins in cell migration

Integrins are glycoproteins that form heterodimeric receptors for extracellular ligands/matrix. An α integrin can pair with a β integrin to form a receptor specific for a set of ligands. The integrin $\alpha 5$ and integrin $\beta 1$ (ITG $\alpha 5\beta 1$) receptor is one of the most well-known and it binds to fibronectin. Currently, 18 integrin α (ITG $\alpha 1$ - $\alpha 11$, ITG αD , ITG αE , ITG αL , ITG αM , ITG αV , ITG $\alpha 2B$ and ITG αX) and 8 integrin β (ITG $\beta 1$ -ITG $\beta 8$) are identified.

Upon binding of the ligand, the integrins cluster into focal contacts. A cell migration process initiates with the formation of protrusions called lamellipodia and filopodia. Within these extensions, focal

contact points with the extracellular matrix (ECM) are formed. Integrins are contained in these contact points which anchor the cytoskeleton to the ECM. The addition of actin monomers to the actin cytoskeletal scaffold pushes the membrane forward and new focal contact complexes are formed. The focal complexes mature into focal adhesions due to the interaction of integrins and the actin cytoskeleton and the creation of a strong interaction with the ECM.

As focal adhesions are formed at the edge of the cell, the same are dispersed at the rear end of the cell. As the cell slides, the contact size of the adhesion is reduced. The adhesions through the integrins serve as traction points for contractile or tensional forces, but they also regulate the activation of Rho GTPases in the protrusions, which control the polymerization of actin and the organization of the actomyosin filament. It is the coordinated regulation of the adhesion and the cytoskeleton organization that enables the cell to migrate (Figure 1.5.2).

Integrin binds to the actin cytoskeleton through actin-associated linking molecules, such as talin, vinculin, zyxin, and α -actinin, without which the adhesion is disassembled. Talin activate integrins enabling them to link to actin. Adhesion disassembly occurs in the presence of calpain, a calcium-dependent protease, which acts on talin or by reducing the affinity of the integrin to the extracellular matrix.

The integrins can change their conformation from a low to high affinity state. Activated integrins show high affinity for their ligand. Extracellular ligands bind to the outer domain of the integrins. The cytoplasmic domain of integrins binds to the actin cytoskeleton, structural molecules and signalling proteins. It is the actin that organizes the adhesion and it associates with the integrins at the leading edge. Actin first interacts with adhesion components such as vinculin and FAK, through its nucleating factor Arp2/3. This targets vinculin and FAK to the adhesion sites. The interaction formed is stabilized by its association to the integrins.

Adhesions require the activation of the Rho GTPases to assemble the actomyosin filament. When the protrusion pauses, the adhesion matures, that is, elongates by the elongation of the contractile filamentous actomyosin. α -actinin seems to have a role in this process. Myosin II is not present at the adhesion site but along the actin filament to cross link the actin bundles and thus mature the adhesion. Rho GTPases are localized in the protrusion as they regulate actin polymerization and disassembly via their effectors Arp2/3, mDia, LIMK, cofilin, MLCK, ROCK, amongst others. These effectors are very important for the formation of actomyosin to generate the contractile force that enables the cell body to move forward. Adhesions contain several proteins that mediate the activation of Rho GTPases, including ERK and PI3K. The integrins can initiate the Rho GTPases signalling cascades and activate other signalling pathways, depending on the composition of the ECM or its ligands.

Activation of signalling pathways typically involves phosphorylation of FAK (Focal adhesion kinase), which co-localizes with the integrins at the focal adhesion sites and which is recruited by talin and

paxillin to anchor it to the integrin. FAK activation attracts Src and these molecules function as docking sites for a variety of signalling molecules.

The interaction between an integrin and its ligand has also a significant role in the linkage between the cytoskeleton and the adhesion components. If the ligand is rigid or inflexible the linkage between the integrin and the cytoskeleton can be weak. Thus, the strength of the linkage depends on the force impinged on it [201-203].

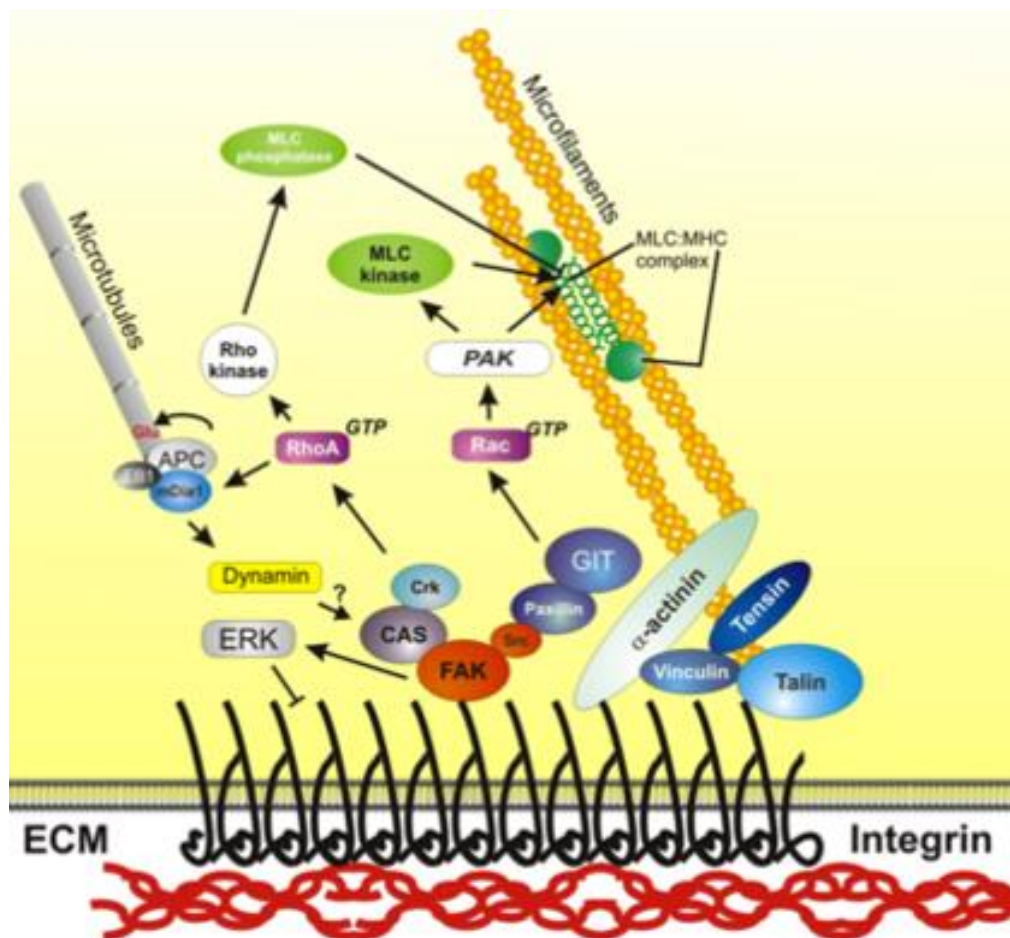


Figure 1.5.2: Integrins in focal adhesions. Integrins connect the extracellular matrix to the internal cytoskeleton in adhesions complexes. Talin, vinculin and α -actinin are actin-linking proteins that connect the integrins to the actin cytoskeleton. FAK and paxillin are signalling adaptors which are recruited to the adhesion complex and upon activation they generate signals that activate Rac to promote actin polymerization. RhoA is also activated and this in turn activates its effectors to enable myosin phosphorylation which generates actomyosin and thus the required contractile force. FAK activates ERK signalling pathway that affects cytoskeleton rearrangement [201].

1.6 The Dickkopf family of proteins

The Dickkopf (Dkk) family of proteins comprises four members of secreted glycoproteins: Dickkopf 1 (Dkk1), Dickkopf 2 (Dkk2), Dickkopf 3 (Dkk3) and Dickkopf 4 (Dkk4). An additional member was later considered in this family, the Dkk3-related protein, termed Soggy (Sgy or Dkk11).

Dkk proteins comprise 255-350 amino acids and a molecular weight of 29 kDa for Dkk1, Dkk2 and Dkk4 and of 38 kDa for Dkk3, which may vary with N-glycosylation and post-translational modifications (Figure 1.6). All the members of the Dkk family contain two conserved cysteine-rich domains separated by a non-conserved linker region. The N-terminal cysteine-rich domain (DKK-N or Cys1) is unique to the Dkks, whereas the C-terminal cysteine-rich domain (Cys2) relates to a functional domain called colipase fold. Colipases are required for the hydrolysis of lipids and for that reason it is suggested that the Cys2 domain of Dkks enables them to interact with lipids in order to regulate Wnt function. The Wnt protein is normally at the cell surface region and a lipid binding may facilitate the Wnt/Dkk interaction at the plasma membrane. Sgy protein lacks the cysteine-rich domain. Dkk3 contain several potential sites for proteolytic cleavage which explains the post-translational modifications that they suffer. In vertebrates, the linker region of Dkk1, 2 and 4 spans 50-55 amino acids but for Dkk3 it is smaller, comprising only 13 amino acids [204-206].

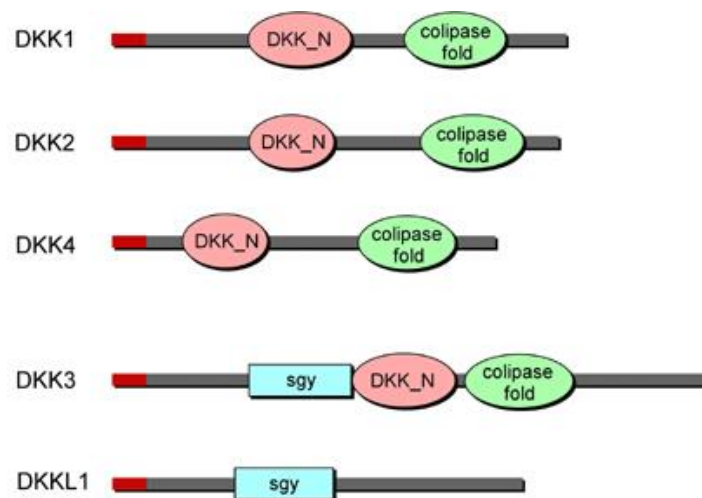


Figure 1.6: Structure of the Dickkopf family of proteins. The structures of Dkk1, 2, 3 and 4 and of the Soggy (Dkk11) protein are shown. Dkk1-4 contain an N-terminal cysteine domain (Dkk_N) and a C-terminal cysteine domain (colipase fold). The soggy domain is only found in Dkk3 and Dkk11. [204].

Notably, Dkk3 is the most divergent member of the family. DNA sequence similarity analysis reveals that Dkk1, 2 and 4 are more related to each other than they are to Dkk3. Additionally, the linker region between the 2 cysteine domains is smaller for Dkk3. The regions before and after the cysteine domains is more extended in Dkk3 than in the other members. The N-terminal region of Dkk3 contains 4 potential glycosylation sites which are not conserved in Dkk1, 2 and 4. The Soggy member shares a sequence similarity with Dkk3 which is not observed for the other Dkks. Human Dkk1, 2 and

4 are located in chromosomes belonging to a paralogous group, which means that they derived from a common ancestral gene due to the structural similarity shared. In contrast, Dkk3 is located is a chromosome which does not belong to the same paralogous group, indicating that this protein arose from a different ancestral gene. Finally, in general, Dkk1, 2 and 4 are known to have an inhibitory role in the regulation of the Wnt signalling, whereas the role of Dkk3 is context specific and it can either induce or inhibit the Wnt signalling [206-208].

One of the main functions of Dkks during embryonic development and this may be related to their interaction with the Wnt signalling pathway. Therefore, Dkks participate in the control of cell fate in embryogenesis. The role of Dkk1 has been particularly explored in embryonic development, where it is known to be a potent head inducer and a regulator of limb formation. Bone formation is regulated by Dkk1 and 2, and so is the development of the eyes and the skin. Knockout of Dkk1 in mice results in embryonic lethality [209].

As the Dkks are modulators of the Wnt signalling, they also play a vital role in cancer. The abnormal expression of specific Dkks is associated with determined cancers. For example, increased expression of Dkk1 is found in myeloma and hepatoblastomas. Enhanced expression of Dkk3 is observed in osteosarcoma, whereas its decreased expression is detected in acute lymphoblastic leukaemia and in prostate cancer. Dkk4 expression is induced in gastric cancer [206-208].

1.6.1 Receptors of Dickkopf proteins

The receptors for Dkk1, 2 and 4 are well identified in the literature. On the other hand, no receptor has been established yet for Dkk3 and the literature presents a great controversy on its identification (Table 1.6.1). Four receptors were proposed for the Dkk proteins. They include Kremen1, Kremen2, Low-density lipoprotein receptor-related protein 5 (LRP5) and low-density lipoprotein receptor-related protein 6 (LRP6).

Table 1.6.1: Receptors proposed for the Dkk proteins

Publication	Dkk1	Dkk2	Dkk3	Dkk4
Mao et al., 2000	Positive for LRP6	Positive for LRP6	Negative for LRP6	NA
Semenov et al., 2001	Positive for LRP6	NA	NA	NA
Bafico et al., 2001	Positive for LRP5 and LRP6	NA	NA	NA
Li et al., 2002	NA	Positive for LRP6	NA	NA
Mao et al., 2002	Positive for Kremen1 and 2	Positive for Kremen1 and 2	Negative for Kremen1 and 2	NA

Publication	Dkk1	Dkk2	Dkk3	Dkk4
Brott et al., 2002	NA	Positive for LRP6	NA	NA
Mao et al., 2003	Positive for Kremen 2	Positive for Kremen 2	Negative for Kremen2	Positive for Kremen 2
Zhang et al., 2004	Potential for LRP5	NA	NA	NA
Wang et al., 2008	Potential for LRP5 and LRP6 Negative for Kremen1 and 2	NA	NA	NA
Chen et al., 2008	NA	Positive for LRP5 and LRP6	NA	NA
Nakamura et al., 2009	Positive for LRP6 Positive for Kremen1 and 2	NA	Negative for LRP6 Potential for Kremen1 and 2	NA
Ahn Ve et al., 2011	Positive for LRP6	NA	NA	NA
Cheng et al., 2011	Positive for LRP6	NA	NA	NA
Bao et al., 2012	Positive for LRP5 and LRP6	NA	NA	NA
Karamariti et al., 2013	NA	NA	Potential for Kremen1	NA
Fujii et al., 2014	NA	NA	Negative for LRP5 and LRP6	NA
Poorebrahim et al., 2016	NA	NA	Potential for LRP5 and LRP6	NA

NA: Not applicable. Green: Positive interaction observed; Orange: Potential for binding, no functional assay shown; Red: Impossibility of interaction confirmed.

LRPs function as Wnt co-receptors. Upon binding of Wnt to LRPs and to Frizzled receptor, LRP is phosphorylated which allows the binding of axin (Wnt signalling pathway). The binding of Dkk to LRP interferes with the receptor's ability to interact with the Wnt-Frizzled system, which blocks the signal transduction (Figure 1.6.1). It is suggested that Dkk binds to LRP through its colipase fold domain.

The colipase fold of Dkk is also proposed to be involved in the binding of Dkk to Kremen receptors. Kremens have a crucial role in potentiating the blocking of the Wnt signalling by Dkks. Kremens form a ternary complex with Dkks and LRPs. Endocytosis of the complex is induced with the removal of LRP from the cell surface. As a result, the canonical Wnt/ β -catenin pathway is blocked and only the non-canonical Wnt pathway - Planar Cell Polarity (PCP) signalling is available for induction [204].

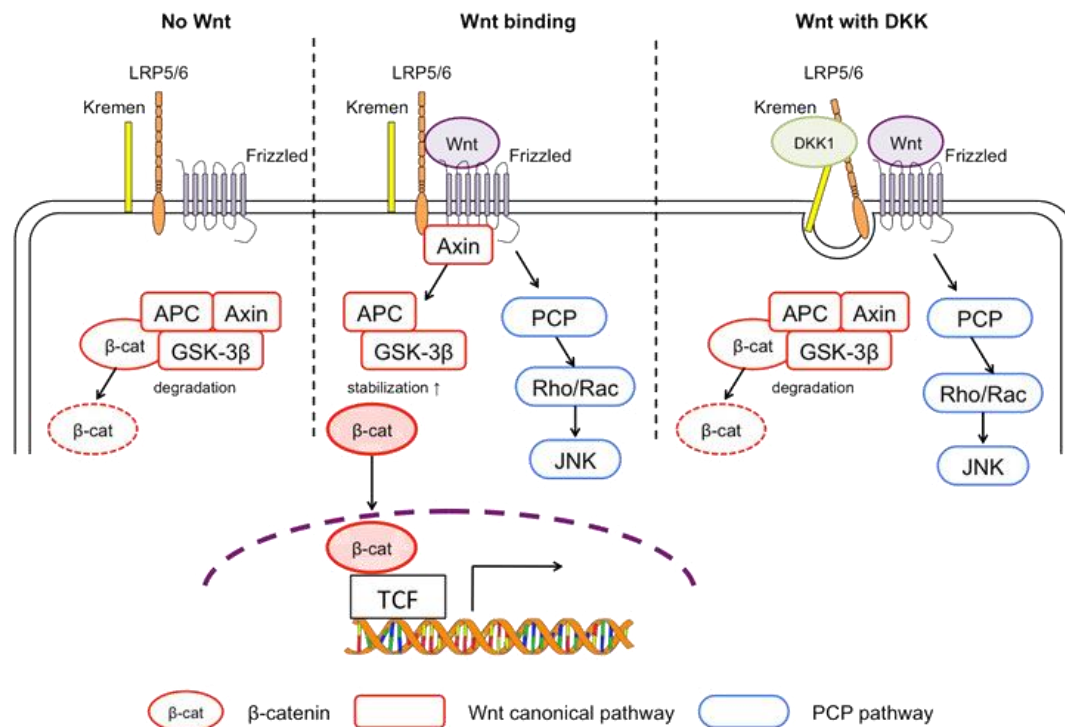


Figure 1.6.1: Wnt signalling modulation by Dkk proteins. The Wnt signalling pathway is divided in two: the canonical Wnt signalling pathway (dependent on β -catenin) and the non-canonical Wnt signalling pathways (independent of β -catenin and which includes the Planar Cell Polarity (PCP) pathway). In the absence of Wnt, cytoplasmic β -catenin is degraded through ubiquitination. Upon binding of Wnt to the receptor complex Frizzled and LRP5/6 the cytoplasmic β -catenin is stabilized and the signalling transduction proceeds. In the presence of Dkk, the LRP5/6 is sequestered in another ternary complex that comprises Dkk, Kremen and LRP and this complex undergoes endocytosis. Thus LRP5/6 are not available for the activation of the canonical Wnt signalling pathway. Instead, the PCP pathway can be induced. (Source: Fedon et al.; Role and function of Wnts in the regulation of myogenesis: When Wnt meets myostatin; 2012; Chapter 4) [210].

1.6.2 Wnt signalling pathway

The Wnt signalling pathway is a vastly explored pathway known to be involved in crucial functions of the cell, including migration, proliferation and differentiation. This pathway has a significant role during early development and later during tissue maintenance. The dysregulation of this pathway has implications in many diseases such as degenerative diseases and in cancer. Furthermore, the Wnt signalling can also regulate lipid and glucose metabolism.

Wnt proteins are secreted glycoproteins comprising 19 family members in humans, which are rich in cysteine residues. These molecules bind to the Frizzled receptor (Fzd), which is a seven transmembrane span protein with a degree of homology with the G protein-coupled receptors.

Upon binding of Wnt with the Frizzled receptor, the signal is transduced to the cytoplasmic phosphoprotein Dishevelled (Dvl), which is recruited and which directly interacts with Fzd. At this stage, the Wnt signalling is divided into two pathways: The canonical Wnt signalling pathway dependent on β -catenin and the non-canonical Wnt signalling pathway which is independent of β -catenin. This latter can branch into two more pathways: The Planar Cell Polarity pathway (PCP) and the Wnt/ Ca^{2+} signalling pathway. Dishevelled protein is the first component of all three branches (Figure 1.6.2) [204, 211, 212].

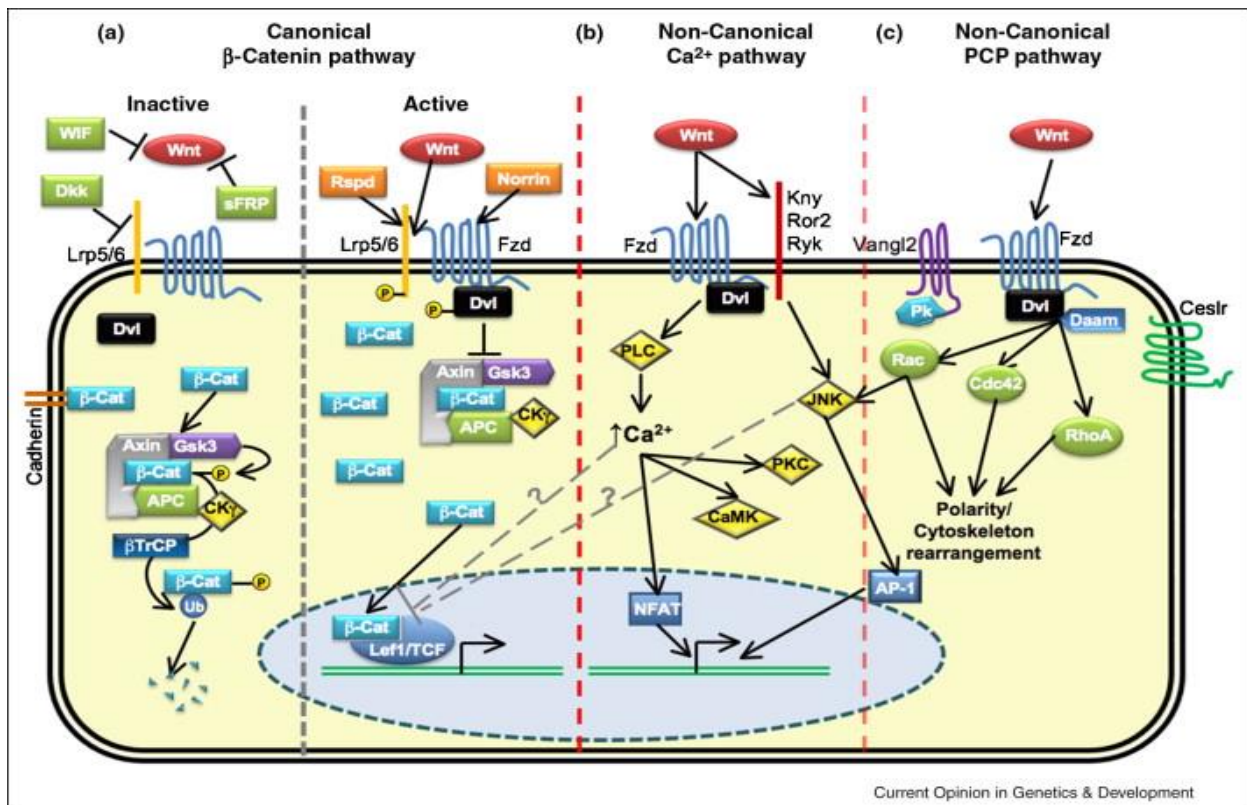


Figure 1.6.2: Wnt signalling pathways. The Wnt signalling pathway comprises the canonical Wnt/ β -catenin pathway (a) and the non-canonical Wnt signalling pathway (b and c). The latter branches into further two pathways: The PCP pathway (b) and the Wnt/ Ca^{2+} pathway (c). In the absence of Wnt stimulation, cytosolic β -catenin is targeted to proteolytic degradation through phosphorylation by the APC–Axin–GSK3–CK1 complex and further ubiquitination through action of β -TrCP-dependent E3 ubiquitin ligase complex. Upon stimulation by Wnt ligands that bind to Fzd receptors and its co-receptors LRP5/6, Dvl is recruited. Dvl inhibits APC–Axin–GSK3–CK1 complex formation by the recruitment and inhibition of GSK3 β , CK1 and Axin to the cytoplasmic membrane. Consequently, β -catenin accumulates in the cytoplasm and enters the nucleus, activating transcription of target genes through association with Lef1/TCF transcription factor family. In the non-canonical Wnt/ Ca^{2+} pathway the interaction of Wnt ligands with Fzd receptors leads to an increase in intracellular calcium level, which subsequently activates CAMKII and PKC in cells, as well as the transcription factor NFAT. In the non-canonical Wnt/PCP pathway Dvl activates Rho GTPases Cdc42, RhoA and Rac1 leading to cytoskeleton rearrangement [210].

1.6.2.1 Canonical Wnt/ β -Catenin signalling pathway

In the canonical Wnt/ β -catenin pathway, Wnt ligands bind not only to Frizzled receptor but also to LRP5 or LRP6. The ternary complex is required for the activation of the pathway. Wnt-Fzd requires the binding of LRP5 or LRP6 (Figure 1.6.2).

In the absence of Wnt, β -catenin is degraded in the cytosol. The scaffolding protein Axin interacts with β -catenin, glycogen synthase kinase 3 (GSK3), adenomatous polyposis (APC) and with casein kinase 1 (CK1) to form a complex. This causes the phosphorylation of β -catenin by GSK3 and CK1 which provides a recognition and binding site for E3-ubiquitin ligase β -Trcp. As a result, β -catenin is ubiquitinated and degraded.

Binding of Wnt to FZD/LRP receptor complex causes the stabilization of β -catenin and its consequential translocation to the nucleus, due to the disruption of the Axin/APC/GSK3 complex. The Dvl protein is crucial for this event to occur as it inhibits GSK3 and it interacts with axin. The PDZ domain of Dvl appears to be central in mediating signalling. β -catenin once translocated into to the nucleus it interacts with T-cell factor (TCF)/lymphocyte-enhancing factor (LEF) and activates transcription of target genes, such as Cyclin D1, c-Myc, vascular endothelial growth factor (VEGF) and interleukin-8 (IL-8).

Dkk proteins are regarded as Wnt antagonist, except for Dkk3 that exhibits a dual role and whose function is described later in this section. As mentioned, Dkks bind to LRP5/6 and through the Kremens they induce LRP5/6 internalization. Therefore, Dkks interfere with the Wnt/ β -catenin pathway and play a negative role in its regulation [211-213].

1.6.2.2. Non-canonical Wnt signalling pathway

In the non-canonical Wnt signalling pathway, the Wnt signal is mediated by Wnt independent of LRP5/6 co-receptors. Here, the signal is again transduced via activation of Dvl.

This β -catenin independent pathway comprises two signalling pathways (Figure 1.6.2): The PCP pathway and the Wnt/ Ca^{2+} pathway. The PCP pathway activates small GTPases, such as Rac, RhoA and Cdc42, which leads to the rearrangement of the cell actin cytoskeleton. The Wnt/ Ca^{2+} pathway involves the release of intracellular Ca^{2+} and this is mediated by G protein signalling. Next, Ca^{2+} -sensitive kinases are activated and they include protein kinase C (PKC) and calcium/calmodulin-dependent kinase II (CamKII). These activate transcription factors, amongst which the nuclear factor of activated T cells (NFAT). Dvl can also directly induce the release of Ca^{2+} and activation of PKC [211, 213, 214].

1.6.3 Dickkopf 3 protein in physiology and pathophysiology

Comparative developmental analysis in murine embryos shows that Dkk proteins are temporally and spatially regulated in a coordinated mode of action [215]. During mouse embryogenesis Dkk3 is expressed in several tissues, including bone, neural epithelium, limb buds, kidney, and heart [216-219]. In adult mice, Dkk3 expression is found in the brain, retina, heart, gastrointestinal tract, adrenal glands, thymus and reproductive system.

In the cardiovascular system, Dkk3 seems to have a cardioprotective role against the development of cardiac remodelling induced by myocardial infarction [219-221]. More recently, a work was published proposing that the Dkk3 expression in macrophages is involved in atherogenesis through modulation of inflammation derived from hyperlipidemia [222]. Dkk3 expression was also found in fibroblasts [223] and in platelets and megakaryocytes under myeloproliferative conditions [224].

Dkk3 participation in tumorigenesis has been extensively explored. In fact, Dkk3 was initially named REIC (Reduced Expression in Immortalized Cells) by Tsuji et al., who observed that Dkk3 expression was downregulated in immortalized cell lines and in a number of tumour-derived cell lines [225]. Today, it is accepted that the role of Dkk3 is context-specific and hence, it depends on the cell type and the surrounding environment. Therefore, Dkk3 can either be an agonist or inhibitor of the Wnt signalling pathway. For example, Dkk3 inhibits prostate cancer growth and lymph nodes metastasis [226, 227]. Additionally, its upregulation attenuates melanoma growth [228]. Contrastingly, there are studies that demonstrate the opposite role for Dkk3. For instance, overexpression of DKK3 promotes proliferation, survival and migration of human hepatoblastoma cells [232], and downregulation of Dkk3 decreases oral squamous carcinoma cell migration and invasion [233].

Still in the context of tumorigenesis, literature reveals that Dkk3 plays a significant role in tumour-related angiogenesis. In blood vessels of glioma, melanoma, colorectal carcinoma and non-Hodgkin lymphoma, the expression of Dkk3 is higher than in normal tissue. Overexpression of this protein increases the microvessel density in a C57/BL6 melanoma model [236, 237]. An attempt to clarify the mechanism involved in the regulation of tumour angiogenesis by Dkk3 indicates a relation between this protein and vascular endothelial growth factor (VEGF) [224, 239, 240]. Considering these findings some researchers postulate that Dkk3 may be considered a pro-angiogenic protein in neovascularization and possibly be a marker for neoangiogenesis in various cancers.

Finally, given that Dkk3 is a secreted protein with potential to induce cell differentiation, it is proposed that Dkk3 is a cytokine protein. Dkk3 can induce the differentiation of monocytes into dendritic-like cells and plays a role in systemic anticancer immunity [241, 242]. Furthermore, this protein is involved in differentiation of embryonic stem cells and pluripotent stem cells into SMCs [243, 244]. At last, the high expression of Dkk3 in tumour vascularization suggests a function for Dkk3 as an endothelial cell differentiation factor [236].

1.7 Protein-protein interaction

Interactions between proteins are intrinsic to basically every cellular process, including ligand-receptor binding, signalling transduction, DNA replication and transcription, cell cycle control, amongst others. Therefore, unveiling novel protein-protein interaction (PPI) provides crucial information that enables the elucidation of the molecular mechanisms behind so many biological processes and the identification of important targets for drug discovery.

Several biophysical and biochemical methods exist to detect PPI, which may also involve the screening of libraries (high throughput techniques). These encompass Surface plasmon resonance (SPR), Isothermal titration calorimetry (ITC), Fluorescence resonance energy transfer (FRET), Mass spectrometry (MS), Co-immunoprecipitation (Co-IP), and Yeast two hybrid system (Y2H), amongst other techniques. More recently, the development of computational tools has been used to predict PPIs by employing the knowledge about the domains present in the interacting molecules [246]. In this section, the Yeast Two Hybrid (Y2H) system will be described.

1.7.1 Yeast Two Hybrid System

The Y2H system is a genetic methodology that uses transcriptional activity to assess PPI. It relies on the modular nature of some transcription factors, which are composed of the DNA-binding domain (DNA-BD) and the Activating domain (AD). Both domains are needed to reconstitute the transcription factor (Figure 1.7.1A).

A major advantage of this technique is that it is an *in vivo* methodology that uses the yeast cell as a living test-tube. Another advantage is that it can be used to screen libraries to identify the proteins that interact with the protein of interest. Hence, the protein of interest X (bait protein) is fused to the transcription factor's binding domain and fragments of a whole genomic DNA (prey proteins) are fused to the transcription factor's activation domain. Upon interaction of protein X with protein Y from the library, both transcription factor (TF) domains are brought into close proximity. As a result, the TF is reconstituted and functional and hence, reporter genes are transcribed.

In the current project the Matchmaker® Gold Y2H system was used, which is a GAL4 transcription factor based assay. GAL4 TF is constituted by the two domains DNA-BD and AD (Figure 1.7.1A).

A Yeast Two Hybrid system GAL4 transcription factor based

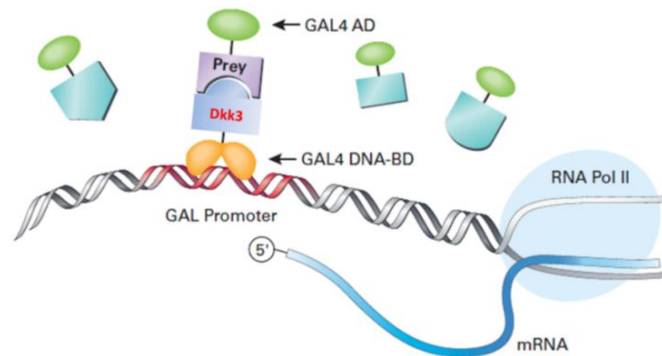


Figure 1.7.1A: Yeast Two Hybrid system GAL4 transcription factor based. GAL4 DNA-BD and GAL4 AD domains are respectively fused to bait and prey proteins. When bait and prey proteins interact with each other, the two GAL4 fragments are brought to close proximity and the transcription factor becomes functional. As a result, reporter genes are transcribed. (Figure adapted from Matchmaker® Gold Yeast Two-Hybrid System User Manual from Clontech).

The yeast *Saccharomyces cerevisiae* represents a good eukaryotic model organism in molecular biology and it reproduces easily. Physiologically, yeast can exist stably in either haploid or diploid states. Upon mating, a diploid cell is formed due to the fusion of the haploid mating cells (Figure 1.7.1B). The diploid yeast cell is stable mitotically. However, under stressful conditions a diploid cell can undergo meiosis. Both haploid and diploid cells divide by mitosis.

In the Matchmaker® Gold Yeast Two-Hybrid System the two haploid mating yeast strain partners used are Y2HGold (mating type a) and Y187 (mating type α). Dkk3 was selected as the bait protein and the Universal mouse cDNA library was considered the prey protein. The bait protein fused to the GAL4 DNA-BD was expressed in the Y2HGold strain and the prey protein fused to GAL4 AD was expressed in the Y187 yeast strain. Both haploid yeast strain partners mate and a diploid yeast cell is formed. In the diploid cell, if the bait and the prey proteins interact, the GAL4 transcription factor is reconstituted and the reporter gene transcription is activated (Figure 1.7.1B) [247-249].

B Yeast mating strategy

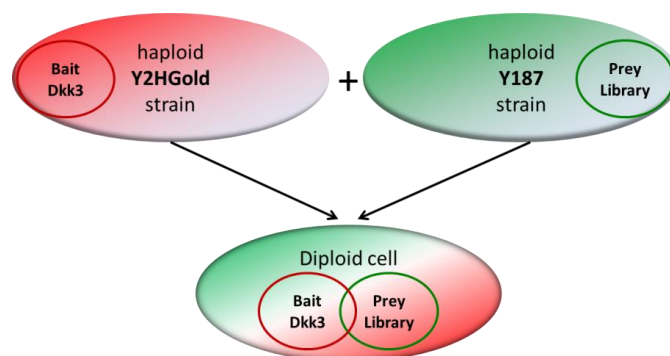


Figure 1.7.1B: Yeast mating strategy. Dkk3 (Bait protein) fused to GAL4-DNA-BD was expressed in the Y2HGold haploid yeast strain. The Universal mouse library (Prey proteins) fused to GAL4 AD domain was expressed in the haploid yeast strain Y187. Both haploid mating partners generate a diploid cell in which if the bait and prey proteins interact, the reporter gene transcription is activated.

All genes in yeast are preceded by an upstream activating region and TATA box regions. Upstream activating sequences (UAS) are regulatory transcription elements relatively close to the TATA box and they constitute the promoter of a yeast gene. Specific transcription activators recognize UAS sequences. GAL4 is a regulatory protein that controls the gene required for galactose metabolism. In the presence of galactose, GAL4 binds to GAL-responsive elements within UAS of galactose genes.

Reporter genes can be integrated into the yeast genome and they are attached to a regulatory sequence of the gene of interest. They are specifically selected to confer certain characteristics to the yeast which normally enable the yeast cells to grow on a selective medium or to change the colour of their colonies. In this case, the reporter genes are under the control of GAL4-responsive promoters. These promoters contain short protein binding sites in the UAS region that are specifically bound by the Gal4 DNA-BD [250-252].

The reporter genes under the control of GAL4-responsive promoters in Y187 strain are lacZ and MEL1. The reporter gene constructs in Y2HGold strain are HIS3, ADE2, AUR1-C and MEL1.

- The **reporter gene HIS3** corresponds to the expression of histidine. Y2HGold is not able to synthesize this amino acid and therefore does not grow on media lacking histidine. His3-responsive to Gal4 is only expressed upon bait and prey proteins' interaction, thus allowing the cell to grow on media lacking histidine.
- **ADE2 reporter gene** leads to the expression of adenine. Y2HGold cannot grow on media that does not contain adenine and, as described for the previous reporter gene, the cells will grow in this media if the protein interaction takes place, thus allowing adenine expression.
- The **reporter gene AUR1-C** encodes the enzyme inositol phosphoryl ceramide synthase. Upon gene transcription activation, the expression of this enzyme confers Y2HGold yeast strain strong resistance to Aureobasidin A, a highly toxic drug which in other conditions would not permit cell growth.
- **MEL1 reporter gene** is transcribed because of bait-prey interaction, which reconstitutes functional GAL4. This results in the expression of α -galactosidase that acts on its substrate X- α -Gal, which turns the yeast colonies blue.

All the four reporter genes in the Y2HGold yeast strain are required to detect the protein interactions in this Yeast Two Hybrid system. The GAL4 DNA-BD expressed in the Y2HGold strain binds to a specific region of the promoters controlling the reporter genes (Upstream Activating Sequence – UAS region). Therefore, the library proteins (prey proteins fused to GAL 4 AD) that would

bind to these regions of the promoter, are screened out, as these UAS regions are already occupied, thus avoiding false positives.

C Reporter gene constructs in Y2HGold and Y187 yeast strains

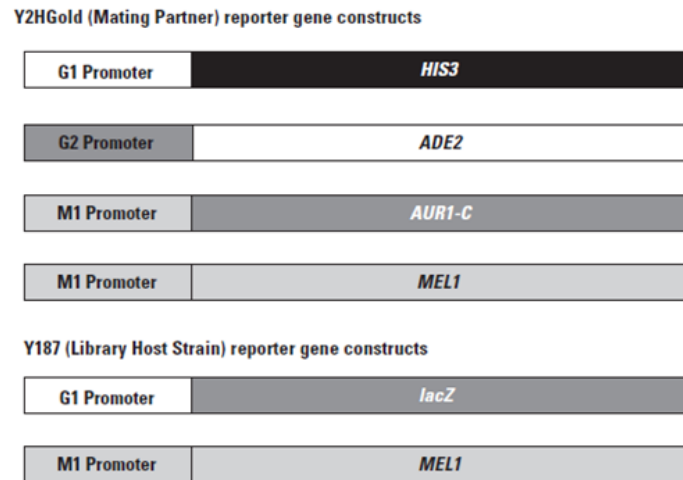


Figure 1.7.1C: Reporter gene constructs in Y2HGold and Y187 yeast strains. Y2HGold strain contains the reporter genes *HIS3*, *ADE2*, *AUR1-C* and *MEL1*, under the control of three different promoters which are responsive to the GAL4: G1, G2 and M1. Y187 yeast strain contains the constructs *lacZ* (under the control of G1 promoter) and *MEL1* (under the control of M1 promoter). The 4 reporter genes in Y2HGold are required to detect protein-protein interaction in the Yeast Two Hybrid system. (Source: Matchmaker® Gold Yeast Two-Hybrid System User Manual from Clontech Laboratories Inc.)

The haploid cell Y2HGold is transformed with the plasmid containing the bait protein fused to GAL4 DNA-BD and encoding for the Tryptophan gene. The haploid mating partner Y187 is transformed with the plasmid containing the fragments of mouse genome and encoding for Leucine gene. Therefore, each haploid strain can grow in a medium lacking the respective nutrient. The diploid cells resultants from the mating process are able to grow on medium lacking both amino acids.

However, when an interaction is observed between the bait protein and a prey-library protein, which results in the activation of GAL4 and consequent transcription of the reporter genes, colonies containing this interaction grow on agar medium lacking the nutrients generated by the transcription of the respective reporter gene. Additionally, colonies only grow in the presence of an antibiotic if the reporter gene transcribed due to a protein-protein interaction confers resistance to it. Likewise, colonies only change colour if they can produce an enzyme that acts upon its substrate, which depends on a bait-prey interaction capable of reconstituting GAL4. On the other hand, no colony grows on the agar medium if the reporter genes are not transcribed due to the absence of bait-prey interaction [253, 254].

Finally, continuous nutrient (histidine) selection through re-scraping the positive colonies eliminates irrelevant library plasmids that may have been co-transformed with the plasmid of interest that initiated reporter gene activity.

False positive interactions may occur. Therefore, the positive interaction found needs to be validated by other methods, such as Co-Immunoprecipitation. Moreover, the plasmids corresponding to the prey proteins from the positive colonies can be rescued, and then transformed in a haploid cell which is submitted to mating with the haploid cell containing the empty plasmid lacking the bait protein. The expected result is absence of growth on the most stringent agar medium lacking all the nutrients and characteristics that only the transcription of the four reporter genes would provide.

1.8 Ligand-Receptor binding

Ligand-receptor binding studies are of great importance in pharmacology for drug-targeted research. They aim at obtaining reliable estimates of the affinity of the proposed ligand for the receptor of interest and at analysing the underlying mechanism of interaction.

Saturation binding experiments involve measuring the binding of an increasing series of concentrations of a ligand to its receptor at equilibrium and the determination of the affinity constant (K_A) or the dissociation constant (K_D). The basic binding reaction relies on the principle that the interaction of the ligand with the receptor is reversible. Equilibrium is reached between the rate of ligand-receptor association and the rate of ligand-receptor dissociation.

$$K_{\text{association}} = K_A = \frac{[RL]}{[R] \times [L]} \qquad K_{\text{dissociation}} = K_D = \frac{[R] \times [L]}{[RL]}$$

[RL]: Concentration of the complex receptor-ligand; **[R]:** Concentration of receptor; **[L]:** Concentration of ligand

The association constant, that is, the strength of binding, is inversely proportional to the dissociation constant. The tighter the ligand binds to the receptor, the lower the value of the dissociation constant and higher the affinity constant.

$$K_A = \frac{1}{K_D}$$

K_A : Association constant (units: nM^{-1} ; mM^{-1} ; M^{-1}); K_D : Dissociation constant (units: nM; mM; M)

To determine empirically the K_D of a system, normally the concentration of the receptor is kept constant, whereas the ligand is added at increasing concentrations. A typically hyperbolic binding curve is obtained by plotting the fraction of ligand bound to the receptor against the concentration

of free ligand (Figure 1.8.1A). To measure the fraction of ligand bound, different methods can be used that involve for instance the measurement of changes in absorbance or luminescence due to binding of ligand to the receptor. Thus, the binding curve representing a saturable system is obtained by plotting the change in absorbance/luminescence against the concentration of free ligand [255-257].

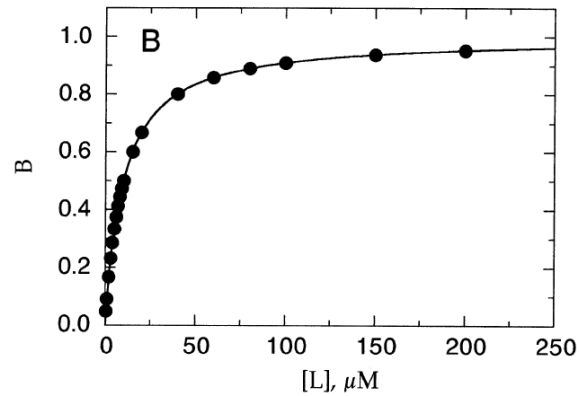


Figure 1.8.1A: Ligand-receptor binding curve. Ligand is added at increasing concentration to a receptor with fixed concentration. Fraction of ligand bound to the receptor (B) is plotted against the concentration of free ligand [L]. Binding curve with hyperbolic shape is obtained [258].

1.9 Hypothesis and Aims of Study

Rationale: A population of progenitor cells was identified within the adventitia of the vessel wall. These cells expressed stem cell markers such as Sca-1+, C-Kit+, CD34+ and Flk1+. The adventitial Sca-1+ cells were shown to differentiate into SMCs and to contribute to neointima lesion [6]. The precise mechanism of migration of the resident vascular progenitor cells is still not understood and the functional roles of these cells require further elucidation. Recently Dickkopf 3 protein (Dkk3) was found to be involved in the differentiation process of stem cells into Smooth muscle cells (SMCs). Additionally, this protein is highly expressed and secreted by SMCs [243, 244]. Studies have also demonstrated a cytokine-like role for Dkk3, where its exogenous administration induces the differentiation of monocytes into dendritic cells [241, 242]. Given these findings, we hypothesized that Dkk3 could potentially play a role as a chemokine-like protein towards the adventitia-derived Sca-1+ vascular progenitor cells (Sca-1+-APCs).

Hypothesis: Dkk3 can induce the migration of murine resident Sca-1+ APCs, *in vitro* and *ex vivo*, in the same manner as the chemokine Sdf-1 α . A potential chemokine receptor is potentially upstream of the migration mechanism of Sca-1+ APCs in response to Dkk3. Dkk3-driven migration could involve the activation of downstream signalling pathways similarly to Sdf-1 α . Functional assays with knockdown or overexpression of the candidate receptor, together with protein-protein interaction assays will provide further support on the identification of Dkk3's receptor and its involvement in the Sca-1+ APCs migration mechanism. Finally, library screening for proteins interacting with Dkk3 could provide further insight into the identification of its receptor. The demonstration of the chemotaxis of Sca-1+ APCs elicited by Dkk3, with the identification of the receptor of this glycoprotein and clarification of the signalling pathways involved in the Dkk3-driven migration mechanism of Sca-1+ APCs will contribute to the development of novel drug-targetted therapy in vascular remodelling.

Aims:

Aim 1: To study the adventitia-derived Sca-1+ vascular progenitor cell migration behaviour in response to Dkk3.

Objective 1.1: To isolate and grow ApoE^{-/-} aortic murine adventitia-derived Sca-1+ vascular progenitor cells (Sca-1+ APCs) and study their migration behaviour, *in vitro* (Transwell and wound healing assays) and *ex vivo* (Aortic ring assay), in response to Dkk3 treatment.

Aim 2: To identify the receptor of Dkk3 involved in the Sca-1+ APCs migration mechanism

Objective 2.1: To investigate the expression of chemokine receptors in Sca-1+ APCs by performing RT-qPCR and Western blot analysis.

Objective 2.2: To perform migration functional assays of Sca-1+ APCs upon receptor knockdown with SiRNA transfection and in response to Dkk3

Objective 2.3: To investigate if receptor overexpression affects the migration of HEK293T cells in response to Dkk3

Objective 2.4: To assess whether Dkk3 co-immunoprecipitates with the receptor candidate of Sca-1+ APCs, showing a physical binding

Objective 2.5: To determine the binding affinity of Dkk3 to the receptor by performing saturation binding assay and calculating the respective dissociation constant

Objective 2.6: To investigate whether the knockdown of the receptor by SiRNA transfection affects the signalling pathways involved in Sca-1+ APC migration in response to Dkk3

Aim 3: To investigate the underlying signalling pathways of the migration mechanism of Sca-1+ APCs driven by Dkk3 treatment.

Objective 3.1: To discover the signalling pathways involved in Dkk3-triggered migration of Sca-1+ APCs through western blot analysis and inhibition of the identified signalling effectors with consequent analysis of the respective functional migration assays.

Chapter 2: Materials and Methods

2.1 Materials

2.1.1 List of cell culture reagents

Table 2.1.1 List of cell culture reagents

Product	Supplier	Catalogue No.
Dulbecco's Modified Eagle's Medium (DMEM) (ATCC Medium)	ATCC	30-2002
DMEM, high glucose, GlutaMAX™ Supplement, pyruvate	ThermoFisher	31966-047
Phosphate-buffered saline (PBS)	ThermoFisher	10010015
Opti-MEM®	ThermoFisher	31985070
EmbryoMax® ES Cell Qualified Fetal Bovine Serum	Millipore	ES-009-B
Fetal Bovine Serum, qualified, E.U.-approved, South America origin	ThermoFisher	10270106
Leukemia Inhibitory Factor Protein, Recombinant human	Millipore	LIF1010
2-Mercaptoethanol (50mM)	ThermoFisher	31350010
Trypsin-EDTA (0.05%), phenol red	ThermoFisher	25300054
Gelatin solution, Type B, 2% in H2O	Sigma-Aldrich	G1393-100ML
Penicillin-Streptomycin (10,000 U/mL)	ThermoFisher	15140122
L-Glutamine (200 mM)	ThermoFisher	25030081
Dimethyl sulfoxide, reagent grade, ≥99.5%	Sigma-Aldrich	D5879
Anti-Sca-1 MicroBead Kit (FITC), mouse	Miltenyi Biotec	130-092-529

2.1.2 List of chemicals and buffers

Table 2.1.2 List of chemicals and buffers

Product	Supplier	Catalogue No.
Ampicillin	Sigma-Aldrich	A0166-25G
Kanamycin	Sigma-Aldrich	K0254-20ML
LB Broth, Miller	ThermoFisher	BP1426-2
Agar	Sigma-Aldrich	A1296-500G
S.O.C. Medium	ThermoFisher	15544034
qPCRBIO SyGreen Mix Hi-ROX	PCR Biosystems	PB20.12-01
Pfu DNA Polymerase	Promega	M7741
dNTP	ThermoFisher	10297-018
1 Kb Plus DNA Ladder	ThermoFisher	10787018
UltraPure Agarose	ThermoFisher	16500500
UltraPure 50x TAE buffer, 1L	ThermoFisher	12361499
SafeView Nucleic Acid Stain	NBS Biologicals	NBS-SV1
Precision Plus Protein Dual Colour ladder	Bio-Rad	1610374
NuPAGE® MOPS SDS Running Buffer	Life Technologies	NP0001
NuPAGE Transfer buffer	Life Technologies	NP0006-1
Bio-Rad Protein Assay Dye Reag. Concent.	Bio-Rad	5000006
Western blotting detection reagents, Amersham ECL	VWR	RPN2106
RIPA Lysis and Extraction Buffer	ThermoFisher	89900
cComplete™ ULTRA Tablets, Mini, EASYpack Protease Inhibitor Cocktail	Sigma-Aldrich/Roche	000000005892970001
TBS Buffer	ThermoFisher	28358
Tween 20	Sigma-Aldrich	P2287-500ML
NuPAGE® LDS Sample Buffer (4X)	ThermoFisher	1621180
NuPAGE™ Sample Reducing Agent	ThermoFisher	17772696
Nitrocellulose Blotting Membrane	GE Healthcare Life Science	10600002
Fugene HD transfection reagent	Promega	E2311

Product	Supplier	Catalogue No.
Lipofectamine RNAimax transfection reagent.	ThermoFisher	13778075
4% Paraformaldehyde solution	Santa Cruz Biotechnology	sc-281692
25% Glutaraldehyde solution	Sigma-Aldrich	G5882
Triton X	Sigma-Aldrich	X100
Matrigel Basement Membrane Matrix	Corning	354234
Crystal violet solution	Sigma-Aldrich	HT90132-1L
Trypan blue	Sigma-Aldrich	T8154
NaHCO ₃ buffer	Sigma-Aldrich	88975-10ML
MgCl ₂	Sigma-Aldrich	M8266
Swine serum	Dako, Agilent Path. Solutions	X090110-8
Bovine Serum Albumin	Santa Cruz Biotechnology	Sc-2323
DAPI	ThermoFisher	D1306
DEPC Treated Water Pyrogen-free	ThermoFisher	46-2224
Glycerol	Sigma-Aldrich	G5516-500ML
UltraPure EDTA 0.5M	ThermoFisher	15575-038

2.1.3 List of Proteins and Inhibitors

Table 2.1.3 List of Proteins and Inhibitors

Product	Supplier	Catalogue No.
DKK3 Recombinant Mouse Protein, His Tag	ThermoFisher	50247-M08H-50
Recombinant Murine SDF-1 α (CXCL12)	PeptoTech	250-20A
Recombinant Human Dkk-3 Protein, CF	R&D Systems	1118-DK-050
Recombinant Human CXCL12/SDF-1a, CF	R&D Systems	350-NS-010/CF
Recombinant Murine PDGF-BB	PeptoTech	315-18
AMD3100	Sigma-Aldrich	A5602-5MG
PD 98059	Calbiochem/Millipore	513000-5MG
LY 294002	Calbiochem/Millipore	19-142
AKT Inhibitor X	Calbiochem/Millipore	124020
NSC23766	Sigma-Aldrich	SML0952-5MG
Y-27632	Calbiochem/Millipore	688000
Rho Inhibitor, Rhosin	Calbiochem/Millipore	555460
β -Catenin/Tcf Inhibitor, FH535	Calbiochem/Millipore	219330
Dvl-PDZ Domain Inhibitor, Peptide Pen-N3	Calbiochem/Millipore	322337

2.1.4 List of kits

Table 2.1.4 List of kits

Product	Supplier	Catalogue No.
QuantiTect Reverse Transcription Kit (400)	Qiagen	205314
QIAshredder (250)	Qiagen	79656
RNeasy Mini Kit (250)	Qiagen	74106
QIAprep Spin Miniprep Kit (250)	Qiagen	27106
QIAquick Gel Extraction Kit (250)	Qiagen	28706
QIAquick PCR Purification Kit (250)	Qiagen	28104
RhoA G-LISA Activation Assay Kit, Colorimetric	Cytoskeleton, Inc.	BK124
Rac1 G-LISA Activation Assay Kit Colorimetric	Cytoskeleton, Inc.	BK128
Cell Proliferation ELISA, BrdU - Colorimetric	Sigma-Aldrich, Roche	000000011647229001
Pierce™ Co-Immunoprecipitation Kit	ThermoFisher	26149
Lightning-Link Alkaline Phosphatase, Labelling Kit	Innova Biosciences	702-0030
NFkB SEAP Reporter Assay Kit	Novus Biologicals	NBP2-25286
SEAP Reporter Gene Assay, chemiluminescent	Sigma-Aldrich/Roche	000000011779842001
Matchmaker Gold Yeast Two-Hybrid System	Takara/Clontech	630489

2.1.5 List of Antibodies

Table 2.1.5 List of Antibodies

Product	Supplier	Catalogue No.
Rabbit anti p-ERK 1/2 (Thr202/Tyr204)	Santa Cruz Biotechnology	sc-16982
Mouse anti ERK 1/2	Santa Cruz Biotechnology	sc-135900
Rabbit anti p-AKT 1/2/3 (Ser473)	Santa Cruz Biotechnology	sc-7985-R
Rabbit anti AKT 1/2/3	Santa Cruz Biotechnology	Sc-8312
Rabbit anti p-MLC 2 (Thr18/Ser19)	Cell Signalling Technology	3674
Rabbit anti MLC 2	Cell Signalling Technology	3672
Rabbit anti p-Cofilin	Cell Signalling Technology	3313
Rabbit anti Cofilin	Cell Signalling Technology	5175
Rabbit anti CXCR2	Abcam	ab14935
Goat anti CXCR4	Santa Cruz Biotechnology	sc-6190
Rabbit anti CXCR7	ThermoFisher	PA3-069
Rabbit anti CXCR7	Novus Biologicals	NBP1-31309
Rabbit IgG Isotype Control	Novus Biologicals	NB810-56910
Goat anti Kremen 1	R&D Systems	AF1647
Rabbit anti Kremen 2	Abcam	ab156007
Goat anti LRP5	Santa Cruz Biotechnology	sc-21390
Mouse anti LRP6	Santa Cruz Biotechnology	sc-25317
Rabbit Integrin α 5	Cell Signalling Technology	4705
Rabbit Integrin β 1	Cell Signalling Technology	4706
Rat anti Integrin β 1	Novus Biologicals	NBP1-43423
Rat IgG2a Kappa	Novus Biologicals	NB410-18450
PE anti-mouse Ly-6A/E (Sca-1)	Biolegend	108107
PE Rat IgG2a, k Isotype Ctrl	Biolegend	400507
Anti HA tag	Abcam	Ab9110
Rabbit anti GAPDH	Santa Cruz Biotechnology	sc-25778

Product	Supplier	Catalogue No.
Goat anti Dkk3	GenScript	Customised
Goat anti Dkk3	Santa Cruz Biotechnology	sc-14959
Mouse anti Actin, α -Smooth Muscle - Cy3	Sigma-Aldrich	C6198
Swine anti Rabbit, HRP	Dako, Agilent Pathology Sol.	P039901-2
Rabbit anti Mouse, HRP	Dako, Agilent Pathology Sol.	P016102-2
Rabbit anti Goat, HRP	Dako, Agilent Pathology Sol.	P044901-2
IRDye 800CW Donkey anti-Rabbit IgG	LI-COR	P/N 926-32213
IRDye 800CW Donkey anti-Mouse IgG	LI-COR	P/N 926-32212
IRDye 800CW Donkey anti-Goat IgG	LI-COR	P/N 926-32214
IRDye 680RD Donkey anti-Rabbit IgG	LI-COR	P/N 926-68073

2.1.6 List of Primers for RT-qPCR

Table 2.1.6 List of Primers

Gene of interest	Forward primer sequence	Reverse primer sequence
GAPDH Murine	5' - CGACTTCAACAGCAACTCCCACTCTTCC - 3'	5' - TGGGTGGTCCAGGGTTTCTTACTCCTT - 3'
Sca-1 Murine	5' - CCCTGATGGAGTCTGTGTTACT - 3'	5' - ATTAGGAGGGCAGATGGGTAAG - 3'
CXCR1 Murine	5' - GCTGGTGATGCTGGTTATCT - 3'	5' - CAAGAAGGGCAGGGTCAAT - 3'
CXCR2 Murine	5' - GCCCTGCCCATCTTAATTCT - 3'	5' - ACCCTCAAACGGGATGTATTG - 3'
CXCR3 Murine	5' - CCTCACCTGCATAGTTGTATGG - 3'	5' - GCTGATCGTAGTTGGCTGATAG - 3'
CXCR5 Murine	5' - GAGGCTGAAGGCTGTGAATAG - 3'	5' - AAGGTGTAGAGCATGGGATTG - 3'
CXCR6 Murine	5' - GGACTCTGACAGATGTGTTTCT - 3'	5' - CACTCATAGGTGCCTGCATAG - 3'
CXCR7 Murine	5' - AACCTCTTTGGGAGCATCTTCTT - 3'	5' - GGTGCCGGTGAAGTAGGTGAT - 3'

Gene of interest	Forward primer sequence	Reverse primer sequence
CX3CR1 Murine	5' - CCCAGTTGTGACATGAAGAGG - 3'	5' - CCGGCAAAGGCGTAGATAAA - 3'
CCR1 Murine	5' - GCTATGCAGGGATCATCAGAAT - 3'	5' - GGTCCAGAGGAGGAAGAATAGA - 3'
CCR2 Murine	5' - TCCACTCTACTCCCTGGTATTC - 3'	5' - TGGCCAAGTTGAGCAGATAG - 3'
CCR3 Murine	5' - CCAGCTGTCAGCAGAGTAAA - 3'	5' - CTCACCAACAAAGGCGTAGA - 3'
CCR4 Murine	5' - CACGCGGTATTCTCCTTGAA - 3'	5' - TGTGGTTGTGCTCTGTGTAG - 3'
CCR5 Murine	5' - TCCGGAGTTATCTCTCAGTGT - 3'	5' - TCTCCTGTGGATCGGGTATAG - 3'
CCR6 Murine	5' - CCCTTGCTGTTTATGGTGTC - 3'	5' - GGATTGCTCTGTGCCTCTT - 3'
CCR7 Murine	5' - GGCTATGAGTTTCTGCTACCTC - 3'	5' - CTACCACCACGGCAATGAT - 3'
CCR8 Murine	5' - TTGGGACTGCGATGTGTAAG - 3'	5' - GCGTGGACAATAGCCAGATA - 3'
CCR9 Murine	5' - GGTCATGGCCTTCTGCTATAC - 3'	5' - GAAGACAGTGAGGACAGTGATG - 3'
CCR10 Murine	5' - GCCTCAATCCGGTGCTTTAT - 3'	5' - TAGGAGCAGAGCAGGAAGAA - 3'
Itga5 Murine	5' - TGCAGTGGTTCGGAGCAAC - 3'	5' - TTTTCTGTGCGCCAGCTATAC - 3'
Itgb1 Murine	5' - ATGCCAAATCTTGCGGAGAAT - 3'	5' - TTTGCTGCGATTGGTGACATT - 3'
Kremen1 Murine	5' - GACTTTCCAGCATCCGTACAA - 3'	5' - CTCACGTCTCCATCTGGATTTC - 3'
Kremen2 Murine	5' - GAGCATCTCCAGAGGATTCAAC - 3'	5' - AGAAGACTCGGGCACCTAT - 3'
LRP5 Murine	5' - CCCCTCTATGACCGGAATCAC - 3'	5' - CGGATATAGTGTGGCCTTTGTG - 3'
LRP6 Murine	5' - CCACCGGGACATGTAAATACACA - 3'	5' - GCACCCACCCACTTTATAATGTTAA - 3'
Pdgfr-β Murine	5' - GGAGACACTGGGAGATGTAGAA - 3'	5' - GGACAGAAGGCATCGGATAAG - 3'
Calponin Murine	5' - GGTCTGCCTACGGCTTGTC - 3'	5' - TCGCAAAGAATGATCCCGTC - 3'
CD31 Murine	5' - CACCCATCACTTACCACCTTATG - 3'	5' - TGTCTCTGGTGGGCTTATCT - 3'

Gene of interest	Forward primer sequence	Reverse primer sequence
GAPDH Human	5' - CATGTTGTCATGGGTGTGAACCA - 3'	5' - AGTGATGGCATGGACTGTGGTCAT - 3'
CXCR2 Human	5' - GCCATGGACTCCTCAAGATT - 3'	5' - AAGTGTGCCCTGAAGAAGAG - 3'
CXCR4 Human	5' - CAAGCAAGGGTGTGAGTTTG - 3'	5' - GGCTCCAAGGAAAGCATAGA - 3'
CXCR7 Human	5' - TTCTCCTACGTGGTGGTCTT - 3'	5' - GCAGGTGAAAGGGATGTAGTG - 3'
Kremen1 Human	5' - CTCTCTGGACTTCGTCATCTTG - 3'	5' - CTGTGGCAGTTCTTCCTTGA - 3'
Kremen2 Human	5' - CTTCTCTTTCTCCTCTTCCTC - 3'	5' - CATTACCTGGAAGCATTTCG - 3'
ItgA5 Human	5' - GGCTTCAACTTAGACGCGGAG - 3'	5' - TGGCTGGTATTAGCCTTGGGT - 3'
ItgB1 Human	5' - CCTACTTCTGCACGATGTGATG - 3'	5' - CCTTTGCTACGGTTGGTTACATT - 3'

2.2 Methods

2.2.1 Study Approval and Murine models

All animal procedures were performed in accordance with the protocols approved by the Institutional Committee for Use and Care of Laboratory Animal.

C57BL/6J mice were purchased from Harlan, UK. ApoE-deficient (ApoE^{-/-}) and Ly6a-GFP (Sca-1-GFP) transgenic mice were purchased from The Jackson Laboratory, USA. To generate transgenic Sca-1-GFP-ApoE^{-/-} mice, Ly6a-GFP mice were crossed with ApoE-deficient mice.

2.2.2 Cell culture of mouse Adventitial Progenitor Cells (APCs), mouse vascular Smooth Muscle Cells (SMCs) and mouse Endothelial Cells (mECs)

2.2.2.1 Adventitia-derived Sca-1+ Vascular Progenitor Cells (Sca-1+ APCs) culture

Adventitial tissue was harvested by carefully detaching it from the media and intima layers of ApoE KO mouse aorta (from the aortic arch and root to the thoracic aorta). The dissected adventitia was cut into 1x1 mm pieces which were then placed in a flask previously coated with 0.02% gelatine (2% Solution Type B from Bovine Skin, Sigma). The flask was placed inverted in a 5% humidified CO₂ atmosphere incubator at 37°C for 3 hours, after which the flask was turned back up and stem cell medium was added: Dulbecco's Modified Eagle's Medium ATCC (American Type Culture Collection, 30-2002), 10% ES cell qualified fetal bovine serum (Embriomax), 10 ng/ml of leukemia inhibitory factor (Merck Millipore, LIF1050), 0.1 mM 2-mercaptoethanol (GIBCO), 100 U/mL penicillin (GIBCO), 100 U/mL streptomycin (GIBCO), 2 mM L-glutamine (GIBCO). During the 5-7 days period of incubation, the medium was changed every 2 days.

To select the Sca-1+ APCs, the cells that outgrew from the adventitia were dispersed with 0.05% trypsin-EDTA (GIBCO) and washed with washing buffer (PBS containing 0.5% FBS and 2 mM EDTA). The cells were then incubated with anti-Sca-1 immunomagnetic beads (MACS Miltenyi Biotec) at 4°C for 10 minutes. After washing the cells and incubating them with microbeads for 15 minutes at 4°C, the cell suspension was added to the MACS column equipped with a magnetic cell separator system. Cells which did not bind to the column were discarded. The Sca-1 cells sorted were flushed out and collected in a tube and cultured in stem cell culture medium on a 0.04% gelatine coated flask.

The Sca-1+ APCs were passaged every other day at a ratio of 1:3. Cells were washed with PBS, detached by using 0.05% trypsin-EDTA, centrifuged and re-suspended with culture medium and transferred to new gelatine coated flasks. After every 5 passages the cells were sorted again for Sca-1+ marker to assure the purity of the cells.

2.2.2.2 Murine Vascular Smooth Muscle Cells (SMCs) culture

The adventitia and the connective tissue were separated from the intima and the media of C57BL/6J mice aorta (from the aortic arch to the thoracic aorta). The intima and the media were carefully dissected and cut into pieces and placed on a gelatine (0.04%) coated flask. The cells were cultured in Dulbecco's Modified Eagle's Medium (GIBCO) supplemented with 10% fetal bovine serum (GIBCO) and 100 U/mL penicillin (GIBCO), 100 U/mL streptomycin (GIBCO), 2 mM L-glutamine (GIBCO), at 37°C in an incubator with humidified atmosphere of 5% CO₂. The medium was changed every 2 days and cells were passaged every other day at a ratio of 1:2. Trypsin-EDTA was used to detach the cells for passaging. These cells were kindly provided by Dr. Baoqi Yu from our group.

2.2.2.3 Mile Sven 1 (MS1) Endothelial Cells culture

The MS1 murine endothelial cells were purchased from American Type Culture Collection (ATCC, CRL-2279™). Cells were cultured in Dulbecco's Modified Eagle's Medium (GIBCO) supplemented with 10% fetal bovine serum (GIBCO) and 100 U/mL penicillin (GIBCO), 100 U/mL streptomycin (GIBCO), 2 mM L-glutamine (GIBCO), at 37°C in a 5% CO₂ atmosphere incubator. The medium was changed every 2 days and cells were passaged at a ratio of 1:4.

2.2.3 Cell culture of Human Embryonic Kidney (HEK) 293T cells

HEK 293T cells were acquired from American Type Culture Collection (ATCC, CRL-11268). The cells were passaged every other day at a ratio of 1:4 and cultured in Dulbecco's Modified Eagle's Medium (GIBCO) supplemented with 10% fetal bovine serum (GIBCO), 100 U/mL penicillin (GIBCO), 100 U/mL streptomycin (GIBCO), 2 mM L-glutamine (GIBCO), in a humidified incubator with 5% CO₂ at 37°C.

2.2.4 Flow Cytometry

Sca-1+ APCs were washed with PBS and trypsinized. After centrifugation, cells were washed again with PBS. Next, cell pellet was resuspended and divided into three BD falcon tubes. Cells were blocked for 15 minutes with blocking buffer (5% swine serum in PBS) on ice and then centrifuged. Following resuspension with blocking buffer, Isotype control PE Rat IgG2ak was added to one tube and PE anti-mouse Ly-6A/E (Sca-1) antibody was added to another tube. The third tube was left unstained. Antibody incubation was carried out for 45 minutes on ice, after which cells were washed with PBS and centrifuged. Finally, cells were resuspended in PBS and analysed using the instrument BD Accuri™ C6. Data analysis was performed using the software FlowJo_V10.

2.2.5 Total RNA extraction

Total RNA was isolated using the RNeasy Mini Kit (Qiagen) was used. RNA extraction was performed according to the protocol provided by the manufacturer. Cells were washed with ice-cold PBS. 350 μ L of RLT lysis buffer was added to each well of a 6 well plate where the cells were previously seeded and treated. The cell lysate was scrapped and pipetted directly into a QIAshredder spin column and centrifuged for 2 minutes for homogenization. In order to promote selective binding of the RNA to the RNeasy silica-based membrane incorporated in the RNeasy Mini spin column, 1 volume of 70% ethanol was added to the homogenized lysate by pipetting up and down. The resulting mixture was applied to the spin column and centrifuged for 30s. The flow-through was discarded and the total RNA bound to the membrane was washed with RW1 and RPE buffers to get rid of contaminants. An additional centrifugation step of 1 minute took place to remove residual flow-through and ethanol that may interfere with downstream reactions. The RNA was eluted with 30 μ L of RNase-free water in a new collection tube and the concentration of the eluted RNA was measured using a Nanodrop Spectrophotometer. The RNA purity was assessed using the ratio of absorbance at 260 nm and 280 nm. Samples presenting A260/A280 ratio values around 2.0 were used for subsequent procedures.

2.2.6 Reverse transcription (RT) of RNA to obtain complementary DNA (cDNA)

In order to synthesise cDNA from the total RNA extracted, the QuantiTect[®] Reverse Transcription Kit (Qiagen) was used as specified by the manufacturer (Table 2.2.6). 1 μ g of total RNA sample was used for each RT reaction. The first step comprised elimination of genomic DNA, where the RNA sample was mixed with 2 μ L of gDNA Wipeout Buffer and the total volume was adjusted to 14 μ L with RNase-free water (Mix 1). The mixture was incubated at 42°C for 2 minutes. During the first step, a master mix was prepared which comprised 1 μ L of Reverse Transcriptase, 1 μ L of the RT Primer Mix and 4 μ L of RT Buffer (Mix 2). The master mix was added to the previously incubated reaction system and the resulting mixture was incubated for 15 minutes at 42°C and then 3 minutes at 95°C. Finally, the cDNA obtained was diluted with 80 μ L of RNase-free water to a concentration of 10 ng/ μ L.

Table 2.2.6 Reverse Transcription components

	Component	Concentration	Volume per sample (μ L)
Mix 1	Template RNA	1 μ g	Variable
	gDNA Wipeout Buffer, 7x	1x	2 μ L
	RNase-free water to volume of 14 μ L	-	Variable
Mix 2	Quantiscript Reverse Transcriptase	Not mentioned	1 μ L
	Quantiscript RT Buffer, 5x	1X	4 μ L
	RT Primer Mix	Not mentioned	1 μ L

2.2.7 Quantitative Real-time Polymerase Chain Reaction (RT-QPCR)

Relative gene expression was quantified by RT-QPCR using the machine Eppendorf Mastercycler® ep realplex. 20 ng of cDNA was added to 18 μL of a master mix made up with 0.75 μL of forward primer (10 μM) and 0.75 μL of reverse primer (10 μM), 10 μL of qPCRBIO SYGreen Mix and 6.5 μL RNase-free water. Primers' sequences are listed in table 2.1.6 and they were all reconstituted with RNase-free water to generate 100 μM stock solutions, which were then diluted to 10 μM as working solutions. cDNA samples were used in duplicates. The QPCR conditions used were as follows: polymerase activation step at 95°C for 2 minutes (1 cycle); denaturation step at 95°C for 5 seconds and combined annealing/extension steps at 60°C for 30 seconds (40 cycles). The threshold cycle (Ct) values were automatically obtained and GAPDH housekeeping gene's Ct value served as the internal endogenous control.

2.2.8 Conventional Polymerase Chain Reaction (PCR)

Polymerase chain reactions were performed using 100ng of cDNA and Pfu DNA Polymerase (Promega). The reaction mix components used are indicated in table 2.2.8.1. The primers specific to the PCR template were designed from human mRNA sequences using the Primer-BLAST tool (<https://www.ncbi.nlm.nih.gov/tools/primer-blast/>) and the plasmid vectors when applicable. Primers' sequences are listed below in table 2.2.8.3 and they were all reconstituted with RNase-free water to generate 100 μM stock solutions, followed by a dilution to 10 μM to use as working solution. The thermal cycling conditions used for Pfu DNA Polymerase-mediated PCR amplification are shown below in table 2.2.8.2.

Table 2.2.8.1 List of reaction mix components

Component	Concentration	Volume per sample (μL)
Cdna	100 ng	Variable
Pfu DNA Polymerase 10X Buffer	10X	5 μL
dNTP mix, 10mM each	200 μM each	1 μL
Forward primer	1.0 μM	1 μL
Reverse primer	1.0 μM	1 μL
Pfu DNA Polymerase	1.25 U	2 μL
Nuclease-Free Water to final volume of 50 μL	-	Variable

Table 2.2.8.2 Thermal cycling conditions for Pfu Polymerase-mediated PCR amplification

Step	Temperature	Time	Number of cycles
Initial Denaturation	95°C	2 minutes	1 cycle
Denaturation	95°C	30 seconds	35 cycles
Annealing	42°C – 65°C*	30 seconds	
Extension	72°C	2 minutes**	
Final Extension	72°C	5 minutes	1 cycle
Hold	4°C	Indefinite	1 cycle

*The annealing temperature depends on primers' sequences.

**2 minutes for every 1 Kb.

Table 2.2.8.3 Conventional PCR primer sequences and parameters

Gene of interest	Forward primer sequence Reverse primer sequence	Annealing Temp. (°C)	Product size (bp)	Source of cDNA
CXCR2 Human	5'-ATATGCTAGCATGGAAGATTTTAACATGGAGA-3' 5'-ATATGTCGACGAGAGTAGTGAAGTGTGCC-3'	56°C	1.033 kb	Human cDNA Clone (Origene; SC321915)
CXCR4 (PCR 1)* Human	5'-AAGCCTGAATTGGTTTTTA-3' 5'-TCTGAAAAATGTGTAACCTA-3'	42.3°C	1.210 kb	HUVEC cDNA (ATCC)
CXCR4 (PCR 2)* Human	5'-ATATGCTAGCATGTCCATTCTTGCCTC-3' 5'-ATATTCTAGAGCTGGAGTGAAAACCTGAAG-3'	54.5°C	1.011 kb	PCR 1 product
CXCR7 (PCR 1)* Human	5'-AGCACAGCCAGGAAGGCGAG-3' 5'-TTTGCTCTAGAAAACCATAG-3'	45.3°C	1.190 kb	HUASMC cDNA (Lonza)
CXCR7 (PCR 2)* Human	5'-ATATGCTAGCATGGATCTGCATCTCT TCGACTA-3' 5'-ATATTCTAGATTTGGTCTCTGCTCCAAGG-3'	57.8°C	1.089 kb	PCR 1 product
Kremen1 Human	5'-ATATGCTAGCATGGCGCCGACCCGCCCGCC-3' 5'-ATATGTCGACGATACTTCTGGGCTGCCCTG-3'	63.4°C	1.476 kb	Human cDNA Clone (Sino Biological Inc.; HG16100-G)
Kremen2 Human	5'-ATATGCTAGCATGGGACACAAGCCCTGCAG-3' 5'-ATATGTCGACGAGAGCGGAGATGAGCGAGCG-3'	64.3°C	1.263 kb	Human cDNA Clone (Dharmacon; MHS6278-202829187)
Dkk3 Murine	5'-CATGGAGGCCGAATTCATGCAGCGGCTCGGGGTATTTTG-3' 5'-GCAGGTCGACGGATCCAATCTCCTCCTCCGCCTAGTGA-3'	67.3°C	1.050 kb	Mouse cDNA Clone (Origene; MR205281)

* PCR 1 was performed as a Nested PCR, where the first product amplified contained an outer larger fragment besides the smaller target fragment. The primers were located outer limits of the template sequence and the number of cycles used for amplification was 40. The resulting product was used in PCR 2, where the primers were specific for the terminals of the target. 35 cycles were set for the amplification of the fragment.

2.2.9 Agarose gel electrophoresis

The gel for electrophoresis was made up with 1.5% Agarose (Sigma) and Tris-acetate EDTA buffer. 0.05% of Ethidium bromide (Sigma) was added to the gel solution and when solidified the gel was placed in the electrophoresis apparatus which was immersed in 1x Tris-Acetate EDTA buffer. The samples were mixed with GelPilot DNA Loading Dye, (Qiagen) and then loaded on the gel. The electric current used to perform the electrophoresis was 165 V for 35 minutes. After the running time the separated bands on the gel were visualized under ultraviolet light.

2.2.10 Treatment with recombinant proteins

To obtain proteins from Sca-1+ APCs, the cells were seeded in 10 cm petri dish and after reaching 50% confluency, the cells were starved overnight. The next day control and treatment media were prepared. The control medium consisted of 0.2% FBS in ATCC medium and the treatment medium consisted of 25 ng/mL of mouse recombinant Dkk3 or mouse recombinant Sdf-1 α , in 0.2% FBS in ATCC medium. After starvation, the cells are washed with PBS and the respective control or treatment media were added at different time points (0 to 60 minutes). Once the required time point was reached, the medium was removed and cells were washed with ice-cold PBS.

2.2.11 Pharmacological inhibition of signalling pathways

Pharmacological agents were used to inhibit signalling pathways (Table 2.2.11). Inhibitors were diluted in 0.2% FBS ATCC medium and the inhibition medium was added to the cells in parallel with the control medium (containing the same amount of vehicle used to reconstitute the inhibitor). For western blot analysis, cells were incubated for 1 hour with the inhibitor prior to replacement with treatment medium. For transwell and scratch migration assays, cells were incubated for 1 hour with the inhibitor prior to performing the assays. Inhibitors were also added to the lower chamber of the transwell insert or to the corresponding well in the scratch assay, during overnight cell migration.

Table 2.2.11: List of pharmacological agents used to inhibit signalling pathways

Inhibitor	Signalling pathway	Concentration (μ M)
PD98059	MEK/ERK	10; 30
AKT Inhibitor X	AKT	2.5, 5
LY294002	PI3K/AKT	10; 25
Rhosin	RhoA/p-MLC	10; 25
Y27632	ROCK/p-MLC	5; 10
NSC23766	Rac1	10; 25

2.2.12 Protein extraction

Cells in Petri dish were washed with ice-cold PBS. 100 μ L of protein lysis buffer (ThermoFisher) was added and the cells were scrapped to an Eppendorf tube on ice. Each sample of cell lysate was sonicated with the Branson Sonifier 150, 2 times for 6 s, at the lowest setting in a cold room (4°C), followed by 30 minutes of incubation on ice. The lysate was then centrifuged at full speed for 10 minutes at 4°C. The supernatant was transferred to a new tube and samples were ready for protein concentration measurement with the Bio-Rad Protein Assay – Bradford method (Bio-Rad). In brief, duplicates for each sample were prepared by mixing 2 μ L of cell lysate with 998 μ L of Bio-Rad Reagent (diluted 1:5 with water) and incubating for 5 minutes at room temperature. The lysis buffer was used as the blank and to prepare a Bovine Serum Albumine (BSA) Standard Curve. The absorbance was measured at 595 nm using the (Bio-Rad Smartspec™ Plus) Spectrophotometer and protein concentration was calculated based on the standard curve prepared.

2.2.13 Western Immunoblotting

20-45 μ g of protein was mixed with 1/4 of NuPage® LDS Sample Loading Buffer (Invitrogen) and 1/10 of NuPAGE® Sample Reducing Agent (Invitrogen). The samples were then incubated at 95°C for 10 minutes. Meanwhile, a NuPage® 4-10% Bis-Tris pre-cast gel (Life Technologies) was immersed in NuPage® MOPS SDS running buffer in the XCell SureLock™ Mini-Cell Electrophoresis System (Life technologies). Precision Plus Protein Ladder (Bio-Rad) and the pre-incubated samples were loaded into the wells of the gel and were run by electrophoresis at 160V constant voltage for 1 hour and 15 minutes. The gel containing the separated proteins was transferred onto a Nitrocellulose Membrane (Amersham Protran) with the XCell II Blot Module (Life Technologies) at 35V for 1 hour and 45 minutes immersed in Transfer Buffer (Life Technologies). Next, the membrane was blocked with 5% milk in PBS-Tween (0.05% of Tween 20 in PBS) for 1 hour at room temperature, followed by an overnight incubation at 4°C with the primary antibody solution (antibody listed in table 2.1.5 in 5% milk in either PBS-Tween or TBS-tween and with 0.02% of sodium azide). Subsequently, the membrane was washed three times, 15 minutes each, with PBS-Tween or TBS-Tween when phospho-antibody was used) and incubated for 2 hours at room temperature with the appropriate secondary antibody diluted in 5% milk in PBS/TBS-Tween. Prior to protein visualization, further washing of the membranes was carried out as described above, with an additional washing step with PBS for 2 minutes. The protein detection method carried out depended on the secondary antibody employed. In the case of HRP (Horseradish peroxidase) conjugated secondary antibodies, the Enhanced Chemiluminescence western blot detection reagents (Amersham ECL Western Blotting Detection Reagent) were added to the membrane for 1 minute and 30 seconds and the chemiluminescent signal was detected by exposing the films (Amersham, Kodak) with the Compact X4 X-Ray film processor (Xograph Imaging system). If the IRDye secondary antibodies (LI-COR Biotechnology) were applied, the respective fluorescence signal was detected with the LI-COR laser-based imaging system (Odyssey CLx Imager).

2.2.14 Co-Immunoprecipitation

Co-Immunoprecipitation assay was performed according to the instructions provided in Pierce Co-Immunoprecipitation Kit (ThermoFisher). Sca-1+ vascular progenitor cells were starved overnight, after which they were treated with 25 ng/mL of Dkk3 for 3 hours. After treatment, the cells were washed with ice-cold PBS and lysed with 500 μ L of ice-cold IP Lysis/Wash Buffer. The cell lysate was harvested and transferred to a microcentrifuge tube. Following centrifugation at 13000 x g for 10 minutes at 4°C, the pelleted cell debris were discarded and the supernatant transferred to a new tube for protein concentration measurement.

To pre-clear the lysate, a Control Agarose Resin column was prepared. For 1mg of lysate, 80 μ L of the Control resin was used, which was added into a spin column. After centrifugation to remove the storage buffer, 100 μ L of Coupling buffer was added to the column to wash the resin. Subsequently, the column was centrifuged and the flow-through was discarded. 1 mg of lysate was placed into the column containing the resin, which was followed by incubation at 4°C for 45 minutes with gentle end-over-end mixing. Finally, the column was centrifuged at 1000 x g for 1 minute and the flow-through was saved to be added later to the immobilized antibody column.

Antibody immobilization columns were prepared as instructed by the supplier (Pierce™ Co-Immunoprecipitation Kit, ThermoFisher). 50 μ L of AminoLink Plus Coupling Resin was added into a Pierce Spin column, which was then centrifuged at 1000 x g for 1 minute. The flow-through was discarded and the resin was washed twice with 200 μ L of Coupling buffer, followed by additional centrifugation and flow-through discarding steps. Antibody solution to be coupled to the resin was prepared, consisting of 50 μ g of antibody, 10 μ L of 20X Coupling Buffer and ultrapure water to adjust the volume to 200 μ L. The solution was added directly to the resin in the spin column and it was followed by the addition of 3 μ L of Sodium Cyanoborohydride solution, in a fume hood. The column was closed with a lid and incubated on a rotator at room temperature for 120 minutes to allow the coupling of the antibody to the resin column. After the incubation period, the column was placed in a collection tube and centrifuged, followed by two washing steps with 200 μ L of Coupling buffer. Next, 200 μ L of Quenching buffer was added to the column. After centrifugation, the flow-through was discarded and the bottom plug inserted. 200 μ L of Quenching buffer and 3 μ L of Sodium Cyanoborohydride were added, and a screw cap was attached. The column was incubated for 15 minutes at room temperature with end-over-end mixing. Next, the column was placed in a collection tube and centrifuged. Two additional washing steps with Coupling Buffer were followed. Finally, the column was washed 6 times with 150 μ L of Wash solution, centrifuging after each wash.

450 μ L of pre-cleared lysate was added to each antibody immobilized column (4 columns: Rabbit anti CXCR7 antibody and respective Rabbit IgG control; Rat anti Integrin β 1 antibody and respective Rat IgG2a Kappa control). A cap and the bottom screw were attached to column, which was submitted to overnight incubation at 4°C with gentle mixing. After the incubation step, the column was placed in a collection tube and centrifuged. Next, 3 times washing steps were followed with 200 μ L of IP Lysis/Wash buffer, with centrifugation after each wash.

10 μL of the Elution buffer were added to the column. After centrifugation, additional 50 μL of elution buffer was added with 5 minutes incubation at room temperature. After centrifugation the flow-through was collected in the same collection tube to accumulate the two elution fractions. The flow-through is analysed by protein measurement to ensure that the antigen has completely eluted. The eluted samples, together with the input sample (pure cell lysate harvested), were used for western blotting to analyse the co-immunoprecipitation of Dkk3 to CXCR7 or Integrin $\beta 1$.

2.2.15 Transwell migration assay

Sca-1+ APCs were starved overnight. The next day, control (0.2% FBS in ATCC medium) and treatment (treatment in 0.2% FBS in ATCC medium) media were prepared. On the lower chamber of transwell inserts with 8.0 μm pore size membrane filters, 800 μL of control or treatment (murine Dkk3 or murine Sdf-1 α ; 0-100 ng/mL) medium was added. Next, 5×10^4 cells resuspended in 200 μL of control medium were loaded into the upper chamber of the transwell insert. After overnight incubation, non-migrating cells on the upper chamber side of the filters were carefully washed with PBS and removed using a cotton bud. The migrated cells (through the pores) on the lower side of the membrane were fixed with 4% PFA in PBS for 10 minutes at room temperature and then stained with 0.1% crystal violet dye for at least 15 minutes at room temperature. A final washing step was followed by carefully submerging the insert in distilled water and drying with cotton bud. Under the microscope, the migrated (stained) cells were counted in 5 different fields of each insert at 10X magnification (Figure 2.2.15). Data was expressed as the fold of migrated Sca-1+ APCs in response to treatment compared to the control. For experiments involving inhibitors, Sca-1+ cells were pre-incubated for 1 hour with the respective inhibitors, after overnight starvation and prior to their transfer to the transwell inserts. Inhibitors were also added to the lower chamber of the transwell inserts.

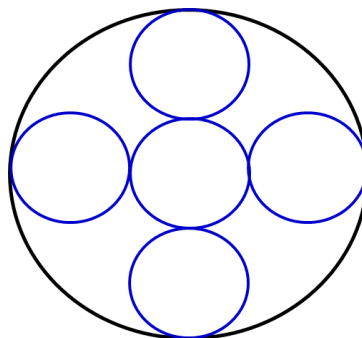


Figure 2.2.15: Layout of fields in each transwell insert at 10X magnification. Sca-1+ migrated cells were counted under the microscope, at 10X magnification, in each field (blue circles). 5 fields were considered for each transwell insert (black circle).

2.2.16 Wound Healing migration assay

Sca-1+ APCs were seeded in 12-well plates until reaching confluency of 80%. Next, cells were starved for at least 6 hours and then washed with PBS. Using a clean 1000 μ L pipette tip a straight scratch was made across the well (Figure 2.2.16). The cell debris were removed with PBS and control (0.2% FBS in ATCC medium) or treatment (0-100 ng/mL of murine Dkk3 or murine Sdf-1 α , in 0.2% FBS in ATCC medium) media were added to the wells. The cells were allowed to migrate (close the scratch/wound) overnight. Subsequently, the medium was removed and the cells were washed with PBS, followed by fixation with 4% PFA in PBS for 10 minutes at room temperature. Finally, after washing with PBS, 0.1% crystal violet dye was used to stain the cells, for at least 15 minutes. After washing the wells with PBS, the cell number of migrated cells was quantified under the microscope at 10X magnification, by counting the cells migrated inside the scratch in 5 different fields. Data was expressed as the fold of migrated Sca-1+ APCs in response to treatment compared to the control. For experiments involving inhibitors, Sca-1+ cells were pre-incubated for 1 hour with the respective inhibitors, prior to making the scratch. Inhibitors were also added to the corresponding wells during overnight cell migration.

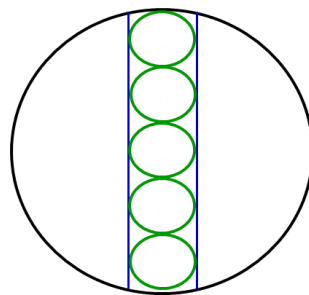


Figure 2.2.16: Layout of fields in each well of a 12-well plate, at 10X magnification. Sca-1+ migrated cells inside the scratch (blue lines) were counted under the microscope, at 10X magnification, in each field (green circles). 5 fields were considered for each well of a 12-well tissue culture plate (black circle).

2.2.17 BrdU Proliferation Assay

The Sca-1+ APC proliferation assay was performed using the Cell Proliferation ELISA BrdU colorimetric Kit (Roche). Sca-1+ APCs were seeded in 96-well plates, followed by at least 6 hours of starvation. Next, control (0.2% FBS in ATCC medium) and treatment (25 and 50 ng/mL of Dkk3 or 10 and 25 ng/mL of Sdf-1 α or 10 ng/mL of Pdgf- β , in 0.2% FBS in ATCC medium) media was added for 16, 24 or 48 hours. After treatment, cells were washed with PBS and BrdU solution (BrdU at 10 μ M in 100 μ L of ATCC medium) was added to each well. Cells were incubated with BrdU solution for 3 hours at 37°C. Subsequently, the labelling medium was removed and 200 μ L of Fixating/Denaturing solution was added to each well with incubation at room temperature for 30 minutes. The

Fixating/Denaturing solution was thoroughly removed from the wells before incubating with 100 μ L of anti-BrdU-POD antibody for 90 minutes at room temperature. Then, the conjugate antibody was removed, and the wells were washed 3 times with 250 μ L of Washing solution. To each well 100 μ L of Substrate solution was added and incubated at room temperature. Once a change in colour was detected, 25 μ L of Stop solution (1M of H₂SO₄) was added to each well. The absorbance of the samples was measured at 450 nm by using a microplate ELISA reader (Infinite M200 PRO, Tecan), with reference to 690 nm for correction. The value obtained for the blank (containing no cells) was subtracted from the value obtained for the samples. Data was expressed as the fold of the values obtained for the treated cells compared to the value of non-treated cells (control).

2.2.18 Aortic ring assay and immunofluorescence staining

Aorta vessels were isolated from Wild type and ApoE^{-/-} mice. After washing with DMEM, the connective and fat tissue were separated from the vessel. Next, transverse cuts were made in order to obtain aortic rings of 1mm size. The resulting rings were extensively rinsed with PBS. Meanwhile, 8-well chamber slides (Ibidi) were filled with 150 μ L of matrigel (Corning) and placed in the 37°C incubator for 30 minutes to allow matrigel solidification. Subsequently, the thoroughly washed aortic rings were carefully inserted in the matrigel and left to incubate at 37°C for 2 hours. During this period of time, control (1% FBS in ATCC medium) and treatment (25 ng/mL of Dkk3, 25 ng/mL of Sdf-1 α , 10 ng/mL of Pdgf- β , in 1% FBS in ATCC medium) media were prepared. After incubation, 200 μ L of the control or treatment media were added to the chambers containing the aortic rings in matrigel. A period of 8 days of incubation at 37°C was followed, with washing of the aortic rings and replacement of the media every other day. For each condition (Wild type versus ApoE^{-/-} mice, control or Dkk3, Sdf-1 α and Pdgf- β treatments) 7 aortic rings were used. On day 8 the cell outgrowth was quantified considering the whole phase contrast view at 10X magnification.

For immunostaining of the aortic rings, transgenic Sca-1-GFP-ApoE^{-/-} mice aortic rings were used. After cell outgrowth, the medium was removed and the aortic rings were washed with PBS. Next, the aortic rings and the cell outgrowth in the matrigel were fixed with a pre-prepared fixing solution (2% PFA and 0.1% glutaraldehyde in PBS). Subsequently, the chamber slides were washed with PBS and then blocked with 5% swine serum in PBS for 45 minutes at room temperature. After removing the blocking solution, the antibody anti-Actin, α -Smooth Muscle-Cy3 (in blocking solution) was added to each aortic ring outgrowth for overnight incubation at 4°C. After incubation, the well chambers were washed with PBS and DAPI was added for 30 minutes at room temperature. Finally, the aortic rings were washed once more with PBS. Images were acquired using Nikon A1R Confocal microscope and processed using ImageJ software. GFP and/or α -SMA positive cells in the cell outgrowth were quantified manually and data was expressed as the fold of cells that outgrew from the aortic rings in response to treatment compared to the control.

2.2.19 Knock-Down of murine receptors with SiRNA

Downregulation of murine receptors (Table 2.2.19) was performed using Lipofectamine RNAiMAX (ThermoFisher) for SiRNA transfection. Sca-1+ APCs were seeded in 6-well plates in complete medium. The next day, upon reaching 70% of confluency, the cells were starved for 3 hours with 1% FBS ATCC medium in the absence of any antibiotics. SiRNA at 10 μ M (3 μ L or 30 pmol) was diluted in 150 μ L of Opti-MEM[®] medium (per well of a 6-well plate) and in a separate tube, Lipofectamine RNAiMAX (9 μ L, considering a ratio of 1:3 for SiRNA:Lipofectamine RNAiMAX) was also diluted in 150 μ L of Opti-MEM medium. The diluted SiRNA was added to the diluted transfection reagent and incubation of 5 minutes at room temperature was followed. The complex SiRNA-lipid formed was added to each well containing the Sca-1+ cells. The following day, complete medium lacking antibiotics was added to the cells. After 48 hours of transfection the cells were washed with PBS and then either harvested for analysis or prepared for transwell or scratch migration assays as explained before.

Table 2.2.19: List of receptor SiRNA and respective control SiRNA

Receptor/Control	SiRNA product	Supplier	Catalogue No.
CXCR2	siGENOME Mouse Cxcr2 siRNA	Dharmacon	D-042157-01-0002
CXCR4	MISSION [®] esiRNA mouse Cxcr4	Sigma-Aldrich	EMU021801-20UG
CXCR4	siGENOME Mouse Cxcr4 siRNA	Dharmacon	D-060184-02-0002
CXCR7	MISSION [®] esiRNA mouse Cxcr7	Sigma-Aldrich	EMU028171-20UG
Kremen1	MISSION [®] esiRNA mouse Kremen1	Sigma-Aldrich	EMU072231-20UG
Kremen2	MISSION [®] esiRNA mouse Kremen2	Sigma-Aldrich	EMU007571-20UG
Integrin α 5	SMARTpool: siGENOME Itga5 siRNA	Dharmacon	M-060502-00-0005
Integrin β 1	SMARTpool: siGENOME Itgb1 siRNA	Dharmacon	M-040783-00-0005
Control GFP	MISSION [®] esiRNA EGFP	Sigma-Aldrich	EHUEGFP-20UG
Control Non-targeting	siGENOME Non-Targeting siRNA #1	Dharmacon	D-001210-01-05
Control Non-targeting (SMART pool)	siGENOME Non-Targeting siRNA #4	Dharmacon	D-001210-04-05

2.2.20 G-LISA Small GTPase Activation Assay

The small GTPases activation assays were performed according to the instructions provided in RhoA and Rac1 G-LISA Activation Assay Kits, in the colorimetric format (Cytoskeleton Inc.). Sac-1+ APCs were seeded in petri dishes and starved overnight the next day. Control (0.2% FBS in ATCC medium) and treatment (25 ng/mL of Dkk3 or Sdf-1 α , in 0.2% FBS in ATCC medium) media were prepared and

added to the cells. Upon reaching the desired time points (0, 3, 5, 10, 13, 15 and 30 minutes of stimulation) cells were washed with ice-cold PBS and 100 μ L of ice-cold Lysis buffer was added to each petri dish. Cells were scrapped from the petri dish placed on ice and transferred to a pre-chilled microcentrifuge tube. The lysates were cleared by centrifugation at 10,000 x g at 4°C for 1 minute. Protein concentration was measured spectrophotometrically using the Protein Assay reagent provided in the kit and it was equalized for all samples with Lysis buffer to attain a protein concentration of 2.0 mg/mL for RhoA activation assay and of 1.0 mg/mL for Rac1 activation assay. A blank was prepared with equal amount of Lysis buffer and Binding buffer. The positive control samples were prepared with Rho control protein or Rac1 control protein, Lysis buffer and Binding Buffer. To the samples to be tested, equal amount of Binding buffer was added. 50 μ L of each test sample, of blank buffer and of positive control sample were pipetted into their corresponding wells and incubated at 4°C for 30 minutes with orbital shaking. After washing the wells with Washing buffer, the Antigen presenting buffer was added, with incubation for 2 minutes at room temperature. Following additional washing, the anti-RhoA or anti-Rac1 primary antibodies were added for incubation at room temperature for 45 minutes, with orbital shaking. Following extensive washing of the wells, the secondary antibody was added for a 45 minutes-period of incubation at room temperature with orbital shaking. Subsequently, the wells were washed and the HRP detection reagent freshly prepared was pipetted into each well. After 10 minutes of incubation at 37°C a yellow colour was developed and the Stop Buffer was added. The resulting signal was read to measure the absorbance at 490 nm in the microplate reader Infinite M200 PRO (Tecan). The absorbance value of the blank was subtracted from the value of the test samples and positive controls and the data was expressed as the fold of the values obtained for the treated cells compared to the value of non-treated cells (control).

2.2.21 Cloning of Human receptors and plasmid amplification

Human receptors CXCR2, CXCR4, CXCR7, Kremen1 and Kremen2 were cloned in a pShuttle-FLAG-HA vector (Figure 2.2.21A). The receptors were cloned using Nhe I and Sal I restriction enzymes (NEB Inc. Biolabs) in order to have the HA tag in C-terminal. The cDNA and primers used to amplify the receptors are shown in table 2.2.8.3. After amplification of the receptors by conventional PCR, the inserts were separated by gel electrophoresis and extracted using the QIAquick Gel Extraction Kit (Qiagen). After confirmation of the respective sequences by sequencing analysis, the receptor inserts were first digested with the Nhe I restriction enzyme, at 37°C for at least 3 hours (Table 2.2.21A). Next, the insert was purified using the QIAquick PCR Purification Kit (Qiagen) and submitted to an overnight digestion at 37°C with the restriction enzyme Sal I. The empty vector was also submitted to digestion (Table 2.2.21B) with both restriction enzymes Nhe I and Sal I, at 37°C for at least 3 hours. The digested insert and empty vector were separated from their respective reaction mixture components by Gel electrophoresis and extracted using again the QIAquick Gel Extraction Kit (Qiagen). Nucleic acid concentration and purity was assessed using the NanoDrop N-1000 spectrophotometer. Next, the ligation step was performed overnight at 14°C with T4 DNA Ligase

(Promega). The ligation reaction mixture was prepared according to Table 2.2.21C. Finally, 100 ng of the resulting product were transformed in JM109 *E. coli* competent cells (Promega, L1001) and the transformed cells were spread in LB-agar plates containing Kanamycin. Selected colonies were amplified overnight and the receptor-HA plasmids were extracted from the transformed cells using QIAprep Spin Miniprep Kit (Qiagen). A restriction enzyme test was performed on the extracted plasmids (37°C, 1 hour, Nhe I and Sal I enzymes) to confirm the success of ligation by visualizing the bands corresponding to the insert and the vector separated in the gel, prior to sequencing the plasmids for the insert. The plasmids pCMV3-ITG α 5-HA and pCMV3-ITG β 1-HA and the vector pCMV3-ORF-HA (Figure 2.2.21B) were acquired ready-made (Sino Biological Inc.) as glycerol stocks and amplified in LB Broth medium containing Kanamycin. The plasmids were extracted from the cells as explained above and stored at -20°C.

A Map of the vector pShuttle-Flag-HA used for cloning

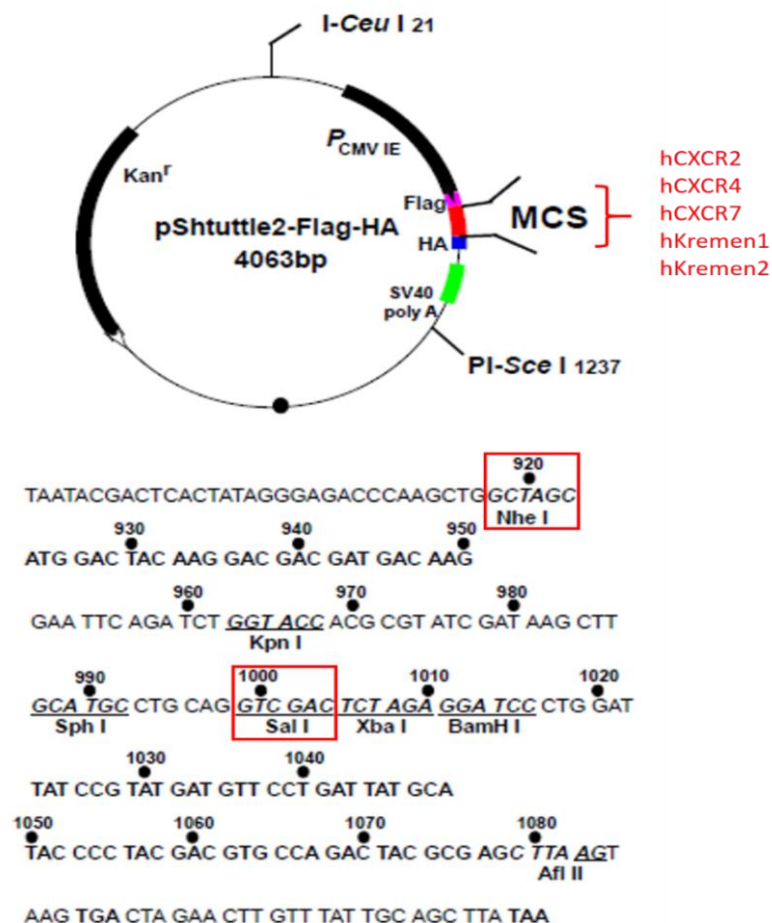


Figure 2.2.21A: Map of the vector pShuttle2-Flag-HA used for cloning. In order to clone the Human receptors (hCXCR2, hCXCR4, hCXCR7, hKremen1 and hKremen2) in the vector with HA in C-terminal, primers containing the sequences of the restriction enzymes Nhe I (for forward primers) and Sal I (for reverse primers) were prepared and cDNA was amplified by PCR.

Table 2.2.21A: Reaction mixture for enzyme digestion of the vector (sequential digestion)

Mixture component	Quantity
Enzyme (Nhe I or Sal I)	1 μ L
Insert	30 μ L
Enzyme Buffer (10X)	4 μ L
Water	5 μ L
Total volume	40 μ L

Table 2.2.21B: Reaction mixture for enzyme digestion of the insert

Mixture component	Quantity
Enzyme (Nhe I + Sal I)	1 μ L + 1 μ L = 2 μ L
Vector	30 μ L
Enzyme Buffer (10X)	4 μ L
Water	4 μ L
Total volume	40 μ L

Table 2.2.21C: Reaction mixture for enzyme digestion of the vector

Mixture component	Quantity
Plasmid	Volume = 100 ng
Insert	$Volume = \frac{500 \text{ ng}}{\text{concentration}} \times \frac{\text{Size of insert}}{\text{Size of vector}}$
Buffer 10X	2 μ L
T4 Ligase	1 μ L
Water	Enough to make up 20 μ L of total volume

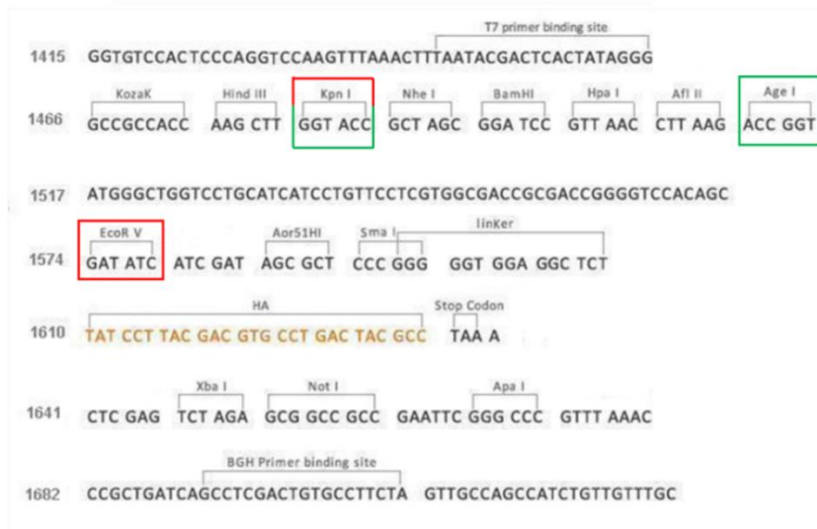
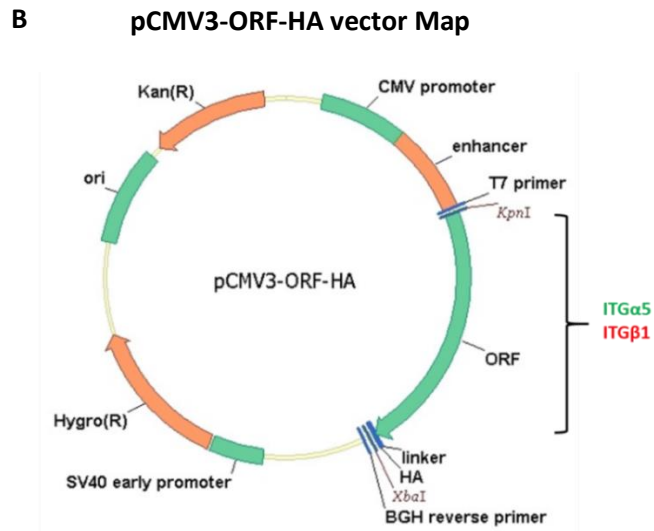


Figure 2.2.21B: Map of the vector pCMV3-HA. ITG α 5 and ITG β 1 are contained in the Open Reading Frame region of the plasmid with HA tag in C-terminal. ITG α 5 was cloned using Kpn I and Age I restriction enzymes. ITG β 1 was cloned with Kpn I and EcoR V restriction enzymes.

2.2.22 Overexpression of receptors on HEK 293T Cells

HEK 293T cells were seeded in 6-well plates and once cell confluency reached 75%, the medium was changed for 1% FBS DMEM without any antibiotics. 3 μ g of the receptor-HA plasmids or of the respective vectors were diluted in 250 μ L of Opti-MEM[®]. Next, 12 μ L of Fugene[®] HD transfection reagent (Promega) were added (ratio of Fugene to DNA: 4:1) in the same tube and the Fugene/DNA mixture was incubated for 15 minutes at room temperature. After incubation, the mixture was added to the well containing the cells to be transfected with the corresponding plasmid or vector. The cells were returned to the incubator and after 12 hours, 5% FBS in DMEM medium lacking antibiotics was added. Following 48 hours of transfection, cells were harvested for either qPCR or Western blot analysis.

2.2.23 Fusion of Dkk3 and Sdf1- α with Alkaline Phosphatase (AP)

Human Dkk3 and Sdf-1 α were reconstituted at concentrations of 200 $\mu\text{g}/\text{mL}$ and 100 $\mu\text{g}/\text{mL}$, respectively. Alkaline Phosphatase (AP) was fused to each recombinant protein using the Lightning-Link[®] Alkaline Phosphatase Conjugation Kit (Innova Biosciences). First, 1 μL of LL-AP modifier reagent was added for each 10 μL of protein and mixed gently. The resulting mixture was pipetted directly onto the lyophilized material contained in the LightningLink[®]-AP vial with gentle resuspension. Overnight incubation was followed at room temperature with protection from light. After incubation, 1 μL of LLquencher reagent was added for every 10 μL of protein used.

The efficiency of AP conjugation was assessed using the NF κ B Secreted Alkaline Phosphatase (SEAP) Reporter Assay Kit (Novus Biologicals). Serially diluted SEAP samples were prepared with SEAP standard provided by the kit, to make a standard curve. Next, hDkk3-AP and hSdf-1 α -AP were serially diluted. Standard curve samples and serially diluted AP-conjugated recombinant protein samples were loaded in the corresponding wells of the microtiter plate. Incubation was followed for 5 minutes at room temperature with gentle shaking. Subsequently, 100 μL of 1 mg/mL of para-Nitrophenylphosphate (PNPP) substrate solution was added to each well and incubated at room temperature for 30 minutes. AP activity was measured by reading the absorbance at 405 nm in the Infinite M200 PRO (Tecan) ELISA plate reader. The concentration of the conjugated-recombinant protein samples was calculated and the efficiency of AP conjugation was determined by calculating the correlation between AP activity and hDkk3-AP or hSdf-1 α -AP concentrations.

2.2.24 Affinity Binding assay and Dissociation Constant (K_D) calculation

White high-binding ELISA 96-well plate (Greiner) was coated overnight at 4 $^{\circ}\text{C}$ with 100 $\mu\text{L}/\text{well}$ of 2 $\mu\text{g}/\text{mL}$ of anti-HA tag antibody (Abcam) in NaHCO_3 buffer (50 mM, pH 9.6). After washing the wells six times with TBS-T, blocking (5% BSA in TBS-T) was followed on a shaker for 1 hour at room temperature. Meanwhile, HEK 293T cells overexpressing hCXCR2, hCXCR4, hCXCR7, hKremen1, hKremen2, hITG α 5 and hITG β 1, after washing with ice-cold PBS, were lysed with RIPA lysis and Extraction buffer (ThermoFisher) containing protease inhibitors. The cell lysate was diluted in blocking buffer. Next, 100 μL of membrane extract lysate was added to the corresponding HA-coated wells and allowed to bind overnight at 4 $^{\circ}\text{C}$ on a shaker. Following extensive washing, the wells were blocked for 1 hour. The blocking buffer was removed and the diluted solutions of hDkk3-AP and hSdf-1 α -AP were added to the wells for 2 hours of incubation at room temperature with gentle shaking. Next, the wells were washed and bound AP activity was measured using chemiluminescent SEAP Reporter Gene Assay (Roche). For each concentration of either hDkk3-AP or hSdf-1-AP, background (wells without cell lysate) binding value was subtracted. The concentration of 0 ng/mL was considered for the wells containing cell lysate in which no AP conjugated recombinant protein was added. Binding curve, Scatchard plot and dissociation constant (K_D) were obtained using GraphPad Prism 7 software.

2.2.25 Yeast Two Hybrid Assay

The Yeast Two Hybrid (Y2H) assay was performed according to the instructions provided in the Matchmaker® Gold Yeast Two-Hybrid System (Clontech/Takara). All the required cells, growth media and accessory kits were either already included or recommended by the Matchmaker® Gold Yeast Two-Hybrid System (Table 2.2.25).

Table 2.2.25: List of items required for Yeast Two Hybrid experiment

Item	Catalogue No.	Supplier
Matchmaker Gold Yeast Two-Hybrid System	630489	Clontech/Takara
Mate & Plate™ Library - Universal Mouse (Normalized)	630483	Clontech/Takara
pGBKT7 DNA-BD Cloning Vector (0.1 µg/µl)	630443	Clontech/Takara
pGADT7 AD Cloning Vector (0.1 µg/µl)	630442	Clontech/Takara
pGBKT7-53 Control Vector (0.1 µg/µl)	---	Clontech/Takara
pGADT7-T Control Vector (0.1 µg/µl)	---	Clontech/Takara
pGBKT7-Lam Control Vector (0.1 µg/µl)	---	Clontech/Takara
MGC Mouse Dkk3 cDNA	MMM1013-202859450	Dharmacon
Y2HGold Yeast Strain	630498	Clontech/Takara
Y187 Yeast Strain	630457	Clontech/Takara
In-Fusion® HD Cloning Plus, 10 Rxns	638909	Clontech/Takara
Yeastmaker Yeast Transformation System 2	630439	Clontech/Takara
Easy Yeast Plasmid Isolation Kit	630467	Clontech/Takara
QIAprep® Spin Miniprep Kit (250)	27106	Qiagen
Yeast Media Set 2	630494	Clontech/Takara
YPDA Broth	630306	Clontech/Takara
YPDA with Agar	630307	Clontech/Takara
SD-Trp Broth	630308	Clontech/Takara
SD-Trp with Agar	630309	Clontech/Takara
SD-Leu Broth	630310	Clontech/Takara
SD-Leu with Agar	630311	Clontech/Takara
SD-Leu/-Trp Broth (DDO)	630316	Clontech/Takara
SD-Leu/-Trp with Agar (DDO)	630317	Clontech/Takara
SD-Ade/-His/-Leu/-Trp Broth (QDO)	630322	Clontech/Takara
SD-Ade/-His/-Leu/-Trp with Agar (QDO)	630323	Clontech/Takara
Aureobasidin A	630466	Clontech/Takara
X-α-Gal	630462	Clontech/Takara

2.2.25.1 Growth of haploid yeast strains Y2HGold and Y187

YPDA agar plates were streaked with Y2HGold and Y187 haploid yeast strains provided as frozen yeast stocks. The plates were incubated upside down at 30°C until colonies were observed (3-5 days). A colony of each strain was inoculated in YPDA medium to allow cell growth, with incubation at 30°C and shaking at 250 rpm, until optical density (OD₆₀₀) of 0.15-0.30 was reached. Cells were centrifuged at 700 g for 5 minutes at room temperature and supernatant was discarded. The cell pellet was resuspended in fresh YPDA medium and let to grow until OD₆₀₀ reached 0.4-0.5 (3-5 hours). The cells were centrifuged and the pellet was resuspended in sterile deionized H₂O. After another centrifugation step, each pellet was resuspended in 1.1 X Tris-EDTA/Lithium Acetate (1.1 X TE/LiAc). The cell suspension was divided into two tubes and centrifuged at high speed for 15 seconds. The supernatant was discarded and the pellets were again resuspended in 1.1 X TE/LiAc. At this stage the yeast haploid cells were ready (competent) for transformation.

2.2.25.2 Control test and yeast transformation

Before proceeding with the mating of mDkk3-transformed cells with the cells transformed with the prey inserts corresponding to the mouse library, control experiments were performed to validate and to be familiar with the Matchmaker® Gold Yeast Two-Hybrid System. For the positive control, Y2HGold yeast strain was transformed with the plasmid pGBKT7-53 (Figure 2.2.25.2B) which encodes GAL4 DNA-BD fused to p53. Y187 yeast strain was transformed with pGADT7-T (Figure 2.2.25.2C) which encodes GAL4 AD fused to SV40 large T-antigen (Figure 2.2.25.2A). For the negative control, Y187 yeast strain was also transformed with pGADT7-T, but the Y2HGold strain was transformed instead with pGBKT7-Lam (Figure 2.2.25.2D), which encodes for GAL4 DNA-BD fused to Human Lamin (Figure 2.2.25.2A).

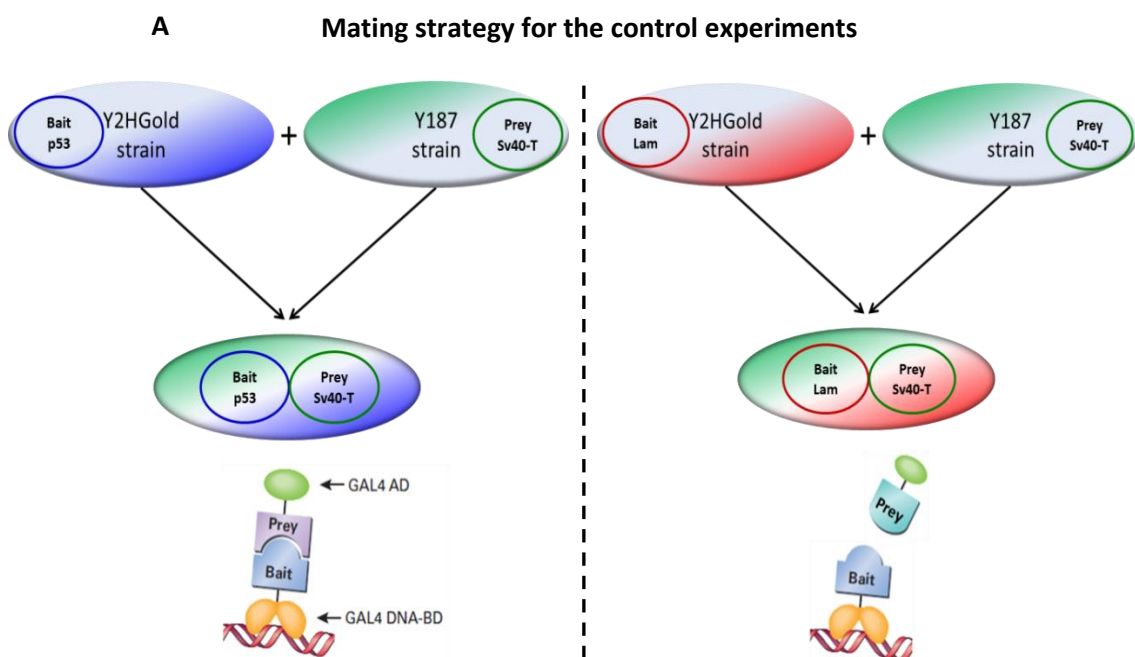


Figure 2.2.25.2A: Mating strategy for the control experiments. Positive control comprised the mating of Y2HGold strain containing the bait plasmid encoding p53 with Y187 strain containing the prey plasmid encoding SV40 Large T-antigen. The negative control comprised the mating of Y2HGold strain containing the bait plasmid encoding Laminin with Y187 strain containing the prey plasmid encoding SV40 Large T-antigen.

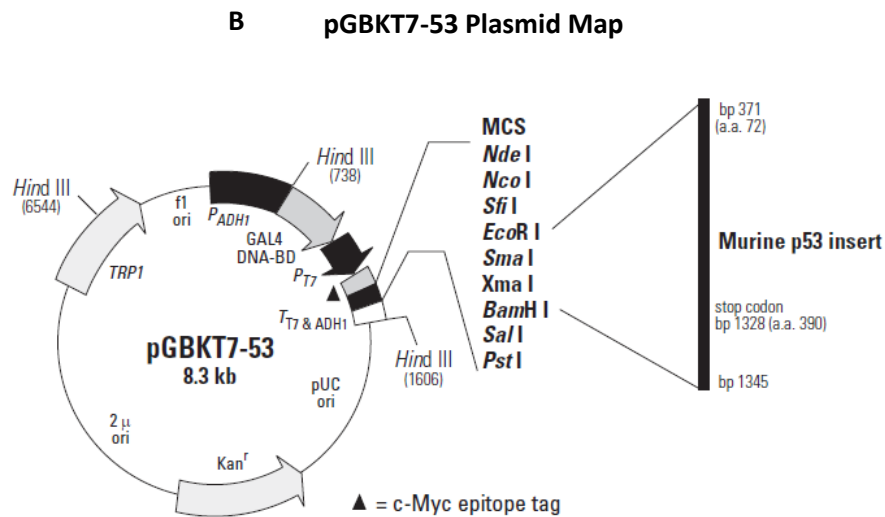


Figure 2.2.25.2B: pGBKT7-53 Plasmid Map. Y2HGold yeast strain was transformed with pGBKT7-53 plasmid, which encodes the murine p53 gene fused to GAL4 DNA-BD. The tryptophan biosynthesis gene is also included in the plasmid, enabling growth of Y2HGold yeast on medium lacking this amino acid.

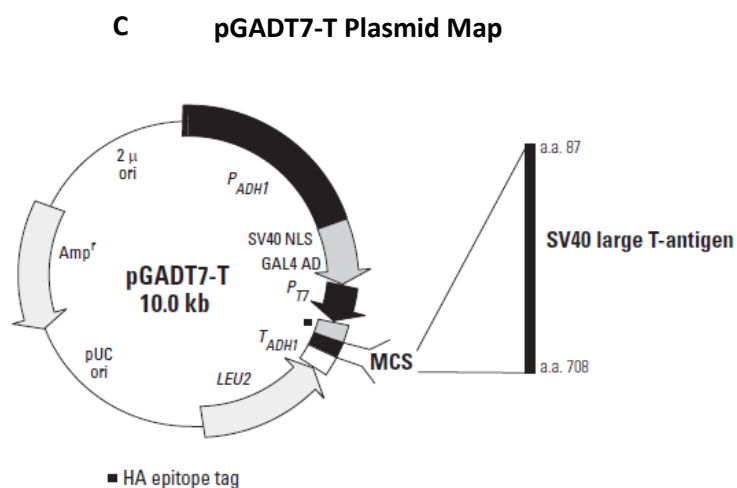


Figure 2.2.25.2C: pGADT7-T Plasmid Map. Y187 yeast strain was transformed with pGADT7-T plasmid, which encodes the SV40 large T-antigen gene fused to GAL4 AD. The leucine biosynthesis gene is also included in the plasmid, enabling growth of Y187 yeast on medium lacking this amino acid.

D pGBKT7-Lam Plasmid Map

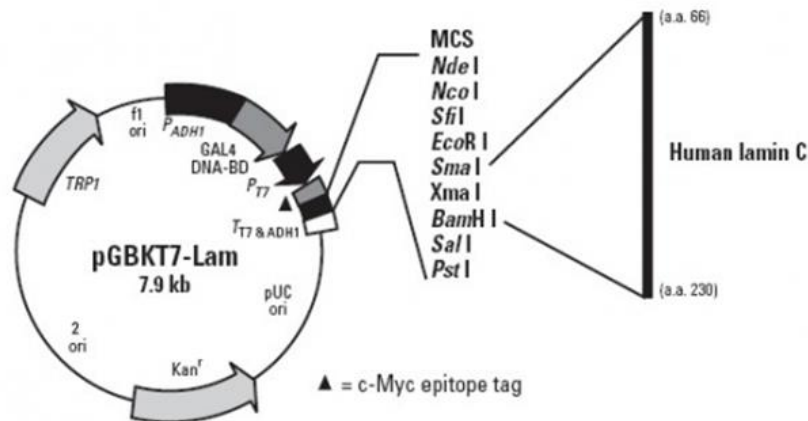


Figure 2.2.25.2D: pGBKT7-Lam Plasmid Map. Y2HGold yeast strain was transformed with pGBKT7-Lam plasmid, which encodes the human lamin C gene fused to GAL4 DNA-BD. The tryptophan biosynthesis gene is also included in the plasmid, enabling growth of Y2HGold yeast on medium lacking this amino acid.

Yeast transformation was performed according to the instructions in Yeastmaker™ Yeast Transformation System 2 (Clontech). In a pre-chilled tube, 100 ng of plasmid was added, followed by 5 µL of Yeastmaker Carrier DNA (10 µg/µL; denatured previously at 95°C for 5 minutes). 50 µL of Yeast competent cells were added, before addition of 500 µL of Polyethylene glycol/Lithium Acetate (PEG/LiAc). The mixture was incubated at 30°C for 30 minutes. Next, 20 µL of Dimethyl sulfoxide (DMSO) was added, with 15 minutes incubation at 42°C in a water bath. Subsequently, the tube was centrifuged at high speed to pellet the cells, which were resuspended with YPD plus medium. Incubation at 30°C, with shaking, was followed for 30 minutes. Cells were then centrifuged at high speed and the cell pellet was resuspended with 1mL of 0.9% sodium chloride (NaCl) solution. 100 µL of 1/10 and 1/100 dilution of the transformed cells were spread onto agar plates containing the appropriate SD selection medium (Table 2.2.25A). The plates were incubated upside down at 30°C until colonies appeared.

Table 2.2.25.2: Yeast transformation strategy

Strain	Transformation plasmid	Agar plate
Y2HGold	pGBKT7-53	SD/-Trp
Y2HGold	pGBKT7-Lam	SD/-Trp
Y187	pGADT7-T	SD/-Leu

The pre-transformed haploid yeast cells were then submitted to a small-scale mating procedure. A colony of Y2HGold cells transformed with pGBKT7-53 and a colony of Y187 cells transformed with pGADT7-T were placed in the same tube containing 2X YPDA medium. Similarly, in another tube, a colony of Y2HGold cells transformed with pGBKT7-Lam and a colony of Y187 cells transformed with pGADT7-T were mixed in 2X YPDA medium. Both tubes were vortexed to mix and then incubated with shaking at 200 rpm at 30°C overnight (minimum 20 hours), to allow the mating of the haploid cells. From the mated culture, 100 µL of 1/10, 1/100, and 1/1,000 dilutions of each tube were spread on the following agar plates: SD/-Trp, SD/-Leu, SD/-Leu/-Trp (DDO), SD/-Leu/-Trp/X-a-Gal/AbA (DDO/X/A). The plates were incubated upside down at 30°C, for 5 days and the assessment of the control test was performed based on the presence or absence of colonies on the plates, according to the expected results.

2.2.25.3 Cloning of mDkk3 into vector pGBKT7 containing GAL4 DNA-BD

Murine Dkk3 cDNA (Figure 2.2.25.3A) cloned in frame with GAL4 DNA-BD of the bait vector pGBKT7 (Figure 2.2.25.3B). The In-Fusion® Advantage HD Cloning Kit (Clontech) was used for this purpose and EcoRI and BamHI enzymes were selected to linearize the vector. The primers required for mDkk3 amplification (Pfu polymerase, Promega) were designed according to the recommended in the In-Fusion® Advantage HD Cloning Kit and the amplified insert did not require enzyme digestion, after DNA purification, as the BamHI and EcoRI sites were included in the sequences of the primers used in mDkk3 amplification. Bait Dkk3 and linearized vector were “fused” using the In-Fusion enzyme, and Stellar™ competent cells (Clontech) were transformed with the plasmid. After amplification of selected colonies, the plasmid was sent for sequencing with a standard T7 primer, to confirm that Dkk3 was cloned in frame with GAL4 DNA-BD. The plasmid pGBKT7 GAL4 DNA-BD-mDkk3 was stored at -20°C.

A Murine Dkk3 cDNA

ATGCAGCGGCTCGGGGGTATTTGCTGTGTACTACTGCTGGCGGCGGCGGTCCCACTGCTCCTGCTCCTTCCCCGACGGTCACTT
GGACTCCGGCGGAGCCGGGCCAGCTCTCAACTACCCTCAGGAGGAAGCTACGCTCAATGAGATGTTTCGAGAGGTGGAGGAG
CTGATGGAAGACTACTCAGCACAACTGCGCAGTGCCGTGGAGGAGATGGAGGCGGAAGAAGCAGCTGCTAAAACGCTCCTCTGA
GGTGAACCTGGCAAGCTTACCTCCCACTATCACAATGAGACCAGCACGGAGACCAGGGTGGGAAATAACACAGTCCATGTGCA
CCAGGAAGTTCACAAGATAACCAACAACCAGAGTGGACAGGTGGTCTTTTCTGAGACAGTCATTACATCTGTAGGGGATGAAGA
AGGCAAGAGGAGCCATGAATGTATCATTGATGAAGACTGTGGGCCACCAGGTACTGCCAGTTTCCAGCTTCAAGTACACCTG
CCAGCCATGCCGGGACCAGCAGATGCTATGCACCCGAGACAGTGAGTGCTGTGGAGACCAGCTGTGTGCCTGGGGTCACTGCA
CCCCAAAGGCCACCAAGGTGGCAATGGGACCATCTGTGACAACCAGAGGGATTGCCAGCCTGGCCTGTGTTGTGCCTTCCAAA
GAGGCCTGCTGTTCCCGTGTGCACACCCCTGCCGTGGAGGGAGAGCTCTGCCATGACCCACCAGCCAGCTGCTGGATCTCA
TCACCTGGGAAGTGGAGCCTGAAGGAGCTTTGGACCGATGCCCTGCGCCAGTGGCCTCCTATGCCAGCCACACAGCCACAGTC
TGGTGTACATGTGCAAGCCAGCCTTCGTGGGCAGCCATGACCACAGTGAGGAGAGCCAGCTGCCAGGGAGGCCCGGATGAG
TACGAAGATGTTGGCTTCATAGGGGAAGTGCGCCAGGAGCTGGAAGACCTGGAGCGGAGCCTAGCCAGGAGATGGCATTG
AGGGCCTGCCCTGTGGAGTCACTAGGCGGAGAGGAGGAGATT

B pGBKT7 plasmid map and partial sequence

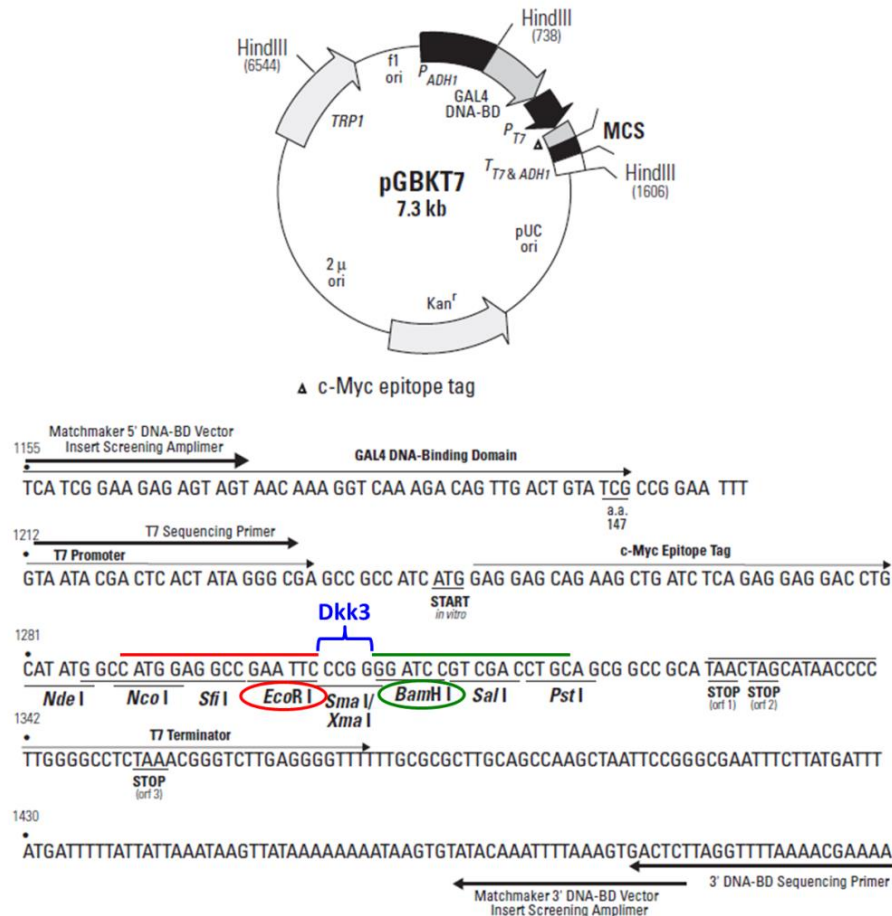


Figure 2.2.25.3: Murine Dkk3 cDNA sequence (A) and pGBKT7 plasmid Map and partial sequence (B). cDNA for murine Dkk3 was purchased from Dharmacon. The sequences highlighted in red were included in the primers used for mDkk3 amplification. Primers were designed according to the In-Fusion® Advantage HD Cloning Kit. EcoRI (red) and BamHI (green) enzymes were selected to linearize the vector. The sequences corresponding to the enzymes were also included in the primers used for murine Dkk3 cDNA amplification. Dkk3 was cloned in frame with GAL4 DNA-BD.

2.2.25.4 mDkk3 bait auto-activation test

Y2HGold competent cells were transformed, as described above, with either 100 ng of the plasmid pGBKT7 GAL4 DNA-BD-mDkk3 or the empty vector pGBKT7. 100 μl of a 1/10 dilution and a 1/100 dilution of the transformed cells were spread onto the following plates: SD/-Trp, SD/-Trp/X-α-Gal, SD/-Trp/X-α-Gal/AbA, SD/-Trp/-Leu (DDO), SD/-Trp/-Leu/X-α-Gal/AbA (DDO/X/A), SD/-Trp/-Leu/-His/-Ade (QDO), SD/-Trp/-Leu/-His/-Ade/X-α-Gal/AbA (QDO/X/A). Plates were incubated upside down at 30°C for 5 days and the assessment of bait (mDkk3) auto-activation was performed based on the presence or absence of colonies on the plates, according to the expected results.

2.2.25.5 Mating of mDkk3 bait containing yeast strain (Y2HGold) with the prey mouse library containing yeast strain (Y187)

Y2hGold haploid yeast strain was previously transformed with mDkk3 bait protein. Normalized Yeast Two-Hybrid mouse cDNA Library was cloned into GAL4 AD vector pGADT7 and transformed into haploid yeast strain Y187. The Normalized Universal Mouse Mate & Plate™ Library was acquired ready made from Clontech.

A concentrated overnight culture of Y2HGold (pGBKT7+mDkk3) was prepared. One fresh colony of the bait strain was incubated in SD/-Trp medium, with shaking at 250 rpm at 30°C, until OD₆₀₀ reached 0.8 (18 hours). The cells were centrifuged at 1000 X g for 5 minutes and the pellet was resuspended with SD/-Trp medium to a cell density of > 1x10⁸ cells/mL (4-5 mL). The 1 mL prey library strain was thawed and combined with the bait strain suspension in a sterile 2 L flask. 45 mL of 2xYPDA medium containing 50 µg/mL of Kanamycin was added to the flask. The library vial was rinsed twice with 1 ml 2xYPDA and added to the 2 L flask. The cell suspension was incubated at 30°C for 20–24 hours, with slowly shaking (30–50 rpm), until zygotes were present in the culture. The 2L flask was next rinsed twice with 50 mL of 0.5xYPDA medium (with 50 µg/ml kanamycin), which was also used to resuspend the cell culture. After centrifugation (1000 x g, 10 minutes) the cell pellet was resuspended in 10 ml of 0.5xYPDA (50 µg/mL Kanamycin) medium. 200 µL of the mated cell culture was spread onto 150 mm DDO/X/A agar plates (55-60 plates). The plates were incubated at 30°C for 3–5 days. Blue colonies (diploid cells) were grown on the plates, and each colony was patched out onto higher stringency QDO/X/A agar plates. The colonies grown after 4 days of incubation at 30°C were re-streaked onto QDO/X/A agar plates and this step was repeated two more times to segregate the genuine blue colonies from white colonies.

2.2.25.6 Library prey plasmid rescue and library screening

The prey plasmid was rescued or isolated from yeast using the Easy Yeast Plasmid Isolation Kit (Clontech). Each colony grown on the last QDO/X/A plate was streaked onto SD/-Leu agar plate (selective medium appropriate for the plasmid pGADT7, corresponding to the prey library). After, incubation at 30°C for 3-5 days, one well-isolated yeast colony from each plate was picked and spread as a 1 cm x 1 cm square on a fresh SD/-Leu agar plate. After the patches grew, half of each was scooped and resuspended in 500 µL of 10mM EDTA in a 1.5 mL centrifuge tube. Cells were centrifuged (11000 x g, 1 minute) and the pellet was resuspended in 200 µL of ZYM buffer. 20 µL of zymolase enzyme was added to the suspension to disrupt the yeast cell wall. The suspension was incubated for 1 hour at 30°C with gentle shaking. The spheroplasts formed were centrifuged at 2000 x g for 10 minutes and 250 µL of Y1 Buffer/RNase A solution was added to resuspend the pellet. Next, 250 µL of Y2 SDS/Alkaline Lysis Buffer was added to the suspension and the tube was inverted 6-8 times to mix the contents, followed by maximum 5 minutes of incubation at room temperature. 300 µL of Y3 Neutralization Buffer was added and after inverting again the tube 6-8 times, the lysate

was clarified by centrifugation (11000 x g, 5 minutes; Room temperature). The supernatant was transferred to a clean tube and the centrifugation step was repeated. The clarified lysate was loaded onto the Yeast Plasmid Spin column placed inside a 2 mL collection tube, and centrifuged at 11000 x g for 1 minute. The flow-through was discarded and the spin column was placed back into the 2 mL collection tube. 450 μ L of Y4 Wash Buffer was added to the spin column, which was then centrifuged at 11000 x g for 3 minutes. Residual Wash Buffer was removed by an additional centrifugation step, after which the spin column was placed in a 1.5 mL tube. 50 μ L of YE Elution Buffer was added to the spin column and incubated for 1 minute at room temperature. Following centrifugation the eluted fraction was collected, as it contained the rescued plasmid.

Stellar competent cells (Clontech) were transformed with 2.5 μ L of the purified yeast plasmid. Transformed competent cells were spread on LB agar plates containing 100 μ g/mL of Ampicillin and then amplified on LB medium/Ampicillin. The plasmid was isolated from the bacterial competent cells using the QIAprep Spin Miniprep Kit (Qiagen) and sent for sequencing with standard T7 primers. The sequencing results allowed the identification of the prey proteins interacting with the bait Dkk3.

2.2.25.7 Confirmation of Positive Interactions

The positive interactions obtained were confirmed by co-transforming in Y2HGold competent cells 100 ng of pGBKT7-mDkk3 with 100 ng of the rescued Prey plasmid (pGADT7-Prey) and, separately, 100 ng of empty pGBKT7 with 100 ng of pGADT7-Prey (Figure 2.2.25.7). 100 μ L of 1/10 and 1/100 dilutions of the transformation mix were spread on the plates: DDO/X and QDO/X/A. After 3-5 days of 30°C incubation the results were assessed based on the presence or absence of colonies, according to the expected results.

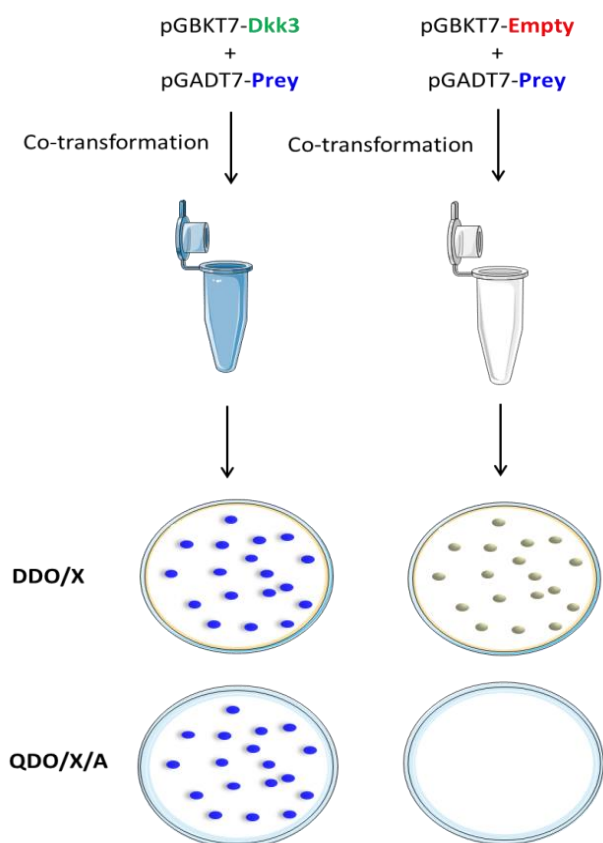


Figure 2.2.25.7: Co-transformation strategy for confirmation of positive interaction. Y2HGold competent yeast cells were co-transformed with the identified prey-plasmid and either Dkk3-bait plasmid or bait-empty vector. The genuine interaction between Dkk3 and ITG α 5/ITG β 1 was confirmed by the presence of blue colonies on both DDO/X and QDO/X/A plates. In contrast, the cells co-transformed with the prey plasmid and the bait-empty vector grew as white colonies on DDO/X but not on QDO/X/A.

2.2.26 Statistical Analysis of Data

Statistical analysis and graphs were performed with GraphPad Prism 7 software. All numerical data were tested for normal distribution using Shapiro-Wilk normality test. To compare two distinct sets of data the two-tailed Student's unpaired t-test was used; To compare more than two sets of data with one variable, One way ANOVA followed by Bonferroni's multiple comparison test was used ; To compare more than two sets of data and more than one variable, Two way ANOVA followed by Bonferroni's multiple comparison test was used. Data was presented as the means \pm Standard Error of Mean (S.E.M.) of at least three independent experiments ($n \geq 3$) and significance was accepted when $p < 0.05$.

Chapter 3: Results

3.1 Purity of Sca-1+ Adventitial Progenitor Cell population

An increasing number of studies has provided evidences on the active role of the adventitia vessel layer in vascular diseases [5, 47, 68-71, 259-262]. In this regard, previous work from our laboratory was one of the pioneers in identifying the presence of a population of vascular stem/progenitor cells resident in the adventitia of the aortic root, which can differentiate into SMCs and accumulate in neointimal lesions. Amongst these progenitor cells, cells positive for stem cell antigen-1 (Sca-1+) were found to be abundant in the adventitia [6].

It has been well established that chemokines, such as Sdf-1 α , recruit and home circulating progenitor cells [263, 264]. The recruitment of the resident Sca-1+ progenitor cells by Sdf-1 α was demonstrated in a study published by our group [102]. Nevertheless, the mechanism driving the migration of the Sca-1+ cells was not described.

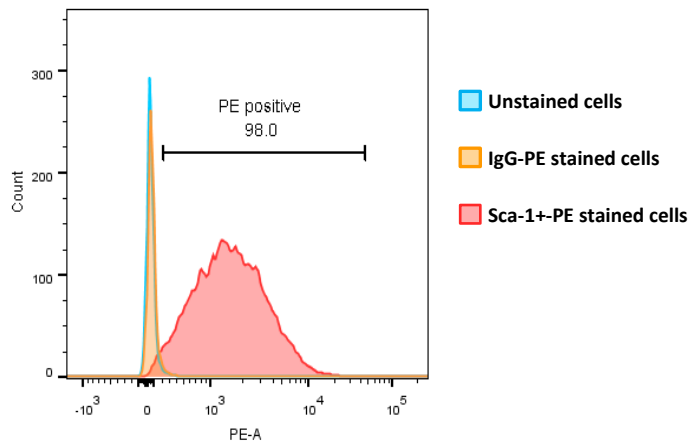
Work from our laboratory has also revealed an important role for the glycoprotein Dkk3 in inducing the differentiation of partially-induced pluripotent stem cells (PiPS) and embryonic stem cells (ESs) into SMCs [243, 244]. These findings suggested that it was important to explore the role of Dkk3 in Sca-1+ cells.

Taken together the above described, this project studied the potential role of Dkk3 in inducing the migration of the Sca-1+ vascular progenitor cells, where Sdf-1 α was used as the positive control.

Sca-1+ adventitia-derived progenitor cells (Sca-1+ APCs) from murine aorta, isolated and selected as described before, were used in this project as the source of the Sca-1+ vascular progenitor cells, from passage 6 to passage 30. Three batches of cells were used in the following experiments. In order to assess if the purity of the Sca-1+ cell population was preserved after every 5 passages (Sca-1+ APCs were sorted by an immunomagnetic sorting system every 5 passages until reaching passage number 30), a flow cytometry analysis was performed.

The cells were incubated with Sca-1 antibody conjugated with the fluorochrome PE. Unstained cells (to detect auto-fluorescence) and IgG-PE incubated cells (to estimate nonspecific binding) were used as negative controls. The results showed an average purity of Sca-1+ cell population of 93% after 5 passages (Figure 3.1), which revealed that not only the immunomagnetic sorting system proves to be an efficient method for selecting the Sca-1+ cells, but also that the purity of the cell population was stable after 5 passages.

A Flow Cytometry analysis of Sca-1+ APCs



B Quantification of Sca-1+ APCs

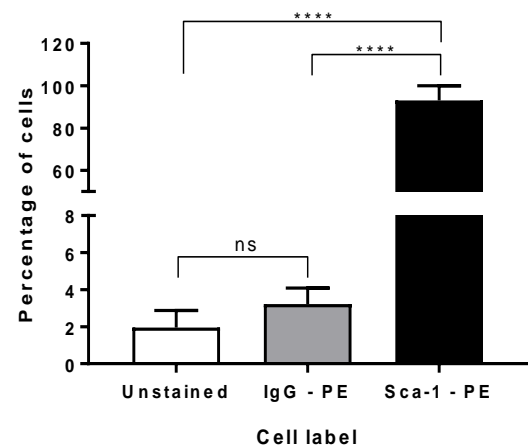


Figure 3.1 Sca-1+ progenitor cell population purity analysis. A: Sca-1+ cell expression in a histogram plot. B: Quantification of Sca-1+ APCs. Adventitia-derived vascular progenitor cells were sorted for Sca-1 marker by an immunomagnetic sorting system. The purity of the cell population was assessed by flow cytometry analysis. After 5 passages, cells were sorted and separated into three groups: Negative control (unstained cells), Isotype control (cells incubated with the IgG-PE conjugated antibody) and cells incubated with the Sca-1-PE conjugated antibody. Sca-1+ cells corresponded to 93.13% of the population on average. (Data shown as mean \pm SEM, **** p <0.0001 by One-way ANOVA, followed by Bonferroni multiple comparison test, $n=4$).

3.2 Dkk3 induced the migration of Sca-1+ vascular progenitor cells, *in vitro* and *ex vivo*

The first step of the study was to investigate whether Dkk3 had a chemotactic effect on adventitia-derived Sca-1+ progenitor cells (Sca-1+ APCs). For that reason, transwell migration and wound healing assays were performed. In previous studies, our group has shown that Sdf-1 α induces the migration of Sca-1+ cells *in vitro* and *ex vivo* in a decellularized vessel model, although the underlying mechanism was not explored [102, 103]. To further confirm the chemotaxis effect of Sdf-1 α and as a positive control for Sca-1+ cell migration, the migratory response of Sca-1+ cells to Sdf-1 α was analysed concomitantly of Dkk3.

3.2.1. Transwell migration assay of Sca-1+ progenitor cells towards Dkk3 and Sdf-1 α treatments

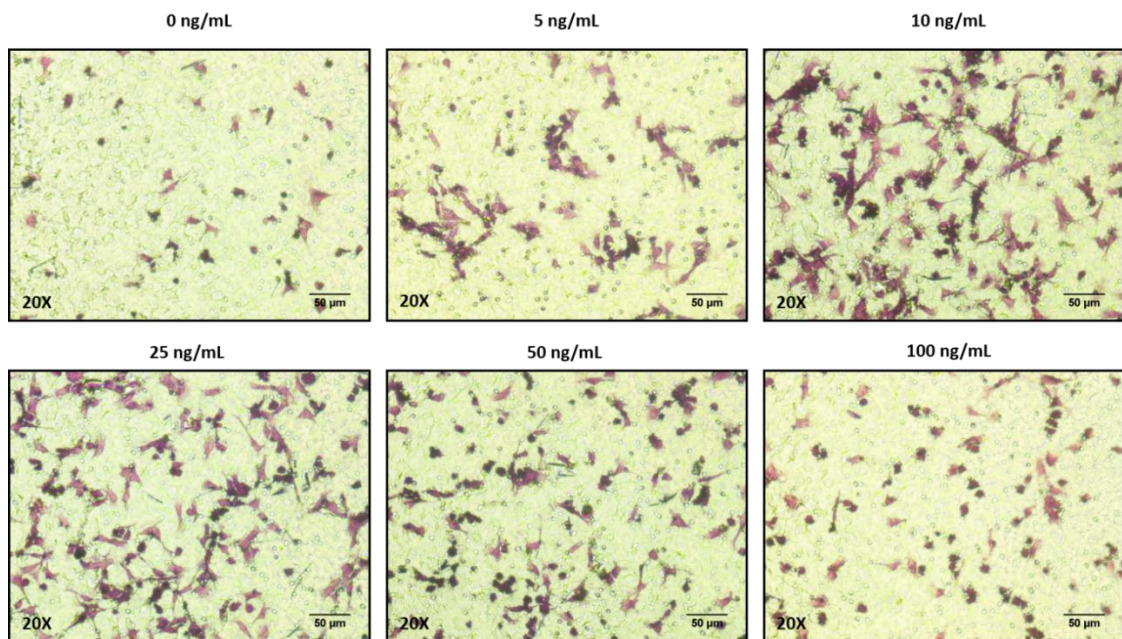
After overnight starvation, Sca-1+ progenitor cells, re-suspended in 0.2% serum medium, were seeded in the upper chamber of 8.0 μ m pore membrane transwells. Increasing concentrations of Dkk3 and Sdf-1 α (0-100 ng/mL) in 0.2% serum medium were loaded in the lower chamber. The cells were allowed to migrate overnight.

After removing the cells from the upper chamber (non-migrated cells), the cells which had migrated to the lower chamber were fixed with PFA and stained with crystal violet dye. Sca-1+ cells were next quantified under the microscope at a magnification of 10X.

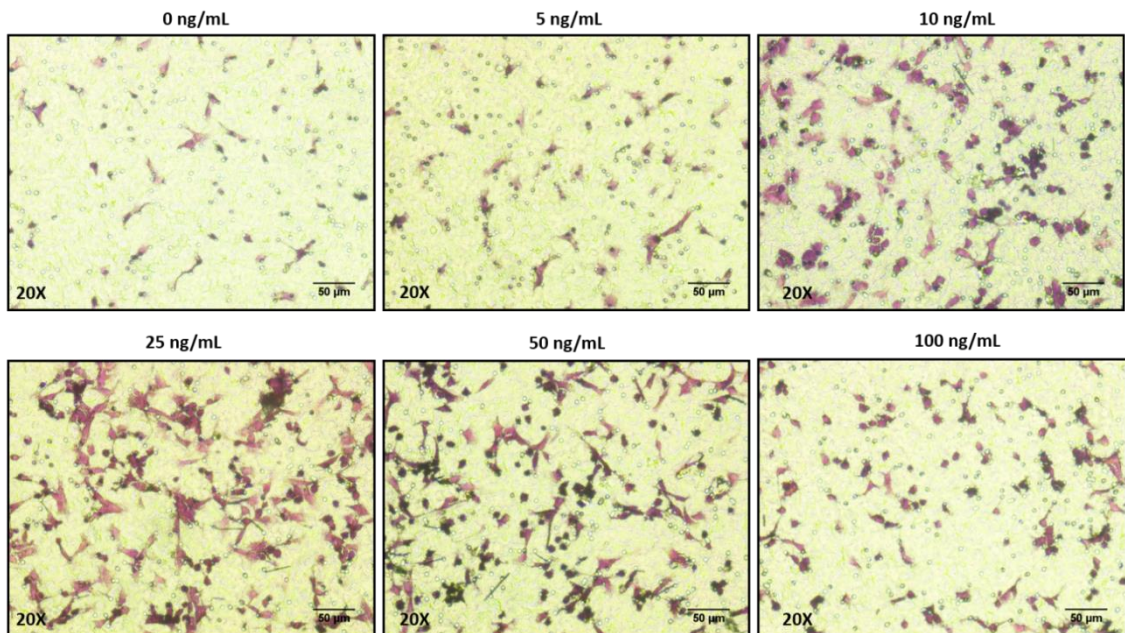
The data obtained revealed that, as previously shown, Sdf-1 α induced the migration of Sca-1+ cell (Figure 3.2.1A, 3.2.1C), with a 1.5 to 2 fold increase in cell migration compared to non-treated cells. No dose effect was observed, as the peak of migration was observed with a concentration of 10 ng/mL of Sdf-1 α , and treatment with 100 ng/mL of Sdf-1 α rendered a migration level of Sca-1+ cells lower than the observed with 5 ng/mL of treatment.

Dkk3 also induced the migration of Sca-1+ APCs, with a 1.3 to 2.1 fold increase compared to non-treated cells (Figure 3.2.1B, 3.2.1D). The migration level reached its peak at the concentration of 25 ng/mL. Similarly, to what was observed with Sdf-1 α treatment, when higher concentration was used, such as 100 ng/mL, the cell migration rate started to decline.

A Sca-1+ progenitor cell migration in response to Sdf-1 α - Transwell migration assay

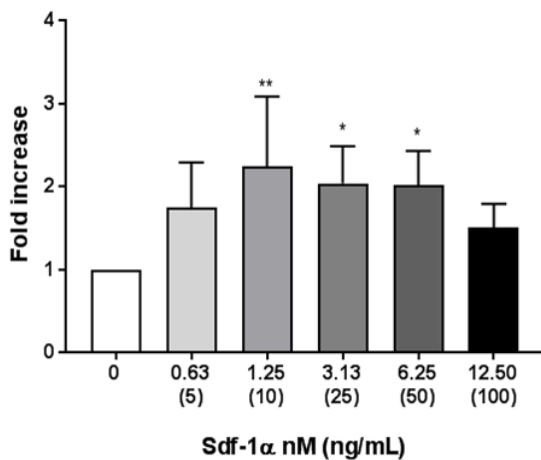


B Sca-1+ progenitor cell migration in response to Dkk3 - Transwell migration assay



The decrease in Sca-1+ APCs migration at the highest doses considered (100 ng/mL) for both Dkk3 and Sdf-1 α treatments could imply the possibility of the cells having passed the saturation point of their migratory response. Shorter time points or even higher doses of treatment could reveal an increased migration of the cells.

C Quantification of Sca-1+ APC migration in response to Sdf-1 α - Transwell assay



D Quantification of Sca-1+ APC migration in response to Dkk3 - Transwell assay

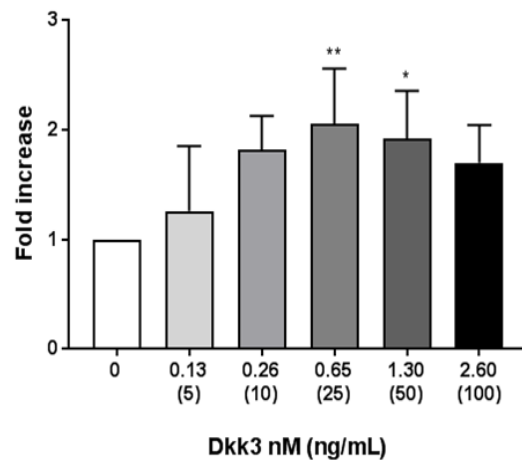


Figure 3.2.1 Dkk3 and Sdf-1 α induce the migration of Sca-1+ progenitor cells in the transwell migration assay. A, B: Representative images of migrated Sca-1+ cells in the transwells, treated respectively with Sdf-1 α and Dkk3, at 20X magnification. C, D: Cell quantification of 5 different fields of each transwell insert at 10X magnification. The Transwell migration assay was performed in order to study the chemotaxis of Sca-1+ resident progenitor cells in response to Dkk3 and Sdf-1 α stimulation at increasing concentration 0-100 ng/mL. The cells were seeded in the upper chamber of the 8.0 μ m pore membrane transwell and the treatment was added in the lower chamber. After overnight incubation, the migrated cells were fixed and stained. The fold was calculated against the 0.2% serum medium control. The Sca-1+ progenitor cell migration was induced toward Dkk3 (particularly at 25 ng/mL) and Sdf-1 α (especially at 10ng/mL) treatments, with statistical significance at 10-50 ng/mL for Sdf-1 α and 25-50 ng/mL for Dkk3. (Data shown as mean \pm SEM, **p<0.001, *p<0.05, by One-way ANOVA, followed by Bonferroni multiple comparison test, n=5).

3.2.2 Wound healing migration assay of Sca-1+ progenitor cells in response to Dkk3 and Sdf-1 α treatments

To further assess if Dkk3 affects the migratory ability of Sca-1+ progenitor cells *in vitro*, a wound healing assay was performed. Sca-1+ APCs were seeded in 12 well plates in complete medium. The next day, they were starved overnight with 0.2% serum medium. After starvation, a scratch was made in each well and increasing concentrations of Dkk3 and Sdf-1 α treatments in 0.2% serum medium were added (0-100 ng/mL). The Sca-1+ progenitor cells were allowed to migrate, i.e., close the wound, overnight. Cell migration was stopped by washing and fixing the cells, which was

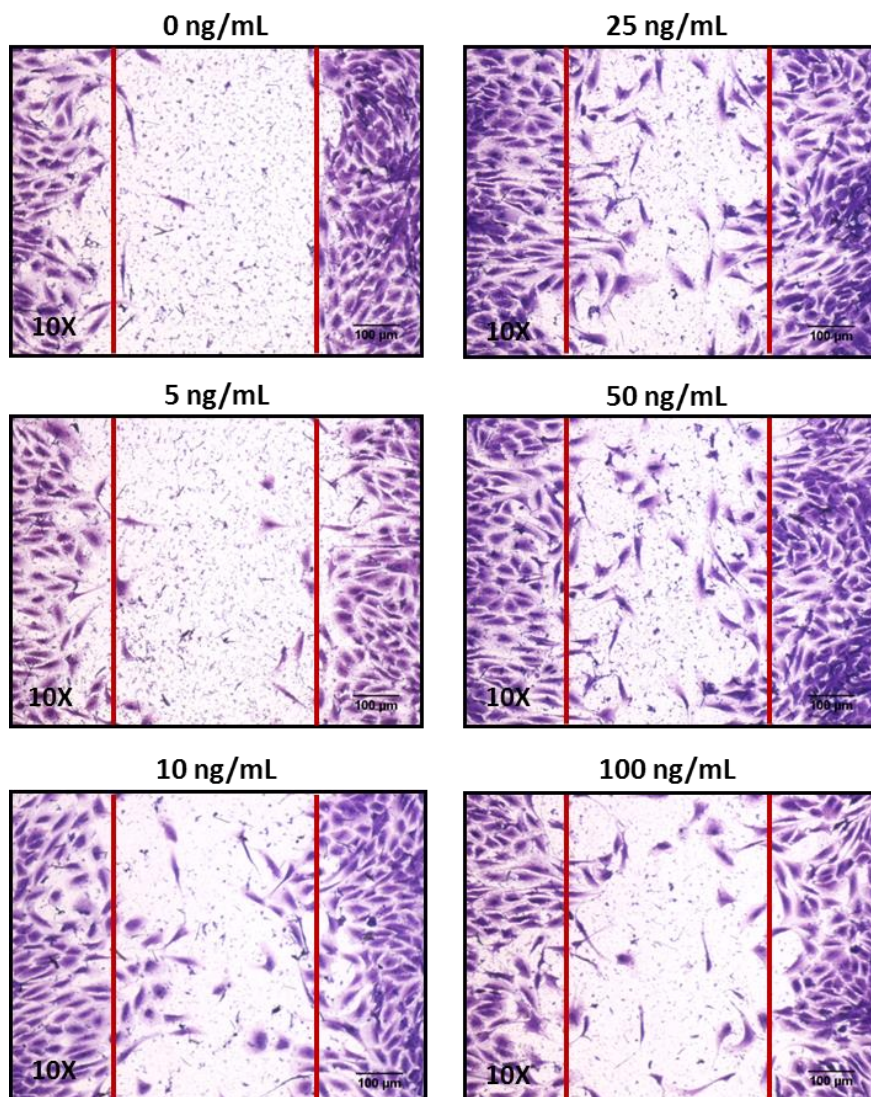
followed by crystal violet staining. Finally, cell quantification was carried out under the microscope at a magnification of 10X.

As anticipated, Sdf-1 α treatment (10-100 ng/mL) induced the migration of Sca-1+ cells. The highest migration rate (1.8 fold increase compared to control) was achieved with 25 ng/mL of Sdf-1 α (Figures 3.2.2A and 3.2.2C).

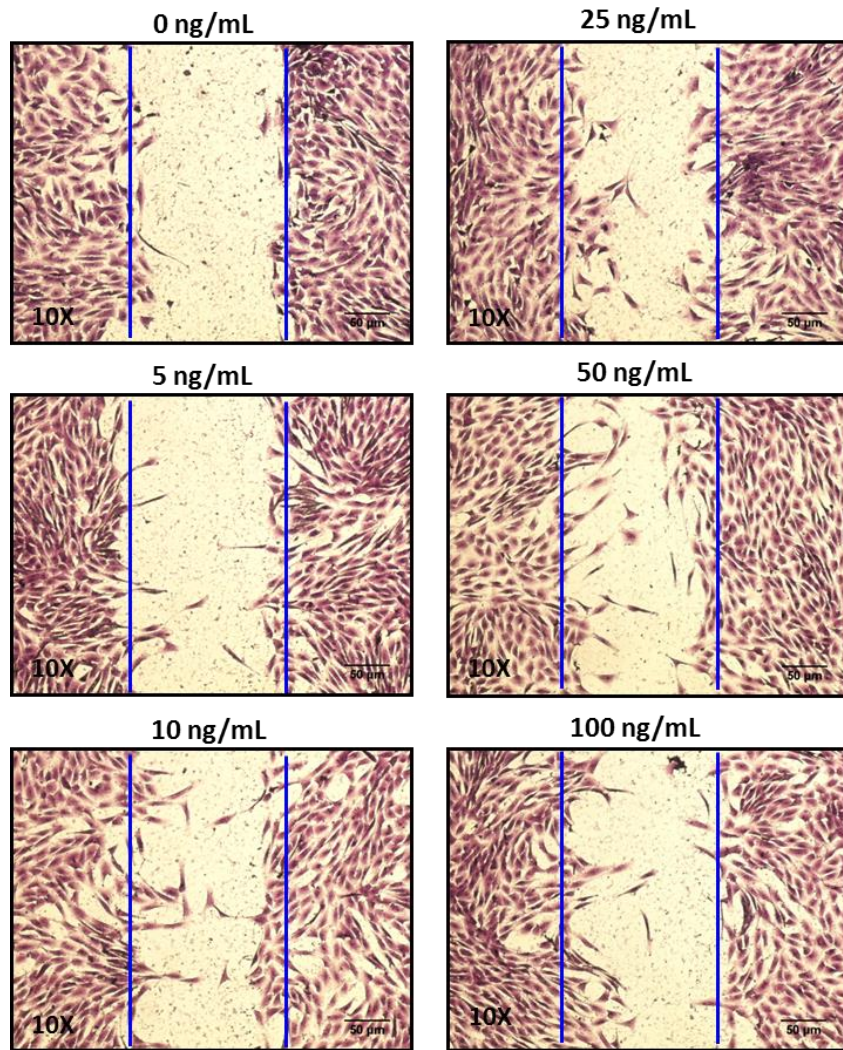
In this migration method, Dkk3 treatment also revealed to promote migration of the Sca-1+ cells, with statistical significance at concentrations 10, 25 and 50 ng/mL and with 1.7, 1.6 and 1.7 fold increase, respectively (Figures 3.2.2B and 3.2.2D).

Interestingly, as observed in the transwell assay, cell migration started to decrease at higher concentration (100 ng/mL) for both Dkk3 and Sdf-1 α treatments.

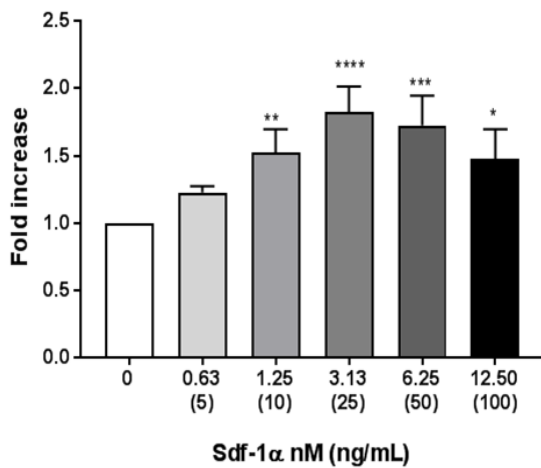
A Sca-1+ progenitor cell migration in response to Sdf-1 α - Wound healing migration assay



B Sca-1+ progenitor cell migration in response to Dkk3 - Wound healing migration assay



C Quantification of Sca-1+ APC migration in response to Sdf-1 α – Wound healing assay



D Quantification of Sca-1+ APC migration in response to Dkk3 – Wound healing assay

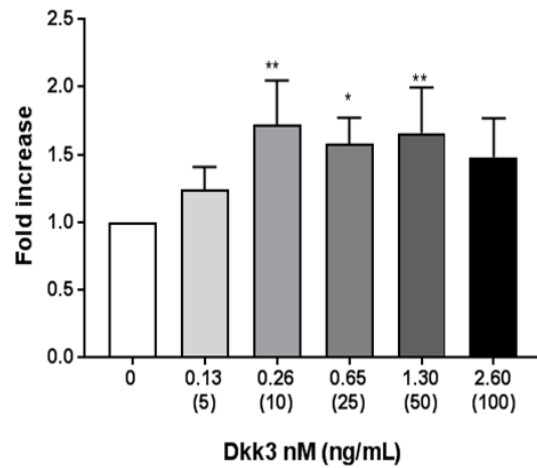


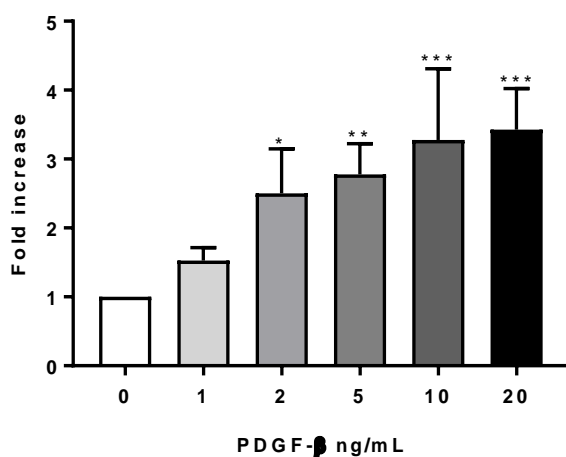
Figure 3.2.2 Dkk3 and Sdf-1 α induce the migration of Sca-1+ progenitor cells. A, B: Representative images of *in vitro* wound healing assay with Sca-1+ cells, treated with Sdf-1 α and Dkk3, respectively, at 20X magnification. The red and blue lines represent the scratch made at 0 h. C, D: Quantification of *in vitro* wound healing assay (5 different microscope fields were counted for each well, at 10X magnification). A wound healing migration assay was performed in order to study the effect of Dkk3 and Sdf-1 α on the Sca-1+ progenitor cells migration. Stimulation was performed with increasing concentrations 0-100 ng/mL. The cells were seeded in 12 well plates in complete medium and starved the next day overnight, prior to the migration assay. The treatment was added after a scratch was made and the Sca-1+ APCs were allowed to migrate overnight. Following washing, the cells were fixed and stained. The fold was calculated against the control (0 ng/mL of Sdf-1 α or Dkk3). Dkk3 and Sdf-1 α induced the migration of the Sca-1+ progenitor cells with statistical significance at 10-100 ng/mL for Sdf-1 α and 10-50 ng/mL for Dkk3. (Data shown as mean \pm SEM, ****p<0.00001, ***p<0.0001, **p<0.01, *p<0.05, by One-way ANOVA and Bonferroni's post-hoc test, n=4).

3.2.3 Pdgf- β induced the migration of Sca-1+ APCs, *in vitro*

In addition to Dkk3 and Sdf-1 α , the chemotactic role of Pdgf- β on Sca-1+ cells was also analysed using migration assays. This growth factor is well known for recruiting, amongst other cell types, vascular smooth muscle- and pericyte- progenitor cells [265-268] and for inducing the differentiation of vascular progenitor cells into SMCs [6]. For this reason, Pdgf- β was considered as a positive control when studying Dkk3 and Sdf-1 α effect *in vitro* and *ex vivo*.

Predictably, in both transwell and wound healing migration assays, Pdgf- β stimulated the migration of Sca-1+ progenitor cells in a dose dependent manner, with statistical significance at concentrations 2, 5, 10 and 20 ng/mL. Pdgf- β induced, respectively, 2.5 to 3.4 and 1.5 to 1.9 fold increase in cell migration in the transwell and wound healing assays.

A Quantification of Sca-1+ APC migration in response to Pdgf- β - Transwell migration assay



B Quantification of Sca-1+ APC migration in response to Pdgf- β - Wound healing assay

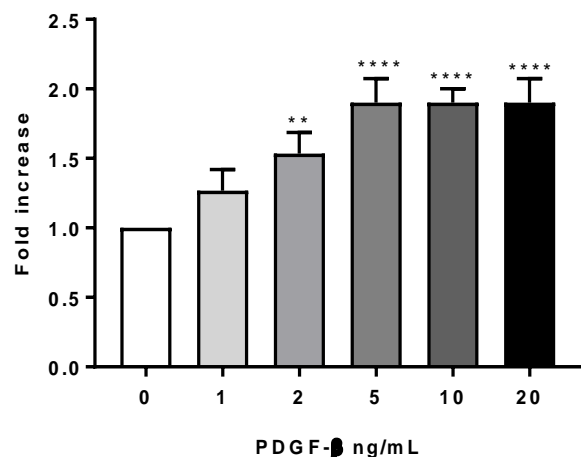


Figure 3.2.3 Pdgf- β induces the migration of Sca-1+ progenitor cells. A, B: Quantification of Sca-1+ cells, from 5 different fields, of the transwell inserts or of the wound healing wells, respectively, at 10X magnification. The fold was calculated against the control (0 ng/mL of Pdgf- β). Sca-1+ progenitor cell migration, stimulated by Pdgf- β , was increased in both migration assays, in a dose-dependent manner, with statistical significance at 2, 5, 10 and 20 ng/mL of treatment. (Data shown as mean \pm SEM, **** p <0.00001, *** p <0.0001, ** p <0.01, * p <0.05, by One-way ANOVA and Bonferroni post-hoc test, n=4).

3.2.4 Dkk3 promoted the migration of Sca-1+ APCs, *ex vivo*

To further explore the role of Dkk3 in the migration of vascular progenitor cells, an *ex vivo* model was used. The aortic ring assay is an explant methodology widely used to study angiogenesis in a three-dimensional model. In this setting, many features can be studied, such as cell migration and proliferation [269].

As mentioned before, Pdgf- β is recognized for its ability to recruit vascular smooth muscle cells, where it can contribute to neointima formation in vascular pathologies, namely in atherosclerosis and restenosis [270-272]. The aortic ring assay has been implemented in many studies to assess the mitogenic ability of Pdgf- β towards the vascular SMCs [273-276].

We sought to apply this explant assay to verify if Dkk3 induces cell outgrowth of the Sca-1+ cells from the aortic rings. Pdgf- β was used as the positive control of the experiment. This model was also used to study for the first time the effect of Sdf-1 α chemokine on the resident Sca-1+ progenitor cells migration in an *ex vivo* model.

Murine aortas were dissected, separated from fat and connective tissue, washed and cut into rings of roughly 1 mm size. In 8 well chamber slides, the rings were embedded in Matrigel and placed in a 37°C incubator. After three hours, control (1% serum medium) and treatment (25 ng/mL of Dkk3, 25 ng/mL of Sdf-1 α and 10 ng/mL of Pdgf- β , in 1% serum medium) medium were added. Every other day the rings were fed with the respective medium and after 8 days, i. e., before reaching the regression phase of the outgrowth, fixation and staining steps were followed.

Wild type and ApoE KO mice aortas were employed in this assay and quantification of the outgrowth took place both before and after fixation and immuno-fluorescence staining.

The wild type mice are relatively resistant to atherosclerosis, reason why ApoE KO mice were also used for the aortic ring assay.

The ApoE KO mouse model (Apolipoprotein E deficiency) constitutes a good model to reproduce the atherosclerotic lesions observed in humans and therefore, it is the most widely used mouse model to study the cellular and molecular mechanisms of atherosclerosis.

ApoE KO mice are apparently healthy, but exhibit significant phenotypic differences in their lipid and lipoprotein profiles in comparison with the wild type mice. The total plasma cholesterol level is markedly increased (hypercholesterolemia) and they develop spontaneous atherosclerotic lesions in several vascular beds, particularly in the aortic root, aortic arch and different branch points along the aorta.

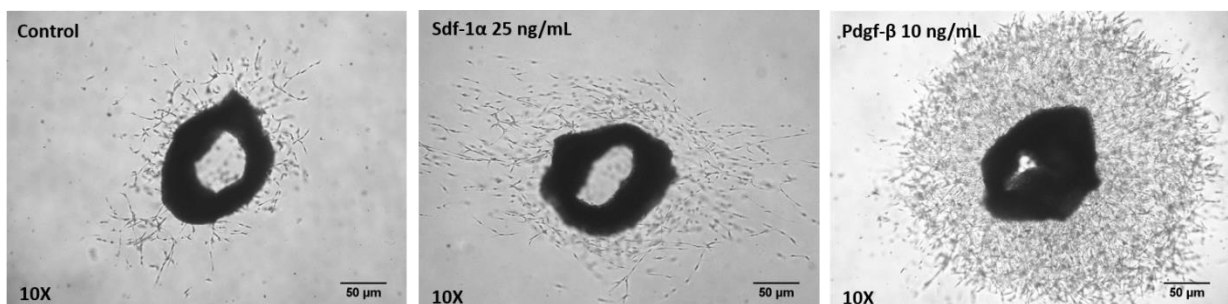
The ApoE KO mice fed with a normal western diet (21% fat, 0.2% cholesterol, 0% cholic acid) show a great increase in their plasma cholesterol and display accelerated atherosclerosis with enhanced inflammation, which has the advantage of avoiding to feed the mice with high fat toxic diet [277, 278].

3.2.4.1 Dkk3 induced cell outgrowth from the aortic rings

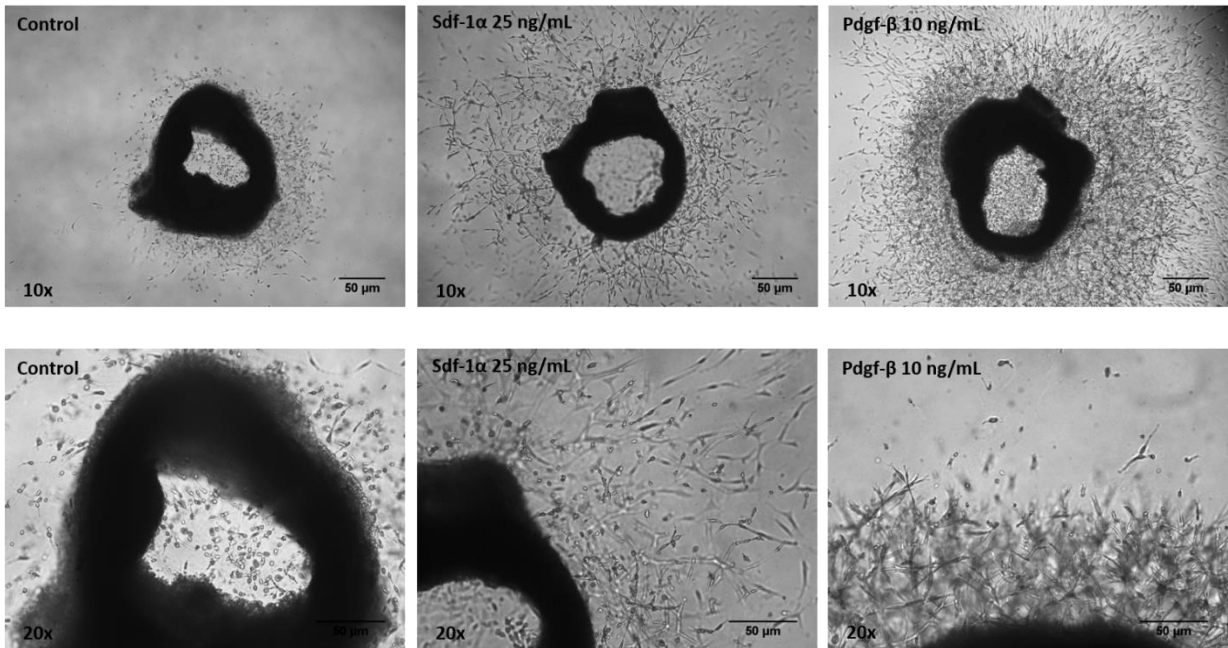
Pdgf- β and Sdf-1 α prompted cell outgrowth from the aortic rings in both wild type (2.2 and 1.3 fold increase, respectively) and ApoE KO mice (2.2 and 1.4 fold increase, respectively), where the growth factor showed a higher impact on cell outgrowth, compared to the chemokine (Figure 3.2.4.1 A-D).

Interestingly, in wild type mice, Dkk3 treatment seemed not to increase significantly cell outgrowth from the aortic rings (Figure 3.2.4.1 E and G). On the other hand, in ApoE KO mice, upon Dkk3 stimulation, a significant 1.4 fold increase in cell outgrowth was observed (Figure 3.2.4.1 F and H). The positive control Pdgf- β also displayed a higher effect on cell outgrowth when compared to Dkk3, in both wild type and ApoE KO mice. Nevertheless, no difference in cell outgrowth was found between the wild type and ApoE KO aortic rings treated with Pdgf- β , as in both conditions, a 2.2 fold increase was observed.

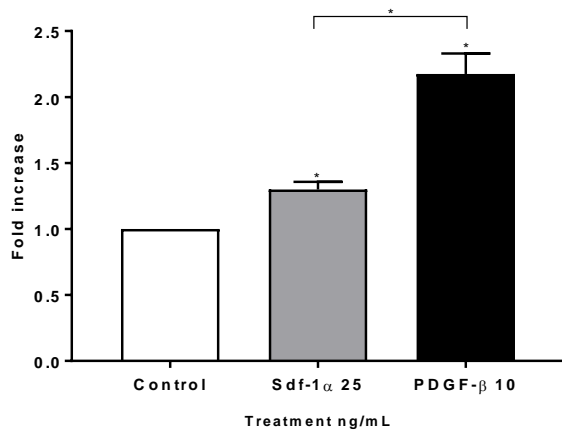
A Cell outgrowth from Wild Type murine aortic rings in response to Sdf-1 α stimulation



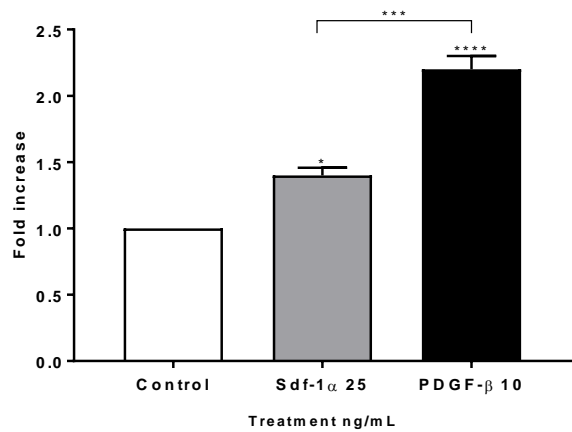
B Cell outgrowth from ApoE KO murine aortic rings in response to Sdf-1 α stimulation



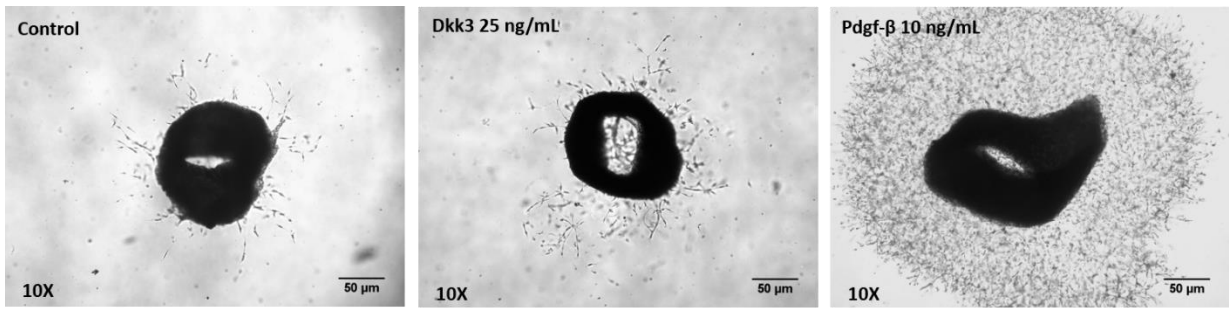
C Quantification of cell outgrowth from Wild type murine aortic rings induced by Sdf-1 α



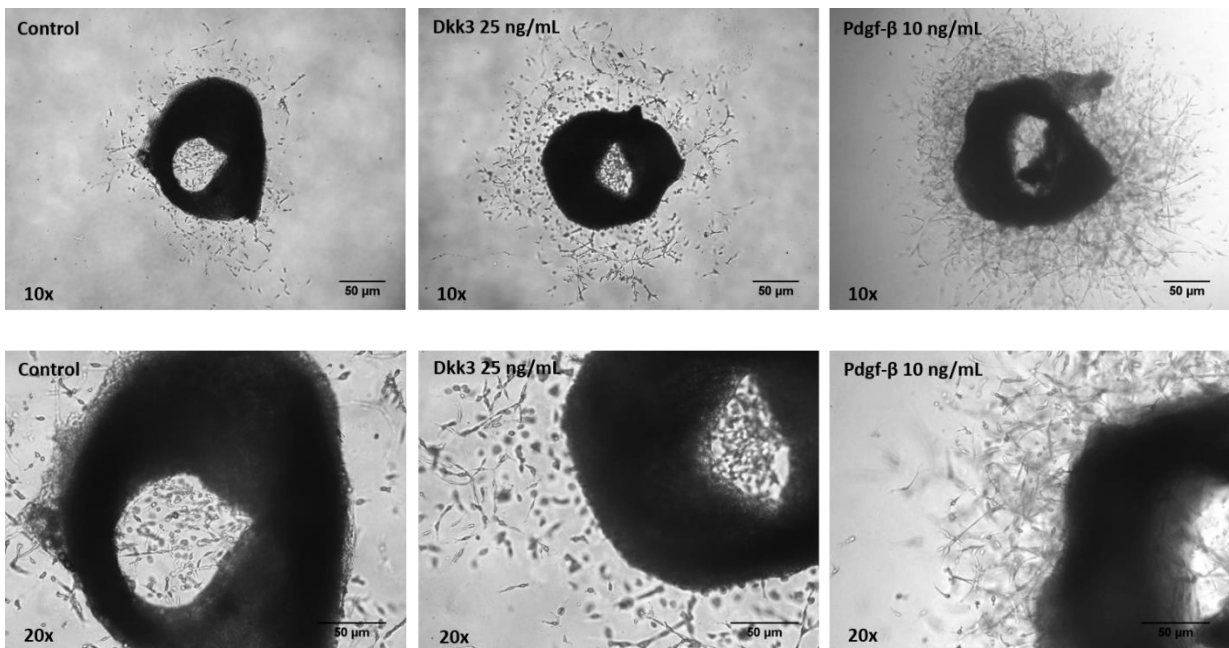
D Quantification of cell outgrowth from ApoE KO murine aortic rings induced by Sdf-1 α



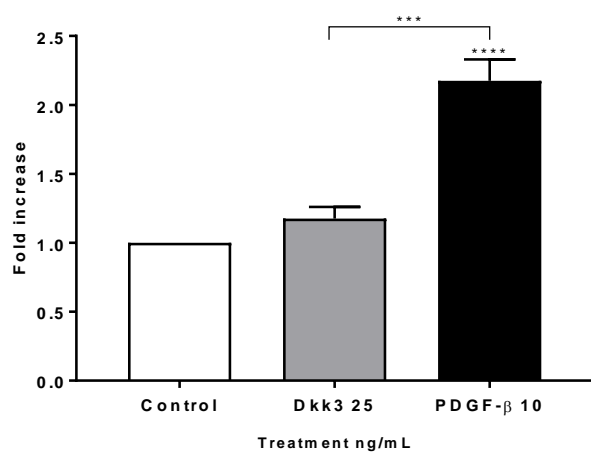
E Cell outgrowth from Wild Type murine aortic rings in response to Dkk3 stimulation



F Cell outgrowth from ApoE KO murine aortic rings in response to Dkk3 stimulation



G Quantification of cell outgrowth from Wild Type murine aortic rings induced by Dkk3



H Quantification of cell outgrowth from ApoE KO murine aortic rings induced by Dkk3

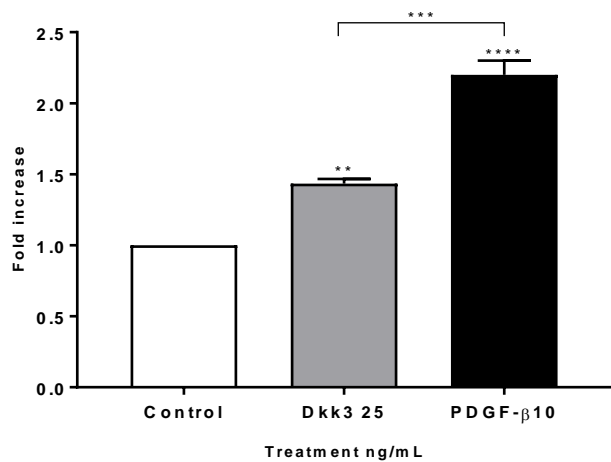


Figure 3.2.4.1 Dkk3 induced cell outgrowth from the aortic rings. Aortic ring explants from Wild type and ApoE KO mice were used to explore the chemotactic role of Dkk3 in a three-dimensional model. Aortic rings were cultured in Matrigel for 7 days in different condition medium (Dkk3 25 ng/mL, Sdf-1 α 25 ng/mL and Pdgf- β 10 ng/mL, in 1% serum) and compared to aortic rings cultured in control medium (1% serum medium). **A, E: Phase-contrast representative images of Wild type mice aortic segments, at 10x magnification, under control or treatment conditions. C, G: Outgrowth quantification of wild type aortic rings, n=4.** Sdf-1 α and Pdgf- β , the positive controls for cell migration, stimulated cell outgrowth from the aortic explants (1.3 and 2.2 fold increase compared to control, respectively). Dkk3 did not induce a significant increase in cell migration of wild type aortic rings. **B, F: Representative photographs of ApoE KO aortic rings, at 10X and 20X magnification. D, H: Quantification of cell outgrowth from ApoE KO aortic explants.** Both Dkk3 and Sdf-1 α significantly increased cell outgrowth in ApoE^{-/-} mice aortic segments, with 1.4 fold increase compared to control. Pdgf- β extensively promoted aortic ring cell outgrowth with 2.2 fold increase. Wild type and ApoE^{-/-} aortic rings stimulated with Pdgf- β showed similar cell outgrowth. On the contrary, increased cell outgrowths were observed in ApoE^{-/-} aortic rings compared to wild type explants, in response to Sdf-1 α and particularly Dkk3 treatment. (Data shown as mean \pm SEM, ****p<0.00001, ***p<0.0001, **p<0.01, *p<0.05, by One-way ANOVA and Bonferroni post-test, N=3).

3.2.4.2 Dkk3 promoted Sca-1+ cell outgrowth from the aortic rings

Cell outgrowth from aortic rings comprises various cell types, including endothelial cells, smooth muscle cells, pericytes, progenitor cells and fibroblasts [279, 280].

To test the hypothesis that Dkk3 can induce Sca-1+ cell outgrowth, aortic rings from transgenic Sca-1-GFP ApoE KO mice were isolated and cultured in the presence of Sdf-1 α and Dkk3. This mouse model allows rapid detection of Sca-1+ cells, as all cells positive for Sca-1+ marker will express green fluorescent protein (GFP).

Confocal microscopy analysis revealed the presence of Sca-1+-GFP cells in the outgrowth, under control condition and under Sdf-1 α and Dkk3 stimulation (Figure 3.2.4.2 A, B and C). Furthermore, the number of Sca-1+ cells, i. e., the number of GFP positive cells was significantly greater when ApoE^{-/-} explants were treated with either Dkk3 or Sdf-1 α , compared to control (1.4 fold increase for both conditions) (Figure 3.2.4.2D).

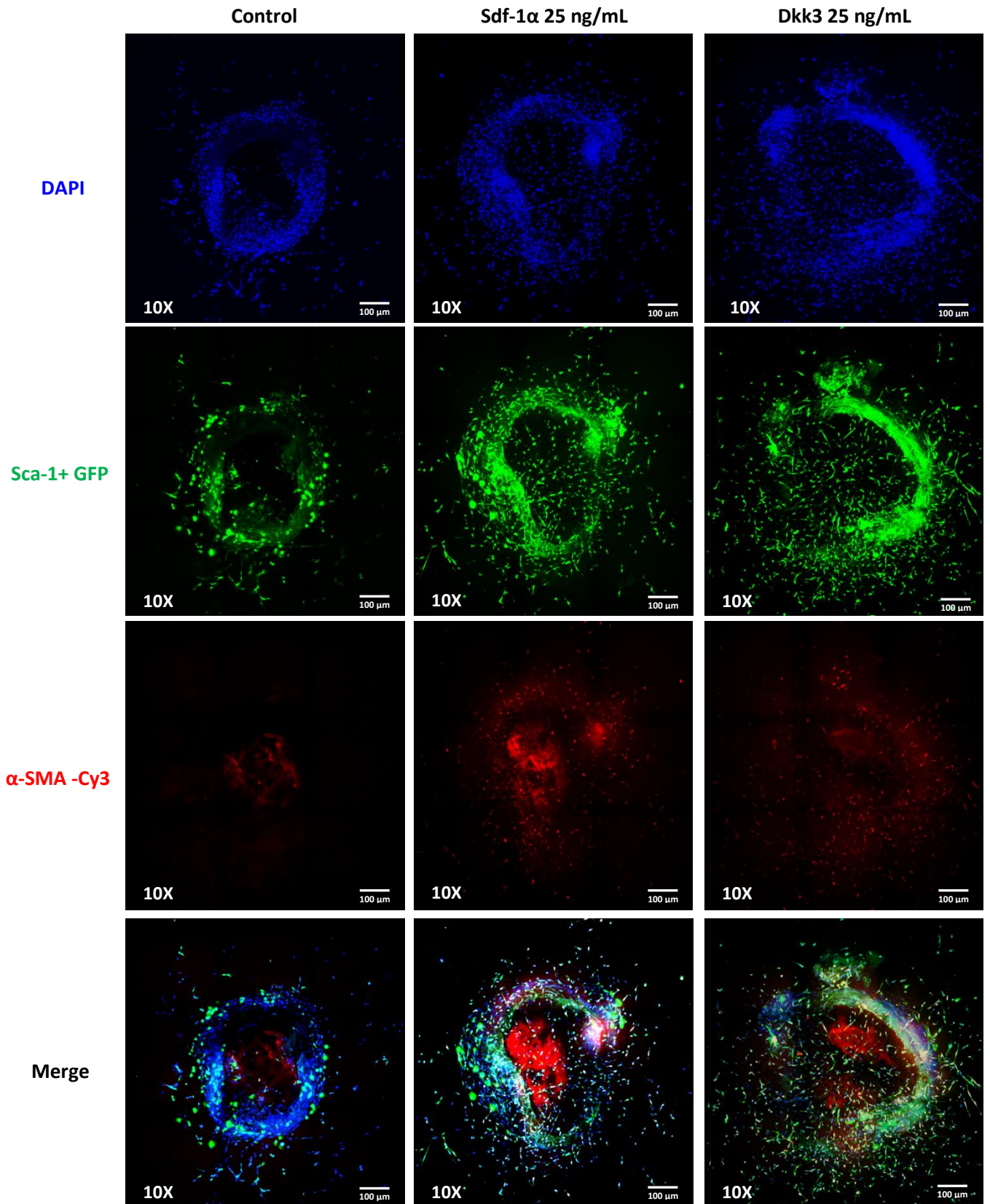
It is well established that SMCs and smooth muscle progenitor cells (SMPCs) are recruited and homed by Sdf-1 α [264, 281]. Additionally, this chemokine can also induce the differentiation of vascular progenitor cells into SMCs [102]. As mentioned previously, Dkk3 is also able to promote the differentiation of stem cells into SMCs *in vitro* [243, 244]. To investigate the role of Dkk3 on SMCs, we performed immunofluorescence staining using α -smooth muscle actin-Cy3 antibody (α -SMA

conjugated with Cy3). The staining enabled to detect the contribution of the SMCs to the outgrowth (Figure 3.2.4.2 A, B and C). Quantification of α -SMA labelled cells showed that both Dkk3 (2.1 fold increase) and Sdf-1 α (1.7 fold increase) induced SMC outgrowth, compared to the control group (Figure 3.2.4.2E).

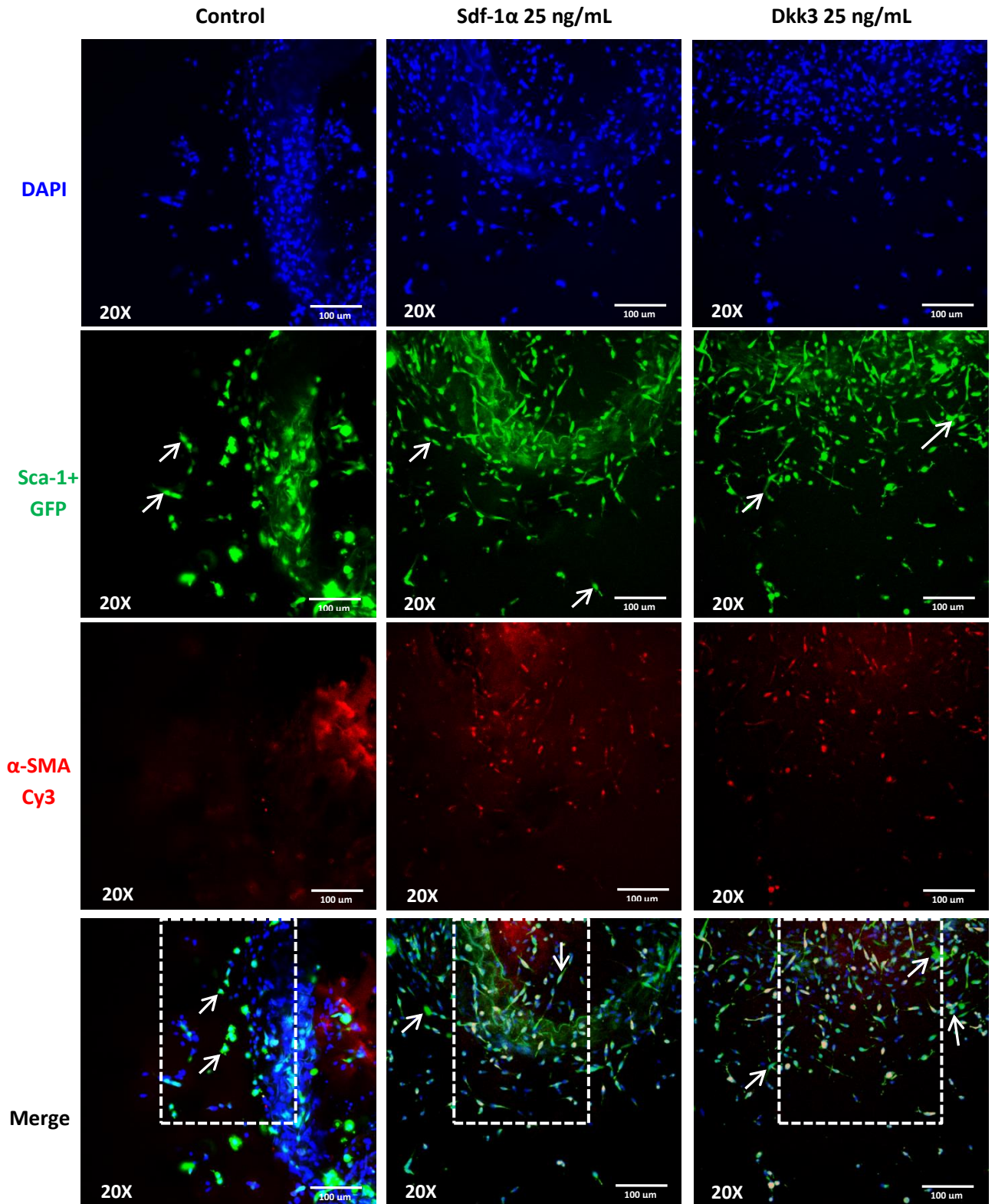
In some cells from the outgrowth, we observed co-localization between the GFP signal and the α -SMA-Cy3 staining. The quantification of the SMA positive GFP cells (Figure 3.2.4.2F) demonstrated that Dkk3 (2.1 fold increase) and Sdf-1 α (1.9 fold increase) equally increased the number of cells positive for Sca-1 marker and smooth muscle cell marker SMA. These cells could represent Sca-1+ cells differentiating into SMCs, and/or SMCs de-differentiating into Sca-1+ cells, when migrating from the aortic ring.

It is worthwhile mentioning that not all the Sca-1-GFP cells were also positive for α -SMA-Cy3 (Figure 3.2.4.2B and C, white arrow). Notably, this was more apparent in the control group.

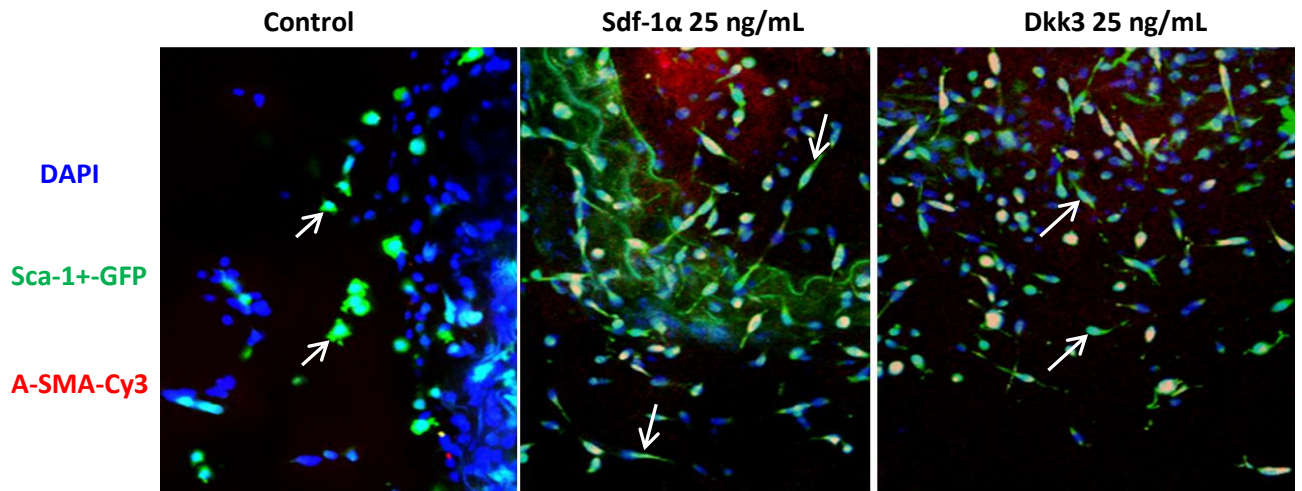
A Dkk3 and Sdf-1 α promoted Sca-1+ vascular progenitor cell outgrowth from mouse ApoE KO aortic rings – 10X magnification



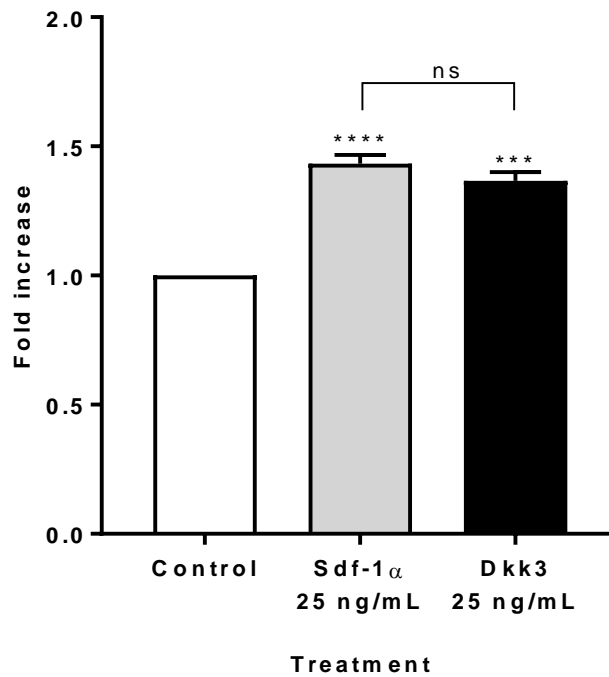
B Dkk3 and Sdf-1 α promoted Sca-1+ vascular progenitor cell outgrowth from mouse ApoE KO aortic rings – 20X magnification



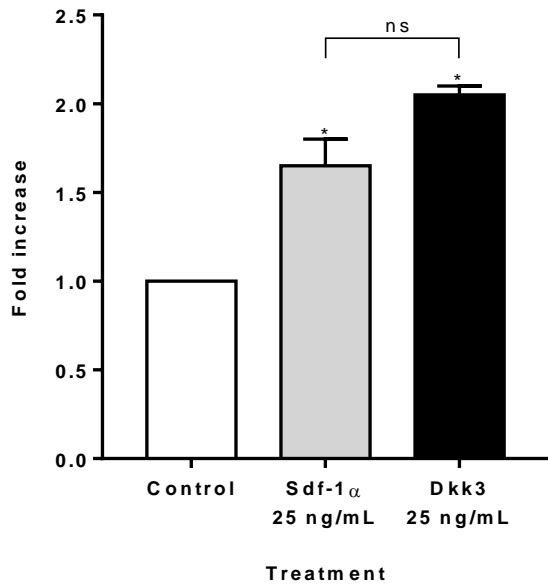
C Dkk3 and Sdf-1 α promoted Sca-1+ vascular progenitor cell outgrowth from mouse ApoE KO aortic rings – Zoom in of 20X magnification images



D Quantification of GFP-Sca-1+ cell outgrowth from mouse ApoE^{-/-} aortic ring, induced by Dkk3 and Sdf-1 α treatments



E Quantification of α -SMA-Cy3 cell outgrowth in ApoE KO aortic ring, induced by Dkk3 or Sdf-1 α treatments



F Quantification of Sca-1+GFP/ α -SMA-Cy3 cell outgrowth in ApoE KO aortic ring, induced by Dkk3 and Sdf-1 α treatments

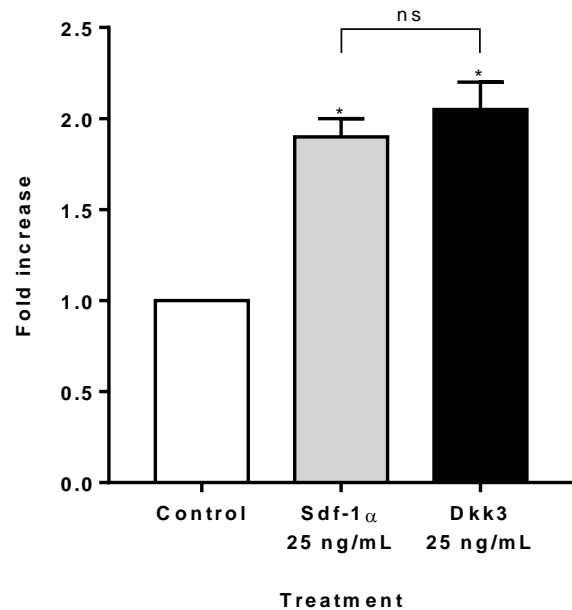


Figure 3.2.4.2 Dkk3 promotes Sca-1+ cell outgrowth from the aortic rings. Sca-1-GFP ApoE KO mice aortas were used in the *ex vivo* assay. Immunofluorescence staining was performed on the aortic rings after fixation and permeabilization steps. α -SMA-Cy3 was used to label the SMCs. **A, B: Respectively, 10X and 20X magnifications of representative images of the rings untreated or stimulated with 25ng/mL of either Sdf-1 α or Dkk3.** The white arrows indicate Sca-1-GFP cells without co-localization with α -SMA-Cy3. Dashed boxes represent the zoomed-in areas. **C: Zoomed-in areas of figure B. D: Quantification of Sca-1-GFP cells in the outgrowth.** Dkk3 and Sdf-1 α equally induced Sca-1+ cell migration/proliferation, with no statistical difference between both treatment groups (1.4 fold increase). **E: Quantification of α -SMA-Cy3 labelled cells, in the cell outgrowth.** Dkk3 exhibited the highest increase in the SMC outgrowth (2.1 fold increase against Control), followed by Sdf-1 α (1.7 fold increase), once more with no statistical significance between both groups. **F: Quantification of the number of cells within the outgrowth presenting co-localization of Sca-1-GFP and α -SMA-Cy3.** Dkk3 (2.1 fold increase) and Sdf-1 α (1.9 fold increase) induced the outgrowth of double positive cells for Sca-1+ and SMC markers, when compared to the untreated group. (Data shown as mean \pm SEM, **** p <0.00001, *** p <0.0001, * p <0.05, by One-way ANOVA and followed by Bonferroni multiple comparison test, n =3).

3.2.5 *In vitro* proliferation of Sca-1+ APCs only took place after 48 hours of Dkk3 treatment

Differences in cell outgrowth could be explained by changes in cell migration or cell proliferation. Therefore, it was important to determine if Dkk3 could also induce *in vitro* the proliferation of the Sca-1+ progenitor cells. BrdU incorporation test was performed.

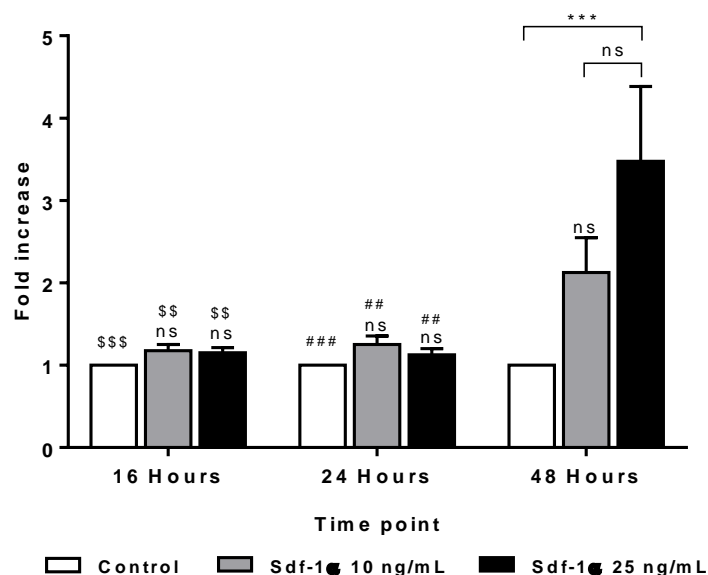
Cells in replication synthesize new DNA, in which the BrdU will be incorporated instead of thymidine. Therefore, when there is a higher number of proliferating cells there will also be a greater level of BrdU incorporation, which can be measured colorimetrically.

For this experiment, 3 time points were selected, 16 hours (the time point used in the migration assays), 24 hours and 48 hours. In addition, for each treatment, the two concentrations that provided the highest rate of migration were also considered. Pdgf- β was used as the positive control.

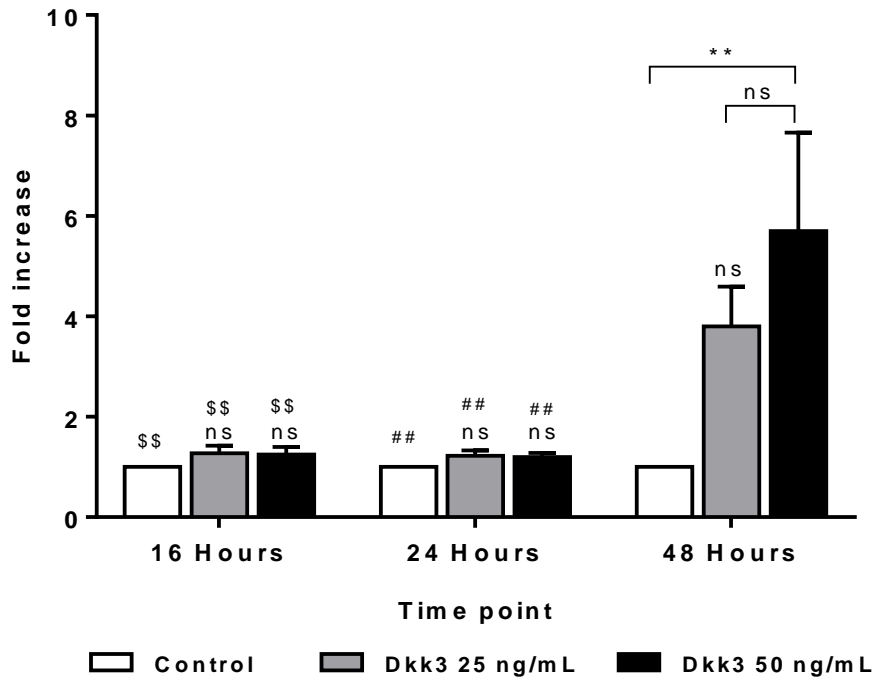
Sca-1+ cells were seeded in 96 well plates in complete medium. The next day, the cells were starved overnight and treated for different periods of time. BrdU was then added and the cells were reincubated for 2 more hours. Next, the wells were washed and the cells were fixed and their DNA was denatured. Finally, anti-BrdU antibody was added and the absorbance was measured after the substrate reaction took place.

The data collected revealed that, for all the conditions (Dkk3, Sdf-1 α and the positive control Pdgf- β) and at all the respective concentrations used, the proliferation rate was only induced after 48 hours of treatment (Figure 3.2.5 A-C). Our *in vitro* migration assays were carried out overnight, i. e., no longer than 16 hours, therefore, it was possible to conclude that Dkk3 primarily promotes Sca-1+ progenitor cell migration. Similarly, the same inference applies when treating the cells with Sdf-1 α and Pdgf- β .

A Proliferation level of Sca-1+ progenitor cells in response to Sdf-1 α BrdU incorporation measurement



**B Proliferation level of Sca-1+ progenitor cells in response to Dkk3
BrdU incorporation measurement**



**C Proliferation level of Sca-1+ progenitor cells in response to Pdgf-β
BrdU incorporation measurement**

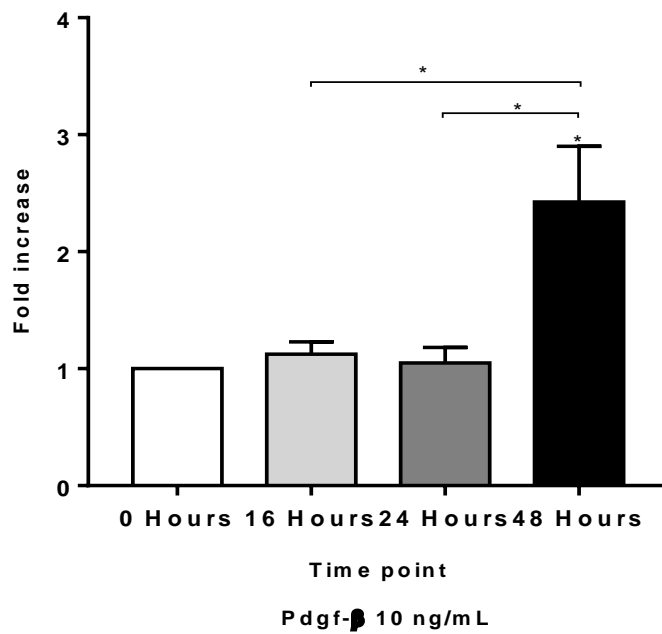


Figure 3.2.5 *In vitro* proliferation of Sca-1+ progenitor cells only takes place after 48 hours of Dkk3 treatment. To measure the proliferation rate of the Sca-1+ progenitor cells, upon Dkk3 stimulation, BrdU incorporation colorimetric method was employed. The level of absorbance correlates to the level of BrdU incorporation during replication and therefore to the rate of cell proliferation. **A, B, C: Quantification of the proliferation rate of Sca-1+ APCs in response to Sdf-1 α , Dkk3 and Pdgf- β stimulation, respectively.** The time points considered were 16 hours, 24 hours and 48 hours. The concentrations selected for each treatment corresponded to those which rendered the greatest degree of cell migration. For all the three conditions, the proliferation rate was only induced at 48 hours of stimulation, at all the concentrations considered. (Data shown as mean \pm SEM, *** p <0.0001, ** p <0.01, * p <0.05, by Two-way ANOVA for A and B and One-way ANOVA for C, followed by Bonferroni post-hoc test, n =4. The symbols *, # and \$ correspond to the fold increase for each time point against the highest concentration at 48 hours).

3.2.6 Conclusion of part 1: Dkk3 induced the migration of Sca-1+ vascular progenitor cells, *in vitro* and *ex vivo*

- This first part of the project disclosed that Dkk3 promoted the migration of the Sca-1+ APCs *in vitro*.
- Furthermore, Dkk3 treatment only promoted the proliferation of Sca-1+ APCs after 48 hours, *in vitro*.
- Dkk3 also induced Sca-1+ cell migration in a three-dimensional model of cell outgrowth (*ex vivo*).
- These evidences together suggested a potential role for Dkk3 as a chemokine-like protein.
- Dkk3 glycoprotein also stimulated the migration/proliferation of SMCs in the cell outgrowth, when compared to the Control condition.
- The concentration of 25 ng/mL of Dkk3 was used in the subsequent experiments, because it provided the highest level of migration *in vitro* and promoted a significant Sca-1+ cell outgrowth *ex vivo*.
- As expected, Pdgf- β and Sdf-1 α also stimulated the Sca-1+ progenitor cell migration. Those factors represent therefore good positive controls to evaluate the migration effect of Dkk3 in the following studies.
- Finally, in the *ex vivo* model, an increased number of Sca-1+ cells (GFP) also exhibiting α -SMA expression in response to Dkk3 treatment could be quantified, indicating either a differentiation or a de-differentiation process mediated by Dkk3.

3.3 CXCR7 is highly expressed in Sca-1+ APCs

The migration mechanism of a cell is activated when a ligand binds to its receptor which is expressed on the cell surface.

The receptors to which Sdf-1 α binds are CXCR4 and CXCR7 [150, 282-284].

No receptor has been identified yet for Dkk3, although studies have proposed Kremen1/2 and LRP5/6 as receptors of the other members of Dkk protein family [204, 208, 285-287].

In view of the chemotactic role of Dkk3 in Sca-1+ progenitor cell migration, also shared by Sdf-1 α , we investigated if a chemokine receptor could be a candidate for Dkk3. Therefore, the first step of the second part of the project consisted of analysing the expression of the chemokine receptors on the Sca-1+ vascular progenitor cells.

3.3.1 Expression profile of chemokine receptors in Sca-1+ APCs

The expression of the whole panel of these receptors was examined in Sca-1+ cells in comparison with their expression in SMCs and ECs, by qPCR analysis (Figure 3.3.1A, fold increase calculated for each receptor in each cell type against the corresponding expression in ECs).

The results obtained demonstrated that the chemokine receptors expression profile of Sca-1+ APCs was between the corresponding profiles of SMCs and ECs, notably except for one receptor – CXCR7 (Figure 3.3A). The expression of CXCR1 to CXCR6 receptors, CX3CR1 and CCR1 to CCR10 receptor, i. e., of all receptors but CXCR7, was not significantly different between the Sca-1+ cells and the ECs and SMCs. On the other hand, the Sca-1+ cell expression of CXCR7 was 5.5-fold greater than its expression on ECs, but not significantly different from its expression on SMCs.

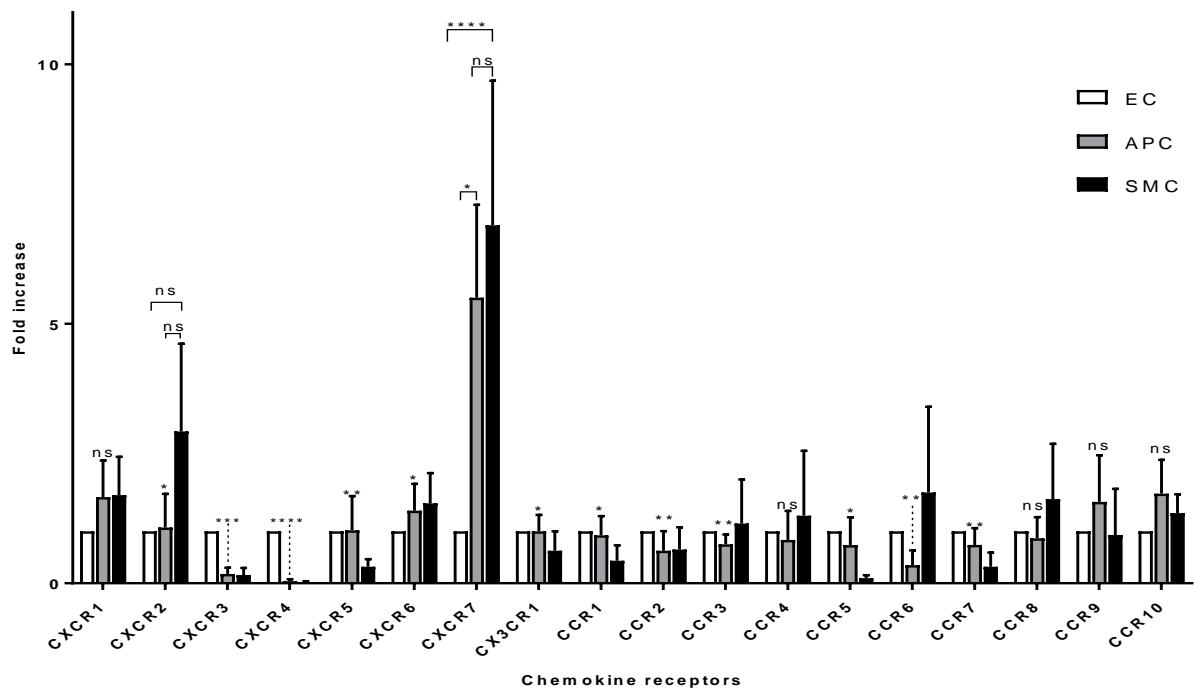
Moreover, compared to all the other receptors expressed on the Sca-1+ cells, CXCR7 was highly expressed in Sca-1+ APCs (5.5-fold increase against ECs). In addition to that, only between CXCR7 and the chemokine receptors CXCR1, CCR4, CCR8, CCR9 and CCR10, no statistical difference was found for the Sca-1+ cells. However, their fold increase against ECs (CXCR1 – 1.7, CCR4-0.8, CCR8-0.9, CCR9-1.6 and CCR10-1.7) was lower than the 5.5-fold increase for CXCR7. CXCR7 was also highly expressed in SMCs. On the other hand, CXCR4 mRNA expression was greater in ECs than in Sca-1+ cells (0.04-fold increase against ECs) or in SMCs (0.02-fold increase against ECs).

Following the mRNA expression analysis, CXCR7, CXCR4 and CXCR2 protein expression was also investigated by western blot (Figure 3.3.1B), which revealed the same trend of expression as the one found in the qPCR analysis, except for CXCR4 which was highly expressed in SMCs. Nevertheless, CXCR4 expression was much lower in the Sca-1+ cells, compared to SMCs and ECs.

CXCR7 protein expression was higher in the Sca-1+ cells and SMCs than in the ECs, similarly to the detected by qPCR.

Correspondingly to the mRNA results, the protein expression of CXCR2 was higher in the SMCs than in the Sca-1+ cells or ECs.

A mRNA expression profile of the chemokine receptors in ECs, Sca-1+ APCs and SMCs



B Protein expression of CXCR2, CXCR4 and CXCR7 receptors in ECs, Sca-1+ APCs and SMCs

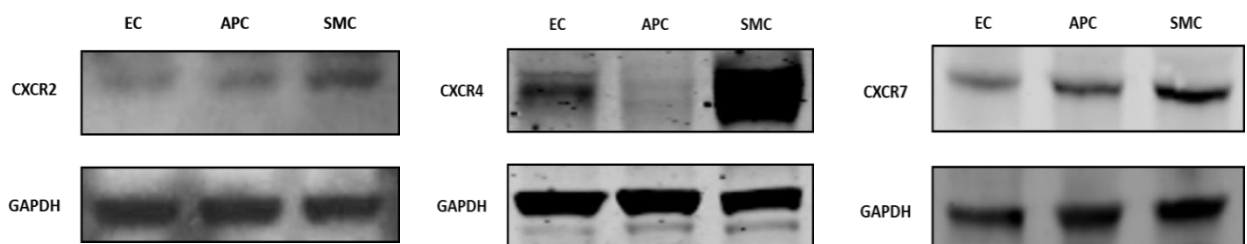


Figure 3.3.1 Expression profile of the chemokine receptors in ECs, Sca-1+ APCs and SMCs. mRNA (by qPCR) and protein (by Western blot) expressions of the chemokine receptors on the three cell types were analysed. **A: mRNA expression profile of the chemokine receptors in ECs, Sca-1+APCs and SMCs.** The fold increase was calculated for each chemokine receptor in each cell type against their corresponding expression in ECs. The statistics shown represent the analysis between CXCR7 and all the other chemokine receptors' expression in Sca-1+ cells. CXCR7 is highly expressed in Sca-1+ APCs and SMCs in comparison with the expression of the other receptors on these two cell types. No significant difference exists between APC and SMC CXCR7 expression, but there is a statistically significant difference between CXCR7 expression in ECs and in Sca-1+ APCs or in SMCs. CXCR4 expression in ECs is significantly higher than its expression on APCs and SMCs. **B: Protein expression of CXCR2, CXCR4 and CXCR7 on ECs, Sca-1+ APCs and SMCs.** CXCR7 protein expression in ECs is lower than in APCs and SMCs. CXCR4 is less expressed in Sca-1+ APCs than in ECs or in SMCs. CXCR2 protein is more expressed in SMCs than in ECs or in Sca-1+ APCs. (Data shown as mean \pm SEM, **** $p < 0.00001$, *** $p < 0.0001$, ** $p < 0.01$, * $p < 0.05$, by Two-way ANOVA and Bonferroni multiple comparison test, $n=5$).

3.3.2 Expression profile of Dkk protein family related receptors, in Sca-1+ vascular progenitor cells

As mentioned before, studies state that Kremen1 and Kremen2 are receptors of Dkk1 and 2. Surprisingly, the same studies further report that Dkk3 cannot bind to Kremen receptors [285, 288].

On the other hand, our group published that Dkk3 co-immunoprecipitates with Kremen1 in human partially-induced pluripotent stem-smooth muscle cells [244].

LRP6 was also indicated to be the receptor of DKK1 and 2, but not of Dkk3 [286, 287].

Taking into consideration the above, we investigated the expression of these receptors in Sca-1+ APCs, comparing it with their expression in ECs and in SMCs.

At the mRNA level, no difference was observed between the three cell types on the Kremen2 expression (Figure 3.3.2A). In contrast, Kremen1 expression in SMCs was significantly higher (3.8-fold increase) than in ECs, but not in APCs. Interestingly, the difference of Kremen1 expression between APCs and ECs was not statistically significant, revealing an intermediate profile of the APCs in terms of Kremen1 expression.

LRP5 and LRP6 expressions were also not statistically different between APCs, ECs and SMCs. What is more, their expression, as well as Kremen2 expression, in the three cell types, was lower than SMC Kremen1 expression.

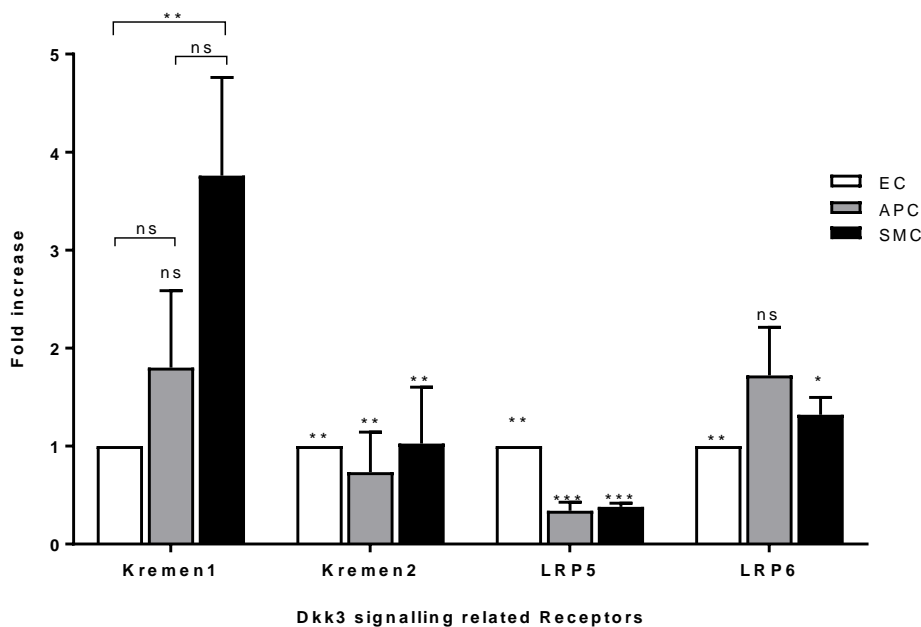
In Sca-1+ APCs, the expression of the 4 receptors, Kremen1, Kremen2, LRP5 and LRP6, was the same, with no statistical difference amongst them.

The western blot assay also showed a greater expression of Kremen1 in SMCs, when compared to Sca-1+ APCs and ECs (Figure 3.3.2B).

Kremen 2 protein expression was low in the three cell types.

LRP5 and LRP6 protein expression was equivalent to their mRNA expression in ECs, APCs and SMCs.

A mRNA Expression of Dkk protein family related receptors in ECs, Sca-1+ APCs and SMCs



B Protein expression of Kremen1, Kremen2, LRP5 and LRP6 receptors in ECs, Sca-1+ APCs and SMCs

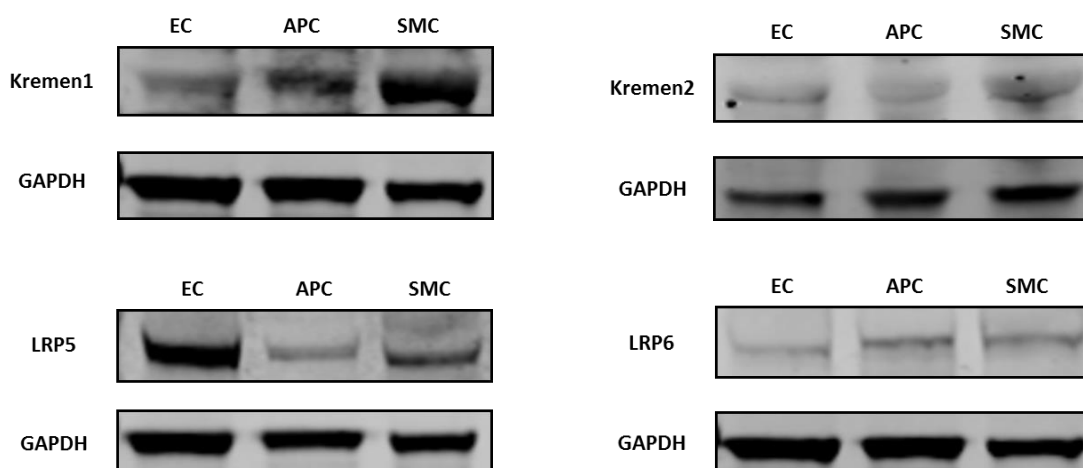


Figure 3.3.2 Expression profile of Dkk protein family related receptors, in ECs, Sca-1+APCs and SMCs. mRNA (by qPCR) and protein (by Western blot) expressions of the Dkk protein family related receptors in the three cell types were analysed. **A: mRNA expression profile of the Dkk protein family related receptors in ECs, Sca-1+ APCs and SMCs.** The fold increase was calculated for each receptor and each cell type against their corresponding expression in ECs. The statistics shown represent the analysis against SMC Kremen1. No statistical difference was observed between Kremen1, Kremen2, LRP5 and LRP6 on Sca-1+ APCs. Kremen1 was highly expressed in SMCs compared to ECs, but no significant difference in its expression was found between SMCs and APCs. On the other hand, Kremen1 expression was also not different between APCs and ECs. Kremen2, LRP5 and LRP6 expression, in the three cell types, was lower than the expression of Kremen1 in SMCs. **B: Protein expression of Kremen1, Kremen2, LRP5 and LRP6 in ECs, Sca-1+ APCs and SMCs.** Kremen1 protein expression in SMCs is greater than in ECs and APCs. Kremen2 expression is low in the three cell types. LRP5 and LRP6 protein expression follows the observed for mRNA expression in ECs, APCs and SMCs. (For each receptor the expression in ECs was considered 1.0-fold increase, but the * symbol represented on all the columns represents comparison against Kremen1 expression in SMCs. Data shown as mean \pm SEM, *** $p < 0.0001$, ** $p < 0.01$, * $p < 0.05$, by Two-way ANOVA and Bonferroni post-hoc test, $n=5$).

3.3.3 Conclusion of part 2: CXCR7 is highly expressed in Sca-1+ APCs

- CXCR7 is highly expressed in Sca-1+ APCs (5.5-fold increase against CXCR7 expression in ECs) in comparison with the other chemokine receptors.
- Interestingly, the same result was obtained for the SMCs, in which CXCR7 is highly expressed, compared to the other chemokine receptors.
- Remarkably, CXCR4 expression in Sca-1+ cells was much lower than in ECs and SMCs.
- Lastly, no difference in the expression of Kremen1, Kremen2, LRP5 and LRP6 was detected in Sca-1+ cells, at the mRNA level.
- Protein analysis showed that Kremen1 is expressed in Sca-1+ APCs, but Kremen2, LRP5 and LRP6 expressions are low.
- In SMCs, Kremen1 is highly expressed.

3.4 CXCR7 is involved in the migration of Sca-1+ APCs promoted by Dkk3 treatment

The study of the expression of the entire panel of chemokine receptors by RT-qPCR analysis showed that CXCR7 is highly expressed in Sca-1+ APCs, and this was confirmed by western blot analysis.

The next step of the project intended to understand whether CXCR7 was involved in the migration of Sca-1+ APCs driven by Dkk3.

The ligands of CXCR7 include Sdf-1 α chemokine, which was herein used as the positive control. Furthermore, as Sdf-1 α is also a ligand of CXCR4 and because CXCR4 and CXCR7 share structural and sequence homology, CXCR4 was considered as well a potential receptor candidate for Dkk3.

CXCR2 was included in the list of candidate receptors also because of its important degree of homology with murine CXCR7 [289] and the fact that the association of CXCR2 and CXCR7 seems to have an essential role in tumour diseases, including acute leukaemia and esophageal cancer [290, 291].

Kremen1 and Kremen2 were as well contemplated, due to reports showing the binding of some Dkk proteins to these receptors and to studies revealing co-immunoprecipitation of Dkk3 with Kremen1 [244, 292].

3.4.1 Downregulation of CXCR7 and Kremen1, by SiRNA transfection, decreased Sca-1+ APC migration driven by Dkk3 treatment

First, we knocked down the receptor candidates, by SiRNA transfection, in Sca-1+ APCs and then we performed transwell migration assays in response to Sdf-1 α and Dkk3.

3.4.1.1 Sca-1+ APCs express low level of CXCR4

Notably, CXCR4 knockdown in the Sca-1+ cells was not achieved (Figure 3.4.1.1C), even by means of two different SiRNA products. The low level of expression of this receptor in the Sca-1+ cells was apparent (Figure 3.4.1.1A and B).

We then implemented a different approach. AMD3100 is a specific antagonist of CXCR4. Treatment of the cells with this agent is known to decrease cell migration induced by Sdf-1 α [293-296].

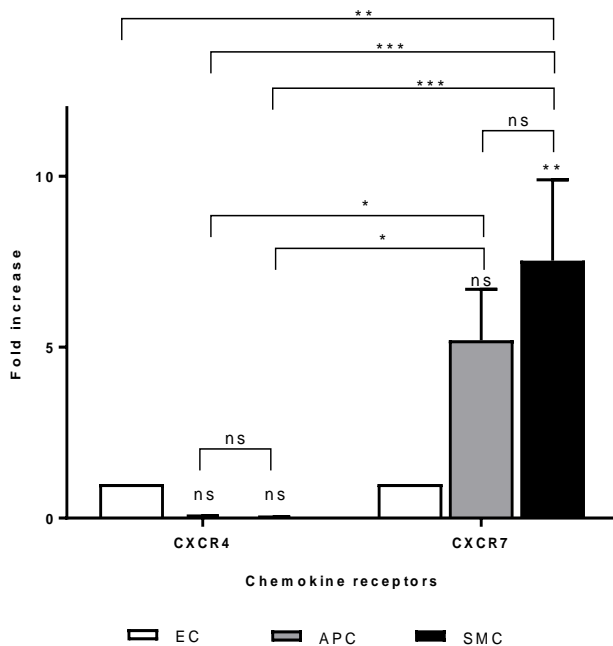
Three different concentrations of the antagonist agent were used and strikingly, Sca-1+ cell migration mediated by Sdf-1 α was not reduced in the presence of the antagonist with any of the concentrations used (Figure 3.4.1.1D).

Likewise, when the Sca-1+ cells were stimulated with Dkk3, the cell migration was not decreased upon AMD3100 treatment (Figure 3.4.1.1E).

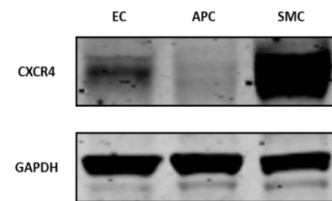
No significant difference was observed between the groups of cells treated with either Sdf-1 α or Dkk3 and the groups of cells in which the antagonist was concomitantly added.

The inability of the CXCR4 antagonist in affecting the migration of the Sca-1+ cells driven by Sdf-1 α could be explained by the low expression of the receptor in the Sca-1+ progenitor cells.

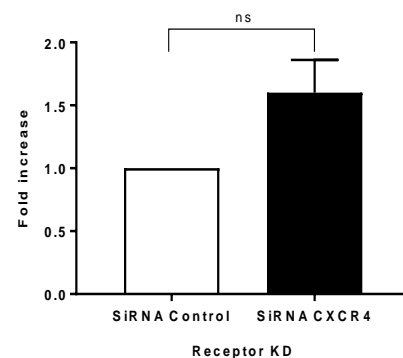
A mRNA Expression of CXCR4 and CXCR7 in ECs, Sca-1+ APCs and SMCs



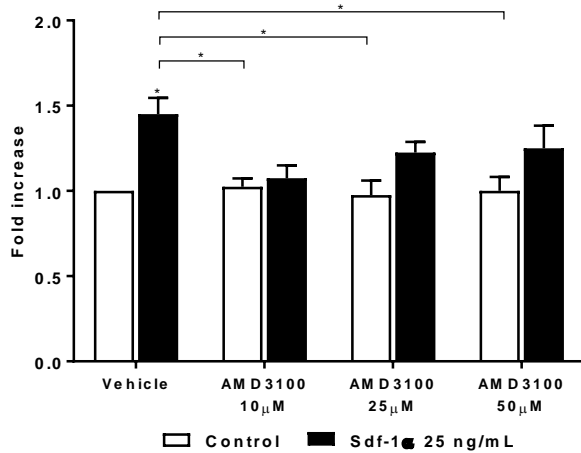
B Protein expression of CXCR4 in ECs, Sca-1+ APCs and SMCs



C qPCR analysis of CXCR4 knockdown



D Sdf-1 α -driven Transwell migration assay of Sca-1+ APCs upon AMD3100 treatment



E Dkk3-driven Transwell migration assay of Sca-1+ APCs upon AMD3100 treatment

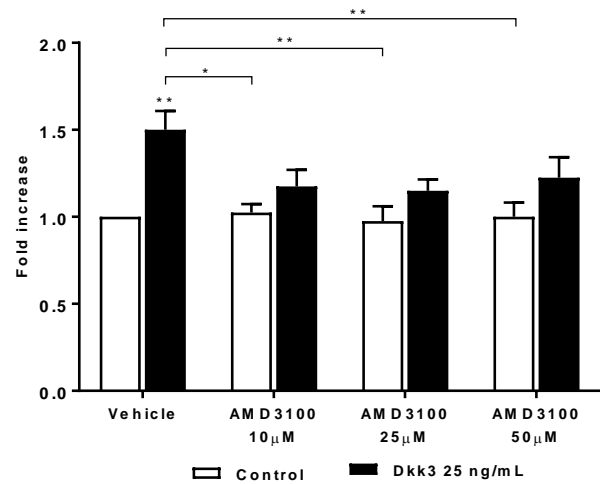


Figure 3.4.1.1 Sca-1+ APCs express low level of CXCR4. CXCR4 expression in Sca-1+ progenitor cells was analysed by qPCR and western blot. In order to assess if the receptor was involved in the migration mechanism driven by Dkk3, knockdown and inhibition of the receptor was undertaken, followed by transwell migration assays. Sdf-1 α was used as a positive control. **A: mRNA expression of CXCR4 and CXCR7 in Sca-1+ APCs, ECs and SMCs.** **B:** Fold increase was calculated for each receptor and each cell type against the corresponding expression in ECs. **Protein expression of CXCR4 in Sca-1+ APCs, ECs and SMCs.** CXCR4 expression in APCs is lower than in ECs or SMCs. CXCR7 expression is higher than CXCR4 expression in APCs and SMCs. **C: mRNA expression of CXCR4 knockdown.** SiRNA transfection of CXCR4 did not accomplish receptor knockdown, probably due to its low expression in the cells. **D, E: Respectively, Sdf-1 α - or Dkk3-driven transwell migration assays of Sca-1+ cells upon AMD3100 treatment.** The Sca-1+ progenitor cell migration, mediated by either Sdf-1 α or Dkk3, was not suppressed with CXCR4 inhibition, as no significant difference was found in the fold increase between Sdf-1 α or Dkk3 treatment groups and the groups in which AMD3100 antagonist was concomitantly added. (Data shown as mean \pm SEM, *** p <0.0001, ** p <0.01, * p <0.05, by Two-way ANOVA, followed by Bonferroni multiple comparison test (A, D, E) and Student's t-test (C); n =4).

3.4.1.2 CXCR7 Knockdown decreased Sca-1+ APC migration induced by Dkk3 or Sdf-1 α stimulation

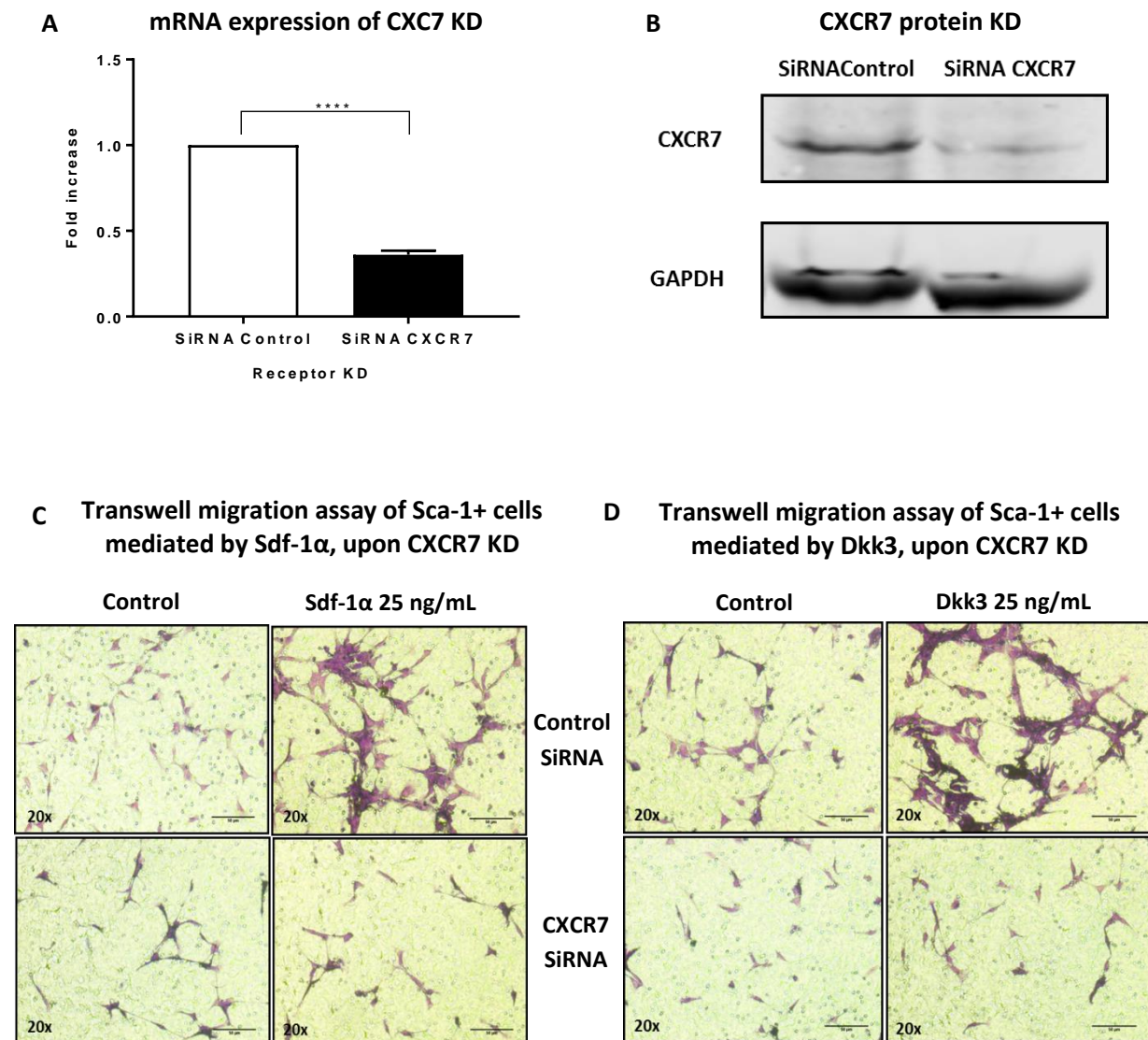
CXCR7 knockdown by SiRNA transfection was easily achieved as confirmed by qPCR analysis (Figure 3.4.1.2A) and western blot assay (Figure 3.4.1.2B).

Sca-1+ progenitor cell migration, stimulated by Sdf-1 α (1.6 fold increase) was remarkably decreased upon CXCR7 knockdown (0.9 fold increase) (Figure 3.4.1.2C, E). This suggested that Sdf-1 α induced the migration of Sca-1+ cells through CXCR7 activation.

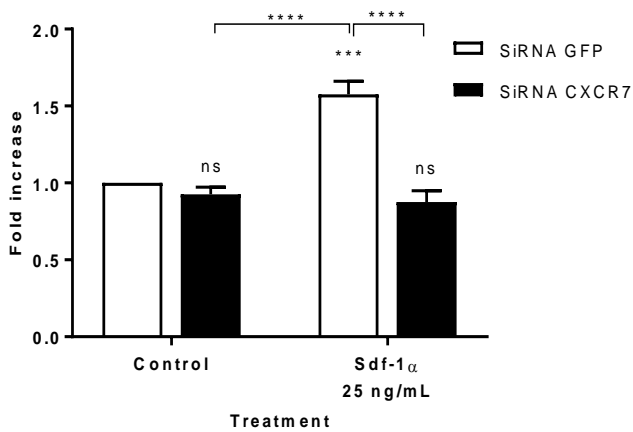
Interestingly, the migration of Sca-1+ cells driven by Dkk3 treatment (1.7 fold increase) was also suppressed when CXCR7 was downregulated (1.1 fold increase) (Figure 3.4.1.2D, F), thus indicating that CXCR7 was involved in the migration of Sca-1+ APCs driven by Dkk3.

These results revealed a similarity in the Sca-1+ APC migration behaviour in response to Sdf-1 α and Dkk3 stimulation.

It is important to mention that no CXCR7 inhibitor or antagonist was available at the time these experiments were performed.



E Quantification of Sdf-1 α mediated migration of Sca-1+ cells, upon CXCR7 KD



F Quantification of Dkk3 mediated migration of Sca-1+ cells, upon CXCR7 KD

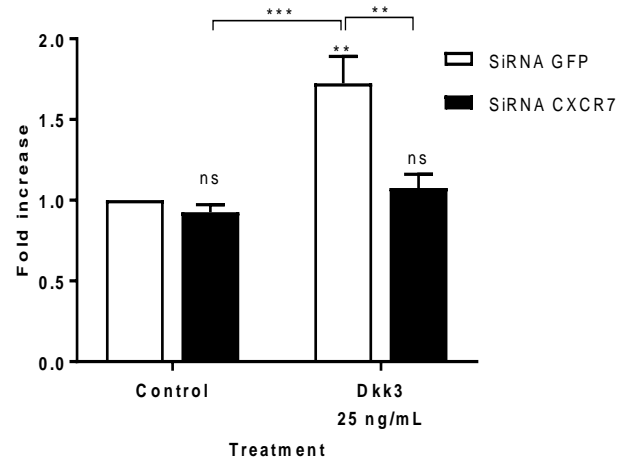


Figure 3.4.1.2 CXCR7 KD decreased Sca-1+ progenitor cell migration induced by Dkk3 or Sdf-1 α stimulation. CXCR7 knockdown was achieved by SiRNA transfection and its efficiency was measured by analysis of the expression of the receptor. **A: mRNA expression of CXCR7 KD. B: CXCR7 KD protein expression.** Transwell migration assays were performed with the SiRNA transfected Sca-1+ cells upon either Sdf-1 α or Dkk3 treatments. **C, D: Respectively, 20X magnification images of the transwell inserts of migrated SiRNA transfected Sca-1+ cells, treated with Sdf-1 α or Dkk3 and under Control condition. E, F: Respectively, quantification of Sdf-1 α - and Dkk3-mediated transwell migration assay, upon CXCR7 KD.** 5 fields at 10X magnification of each insert for each condition were considered for quantification of cell migration. Duplicates were used for each treatment and SiRNA transfection. For both treatments, Sdf-1 α and Dkk3, the migration of Sca-1+ cells was significantly reduced upon CXCR7 downregulation. The fold increase of the cells treated with Sdf-1 α decreased from 1.6 to 0.9. In the case of the Dkk3 stimulated cells, the fold increase was suppressed from 1.7 to 1.1. (Data shown as mean \pm SEM, **** p <0.00001, *** p <0.0001, by Student's t-test for A and Two-way ANOVA for E and F, followed by Bonferroni post-hoc test, $n=4$).

3.4.1.3 *Sca-1+* APC migration induced by *Dkk3* was not decreased upon *CXCR2* downregulation

CXCR2 knockdown by SiRNA transfection was confirmed by qPCR and western blot (Figure 3.4.1.3A and B).

Transwell migration assay was performed on the transfected *Sca-1+* cells, in response to *Dkk3* (Figure 3.4.1.3C and D).

The results obtained showed that the downregulation of *CXCR2* did not affect the migration induced by *Dkk3*, which questions its involvement in *Dkk3*-driven migration of *Sca-1+* progenitor cells.

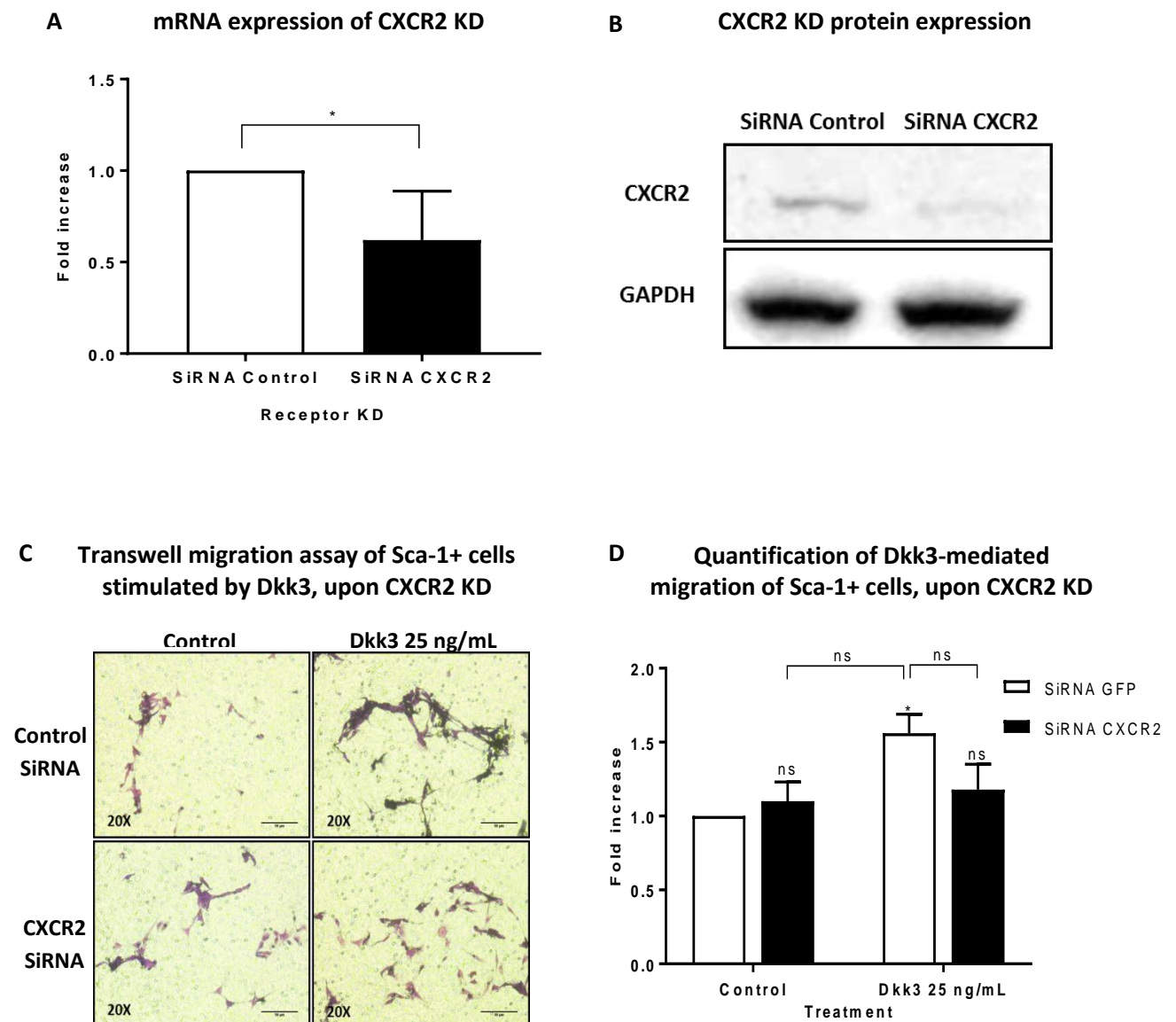


Figure 3.4.1.3 Sca-1+ progenitor cell migration induced by Dkk3 was not decreased by CXCR2 downregulation. CXCR2 knockdown was achieved by SiRNA transfection in Sca-1+ progenitor cells. qPCR and western blot techniques were used for transfection validation. **A: mRNA expression of CXCR2 downregulation.** **B: CXCR2 knockdown protein expression.** **C: Representative images at 20X magnification of migrated Sca-1+ cells transfected with SiRNA, under Control or Dkk3 treatment conditions.** **D: Quantification of Dkk3-mediated Sca-1+ cell migration, upon CXCR2 knockdown.** For each condition 5 fields at 10X magnification were considered to quantify the number of cells migrated. No significant difference was found between Dkk3 treated cells transfected with Control SiRNA and Dkk3 treated cells transfected with CXCR2 SiRNA, indicating that the downregulation of CXCR2 had no effect in the Dkk3-driven migration of Sca-1+ cells. (Data shown as mean \pm SEM, * $p < 0.05$, by Student's t-test for A and Two-way ANOVA for D, followed by Bonferroni multiple comparison test, $n=5$).

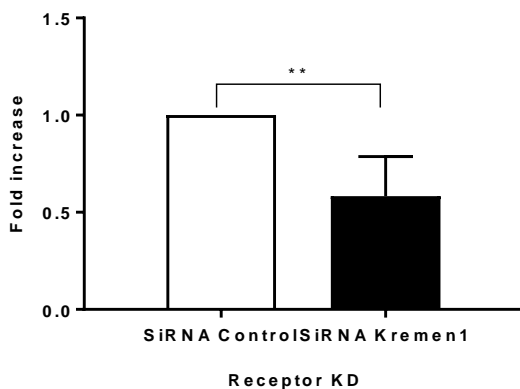
3.4.1.4 Kremen1 Knockdown decreased Sca-1+ APCs migration driven by Dkk3

Sca-1+ progenitor cell migration upon Kremen1 downregulation was assessed.

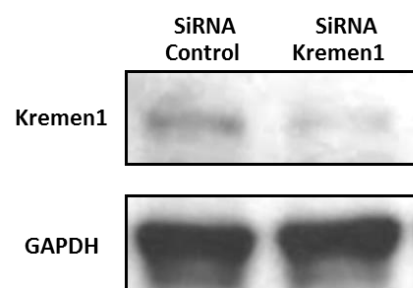
The qPCR and western blot analysis validated the success of Kremen1 knockdown (Figure 3.4.1.4A and B).

The transwell migration assay revealed that, by knocking down Kremen1, the Sca-1+ cell migration induced by Dkk3 was reduced from 1.6 fold increase to 1.0 fold increase (Figure 3.4.1.4C and D). This finding supported the notion that Kremen1 could be involved in the migration of Sca-1+ cells promoted by Dkk3.

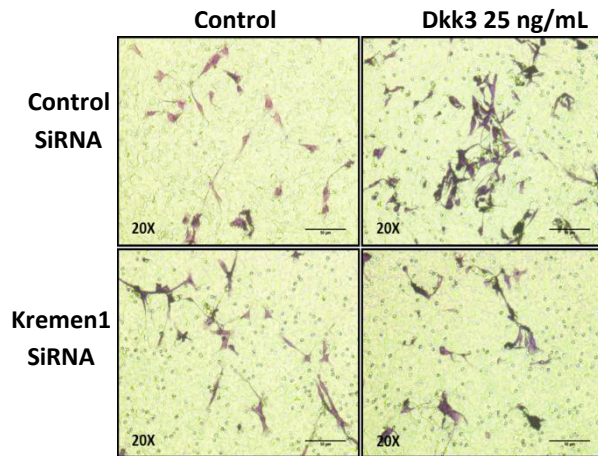
A mRNA expression of Kremen1 KD



B Kremen1 KD protein expression



C Transwell migration assay of Sca-1+ cells stimulated by Dkk3, upon Kremen1 KD



D Quantification of Dkk3 mediated migration of Sca-1+ cells, upon Kremen1 KD

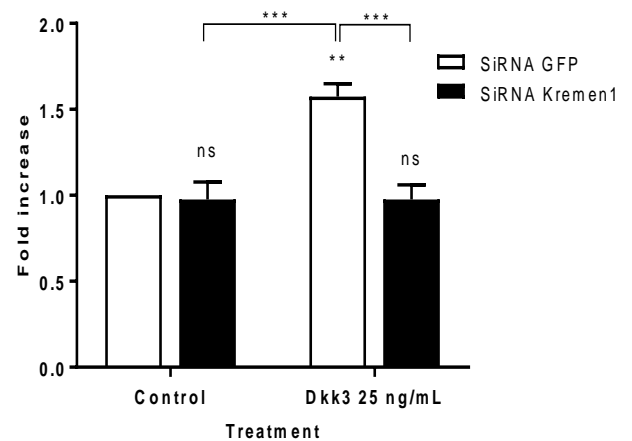


Figure 3.4.1.4 Kremen1 Knockdown decreased Sca-1+ progenitor cell migration driven by Dkk3. SiRNA transfection was performed in Sca-1+ cells to knockdown Kremen1. qPCR and Western blot methods were used to validate the success of the transfection. **A: mRNA expression of Kremen1 knockdown. B: Protein expression of Kremen1 downregulation.** Transwell migration assay was performed with the transfected cells, upon Dkk3 treatment. **C: 20X magnification images of the transwell inserts with the Sca-1+ cells that have migrated under Control or Dkk3 treatments. D: Quantification of the Dkk3-driven migration of Sca-1+ cells transfected with Kremen1 SiRNA.** Kremen1 downregulation affected negatively the migration of the Sca-1+ cells driven by Dkk3, as the fold increase decreased from 1.6 to 1.0. This result supported the notion that Kremen1 could be involved in the migration mechanism of Sca-1+ cells induced by Dkk3. (Data shown as mean \pm SEM, *** p <0.0001, ** p <0.01, by Student's t-test for A and Two-way ANOVA for D, followed by Bonferroni post-hoc test, $n=4$).

3.4.1.5 Sca-1+ APCs express low level of Kremen2

Kremen2 level of expression in the Sca-1+ APCs is low, as detected by western blot (Figure 3.1.4.5B). Therefore, knockdown of this receptor was not attained (Figure 3.4.1.5A), as it is difficult to knockdown a receptor which exhibits a low expression in the cells.

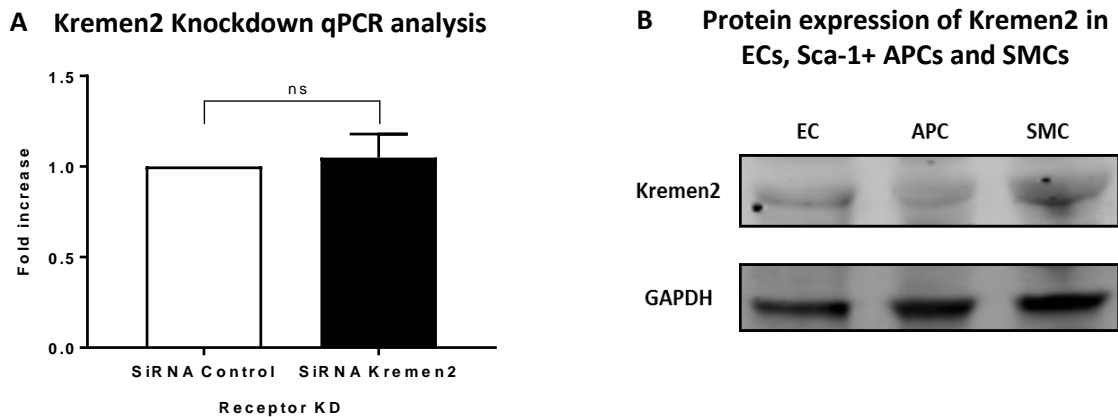


Figure 3.4.1.5 Sca-1+ progenitor cells express low level of Kremen2. Kremen2 SiRNA transfection was carried out in Sca-1+ progenitor cells. **A: qPCR analysis of Kremen2 Knockdown.** Downregulation of Kremen2 was not achieved in Sca-1+ progenitor cells. **B: Kremen2 protein expression by western blot on ECs, APCs and SMCs.** The expression of Kremen2 in Sca-1+ cells is low, which could be the reason for the unsuccessful knockdown of the receptor, since it is difficult to knockdown a receptor which has a low expression in the cell. (Data shown as mean \pm SEM, by Student's t-test, n=4).

3.4.1.6 Conclusion of part 3: Downregulation of CXCR7 and Kremen1, by SiRNA transfection, decreased Sca-1+ APCs migration driven by Dkk3 treatment

- Three chemokine receptors, CXCR2, CXCR4 and CXCR7, were selected as candidates for Dkk3, due to their expression in Sca-1+ APCs and their structural and sequence homology.
- Kremen1 and Kremen2 were also considered as candidate receptors for Dkk3, due to studies reporting their involvement with some Dkk proteins.
- CXCR4 and Kremen2 expression was substantially low in Sca-1+ cells, especially when compared to ECs and SMCs. Consequently, knockdown of these receptors was not possible.
- CXCR4 is the cognate receptor of Sdf-1 α . Therefore, its antagonist AMD3100 was used in the transwell assay, by pre-incubating the Sca-1+ cells with this agent and then stimulating them with Sdf-1 α . Interestingly, Sdf-1 α -driven migration of the Sca-1+ cells was not attenuated. Similarly, Dkk3-mediated migration of Sca-1+ APCs was also not reduced. We speculated that this occurred due to the low expression of CXCR4 in Sca-1+ APCs. The same rationale was applied to Kremen2, whose expression was also low in Sca-1+ APCs.
- CXCR7 is highly expressed in Sca-1+ APCs, which also express Kremen1. These receptors seem to be involved in the Sca-1+ APC migration stimulated by Dkk3, as the knockdown of these receptors affected negatively the Dkk3-driven migration of Sca-1+ progenitor cells.
- Likewise, CXCR7 downregulation decreased the migration of Sca-1+ cells treated with Sdf-1 α .
- Based on the data presented, we postulate that CXCR7 and Kremen1 were involved in the migration mechanism of Sca-1+ APCs induced by Dkk3.

3.4.2 Overexpression of CXCR7 induced Dkk3-driven cell migration

We employed another strategy to investigate the involvement of the candidate receptors in the migration mechanism promoted by Dkk3. Receptors were overexpressed in HEK 293T cells and then functional migration assays were performed.

3.4.2.1 *Sdf-1 α* , but not *Dkk3* stimulation, increased the migration of HEK 293T cells overexpressing CXCR4

The first receptor tested was CXCR4. Upregulation of CXCR4 in HEK 293T cells was confirmed by qPCR (Figure 3.4.2.1A).

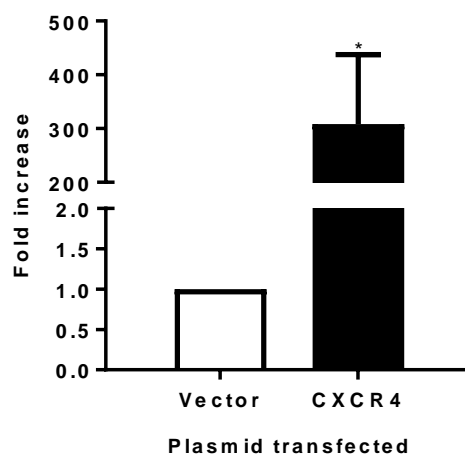
Next, transwell migration assay on the cells was performed with either Sdf-1 α or Dkk3 treatment (Figure 3.4.2.1B).

It was expected that the treatment with Sdf-1 α chemokine on the CXCR4 overexpressing cells would increase their migration rate, as CXCR4 has been established in the literature Sdf-1 α receptor.

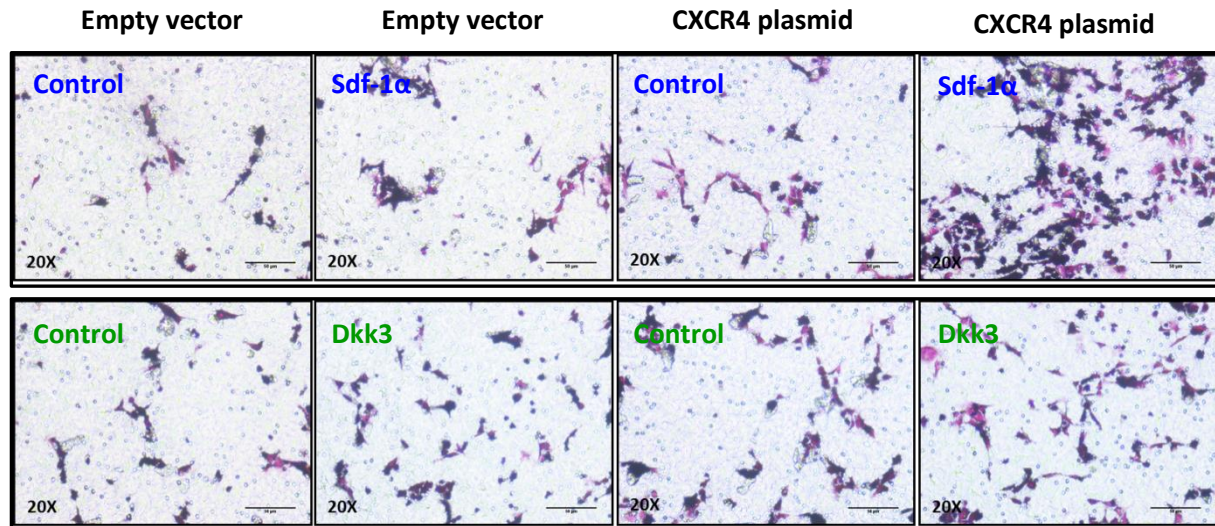
The data obtained revealed that 25 ng/mL of hSdf-1 α increased the migration rate of the HEK 293T cells overexpressing hCXCR4 by 1.8 fold increase (Figure 3.4.2.1C). Additionally, when only the empty vector was transfected, Sdf-1 α did not induce the migration of the HEK cells. hCXCR4 plasmid transfection by itself did not affect the cell migration rate, since no significant difference was found between the migration rate of the cells transfected with the empty vector and with the hCXCR4 plasmid.

On the other hand, when hCXCR4 overexpressing cells were treated with 25 ng/mL of hDkk3, no difference was found on the cell migration level between any of the conditions (Figure 3.4.2.1B and D). This implicated that CXCR4 was possibly not involved in the migration mechanism driven by Dkk3.

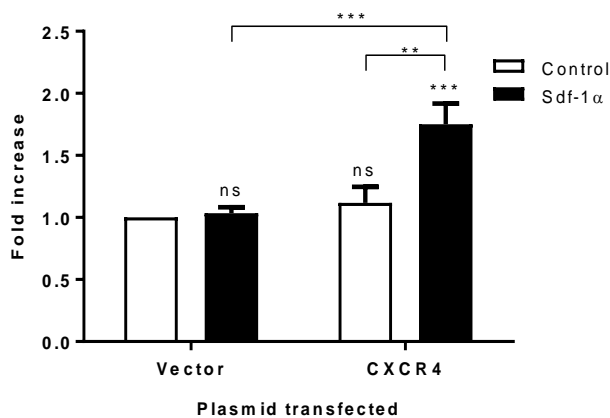
A hCXCR4 upregulation in HEK 293T cells – mRNA expression



B hSdf-1 α and hDkk3 mediated transwell migration assay of HEK 293T cells overexpressing hCXCR4



C Quantification of Sdf-1 α mediated migration of HEK 293T cells overexpressing CXCR4



D Quantification of Dkk3 mediated migration of HEK 293T cells overexpressing CXCR4

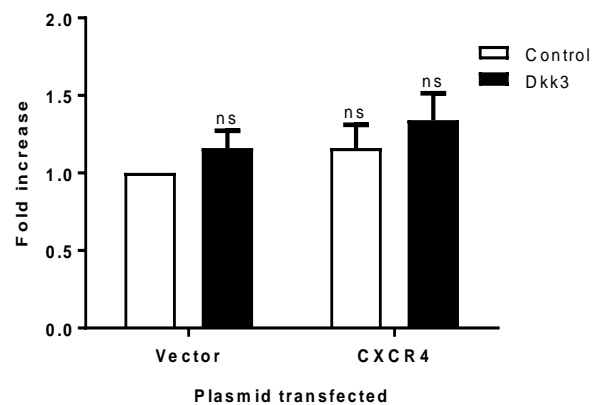


Figure 3.4.2.1 Sdf-1 α , but not Dkk3 stimulation, increased the migration of HEK 293T cells overexpressing CXCR4. Empty vector pShuttle2-Flag-HA and plasmid pShuttle2-Flag-hCXCR4-HA were transfected into HEK 293T cells. Transwell migration assays on these cells were performed with either 25 ng/mL of hSdf-1 α or 25 ng/mL of hDkk3. **A:** mRNA expression of HEK 293T cells overexpressing CXCR4. **B:** 20X magnification representative images of HEK 293T-migrated cells transfected with either empty vector or hCXCR4 plasmid and stimulated with either hSdf-1 α or hDkk3. **C, D:** Respectively, quantification hSdf-1 α - or hDkk3- mediated migration of HEK 293T cells overexpressing hCXCR4. hSdf-1 α induced the migration of hCXCR4 transfected cells (1.8-fold increase) in comparison with the cells transfected with the empty vector. Dkk3 did not affect the migration of the cells in any transfection condition. (Data shown as mean \pm SEM, *** p <0.001, ** p <0.01, * p <0.05, by Student's t-test (A) and Two-way ANOVA followed by Bonferroni post-hoc test (C, D), n =5).

3.4.2.2 Dkk3 and Sdf-1 α promoted the migration of HEK 293T cells overexpressing CXCR7

Human CXCR7 was transfected into HEK 293T cells, which was confirmed by qPCR (Figure 3.4.2.2A).

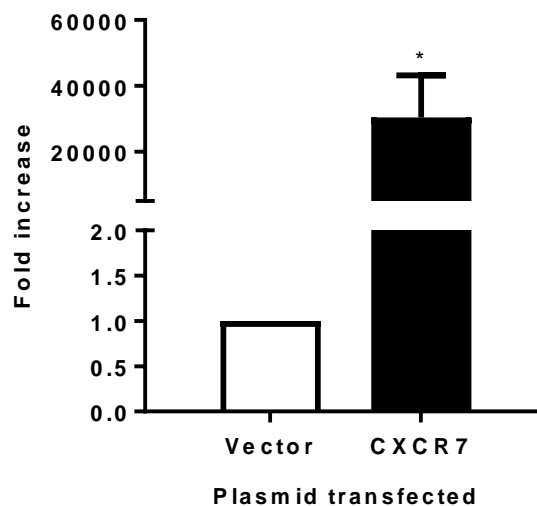
The cells overexpressing CXCR7 were submitted to transwell migration assay with either 25 ng/mL of hSdf-1 α or 25 ng/mL of hDkk3 stimulation (Figure 3.4.2.2B).

Treatment with hSdf-1 α on HEK cells transfected with hCXCR7 prompted an increase in the migration level of these cells, with a fold increase of 1.4, when compared to the cells transfected with the empty vector (Figure 3.4.2.2.B and C). Impressively, when the CXCR7 overexpressing cells were stimulated with Dkk3, the migration rate was also induced to a significant fold increase of 1.9, in comparison with cells transfected with empty vector (Figure 3.4.2.2.B and D).

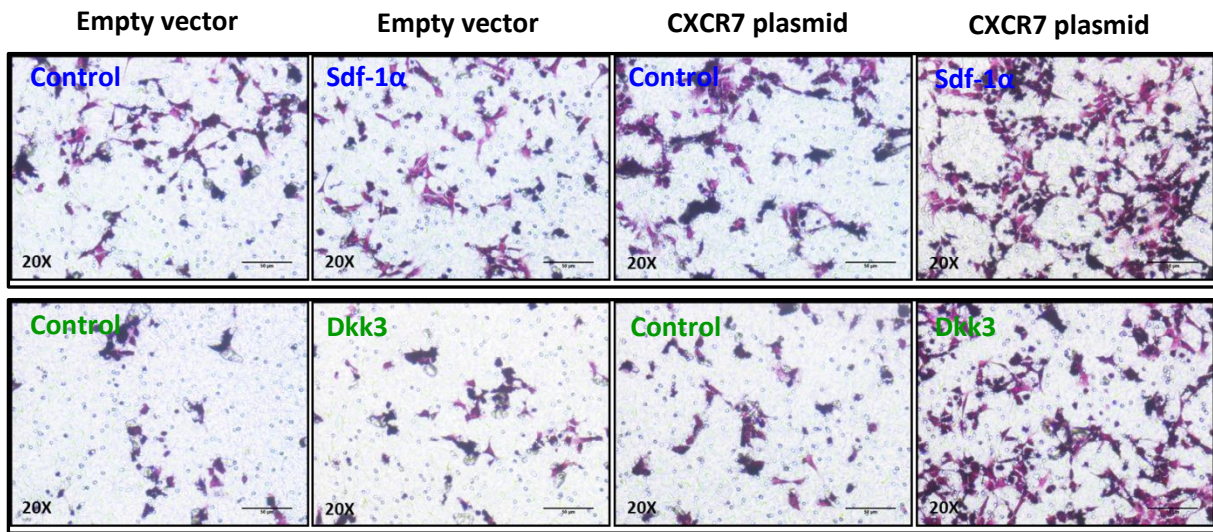
HEK 293T cell transfection with hCXCR7 plasmid did not affect by itself the cell migration rate. Additionally, Sdf-1 α and Dkk3 stimulation of the cells transfected with empty vector had no effect on their migratory response.

The results obtained herein were consistent with what was found before, where knockdown of CXCR7 played a negative role in the migration rate of Sca-1+APCs treated with either Sdf-1 α or Dkk3 (Figure 3.4.1.2 E and F).

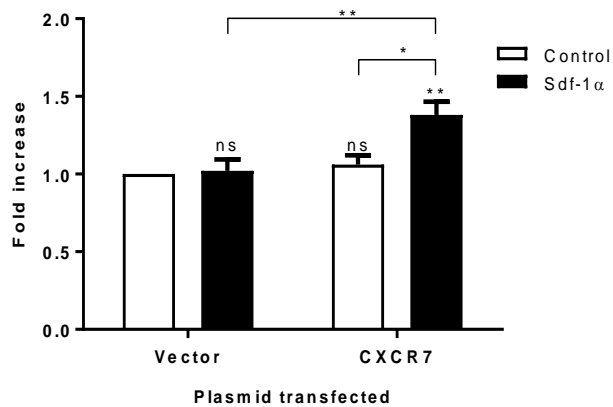
A CXCR7 overexpression in HEK 293T cells – qPCR analysis



B Sdf-1 α and Dkk3 driven Transwell migration assay of HEK 293T cells overexpressing CXCR7



C Quantification of Sdf-1 α driven migration of HEK 293T cells overexpressing CXCR7



D Quantification of Dkk3 driven migration of HEK 293T cells overexpressing CXCR7

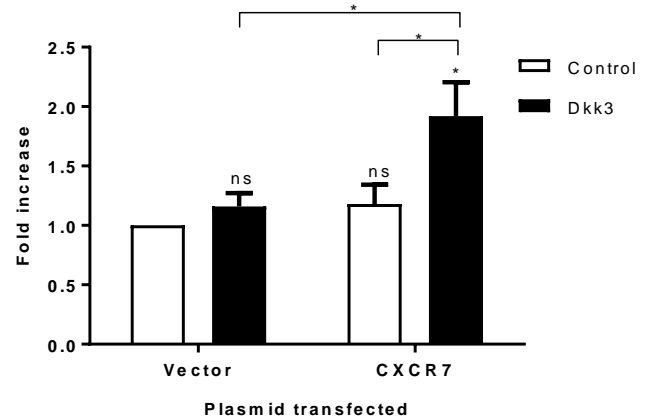


Figure 3.4.2.2 Dkk3 and Sdf-1 α promoted the migration of CXCR7 overexpressing HEK 293T cells. Empty vector pShuttle2-Flag-HA and plasmid pShuttle2-Flag-hCXCR7-HA were transfected into HEK 293T cells. Transwell migration assays on these cells were performed with either 25 ng/mL of hSdf-1 α or 25 ng/mL of hDkk3 treatment. **A: hCXCR7 upregulation in HEK 293T cells – qPCR analysis.** **B: 20X magnification representative images of HEK 293T-migrated cells transfected with either empty vector or hCXCR7 plasmid and stimulated with either hSdf-1 α or hDkk3.** **C, D: Respectively, quantification hSdf-1 α - or hDkk3- mediated migration of HEK 293T cells overexpressing hCXCR7.** Plasmid hCXCR7 transfection by itself did not affect cell migration. Upon stimulation of the CXCR7 overexpressing cells with either hSdf-1 α or hDkk3, the migration level was induced by 1.4 or 1.9 fold increase, respectively. (Data shown as mean \pm SEM, ** p <0.01, * p <0.05, by Student's t-test (A) and Two-way ANOVA followed by Bonferroni multiple comparison test (C, D), n =5).

3.4.2.3 Dkk3 treatment had no effect on the migration response of CXCR2 overexpressing HEK 293T cells

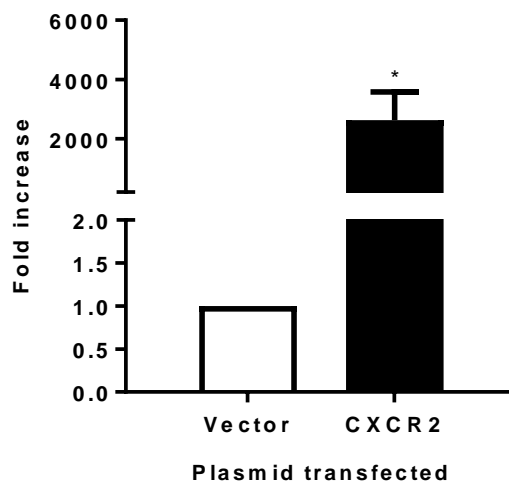
The chemokine receptor hCXCR2 was also transfected into HEK 293T cells. We confirmed by qPCR analysis the achievement of the transfection (Figure 3.4.2.3A).

The transwell migration assay of the transfected cells revealed that the overexpression of the receptor, without the stimulation by any treatment, promoted by itself an increase in the migration of HEK 293T cells, although with no statistical significance (Figure 3.4.2.3.B, C, D).

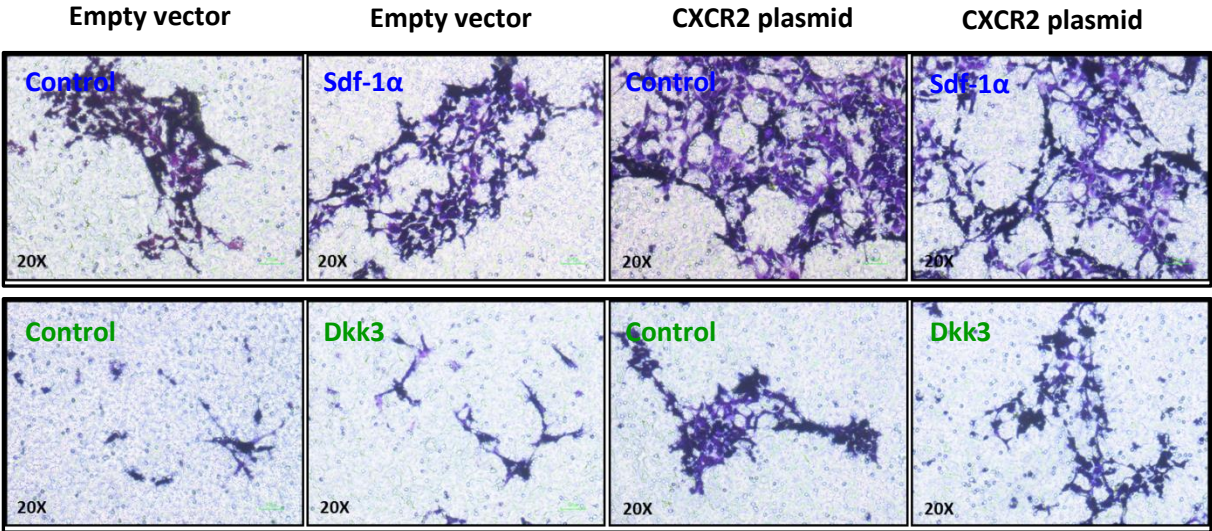
As anticipated, hSdf-1 α treatment did not induce the migration of the cells overexpressing hCXCR2. CXCR2 has not been recognized as an Sdf-1 α receptor, which explains the result obtained (Figure 3.4.2.3C).

Dkk3 stimulation also had no effect on the migration rate of the transfected cells, as no difference was found in the migration rate amongst all groups of cells (Figure 3.4.2.3D). Notably, this finding was consistent with the result obtained in the previous section of the project, where CXCR2 downregulation also had no influence on the Dkk3-mediated migration level of Sca-1+ cells (Figure 3.4.1.3D).

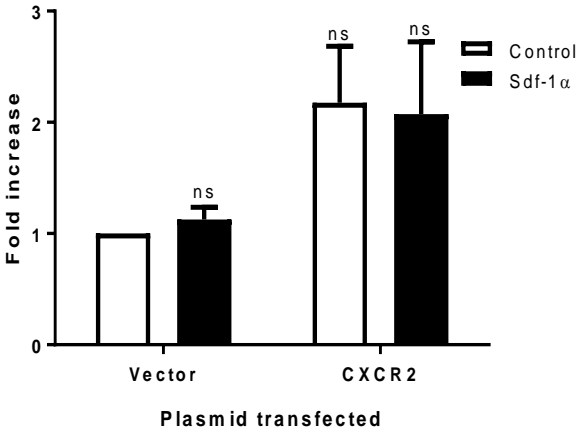
A mRNA Expression of CXCR2 upregulation in HEK 293T cells



B hSdf-1 α and hDkk3 mediated Transwell migration assay of HEK 293T cells overexpressing hCXCR2



C Quantification of Sdf-1 α mediated migration of HEK 293T cells upon CXCR2 upregulation



D Quantification of Dkk3 mediated migration of HEK 293T cells upon CXCR2 upregulation

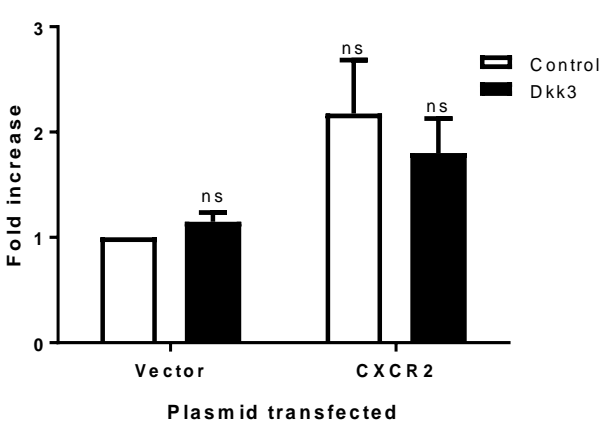


Figure 3.4.2.3 Dkk3 and Sdf-1 α treatments had no effect on the migration level of CXCR2 overexpressing HEK 293T cells. Empty vector pShuttle2-Flag-HA and plasmid pShuttle2-Flag-hCXCR2-HA were transfected into HEK 293T cells. Transwell migration assays on these cells were performed with either 25 ng/mL of hSdf-1 α or 25 ng/mL of hDkk3 treatment. **A: mRNA expression of hCXCR2 upregulation in HEK 293T cells. B: 20X magnification representative images of HEK 293T-migrated cells transfected with either empty vector or hCXCR2 plasmid and stimulated with either hSdf-1 α or hDkk3. C, D: Respectively, quantification hSdf-1 α - or hDkk3- mediated migration of HEK 293T cells overexpressing hCXCR2.** Plasmid hCXCR2 transfection, without any treatment, induced by itself the migration of HEK 293T cells, although with no statistical significance. Upon stimulation of the hCXCR2 overexpressing cells with either hSdf-1 α or hDkk3, no effect was found on the cell migration response. (Data shown as mean \pm SEM, * p <0.05, by Student's t-test (A) and Two-way ANOVA followed by Bonferroni multiple comparison test (C, D), n =4).

3.4.2.4 Dkk3 stimulation had no effect on the migration of Kremen1 or Kremen2 overexpressing HEK 293T cells

hKremen1 and hKremen2 receptors were transfected into HEK 293T cells and this was confirmed by the analysis of mRNA expression through qPCR (Figure 3.4.2.4A and B).

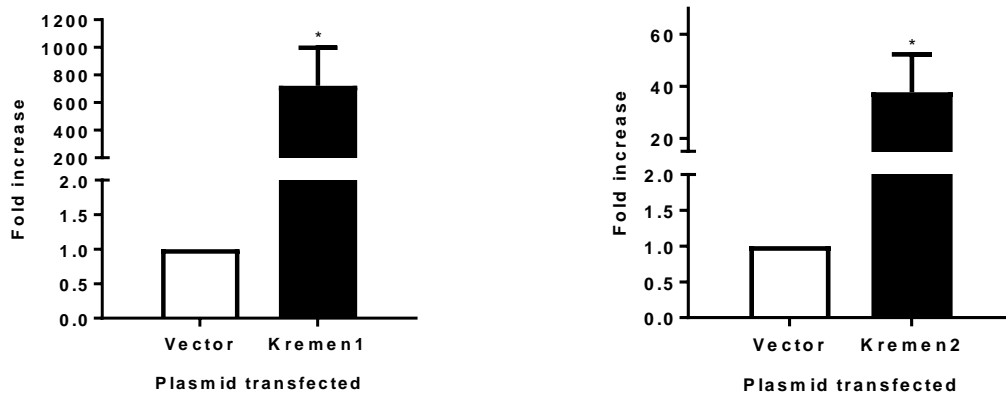
The transfected cells were then used in transwell migration assay with 25 ng/mL of hDkk3 (Figure 3.4.2.4C).

The data obtained demonstrated that overexpression of either receptor, by itself, had no impact on the migration level of the cells. Likewise, Dkk3 treatment of HEK 293T cells overexpressing either Kremen1 or Kremen2 had no effect on the cell migratory response compared to the cells transfected with the empty vector (Figure 3.4.2.4D and E). In fact, no significant difference was found amongst any of the treatment and transfection conditions.

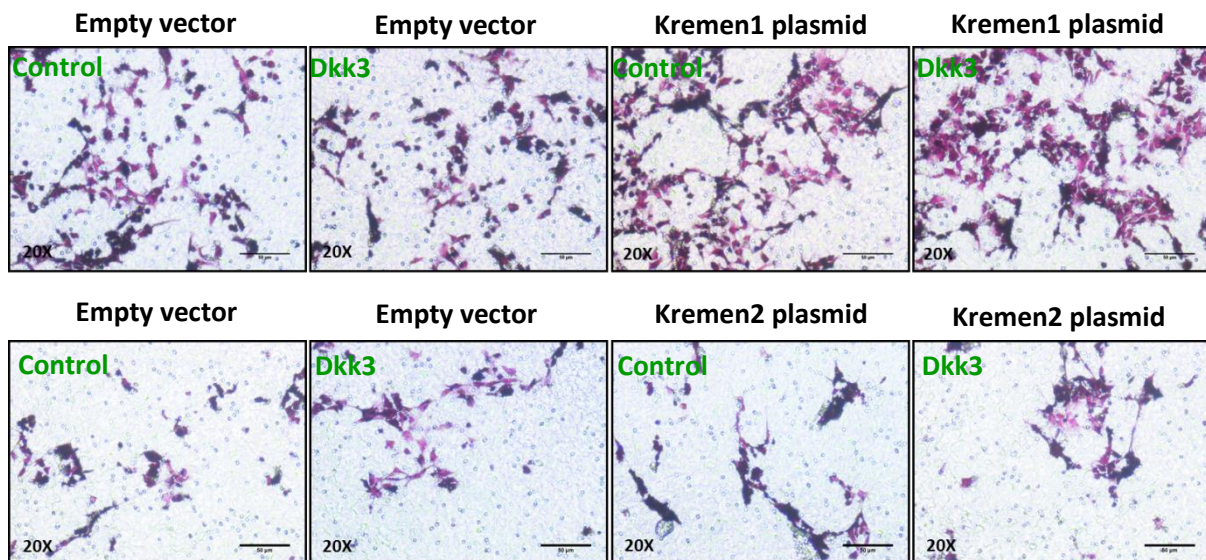
The data herein obtained regarding the receptor Kremen1 was notably conflicting with the previous finding (Figure 3.4.1.4D), where downregulation of Kremen1 had decreased the Dkk3-driven migration rate of the Sca-1+ progenitor cells.

A **Kremen1 upregulation in HEK 293T cells - mRNA Expression**

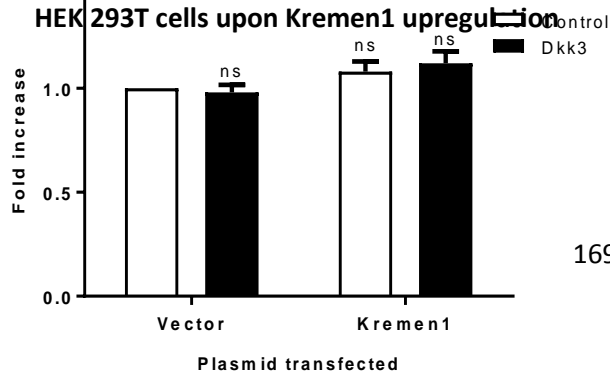
B **Kremen2 upregulation in HEK 293T cells - mRNA Expression**



C Dkk3 mediated Transwell migration assay of HEK 293T cells overexpressing either Kremen1 or Kremen2



D Quantification of Dkk3 mediated migration of HEK 293T cells upon Kremen1 upregulation



E Quantification of Dkk3 mediated migration of HEK 293T cells, upon Kremen2 upregulation

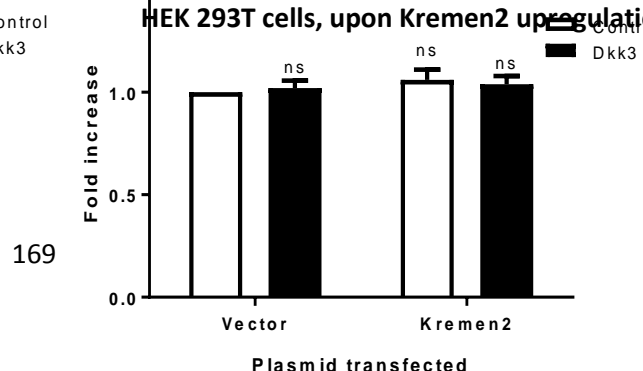


Figure 3.4.2.4 Dkk3 stimulation had no effect on the migration of HEK 293T cells overexpressing either Kremen1 or Kremen2. Empty vector pShuttle2-Flag-HA and cloned plasmids pShuttle2-Flag-hKremen1-HA and pShuttle2-Flag-hKremen2-HA were transfected into HEK 293T cells. Transwell migration assays on these cells were performed with 25 ng/mL of hDkk3 treatment. **A, B: Respectively, hKremen1 and hKremen2 upregulation mRNA expression in HEK 293T cells. C: 20X magnification representative images of HEK 293T-migrated cells transfected with either empty vector or hKremen1 or hKremen2 plasmids, under Control or hDkk3 treatment conditions. D, E: Correspondingly, quantification of hDkk3-mediated migration of HEK 293T cells overexpressing hKremen1 or hKremen2.** Dkk3 treatment did not stimulate the migration of the HEK 293T cells transfected with either the empty vector or with the cloned plasmids hKremen1 and hKremen2. (Data shown as mean \pm SEM, * $p < 0.05$, by Student's t-test (A, B) and Two-way ANOVA and Bonferroni post-hoc test, $n = 5$).

3.4.2.5 Conclusion of part 4: Overexpression of CXCR7 induced Dkk3-driven cell migration

- hCXCR2, hCXCR4, hCXCR7, hKremen1 and hKremen2 were cloned in a pShuttle2-Flag-HA vector and transfected into HEK 293T cells.
- Transwell migration assays were performed on the transfected cells upon stimulation with either 25 ng/mL of hSdf-1 α or hDkk3.
- Overexpression of CXCR2 did not affect the migration level of HEK 293T cells with either Sdf-1 α or Dkk3 treatments.
- Upregulation of CXCR4 increased the migration rate of the cells upon Sdf-1 α stimulation (1.8 fold increase), but no difference was found when treating the cells with Dkk3.
- Dkk3 (1.9 fold increase) and Sdf-1 α (1.4 fold increase) induced the migration of CXCR7 overexpressing cells.
- Interestingly, Kremen1 overexpression did not affect cell migration upon Dkk3 stimulation. This finding contrasted with the result obtained previously, which showed that downregulation of Kremen1 by SiRNA transfection decreased the Dkk3-driven Sca-1 $^+$ APC migration.
- Finally, Dkk3 did not show an effect on the migration of cells overexpressing Kremen2.
- This part of the project supported what we hypothesised before: CXCR7 was involved in cell migration driven by Dkk3.

3.4.3 Dkk3 binds to CXCR7

With the aim of confirming the physical interaction between Dkk3 and CXCR7, we performed the Co-Immunoprecipitation (Co-IP) assay and developed a methodology that enabled measuring the binding affinity of Dkk3 to CXCR7.

3.4.3.1 Dkk3 co-immunoprecipitated with CXCR7

Co-IP was performed to verify if Dkk3 physically associates with endogenous CXCR7 in Sca-1+ APCs.

The result obtained revealed that Dkk3 binds to CXCR7, as a band was observed for the samples added into the CXCR7-coupled spin columns (Figure 3.4.3.1). No band was found for the samples loaded onto the IgG-coupled spin column, confirming that the band obtained did not correspond to unspecific binding.

Moreover, a matching band was displayed for the input sample, which validated the band corresponding to Dkk3-CXCR7 complex.

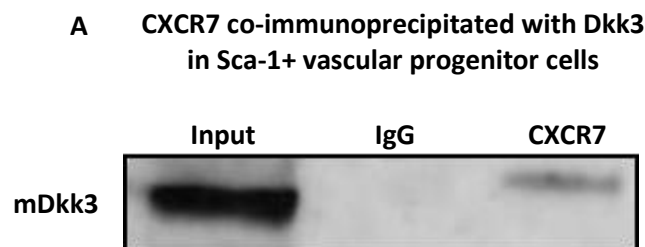
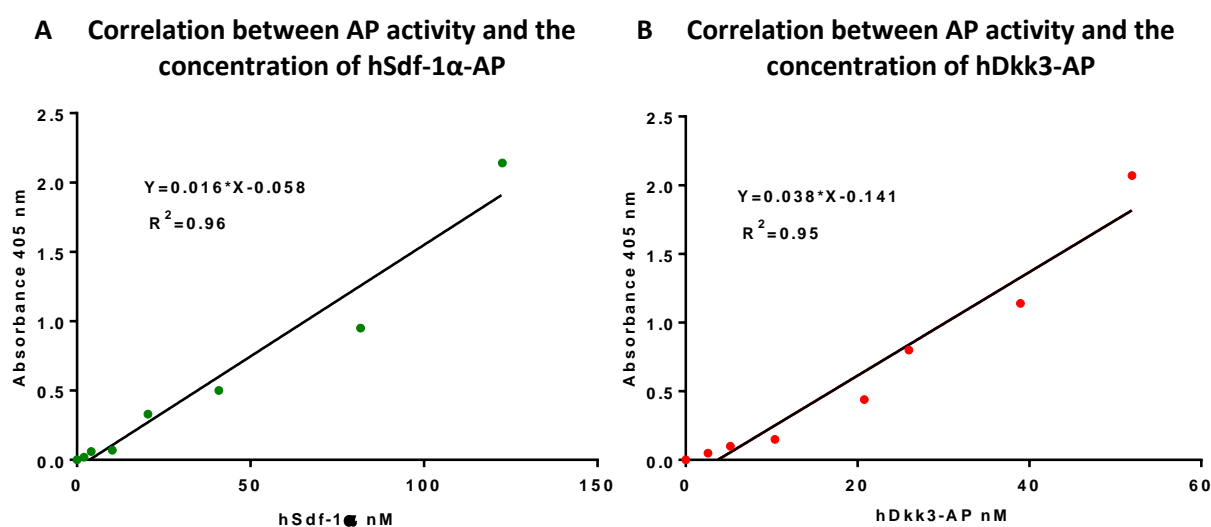


Figure 3.4.3.1: Dkk3 co-immunoprecipitated with CXCR7 in Sca-1+ vascular progenitor cells. Sca-1+ progenitor cells were treated with Dkk3 for 3 hours. Cell lysates were pre-cleared and loaded onto IgG- or CXCR7- coupled Resin spin columns. The eluted and input samples were used in western blot with anti-Dkk3 antibody incubation. Immunoblot analysis demonstrated that Dkk3 co-immunoprecipitated with CXCR7. A matching band was present in the input sample, which stands for the whole cell lysate. No band was observed for the samples loaded onto IgG-coupled spin columns.

3.4.3.2 CXCR7 has high binding affinity for Dkk3

Having confirmed the physical interaction between Dkk3 and CXCR7, we sought to measure their binding affinity by calculating the dissociation constant (K_D) through a saturation binding assay.

First, we confirmed the AP conjugation to the ligands Dkk3 and Sdf-1 α . A correlation was observed between the AP activity and the concentration of hDkk3-AP ($R^2=0.95$) and of hSdf-1 α ($R^2=0.96$), (Figure 3.4.3.2A and B). These results showed that the conjugation of AP to each ligand was successful.



Next, we measured the affinity binding of hDkk3-AP and of hSdf-1 α for the receptors hCXCR2-HA, hCXCR4-HA, hCXCR7-HA, hKremen1-HA and hKremen2-HA.

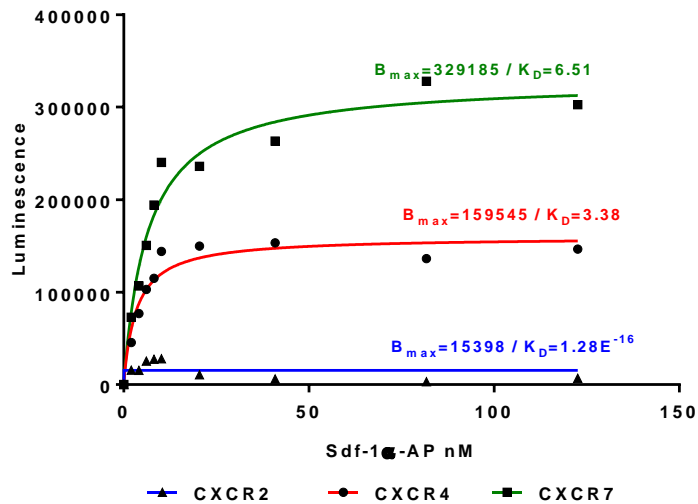
Sdf-1 α had a high binding affinity for both CXCR4 ($K_D=3.38$) and CXCR7 ($K_D=6.51$) receptors, but it did not bind to CXCR2, as no characteristic hyperbolic saturation binding curve was observed for this receptor (Figure 3.4.3.2C and D). Furthermore, the data obtained revealed that Sdf-1 α had bound more strongly to CXCR4 than to CXCR7, since the dissociation constant (K_D) of the first was lower than the K_D of CXCR7. In other words, it needed a lower concentration of the ligand Sdf-1 α to occupy half of the binding sites of CXCR4 than of CXCR7.

The method developed herein to assess the binding affinity of a ligand-AP for the corresponding receptor(s) was validated, since the results obtained for the binding of Sdf-1 α to CXCR4 and CXCR7 were consistent with the expected and reported in the literature [297, 298].

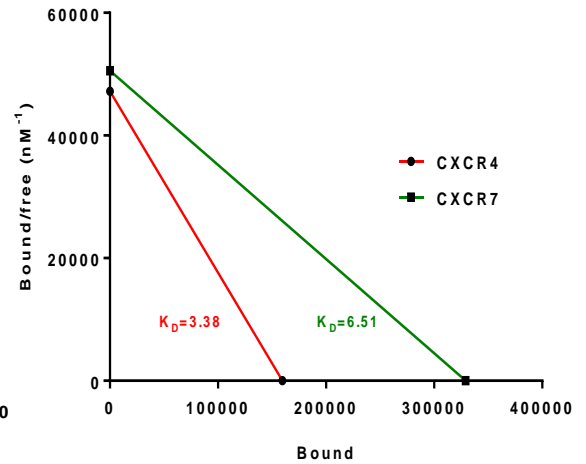
Remarkably, Dkk3 also had a high binding affinity for CXCR7 ($K_D=10.61$), but it did not bind to CXCR4 ($K_D=1.36E^{+16}$), Kremen1 ($K_D=1.29E^{+15}$) and Kremen2 (Figure 3.4.3.2.E and F). A hyperbolic curve was achieved for the binding of Dkk3 to CXCR7, but ambiguous curves were exhibited for CXCR4 and Kremen1. Additionally, the incredibly high values of K_D for CXCR4 and Kremen1 revealed that the

binding affinity of Dkk3 for these receptors was very low. No curve was possible to display for the binding of Dkk3 to Kremen2.

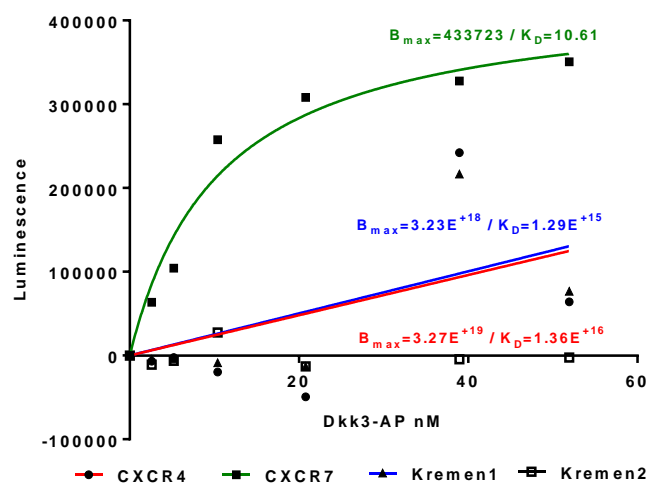
C Binding of hSdf-1 α -AP to hCXCR2, hCXCR4 and hCXCR7 293T transfected cells



D Scatchard analysis of the binding of hSdf-1 α -AP to hCXCR4 and hCXCR7 293T transfected cells



E Binding of hDkk3-AP to hCXCR4, hCXCR7, hKremen1 and hKremen2 293T transfected cells



F Scatchard analysis of the binding of hDkk3-AP to hCXCR4, hCXCR7, hKremen1 and hKremen2 293T transfected cells

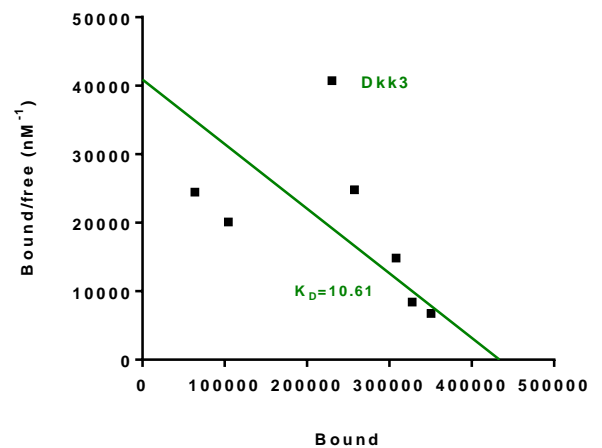


Figure 3.4.3.2: CXCR7 has high binding affinity for Dkk3. Alkaline Phosphatase was conjugated to hDkk3 and hSdf-1 α , followed by a serial dilution of these ligands. **A, B: Respectively, correlation between AP activity and the concentration of either hSdf-1 α -AP or hDkk3-AP.** After adding PNPP to each well of a 96-well plate containing the serially diluted ligands, absorbance at 405 nm was measured. The AP activity increased with the concentration of either hSdf-1 α -AP or hDkk3-AP, confirming the success of AP labelling process. Cloned plasmids hCXCR2, hCXCR4, hCXCR7, hKremen1 and hKremen2 and the empty vector pShuttle2-Flag-HA were transfected into HEK 293T cells. After lysis, the 293T transfected cell membrane extracts were added to HA antibody coated wells of high binding 96-well ELISA plates. HSdf-1 α -AP and hDkk3-AP solutions were placed in the wells with 2 hours of incubation. AP activity was measured by chemiluminescence due to the hydrolysis of PNPP substrate. **C, D: Binding curve and Scatchard analysis plot of the binding of hSdf-1 α -AP to hCXCR4, hCXCR7 and hCXCR2 293T transfected cells.** Sdf-1 α binds with high affinity to CXCR4 ($K_D=3.38$) and to CXCR7 ($K_D=6.51$), but does not bind to CXCR2. **E, F: Binding curve and Scatchard analysis plot of the binding of hDkk3-AP to hCXCR4, hCXCR7, hKremen1 and hKremen2.** Dkk3 binds with high affinity to CXCR7 ($K_D=10.61$), but it does not bind to CXCR4, Kremen1 and Kremen2. (Data represents the average of two independent experiments).

3.4.4 Conclusion of part 5: Dkk3 binds to CXCR7

- Alkaline Phosphatase was successfully conjugated to Dkk3 and Sdf-1 α .
- As expected, Sdf-1 α bound to CXCR4 and CXCR7, but not to CXCR2.
- The results obtained for Sdf-1 α validated the method developed to assess the binding affinity of a ligand for its receptor.
- Dkk3 had a high binding affinity to CXCR7, but not to CXCR4, Kremen1 and Kremen2.
- Dkk3 co-immunoprecipitated with CXCR7 of Sca-1+ vascular progenitor cells.
- These findings revealed that, in fact, Dkk3 binds to CXCR7.

3.5 Signalling pathways involved in the migration mechanism of Sca-1+ vascular progenitor cells induced by Dkk3 treatment

Cell migration mechanism is a complex phenomenon that implicates different signalling pathways, which in turn can be interconnected.

We explored diverse signalling pathways to elucidate on the Sca-1+ APC migration mechanism triggered by Dkk3 treatment.

3.5.1 ERK activation is involved in Dkk3-driven migration mechanism of Sca-1+ APCs

First, we analysed whether ERK activation was affected by Dkk3 stimulation.

ERK 1/2 are phosphorylated by MEK 1/2. For this reason, we investigated if MEK 1/2 activation level was induced by Dkk3 treatment.

Phosphorylation of MEK 1/2 was observed from as early as 3 minutes of Dkk3 stimulation and it was maintained until at least 60 minutes of treatment (Figure 3.5.1.A).

As a result, ERK 1/2 early activation was also observed upon Dkk3 treatment, throughout the time points considered (Figure 3.5.1.B).

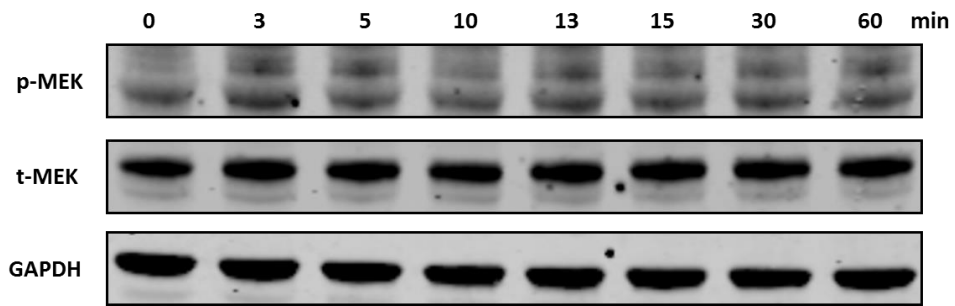
The activation of a signalling effector by itself is not sufficient to infer about its involvement in the cell migration mechanism. It is also necessary to verify if, by inhibiting this protein, the cell migration is consequently decreased.

PD98059 inhibits the activation of MEK 1/2, suppressing thus the phosphorylation of ERK1/2.

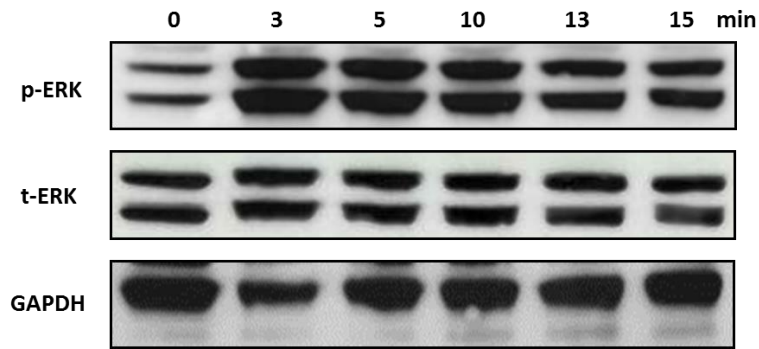
Two different concentrations of this inhibitor were used in the migration assay and both repressed the cell migration induced by Dkk3 stimulation (Figure 3.5.1.C). 10 μ M of PD98059 decreased the Sca-1+ cell migration driven by Dkk3 from 1.6 to 1.1 fold increase. Likewise, 30 μ M of the inhibitor reduced the migration rate to 0.8 fold increase.

The inhibition of ERK phosphorylation upon PD98059 treatment was confirmed by western blot, at the time points 5 and 10 minutes (Figure 3.5.1D).

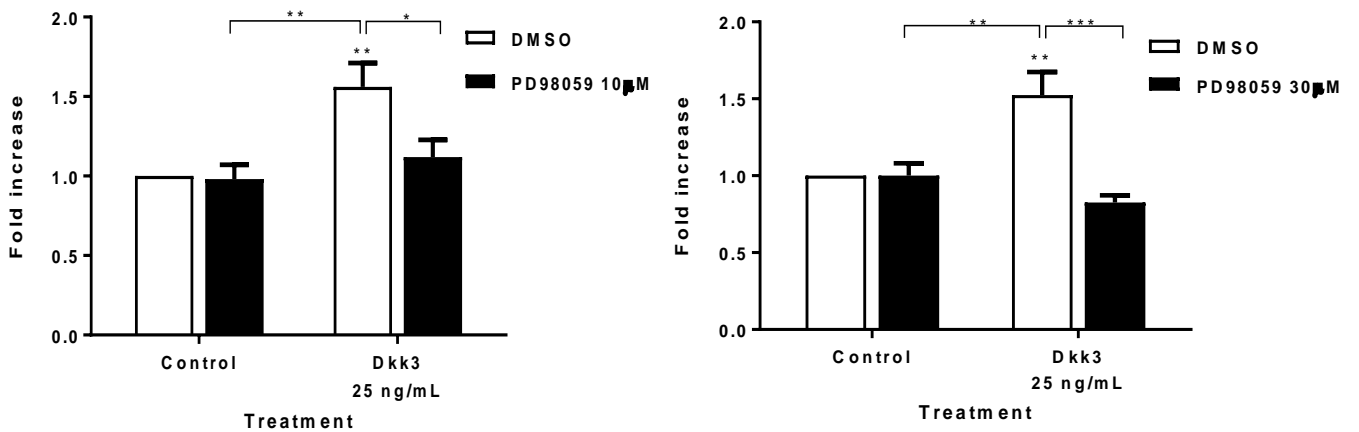
A Dkk3 induced MEK activation



B Dkk3 triggered ERK phosphorylation



C MEK/ERK inhibition by PD98059 played a negative role in the migration of Sca-1+ cells stimulated by Dkk3



D PD98059 inhibited ERK phosphorylation under Control and Dkk3 treatment conditions

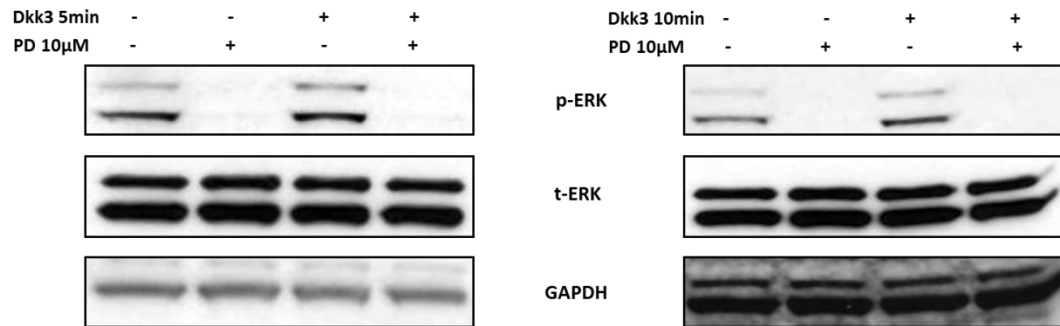


Figure 3.5.1 ERK activation is involved in Dkk3-driven migration mechanism of Sca-1+ vascular progenitor cells. MAPK signalling cascade's involvement in the migration mechanism of Sca-1+ cells was assessed by investigating whether Dkk3 stimulation induced the phosphorylation of MEK 1/2 and ERK 1/2. **A: Dkk3 induced MEK 1/2 activation.** MEK activation was induced from as early as 3 minutes and was maintained until at least 60 minutes of Dkk3 treatment. **B: Dkk3 triggered ERK 1/2 phosphorylation.** Dkk3 induced ERK phosphorylation at all time points considered, from 3 minutes to 15 minutes of Dkk3 treatment. **C: MEK/ERK inhibition by PD98059 played a negative role in the migration of Sca-1+ cells stimulated by Dkk3.** **D: PD98059 inhibited ERK phosphorylation under Control and Dkk3 treatment conditions.** Sca-1+ cells were pre-incubated for 1 hour with ERK inhibitor prior to western blot and migration assays under Dkk3 treatment. Both 10 μM and 30 μM of PD98059 inhibited the migration of the Sca-1+ cells by decreasing, respectively, the migration fold increase from 1.6 to 1.1 and 1.5 to 0.8. Phosphorylation of ERK was inhibited at 5 and 10 minutes upon PD98059 treatment. (Data shown as mean ±SEM, ***p<0.001, **p<0.01, *p<0.05, by Two-way ANOVA and Bonferroni post-hoc test, N=4).

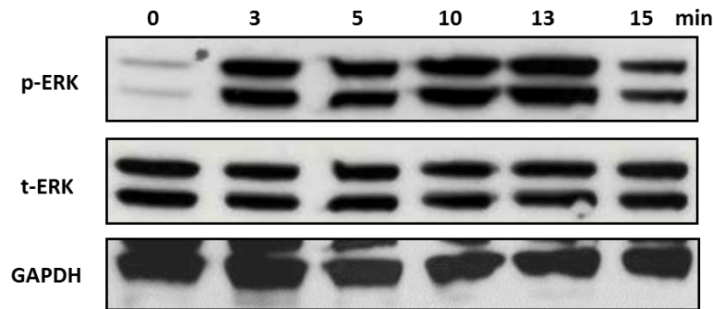
3.5.2 Sdf-1α mediated migration of Sca-1+ cells also involved ERK activation

Sdf-1α also induced the phosphorylation of ERK from 3 minutes to at least 15 minutes of stimulation (Figure 3.5.2A).

Additionally, 10 and 30 μM of PD98059 also suppressed the Sca-1+ cell migration mediated by Sdf-1α treatment, with a reduction in the fold increase from 1.5 to 0.9 and 0.8, respectively (Figure 3.5.2B).

These results suggested that the MAPK kinase signalling transduction cascade was involved in the Sca-1+ cell migration mechanism driven by either Dkk3 or Sdf-1α.

A Sdf-1 α triggered ERK phosphorylation



B MEK/ERK inhibition by PD98059 played a negative role in the migration of Sca-1+ cells stimulated by Sdf-1 α

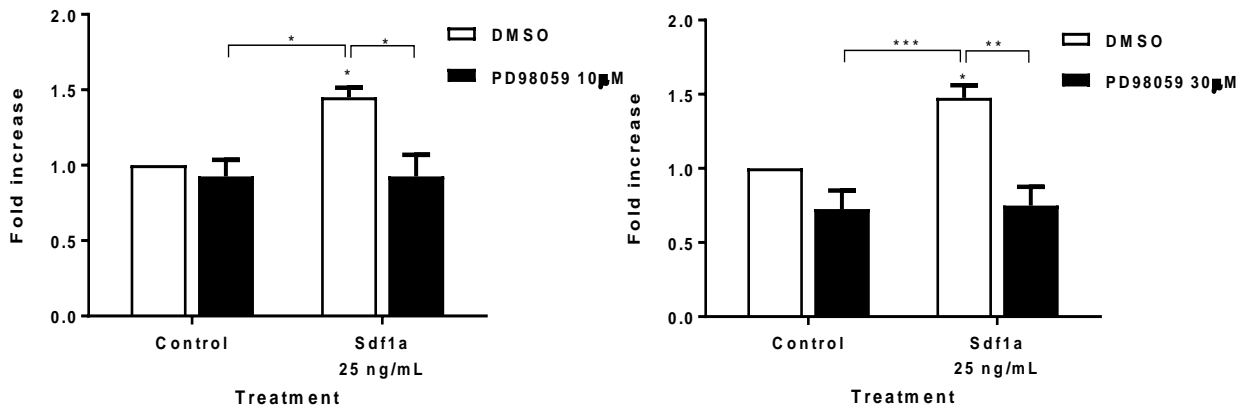


Figure 3.5.2 Sdf-1 α mediated migration of Sca-1+ cells also involved ERK activation. MAPK signalling cascade's involvement in the Sdf-1 α -mediated migration of Sca-1+ cells was assessed by investigating whether Sdf-1 α induced the phosphorylation of ERK 1/2. **A: Sdf-1 α triggered ERK phosphorylation.** ERK activation was induced from as early as 3 minutes and was maintained until at least 15 minutes of Sdf-1 α treatment. **B: MEK/ERK inhibition by PD98059 played a negative role in the migration of Sca-1+ cells stimulated by Sdf-1 α .** Both 10 and 30 μ M of PD98059 inhibition reduced the migration of Sdf-1 α -mediated migration, by decreasing, respectively, the migration fold increase from 1.5 to 0.9 and 0.8. (Data shown as mean \pm SEM, *** p <0.001, ** p <0.01, * p <0.05, by Two-way ANOVA and followed by Bonferroni post-hoc test, N=4).

3.5.3 PI3K/AKT signalling pathway is involved in Sca-1+ progenitor cell migration promoted by Dkk3

The PI3K/AKT signalling transduction pathway is another pathway largely associated with cell migration. Therefore, we analysed the phosphorylation level of AKT in response to Dkk3 and then assessed if PI3K inhibitor LY29004 affected the phosphorylation level of AKT and the Sca-1+ cell migration stimulated by Dkk3.

The activation of AKT was induced from 3 minutes until at least 60 minutes of Dkk3 treatment (Figure 3.5.3A).

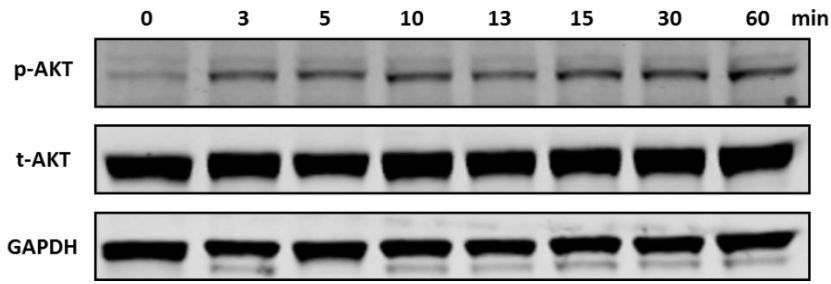
The AKT phosphorylation can be inhibited by the AKT Inhibitor X. Therefore we assessed if the inhibition of AKT activation had a negative effect on the Sca-1+ cell migration in response to Dkk3 treatment.

The Dkk3-driven Sca-1+ cell migration was decreased upon 2.5 μ M (fold increase of 1) and 5 μ M (fold increase of 0.9) of AKT Inhibitor X treatment (Figure 3.5.3B). Due to the knowledge of the role of AKT signalling in cell survival, we wished to assess whether AKT inhibition affected the rate of Sca-1+ cell survival. For this purpose, a quantification of cell death upon AKT inhibitor X and Dkk3 treatments was carried out. After incubating the cells for two hours with the inhibitor and with Dkk3, a trypan blue staining was performed and the number of cells stained (dead cells) was quantified, under the microscope (Figure 3.5.3C). Neither Dkk3 nor AKT inhibitor promoted Sca-1+ cell death, as no significant difference was found in the number of dead cells (Figure 3.5.3D).

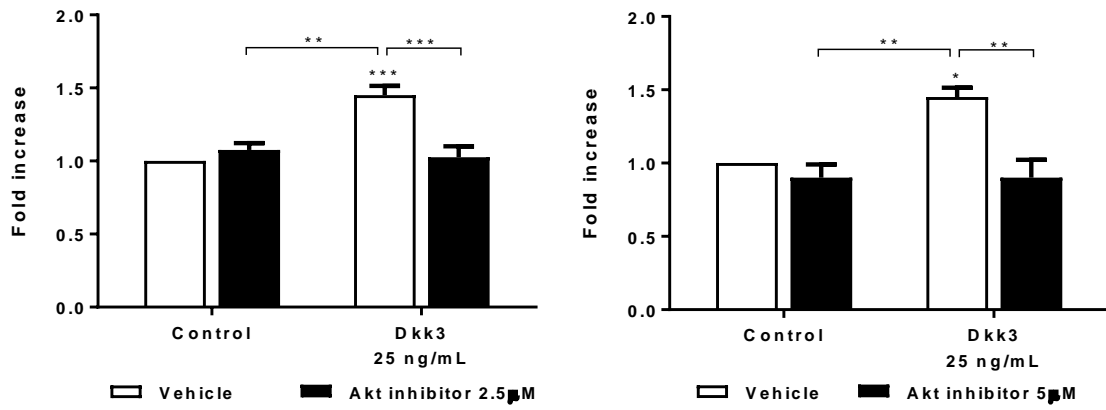
AKT is activated by PI3K, therefore, we investigated whether the inhibition of the PI3K activity would block the AKT phosphorylation induced by Dkk3. LY29004 is a widely used inhibitor of PI3K activity [299-301]. Sca-1+ cells were pre-incubated with either 10 or 25 μ M of LY29004, followed by Dkk3 treatment and western blot and migration assays. Both inhibitor concentrations decreased the Dkk3-driven Sca-1+ progenitor cell migration, from 1.5 to 1.1 fold increase (10 μ M LY29004) and 1.7 to 1.0 fold increase (25 μ M LY29004), (Figure 3.5.3E). AKT phosphorylation induced by DKK3 was inhibited at 5 and 10 minutes with 10 μ M of LY29004 inhibitor (Figure 3.5.3F).

The data herein obtained proved that the PI3K/AKT signalling pathway is part of the Dkk3-driven migration mechanism of Sca-1+ progenitor cells.

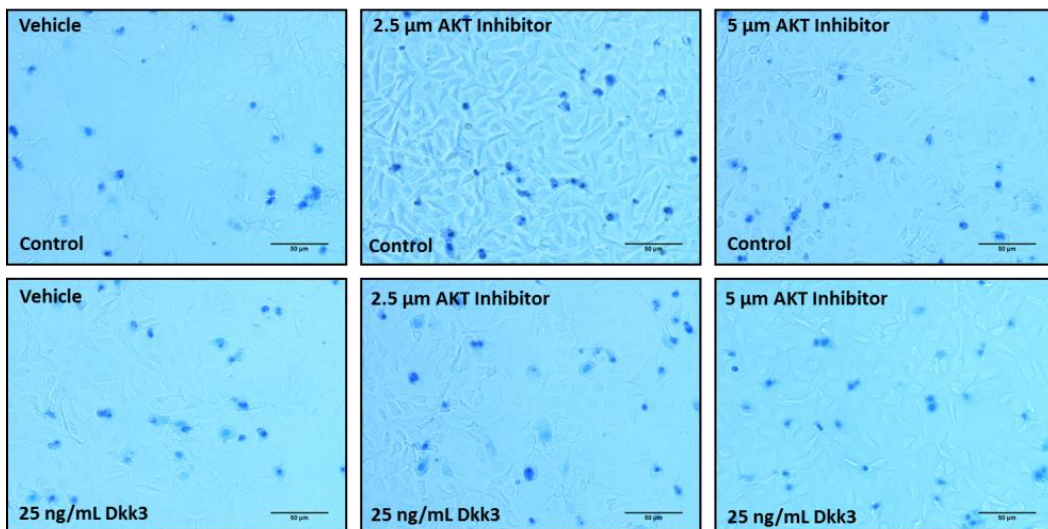
A Dkk3 induced AKT phosphorylation



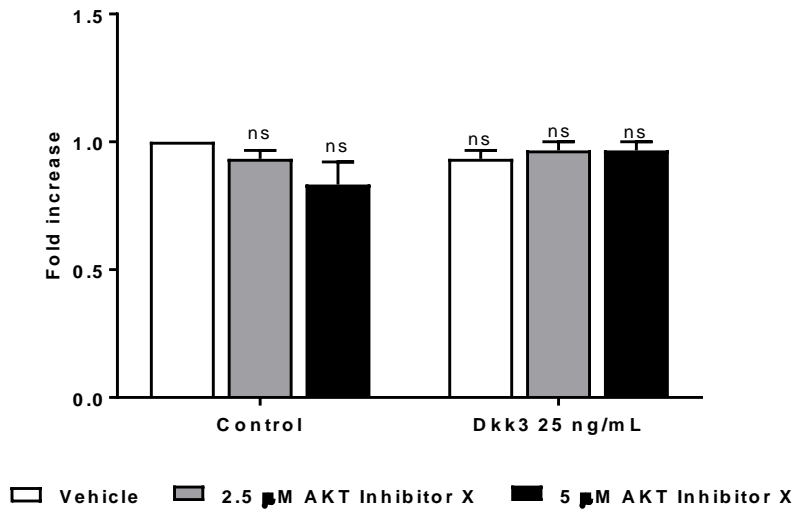
B AKT inhibitor X decreased Dkk3 driven Sca-1+ cell migration



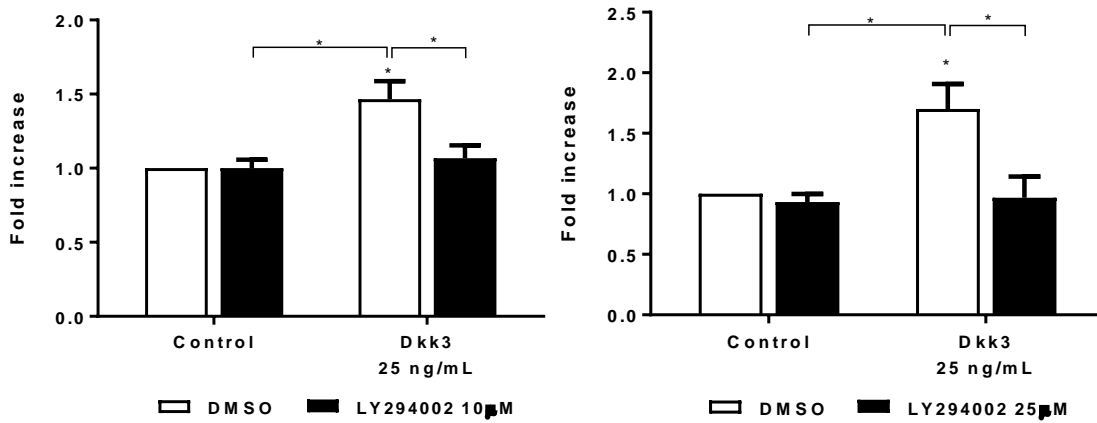
C Trypan blue staining of Sca-1+ cells after Dkk3 and AKT Inhibitor X treatments



D Quantification of cell death upon Dkk3 and AKT Inhibitor X treatments



E PI3K inhibitor LY294002 reduced the migration of Sca-1+ APCs induced by Dkk3 treatment



F LY294002 inhibitor repressed AKT phosphorylation in Sca-1+ progenitor cells both under Control and Dkk3 treatment conditions

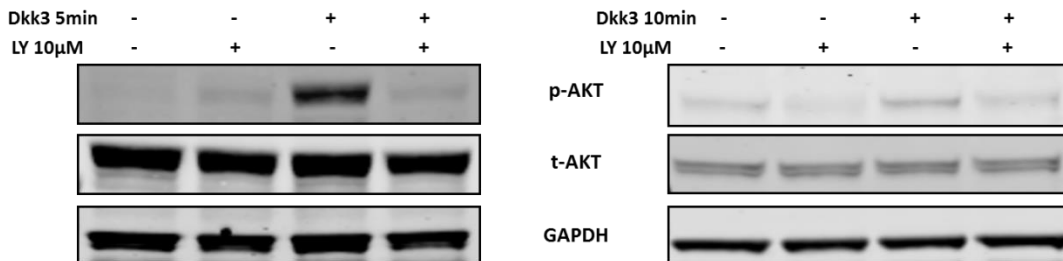


Figure 3.5.3 PI3K/AKT signalling pathway is involved in Sca-1+ progenitor cell migration promoted by Dkk3. PI3K/AKT signalling pathway involvement in the migration mechanism of Sca-1+ progenitor cells was assessed by investigating whether Dkk3 stimulation induced the phosphorylation of AKT. **A: Dkk3 induced AKT phosphorylation.** AKT activation was induced from as early as 3 minutes and was maintained for at least 60 minutes of Dkk3 treatment. **B: AKT Inhibitor X decreased Dkk3-driven Sca-1+ cell migration.** AKT inhibitor X decreased Dkk3-driven Sca-1+ cell migration at 2.5 μM (1.5 to 1.0 fold increase) and 5 μM (1.5 to 0.9 fold increase) concentrations; N=4. **C: Trypan blue staining of Sca-1+ cells after Dkk3 and AKT Inhibitor X treatments.** 20X magnification representative images of Sca-1+ cells stained with trypan blue after 2 hours of incubation with Dkk3 and AKT Inhibitor X. **D: Cell death quantification upon Dkk3 and AKT Inhibitor X treatments.** Neither Dkk3 stimulation nor AKT inhibitor incubation induced cell death, as no significant difference was found in the number of dead cells, in any of the conditions; N=3 **E: PI3K inhibitor LY29004 reduced the migration of Sca-1+ progenitor cells induced by Dkk3 treatment.** Dkk3-driven Sca-1+ cell migration was negatively affected by treatment with LY29004 at 10 μM (1.5 to 1.1 fold increase) and 25 μM (1.7 to 1.0 fold increase) concentrations, N=3. **F: LY29004 inhibitor repressed AKT phosphorylation at 5 and 10 minutes of Dkk3 stimulation.** Phosphorylation of AKT was inhibited at 5 and 10 minutes upon 10 μM LY29004 treatment. (Data shown as mean \pm SEM, ***p<0.001, **p<0.01, *p<0.05, by Two-way ANOVA followed by Bonferroni multiple comparison test).

3.5.4 PI3K/AKT pathway is also involved in the migration of Sca-1+ cells upon Sdf-1 α stimulation

The involvement of PI3K/AKT signalling pathway was also verified in Sca-1+ progenitor cell migration promoted by Sdf-1 α .

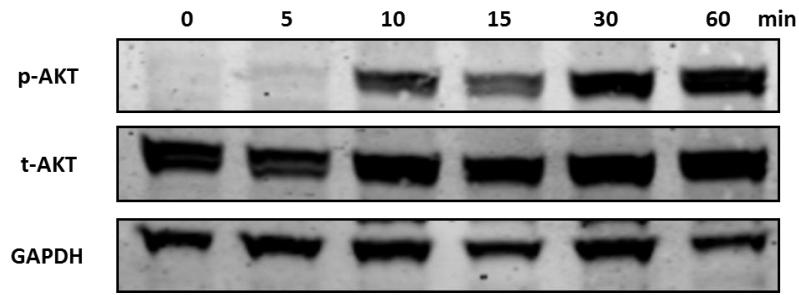
AKT phosphorylation was induced from as early as 5 minutes and maintained for at least 60 minutes of Sdf-1 α stimulation (Figure 3.5.4.A).

Sdf-1 α -driven migration of Sca-1+ cells was negatively affected upon AKT Inhibitor X treatment, with 2.5 μM (1.8 to 1.0-fold increase) and 5 μM (1.8 to 1.1 fold increase) concentrations (Figure 3.5.4.B).

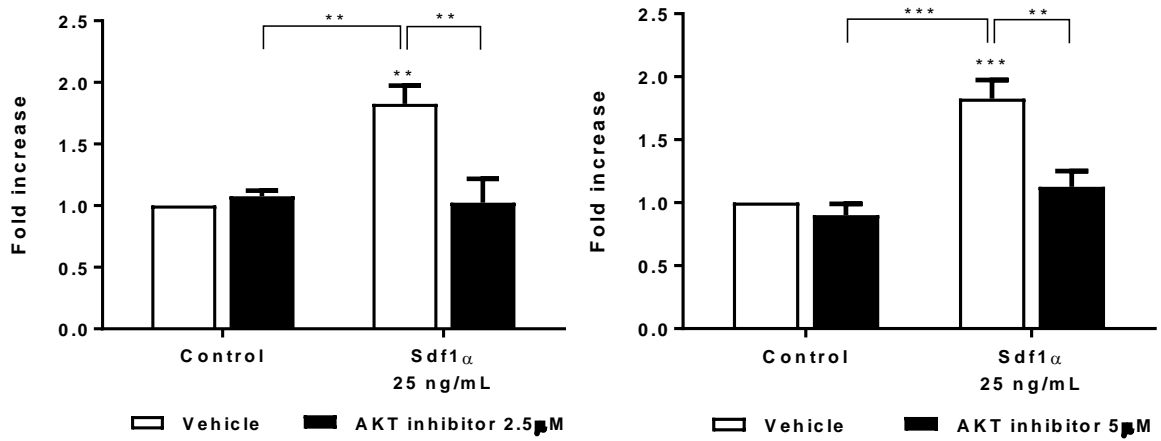
Likewise, PI3K inhibitor LY29004 also reduced Sca-1+ cell migration induced by Sdf-1 α , with concentrations of 10 μM (1.5 to 1.0 fold increase) and 25 μM (1.8 to 1.1 fold increase) (Figure 3.5.4C).

As a result, we concluded that PI3K/AKT signalling pathway was also implicated in Sca-1+ progenitor cell migration mediated by Sdf-1 α .

A Sdf-1 α activated AKT



B AKT inhibitor X decreased Sdf-1 α -driven Sca-1+ cell migration



C PI3K inhibition by LY294002 decreased Sca-1+ cell migration induced by Sdf-1 α

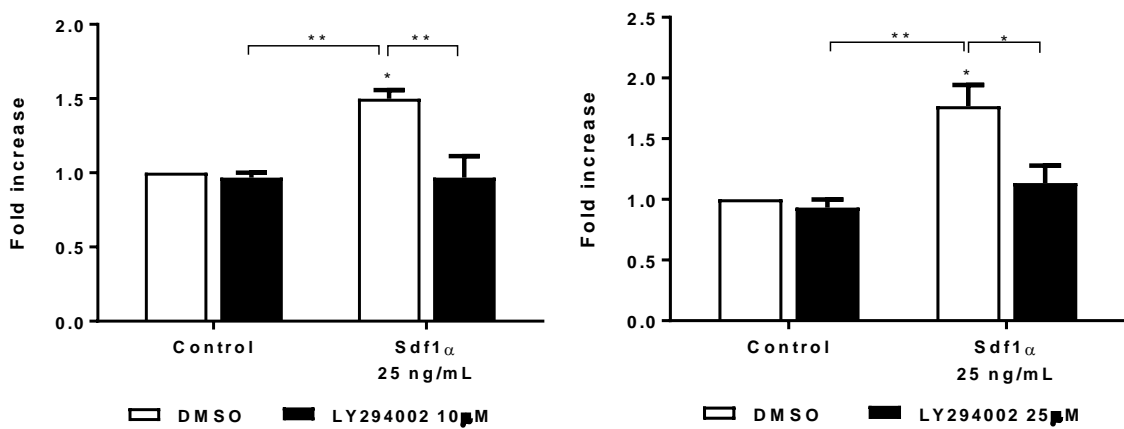


Figure 3.5.4 PI3K/AKT pathway is involved in the migration of Sca-1+ progenitor cells upon Sdf-1 α stimulation. PI3K/AKT signalling pathway involvement in the migration mechanism of Sca-1+ progenitor cells induced by Sdf-1 α was assessed. **A: Sdf-1 α activated AKT.** AKT phosphorylation was induced from as early as 5 minutes and was maintained for at least 60 minutes of Sdf-1 α treatment. **B: AKT Inhibitor X decreased Sdf-1 α -driven Sca-1+ cell migration.** AKT inhibitor X decreased Sdf-1 α -driven Sca-1+ cell migration with concentrations of 2.5 μ M (1.8 to 1.0 fold increase) and 5 μ M (1.8 to 1.1 fold increase); N=4. **C: PI3K inhibition by LY29004 decreased the migration of Sca-1+ progenitor cells induced by Sdf-1 α treatment.** Sdf-1 α -driven Sca-1+ cell migration was negatively affected by treatment with LY29004 at 10 μ M (1.5 to 1.0 fold increase) and 25 μ M (1.8 to 1.1 fold increase) concentrations, N=3. (Data shown as mean \pm SEM, ***p<0.001, **p<0.01, *p<0.05, by Two-way ANOVA followed by Bonferroni multiple comparison test).

3.5.5 Activation of Rho GTPases is implicated in Sca-1+ APC migration mechanism induced by Dkk3

Due to the crucial importance of Rho GTPases in cell migration mechanism, their activation level mediated by Dkk3 and Sdf-1 α was assessed at 0, 3, 5, 10, 13, 15 and 30 minutes of stimulation.

3.5.5.1 Rac1 activation is involved in the Sca-1+ cell migration mechanism induced by Dkk3

25 ng/mL of Dkk3 induced the activation of Rac1 at all time points, with statistical significance at 10 (1.4 fold increase), 13 (1.6 fold increase) and 15 (1.4 fold increase) minutes of stimulation (Figure 3.5.5.1A).

Similarly, 25 ng/mL of Sdf-1 α also induced Rac1 activation with statistical significance at 13 (1.5 fold increase) and 15 (1.4 fold increase) minutes of treatment (Figure 3.5.5.1A).

Next, we used the compound NSC23766, a Rac1 activation inhibitor, to assess if the Dkk3-driven Sca-1+ cell migration was affected. Indeed, the cell migration was decreased with 10 μ M (1.7 to 1.3 fold increase) and 25 μ M (1.7 to 1.1 fold increase) of NSC23766 concentrations (Figure 3.5.5.1C).

Rac1 activation induced by Dkk3 treatment was also inhibited at 10 minutes (1.4 to 0.9 fold increase) and 15 minutes (1.4 to 1.0 fold increase) of stimulation, upon 25 μ M of NSC23766 treatment (Figure 3.5.5.1B).

These findings demonstrated that Rac1 activation is implicated in the migration mechanism of Sca-1+ progenitor cells induced by Dkk3 and potentially by Sdf-1 α as well.

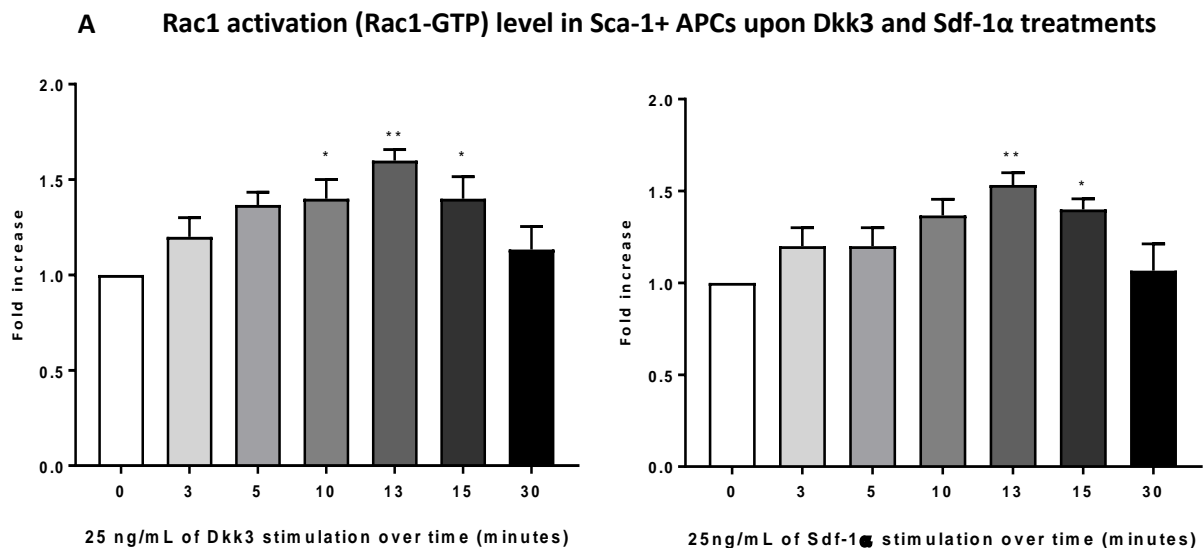
At this stage, we aimed at understanding whether Rac1 activation was upstream or downstream of MEK/ERK and PI3K/AKT signalling pathways, which were previously demonstrated to be involved in the Dkk3-mediated Sca-1+ progenitor cell migration.

Hence, we investigated if ERK phosphorylation was influenced by Rac1 activation inhibition. By treating the cells with 10 μ M of NSC23766, ERK phosphorylation was repressed at 10 and 15 minutes of Dkk3 stimulation (Figure 3.5.5.1D). This suggested that Rac1 activation was upstream of ERK phosphorylation.

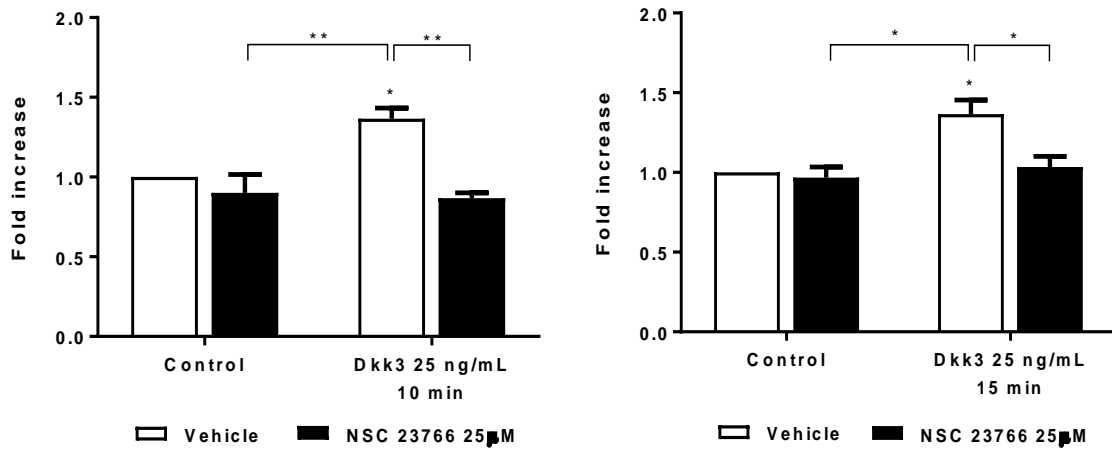
However, we examined as well whether ERK inhibitor PD98059 reduced the activation level of Rac1. Strikingly, Rac1 activation was suppressed at 10 minutes (1.4 to 0.9 fold increase) and 15 minutes (1.5 to 1.1 fold increase) with 10 μ M of NSC23766 treatment (Figure 3.5.5.1E).

The fact that ERK inhibition decreased the level of Rac1 activation and, in turn, Rac1 activation inhibition suppressed ERK phosphorylation, revealed that a feedback mechanism was taking place between Rac1 GTPase and ERK.

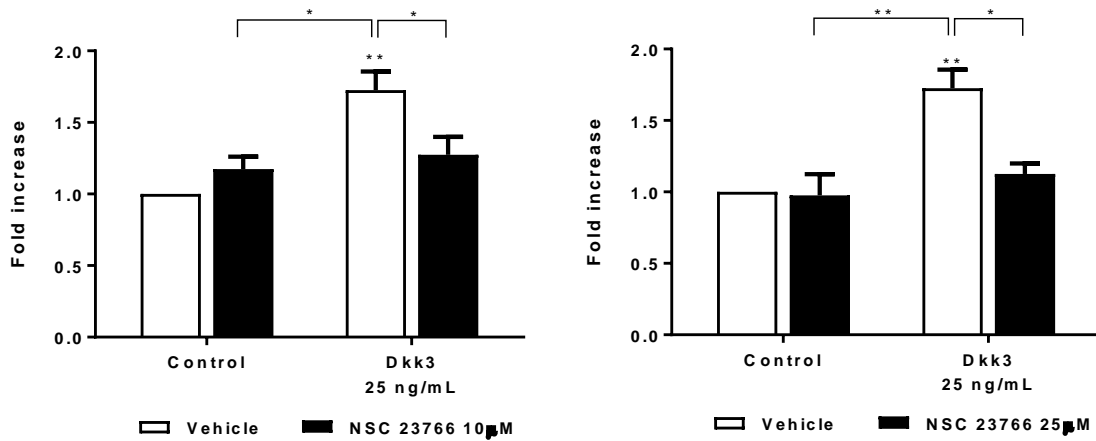
Finally, Rac1 activation was also tested upon PI3K/AKT inhibition. 10 μ M of LY29004 had no impact in the Rac1 activation level at both 10 and 15 minutes of Dkk3 stimulation (Figure 3.5.5.1F). We thus inferred that AKT phosphorylation was not upstream of Rac1 GTPase pathway.



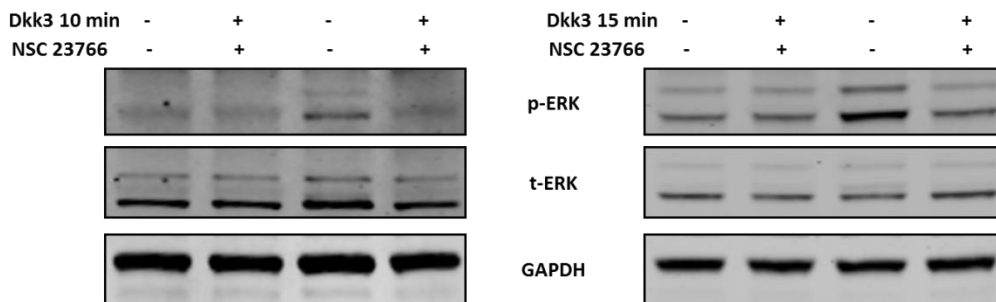
B NSC23766 suppressed the activation of Rac1 in Sca-1+ APCs under control and Dkk3 treatment conditions



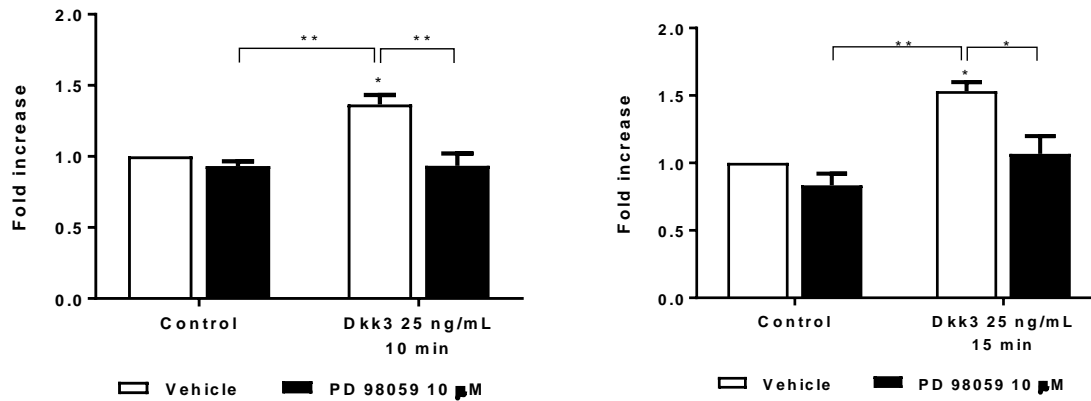
C Rac1 activation inhibitor NSC23766 suppressed Sca-1+ APCs migration driven by Dkk3 treatment



D Rac1 activation inhibitor repressed ERK phosphorylation in Dkk3-mediated migration of Sca-1+ APCs



E ERK inhibition by PD98059 suppressed Rac1 activation in Sca-1+APCs stimulated by Dkk3



F LY294002 did not affect the level of activation of Rac1 in Sca-1+ APCs treated with Dkk3

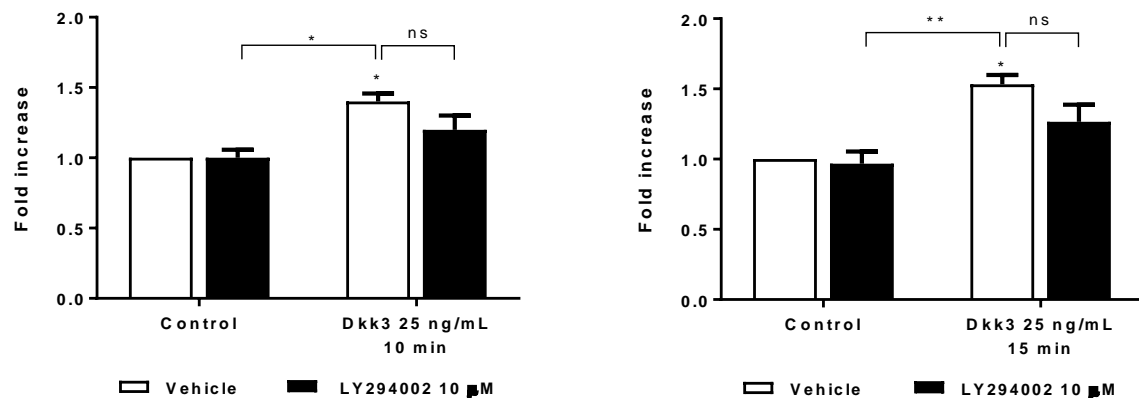


Figure 3.5.5.1 Rac1 activation is involved in Sca-1+ cell migration mechanism induced by Dkk3. Rac1 GTPase protein's role, in Dkk3-driven Sca-1+ cell migration, was investigated. **A: Rac1 activation (Rac1-GTP) level in Sca-1+ APCs upon Dkk3 and Sdf-1 α treatments.** Dkk3 induced Rac1 activation at all time points, with statistical significance at 10 (1.4 fold increase), 13 (1.6 fold increase) and 15 minutes (1.4 fold increase) of stimulation; N=3. **B: NSC23766 suppressed the activation of Rac1 in Sca-1+ APCs under control and Dkk3 treatment conditions.** Rac1 activation induced by Dkk3 was inhibited at 10 minutes (1.4 to 0.9 fold increase) and 15 minutes (1.4 to 1.0 fold increase), upon 25 μ M of NSC23766 treatment; N=3. **C: Rac1 activation inhibitor NSC23766 suppressed the migration of Sca-1+ APCs driven by Dkk3 treatment.** Sca-1+ cell migration decreased with 10 μ M (1.7 to 1.3 fold increase) and 25 μ M (1.7 to 1.1 fold increase) of NSC23766 treatment; N=4. **D: Rac1 activation inhibition repressed ERK phosphorylation in Dkk3-mediated migration of Sca-1+ progenitor cells.** Treatment with 10 μ M of NSC23766 repressed ERK phosphorylation at 10 and 15 minutes of Dkk3 stimulation. **E: ERK inhibition by PD 98059 suppressed Rac1 activation in Sca-1+ progenitor cells stimulated with Dkk3.** Rac1 activation was suppressed at 10 minutes (1.4 to 0.9 fold increase) and 15 minutes (1.5 to 1.1 fold increase) with 10 μ M of NSC23766 treatment; N=3. **F: LY294002 did not affect the level of activation of Rac1 in Sca-1+ progenitor cells treated with Dkk3.** 10 μ M of LY29004 had no impact in the Rac1 activation level at both 10 and 15 minutes of Dkk3 stimulation; N=3. (Data shown as mean \pm SEM, ** p <0.01, * p <0.05, by One-Way ANOVA (A) and Two-way ANOVA (B, C, E and F), followed by Bonferroni multiple comparison test).

3.5.5.2 RhoA signalling pathway is implicated in Sca-1+ APC migration mechanism induced by Dkk3 treatment

Another essential member of the Rho GTPase family is RhoA. Downstream of its signalling cascade is Myosin Light Chain (MLC), whose phosphorylation is dependent on the activation of Rho-associated Kinases (ROCK). These molecular events are pivotal in the regulation of the cell cytoskeleton and consequently cell motility [302-305].

We first analysed the activation level of the downstream effectors of RhoA in Sca-1+ cells. MLC phosphorylation (activation) was induced by both Dkk3 and Sdf-1 α treatments, from as early as 3 minutes of stimulation (Figure 3.5.5.2A).

On the other hand, cofilin phosphorylation (inactivation) level was not altered upon Dkk3 or Sdf-1 α stimulation. Cofilin was found already phosphorylated (inactive state) in the Control condition and neither Dkk3 nor Sdf-1 α treatments were able to alter this state at any of the time points considered (Figure 3.5.5.2B).

We then measured the activation degree of RhoA. Dkk3 treatment induced RhoA activation at mostly all the time points considered, with statistical significance at 3 (1.4 fold increase), 13 (1.7 fold increase), 15 (1.4 fold increase) and 30 minutes (1.3 fold increase) of stimulation. Equally, Sdf-1 α treatment also induced RhoA activation with significant increase at 13 (1.5 fold increase), 15 (1.4 fold increase) and 30 minutes (1.4 fold increase) of stimulation (Figure 3.5.5.2C).

In order to assess whether RhoA activation was involved in the Dkk3-driven migration mechanism of Sca-1+ progenitor cells, Rhosin compound was used in a transwell migration assay. Rhosin is a RhoA activation inhibitor and it decreased cell migration at 10 μ M (1.5 to 1.1-fold increase) and 25 μ M (1.6 to 1.0 fold increase) concentrations (Figure 3.5.5.2E).

RhoA activation was also suppressed by 10 μ M of Rhosin inhibitor at 13 (1.6 to 0.9 fold increase) and 15 minutes (1.5 and 1.1 fold increase) of Dkk3 stimulation (Figure 3.5.5.2D).

Cell actomyosin contractility is induced by MLC phosphorylation, which occurs either directly by ROCK or due to inhibition of Myosin Phosphatase. RhoA is upstream of all these processes and we therefore investigated whether RhoA activation inhibition had an effect in the phosphorylation level of MLC induced by Dkk3 stimulation. Verily, MLC phosphorylation was repressed by 10 μ M of Rhosin inhibitor treatment at 13 minutes of Dkk3 stimulation (Figure 3.5.5.2F).

The implication of ROCK in the Dkk3-driven Sca-1+ cell migration mechanism was also assessed. Y27632 is a ROCK inhibitor and it decreased the cell migration rate at 5 μ M (1.7 to 1.2 fold increase) and 10 μ M (1.7 to 1.1 fold increase) concentrations (Figure 3.5.5.2.G).

Additionally, MLC phosphorylation was also reduced by 5 μ M of Y27632 inhibitor at 13 minutes of Dkk3 stimulation (Figure 3.5.5.2H).

The data here presented proved that Dkk3 triggered RhoA activation, which in turn activated ROCK and promoted MLC phosphorylation. This signalling cascade seems to be involved as well in Sca-1+ APCs migration driven by Sdf-1 α treatment.

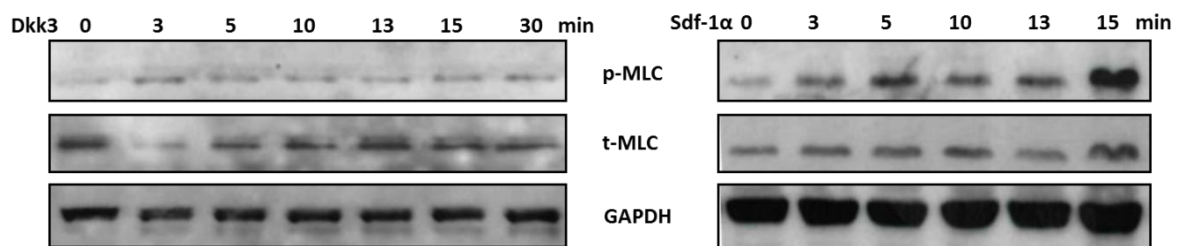
Lastly, with the intention of studying the cross-talk between RhoA signalling cascade and other signalling pathways, we measured RhoA activation level in response to ERK and PI3K/AKT inhibition.

PD98059 at 10 μ M concentration did not repress RhoA activation at 13 and 15 minutes of Dkk3 stimulation (Figure 3.5.5.2I).

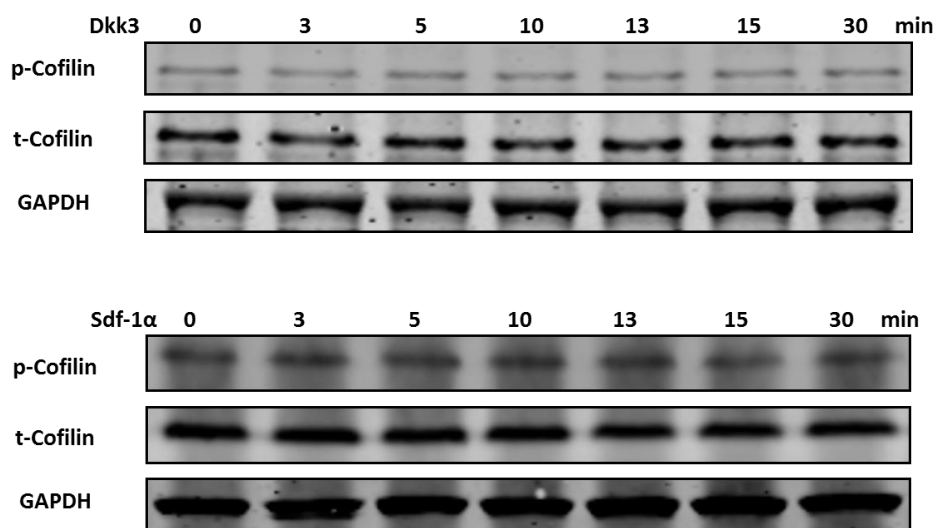
Intriguingly, PI3K/AKT inhibitor LY29004 at 10 μ M concentration also did not attenuate the activation level of RhoA at 13 and 15 minutes of Dkk3 stimulation (Figure 3.5.5.2J).

These results showed that MAPK and PI3K/AKT signalling pathways were not upstream of RhoA signalling cascade and therefore, they were either independent or downstream of RhoA pathway.

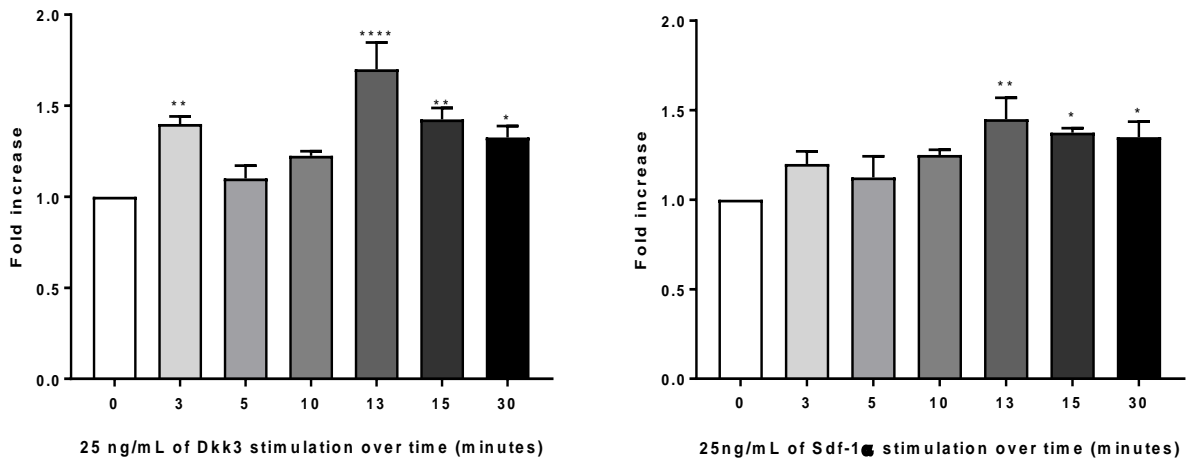
A Dkk3 and Sdf-1 α induced the phosphorylation of Myosin Light Chain in Sca-1+ APCs



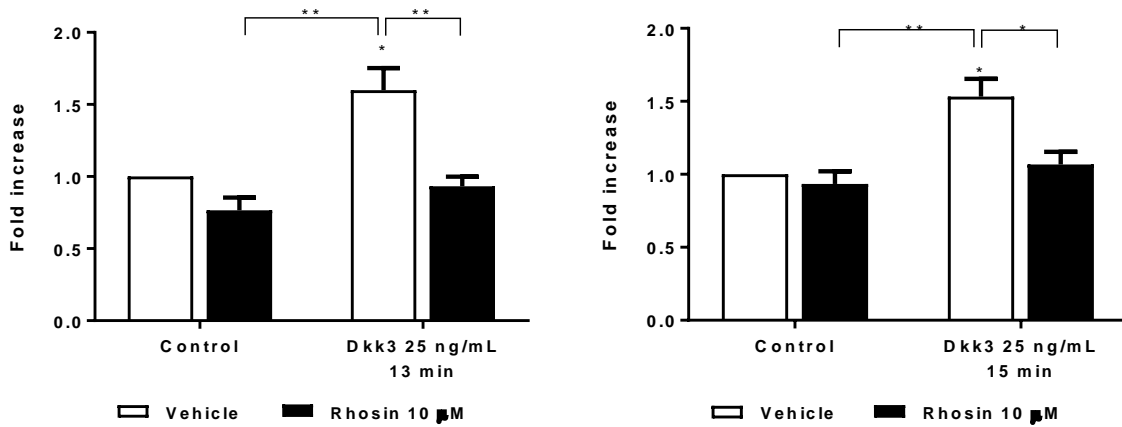
B Cofilin phosphorylation level was not affected by Dkk3 or Sdf-1 α stimulation



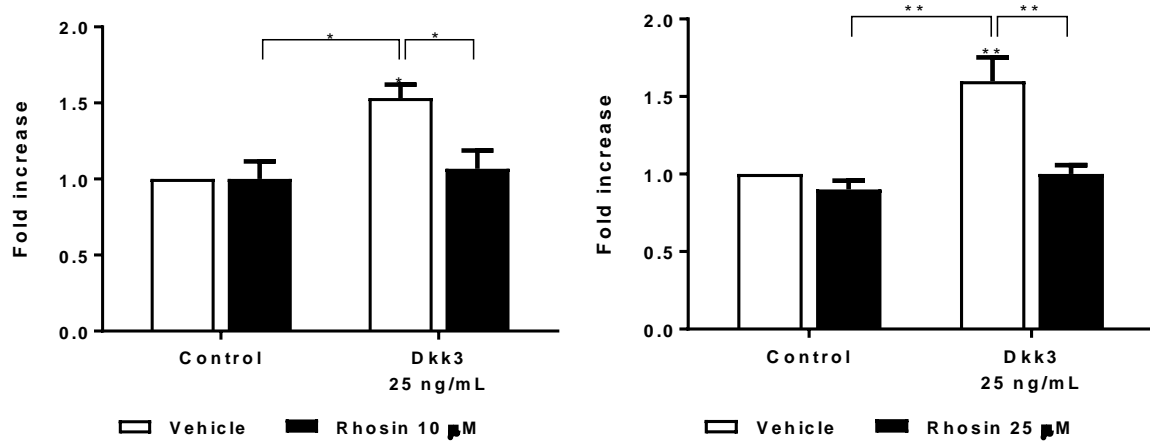
C RhoA activation (RhoA-GTP) level in Sca-1+ APCs upon Dkk3 or Sdf-1 α treatments



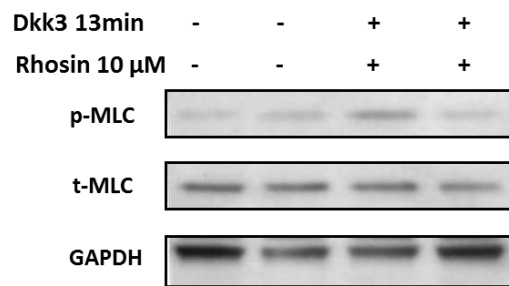
D Rhosin (G04) inhibited RhoA activation triggered by Dkk3 stimulation in Sca-1+ APCs



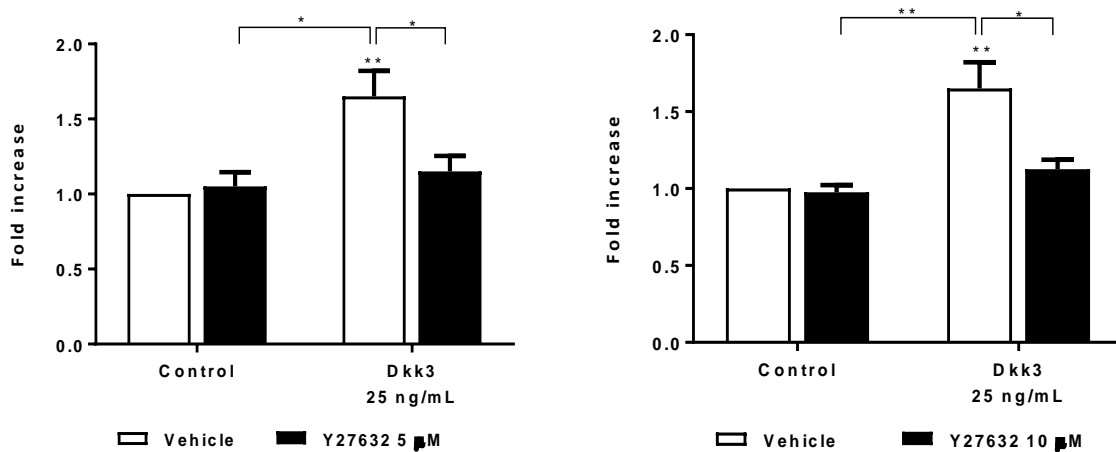
E Rhosin inhibitor decreased the migration of Sca-1+ APCs stimulated by Dkk3 treatment



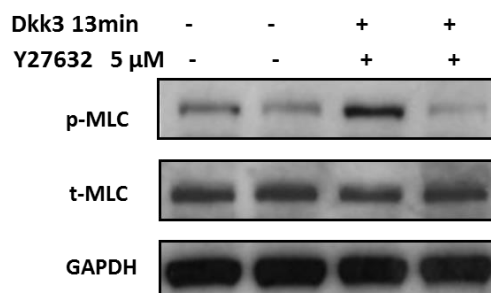
F RhoA activation inhibitor Rhosin reduced the phosphorylation of Myosin Light chain in Sca-1+ APCs stimulated with Dkk3



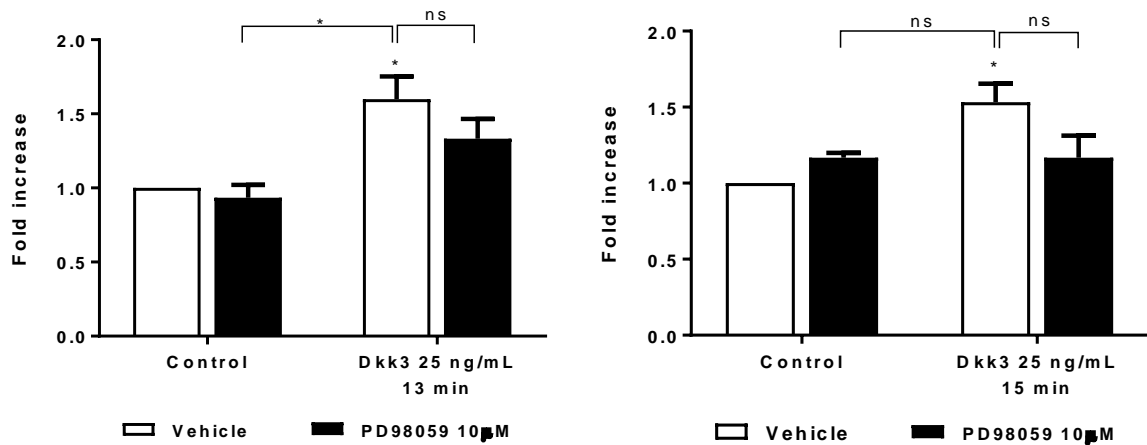
G ROCK inhibitor Y27632 decreased the migration of Sca-1+ APCs induced by Dkk3 treatment



H Myosin Light Chain phosphorylation triggered by Dkk3 stimulation was suppressed in Sca-1+ APCs upon Y27632 treatment



I ERK inhibition with PD98509 did not affect the activation level of RhoA in Sca-1+ progenitor cells stimulated with Dkk3



J PI3K inhibition by LY294002 did not affect the activation level of RhoA in Sca-1+ APCs treated with Dkk3

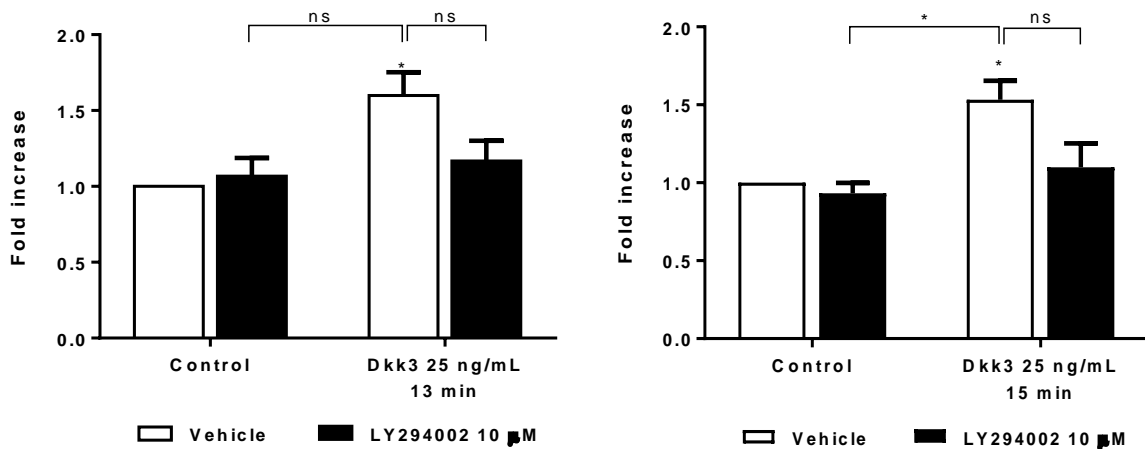


Figure 3.5.5.2 RhoA signalling pathway is implicated in Sca-1+ progenitor cell migration mechanism stimulated by Dkk3 treatment. RhoA signalling pathway's implication in Dkk3-driven Sca-1+ cell migration was investigated. **A: Dkk3 and Sdf-1 α induced the phosphorylation of MLC in Sca-1+ progenitor cells.** Phosphorylation of MLC was observed from as early as 3 minutes of stimulation with Dkk3 or Sdf-1 α . **B: Cofilin phosphorylation level was not affected by Dkk3 or Sdf-1 α stimulation.** Cofilin was found to be already phosphorylated in the Control condition and neither Dkk3 nor Sdf-1 α treatments changed its phosphorylation state at any of the time points considered. **C: RhoA activation (RhoA-GTP) level in Sca-1+ APCs upon Dkk3 or Sdf-1 α treatments.** Dkk3 induced RhoA activation at mostly all the time points considered, with statistical significance at 3 (1.4 fold

increase), 13 (1.7 fold increase), 15 (1.4 fold increase) and 30 minutes (1.3 fold increase) of stimulation. Equally, Sdf-1 α treatment also induced RhoA activation with significant increase at 13 (1.5 fold increase), 15 (1.4 fold increase) and 30 minutes (1.4 fold increase) of stimulation. **D: Rhosin (G04) inhibited RhoA activation triggered by Dkk3 stimulation in Sca-1+ APCs.** RhoA activation was suppressed by 10 μ M of Rhosin inhibitor at 13 (1.6 to 0.9 fold increase) and 15 minutes (1.5 and 1.1 fold increase) of Dkk3 stimulation. **E: Rhosin inhibitor decreased the migration of Sca-1+ vascular progenitor cells induced by Dkk3 treatment.** Rhosin inhibitor decreased the Dkk3-driven cell migration with 10 μ M (1.5 to 1.1-fold increase) and 25 μ M (1.6 to 1.0 fold increase) concentrations. **F: RhoA activation inhibitor Rhosin reduced the phosphorylation of Myosin Light chain in Sca-1+ APCs stimulated with Dkk3.** MLC phosphorylation was repressed by 10 μ M of Rhosin inhibitor at 13 minutes of Dkk3 stimulation. **G: ROCK inhibitor Y27632 decreased the migration of Sca-1+ APCs stimulated by Dkk3.** Y27632 treatment decreased the cell migration rate at 5 μ M (1.7 to 1.2 fold increase) and 10 μ M (1.7 to 1.1 fold increase) concentrations. **H: Myosin Light Chain activation was suppressed in Sca-1+ APCs treated with Dkk3.** MLC phosphorylation was reduced by 5 μ M of Y27632 inhibitor at 13 minutes of Dkk3 stimulation. **I: ERK inhibition with PD98509 did not affect the activation of RhoA in Sca-1+ progenitor cells stimulated with Dkk3.** 10 μ M of PD98059 did not repress RhoA activation at 13 and 15 minutes of Dkk3 stimulation. **J: PI3K inhibition by LY294002 did not affect the activation of RhoA in Sca-1+ progenitor cells treated with Dkk3.** 10 μ M of LY29004 did not attenuate the activation of RhoA induced by 13 and 15 minutes of Dkk3 stimulation. (Data shown as mean \pm SEM, **p<0.01, *p<0.05, by One-Way ANOVA (C) and Two-way ANOVA (D, E, G, I and J), followed by Bonferroni multiple comparison test).

3.5.6 Conclusion of part 6: Signalling pathways involved in the migration mechanism of Sca-1+ APCs induced by Dkk3 treatment

- MEK 1/2 and ERK 1/2 phosphorylation was stimulated from as early as 3 minutes of Dkk3 stimulation and was maintained until at least 60 minutes of treatment.
- Sdf-1 α also induced ERK phosphorylation at early time points.
- MEK/ERK inhibitor PD98059 significantly decreased the Dkk3- and Sdf-1 α -driven migration of Sca-1+ progenitor cells and suppressed ERK phosphorylation at both Control and Dkk3 treatment conditions.
- MAPK kinase signalling pathway is involved in the Sca-1+ progenitor cell migration mechanism induced by Dkk3 and Sdf-1 α .
- AKT activation was promoted by Dkk3 and Sdf-1 α at early time points.
- Inhibition of AKT phosphorylation by AKT Inhibitor X reduced the Sca-1+ cell migration mediated by either Dkk3 or Sdf-1 α .

- Likewise, PI3K inhibitor LY29004 also suppressed the Dkk3 or Sdf-1 α mediated migration of Sca-1+ progenitor cells.
- Additionally, LY29004 repressed the AKT phosphorylation stimulated by Dkk3.
- The PI3K/AKT signalling transduction pathway is implicated in the Sca-1+ vascular progenitor cell migration mechanism triggered by Dkk3 or Sdf-1 α treatments.
- Both Dkk3 and Sdf-1 α prompted the activation of Rac1 and RhoA, particularly at 3, 13, 15 and 30 minutes of stimulation.
- Rac1 activation inhibitor NSC23766 suppressed the Dkk3 mediated cell migration.
- NSC23766, not only attenuated Rac1 activation but also repressed ERK phosphorylation, induced by Dkk3.
- PD98059 reduced Rac1 activation stimulated by Dkk3 in Sca-1+ APCs.
- ERK and Rac1 signalling pathways cross-talk with each other in a feedback manner.
- PI3K/AKT inhibitor LY29004 did not affect Rac1 activation level triggered by Dkk3 treatment.
- Dkk3 and Sdf-1 α treatments resulted in an increase in MLC phosphorylation level, but did not alter the initial phosphorylated state of cofilin.
- RhoA activation inhibitor Rhosin and ROCK inhibitor Y27632 both decreased the migration rate of Sca-1+ progenitor cells driven by Dkk3.
- Rhosin and Y27632 agents inhibited as well MLC phosphorylation promoted by Dkk3 treatment.
- Dkk3-triggered activation of RhoA was prevented upon Rhosin treatment.
- The data gathered demonstrated that the Rho GTPase family of proteins, namely Rac1 and RhoA, played an important role in Sca-1+ APC migration mediated by Dkk3 or Sdf-1 α .
- PD98059 and LY29004 inhibitors did not affect the level of RhoA activation induced by Dkk3, suggesting that ERK and PI3K/AKT pathways were either independent or downstream of the RhoA signalling cascade.

3.5.7 The Wnt signalling pathway is not involved in Sca-1+ APCs migration mechanism stimulated by Dkk3 treatment

Dkk3 was shown to regulate the Wnt signalling pathway in a context specific way, depending thus on the cell type involved [204, 292, 306-311].

We wished to understand if the Wnt signalling pathway was involved in Sca-1+ cell migration induced by Dkk3.

3.5.7.1 β -Catenin inhibition by FH535 had no effect in Dkk3-mediated migration mechanism of Sca-1+ APCs

The canonical Wnt/ β -Catenin pathway was proved to be involved in cell migration, with great importance in cancer development. Dkk proteins can bind to LRP5/6, which are co-receptors of the Frizzled receptor. Wnt binds to the receptor complex Frizzled and LRP5/6, leading to accumulation of β -Catenin in the cytoplasm. Thus, Dkk interaction with LRP5/6 receptor affects the cell response modulated by β -Catenin activation [212, 312-315].

With the purpose of understanding if β -Catenin played a role in Sca-1+ cell migration mechanism induced by Dkk3, we performed the transwell migration assay with the Wnt/ β -Catenin signalling inhibitor FH535.

The results revealed that inhibition of the Wnt/ β -Catenin signalling by itself, at concentrations of 5 μ M and 15 μ M of FH535, surprisingly induced the migration of the Sca-1+ cells in the same manner as when the cells were treated with Dkk3. Furthermore, an identical migration rate was observed for the group in which FH535 was added to the cells together with Dkk3. There was no statistical difference between all these conditions (Figure 3.5.7.1A). These findings suggested that the Dkk3-driven migration of Sca-1+ APCs was not affected by the inhibition of the Wnt/ β -Catenin signalling pathway.

A β -Catenin inhibitor FH535 had no effect in the Dkk3-mediated migration of Sca-1+APCs

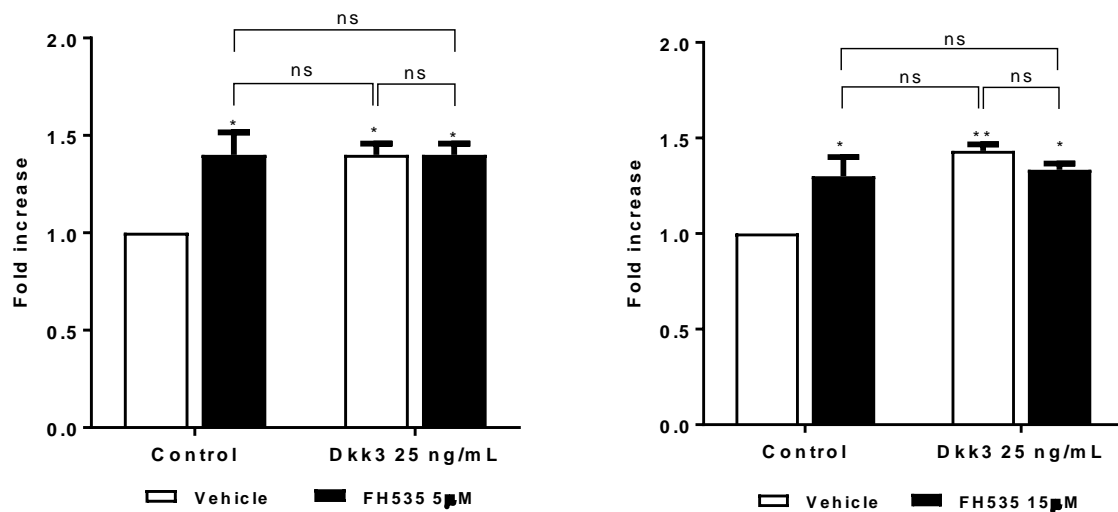


Figure 3.5.7.1A β -Catenin inhibition by FH535 had no effect in the Dkk3-mediated migration mechanism of Sca-1+ APCs. The role of the canonical Wnt/ β -Catenin signalling pathway, in the migration mechanism of Sca-1+ cells induced by Dkk3, was assessed by performing a transwell migration assay with the inhibitor FH535 at 5 μ M and 15 μ M concentrations. In comparison with the control group, cell migration was induced by FH535, Dkk3 and Dkk3 with FH535, in the same manner, with no statistical difference between any of the groups. (Data shown as mean \pm SEM, ** p <0.01, * p <0.05, by Two-way ANOVA, followed by Bonferroni multiple comparison test, N=4).

3.5.7.2 DVL inhibition by Peptide Pen-N3 had no effect in the Dkk3-driven migration mechanism of Sca-1+ APCs

In the classical canonical Wnt signalling, the ligand's binding to the receptor complex FZD-LRP5/6, triggers the phosphorylation of the Dishevelled (Dvl) protein and the consequent signal transduction which leads to the stabilization and accumulation of β -Catenin in the cytoplasm and translocation to the nucleus. As a result, target gene transcription takes place followed by cellular response, such as migration and proliferation.

On the other hand, in the non-canonical Wnt signalling pathway, upon FZD-mediated DVL activation, the signal transduction through Rac1 and RhoA activation is generated independently of the β -Catenin pathway [316-323].

To further support the assumption that the Dkk3-driven Sca-1+ APC migration did not implicate the Wnt signalling pathway, we carried out another transwell migration assay using now the peptide Pen-N3 (inhibitor of the PDZ domain of DVL), which disrupts the FZD-DVL interaction.

Peptide Pen-N3, at 5 μ M or 15 μ M of concentration, did not affect the Dkk3-driven Sca-1+ APC migration, as no significant difference was found between the condition in which Dkk3 was used alone and the condition where it was used together with the inhibitor (Figure 3.5.7.2A).

We thus inferred that the Wnt signalling pathway, through DVL signalling transduction, was potentially not involved in the migration mechanism of Sca-1+ cells induced by Dkk3.

A DVL inhibition by Peptide Pen-N3 had no effect in the Dkk3-driven migration of Sca-1+ APCs

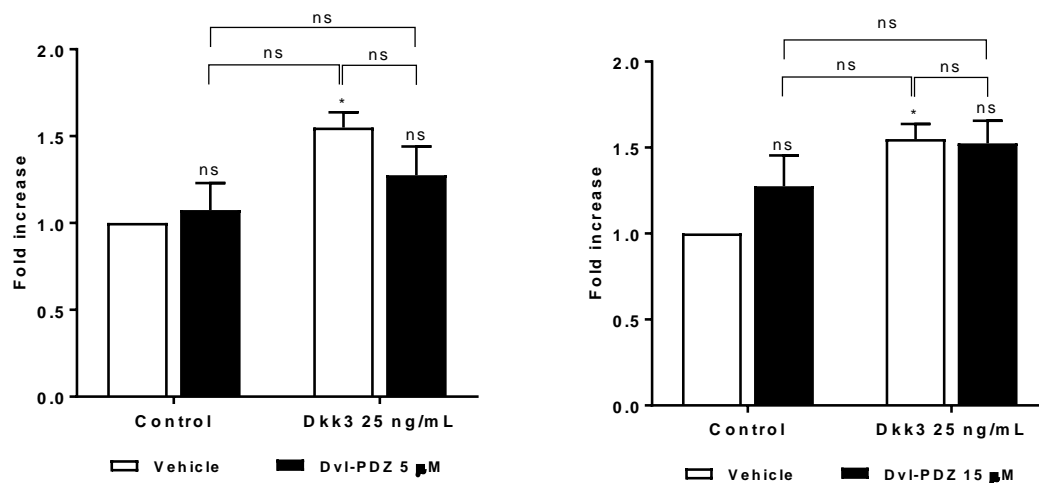


Figure 3.5.7.2A: DVL inhibition by Peptide Pen-N3 had no effect in the Dkk3-driven migration mechanism of Sca-1+ APCs. The involvement of DVL, an important protein included in the Wnt signalling pathway, in the Dkk3-driven migration mechanism of Sca-1+ APCs was assessed. Treatment of the cells with the DVL-PDZ inhibitor (Peptide Pen-N3) did not affect the Dkk3-driven migration of APCs, as no significant difference was found between the Dkk3 treatment group and the group with both Dkk3 and DVL-PDZ inhibitor treatments. (Data shown as mean \pm SEM, * p <0.05, by Two-way ANOVA, followed by Bonferroni multiple comparison test, N=4).

3.5.7.3 Conclusion of part7: The Wnt signalling pathway is not involved in the Sca-1+ APC migration mechanism stimulated by Dkk3 treatment

- Inhibition of the Wnt/ β -Catenin signalling pathway by FH535 treatment significantly promoted Sca-1+ cell migration.
- Nevertheless, no difference was found in the cell migration level between the condition in which Dkk3 was used alone and the condition in which it was used together with the inhibitor.
- For this reason, we inferred that the canonical Wnt/ β -Catenin signalling pathway was not involved in the Dkk3-mediated migration mechanism of Sca-1+ progenitor cells.
- Dishevelled protein inhibition by Peptide Pen-N3 (DVL-PDZ inhibitor) did not affect the Dkk3-mediated Sca-1+ cell migration.
- The results obtained showed that the Wnt signalling pathway, through the Dishevelled protein signalling transduction, was not implicated in the Sca-1+ APC migration induced by Dkk3.

3.6 CXCR7 is upstream of Dkk3-driven migration mechanism of Sca-1+ APCs

Up until now we showed that Dkk3 induced the migration of Sca-1+ APCs and that it binds to CXCR7.

The signalling pathways involved in the underlying Sca-1+ APC migration mechanism have been uncovered as well.

Finally, we investigated whether CXCR7 activation by Dkk3 was upstream of the signalling pathways involved in Sca-1+ APC migration mechanism above elucidated.

To this end, we transfected Sca-1+ APCs with CXCR7 SiRNA and assessed its effect on the signalling pathways triggered by Dkk3 treatment.

3.6.1 CXCR7 downregulation repressed ERK phosphorylation in Sca-1+ APCs induced by Dkk3

Dkk3 treatment increased ERK phosphorylation in the cells transfected with Control SiRNA. Upon CXCR7 downregulation ERK phosphorylation was reduced at 10 and 15 minutes of Dkk3 treatment (Figure 3.6.1A).

This result revealed that CXCR7 receptor is important for ERK activation by Dkk3 in Sca-1+ APCs.

A CXCR7 downregulation repressed ERK phosphorylation in Sca-1+ APCs induced by Dkk3

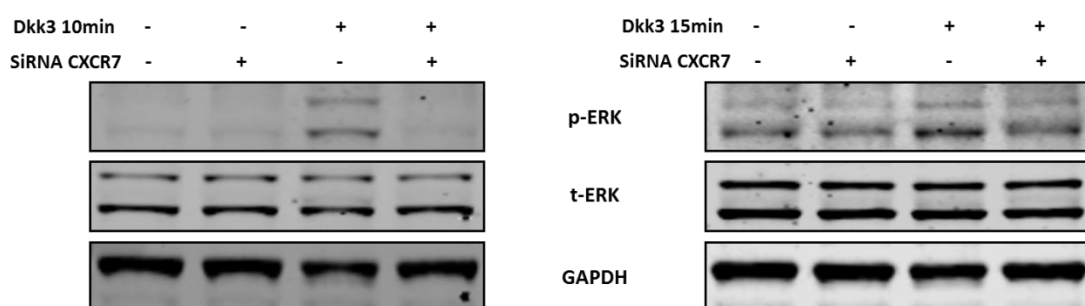


Figure 3.6.1A CXCR7 downregulation repressed ERK phosphorylation in Sca-1+ APCs induced by Dkk3. CXCR7 downregulation was achieved by SiRNA transfection and the level of ERK phosphorylation was assessed. Dkk3 treatment for 10 and 15 minutes increased ERK phosphorylation in Control SiRNA transfected cells. CXCR7 downregulation reduced ERK phosphorylation induced by Dkk3 in Sca-1+ APCs.

3.6.2 CXCR7 knockdown by SiRNA transfection suppressed AKT phosphorylation in Sca-1+ APCs stimulated by Dkk3

AKT activation by Dkk3 upon CXCR7 downregulation by SiRNA transfection was also analysed.

Control and CXCR7 SiRNA transfection did not activate AKT (Figure 3.6.2A).

Dkk3 treatment for 5 and 10 minutes induced AKT phosphorylation in the Control condition.

Upon CXCR7 knockdown Dkk3-triggered AKT phosphorylation was repressed.

We thus proved that CXCR7 is essential for AKT activation in Dkk3-mediated Sca-1+ APC migration.

A CXCR7 knockdown suppressed Dkk3-triggered AKT phosphorylation in Sca-1+ APCs

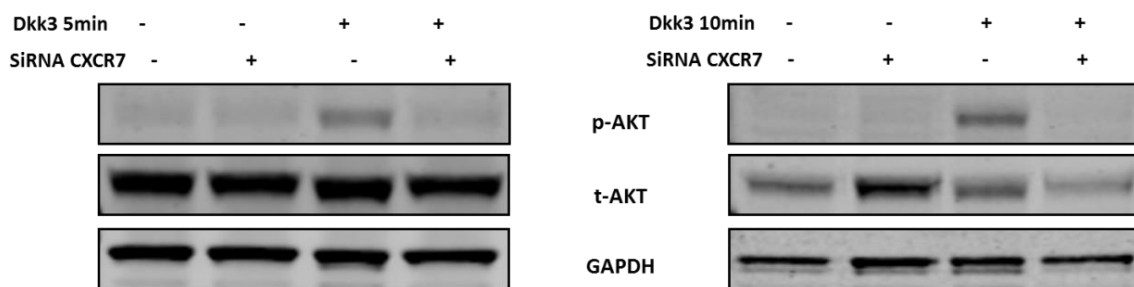


Figure 3.6.2A CXCR7 knockdown by SiRNA transfection suppressed Dkk3-triggered AKT phosphorylation in Sca-1+ APCs. AKT activation by Dkk3 upon CXCR7 downregulation was analysed. Control and CXCR7 SiRNA transfection did not activate AKT. Dkk3 treatment for 5 and 10 minutes induced AKT phosphorylation in the Control condition. Upon CXCR7 knockdown AKT phosphorylation was repressed.

3.6.3 Rac1 activation induced by Dkk3 is decreased in Sca-1+ cells transfected with CXCR7 SiRNA

Rac1-GTP level was measured upon CXCR7 knockdown in Sca-1+ APCs.

Control and CXCR7 SiRNA transfection did not stimulate Rac1 activation (Figure 3.6.3A).

Dkk3 treatment triggered Rac1 activation at 13 (1.5 fold increase) and 15 minutes (1.5 fold increase) of stimulation in the Control condition, but it did not affect Rac1-GTP level in the CXCR7 knockdown condition.

The data obtained proved that CXCR7 was essential for Rac1 activation triggered by Dkk3 in Sca-1+ progenitor cells.

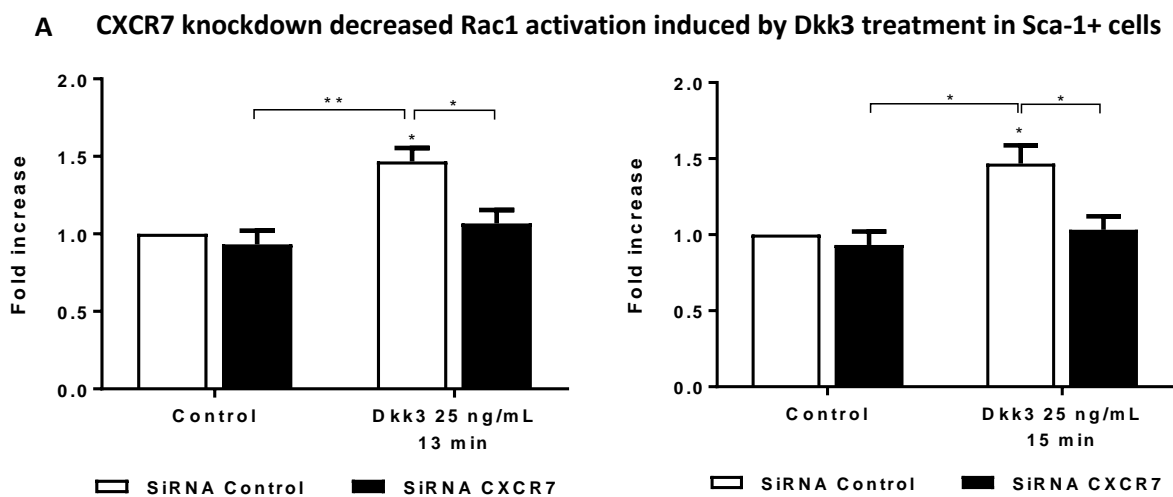


Figure 3.6.3A: Rac1 activation induced by Dkk3 was decreased in Sca-1+ cells transfected with CXCR7 SiRNA. Rac1-GTP level was measured upon CXCR7 knockdown in Sca-1+ progenitor cells. Control and CXCR7 SiRNA transfection did not stimulate Rac1 activation. Dkk3 treatment triggered Rac1 activation at 13 and 15 minutes of stimulation in the Control condition, but it did not affect Rac1-GTP level in the CXCR7 knockdown condition (Data shown as mean \pm SEM, ** $p < 0.01$, * $p < 0.05$, by Two-way ANOVA, followed by Bonferroni multiple comparison test, $N=3$).

3.6.4 Dkk3-driven RhoA activation in Sca-1+ cells was reduced upon CXCR7 downregulation

RhoA activation level was assessed upon CXCR7 downregulation in Sca-1+ progenitor cells.

The transfection of Control or CXCR7 SiRNA did not affect the Rho-GTP level (Figure 3.6.4A).

Once Dkk3 treatment was added for 13 (1.7 fold increase) and 15 minutes (1.3 fold increase), RhoA activation was promoted in the Control condition. However, in the CXCR7 knockdown condition, RhoA activation was not induced.

Therefore, CXCR7 was implicated in RhoA activation stimulated by Dkk3 in Sca-1+ APCs.

A Dkk3-driven RhoA activation in Sca-1+ APCs was reduced upon CXCR7 downregulation

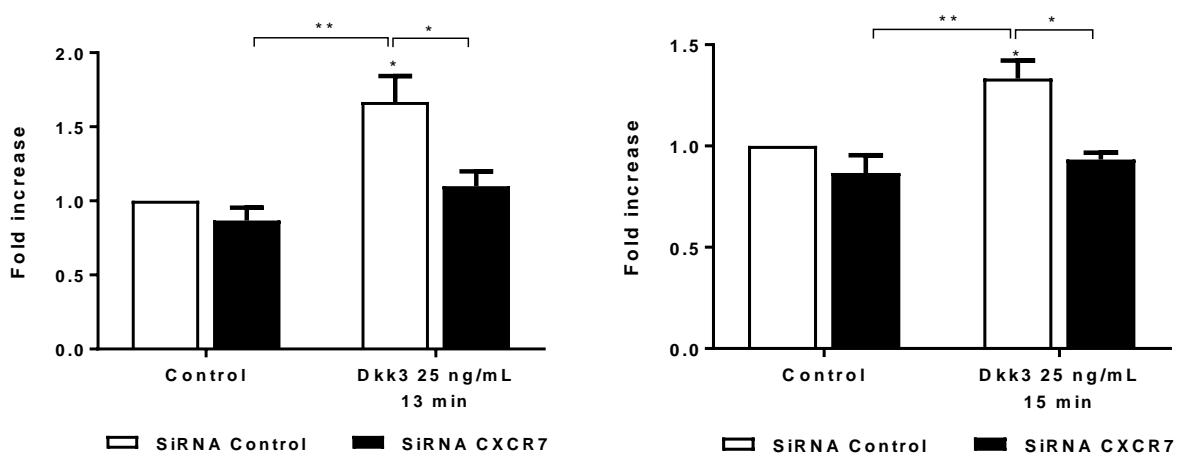


Figure 3.6.4A Dkk3-driven RhoA activation in Sca-1+ APCs was reduced upon CXCR7 downregulation. RhoA activation level was assessed upon CXCR7 downregulation in Sca-1+ progenitor cells. Control or CXCR7 SiRNA transfection did not affect the Rho-GTP level. Dkk3 treatment promoted RhoA activation at 13 (1.7 fold increase) and 15 minutes (1.3 fold increase) of stimulation, in the Control condition. However, in the CXCR7 knockdown condition, RhoA activation was not induced. (Data shown as mean \pm SEM, **p<0.01, *p<0.05, by Two-way ANOVA, followed by Bonferroni multiple comparison test, N=3)

3.6.5 Conclusion of part 7: CXCR7 is upstream of Dkk3-driven migration mechanism of Sca-1+ APCs

- ERK phosphorylation induced by Dkk3 was suppressed in Sca-1+ cells transfected with CXCR7 SiRNA.
- AKT activation promoted by Dkk3 treatment was reduced upon CXCR7 downregulation.
- CXCR7 knockdown repressed Rac1 activation driven by Dkk3 stimulation in Sca-1+ progenitor cells.
- Dkk3 mediated RhoA activation was decreased in the cells transfected with CXCR7 SiRNA.
- CXCR7 is essential in Sca-1+ progenitor cell migration mechanism induced by Dkk3 treatment.

3.7 Summary 1

- Dkk3 induced Sca-1+ APCs migration, *in vitro* and *ex vivo*.
- Dkk3 binds to CXCR7 with high affinity.
- MAPK Kinase signalling pathway is involved in Sca-1+ cell migration mechanism induced by Dkk3.
- PI3K/AKT signalling pathway is implicated in Dkk3-driven Sca-1+ APC migration mechanism.
- Rho GTPase signalling cascade, including Rac1 and RhoA pathways, was induced by Dkk3 treatment in Sca-1+ progenitor cells.
- CXCR7 receptor is upstream of the signalling pathways comprised in the Sca-1+ vascular progenitor cell migration mechanism stimulated by Dkk3.

3.8 Dkk3 binds to Integrins $\alpha 5$ and $\beta 1$, through which it induces the migration of Sca-1+ vascular progenitor cells

Protein-protein interaction can be studied by various different methodologies, including Co-Immunoprecipitation, Pull-down assays, Mass Spectrometry, Phage display assay, Yeast-Two-Hybrid technique, amongst others. [324]

In order to detect which proteins, especially receptors, interact with Dkk3, we selected a library-based method. The Yeast-Two-Hybrid system is a well-established technique which has successfully identified many protein-protein interactions, similar to the ones we wished to seek (Ligand-Receptor interaction) [251, 325, 326].

We developed in our laboratory the Matchmaker[®] Gold Yeast Two-Hybrid System by following thoroughly the instructions given by the manufacturer Clontech-Takara.

The ligand murine Dkk3 was used as the bait of this system and the Normalized Universal mouse cDNA library was used as the prey.

3.8.1 The Yeast-Two-Hybrid system revealed that Dkk3 interacted with Integrin $\alpha 5$ and Integrin $\beta 1$

3.8.1.1 Control experiments

The first step of this assay consisted of performing the control experiments, which allowed understanding the functioning of the Yeast Two Hybrid (Y2H) System herein implemented.

The positive control consisted of the known interaction between murine p53 and the SV40 large T-antigen in an Y2H system [327]. Y2HGold yeast strain was transformed with the plasmid pGBKT7-53, which encodes GAL4 DNA-BD fused to p53. Y187 yeast strain was transformed with pGADT7-T, which encodes GAL4 AD fused to SV40 large T-antigen (Table 3.8.1.1A).

The negative control comprised as well Y187 yeast strain transformed with pGADT7-T, but the Y2HGold was transformed instead with pGBKT7-Lam, which encodes for GAL4 DNA-BD fused to Human Lamin.

In the positive control, the resulting diploid cell should show an activation of the 4 reporter genes, due to the interaction of p53 protein with SV40 large T-antigen. On the contrary, in the negative

control, because Lamin and T-antigen do not interact with each other, the diploid cell should not present the activation of the reporter genes.

The plasmids pGBKT7-53 and pGBKT7-Lam encode the tryptophan gene and hence, the cells transformed with any of them (Y2HGold yeast strain cells) can grow on medium lacking this amino acid. The plasmid pGADT7-T encodes for leucine, so Y187 cells transformed with this plasmid can grow on medium that does not contain leucine. Diploid cells can grow on medium lacking both tryptophan and leucine as they will contain both plasmids.

Table 3.8.1.1A: Yeast transformation strategy


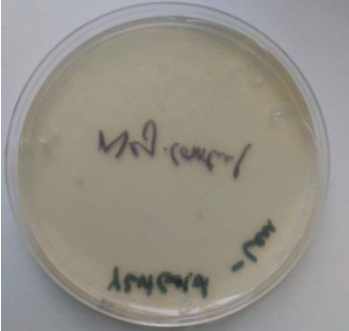
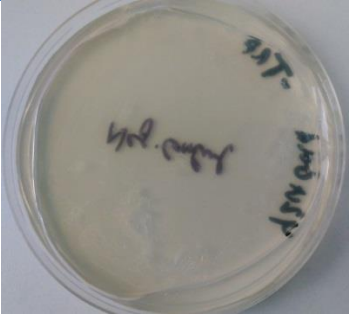
Strain	Transformation plasmid	Agar plate
Y2HGold	pGBKT7-53	SD/-Trp
Y2HGold	pGBKT7-Lam	SD/-Trp
Y187	pGADT7-T	SD/-Leu



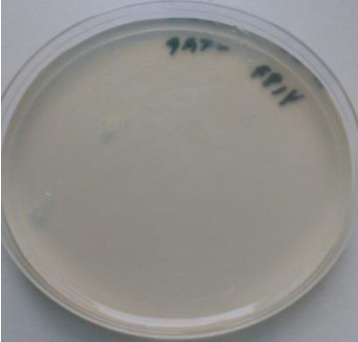

As expected, Y2HGold and Y187 yeast strains only grew on YPDA agar plates and no colony was observed on Single Drop Out agar plates which lacked either tryptophan or leucine amino acids (Table 3.8.1.1B).

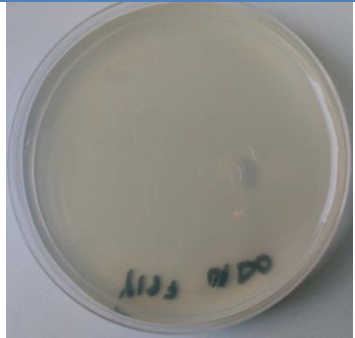
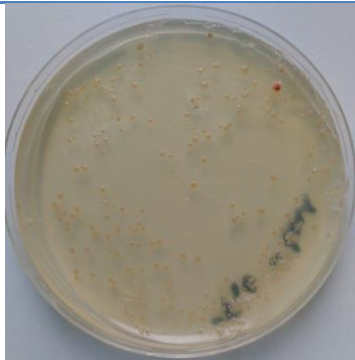
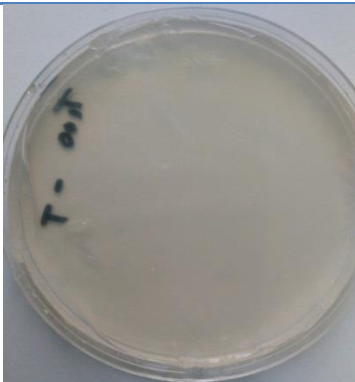

Y2HGold cells transformed with either pGBKT7-53 or pGBKT7-Lam were able to grow on SD/-Trp but not on SD/-Leu. On the other hand, Y187 cells transformed with pGADT7-T grew on SD/-Leu agar plates and not on SD/-Trp.

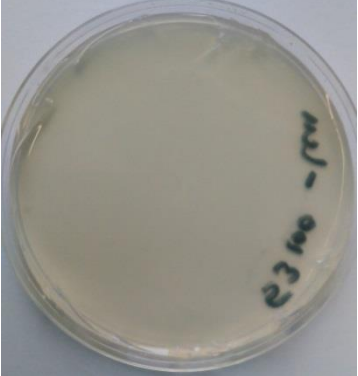



Following mating, diploid cell colonies were displayed on DDO plates (SD/-Trp/-Leu). However, only diploid cells containing the plasmids pGADT7-T and pGBKT7-53 were able to grow on DDO/X/A agar plates, due to the interaction of p53 with the SV40 large T-antigen, which conferred the cells resistance to the drug Aureobasidin A and which expressed α -galactosidase that hydrolyses X- α -Gal substrate, thus turning the colonies blue. As no interaction occurs between lamin and SV40 T-antigen, the corresponding diploid cells were not able to grow on DDO/X/A.




Table 3.8.1.1B: Positive and negative control results

Mating strain and vector	Plate on SD Minimal Agar Medium	Expected result	Result observed
Y2HGold	2xYPDA	White colonies	 <p data-bbox="1121 703 1305 734">White colonies</p>
Y187	2xYPDA	White colonies	 <p data-bbox="1121 1113 1305 1144">White colonies</p>
Y2HGold	SD/-Leu	No colonies	 <p data-bbox="1139 1482 1287 1514">No colonies</p>
Y2HGold	SD/-Trp	No colonies	 <p data-bbox="1139 1834 1287 1863">No colonies</p>

Mating strain and vector	Plate on SD Minimal Agar Medium	Expected result	Result observed
Y2HGold	SD-Leu/-Trp (DDO)	No colonies	 <p data-bbox="1139 611 1286 645">No colonies</p>
Y2HGold	SD-Leu/-Trp/X- α -Gal/AbA (DDO/X/A)	No colonies	 <p data-bbox="1139 969 1286 1003">No colonies</p>
Y187	SD/-Trp	No colonies	 <p data-bbox="1139 1350 1286 1384">No colonies</p>
Y187	SD-Leu/-Trp (DDO)	No colonies	 <p data-bbox="1139 1731 1286 1765">No colonies</p>

Mating strain and vector	Plate on SD Minimal Agar Medium	Expected result	Result observed
Y187	SD-Leu/-Trp/X- α -Gal/AbA (DDO/X/A)	No colonies	 <p data-bbox="1139 622 1286 658">No colonies</p>
Y187 – pGADT7-T	SD/-Leu	White/Red colonies	 <p data-bbox="1091 1016 1334 1055">White/Red colonies</p>
Y187 – pGADT7-T	SD/-Trp	No colonies	 <p data-bbox="1139 1435 1286 1473">No colonies</p>
Y2HGold – pGBKT7-53	SD/-Trp	White/Red colonies	 <p data-bbox="1091 1809 1334 1843">White/Red colonies</p>

Mating strain and vector	Plate on SD Minimal Agar Medium	Expected result	Result observed
Y2HGold – pGBKT7-53	SD/-Leu	No colonies	 <p data-bbox="1141 674 1289 703">No colonies</p>
Y2HGold – pGBKT7-Lam	SD/-Trp	White/Red colonies	 <p data-bbox="1093 1055 1334 1084">White/Red colonies</p>
Y2HGold – pGBKT7-Lam	SD/-Leu	No colonies	 <p data-bbox="1141 1473 1289 1503">No colonies</p>
Y187 – pGADT7-T X Y2HGold – pGBKT7-53	SD-Leu/-Trp (DDO)	White/Red colonies	 <p data-bbox="1093 1906 1334 1935">White/Red colonies</p>


Mating strain and vector	Plate on SD Minimal Agar Medium	Expected result	Result observed
Y187 – pGADT7-T X Y2HGold – pGBKT7-53	SD-Leu/-Trp/X- α -Gal/AbA (DDO/X/A)	Blue colonies	 <p data-bbox="1129 645 1294 674">Blue colonies</p>
Y187 – pGADT7-T X Y2HGold – pGBKT7-Lam	SD-Leu/-Trp (DDO)	White/Red colonies	 <p data-bbox="1091 1048 1334 1077">White/Red colonies</p>
Y187 – pGADT7-T X Y2HGold – pGBKT7-Lam	SD-Leu/-Trp/X- α -Gal/AbA (DDO/X/A)	No colonies	 <p data-bbox="1139 1451 1286 1480">No colonies</p>





3.8.1.2 Test for auto-activation of the bait Dkk3

Another important control required was the confirmation that Dkk3 could not autonomously activate any of the reporter genes in Y2HGold yeast cell without the presence of the prey protein. Therefore, we transformed Y2HGold cells with the previously cloned plasmid comprising Dkk3 fused to GAL4 DNA-BD and spread the cells on SD/-Trp, SD/-Leu, SD/-Trp/X/A, DDO, DDO/X/A and Quadruple Drop Out –Trp/-Leu/Ade/-His (QDO) agar plates. The QDO medium is the most stringent condition, as it does not contain tryptophan, leucine, adenine and histidine, which would only be produced by diploid cells with GAL4 fully functional and reconstituted due to bait-prey interaction.

The data obtained revealed that Dkk3, in the absence of the prey protein, was not able to auto-activate the reporter genes of the Y2HGold cells (Table 3.8.1.2), as no colonies were present on the plates SD/-Leu, SD/-Trp/X/A, DDO, DDO/X/A and QDO. Colonies were observed only on plates SD/-Trp plates.

Table 3.8.1.2: Test for Dkk3 auto-activation

Selective agar plate	Expected result	Result observed
SD/-Trp	White/Red colonies	 White/Red colonies
SD/-Leu	No colonies	 No colonies

Selective agar plate	Expected result	Result observed
SD/-Trp/X- α -Gal/AbA	No colonies	 <p>No colonies</p>
SD/-Trp/-Leu (DDO)	No colonies	 <p>No colonies</p>
SD/-Trp/-Leu/X- α -Gal/AbA (DDO/X/A)	No colonies	 <p>No colonies</p>
SD/-Trp/-Leu/-His/-Ade (QDO)	No colonies	 <p>No colonies</p>

3.8.1.3 *Screening of the Normalized Universal Mouse Yeast Two Hybrid cDNA Library*

Mate & Plate™ Universal Mouse Library in Y187 cells frozen stock was mixed with a concentrated culture of the Y2HGold cells previously transformed with the bait Dkk3 plasmid, followed by incubation overnight to allow mating.

The obtained diploid cells were spread on SD/-Trp, SD/-Leu, DDO and DDO/X/A agar plates. From the latter ones, the colonies that had grown were separately streaked on QDO/X/A plates, which have higher stringency. Additional two times re-streaking on QDO/X/A were followed in order to thoroughly segregate the white colonies from the blue target colonies.

In parallel, Y187 cells were transformed with the empty vector pGADT7 (corresponding to the vector used to clone the prey - mouse library) and Y2HGold cells were transformed with the empty vector pGBDT7 (empty vector used for bait cloning). These haploid cells were allowed to mate overnight. Since no bait or prey proteins were cloned in these plasmids, it was expected that the resulting diploid cells would not express the reporter genes.

Cells transformed with the Dkk3 bait plasmid were also submitted to mating with Y187 cells transformed with the empty vector, in order to assess the possibility of the existence of false positives.

All the mated diploid cells were plated on SD/-trp, SD/-Leu, DDO, DDO/X/A and QDO/X/A agar plates and incubated for 3-5 days at 30°C.

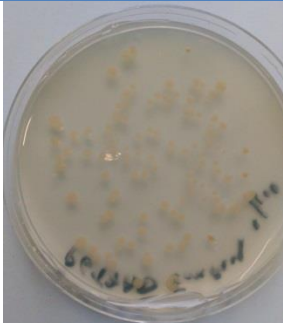



Not surprisingly, pGADT7 transformed cells (Y187 strain) grew on SD/-Leu plates and pGBKT7 transformed cells (Y2HGold strain) grew on SD/-Trp agar plates (Table 3.8.1.3A). Furthermore, DDO plates also exhibited colonies of diploid cells resultant from the mating of these empty vector-transformed haploid cells. Nevertheless, no colonies were observed in DDO/X/A and QDO/X/A agar plates, since no bait or prey proteins were expressed.






Upon mating of Y2HGold cells transformed with the bait Dkk3 fused to GAL4 DNA-BD and the Y187 cells transformed with the empty vector without any prey protein, colonies were displayed on DDO plates (because empty bait and prey vectors encode for tryptophane and leucine, respectively) but not on DDO/X/A and QDO/X/A agar plates, as no prey protein was present to interact with Dkk3.



In contrast, on all the DDO, DDO/X/A and QDO/X/A agar plates, because in the diploid cells, obtained by mating Y2HGold cells transformed with bait Dkk3 with Y187 cells transformed with mouse cDNA library, bait-prey interaction had occurred, distinct colonies were present. White/red colonies were observed in DDO plates and blue colonies were detected on DDO/X/A and QDO/X/A agar plates. These findings revealed that Dkk3 had interacted with prey proteins of the mouse library.

Nonetheless, it was necessary to identify the prey proteins with which Dkk3 had interacted and more importantly, to rule out false positive results.

Table 3.8.1.3A: Screening of the Universal mouse normalized Two-Hybrid Library

Mating strain and vector	Selective agar plate	Expected result	Result observed
Y187 – pGADT7 (empty vector)	SD/-Leu	White/Red colonies	 White/Red colonies
Y2HGold – pGBKT7 (empty vector)	SD/-Trp	White/Red colonies	 White/Red colonies
Y187 – pGADT7 (empty vector) X Y2HGold – pGBKT7 (empty vector)	SD/-Trp/-Leu (DDO)	White/Red colonies	 White/Red colonies
Y187 – pGADT7 (empty vector) X Y2HGold – pGBKT7 (empty vector)	SD/-Trp/-Leu/X- α - Gal/AbA (DDO/X/A)	No colonies	 No colonies

Mating strain and vector	Selective agar plate	Expected result	Result observed
Y187 – pGADT7 (empty vector) X Y2HGold – pGBKT7 (empty vector)	SD/-Trp/-Leu/-His/-Ade/X- α -Gal/AbA (QDO/X/A)	No colonies	 No colonies
Y187 – pGADT7 (empty vector) X Y2HGold – pGBKT7-Dkk3	SD/-Trp/-Leu (DDO)	White/Red colonies	 White/Red colonies
Y187 – pGADT7 (empty vector) X Y2HGold – pGBKT7-Dkk3	SD/-Trp/-Leu/X- α -Gal/AbA (DDO/X/A)	No colonies	 No colonies
Y187 – pGADT7 (empty vector) X Y2HGold – pGBKT7-Dkk3	SD/-Trp/-Leu/-His/-Ade/X- α -Gal/AbA (QDO/X/A)	No colonies	 No colonies
Y187 – pGADT7 – mouse Library X Y2HGold – pGBKT7-Dkk3	SD/-Trp/-Leu (DDO)	White/Red colonies	 White/Red colonies

Mating strain and vector	Selective agar plate	Expected result	Result observed
Y187 – pGADT7 – mouse Library X Y2HGold – pGBKT7-Dkk3	SD/-Trp/-Leu/X- α -Gal/AbA (DDO/X/A)	Blue colonies	 Blue colonies
Y187 – pGADT7 – mouse Library X Y2HGold – pGBKT7-Dkk3	SD/-Trp/-Leu/-His/-Ade/X- α -Gal/AbA (QDO/X/A)	Blue colonies	 Blue colonies

From the positive blue colonies obtained, the prey plasmids were rescued and sent for sequencing. The sequencing results enabled the identification of 69 proteins that interacted with murine Dkk3 (Table 3.8.1.3B).

Amongst these, we were more interested in identifying membrane bound proteins, that is, receptors. Remarkably, 4 receptors were found: Integrin β 1 (two hits), Robo1 (one hit), Integrin α 5 (one hit) and GPR116 (1 hit).

The identification of the Integrins α 5 and β 1 as receptors to which Dkk3 binds was a remarkable evidence of the important role of Dkk3 in cell migration, as these particular integrins are well known for their implication in cell migration mechanism of various cell types [328, 329]. Interestingly, ITG α 5 β 1 has been recognised as the receptor of fibronectin [330, 331]. What is more, Fibulin 5 was also detected as a protein interacting with Dkk3 and studies have shown that ITG α 5 β 1 actually binds to Fibulin 5 [332, 333].

Considering the just described, we decided to focus on the receptors ITG α 5 and ITG β 1.

Table 3.8.1.3B: Identification of the library prey proteins that interacted with the bait Dkk3

Plasmid #	NCBI Reference Sequence	Symbol	Full name	Cellular component
1	NM_013669.2	SNAP91	Synaptosomal-associated protein 91	Clathrin-coated vesicle; AP-2 adaptor complex; Pre-and Post-synaptic membrane; Membrane
2	NM_009632.2	Parp2	Poly (ADP-ribose) polymerase family, member 2	Cytoplasm; Nucleolus; Nucleus
3	NM_027415.2	Tmem70	Transmembrane protein 70	Integral component of mitochondrial membrane
4	NM_013669.2	SNAP91	Synaptosomal-associated protein 91	Clathrin-coated vesicle; AP-2 adaptor complex; Pre and Post synaptic membrane; Membrane
5	NM_009396.2	Tnfaip2	Tumor necrosis factor, alpha-induced protein 2	Cytoplasm
6	NM_007399.4	Adam10	A desintegrin and metallopeptidase domain 10	Cell membrane; Golgi apparatus; Nucleus
7	NM_001102458.1	Azin1	Antizyme inhibitor 1	Cytoplasm; Nucleus
8	NM_001163456.1	Cox18	Cytochrome c oxidase assembly protein 18	Integral component of mitochondrial inner membrane
9	NM_152220.2	Stx3	Syntaxin 3	SNARE complex; Cell membrane; Dendrite
10	NM_030557.3	Mynn	Myoneurin	Nucleus
11	NM_010578.2	Itgb1	Integrin beta 1 (fibronectin receptor beta)	Cell membrane; Filopodium; Focal adhesion
12	NM_010578.2	Itgb1	Integrin beta 1 (fibronectin receptor beta)	Cell membrane; Filopodium; Focal adhesion
13	NM_011327.4	Scp2	Sterol carrier protein 2, liver	Cytoplasm; Mitochondrion; Peroxisome
14	NM_001252070.1	Dnah7a	Dynein, axonemal, heavy chain 7A	Cytosol; Cilium; Inner dynein arm
15	NM_026242.3	Mrfap1	Morf4 family associated protein 1	Cytoplasm; Nucleus
16	NM_001319151.1	Myo16	Myosin XVI	Cytoplasm; Myosin complex
17	NM_026470.3	Spata6	Spermatogenesis associated 6	Cell projection; Sperm connecting piece

Plasmid #	NCBI Reference Sequence	Symbol	Full name	Cellular component
18	NM_007796.2	Ctla2a	Cytotoxic T lymphocyte-associated protein 2 alpha	Dendrite
19	NM_009396.2	Tnfaip2	Tumor necrosis factor, alpha-induced protein 2	Cytoplasm
20	NM_001014973.2	Snx13	Sorting nexin 13	Endosome; Membrane
21	NM_001077495.2	Pik3r1	Phosphatidylinositol 3-kinase, regulatory subunit, polypeptide 1 (p85 alpha)	Cytoplasm; Membrane; Perinuclear endoplasmic reticulum membrane
22	NM_207635.1	Rps24	Ribosomal protein S24	Ribosome; Nucleus
23	NM_001170433.1	Ppfibp1	PTPRF interacting protein, binding protein (liprin beta 1)	Focal adhesion
24	NM_144807.3	Chpt1	Choline phosphotransferase 1	Golgi apparatus
25	NM_009274.2	Srpk2	Serine/arginine-rich protein specific kinase 2	Cytoplasm; Nucleus
26	NM_026887.3	Ap1s2	Adaptor-related protein complex 1, sigma 2 subunit	Golgi apparatus; Clathrin-coated pit
27	NM_019413.2	Robo1	Roundabout guidance receptor 1	Axolemma; Cell membrane
28	NM_009096.3	Rps6	Ribosomal protein S6	Cytoplasm; Ribosome
29	NM_007700.2	Chuk	Conserved helix-loop-helix ubiquitous kinase	Cytoplasm; Nucleus; CD40 receptor complex; IkkappaB kinase complex
30	NM_027022.4	Cmtm2a	CKLF-like MARVEL transmembrane domain containing 2A	Cytoplasm; Extracellular space; Integral component of membrane; Nucleus
31	NM_001037841.3	Ck1f	Chemokine-like factor	Extracellular region; Integral component of membrane
32	NM_001113384.1	Gnao1	Guanine nucleotide binding protein, alpha O	heterotrimeric G-protein complex; Membrane; Dendrite
33	NM_010948.3	Nudc	NudC nuclear distribution protein	Golgi apparatus; Cytoplasm; Cytoskeleton
34	NM_011812.4	Fbln5	Fibulin 5	Extracellular matrix; Colocalization with elastic fiber
35	NM_001014973.2	Snx13	Sorting nexin 13	Endosome; Membrane

Plasmid #	NCBI Reference Sequence	Symbol	Full name	Cellular component
36	NM_008402.3	Itgav	Integrin alpha V	Plasma membrane; Focal adhesion; Filopodium; Lamellipodium
37	NM_030028.1	Tmem190	Transmembrane protein 190	Inner acrosomal membrane; Nucleus
38	NM_001164838.1	Lrrfip2	Leucine rich repeat (in FLII) interacting protein 2	Nucleus
39	NM_024406.2	Fabp4	Fatty acid binding protein 4, adipocyte	Cytoplasm
40	NM_001286062.1	Angpt1	Angiopoietin 1	Extracellular
41	NM_054077.4	Prelp	Proline arginine-rich end leucine-rich repeat	Extracellular
42	NM_054077.4	Prelp	Proline arginine-rich end leucine-rich repeat	Extracellular
43	NM_001243064.1	Cav1	Caveolin 1, caveolae protein	Caveola; Golgi apparatus; Endoplasmic reticulum; Plasma membrane
44	NM_177025.5	Cobll1	CobI-like 1	Extracellular exosome
45	NM_001164838.1	Lrrfip2	Leucine rich repeat (in FLII) interacting protein 2	Nucleus
46	NM_172675.4	Stx16	Syntaxin 16	Golgi apparatus; SNARE complex; Focal adhesion
47	NM_026759.3	Mrpl13	Mitochondrial ribosomal protein L13	Mitochondrion; Ribosome
48	NM_023785.3	Ppbp	Pro-platelet basic protein	Extracellular
49	NM_010518.2	Igfbp5	Insulin-like growth factor binding protein 5	Extracellular; Insulin-like growth factor binding protein complex
50	NM_178790.4	Abi3bp	ABI gene family, member 3 (NESH) binding protein	Extracellular matrix
51	NM_180599.1	Mfap3	Microfibrillar-associated protein 3	Membrane
52	NM_001160017.1	Gnb1	Guanine nucleotide binding protein (G protein), beta 1	Heterotrimeric G-protein complex; Dendrite; Photoreceptor inner and outer segment
53	NM_173753.4	Fnip1	Folliculin interacting protein 1	Cytoplasm

Plasmid #	NCBI Reference Sequence	Symbol	Full name	Cellular component
54	NM_010578.2	Itgb1	Integrin beta 1 (fibronectin receptor beta)	Cell membrane; Filopodium; Focal adhesion
55	NM_009063.4	Rgs5	Regulator of G-protein signalling 5	Cytoplasm; Membrane
56	NM_198297.3	Trat1	T cell receptor associated transmembrane adaptor1	T cell receptor complex; Plasma membrane
57	NM_001081178.1	Adgrf5 GPR116	Adhesion G protein-coupled receptor F5	Plasma membrane
58	NM_009063.4	Rgs5	Regulator of G-protein signalling 5	Cytoplasm; Membrane
59	NM_010518.2	Igfbp5	Insulin-like growth factor binding protein 5	Extracellular; Insulin-like growth factor binding protein complex
60	NM_011812.4	Fbln5	Fibulin 5	Extracellular matrix; Colocalization with elastic fiber
61	NM_001317243.1	Mtch2	Mitochondrial carrier 2	Mitochondrion
62	NM_009443.3	Tgoln1	Trans-golgi network protein	Golgi apparatus
63	NM_027409.5	Mospd1	Motile sperm domain containing 1	Cytoplasm; Perinuclear region of cytoplasm; Membrane
64	NM_001243008.1	Col6a3	Collagen, type VI, alpha 3	Extracellular matrix
65	NM_001243008.1	Col6a3	Collagen, type VI, alpha 3	Extracellular matrix
66	NM_001243008.1	Col6a3	Collagen, type VI, alpha 3	Extracellular matrix
67	NM_026433.2	Tmem100	Transmembrane protein 100	Cytoplasm; Endoplasmic reticulum; Membrane; Perinuclear region of cytoplasm
68	NM_010948.3	Nudc	NudC nuclear distribution protein	Golgi apparatus; Cytoplasm; Cytoskeleton
69	NM_134034.2	Ppp4r3b	Protein phosphatase 4 regulatory subunit 3B	Cytoplasm; Protein phosphatase 4 complex

3.8.1.4 Confirmation of the positive interactions

To rule out the possibility of false positive interactions, we co-transformed Y2HGold competent yeast cells with the identified prey plasmids and with either Dkk3 bait plasmid or bait empty vector (Figure 3.8.1.4).

The co-transformation mix was spread on DDO/X, followed by QDO/X/A plates. Upon interaction of Dkk3 with either ITG α 5 or ITG β 1, blue colonies should grow on both plates, as the GAL4 transcription activator would be reconstituted and functional. In contrast, no colonies should be observed on QDO/X/A corresponding to the yeast co-transformed with bait empty vector and with the identified prey plasmids, since Dkk3 would not be present to interact with the prey proteins and thus activate the reporter genes.

The results obtained proved that the Dkk3-ITG α 5 and Dkk3-ITG β 1 interactions were genuine, because blue colonies were detected on both DDO/X and QDO/X/A plates, which did not occur when empty vectors were used, as white colonies were present on DDO/X plates but colonies were absent on QDO/X/A agar plates (Table 3.8.1.4).

A Co-transformation strategy for confirmation of positive interactions

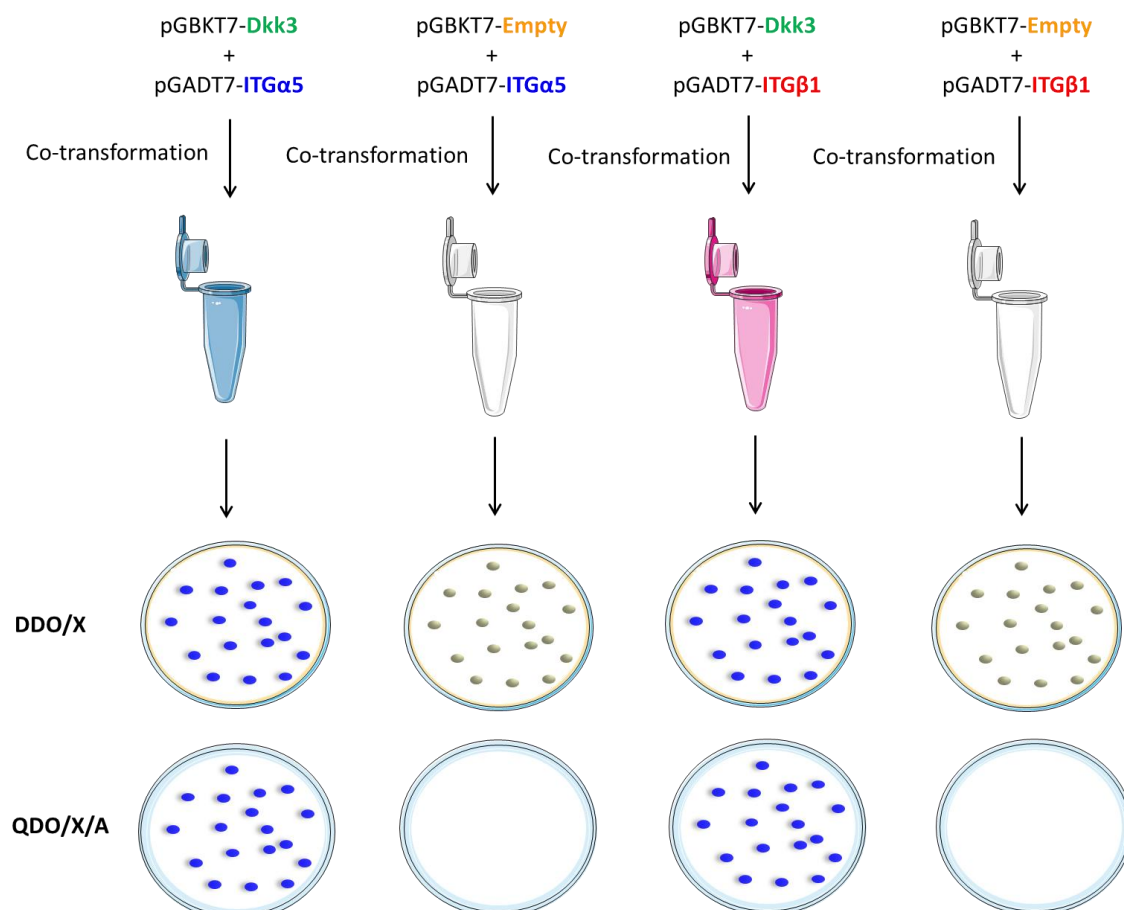
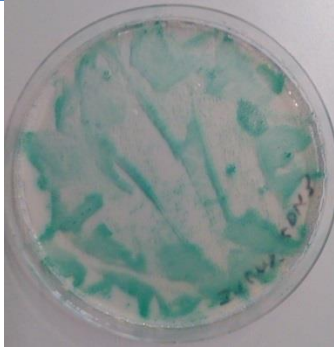
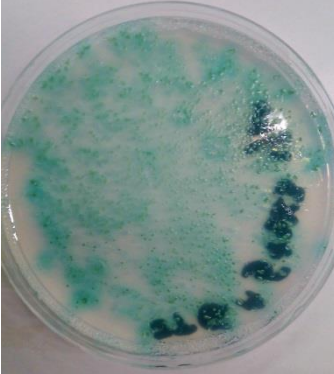




Figure 3.8.1.4: Co-transformation strategy for confirmation of positive interaction. Y2HGold competent yeast cells were co-transformed with the identified prey plasmid and either Dkk3 bait plasmid or bait empty vector. The genuine interaction between Dkk3 and ITG α 5/ITG β 1 was confirmed by the presence of blue colonies on both DDO/X and QDO/X/A plates. In contrast, the cells co-transformed with the prey plasmid and the bait empty vector grew as white colonies on DDO/X, but no colonies were observed on QDO/X/A.

Table 3.8.1.4: Results for the positive interaction confirmation test

Mating strain and vector	Selective agar plate	Expected result	Result observed
pGBKT7-Dkk3 X pGADT7-ITG α 5	DDO/X	Blue colonies	 Blue colonies
pGBKT7-Dkk3 X pGADT7-ITG α 5	QDO/X/A	Blue colonies	 Blue colonies
pGBKT7-Empty X pGADT7-ITG α 5	DDO/X	White colonies	 White colonies

Mating strain and vector	Selective agar plate	Expected result	Result observed
pGBKT7-Empty X pGADT7-ITG α 5	QDO/X/A	No colonies	 <p data-bbox="1129 622 1278 656">No colonies</p>
pGBKT7-Dkk3 X pGADT7-ITG β 1	DDO/X	Blue colonies	 <p data-bbox="1121 976 1286 1014">Blue colonies</p>
pGBKT7-Dkk3 X pGADT7-ITG β 1	QDO/X/A	Blue colonies	 <p data-bbox="1121 1361 1286 1397">Blue colonies</p>
pGBKT7-Empty X pGADT7-ITG β 1	DDO/X	White colonies	 <p data-bbox="1110 1711 1299 1749">White colonies</p>

Mating strain and vector	Selective agar plate	Expected result	Result observed
pGBKT7-Empty X pGADT7-ITGβ1	QDO/X/A	No colonies	 No colonies

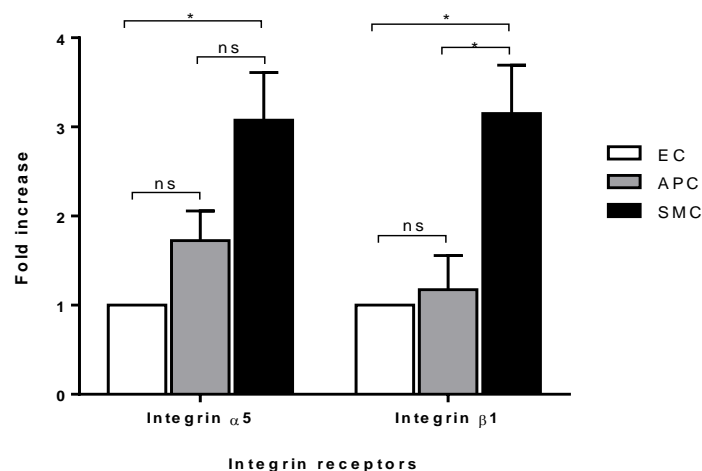
3.8.2 Integrins α5 and β1 expression in Sca-1+ vascular progenitor cells

In view of the previous findings, we analysed the expression of ITGα5 and ITGβ1 in Sca-1+ progenitor cells, to understand whether the Dkk3-driven migration mechanism of the Sca-1+ APCs involved the interaction of this ligand with ITGα5 and ITGβ1.

We performed a qPCR analysis on Sca-1+-APCs, SMCs and ECS (Figure 3.8.2A) and the results revealed that the expression of both ITGα5 and ITGβ1 is higher on Sca-1+-APCs than on ECs, although with no statistical significance, and lower than on SMCs with significant difference for ITGβ1.

The protein expression by western blot showed that both proteins are expressed in Sca-1+ APCs, however less than in SMCs (Figure 3.8.2B).

A mRNA Expression of ITGα5 and ITGβ1 in ECs, Sca-1+ APCs and SMCs



B Protein expression of ITG α 5 and ITG β 1 in ECs, Sca-1+ APCs and SMCs

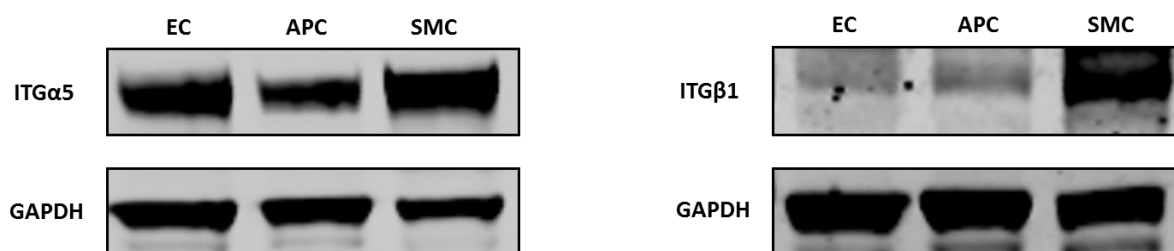


Figure 3.8.2 ITG α 5 and ITG β 1 expression in Sca-1+ APCs, ECs and SMCs. A: mRNA Expression by qPCR; B: Protein expression by western blot. The expression of both ITG α 5 and ITG β 1 is higher in Sca-1+ APCs than in ECs, although with no statistical significance, and lower than in SMCs with significant difference for ITG β 1. Protein expression showed that Sca-1+ APCs express ITG α 5 and ITG β 1, however at lower level than SMCs. (Data shown as mean \pm SEM, * p <0.05, by Two-way ANOVA and Bonferroni multiple comparison test, N=5).

3.8.3 Dkk3 binds to Integrins α 5 and β 1 in Sca-1+ progenitor cells

After confirming the expression of ITG α 5 and ITG β 1 in Sca-1+ cells we carried out a Co-Immunoprecipitation assay.

The AminoLink Plus Coupling Resin spin columns (Thermofisher) coupled with Rabbit anti-ITG β 1 or Rabbit IgG were prepared.

The Dkk3 treated cell lysates were pre-cleared through Control Agarose Resin slurry spin columns and incubated overnight at 4°C with either the Rabbit IgG- or Anti-ITG β 1-Coupling Resin spin columns.

After antibody coupling to the resin columns, the lysates were eluted and the western blot was performed on the eluted and input samples.

Following Dkk3 antibody incubation, the results obtained showed that Dkk3 bound to ITG β 1, as a band was observed for the samples added to the ITG β 1-coupled spin column (test sample) that matched a band displayed for the input sample, thus validating the Dkk3-ITG β 1 band size (Figure 3.8.3A). Although a slight band was apparent in the IgG control, this was so faint in comparison to the band observed for the test sample, that it was dismissed as either a fall over from the input or an artefact of the experiment. We therefore concluded that a specific binding was obtained.

We next incubated the membrane with ITG α 5 antibody and interestingly, the corresponding band was detected, which indicated that ITG α 5 binds to ITG β 1 and this receptor complex can potentially bind to Dkk3. No band was present in the samples passed through the IgG-coupled columns, revealing the absence of unspecific binding. Once more, the input sample displayed a matching band, which validated the size of the band acquired.

A Dkk3 and ITG α 5 co-Immunoprecipitated with ITG β 1 in Sca-1+ APCs

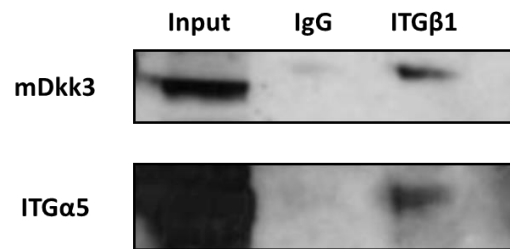


Figure 3.8.3A Dkk3 and ITG α 5 co-Immunoprecipitated with ITG β 1 in Sca-1+ progenitor cells. ITG β 1 antibody or Rabbit IgG were coupled to Resin spin columns in order to verify if Dkk3 and ITG α 5 could co-immunoprecipitate with ITG β 1. Western blot analysis revealed that Dkk3 bound to ITG β 1, with no bands observed corresponding to IgG. The input sample exhibited a matching band. After re-incubation of the membrane with ITG α 5 antibody, it was observed that ITG α 5 also immunoprecipitated with ITG β 1. The input sample once more validated the band size and no band was found for IgG.

3.8.4 Integrins α 5 and β 1 are high affinity binding receptors for Dkk3

Next, we analysed the binding affinity of Dkk3 for ITG α 5 and TG β 1 and calculated the corresponding dissociation constants (K_D) through a saturation binding assay.

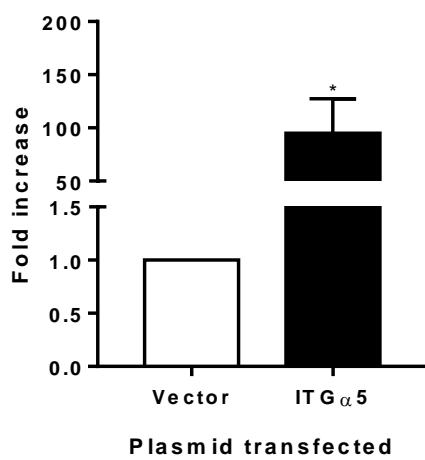
HEK 293T cells were transfected with empty vector pCMV3-ORF-HA or with plasmids pCMV3-ITG α 5-HA and pCMV3-ITG β 1-HA (Sino Biological Inc.). After 48 hours of transfection, the cells were washed with ice cold PBS and lysed to obtain the membrane extracts containing the overexpressed receptors.

In parallel, HA coated ELISA 96-well plates were prepared and the transfected HEK cell membrane extracts were loaded onto to the anti-HA coated wells. Serially diluted hDkk3-AP ligand was added to the wells and the AP activity was measured by adding PNPP to the wells and reading the chemiluminescence signal. For each ligand concentration, the background binding value (membrane extracts of cells transfected with empty vector) was subtracted. The values of non-conjugated hDkk3 were used as the blank.

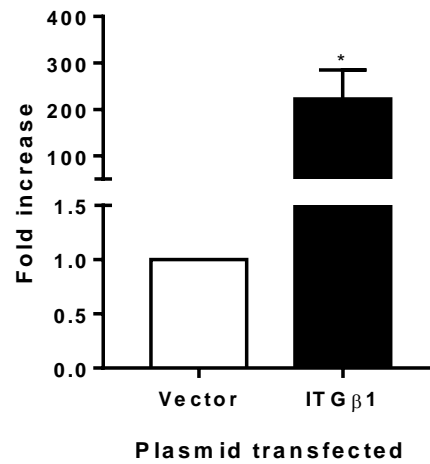
The qPCR analysis confirmed the ITG α 5 and ITG β 1 overexpression in HEK 293T cells (Figure 3.8.4A and B).

The binding curves obtained for both ITG α 5 and ITG β 1 were characteristically hyperbolic (Figure 3.8.4D) and the dissociation constants obtained, $K_D=18.15$ (ITG β 1) and $K_D=14.85$ (ITG α 5), demonstrated that Dkk3 bound with high affinity to ITG α 5 and to ITG β 1 (Figure 3.8.4C and D).

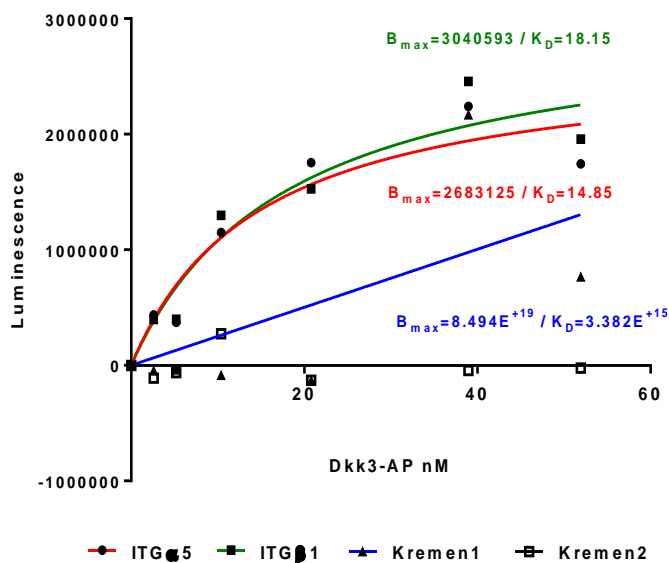
A mRNA expression of ITG α 5 upregulation in HEK 293T transfected cells



B mRNA expression of ITG β 1 upregulation in HEK 293T transfected cells



C Binding of hDkk3-AP to hITG α 5 and hITG β 1 HEK transfected cells



D Scatchard analysis of hDkk3-AP binding to hITG α 5 and hITG β 1 HEK transfected cells

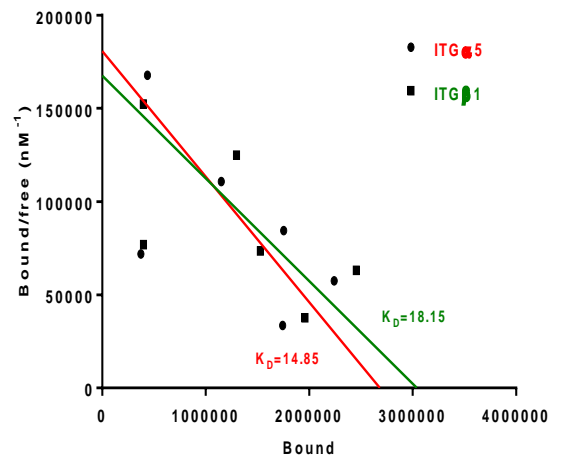


Figure 3.8.4 Integrins $\alpha 5$ and $\beta 1$ are high affinity binding receptors for Dkk3. The binding affinity of Dkk3 to ITG $\alpha 5$ and ITG $\beta 1$ was assessed with the calculation of the respective dissociation constants. HEK 293T cells were transfected with either empty vector pCMV3-ORF-HA or with the plasmids pCMV3-ITG $\alpha 5$ -HA and pCMV3-ITG $\beta 1$ -HA. **A, B: Respectively, mRNA Expression of ITG $\alpha 5$ and ITG $\beta 1$ upregulation in HEK 293T cells.** Overexpression of ITG $\alpha 5$ and ITG $\beta 1$ was confirmed by qPCR. The transfected cell lysates were loaded onto the wells of a high binding 96-well ELISA-plate previously coated with HA-antibody. hDkk3-AP serially diluted solutions were allowed to bind for 2 hours to the receptors of the cell extracts. The AP activity was measured by chemiluminescence. **C: Binding of hDkk3-AP to hITG $\alpha 5$ and hITG $\beta 1$ HEK 293T transfected cells. D: Scatchard analysis of hDkk3-AP to hITG $\alpha 5$ and hITG $\beta 1$ HEK 293T transfected cells.** Dkk3 bound with high affinity to ITG $\alpha 5$ (KD=14.85) and ITG $\beta 1$ (KD=18.15). (Data shown as mean \pm SEM, by Student's t-test for A and B. Data represented in C and D correspond to the average of two independent experiments).

3.8.5 Downregulation of Integrins $\alpha 5$ and $\beta 1$ suppressed the migration of Sca-1+ APCs driven by Dkk3 stimulation

Up until now we confirmed that Dkk3 binds to ITG $\alpha 5$ and ITG $\beta 1$. We next sought to verify whether the downregulation of these receptors was involved in the migration of the Sca-1+ progenitor cells stimulated by Dkk3 treatment.

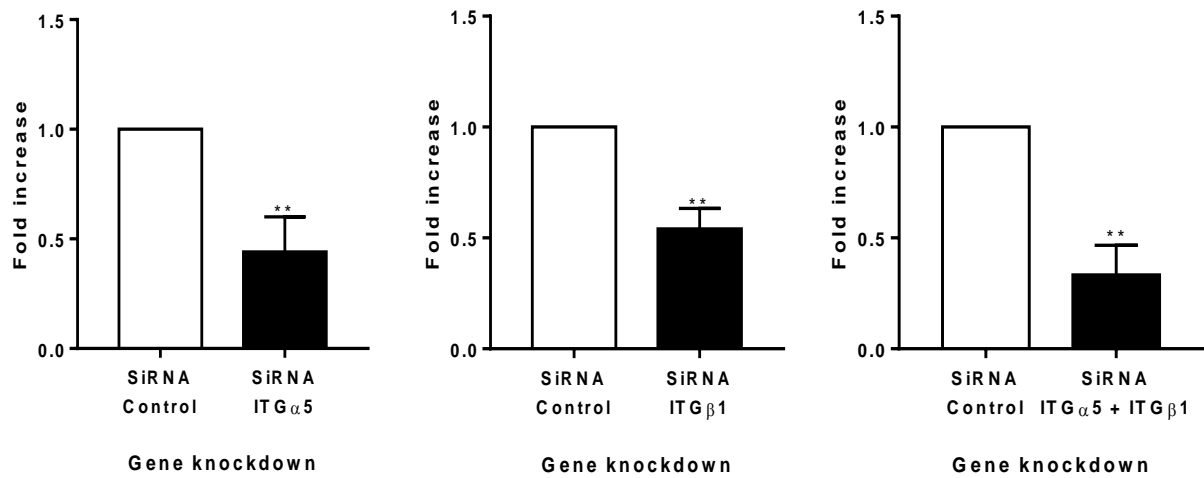
Therefore, Sca-1+ APCs were transfected with ITG $\alpha 5$, ITG $\beta 1$ or ITG $\alpha 5$ +ITG $\beta 1$ SiRNAs. After 48 hours of transfection, the cells were submitted to wound healing assay overnight (15 hours) under Control or Dkk3 treatment conditions (Figure 3.8.5B).

The analysis of mRNA expression showed that the SiRNA transfection was successfully achieved (Figure 3.8.5A).

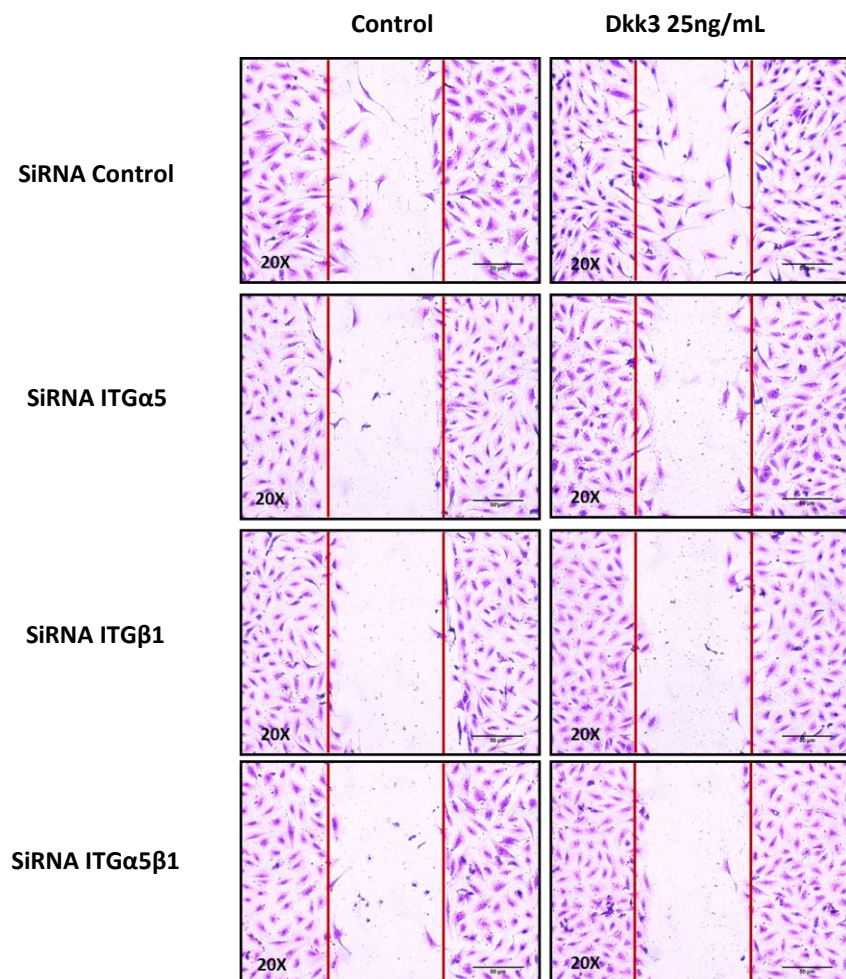
Dkk3-mediated Sca-1+ cell migration (1.6 fold increase compared to control) was repressed upon ITG $\alpha 5$, ITG $\beta 1$ and ITG $\alpha 5$ +ITG $\beta 1$ downregulation (Figure 3.8.5C).

This result proved that ITG $\alpha 5$ and ITG $\beta 1$ are implicated in the Dkk3-triggered Sca-1+ progenitor cell migration mechanism.

A Downregulation of ITG α 5 and ITG β 1 by SiRNA transfection in Sca-1+ APCs – qPCR analysis



B Wound healing assay of Sca-1+ APCs treated with Dkk3, upon knockdown of ITG α 5 and ITG β 1 by SiRNA transfection



C Quantification of Dkk3-driven migration of Sca-1+ APCs upon downregulation of ITG α 5 and ITG β 1 by SiRNA transfection

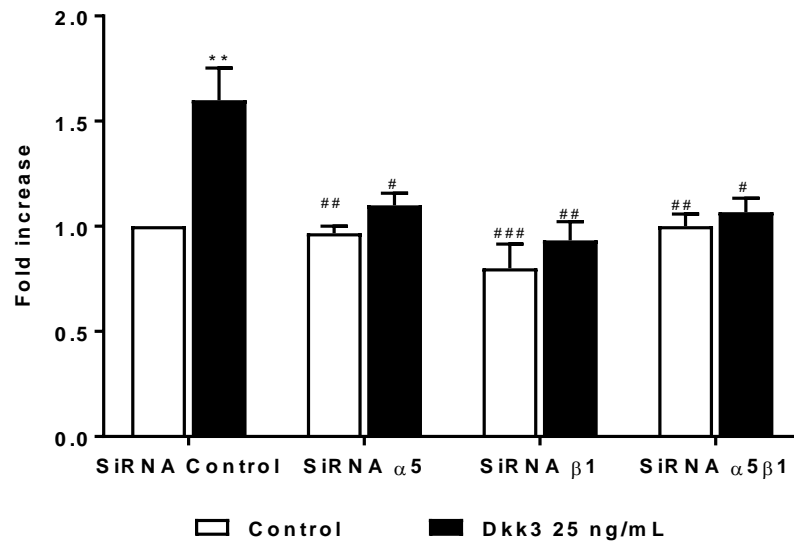


Figure 3.8.5 Downregulation of Integrins α 5 and β 1 suppressed Dkk3-driven Sca-1+ APC migration. Sca-1+ vascular progenitor cells were transfected with ITG α 5 and ITG β 1 SiRNAs. **A: Downregulation of ITG α 5 and ITG β 1 by SiRNA transfection in Sca-1+ APCs – qPCR analysis.** The mRNA expression analysis demonstrated that ITG α 5 and ITG β 1 were successfully downregulated in Sca-1+ APCs; N=5. **B: Wound healing assay of Sca-1+ vascular progenitor cells treated with Dkk3, upon knockdown of ITG α 5 and ITG β 1 by SiRNA transfection.** The SiRNA transfected cells were submitted to wound healing assay overnight (15 hours) upon Control and Dkk3 treatments. **C: Quantification of Dkk3-driven migration of Sca-1+ APCs upon downregulation of ITG α 5 and ITG β 1 by SiRNA transfection.** ITG α 5 and ITG β 1 downregulation suppressed Dkk3-mediated Sca-1+ APC migration. (Data shown as mean \pm SEM, **p<0.01, ###p<0.001, ##p<0.01, #p<0.05, by Student's T test (A) and Two-way ANOVA (C), followed by Bonferroni multiple comparison test, N=3. The symbol * corresponds to the fold increase between the Dkk3 treated cells and the untreated cells, both in the Control SiRNA transfection condition; the symbol # corresponds to the fold increase between the Dkk3 treated Control SiRNA transfected cells and all the other groups of cells).

3.9 Summary 2

- The Yeast Two Hybrid system revealed that Dkk3 interacts with Integrin α 5 and Integrin β 1.
- The Co-Immunoprecipitation assay showed that Dkk3 and Integrin α 5 bind to Integrin β 1, possibly forming a ternary complex.
- Integrin α 5 and Integrin β 1 are high affinity binding receptors for Dkk3.
- Downregulation of Integrin α 5 and Integrin β 1 reduced the Dkk3-driven Sca-1+ vascular progenitor cell migration.
- ITG α 5 β 1 was involved in the Dkk3-mediated Sca-1+ APCs migration.

Chapter 4: Discussion

4.1 Brief Overview and Summary of the Major Findings

In 2012, cardiovascular diseases were reported to be the major cause of premature death worldwide, representing 31% of all global deaths. These diseases include hypertension, hyperlipidaemia-induced atherosclerosis, transplant arteriosclerosis, restenosis resulting from angioplasty, vein graft atherosclerosis and aneurysms, which exhibit a paramount underlying process known as vascular remodelling, which is characterized by an alteration of the structure of the blood vessels, due to cell migration, proliferation, growth, death and secretion of matrix degradation enzymes [334-336]. This process can occur in response to cytokines, including chemokines, produced by activated endothelial cells (ECs), Smooth muscle cells (SMCs), inflammatory cells, platelets, amongst others [142, 337-344].

In this context, one important therapeutic strategy is to control or regulate cell migration and/or proliferation. Sdf-1 α is a chemokine well-known for playing a key role in the recruitment and homing of cells which contribute to neointima formation, comprising hematopoietic stem cells (HSC), endothelial progenitor cells (EPCs), smooth muscle cells, inflammatory cells, and platelets [142, 149, 150, 345-351]. The cognate receptors of Sdf-1 α are CXCR4 and CXCR7 [149, 284, 352-359]. Inhibition of CXCR4 by AMD3100, commercially available as Plerixafor, has shown to prevent cell migration, thus reducing abnormal cell accumulation in neointimal hyperplasia. On the other hand, hematopoietic stem cell mobilization driven by CXCR4 antagonism is required and beneficial in stem cell transplantation therapies against many cancers, as blocking CXCR4 inhibits the retention of the cells in the bone marrow via Sdf-1 α [102] [294, 360-370].

Studies have demonstrated that the cells contributing to neointima thickening originate not only from local media SMC migration and proliferation but also from circulating progenitor cells, which are able to differentiate into different cell types [24, 38, 43, 336, 371-374]. More recently, our group revealed that progenitor cells also reside in the adventitia of the vessel wall, expressing stem cell markers, such as Sca-1+, c-kit+, CD34 and Flk1 and that they can also differentiate into SMCs [6]. An increasing number of studies has further supported this notion of the existence of resident progenitor cells in the vessel wall and demonstrated that the understanding of the function and behaviour of these cells is of great importance, especially regarding the development of new therapeutic approaches in cardiovascular diseases [3, 5, 9, 10, 47, 75, 100, 259-262, 335, 375-382].

The discovery of new cytokines/chemokines involved in cell migration and differentiation during the process of remodelling as well as the elucidation of the underlying mechanisms of action could give rise to novel potential therapies for the treatment of several cardiovascular disorders. Furthermore, the identification on the surface of migratory cells of the receptor mediating the cellular response to these cytokines/chemokines is central in the development of drug targeted therapy [367, 383-387].

Our laboratory has investigated the role of Dkk3 using several models. A microarray analysis of partially induced pluripotent stem cells (PiPSCs) subjected to differentiation into SMCs revealed that Dkk3 expression was elevated alongside the expression of SMC markers, such as Calponin and SM22,

during the differentiation process. Moreover, overexpression of and stimulation with Dkk3 led to an additional increase in the expression of the SMC markers. The supernatant of differentiated cells also exhibited a greater concentration of Dkk3 [244].

Similarly, Dkk3 was shown to be involved in the differentiation of Embryonic Stem Cells (ESCs) into SMCs, as the knockdown of Dkk3 reduced the expression of the SMC markers. Furthermore, overexpression of Dkk3 promoted its secretion and the expression of Myocardin, a SMC gene transcription activator [243].

The hypothesis that Dkk3 could act as a cytokine, was supported by Watanabe et al., whose study demonstrated the ability of exogenous Dkk3 to induce the differentiation of monocytes into a novel cell type resembling immature dendritic cells [241] and reinforced by Kinoshita et al., who verified that Dkk3 protein injection produced a cytokine-like effect which induced the differentiation of monocytes into dendritic-like cells, thus allowing Dkk3 to play a systemic anticancer immunity role [242].

Dkk3 involvement in cardiovascular pathology is supported by the observation that it is overexpressed in cross-sections of ApoE^{-/-} mice aortic roots compared to wild type mice aortas (unpublished data). Consequently, our hypothesis is that Dkk3 is a chemokine-like protein capable of inducing the chemotaxis of the adventitia-derived Sca-1⁺ vascular progenitor cells (Sca-1⁺ APCs).

The current project aimed at studying the migration of Sca-1⁺ APCs in response to Dkk3 and identifying the underlying mechanisms including the identification of the receptor mediating Dkk3 response.

We have demonstrated that Dkk3 induces the migration of resident Sca-1⁺ APCs, *in vitro* and *ex vivo*, in the same manner as Sdf-1 α . Additionally, receptor-ligand assays revealed that Dkk3, like Sdf-1 α , binds with high affinity to CXCR7, which was further confirmed by Co-Immunoprecipitation analysis. Functional migration assays including overexpression and knockdown of the receptor further proved the involvement of CXCR7 in the Dkk3 driven migration of Sca-1⁺ APCs. The study of the signalling pathways triggered in response to Dkk3 treatment showed that MAPK kinase signalling cascade, PI3K/AKT signalling pathway and Rho GTPases family members RhoA and Rac1 were implicated in Sca-1⁺ APCs cell migration. Remarkably, Dkk3 and chemokine Sdf-1 α activated the same downstream signalling pathways in Sca-1⁺ cells. Finally, the downregulation of CXCR7 affected the signalling pathways activated by Dkk3 stimulation, thus confirming the upstream role of this receptor in the Sca-1⁺ progenitor cell migration.

To achieve a complete screen of the potential receptors that could interact with Dkk3 we performed a Yeast Two Hybrid experiment. Our results indicated that, amongst other proteins, Integrin α 5 (ITG α 5) and Integrin β 1 (ITG β 1) interacted with Dkk3. Co-immunoprecipitation and Ligand-receptor binding affinity studies confirmed the interaction discovered. To investigate whether these receptors are involved in the migration of Sca-1⁺ APCs promoted by Dkk3, their expression was knocked down

by SiRNA transfection in the cells before migration assays were performed. Notably, Dkk3-mediated Sca-1+ cell migration was repressed upon the downregulation of ITG α 5 and ITG β 1.

The data herein presented are the first to show that Dkk3 can elicit a chemotactic response in adventitia-derived Sca-1+ vascular progenitor cells. Moreover, our work finally provided the first evidences of high affinity binding receptors of Dkk3, which had not been identified thus far. These findings will be discussed in detail in the following paragraphs.

4.2 The role of Dkk3 as a chemokine-like protein capable of inducing chemotaxis in Adventitia-derived Sca-1+ vascular Progenitor Cells

In 2004, *Hu et al.*, were the first to reveal that a population of stem/progenitor cells resides in the Adventitia of ApoE^{-/-} mice aortic roots and that these cells express the stem cell markers Sca-1+, c-Kit+, CD34 and Flk-1. The same study showed that isolated adventitial Sca-1+ cells could differentiate *In vitro* into SMCs in response to Pdgf- β . Additionally, the capacity *In vivo* of the adventitial Sca-1+ cells to migrate across the vessel wall and subsequently differentiate into SMCs thus contributing to neointima formation, was proved when Sca-1+ β -gal⁻ cells carrying the SM22-LacZ gene applied on the adventitial side of vein grafts in ApoE^{-/-} mice were detected after 4 weeks differentiated into SMCs (β -gal⁺) in the neointima [6].

Later, our group studied the function of Sca-1+ progenitor cells in pathological vessels and concluded that these cells are present in the adventitia of vein grafts 4 weeks after implantation. Adventitial Sca-1+ cells possessed a multipotent capacity to differentiate *in vitro* not only into SMCs but also into other cell types such as adipogenic, osteogenic, or chondrogenic lineages. In the *ex vivo* bioreactor system, Sca-1+ cells also proved to have a migratory ability from the external side of the vessel scaffold towards Sdf-1 α added in the circulating medium. SMC markers were also expressed in these migratory cells present in the decellularized vessel wall. Finally, carotid artery vein graft implanted in ApoE^{-/-} mice, after being enveloped with adventitial Sca-1+ progenitor cells, displayed an exacerbation of the atherosclerotic lesions, in comparison to the grafts with no Sca-1+ cell seeding. Taken together it was determined that the adventitia-derived Sca-1+ vascular progenitor cells actively participate in the pathogenesis of vein graft atherosclerosis, via migration and differentiation into SMCs [103].

More recently, another work from our laboratory demonstrated that SMCs secrete chemokines, such as CCL2 and CXCL1, which in turn stimulates the migration of resident Sca-1+ progenitor cells to the neointima [78].

The above studies draw the attention to the fact that the migration of stem/progenitor cells, which participate in the vascular remodelling phenomenon, is driven by the presence of chemotactic

proteins produced by different cell types, although the underlying migration mechanisms still require clarification.

We sought to investigate whether Dkk3 is a chemokine-like protein involved in the migration of the Sca-1+ cells. Furthermore, as no receptor has been truly recognised yet for this protein, we aimed at identifying the receptor of Dkk3.

4.2.1 Dkk3 induces the migration of Sca-1+ vascular progenitor cells

SMCs are activated in response to vessel injury. As a consequence, these cells undergo proliferation and migration, thus contributing to neointima formation [388-390]. Additionally, cytokines and growth factors are released, leading to the development of an inflammatory microenvironment and the recruitment and mobilization of inflammatory cells and circulating progenitor cells [119, 343, 391]. Many studies have already proven that resident progenitor cells also participate in neointimal hyperplasia via migration and differentiation processes [5, 6, 75, 392].

Our project focuses on Adventitia-derived Sca-1+ vascular progenitor cells (Sca-1+ APCs) to further investigate their contribution to vascular remodelling, in particular through to their migration behaviour, which thus far lacks insight.

The Sca-1+ APCs were isolated from and sorted by Immunomagnetic beads selection. The sorting method efficiency and the establishment of the purity of the cell population after *n* passages, were assessed by flow cytometry analysis. The results proved that the purity of the Sca-1+ cell population was preserved even following 5 passages, as an average of 93% of Sca-1+ cells was detected (Figure 3.1). Therefore, the cells were sorted using Sca-1+ marker every 5 passages.

Sdf-1 α is one of the most well-known chemokines with an established role in inducing migration, proliferation and differentiation of various cell types, namely circulating and resident stem/progenitor cells [102, 393]. Therefore, this chemokine was used as the positive control in the functional migration assays.

Two types of migration methods were implemented due to their distinctive characteristics and the need to explore different modes of cell migration. In the transwell migration assay the cells are loaded in the upper side of a porous membrane insert and the chemokine medium is placed in the lower chamber. A chemoattractant gradient is formed, towards which the cells migrate through the porous membrane (physical barrier). Cell quantification of the migrated cells on the lower side of the membrane is followed under the microscope. Thus, this type of migration assay is an end-point chemotaxis study, as fixing and staining steps are required for cell quantification. Invasion studies may also be carried out by the transwell assay, with the addition of an extracellular matrix on top of the porous membrane. On the other hand, the Wound healing assay, also known as Scratch assay, is

a simple approach which only requires doing a scratch with a tip on a cell monolayer. The wound closure can thus be monitored, in response to different treatments. In this type of migration study, the speed of cell migration can also be assessed as well as single cell migratory behaviour. This method is a two-dimensional assay and no chemotaxis gradient is achieved. Furthermore, cell proliferation can also affect the outcome of the experiment. However, when treating the cells with inhibitors that can change the cell morphology/cytoskeleton, it might be preferable to perform the Scratch assay to assure that the result which we obtained is actually due to the treatment in study and not to the secondary effect observed on the cell morphology. For example, if an inhibitor suppresses filopodia/lamellipodia formation in the cells, these can show a reduced size and thus pass more easily through the pores of the transwell insert. Nevertheless, in the scratch assay, the wound closure could be slower in response to the same inhibitor, as reduced number of filopodia/lamellipodia could represent a poorer migratory ability of the cell. Hence, the selection of the migration assay to be used should be cautious and adequate to the intent of the analysis and to the type of cell, as only adherent cells can be used in the Wound healing assay. Table 4.2.1 succinctly compares both *In vitro* migration assays [394-397].

Table 4.2.1 Comparison between Transwell and Wound healing migration assays

Feature	Transwell Migration assay	Wound healing assay
Cost	Costs associated with the acquisition of the transwell insert	More economical
Cell compatibility	Adherent and suspension cells	Adherent cells
Detection time	End-point	End-point or Real-time
Type of analysis	Quantitative	Quantitative and Qualitative
Chemotaxis gradient	Yes	No
Adaptability to automation	Difficult	Easy
Reproducibility	Good	Fair
Dimensionality	2D and 3D	2D
Direction of movement	Mainly Vertical	Horizontal
Measurement	Cell count	Cell count; Wound closure
Live imaging and/or Single cell tracking	No	Yes

The Sdf-1 α concentration range (0-100 ng/mL) used to promote Sca-1+ APC migration *in vitro* and *ex vivo* was selected according to the found in the literature and performed previously in our laboratory [102, 103]. Sdf-1 α -driven migration assay showed that the migration fold increase peaked at 10-50 ng/mL of treatment and started to slightly reduce at higher concentration, although still above the control condition (Figures 3.2.1.C and 3.2.2.C). This could suggest that the receptors CXCR4 and/or

CXCR7 mediating Sdf-1 α response were at the beginning progressively activated until a saturation state was reached upon increasing chemokine treatment [136, 398]. Furthermore, chemokine receptor internalization after activation has been demonstrated by many studies [399, 400]. Therefore, internalization of the CXCR4 and CXCR7 could possibly have occurred, thus leaving less available receptors on the cell surface for additional ligand binding and consequent cell migration stimulation.

No report has been published so far on the direct migratory effect of Dkk3 on vascular progenitor cells. Dkk3 protein has always been associated with tumour development, particularly regarding its role in cell apoptosis, proliferation, migration and invasion. Contrasting studies on the role of Dkk3 in cancer have emerged over time as Dkk3 has both been recognised as a tumour suppressor agent [226-231] and associated with the development of tumour pathogenesis [232-235]. Studies on the role of Dkk3 on cell migration in cancer have been published. Huo et al., showed that Dkk3 overexpression attenuated the miR-25-induced motility of MV3 cells (Human melanoma cell line) [228]. Romero et al., demonstrated that culture medium from cells transfected with Dkk-3 plasmids, compared to control culture medium, inhibited TGF- β -induced PC3 cell (human prostate cancer cell lines) migration [227]. Consistently, Xiang et al., verified that Dkk3 overexpressing breast cancer cells migrated in a slower rate than control cells [229]. Contrastingly, Pei et al., found that DKK3 knockdown decreased the migration of Huh6 cells (human hepatoblastoma cell line) [232]. Katase et al., revealed that Dkk3 knockdown by siRNA transfection reduced the migration of Ca9-22 cells (oral squamous cell carcinoma cell line) [233]. We wished to investigate whether Dkk3 treatment stimulated the migration of Sca-1+ APCs.

The Dkk3 concentration range used in *in vitro* and *ex vivo* migration assays was selected according to the used in studies published by our group regarding the stem cell differentiation into SMC in response to Dkk3 [243, 244]. Furthermore, the concentrations considered are in accordance with the level of Dkk3 measured in human serum in a period of time of 5 years (unpublished data) (Figure 4.2.2B).

Remarkably, as observed with Sdf-1 α , a significant increase of Sca-1+ progenitor cell migration was observed in response to Dkk3 stimulation. The highest rate of migration was achieved at 25-50 ng/mL of Dkk3 concentration (Figure 3.2.1D and 3.2.2.D). In addition, although greater than in the control condition, the increase in cell migration also dropped upon 100 ng/mL of Dkk3 treatment. We postulated that, as it was detected with Sdf-1 α , at increasing protein concentration the corresponding receptor becomes either saturated or is internalized [136, 398-402].

Growth factors have also been reported to play an important role in the migration of several cell types. Pdgf- β is capable of inducing the migration of SMCs and the differentiation of stem/progenitor cells into SMCs, processes of crucial significance in the pathogenesis of atherosclerosis [101, 265, 403-405]. To further understand the migration behaviour of Sca-1+APCs we conducted migration assays in response to Pdgf- β . As anticipated, this growth factor stimulated

their cell migration and in a dose-dependent manner (Figures 3.2.3A and B). This finding proved that Pdgf- β could also be used as a positive control in the following experiments.

We also investigated if Dkk3 affected cell proliferation, a process implicated in vascular remodelling. The BrdU incorporation assay was carried out and three stimulation time points were selected, including the 16 hours-time course applied in the migration assays. Interestingly, Sca-1+AdvPC proliferation was only promoted after 48 hours of stimulation with either Dkk3, or Sdf-1 α or Pdgf- β , at any of the concentrations considered (Figures 3.2.5A, B and C). We thus inferred that these protein treatments primarily induce Sca-1+ APC migration, which is later followed by proliferation, in response to persistent stimulation.

The Aortic ring assay is a well-established method to study cell migration three-dimensionally, which is closer to the *In vivo* setting and provides more information. In this context, Pdgf- β has been widely used to prove its ability to promote cell migration, proliferation and differentiation [276, 406-408].

As a consequence, we explanted aortic arteries from Wild type and ApoE^{-/-} mice and performed aortic ring assay. Cell outgrowth started at days 2-4 days and culminated at 7-9 days, after which the ingrowth began.

Predictably and consistent with the described in the literature, Pdgf- β substantially induced the cell outgrowth from both Wild type and ApoE^{-/-} mice aortic rings (Figures 3.2.4.1A-H).

Likewise, cell outgrowth from Wild type and ApoE^{-/-} explants was also significantly promoted in response to Sdf-1 α (Figures 3.2.4.1A-D). Although this study is the first to use a 3D model, the results obtained are not surprising, as it has already been shown that Sdf-1 α can induce the migration and proliferation of SMCs, ECs and resident progenitor cells [102, 144, 164, 295, 409, 410].

What was striking to us was the same capacity exhibited by Dkk3 in stimulating the cell outgrowth, which revealed statistical significance for the ApoE^{-/-} mice group of rings (Figure 3.2.4.1E-H). This fact was interesting and it has two potential reasons. Firstly, ApoE-deficient aortas are characterised by the presence of atherosclerotic lesions which comprises hyperplasia and neointima formation [277, 411-413]. Therefore, because more cells are present in the ApoE^{-/-} aortas compared to the Wild type aortas, it is highly likely that the corresponding cell outgrowth is also greater in response to a particular treatment. Secondly, ApoE-deficient mice vessel walls also possess an increased number of stem/progenitor cells, particularly Sca-1+ progenitor cells, susceptible to migrate and to differentiate and thus to contribute to neointima formation [6, 277, 412]. Cell outgrowth from ApoE^{-/-} mice aortic rings is higher than the outgrowth from Wild type aortic explants upon certain stimulation.

The aortic rings isolated from ApoE^{-/-} mice were submitted to immunostaining in order to characterise the cell types present in the Dkk3-triggered cell outgrowth. The SMCs were labelled by incubation with an antibody for alpha-Smooth Muscle-actin (α -SMA). Sca-1-GFP transgenic mice

crossed with ApoE^{-/-} mice were used, therefore Sca-1⁺ cells could be directly identified through their GFP expression.

We observed that the aortic ring cell outgrowth in the control and in any of the treatment conditions included Sca-1⁺-GFP cells (Figure 3.2.4.2.A-D). In addition, the number of Sca-1⁺ cells in the outgrowth was higher upon Dkk3 or Sdf-1 α stimulation, which further proved that these proteins induce the migration and/or proliferation of resident Sca-1⁺ vascular progenitor cells, in a three-dimensional setting, which better mimics the *in vivo* scenario than the *in vitro* migration assays.

As it has been previously described in many studies, neointima formation and hyperplasia involve vascular remodelling, due to cell migration, proliferation, differentiation in response to different signals. SMCs have been considered one of the main players in this process [44, 49, 50, 57, 60, 99, 414-419]. Therefore, it was expected to find a higher number of cells labelled with the SMC marker α -SMA in the cell outgrowth from the aortic rings treated with Sdf-1 α and with Dkk3 (Figure 3.2.4.2.E). In fact, the SMC outgrowth was more pronounced in the aortic rings stimulated by Dkk3. Notably, Dkk3- and Sdf-1 α -stimulated cell outgrowths included also a higher number of cells displaying both Sca-1⁺ and α -SMA markers, i. e., cells with co-localization of Sca-1⁺-GFP and α -SMA-Cy3 staining (Figure 3.2.4.2.F). Two mechanisms could explain those results.

The first mechanism could be that Sca-1⁺ progenitor cells have differentiated into SMCs. Hu et al., in the vein graft model, elegantly showed that adventitia⁻Sca-1⁺ vascular progenitor cells are one source of SMCs, as many β -gal⁺ cells were found in the neointimal lesions, after applying the Sca-1⁺ progenitor cells carrying the LacZ gene under the control of SM22 promoter to the outer side of the vein grafts in ApoE^{-/-} mice [6]. Another work from the same group also demonstrated that Sca-1⁺ APCs have a significant role in the pathogenesis of vein graft-derived atherosclerosis, due their migratory and differentiation abilities. In this study, Sca-1⁺ APCs were able to differentiate into SMCs *in vitro*. It was also showed that Sca-1⁺ progenitor cells could migrate through the scaffold of the decellularized mice aorta in response to Sdf-1 α and differentiate into SMCs in this *ex vivo* bioreactor model [103]. In their study, Wong et al., disclosed that restenosis after Sirolimus-eluting stent therapy is the result of induced Sca-1⁺ vascular progenitor cell migration and differentiation into SMCs. *In vitro* assays revealed an increased migration rate of the Sca-1⁺ cells in response to Sirolimus, through CXCR4 activation. The *ex vivo* bioreactor system also presented a Sirolimus-driven induction of the Sca-1⁺ cell migration, as the cells seeded on the outer side of the decellularized vessel were observed in the inner layer of the vessel wall and immunostaining confirmed that these cells had differentiated into SMCs expressing Calponin and SM-22 α markers [102]. Karamariti et al., proved in their study that Dkk3 is involved in the differentiation process of partially induced Pluripotent Stem cells into SMCs, by regulating the expression of SMC-related genes, such SM22 [244]. Wang et al., further confirmed the implication of Dkk3 in inducing the differentiation of Embryonic stem cells (ESCs) into SMCs, with an increase in Dkk3 expression and secretion from the differentiated SMCs [243]. Hence, there is enough body of work to assume that the increased number of SMCs and cells co-stained with both Sca-1⁺ and α -SMA, in the cell outgrowth induced by Sdf-1 α or Dkk3, could be explained by migration and possible differentiation of Sca-1⁺ cells.

The second possible mechanism to explain the increase of SMA+/Sca-1+ cells is that SMCs could have started dedifferentiating upon Dkk3 treatment. Several studies have described the switching of SMC phenotype in atherogenesis, in response to environmental signals, including cytokines and mechanical forces. Under normal conditions, the SMCs in the vessel wall media are displayed in concentric layers with a contractile phenotype and elongated morphology, with abundant myofilaments and a low proliferation rate. In contrast, the SMCs present in neointima lesions exhibit a synthetic phenotype, a more flattened morphology and less inner myofilaments. Abundant golgi and rough endoplasmic reticulum bodies are present, which indicates increased synthetic and secretory activities. Hence, plastic SMCs are more prone to migrate and proliferate. This is accompanied by a decrease in the expression of the SMC differentiation markers, such as Actin- α -SM, SM-22 α , SM-MHC and ACTA2 [93, 374, 420-424]. On the other hand, progenitor cell markers can potentially be expressed in the dedifferentiated SMCs, such as the Sca-1+ marker. There is evidence regarding the participation of Krüppel-Like Factor-4 (Klf4) in the SMC phenotype modulation in atherosclerosis. Klf4 is a transcription factor recognised for its role in maintaining the pluripotency in ESCs and in reprogramming somatic cells into pluripotent stem cells, thus it is expected to have very low expression in adult somatic cells, such as SMCs. Nevertheless, studies revealed that its expression is increased in response to vascular injury or in ApoE^{-/-} mice and it is associated with SMC migration and proliferation to the neointima [95, 405, 425-427]. More recently, Majesky et al., showed that Sca-1+ vascular progenitor cell population is generated from adventitial-SMC dedifferentiation, thus contributing to adventitia remodelling. These Sca-1+ cells, due to their multipotency capacity, are able to differentiate *In vivo* into mature SMCs and other cell types. Once more, it was demonstrated that the Adventitia is a highly dynamic vessel layer, containing various cell types and that it has a participative role in normal and pathological physiology. Fate mapping and lineage tracing strategies were employed in this study, in which Myh11-CreERT- β Gal/YFP mice were used to understand the fate of mature SMCs upon vascular injury. Tamoxifen was injected before injury, which allowed permanent labelling and tracking the SMCs expressing SM-MHC and their progeny throughout the experiments, even if they lose when SM-MHC expression at later time points. This approach revealed that medial SMCs not only contribute to neointima formation but also migrate to the Adventitia, where they lose the SMC marker and gain stem cell markers, such as Sca-1+ and CD34. Therefore, these Sca-1+ cells derived from dedifferentiated SMCs contribute to the resident adventitial Sca-1+ progenitor cell pool. In addition, the SMC phenotype transition with generation of progenitor cells encompassed induction of the Klf4 factor *in vivo* [376]. Shankman et al., provided insight as well in the dedifferentiation process of the SMCs by using a SMC lineage tracing method. In SMC-YFP^{+/+}-ApoE^{-/-} mice arteries most of the medial SMCs were MHC11-YFP labelled upon tamoxifen injection. After prolonged western diet, 30% of the YFP⁺-SMCs in the atherosclerotic lesion were phenotypically modulated, as ACTA2 expression was not detected and, many YFP⁺ACTA2⁻-SMCs exhibited Sca-1+ marker expression. Interestingly, many YFP⁺-SMCs also expressed KLF4. The lesion size of arteries from mice with Klf4 deficiency in the SMCs (SMC YFP^{+/+}Klf4 ^{Δ/Δ} ApoE^{-/-}) was highly reduced when compared to the arteries of the control mice (SMC YFP^{+/+}Klf4^{+/+}ApoE^{-/-}) and the number of YFP⁺ACTA2⁻Sca-1+ SMCs in the media area underlying the lesion had also decreased. Therefore, this study also proved

that Klf4 is involved in the SMC phenotype transition [95]. Whether this dynamic process is dependent on Klf4 in the cell outgrowth mechanism driven by Dkk3, more studies are required.

We should not rule out the possibility that Dkk3 could have also promoted the migration and/or proliferation of endothelial cells or induced the differentiation of the Sca-1+ vascular progenitor cells into ECs. Angiogenesis is a crucial event in tumorigenesis, as the blood supply provides the required oxygen and nutrients. Once more, divergent studies have been published concerning the role of Dkk3 in tumour-related neovascularization. Untergasser et al., found an increase in the number of blood vessels expressing Dkk3 in certain neoplasms and carcinomas when comparing to normal tissues and an increase in the microvessel density in C57/BL6 mouse model in response to Dkk3 overexpression in skin melanoma cells [236]. In 2009, Fong et al., proposed that Dkk3 could be a specific marker for tumour endothelial cells, as Dkk3-positive vessels were found only in tumour tissue but no in normal tissue. Additionally, they suggested that patients suffering from pancreatic adenocarcinoma who showed Dkk3-expressing microvessels could benefit more from chemotherapy, due to a more efficient inhibition of endothelial cell outgrowth in response to chemotherapeutic drugs [428]. Zitt and Mühlmann et al., in their first study concluded that Dkk3 was a proangiogenic factor involved in neovascularisation during colorectal tumour growth [237] and in a subsequent work they observed an overexpression of Dkk3 in microvessels of gastric carcinoma [238]. Interestingly, Medinger et al., detected that Dkk3 was produced by megakaryocytes and co-localised with VEGF in platelets and that it was released similarly to VEGF upon platelet stimulation [224]. Kim et al., demonstrated an association between Dkk3 expression and VEGFR-2/PI3K/Akt signalling pathway, as overexpression of Dkk3 suppressed the β m2 -driven VEGFR-2/AKT/mTOR signalling pathway [239]. All these data provide enough evidence to recognise a role for Dkk3 in vascular biology.

Rigorous lineage-tracing methodology and confocal analysis of mice model, resulting from the crossing of knock in Sca-1-CreER^{T2} mice with Cre expression under the control of Sca-1 endogenous promoter, with ROSA26 fluorescent reporter mice, would provide answers to the following questions when used *in vivo* and in herein exposed explant model. Does Dkk3 induce the migration, proliferation and/or differentiation of the resident Sca-1+ vascular progenitor cells? Is Dkk3 responsible for the SMC dedifferentiation process, either under normal or pathological conditions? Could Dkk3 induce as well the differentiation of the Sca-1+ vascular progenitor cells into ECs? Does the Dkk3-driven Sca-1+ progenitor cell migration process occur prior to the differentiation process in the atherosclerotic lesions? Is there a possible fusion of the Sca-1+ progenitor cells with pre-existing SMCs? Is the Dkk3-triggered Sca-1+ cell differentiation phenomenon confined to the SMC or EC lineages or can it also comprise for example inflammatory cell lineages? What is the exact role of Dkk3-mediated Sca-1+ progenitor cell migration and differentiation during atherogenesis?

This and much more information could be gained from the proposed lineage tracing methodology. Nevertheless, we have produced the first evidence of the ability of Dkk3 to induce the migration of resident Sca-1+ vascular progenitor cells, *in vitro* and *ex vivo*.

4.2.2 Dkk3 binds with high affinity to CXCR7

Having established the chemotactic role of Dkk3 on the resident Sca-1+ vascular progenitor cells, the next step consisted of dissecting the underlying migration mechanism, which raised the essential question of which is the receptor Dkk3 binds to and mediates Sca-1+ progenitor cell migration?

A detailed search in the literature clearly shows that there is a great controversy over the identification of Dkk3 receptor. In fact, until very recently, no receptor was yet proposed. On the other hand, the receptors for the other three members of the Dkk family of proteins, Dkk1, 2 and 4, have been identified.

In 2000, Mao et al., demonstrated that Human LRP6 is a high-affinity binding receptor of Dkk1 and Dkk2. Furthermore, they showed that Dkk3 was actually not able to bind to this receptor [286]. Subsequently, a series of studies progressively supported those findings. Semenov et al., observed the binding of Dkk1 to LRP6 through affinity binding and co-immunoprecipitation assays [429] and Bafico et al., detected that Dkk1 not only binds to LRP6 but also to a lesser extent to LRP5 [430]. Li et al., confirmed that Dkk2 binds to LRP6 [431]. Later in 2014, Fujii et al., through modelling simulation studies provided support to the lack of affinity between Dkk3 and LRP5/6 receptors [432].

In another study, Mao et al., disclosed two more candidate receptors for Dkk1 and Dkk2. In this work, they concluded that both Dkk1 and Dkk2 could bind with high affinity to Kremen1 or Kremen2. Contrarily, Dkk3 could not bind to these receptors. Co-immunoprecipitation was performed proving the binding of Dkk1 to Kremen2 and interestingly, it was inferred that Dkk1 could bridge LRP6 with either of the Kremens, forming a ternary complex [285]. In 2003, the same team proved that Kremen2 co-operates with Dkk1, 2 and 4 to inhibit the Wnt signalling, but not with Dkk3 [287].

In the following years, more effort was put on the elucidation of the signalling mechanisms and the specific molecular domains involved in the binding of Dkk1 and Dkk2 to LRP5, LRP6, Kremen1 and Kremen2, resulting in divergent evidences on their underlying function [213, 433-438]. In 2009, Nakamura et al., stated that Dkk1 and Dkk3 are associated with Kremen1 and Kremen2, as their GST pull down and co-immunoprecipitation assays demonstrated that these two Dkk proteins could form complexes with the Kremens. Nevertheless, Dkk3 did not interact with LRP6 as Dkk1 did [292]. Following this, Karamariti et al., proposed that Dkk3 activates the Wnt signalling pathway through Kremen1, in the differentiation process of partially-induced pluripotent stem cells (PiPSCs) into SMCs. This was supported by the evidence of co-immunoprecipitation of Dkk3 with Kremen1 and immunostaining showing co-localisation of the glycoprotein with the receptor in PiPSC-SMCs in a perinuclear pattern [244].

In 2016, Mohammadpour et al., carried out an *In silico* study to determine the structure of Dkk3 and to understand whether Dkk3 was capable of interacting with the Kremens, LRP5/LRP6 receptors and EGFR. By taking advantage of different bioinformatic tools the authors predicted that Dkk3 is capable of interacting with the Kremens, the LRPs and the EGFR proteins. However, no functional

assays were presented and the study was based merely on software analysis [439]. More recently, Poorebrahim et al., also performed an *In silico* evaluation of Dkk3 and concluded that, similar to the other family members, Dkk3 can interact with the EGF-like domain (PE) of LRP5/6, through its Cys-rich domain 2 (CRD2) domain. Intriguingly, they detected that this CRD2 domain alone could bind more tightly to the LRP5/6 than the whole structure of Dkk3 and that the binding affinity of Dkk1 to LRP6 was higher than the binding affinity of the Dkk3-LRP6 complex [440].

In light of these conflicting reports, it was not yet possible to recognise the receptor for Dkk3.

As we had shown that Dkk3 promotes the chemotaxis of Sca-1⁺ APCs, we sought to investigate whether Dkk3 could bind to a chemokine receptor. We analysed the expression of the chemokine receptors in mouse aortic Sca-1⁺ APCs, mouse pancreatic endothelial cells - MS1 cells (ECs) and mouse aortic smooth muscle cells (SMCs). No significant difference was found for the expression of CXCR1-CXCR6, CCR1-CCR10 and CX3CR1 in the three cell types considered (Figure 3.3.1A). However, CXCR7 expression in Sca-1⁺ APCs was significantly higher than in the ECs, but its expression was equivalent to the level detected in the SMCs. Consistent with our findings, Yu et al., by performing a qPCR array also found that CXCR7 receptor is highly expressed in VPCs [78].

CXCR7, alongside CXCR4, is recognised as the receptor of the chemokine Sdf-1 α [150, 153, 282, 284]. Intriguingly, our qPCR results showed that CXCR4 expression was lower in the Sca-1⁺-AdvPCs and in SMCs than in the ECS. This low expression of CXCR4 in the Sca-1⁺ progenitor cells was also observed at the protein level. Nevertheless, CXCR4 protein expression was high in both ECs and SMCs. At the protein level, CXCR7 was greatly expressed in both Sca-1⁺ A-PCs and SMCs, which is in accordance with what we observed at the mRNA level (Figure 3.3.1B).

We demonstrated that Dkk3 had a similar positive effect as Sdf-1 α on the migration behaviour of the Sca-1⁺ vascular progenitor cells. Considering that CXCR4 and CXCR7 are the cognate receptors of Sdf-1 α and, given the strikingly high and differential expression of CXCR7 in the Sca-1⁺-AdvPCs and SMCs, compared to the expression of the other chemokine receptors, we postulated that the Dkk3-driven migration mechanisms of Sca-1⁺ APCs could involve CXCR7 activation. Moreover, this hypothesis seemed to be supported by the reports on the implication of Dkk3 in the differentiation of stem cells into SMCs [243, 244].

Firstly, we intended to verify if the downregulation of CXCR7 in the Sca-1⁺ progenitor cells, by SiRNA transfection, would affect the Dkk3-driven migration. Sdf-1 α was used as a positive control. Sdf-1 α -mediated Sca-1⁺ vascular progenitor cell migration was significantly reduced upon CXCR7 knockdown (Figure 3.4.1.2.C and E). This result was expected as studies have shown that CXCR7 activation by Sdf-1 α can be involved in cell migration. Chen et al., revealed that cardiac stem cell migration induced by Sdf-1 α was suppressed by CXCR7 and CXCR4 downregulation. In the context of atherosclerosis-related inflammation, Ma et al., found that Sdf-1 α stimulation significantly increased macrophage migration mediated by CXCR7 [441]. Although CXCR7 was initially accepted as an orphan and decoy receptor with no functional role [289, 297, 442-444], an increasing number of

studies has been demonstrating that CXCR7 does have an active role in the regulation of cell function, such as cell migration [297, 357, 445-447]. Therefore, CXCR7 is not recognised now as only a scavenger receptor [354, 448-450].

Due to the homology between CXCR7 and CXCR4 receptors [451, 452] [453] and their binding affinity for the chemokine Sdf-1 α , we intended to assess whether the migration of the progenitor cells induced by Dkk3 or Sdf-1 α involved the receptor CXCR4. The Sdf-1 α /CXCR4 axis is notorious for its role in inducing cell migration and homing, especially concerning the Hematopoietic stem cell chemotaxis [454-457]. Therefore, we attempted to knockdown the receptor by SiRNA transfection and then perform the migration assay. Surprisingly, CXCR4 downregulation was not achieved, even though 2 different SiRNA were used (Figure 3.4.1.1B). This might be due to the low expression of CXCR4 on the Sca-1 $^+$ progenitor cells (Figure 3.4.1.1A and B). As a result, we opted for a different approach, based on the use of a chemical antagonist. We performed migration assays by first pre-incubating the cells with the CXCR4 antagonist AMD3100. Neither Sdf1- α - nor Dkk3-driven Sca-1 $^+$ progenitor cell migration was affected by CXCR4 inhibition, as no difference was found between the Sdf-1 α /Dkk3 stimulated groups with and without AMD3100 treatment (Figure 3.4.1.1.D and E). Once more, the low expression of CXCR4 on the Sca-1 $^+$ APCs could explain these findings. Indeed, Burns et al., showed that the bicyclam AMD3100 did not inhibit the binding of Sdf-1 α in the breast tumour cell line MCF-7 which did not express functional CXCR4 on their surface. In addition, they used human breast tumour cells which did not express CXCR4 and CXCR7. Upon transfection of CXCR7, AMD3100 was not able to compete with the binding of the chemokine [354]. Zabel et al., in their study of trans-endothelial migration (TEM) of cancer cells found that, although the NC-37 cells (human Burkitt's lymphoma cell line) expressed both CXCR4 and CXCR7 receptors, the CXCR7-specific antagonists were more effective in inhibiting the Sdf-1 α -triggered migration than the AMD3100 agent [357]. Finally, Grymula et al., showed that CXCR4 inhibition by AMD3100 was not sufficient to inhibit the Sdf-1 α -mediated migration of rhabdomyosarcoma metastatic cells, as these expressed not only CXCR4 but also CXCR7, thus concluding that a simultaneous blockage of both receptors would render a more efficient strategy [458]. Interestingly, Kalatskaya et al., observed that AMD3100 could be an agonist of CXCR7 with potentiation of Sdf-1 α binding to this receptor [459]. The agonistic activity of the bicyclam inhibitor towards CXCR7 was also demonstrated by Gravel et al., [460]. We did not detect an increase of the Sca-1 $^+$ APCs migration in response to Sdf-1 α or Dkk3 in AMD3100 treated cells.

Hessen et al., observed a 43% amino acid similarity, in both rabbit and mouse species, between CXCR7 and CXCR2 protein sequences [451]. In addition, some ligands were found to be promiscuous towards CXCR2, CXCR4 and CXCR7, as is the case of Macrophage migration-inhibitory factor (MIF) [461-463]. As a consequence, we sought to analyse whether the downregulation of CXCR2 would affect the migration of Sca-1 $^+$ APCs in response to Dkk3. The transfection SiRNA specific for CXCR2 did not affect the migration rate of the cells (Figure 3.3.1.3) indicating that CXCR2 is presumably not involved the Dkk3-driven migration mechanism of the Sca-1 $^+$ progenitor cells.

Finally, as the Kremen receptors have been associated with the Dkk protein family, we assessed their possible implication in the Sca-1+ migration mechanism induced by Dkk3. Kremen1 expression on the Sca-1+Adv-PCs was detected at the mRNA and protein levels and the receptor knockdown was successfully achieved. Notably, the Dkk3-mediated migration of the Sca-1+ progenitor cells was reduced in the cells transfected with Kremen1 SiRNA (Figure 3.4.1.4). On the other hand, we detected a low expression of Kremen2 in the Sca-1+ progenitor cells (Figure 3.4.1.5), which understandably resulted in unsuccessful knockdown by SiRNA transfection.

Sca-1+ APCs expressed also low levels of LRP5 and LRP6 (Figure 3.3.2). Consequently, we didn't pursue with the respective SiRNA transfection and subsequent migration assay in response to Dkk3.

Our next strategy, to further clarify which receptors remain as candidates for Dkk3 protein, was to overexpress the receptors on the HEK 293T cells by plasmid transfection and then to perform migration assays with Dkk3 stimulation. Sdf-1 α was used as the positive control of the experiment. Human CXCR2, CXCR4, CXCR7, Kremen1 and Kremen2 were cloned in a pShuttle-Flag-HA vector and transfected in the 293T cells, before the cells were submitted to transwell migration assay.

As anticipated, Sdf-1 α induced the migration of 293T cells overexpressing either CXCR4 or CXCR7 (Figure3.4.2.1. and Figure3.4.2.2.) but not in the cells transfected with the control vector or overexpressing CXCR2, which validated the design of this experiment (Figure 3.4.2.3). Interestingly, Dkk3 induced the migration of HEK 293T cells overexpressing CXCR7, but had no effect on cells overexpressing CXCR4 or CXCR2, which was consistent with the result obtained in the SiRNA transfection experiment. This reinforced the hypothesis that CXCR7 is potentially involved in Dkk3-triggered cell migration.

Surprisingly and in opposition with the results observed following the downregulation assay of the receptors, the migration of the HEK cells upon Kremen1 overexpression was not induced (Figure 3.4.2.4.). Hence the involvement of this receptor in the Dkk3-driven cell migration still requires further clarification.

Our third experimental approach consisted of measuring the binding affinity of the candidate receptors to Dkk3. We followed the methodology described by Mao et al., [285, 286], in which alkaline phosphatase (AP) was fused to the ligand and the degree of ligand-receptor binding was measured by the activity of the enzyme. Sdf-1 α -AP exhibited a high binding affinity for CXCR4 ($K_D=3.38nM$) and CXCR7 ($K_D=6.51nM$) and as expected, this chemokine did not bind to CXCR2 (Figure 3.4.3.2). The binding of Sdf-1 α to CXCR4 and CXCR7 has been extensively described in the literature, as mentioned before. The dissociation constants we measured were in accordance with the found in the literature. Balabanian et al., provided a K_D of 0.4 nM for CXCR7 [297] and Crump et al., calculated a K_D of 3.6 nM for CXCR4 [464]. The small discrepancies observed between the K_D values we obtained and the values found in the literature are due to the different methodologies applied for the measurement of the dissociation constant. Therefore, we validated this method and applied it to measure the binding affinities of Dkk3 to the candidate receptors.

Remarkably, Dkk3 exhibited a high binding affinity for CXCR7 ($K_D=10.61\text{nM}$), but it did not bind to CXCR4 ($K_D=1.36\text{E}^{+16}\text{nM}$) and Kremen1 ($K_D=1.29\text{E}^{+15}\text{nM}$), as ambiguous binding curves were obtained and the values of their respective dissociation constants were extremely high (Figure 3.4.3.2.E and F). The binding of Dkk3 to CXCR7 was represented by a characteristic hyperbolic saturation curve, but no curve was obtained regarding the binding of Dkk3 to Kremen2. Our results are consistent with what Mao et al., reported: Dkk3 does not bind to Kremen1 and Kremen2 [285].

Although Karamariti et al., demonstrated that Dkk3 can co-immunoprecipitate with Kremen1 in differentiated SMCs [244] and Nakamura et al. showed by pull down and co-immunoprecipitation analysis that Dkk3 can be associated with Kremen1 and Kremen2 [292] and finally, Mohammadpour et al., suggested through their *in silico* study that Dkk3 was capable of interacting with the Kremens [439], no cell functional assays or affinity binding experiments had been performed so far. In addition to the functional assays, we also performed a co-immunoprecipitation assay which confirmed the binding of Dkk3 to endogenous CXCR7 expressed on the Sca-1+ vascular progenitor cells (Figure 3.4.3.1). Our work is the first to present evidence on the high binding affinity of Dkk3 to CXCR7, and to confirm the involvement of CXCR7 in Dkk3-induced migration by cell functional migration assays. Cell migration is a key process involved in neointimal hyperplasia. The identification and functional validation of chemokine receptor, CXCR7, as the receptor involved in Dkk3-induced chemotaxis of adventitia-derived Sca-1+ vascular progenitor cells, unveils new potential drug-targeted therapeutic strategies against vascular diseases.

In vascular remodelling, the recruitment of SMCs and progenitors cells expressing CXCR4 is known to contribute to neointima formation [281, 465, 466]. Conversely, it is also recognised that the CXCR4/Sdf-1 α axis plays a role in the regulation of neutrophils recruitment in atherosclerosis [467]. Unlike CXCR4, the role of CXCR7 has not been exhaustively investigated in vascular biology.

CXCR7 mice knockout results in postnatal lethality and only 30% of the mice survive. The mice displayed cardiac hyperplasia, myocardial degeneration with ventricular septal defects and semilunar heart valve malformation and fibrosis. The death of the CXCR7 $^{-/-}$ mice 1 week after birth was associated with the lack of expression of this receptor in vascular endothelial cells of the lungs and heart, in cardiomyocytes, cerebral cortex and bone cells. The data gathered revealed an important role for CXCR7 in cardiovascular biology [468-470].

Li et al., studied the role of CXCR7 concerning inflammation and lipidemia in atherosclerosis and vascular remodelling. Interestingly, these authors showed that CXCR7 was highly expressed in adipose and arterial tissues, the heart and, to a lesser extent in bone marrow cells and platelets. In addition, activation of CXCR7 was observed in endothelial and adventitial cells of the aorta. Conditional deletion of CXCR7 in ApoE $^{-/-}$ mice was carried out and the wire injury of the carotid artery was performed. CXCR7 deficiency exacerbated neointimal hyperplasia, with an increase in the number of macrophages and in the level of cholesterol in the serum. Injection of the CXCR7 synthetic antagonist CCX771 ameliorated the neointimal lesion by reducing the neointimal area, the serum concentration of cholesterol and the consequent macrophage accumulation. Although the

authors did not have any indication regarding the role of CXCR7 on progenitor cell recruitment and SMC accumulation, they did suggest that in CXCR7^{-/-}-APoE^{-/-} mice the hyperlipidemia could have promoted the transformation of the SMCs into foam cells. Thus, the authors concluded that CXCR7 activation could have a beneficial effect in atherosclerosis due to the improvement of the hyperlipidemia-induced monocytosis mechanism [166]. Likewise, Ma et al., also showed that macrophages present in the aortic atheroma of ApoE^{-/-} mice expressed CXCR7. Furthermore, activation of the receptor increased the phagocytic activity of the macrophages, hence contributing to atherogenesis [352].

Hao et al., used a different approach to study the role of CXCR7 in vascular biology. In their work, CXCR7 deletion was restricted to the endothelium, as a CXCR7^{fl/fl}-Cdh5-CreERT2⁺ mouse model was used. Analysis of CXCR7 expression revealed that it was upregulated in endothelial cells of the neointima following artery injury. Conditional deletion of endothelial CXCR7 increased the neointimal area. Conversely, cytokine-induced upregulation of CXCR7 promoted endothelial regeneration after endothelial denudation injury [471]. Zhang et al., proposed that treatments enabling CXCR7 upregulation could represent a potential therapy for endothelial repair in patients suffering with hypertension [472]. Dai et al., showed that, together with CXCR4, the receptor CXCR7 was also essential to stimulate the transendothelial migration of the endothelial progenitor cells and the tube formation induced by Sdf-1 α [473]. The suggested angiogenic property of CXCR7 is further supported by many other reports, especially related to the tumour vasculature [357, 359, 472-480].

This leads us to speculate that Dkk3-triggered activation of CXCR7 and consequent induction of Sca-1⁺ APCs migration and potential differentiation into SMCs could result in a protective role against atherosclerosis. This assumption was based on the preliminary results obtained from two studies developed by our collaborators (Unpublished data).

In one study, Dkk3 was loaded in nano-structured collagen fibres constituent of vascular grafts in order to promote the regeneration of functional vascular smooth muscle cells. The dkk3-loaded vascular grafts were transplanted in abdominal aortas of rats and Dkk3 was progressively released upon collagen fibre degradation. The immuno-staining analysis revealed that the neotissue formation and the endothelization was similar between both Dkk3 and control (absence of Dkk3 in the nano-structured collagen fibers) groups at two and four weeks of grafting. However, the secretion of collagen and elastin was increased in response to Dkk3 and the difference in the extracellular matrix (ECM) between both groups was more pronounced after 4 weeks. Additionally, Dkk3-loaded vessels exhibited a higher number of Sca-1⁺ vascular progenitor cells infiltrated in the vascular grafts. At two weeks of grafting, the neotissue formed in the Dkk3 group showed a greater number of cells co-stained for Sca-1⁺ and α -SMA markers. After four weeks of regeneration, the Sca-1⁺ marker was hardly observed and the SMC marker persisted, which indicated that the Sca-1⁺ progenitor cells had differentiated into SMCs (Figure 4.2.2.A).

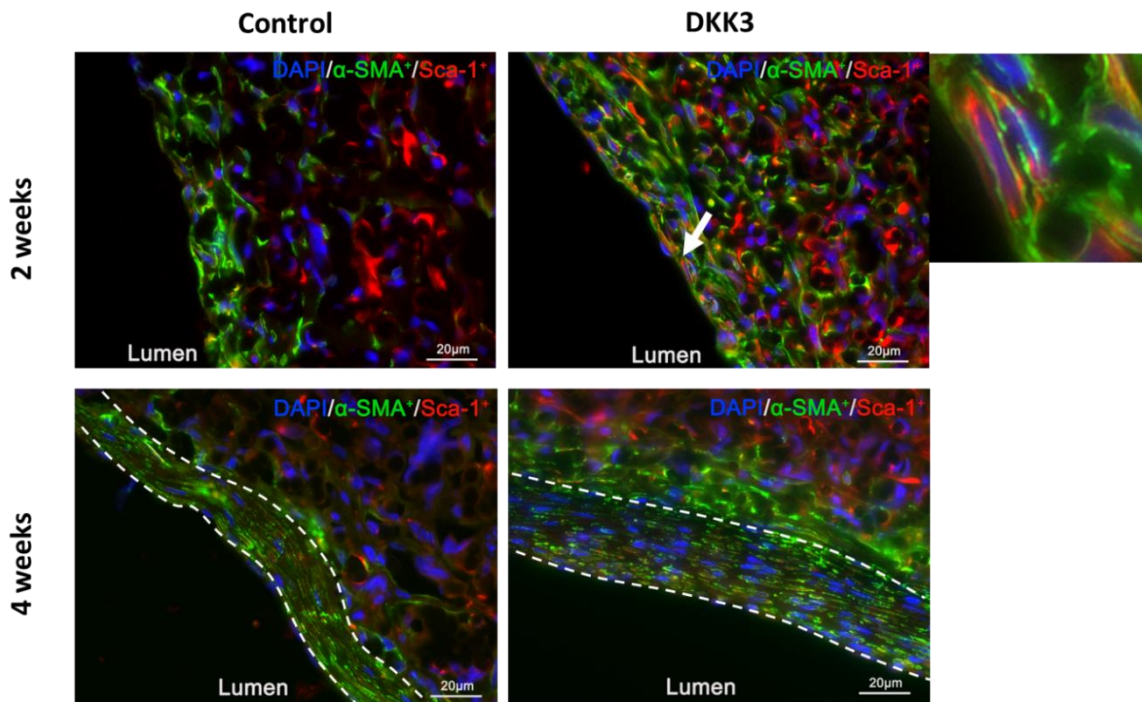


Figure 4.2.2.A: Sca-1⁺ expression on artificial vessel model. Dkk3 was loaded in nano-structured collagen fibres constituent of vascular grafts. After 2 weeks of grafting, Dkk3-loaded grafts exhibited a higher number of Sca-1⁺ cell (red) in the neotissue, compared to grafts lacking Dkk3 loading. Sca-1 marker and α -SMA co-expressing cells were also present in the Dkk3-loaded grafts. After 4 weeks, all Sca-1⁺ cells seem to have differentiated into SMCs.

These results implied that local delivery of Dkk3 recruits Sca-1⁺ vascular progenitor cells and promotes their differentiation into mature SMCs, with an increase in the ECM production. Akhtar et al., demonstrated that injection of Sdf-1 α induced the motility of SMCs, increased the thickness of the fibrous cap and the collagen content in the neointimal lesion and thus promoted the stabilization of the atherosclerotic plaque [465]. Dkk3 could thus potentially also have a protective role in atherogenesis by promoting plaque stabilization. Additional experiments are required to further support this hypothesis.

Another work from our collaborators included the Bruneck study, which consisted of a prospective study on atherosclerosis based on human samples. Dkk3 concentration was measured and, according to the level of Dkk3 in the sera, the population was divided into three groups: Group 1 (Dkk3 < 65 ng/mL); Group 2 (Dkk3 65-74 ng/mL); Group 3 (Dkk3 > 75 ng/mL). The results obtained revealed that the Dkk3 plasma level inversely correlated with intimal thickening of the carotid artery ($p=0.008$) and the incidence of atherosclerosis and stenosis (Figure 4.2.2B).

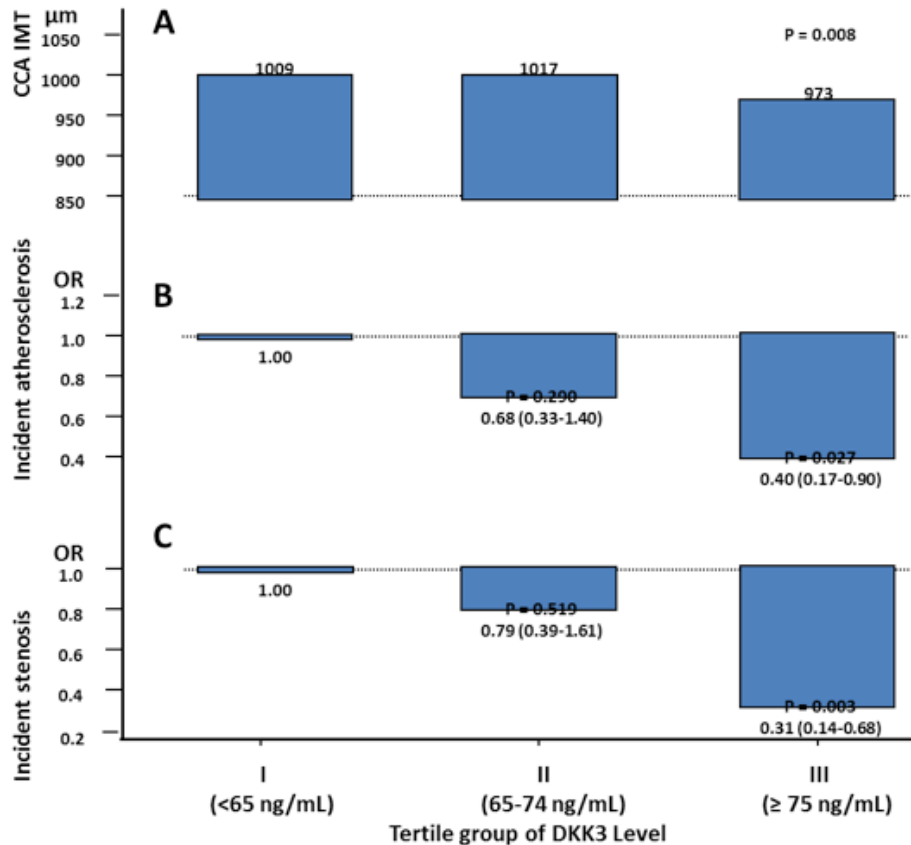


Figure 4.2.2.B: Relation between Dkk3 plasmatic concentration and the risk of atherogenesis. In the Bruneck study, Dkk3 concentration was measured in human plasma samples and according to the values obtained, the samples were divided into three groups: Group I <65 ng/mL; Group II 65-74 ng/mL; group III ≥75 ng/mL). Intimal thickening of the common carotid artery (CCA IMT), incidence of atherosclerosis and incidence of stenosis were inversely correlated with Dkk3 plasma level.

Previous work from our group (unpublished data) correlates the Bruneck study. Immunostaining was performed in frozen sections of the aortic roots of Wild type and ApoE^{-/-} mice. The latter group displayed a higher expression of Dkk3 compared to the Wild type group. Furthermore, Dkk3 expression in ApoE^{-/-} co-localised with the expression of SMC cell markers (α-SMA). Analysis of Dkk3 concentration in ApoE^{-/-} mice sera showed that the Dkk3 level reduced with the aging of the mice (6 to 12 months of age; p<0.01 by unpaired Student's T-test).

Dkk3 blood level is thus inversely correlated with cardiovascular pathologies, hence suggesting a protective role for Dkk3. Moreover, the ability of Dkk3 to induce the migration of the Sca-1+ vascular progenitor cells to the neointima and their further differentiation into mature SMCs, suggests a possible function in atheroma plaque stabilization. In fact, Karamariti et al., and Wang et al., proved that Dkk3 is involved in the differentiation process of stem cells into SMCs [243, 244].

Interestingly, Cheng et al., published a study revealing that Dkk3 ablation reduced the pathogenesis of atherosclerosis in ApoE^{-/-} mice. The authors first detected an increase in the Dkk3 expression in

ApoE^{-/-} mice aortas, which is consistent with what our group observed. But, they concluded that this strong expression of Dkk3 was localized in the macrophages present in the atherosclerotic plaques of patients with coronary heart disease and of hyperlipidemic mice and, that the SMCs exhibited only a modest expression of Dkk3. They also observed that Dkk3^{-/-}-ApoE^{-/-} mice displayed a decrease in the atherosclerotic lesion of their aorta, with a reduction of the necrotic core size, increase in the number of SMCs, greater secretion of collagen, reduction of macrophages recruitment and decrease in the lipidic content, all contributing to the plaque stability [222]. Although this report seems to apparently contradict our assumption of a protective role for Dkk3, three major points need to be addressed. Firstly, the study only focused on the role of Dkk3 in the inflammatory and lipidemic aspect of the atherosclerosis. Secondly, the differences reported between the Dkk3^{-/-}-ApoE^{-/-} mice and the ApoE^{-/-} littermates, regarding the lesions, were mainly observed when a high fat diet (HFD) was applied and no differences were found between both groups fed with a normal chow. Thirdly, it was surprising to observe that in ApoE^{-/-} mice aorta the α -SMA staining was barely detectable. Furthermore, the quantification of the SMC content in ApoE^{-/-} mice and Dkk3^{-/-}-ApoE^{-/-} mice was solely based on this SMC marker. Our data depict contrasting results regarding the expression of Dkk3 in vascular SMCs of ApoE^{-/-} mice (unpublished data). Moreover, studies have demonstrated an increased expression of Dkk3 in differentiated mature SMCs [243, 244]. We therefore believe that more analysis of these mouse models should be completed in respect to the function of Dkk3 in atherogenesis and inherent SMC hyperplasia and endothelial barrier dysfunction. Furthermore, the study of the function of Dkk3 in other vascular disease animal models that involve hyperplasia and neointima formation, such as wire injury or vein grafting, would provide more insight and help to clarify the role of Dkk3 in vascular biology. Finally, we have to consider that the function of Dkk3 could be context-specific, as it was shown in the field of cancer that this glycoprotein can either be a tumour suppressor [481-483] or a cancer growth promoter [232, 233, 484], depending on the cancer cell type involved.

The use of Sca-1+ lineage tracing strategy coupled with mouse models of cardiovascular diseases, to study the function of Dkk3 would provide crucial information and enable to elucidate on important strategies to develop novel therapies in cardiovascular diseases. In addition, these models could be used to investigate in vivo the role of CXCR7 and identify if it is a valuable potential target for drug-targeted therapy.

4.2.3 Signalling pathways involved in the Dkk3-driven Sca-1+ vascular progenitor cell migration mechanism

The clarification of the signalling pathways governing the cell response to stimulus is crucial for the understanding of physiological and pathological processes and for the design of novel therapies.

After determining that Dkk3 played a role in vascular biology, by inducing the migration of Sca-1+ APCs, we focused on uncovering signalling pathways downstream of CXCR7 in Dkk3-mediated migration.

Cell migration comprises many signalling cascades vastly described in the literature. The MAPK family is one of them and therefore, we first investigated whether it played a role in Sca-1+ APCs migration induced by Dkk3.

The extracellular signal-regulated kinases (ERK) are a sub-family of the MAPK family which are activated by cytokines and growth factors. ERK1 and ERK2 proteins are substrates of MAPK kinases MEK1 and MEK2 and they can phosphorylate cytoskeleton-related proteins and migration-related transcription factors [186, 188, 485]. Treatment of the Sca-1+ cells with Dkk3 induced the activation of MEK1/2 which in turn led to the phosphorylation of ERK1/2 (Figure 3.5.1). Interestingly, the same result was observed upon treatment of the Sca-1+ progenitor cells with Sdf-1 α (Figure 3.5.2). To confirm whether the activation of this signalling pathway regulated the Dkk3-mediated Sca-1+ progenitor cell migration, we performed a transwell migration assay with the MEK/ERK activation inhibitor PD 98059. Sca-1+ cell migration in response to Dkk3 was suppressed upon inhibition of the MEK/ERK phosphorylation. Likewise, Sdf-1 α driven migration was also decreased, thus implying that both Dkk3 and Sdf-1 α share the same signalling pathway in Sca-1+ progenitor cell migration.

The involvement of ERK signalling in cell migration induced by Dkk3 has not been shown thus far. Nevertheless, it is known that the ERK signalling pathway is involved in the regulation of other functions of Dkk3. Wang et al., concluded that, in the course of differentiation of embryonic stem cells into SMCs, the induction of the transcription factor ATF6 and activation of myocardin transcription upon Dkk3 treatment, required inhibition of ERK 1/2 [243]. Similarly, Gu et al., found that overexpression of Dkk3 in pancreatic cancer cells led to the downregulation of ERK phosphorylation after 48 and 72 hours and consequent suppression of pancreatic cell growth [482]. XY Wang et al., showed that the proliferation of mammary epithelial cells is associated with a decrease in Dkk3 secretion, which is related to increased ERK phosphorylation [486]. Interestingly, Xia et al., demonstrated that Dkk3 suppressed the CD133 induced-antitumor activity in NK cells by inhibiting ERK pathway [487]. Although these reports indicate that Dkk3 could inhibit the ERK pathway, they all refer to long-term processes, longer than 24 hours, such as cell differentiation and cell proliferation. In our study, Sca-1+ cell migration was assessed within 16 hours and ERK phosphorylation induction was detected at time points as early as 3-5 minutes until 60 minutes of Dkk3 stimulation.

ERK activation in cell migration has been demonstrated in several studies, which supports our findings. For instance, Sdf-1 α -mediated ERK phosphorylation and consequent induction of cell migration was found in aortic SMCs [294], bone marrow-derived megakaryocytes [488], cardiac stem cells [489], human umbilical cord blood mesenchymal stem cells [490], bone marrow lymphoma cells [491], multiple myeloma cells [492], neural progenitor cells [158], melanocytes [493], amongst other cell types.

PI3K/AKT signalling pathway has also been implicated in cell chemotaxis. For example, Sdf-1 α promoted cell migration via AKT phosphorylation in endothelial progenitor cells [494], bone marrow-derived mesenchymal stem cells [495], human umbilical cord blood mesenchymal stem cells [496], cardiac stem/progenitor cells [489], adipose-derived stem cells [497], neural-like cells [498] and breast cancer cells [499].

We verified the increase in AKT phosphorylation in the Sca-1 $^{+}$ APCs, in response to Dkk3 and Sdf-1 α stimulation (Figure 3.5.3 and 3.5.4). Furthermore, inhibition of AKT phosphorylation with either AKT specific inhibitor or with PI3K inhibitor LY29004 abrogated the Dkk3- and Sdf-1 α -driven Sca-1 $^{+}$ cell migration.

AKT activation also regulates cell proliferation [409, 500-502] and survival [503-505], and we therefore assessed if Dkk3 was regulating these two processes in Sca-1 $^{+}$ cells. The BrdU proliferation assay showed that the Sca-1 $^{+}$ cell proliferation induced by either Dkk3 or Sdf-1 α only occurs at 48 hours of stimulation, with no difference in the proliferation rate between the control and the treated groups at 16 and 24 hours of treatment (Figure 3.2.5). AKT phosphorylation was observed at early time points (0-60 minutes) and the migration assays were carried out overnight, so we assumed that the rapid AKT activation modulated primarily Sca-1 $^{+}$ cell migration mechanism, rather than the proliferation. Nevertheless, the increase in the number of the Sca-1 $^{+}$ vascular progenitor cells observed in the cell outgrowth from the aortic rings (*ex vivo*) and in the neotissue of the vascular grafts (*in vivo*) could be the result of both cell migration and cell proliferation stimulated by Dkk3 treatment.

To assess whether the AKT phosphorylation-triggered by Dkk3 treatment was involved in the progenitor cell survival, we quantified the number of cells stained with trypan blue after incubation with Dkk3 and AKT inhibitor for 3 hours. The results confirmed that Dkk3 did not promote either cell death or cell survival, as no difference was found in the number of dead cells in both treated and untreated groups. Upon incubation with AKT inhibitor, the same level of cell death was detected in all the conditions (Figure 3.5.3C), which showed that neither Dkk3 nor the inhibitor had any effect on the Sca-1 $^{+}$ progenitor cell survival rate at the time points used to analyse the Sca-1 $^{+}$ progenitor cell migration mechanism.

Few studies have linked AKT phosphorylation and Dkk3. Kim et al., showed that overexpression of Dkk3 in ovarian carcinoma cells leads to the suppression of β 2M-mediated AKT phosphorylation and consequent tumour growth [239]. Zenzmaier et al, demonstrated that Dkk3 knockdown in prostatic

stromal cells attenuates AKT phosphorylation, thus reducing the fibroblast proliferation level and the myofibroblast differentiation [506]. Xu et al., similarly detected that AKT phosphorylation was downregulated in gastric carcinoma cells overexpressing Dkk3, leading to a decrease in their proliferation rate [507]. Finally, the inhibitory effect of Dkk3 in osteosarcoma progression via AKT activation suppression was also proven by Lin et al., [508]. Here, we provide the first evidence of the implication of the PI3K/AKT pathway in a cell migration mechanism promoted by Dkk3.

The Rho GTPases family is one of the most well studied families of signalling molecules in cell migration. It is known to regulate the cell cytoskeleton and to promote cell movement, by switching from an inactive state (GDP bound) to an active state (GTP bound). They enable the communication between the outside stimulus, such as chemokine binding to its receptor, and the cytoskeleton dynamics [509-511]. It is thus not surprising to find numerous amounts of studies on the activation of Rho GTPases in response to Sdf-1 α for instance [512-516].

We explored whether members of the Rho GTPases family participated in the mechanism of the Sca-1+ APCs migration induced by Dkk3.

In the literature, cell migration induced by a Dkk protein has been associated with the Wnt signalling pathway. The role of Dkks is mainly known in the cancer field where it is related to the regulation of cell migration, invasion, proliferation, amongst other cell functions, and it is dependent on the tumour cell context. Unlike the other members of the Dkk family, which are Wnt signalling antagonists, Dkk3 can either be an agonist [292, 517, 518] or inhibitor [229, 508, 519]. The Wnt signalling comprises the canonical Wnt/ β -catenin pathway and the non-canonical (β -catenin independent) pathway. The Rho GTPases signalling cascades involved in cell migration mechanism are known to belong to the non-canonical pathway, which branches into further two pathways: The Planar Cell Polarity (PCP) pathway and the Wnt/Ca²⁺ pathway. Actin cytoskeleton regulation is a feature of the PCP pathway, which includes Rac/Rho activation [211, 312, 520, 521].

Rac1 is a member of the Rac subfamily belonging to the Rho GTPases family, which is responsible for the formation of lamellipodial protrusions in cells. Tsujimura et al., demonstrated that Dkk3 knockdown inactivated Rac1 in bladder cancer cells [234]. Veeck et al., suggested that the downregulation of Dkk3 expression in malignant tumours, such as breast cancer, disrupts the PCP pathway of the non-canonical Wnt signalling, which encompasses Rho/Rac recruitment. As a result, the network of cell migration and polarity are altered and the tumour aggressiveness is enhanced [522]. On the other hand, Katase et al., showed that Dkk3 knockdown in oral squamous cell carcinoma-derived cells does not affect the expression of Rac1. However, only Rac1 expression was analysed and not its activation level [233]. Our data revealed that the treatment of Sca-1+ progenitor cells with Dkk3 induced the activation of Rac1, at 10-15 minutes of stimulation, just as Sdf-1 α treatment did (Figure 3.5.5.1). This activation was suppressed upon treatment with the Rac1 activation inhibitor NSC 23766.

Next, we investigated whether the observed Rac1 activation in response to Dkk3 was upstream or downstream of the previous signalling pathways discussed.

Rac1 activation in response to MEK/ERK signalling pathway activation has been demonstrated in the literature [523]. Conversely, the requirement of Rac1 for MEK/ERK signalling pathway activation has been also reported [158, 524]. We used the MEK/ERK phosphorylation inhibitor PD 98059 to verify if it affected Rac1 activation. Remarkably, Rac1 activation triggered by Dkk3 treatment was suppressed at 10 and 15 minutes of stimulation upon PD98059 treatment (Figure 3.5.5.1E), suggesting that ERK activation is upstream of Rac1 activation. However, Rac1 inhibitor NSC23766 also repressed the ERK phosphorylation-driven by Dkk3 at 10 and 15 minutes of stimulation (Figure 3.5.5.2D). We thus inferred that ERK and Rac1 activation are both involved in the Dkk3-mediated Sca-1+ progenitor cell migration and that they mutually regulate each other in a feedback loop manner. Interestingly, treatment of the Sca-1+ progenitor cells with the PI3K inhibitor LY29004 did not repress Rac1 activation induced by Dkk3 (Figure 3.5.5.1F), which indicates that the PI3K/AKT signalling pathway is either downstream or independent of Rac1 activation.

RhoA is another important member of the Rho GTPases family. It regulates stress fiber formation and cell contraction, reflecting in cell body contractility and tail retraction. One of the effectors of RhoA is Rho-associated protein kinase (ROCK), which can either directly phosphorylate MLC at Ser19 or suppress the activity of MLC phosphatase, thus resulting in an increase in p-MLC. p-MLC is important for maintenance of stress fibers and focal adhesions. Rho kinase can also induce LIM Kinase activation which results in cofilin phosphorylation (inhibition). Cofilin is known to depolymerise actin filaments and hence severe actin barbed ends, necessary for actin filaments turnover [174, 525, 526].

We first investigated the phosphorylation levels of MLC and cofilin in response to Dkk3 treatment. The western blot analysis revealed that MLC phosphorylation was increased, similarly to the trend observed upon Sdf-1 α stimulation, but no change was observed in the cofilin phosphorylation level (Figure 3.5.5.2B). To understand if RhoA GTPase was the driver of MLC activation, we assessed the RhoA activation degree in Sca-1+ progenitor cells stimulated with either Dkk3 or Sdf-1 α . Both proteins triggered RhoA activation, with significant increase at 13-30 minutes of treatment (Figure 3.5.5.2C). Furthermore, RhoA activation was abolished upon Rhosin treatment, which is a RhoA GTPase activation site inhibitor and consequently, MLC phosphorylation induced by Dkk3 treatment was abolished (Figure 3.5.5.2F). Next, we questioned whether the Rho associated protein kinases (ROCKs) intervene in this pathway and therefore, we performed the wound healing assay with the inhibitor Y27632. The ROCK inhibitor not only reduced the Sca-1+ progenitor cell migration driven by Dkk3 but it also reduced the phosphorylation level of MLC (Figure 3.5.5.2H). In view of these finding, we concluded that Dkk3 induces RhoA activation, which in turn leads either to ROCK activation or direct MLC phosphorylation.

Thus far, only one study links RhoA to Dkk3. Katase et al., showed that RhoA expression was not changed in oral squamous cell carcinoma-derived cells upon Dkk3 knockdown. However, only RhoA expression was assessed, but not its activation level [233]. Different studies were published showing the participation of RhoA in Dkk1-triggered signalling pathways. Krause et al., showed that Dkk1 enhanced the osteosarcoma cell resistance to stress through activation of RhoA and JNK, which are comprised in the non-canonical Wnt signalling pathway [527]. Rachner et al., detected that inhibition of Cdc42 and Rho resulted in suppression of DKK1 expression and protein secretion in breast cancer cells *in vitro* [528]. Shusterman et al., demonstrated that inhibition of the Wnt pathway with Dkk1 treatment led to a decrease in RhoA and ROCK activity in ameloblast-lineage cells [529]. We provide evidence on the involvement of RhoA activation in the Dkk3-mediated Sca-1+ APCs migration mechanism. Several studies had already described the activation of RhoA in response to chemokine stimulation to drive cell migration [530-533].

To understand whether the RhoA signalling cascade is regulated by any of the other signalling pathways previously described, we carried out the RhoA activation assay with the MEK/ERK inhibitor PD98059 and the PI3K/AKT inhibitor LY29004. In our hands, none of the inhibitors affected the Dkk3-driven RhoA activation in the Sca-1+ APCs (Figure 3.5.5.2 I and J), hence revealing that these signalling pathways are either downstream or independent of the RhoA signalling cascade.

Considering the data presented, one crucial question remained: Is Dkk3 activating all the above signalling pathways through the Wnt signalling pathway or are these pathways regulated by another mechanism triggered by the binding of Dkk3 to its receptor?

All the Dkk proteins, except for Dkk3, are known to be antagonist of the Wnt signalling pathway [204, 433, 435]. As mentioned before, Dkk3 protein can either be an agonist or an inhibitor of the Wnt pathway, depending on the physio-pathological context.

We performed a transwell migration assay with the Wnt/ β -catenin antagonist FH535 on the Sca-1+ APCs. Notably, addition of the antagonist by itself resulted in an increase of the Sca-1+ cell migration, with a migration rate comparable to the one obtained for the Dkk3 treatment. We could then speculate that Dkk3 could act as an antagonist of the Wnt/ β -catenin signalling pathway. However, the Dkk3-promoted Sca-1+ cell migration level was not affected upon FH535 treatment and no cumulative antagonism was observed (Figure 3.5.7.1). We thus assumed that the canonical Wnt/ β -catenin pathway was not involved in the Sca-1+ vascular progenitor cell migration mechanism.

The Dishevelled (Dvl) protein is a critical component of both the canonical and non-canonical Wnt signaling pathways, as its PDZ domain interacts with the Frizzled receptor of Wnt. In the canonical pathway Wnt binds to the Frizzled and LRP5/6 receptor complex which leads to β -catenin stabilization and subsequent translocation to the nucleus for gene transcription activation. In the non-canonical pathway, Wnt signalling is transduced through Frizzled,

independent of LPR5/6, where Dvl activates the Rho GTPases thus modulating the cytoskeleton rearrangement (PCP pathway) or where Dvl leads to release of intracellular calcium, involved in cell motility (Wnt-Ca²⁺ pathway) [211, 312, 520, 534].

Inhibition of the Dishevelled protein, with the Dvl-PDZ inhibitor which targets the PDZ domain of Dvl, did not repress the Dkk3-driven migration of the cells. No difference was found between the Dkk3 treated group and the Inhibitor treated groups (Figure 3.5.7.2). We thus obtained further evidence that the canonical Wnt signalling is not involved in the Dkk3-driven Sca-1⁺ progenitor cell migration. Likewise, the non-canonical Wnt pathway is also potentially not implicated in the mechanism driving Dkk3 induced migration.

Our data proves that Dkk3-induced Sca-1⁺ progenitor cell migration mechanism involves the activation of the MEK/ERK and PI3K/AKT signalling pathways and implicates activation of Rho GTPases, such as Rac1 and RhoA, with consequent cytoskeleton rearrangement for cell motility promotion. Remarkably, we provide the first evidence that Wnt signalling pathways classically associated with Dkk proteins do not have a role in the migration mechanism herein described.

With the identification of Dkk3 receptor and the dissection of the migration mechanism of the Sca-1⁺ vascular progenitor cells stimulated by Dkk3, we next investigated if the binding of Dkk3 to CXCR7 was activating the identified downstream signalling pathways involved in Sca-1⁺ cell migration.

4.2.4 CXCR7 is upstream of the Sca-1⁺ vascular progenitor cell migration mechanism stimulated by Dkk3

To assess whether CXCR7 is upstream of the ERK activation upon Dkk3 stimulation, we performed CXCR7 SiRNA transfection in the Sca-1⁺ vascular progenitor cells. ERK phosphorylation level was suppressed upon CXCR7 downregulation at 10 and 15 minutes of Dkk3 stimulation (Figure 3.6.1A), which proved that CXCR7 activation through Dkk3 binding is responsible for ERK activation.

Several studies support the CXCR7 regulation of the ERK signalling pathway. Grymula et al., showed that Sdf-1 α and another ligand of CXCR7, ITAC, both induced ERK phosphorylation and consequent migration of different rhabdomyosarcoma cell lines [458]. Tarnowski et al., concluded that ITAC-induced activation of CXCR7 in human hematopoietic cell lines leads to ERK phosphorylation and enhanced cell adhesion and slightly cell migration [356]. Additionally, Inaguma et al., demonstrated that CXCR7 inhibition blocked the Sdf-1 α -induced ERK phosphorylation and breast cancer cell migration [446]. Similarly, Chen et al., revealed that Sdf-1 α driven migration of neural progenitor cells is mediated by CXCR7, independently of CXCR4 and involves ERK phosphorylation [158]. Interestingly, Kumar et al., also observed T cell chemotaxis induced by ERK phosphorylation triggered by Sdf-1 α binding to CXCR7, upon CXCR4 blocking

[535]. Odemis et al., proved that CXCR7 activation by Sdf-1 α promotes ERK phosphorylation in astrocytes and Schwann cells [536].

Next, we analysed the AKT phosphorylation level in CXCR7 downregulated Sca-1+ progenitor cells. The activation of AKT in response to Dkk3 treatment was abrogated with CXCR7 knockdown (Figure 3.6.2.A). AKT regulation by CXCR7 has been reported elsewhere. Dai et al., demonstrated that upregulation of CXCR7 rescues the angiogenic function of endothelial progenitor cells of a diabetic mouse model and that inhibition of the PI3K/AKT signalling pathway prevents SDF-1/CXCR7-mediated angiogenic repair [474]. Chen et al., concluded that SDF-1/CXCR7/Akt pathway played an important role in cardiac stem cell migration [489]. Odemis et al., showed that SDF-1 α -driven activation of AKT remained fully inducible in astrocytes from CXCR4-deficient mice, but was abrogated in astrocytes transfected with CXCR7 siRNA [536]. Finally, Grymula et al., observed the chemotaxis of rhabdomyosarcoma cells in response to Sdf-1 α and ITAC binding to CXCR7, via AKT signalling pathway activation [458].

The regulation of the Rho GTPases family by CXCR7 activation upon Dkk3 treatment was also analysed. Strikingly, Rac1 and RhoA activation was repressed in Sca-1+ progenitor cells transfected with CXCR7 siRNA and it remained abrogated with Dkk3 stimulation, thus confirming that CXCR7 modulates Rac1 and RhoA activation in response to Dkk3 treatment (Figure 3.6.3A and Figure 3.6.4A). Reports exist showing the functional role of CXCR7 on the modulation of Rho GTPases. For instance, Chen et al., demonstrated that Rac1 activation via CXCR7/Sdf-1 α is required for neural progenitor cell migration [158]. Guo et al., revealed that Rho/ROCK pathway is involved in the migration and invasion of pancreatic cancer cells via CXCR7 activation by Sdf-1 α [537].

Collectively, the data obtained proved that the binding of Dkk3 to CXCR7 is upstream of the signalling pathways involved in the migration mechanism of the Sca-1+ vascular progenitor cells. Figure 4.6 summarizes schematically the Sca-1+ APC migration mechanism induced by Dkk3.

4.3 The Yeast Two Hybrid system reveals that Dkk3 interacts with Integrin α 5 and Integrin β 1

In an attempt to investigate which proteins interact with Dkk3, potentially including receptors, we used a methodology which encompassed the screening of a mouse genome library. The Yeast Two Hybrid System (Y2H) consists of the identification of protein-protein interactions resultant of the reconstitution of the transcription factor GAL4 in yeast cells.

Kim et al., used the yeast two-hybrid system to characterize Dkk3-dependent signalling cascades and they found that Dkk3 binds to β 2M [538]. Ochiai et al., by performing the Y2H and pull-down assays, determined that the N-terminal regions of both Dkk3 and SGTA (small glutamine-rich tetratricopeptide repeat containing protein α) mediated their interaction [539]. The Y2H system has been widely used to identify protein-protein interactions, including the work of Rocchi et al., which analysed the interaction between SH2-containing protein tyrosine phosphatase 2 (SHP-2) with the receptors IR (insulin receptor) and IRS-1 (insulin-like growth factor-I receptor) [540]. Oakley et al., through Y2H analysis, identified MyoD family inhibitor domain-containing protein (MDFIC) as a binding partner for glucocorticoid receptor (GR) [541].

We fused GAL4 DNA binding domain (GAL4 DNA-BD) was fused to mouse Dkk3 (bait protein), whereas as the ready-made GAL4 activation domain (GAL4 AD) fused to the mouse genome library cDNA inserts (prey proteins) was provided by the supplier. After mating the two transformed haploid yeast strains and spreading the resulting diploid cells on increasing stringent and selective agar medium plates, we analysed the colonies obtained.

4.3.1 Yeast Two Hybrid control tests

As it was very important to first validate and understand the functioning of the Y2H system, we performed the recommended control experiments.

As expected, DDO/X/A agar plates for the positive control exhibited blue colonies due to the known interaction of murine p53 with the SV40 large T-antigen, which resulted in the activation of the reporter genes, thus conferring the cells resistance to the drug Aureobasidin A, present in the agar medium, and enabling the expression of α -galactosidase that hydrolyses X- α -Gal substrate, which renders the blue colour to the colonies (Table 3.8.1.1.B).

On the contrary, in the negative control, because Lamin and T-antigen do not interact with each other, the diploid yeast cell was not able to grow on the DDO/X/A agar plates, as the reporter genes could not be transcribed (Table 3.8.1.1.B).

Next, we tested the potential of Dkk3 to auto-activate any of the reporter genes in the Y2HGold yeast cell in the absence of any prey protein. If positive results were obtained, the Y2H system could not be used anymore, because it relies on the activation of these reporter genes upon interaction of Dkk3 with another protein

The data obtained revealed that Dkk3 did not auto-activate the reporter genes, as no colonies were present on the SD/-Trp/X/A, DDO/X/A and QDO selective plates, but only on SD/-Trp agar plates, in which only tryptophan is missing, an amino acid produced by the haploid Y2HGold cell since it was transformed with Dkk3-GAL 4 DNA-BD plasmid containing the gene encoding for Tryptophan (Table 3.8.1.2).

Finally, we wished to verify whether Dkk3-GAL4 DNA-BD would interact with the empty vector encoding for GAL4 AD, that is, in the absence of library prey protein, upon mating of the respective transformed haploid cells, which would reveal the likelihood of false positive results. DDO/X/A and QDO/X/A agar plates did not exhibit colonies, thus showing that the possibility of observing false positives resultant from Dkk3 interaction with GAL4 AD in the absence of any library prey protein would be small.

We thus validated the methodology of the Y2H system developed for the first time in our laboratory and proceeded with the screening of the mouse library with Dkk3.

4.3.2 Screening of the Universal mouse normalized Library

The most stringent plate, QDO/X/A, displayed distinct blue colonies, indicating interaction between Dkk3 and some of the mouse library prey proteins (Table 3.8.1.3A). Following plasmid rescue and sequencing, we identified extracellular matrix and membrane-bound proteins which interacted with Dkk3 (Table 3.8.1.3.B).

Remarkably, four receptors were recognised: Integrin $\beta 1$ (two hits), Robo1 (one hit), Integrin $\alpha 5$ (one hit) and GPR116 (1 hit). Amongst the extracellular matrix components, Fibulin 5 reproducibly activated the reporters two times, as two colonies were positive for this protein.

Strikingly, studies have revealed that Integrin $\alpha 5$ (ITG $\alpha 5$) and Integrin $\beta 1$ (ITG $\beta 1$), as a receptor complex, bind to Fibulin 5. Lomas et al., reported that Fibulin 5 binds to human SMCs through $\alpha 5\beta 1$ and $\alpha 4\beta 1$ integrins [332]. Nakamura et al., revealed that the N-terminal of fibulin-5 binds to integrins $\alpha V\beta 3$, $\alpha V\beta 5$ and $\alpha 9\beta 1$, which are known to be expressed by vascular cells [542]. Williamson et al., concluded that HUVEC attachment to fibulin 5 and fibrillin-1 is mediated by integrins $\beta 1$, αv , $\alpha 3$, $\alpha 4$ and $\alpha 5$ [543].

Integrins are notably known for their role in cell migration [201, 203, 544]. Several studies have specifically demonstrated the important role of ITG $\alpha 5$ and ITG $\beta 1$ in regulating cell migration.

Marchetti et al., showed that the integrins $\alpha 5$ and $\beta 1$ are required for the control of cortical neuron cell migration during the development of mouse brain [545]. Veevers-Lowe et al., indicated that the migration of mesenchymal stem cells at sites of vascular remodelling is controlled by the crosstalk between Pdgfr- β and ITG $\alpha 5\beta 1$ [546]. Caswell et al., revealed that tumour cell invasion is enhanced by the Rab25-driven recycling of ITG $\alpha 5\beta 1$ [547]. The same author demonstrated in another study that the recycling of ITG $\alpha 5\beta 1$ and ITG $\alpha 5\beta 3$ regulates persistent cell migration by activating the RhoA signalling cascade [548]. Kabir-Salmani et al., concluded that the migration of extravillous trophoblast cells induced by IGF-I involves ITG $\alpha 5\beta 1$ activation [549].

Furthermore, ITG $\alpha 5$ and ITG $\beta 1$ are also greatly recognised for their function in vascular biology. Davenpeck et al., inferred that ITG $\alpha 5\beta 1$ has a role in SMC growth and in regulating coronary SMC phenotype [550]. Later, Xiao et al., showed that the differentiation of Sca-1+ vascular progenitor cells into SMCs involves collagen IV and integrins $\alpha 1$, $\alpha 5$ and $\beta 1$ [101]. Interestingly Wijelath et al., concluded that the differentiation of endothelial progenitor cells into mature endothelium is mediated by VEGF and fibronectin and that this process is regulated by ITG $\alpha 5\beta 1$ [551]. Cascone et al., revealed that the Ang-1/Tie2 axis cross-talks with ITG $\alpha 5\beta 1$ in angiogenesis, thus modulating endothelial cell motility [552]. Concerning a potential contribution in the progression of vascular diseases, Yurdagul et al., indicated that the inflammation in early stage of atherogenesis is regulated by the cross-talk between fibronectin and oxidized low-density lipoprotein, which in turn is mediated by ITG $\alpha 5\beta 1$ [553].

We therefore postulated that the Sca-1+ vascular progenitor cell migration could also be triggered by the binding of Dkk3 to ITG $\alpha 5\beta 1$. Our Y2H results obtained confirmed that the interactions identified were in fact positive interactions, as no colonies were detected on QDO/X/A agar plates when ITG $\alpha 5$ and ITG $\beta 1$ plasmids were co-transformed with the empty vector GAL4 DNA-BD (absence of the bait Dkk3 protein) (Table 3.8.1.4).

We had thus identified a genuine interaction between Dkk3 and ITG $\alpha 5$ and ITG $\beta 1$.

4.4 Dkk3 binds with high affinity to Integrin $\alpha 5$ and Integrin $\beta 1$

To understand if Dkk3 can bind to ITG $\alpha 5\beta 1$ and thus promote the Sca-1+ vascular progenitor cell migration, we first analysed the expression of these integrins on the Sca-1+ progenitor cells. mRNA and protein analysis demonstrated that ITG $\alpha 5$ expression on the Sca-1+ cells was between the level of expression on ECs and on SMCs, although with no significant difference amongst the three types of cells. On the other hand, ITG $\beta 1$ expression on Sca-1+ cells was significantly lower than on SMCs, but similar to its expression on ECs. We thus detected that both integrin receptors were present on Sca-1+ vascular progenitor cells (Figure 3.8.2).

Two assays were next performed to assess the binding of Dkk3 to ITG α 5 and ITG β 1: Co-Immunoprecipitation assay and Affinity binding analysis.

After immunoprecipitating ITG β 1 from Sca-1+ vascular progenitor cells, previously treated with Dkk3, we assessed whether this glycoprotein and the receptor ITG α 5 were bound to ITG β 1. The data obtained showed that both Dkk3 and ITG α 5 co-immunoprecipitated with ITG β 1, suggesting the formation of a complex ITG α 5 β 1-Dkk3 in Sca-1+ progenitor cells (Figure 3.8.3.A).

Subsequently, we followed the methodology described by Mao et al., [285, 286] to measure the binding affinity of Dkk3 to ITG α 5 and ITG β 1. Briefly, alkaline phosphatase (AP) was fused to the Dkk3, the serially diluted Dkk3-AP was added to the HEK 293T cells overexpressing ITG α 5 or ITG β 1 and the activity of the enzyme was measured by chemiluminescence, which provided the binding curves for each receptor (Figure 3.8.4).

Remarkably, the binding curves obtained for both ITG α 5 and ITG β 1 were characteristically hyperbolic and the dissociation constants obtained, $K_D=18.15$ (ITG β 1) and $K_D=14.85$ (ITG α 5), revealed that Dkk3 binds with high affinity to ITG α 5 and to ITG β 1 (Figure 3.8.4D and E). The K_D values calculated are in agreement with typical values for the high affinity of a ligand to its receptor (nanomolar range) [554-557].

We provided the first evidence of the binding of Dkk3 to ITG α 5 and ITG β 1 through different approaches. Nevertheless, to assess whether it had a role on the Sca-1+ progenitor cell migration mechanism, functional assays were required.

It is interesting to note that Fu et al., showed that in Zebrafish Dkk3a (in zebrafish two *dkk3* genes have been reported: *dkk3a* and *dkk3b*, where Dkk3a is expressed in neuronal structures of the head and whereas *dkk3b* is expressed in the endocrine cells of the pancreas and brachial arches) binds to ITG α 6b [558]. This finding supports our result regarding the binding of Dkk3 to integrins, α 5 and β 1. Additionally, although a different integrin was identified by Fu et al., we should consider that it was mentioned that Dkk3a is mainly expressed in the neural tissue of Zebrafish and furthermore, this species is far more distinct from the human species than the mouse species, which shares 84.31% of homology with the human Dkk3 gene, whereas the Dkk3a gene of Zebrafish shares only 37% of similarity [559].

Later, in 2015, Shimazu et al., attempted to associate Dkk3 protein's function and integrins. This work shows that the combination therapy comprising adenovirus-Dkk3 (Ad-Dkk3) and cRGD (integrin antagonist) treatments provides a significant increase in mice survival when compared to monotherapy with Ad-Dkk3, in malignant glioma, as the proliferative rate of the malignant glioma cells was significantly reduced [560]. cRGD is an antagonist of different integrins, such as α 3 β 1, α 8 β 1, α 5 β 3, α 5 β 1, α 5 β 5, α 5 β 6 and α 11 β 3, therefore it is not specific to one integrin receptor, thus having a wide spread effect [561]. In addition, as explained before, Dkk3 function is context-dependent, as it can either inhibit or promote cell migration, proliferation or survival according to

the existing cell type and microenvironment. The analysis of the effect of cRGD antagonist treatment on the Dkk3-driven Sca-1+ progenitor cell migration behaviour would give clues on the role of the integrins in this migration mechanism. Nevertheless, more specific integrin-related approaches would be required to complement the peptide inhibition studies in the assessment of the function of Dkk3 binding to ITG α 5 β 1 receptor in the Sca-1+ progenitor cell migration mechanism.

We reveal for the first time that ITG α 5 β 1 are high affinity binding receptors of Dkk3 and that this receptor-ligand interaction is potentially involved in the Sca-1+ vascular progenitor cell migration mechanism.

4.5 Integrin α 5 and Integrin β 1 are involved in the migration behaviour of Sca-1+ progenitor cells promoted by Dkk3

To elucidate on the function of the binding of Dkk3 to ITG α 5 and ITG β 1 on the Sca-1+ progenitor cells we downregulated the integrins by SiRNA transfection.

Notably, the data gathered demonstrated that the Dkk3-mediated Sca-1+ cell migration was repressed upon downregulation of ITG α 5, ITG β 1 and ITG α 5+ITG β 1, with significant difference against the group of cells transfected with Control SiRNA and stimulated with Dkk3 (Figure 3.8.5). We thus concluded that ITG α 5 and ITG β 1 are potentially implicated in the Dkk3-triggered Sca-1+ progenitor cell migration mechanism.

The well-established involvement of ITG α 5 β 1 in the migration mechanism of many different cell types supports our inference [328, 329, 545, 546, 548, 549, 562].

The dissection of the signalling pathways triggered by the binding of Dkk3 to ITG α 5 β 1 requires additional experiments, namely the verification of the activation/phosphorylation levels of the signalling cascades described in this work after downregulation of integrin receptors by SiRNA transfection. The probable abrogation of the Dkk3-activated signalling pathways would thus confirm the functional role of ITG α 5 and ITG β 1 on the Sca-1+ APCs migration.

The PI3K/AKT axis, the MAPK kinase signalling pathway and the Rho GTPases family have all been proved to be regulated by integrins in cell migration mechanisms [202, 203, 530, 546, 563, 564] and, as these were shown herein to be implicated in the Sca-1+ progenitor cell migration behaviour induced by Dkk3, we propose the below scheme displaying the signalling pathways possibly activated by the binding of Dkk3 to ITG α 5 β 1 in Sca-1+ vascular progenitor cells (Figure 4.6).

4.6 Schematic overview of Dkk3-mediated Sca-1+ APC migration mechanism

The signalling network implicated in the migration mechanism of Sca-1+ vascular progenitor cells in response to Dkk3 binding to CXCR7 and/or ITG α 5 β 1 is represented in the scheme below.

Dkk3 binds to CXCR7 and/or ITG α 5 β 1 and triggers the activation of a network of signalling pathways involved in the Sca-1+ vascular progenitor cell migration mechanism. Upon Dkk3 binding MEK1/2 is activated and it induces the phosphorylation of ERK1/2. ERK1/2 either activates Rac1 or directly modulates cytoskeleton rearrangement to promote cell migration. Rac1 activation also results from Dkk3 binding to CXCR7, which in turn directly regulates cell migration and/or stimulates ERK phosphorylation. Rac1 and ERK activation seem to work in a feedback manner controlling each other's activation level to regulate cell migration. Binding of Dkk3 to CXCR7 and/or ITG α 5 β 1 promotes AKT phosphorylation via PI3K, which leads to cytoskeleton rearrangement. PI3K/AKT signalling pathway does not control RhoA and Rac1 activation and hence it can either be a downstream pathway of the Rho GTPases signalling cascade or an independent signalling pathway. RhoA activation level is increased in response to Dkk3 binding, which leads to MLC phosphorylation either directly or via ROCK activation. MLC activation results in actomyosin contraction required for cell migration (Figure 4.6).

Because Dkk3 was shown to bind to both CXCR7 and ITG α 5 β 1 and, as reports exist demonstrating the interaction of integrins to other receptors to regulate cell function [565-567], it could be interesting to investigate whether CXCR7 interacts with ITG α 5 β 1 in Sca-1+ progenitor cell migration or, whether the activation of these receptors are independent processes and promoters of Sca-1+ cell migration.

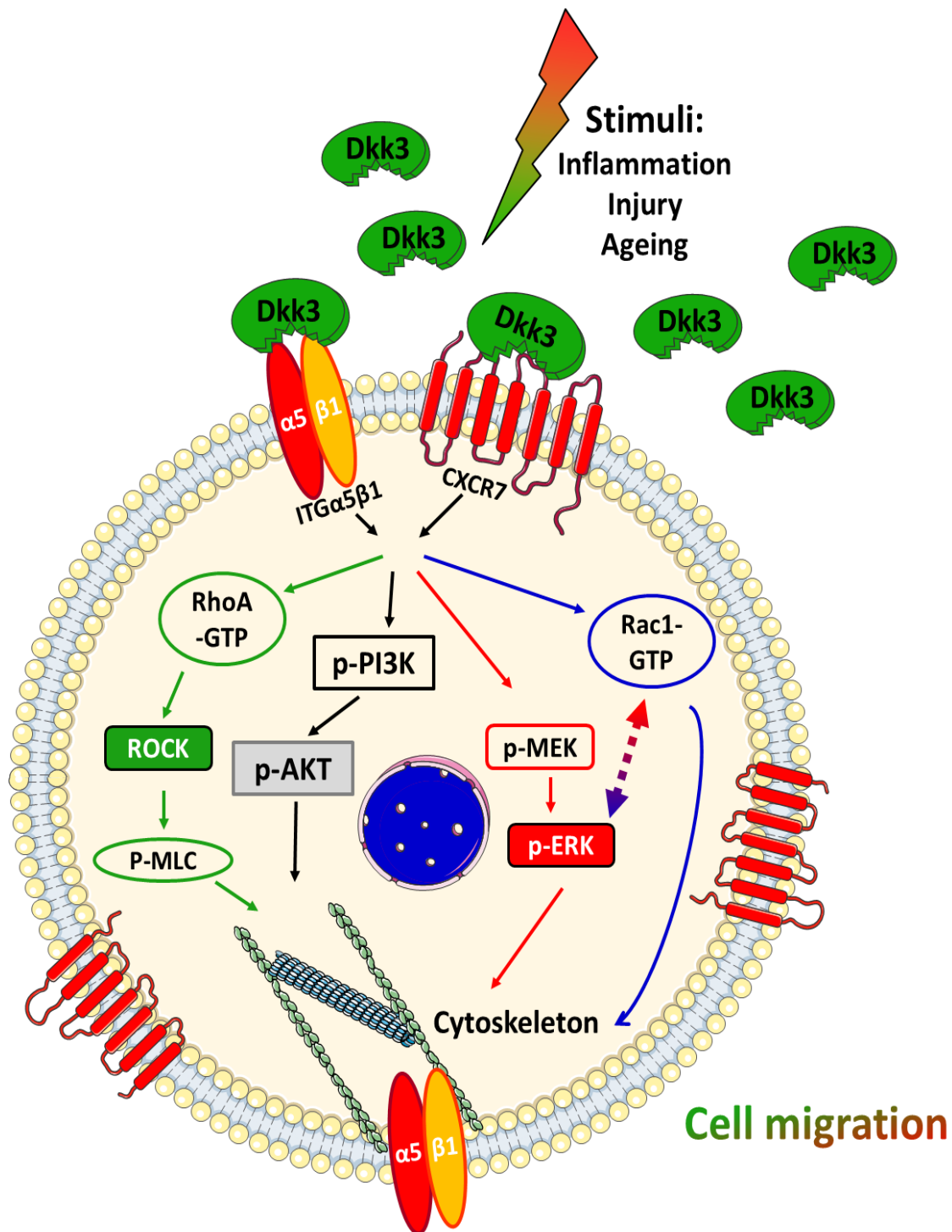


Figure 4.6: Dkk3-driven Sca-1+ vascular progenitor cell migration mechanism. Dkk3 binds to ITGα5β1 and, as a result, it triggers the activation of MEK1/2, which induces the phosphorylation of ERK1/2. ERK1/2 either activates Rac1 or directly modulates cytoskeleton rearrangement to promote cell migration. On the other hand, Rac1 activation can occur upstream of ERK activation upon Dkk3 binding to ITGα5β1, which in turn regulates cell cytoskeleton and/or stimulates ERK phosphorylation. The Dkk3/ITGα5β1 axis also promotes AKT phosphorylation via PI3K, leading to cytoskeleton reorganization. RhoA activation level increases in response to the binding of Dkk3 to ITGα5β1, which induces MLC phosphorylation, either directly or via ROCK activation.

Chapter 5: Conclusions

5.1 Conclusions

- Dkk3, similarly to Sdf-1 α , induces the chemotaxis of resident Sca-1+ vascular progenitor cells *in vitro*.
- Cell outgrowth from ApoE^{-/-} mouse aortic rings, promoted by Dkk3 treatment, comprises Sca-1+ vascular progenitor cells, SMCs and cells exhibiting both Sca-1+ and α -SMA markers.
- Downregulation or overexpression of CXCR7 drives, respectively, reduction or increase of cell migration stimulated by either Dkk3 or Sdf-1 α treatments.
- Dkk3 co-immunoprecipitates with CXCR7 and, similarly to chemokine Sdf-1 α , it binds with high affinity to CXCR7.
- Kremen1 and Kremen2 are not high binding affinity receptors for Dkk3.
- The PI3K/AKT axis, the MAPK kinase signalling pathway and the Rho GTPases family are involved in the Dkk3-mediated migration mechanism of Sca-1+ vascular progenitor cells, which is shared by Sdf-1 α treatment.
- CXCR7 downregulation suppresses the signalling cascades triggered by Dkk3 stimulation.
- We conclude that Dkk3 is a chemokine-like protein which binds to CXCR7 and promotes the Sca-1+ vascular progenitor cell migration, in an equivalent manner to Sdf-1 α .
- Integrin α 5 and integrin β 1 interact with Dkk3 protein.
- Dkk3 binds with high affinity to ITG α 5 and ITG β 1 and co-immunoprecipitates with these receptors as a complex in Sca-1+ progenitor cells.
- Downregulation of ITG α 5 and ITG β 1 represses the Sca-1 progenitor cell migration in response to Dkk3.
- Dkk3 binds to ITG α 5 β 1 to promote Sca-1+ vascular progenitor cell migration.

Chapter 6: Future work

6.1 Future work and perspectives

We have successfully demonstrated for the first time that Dkk3 induces the migration of Sca-1+ APCs. As other stem/progenitor cells, such as c-Kit+, CD34 and Flk1+ cells were also found to reside in the vascular adventitia [6], which is now recognised to be a highly active vessel layer [3-5, 75, 261, 568], it could be interesting to study whether these cells can also migrate in response to Dkk3 and perhaps even differentiate into SMCs, thus contributing to neointima hyperplasia.

Our aortic ring assay showed that Dkk3 induces resident Sca-1+ APC migration, proliferation and potentially differentiation into SMCs. These findings are supported by the artificial vessel graft study performed by a collaborating group, which demonstrated that Dkk3 induces *in vivo* Sca-1+ APC recruitment to neotissue and potential differentiation into SMCs, with increased ECM production (unpublished data). On this matter, studies have revealed that Dkk3 is involved in the differentiation mechanism of stem cells into SMCs [243, 244]. We believe that the study of the differentiation mechanisms underlying the Sca-1+ progenitor cell differentiation into SMCs could provide valuable information to further clarify how the Sca-1+ cells contribute to atherosclerotic hyperplasia.

We used aortic rings derived from transgenic Sca-1-GFP mice in our study. This model is not sufficient to assess if the Dkk3-induced migration of Sca-1+ APCs was followed by SMC differentiation, or if on the other hand, the SMCs migrated in response to Dkk3 and then de-differentiated, thus exhibiting the Sca-1+ marker. Application of the Sca-1+ lineage tracing strategy could provide the answer to this question, as well as to others, such as whether Dkk3 induces the fusion of Sca-1+ cells with other cell types, such as SMCs. The lineage tracing model would therefore provide a better understanding on the origin of the increased number of cells exhibiting the co-expression of Sca-1+ cell marker and α -SMA marker in response to Dkk3. Additionally, clarification would be obtained regarding the ability of Dkk3 to potentially induce Sca-1+ cell differentiation into ECs or other cell types, or to induce the migration of ECs or inflammatory cells. Finally, crucial information would be gathered concerning Dkk3 protein's role, revealing whether it is a protective or a disruptive agent in atherogenesis.

In respect to *in vivo* studies, in addition to the Dkk3-loaded artificial vessel model previously mentioned, other different vascular diseases mouse models could be used to elucidate the role of Dkk3 in inducing the adventitial Sca-1+ APCs migration in atherogenesis. The ApoE^{-/-} mouse model and other experimental models of injury, such as the Wire Injury, the Vein Graft model, the Cuff-Induced Neointimal Formation and the artery Ligation, are useful tools to study neointima formation. Comparing Wild type and Dkk3^{-/-} mice in these models would allow us to study the effect of Dkk3 on neointima formation and on Sca-1+ cells behaviour and distribution in the vascular wall in the context of pathology. The use of a Dkk3 blocking antibody could also be administered, either locally or systemically, and the level of Sca-1+ progenitor cell migration towards the neointima could be assessed. In another approach, Dkk3 could be administered either locally or systemically in injured or uninjured arteries, and the number of Sca-1+ cells that migrated from the outer side of

the vessel to the neointima could be analysed. What is more, the study of the effect of other cytokines on the neointima formation could be evaluated in response to the expression or absence of Dkk3. For example, it would be very useful to understand how Dkk3 expression affects the Sdf-1 α mediated neointima formation in ApoE^{-/-} mice and/or injured arteries. Finally, the bioreactor model comprising a decellularized vessel, could similarly to the artificial *in vivo* setting, aid in the clarification of the *ex vivo* mechanism of Sca-1+ progenitor cell migration from the outer layer through the vessel wall in response to Dkk3 treatment.

As a substantial number of studies has shown that Dkk3 is involved in tumour-related angiogenesis [236, 239, 240], we think that it is worthwhile to investigate whether Dkk3 influences the endothelial cell migration, proliferation or survival in vascular diseases, such as in atherosclerosis, and if this effect has either a protective or disruptive role in atherogenesis. In this regard, a study with Dkk3^{-/-} mice and ApoE^{-/-}-Dkk3^{-/-} mice has been recently carried out to analyse the function of Dkk3 on endothelial layer repair and to assess the migration of HUVECs in response to Dkk3 treatment and overexpression (unpublished data). We could thus obtain more information on Dkk3 specific function on different cell types of the vascular wall in the context of vascular diseases.

Reports have concluded that there is an association between Dkk3 and inflammation [222, 241, 242]. Therefore, we propose to further explore if Dkk3 recruits inflammatory cells to the neointima during the progression of atherosclerosis or if these are the source of Dkk3 which then mobilizes the progenitor cells or SMCs.

Dkk3 is highly expressed in SMCs [243, 244], megakaryocytes [224], macrophages [222, 241, 242] and tumour-associated ECs [236, 240]. It could be of great interest to compare the level of Dkk3 secretion from these cell types with the amount of Dkk3 secreted by the Sca-1+ APCs to further understand whether a consequent paracrine or local effect exists. Additionally, because other cytokines and growth factors may participate in progenitor cell migration, a proteomic study or ELISA array could be performed on the conditioned medium of the different vascular cell types upon Dkk3 treatment, to understand whether it stimulates the production of chemoattractants, which could also influence Sca-1+ APC migration. Finally, performing an array of human serum/plasma to analyse the level of secreted Dkk3 at different physiological and pathological conditions would provide further insight into the role of Dkk3, which could add clinical relevance to our study.

Our Yeast Two Hybrid assay, showed that Dkk3 interacts with Fabp4 (Fatty Acid Binding Protein 4), which as marker used for adipocytes and which is involved in fatty acid uptake, transport and metabolism [569-571]. Xie et al., concluded that Dkk3 alleviates fatty liver in obese mice [572]. Cheng et al., inferred that Dkk3 can increase lipid accumulation in atheroma [222]. We thus postulate that Dkk3 could play a role in the lipid metabolism and this should be further clarified.

Fabp4 is also associated with diabetes [573-575] and our Y2H analysis also identified the interaction of Insulin Like Growth Factor Binding Protein 5 (IGFBP5) with Dkk3. This finding suggests a possible link between Dkk3 and the development of diabetes, which should be addressed.

The data obtained in this work revealed that CXCR7 is a high affinity binding receptor of Dkk3. Unfortunately, CXCR7 complete deletion causes perinatal lethality. Hence, we cannot use this mouse model in our experiments. Additionally, CXCR7 antagonists are not available commercially. We could attempt to generate Sca1⁺-CreER^{T2}-CXCR7^{fllox/-} mice to obtain CXCR7 deleted specifically in Sca-1⁺ progenitor cells and then study *in vivo* the involvement of CXCR7 receptor in the migration mechanism of Sca-1⁺ progenitor cells in response to Dkk3, under normal and atherosclerotic conditions. Another different approach involves seeding the Sca-1⁺ cells exhibiting CXCR7 downregulation, on the adventitial side of injured and uninjured arteries, and then assess whether these cells contribute less or more to neointima formation in response to Dkk3 administration.

The signalling pathways involved in the Sca-1⁺ APC migration mechanism induced by Dkk3, through CXCR7 activation, have been described in this work and they consist of the PI3K/AKT axis, the MAPK kinase signalling cascade and the Rho GTPases family. The confirmation of these pathways *in vivo* could be achieved with local or systemic administration of the corresponding inhibitors in the different vascular diseases mouse models above mentioned, with or without Dkk3 expression or administration. However, we should consider that not only the Sca-1⁺ cells would be affected but also other susceptible cells. Consequently, the approach of adding the inhibitor together with the Sca-1⁺ cells applied on the adventitial side of injured arteries would be more informative. Sca-1⁺ cells transfected with ERK or AKT siRNA, or with constructs encoding for constitutively-active or dominant-negative mutant of either Rac1 or RhoA, could also be used to verify *in vivo* the involvement of these signalling effectors in the Dkk3-driven Sca-1⁺ APC migration mechanism.

RNA microarray analysis would provide information on additional signalling pathways induced or repressed in Sca-1⁺ vascular progenitor cells in response to Dkk3 stimulation, which could enlighten on the Dkk3-triggered cell migration, proliferation and differentiation mechanisms, amongst others.

The Yeast Two hybrid methodology revealed that Dkk3 interacts with integrin $\alpha 5$ and integrin $\beta 1$, which was further confirmed by co-immunoprecipitation and affinity binding assays. Migration functional assay confirmed the role of ITG $\alpha 5$ and ITG $\beta 1$ in Sca-1⁺ cell migration. Integrin $\alpha 5$ Knock Out causes lethality. ITG $\beta 1$ ^{-/-} mouse model is available and could be used to study *in vivo* the role ITG $\beta 1$ in the neointima formation in response to Dkk3. Moreover, Wild type and ITG $\beta 1$ ^{-/-} mice Sca-1⁺ cells could be seeded on the outer side of injured arteries and their contribution to neointima could be examined in response to Dkk3 administration. Furthermore, ITG $\beta 1$ ^{fllox/-} mice could be crossed with Sca1⁺-CreER^{T2} to conditionally delete ITG $\beta 1$ in Sca-1 cells and thus the *in vivo* effect of Dkk3 on these cells could be assessed, under normal and atherosclerotic conditions. This same approach could be implemented for ITG $\alpha 5$, with the generation of a Sca1⁺-CreER^{T2}-ITG $\alpha 5$ ^{fllox/-} mouse model. Blocking antibodies or specific siRNA for ITG $\alpha 5$, ITG $\beta 1$ and ITG $\alpha 5\beta 1$ could also be placed together with the Sca-1⁺ cells on the adventitial side of injured and uninjured arteries and their migration to the inner side of the vessel in response to Dkk3 could be analysed.

The signalling pathways implicated in ITG $\alpha 5$ and ITG $\beta 1$ mediated Sca-1⁺ cell migration was not analysed in this study. We therefore aim at completing this step in our future work.

With the identification of two receptors for Dkk3, a possible interaction between CXCR7 and ITG α 5 β 1 will be explored. We thus intend to perform a Co-immunoprecipitation experiment to see if CXCR7 binds to ITG α 5 β 1. To analyse if one receptor regulates the other, downregulation and overexpression assays followed by the measurement of the receptor expression and/or activation will be executed. The cross-talk of integrins with growth factor receptors and chemokine receptors, with synergistic effect on cell migration in some cases, has been reported elsewhere [576-578].

The analysis of the expression of the receptors CXCR7 and ITG α 5 β 1, and possible co-localization with Dkk3 in Sca-1+ cells in models of neointima formation, such as injury models or ApoE^{-/-} mouse model, would be of interest. Likewise, time lapse *in vivo* immunofluorescence imaging of the Dkk3 treated Sca-1+ cells versus untreated cells showing the expression of the receptors co-localized with Dkk3, would furnish additional confirmation.

To identify the Dkk3 domain that binds to either CXCR7 or ITG α 5 β 1, we could engineer Dkk3 constructs with deletions of different domains and then perform competitive ligand-receptor binding assays. This would give crucial information required for the development of drug-targeted therapy with Dkk3 in not only vascular diseases but also tumour diseases.

Finally, in our understanding, it should not be ignored the fact that the Y2H system enabled the identification of Fibulin 5 as one of the proteins that interacts with Dkk3. Fibulin 5 is a component of the ECM, which contributes to the formation of elastic fibers and binds to a set of integrins receptors, including ITG α 5 β 1 [332, 542, 579-581]. Lomas et al., showed that Fibulin 5 supports the attachment of human aortic SMCs through ITG α 5 β 1 and that its interaction can be vital for the ordered formation of elastic fibers [332]. Spencer et al., revealed that in the absence of Fibulin 5, the mutant mice displayed an increased vascular remodelling with thickening of the neointima and that SMCs from Fbln-5^{-/-} mice exhibited an enhanced migratory and proliferative response to mitogenic stimulation [582]. These data, together with our results regarding the interaction of Dkk3 with Fibulin 5, ITG α 5 and ITG5 β 1 and considering the different roles of Dkk3 on Sca-1+ cells, lead us to postulate that the formation of the Fibulin 5-Dkk3-ITG α 5 β 1 trimeric complex could participate in Sca-1+ cell migration and vascular wall hyperplasia.

Our data reveals the emergence of Dkk3 as a novel chemokine-like protein towards Sca-1+ APCs. We also identified Dkk3 protein's receptors, CXCR7 and ITG α 5 β 1. Furthermore, we provided elucidation on the signalling pathways activated by the binding of Dkk3 to CXCR7. These findings are very relevant in the development of potential new therapies for cardiovascular diseases, such as atherosclerosis, which are characterized by exacerbated cell migration and proliferation. We strongly believe that our work, which highlights the role of Dkk3 on Sca-1+ cells behaviour, could contribute for the future development of drug-targeted therapy in atherosclerosis.

Chapter 7: Publications and Abstracts

7.1 Published

Simpson, R. M. L., Hong, X., Wong, M. M., Karamariti, E., **Bhaloo, S. I.**, Warren, D., Kong, W., Hu, Y. & Xu, Q., ***Hyaluronan Is Crucial for Stem Cell Differentiation into Smooth Muscle Lineage.*** Stem Cells, 2016. 34(5): p.1225-1238.

7.2 In Revision

Le Bras, A., Yu, b., **Bhaloo, S. I.**, Hong, x., Zhang, Z., Hu, Y., Xu, Q. **Adventitial Sca1+ cells transduced with ETV2 are committed to the endothelial fate and improve vascular remodeling following injury** (Submitted manuscript – 2017)

7.3 In Peer Review

Xie, Y., Potter, C., Le Bras, A., **Bhaloo, S. I.**, Nowak, W., Gu, W., Zhang, Z., Hu, Y., Zhang, L., Xu. Q., **Leptin Induces Sca-1+ Progenitor Cell Migration Enhancing Neointimal Lesions in Vessel-Injury Mouse Models** (Submitted manuscript – 2017)

7.4 In Preparation

Bhaloo, S. I., Le Bras, A., Zhang, Z., Hu, Y., Xu, Q., **Dkk3 induces Adventitial Sca-1+ progenitor cell chemotaxis through CXCR7 – The emergence of a novel chemokine-like protein**

Gu, W., Yao, X, Nowak, W., Le Bras, A., **Bhaloo, S. I.**, Hong, X., Zhang, Z., Hu, Y., Xu, Q. **Smooth muscle cells differentiate from perivascular adipose tissue-derived stem cells, through Apelin inhibition and metabolic profile change**

7.5 Abstracts presented in meetings

Bhaloo, S. I., Wong, M., A., Zhang, Z., Hu, Y., Xu, Q., Vascular Stem/Progenitor Cell Migration in Vascular Diseases in response to chemokines, German Matrix Meeting (Extracellular Matrix), University of Munster, Germany, 12-14 March 2015 (Poster presentation)

Bhaloo, S. I., Le Bras, A., Zhang, Z., Hu, Y., Xu, Q., Sca-1+ vascular progenitor cell migration is induced by SDF-1 α release in atherosclerosis, BHF Centre of Research Excellence Postgraduate Symposium, King's College London, United Kingdom, 27 April 2015 (Poster presentation)

Bhaloo, S. I., Le Bras, A., Zhang, Z., Hu, Y., Xu, Q., Vascular Progenitor Cell Migration in Vascular Diseases in response to chemokine Sdf1- α and chemokine-like protein Dkk3, Vascular Biology: MicroRNAs and proteomics - European SmArTeR Summer School, King's College London, United Kingdom, 15-19 November 2015 (Oral and Poster presentation)

Bhaloo, S. I., Le Bras, A., Zhang, Z., Hu, Y., Xu, Q., Vascular Progenitor Cell Migration in Vascular Diseases in response to chemokine-like protein Dkk3, SmArTeR Meeting Network Symposium on Imaging and Image Analysis (Advanced confocal microscopy), Ludwig-Maximilians-Universität, Munich, Germany, 30 May-5 June, 2016 (Oral presentation)

Bhaloo, S. I., Le Bras, A., Zhang, Z., Hu, Y., Xu, Q., Vascular Progenitor Cell Migration in Vascular Diseases in response to chemokine Sdf1- α and chemokine-like protein Dkk3, Small Artery Remodelling (SmArTeR) 2016 Symposium on Vascular remodeling: Novel developments in progenitor cell biology and gene regulation, University of Fribourg, Switzerland, 7-9 November, 2016 (Poster presentation)

Nowak, W., Gu, W., Yao, X., Le Bras, A., **Bhaloo, S. I., Smooth muscle cells differentiate from perivascular adipose tissue-derived stem cells, through Apelin inhibition and metabolic profile change**, EMBO Symposia, Heidelberg, Germany, 21-23 May 2017 (Poster presentation)

Bhaloo, S. I., Le Bras, A., Zhang, Z., Hu, Y., Xu, Q., Vascular Progenitor Cell Migration in Vascular Diseases in response to chemokines – The emergence of a novel chemokine-like protein Dkk3, ISSCR 2017 Annual Meeting, Boston, United States of America, 14-17 June 2017 (Poster presentation)

Chapter 8: References

- [1] Levy B I and Tedgui A 1999 Biology of the Arterial Wall *Basic Science for the Cardiologist* Volume 1
- [2] Pugsley M K and Tabrizchi R 2000 The vascular system: An overview of structure and function *Journal of Pharmacological and Toxicological Methods* 44 333-40
- [3] Majesky M W, Dong X R, Hoglund V, Daum G and Mahoney W M, Jr. 2012 The adventitia: a progenitor cell niche for the vessel wall *Cells, tissues, organs* 195 73-81
- [4] Hu Y and Xu Q 2011 Adventitial Biology *Differentiation and Function* 31 1523-9
- [5] Majesky M W, Dong X R, Hoglund V, Mahoney W M, Jr. and Daum G 2011 The adventitia: a dynamic interface containing resident progenitor cells *Arteriosclerosis, thrombosis, and vascular biology* 31 1530-9
- [6] Hu Y, Zhang Z, Torsney E, Afzal A R, Davison F, Metzler B and Xu Q 2004 Abundant progenitor cells in the adventitia contribute to atherosclerosis of vein grafts in ApoE-deficient mice *Journal of Clinical Investigation* 113 1258-65
- [7] Passman J N, Dong X R, Wu S-P, Maguire C T, Hogan K A, Bautch V L and Majesky M W 2008 A sonic hedgehog signaling domain in the arterial adventitia supports resident Sca1+ smooth muscle progenitor cells *Proceedings of the National Academy of Sciences* 105 9349-54
- [8] Campagnolo P, Cesselli D, Al Haj Zen A, Beltrami A P, Kränkel N, Katare R, Angelini G, Emanuelli C and Madeddu P 2010 Human Adult Vena Saphena Contains Perivascular Progenitor Cells Endowed With Clonogenic and Proangiogenic Potential *Circulation* 121 1735-45
- [9] Zengin E, Chalajour F, Gehling U M, Ito W D, Treede H, Lauke H, Weil J, Reichenspurner H, Kilic N and Ergun S 2006 Vascular wall resident progenitor cells: a source for postnatal vasculogenesis *Development (Cambridge, England)* 133 1543-51
- [10] Psaltis P J, Puranik A S, Spoon D B, Chue C D, Hoffman S J, Witt T A, Delacroix S, Kleppe L S, Mueske C S, Pan S, Gulati R and Simari R D 2014 Characterization of a resident population of adventitial macrophage progenitor cells in postnatal vasculature *Circulation research* 115 364-75
- [11] Hoshino A, Chiba H, Nagai K, Ishii G and Ochiai A 2008 Human vascular adventitial fibroblasts contain mesenchymal stem/progenitor cells *Biochemical and Biophysical Research Communications* 368 305-10
- [12] Kramann R, Goettsch C, Wongboonsin J, Iwata H, Schneider R K, Kuppe C, Kaesler N, Chang-Panesso M, Machado F G, Gratwohl S, Madhurima K, Hutcheson J D, Jain S, Aikawa E and Humphreys B D 2016 Adventitial MSC-like Cells Are Progenitors of Vascular Smooth Muscle Cells and Drive Vascular Calcification in Chronic Kidney Disease *Cell stem cell* 19 628-42
- [13] Lin C S and Lue T F 2013 Defining vascular stem cells *Stem cells and development* 22 1018-26
- [14] Gómez-Gavero M V, Lovell-Badge R, Fernández-Avilés F and Lara-Pezzi E 2012 The Vascular Stem Cell Niche *Journal of Cardiovascular Translational Research* 5 618-30
- [15] Asahara T, Kawamoto A and Masuda H 2011 Concise Review: Circulating Endothelial Progenitor Cells for Vascular Medicine *Stem Cells (Dayton, Ohio)* 29 1650-5
- [16] Aicher A, Rentsch M, Sasaki K-i, Ellwart J W, Fändrich F, Siebert R, Cooke J P, Dimmeler S and Heeschen C 2007 Nonbone Marrow-Derived Circulating Progenitor Cells Contribute to Postnatal Neovascularization Following Tissue Ischemia *Circulation Research* 100 581-9
- [17] Kuwana M, Okazaki Y, Kodama H, Izumi K, Yasuoka H, Ogawa Y, Kawakami Y and Ikeda Y 2003 Human circulating CD14+ monocytes as a source of progenitors that exhibit mesenchymal cell differentiation *Journal of leukocyte biology* 74 833-45

- [18] Wang Y, Johnsen H E, Mortensen S, Bindselev L, Ripa R S, Haack-Sorensen M, Jorgensen E, Fang W and Kastrup J 2006 Changes in circulating mesenchymal stem cells, stem cell homing factor, and vascular growth factors in patients with acute ST elevation myocardial infarction treated with primary percutaneous coronary intervention *Heart (British Cardiac Society)* 92 768-74
- [19] Marketou M E, Parthenakis F I, Kalyva A, Pontikoglou C, Maragkoudakis S, Kontaraki J E, Zacharis E A, Patrianakos A, Chlouverakis G, Papadaki H A and Vardas P E 2015 Circulating mesenchymal stem cells in patients with hypertrophic cardiomyopathy *Cardiovascular pathology : the official journal of the Society for Cardiovascular Pathology* 24 149-53
- [20] Zvaifler N J, Marinova-Mutafchieva L, Adams G, Edwards C J, Moss J, Burger J A and Maini R N 2000 Mesenchymal precursor cells in the blood of normal individuals *Arthritis Research & Therapy* 2 477
- [21] Wojakowski W, Tendera M, Kucia M, Zuba-Surma E, Paczkowska E, Ciosek J, Hałasa M, Król M, Kazmierski M, Buszman P, Ochała A, Ratajczak J, Machaliński B and Ratajczak M Z 2009 Mobilization of Bone Marrow-Derived Oct-4+ SSEA-4+ Very Small Embryonic-Like Stem Cells in Patients With Acute Myocardial Infarction *Journal of the American College of Cardiology* 53 1-9
- [22] Kucia M, Reza R, Campbell F R, Zuba-Surma E, Majka M, Ratajczak J and Ratajczak M Z 2006 A population of very small embryonic-like (VSEL) CXCR4+SSEA-1+Oct-4+ stem cells identified in adult bone marrow *Leukemia* 20 857-69
- [23] Dimmeler S and Zeiher A M 2004 Vascular repair by circulating endothelial progenitor cells: the missing link in atherosclerosis? *Journal of molecular medicine (Berlin, Germany)* 82 671-7
- [24] Briasoulis A, Tousoulis D, Antoniadou C, Papageorgiou N and Stefanadis C 2011 The role of endothelial progenitor cells in vascular repair after arterial injury and atherosclerotic plaque development *Cardiovascular therapeutics* 29 125-39
- [25] Yoder M C 2012 Human Endothelial Progenitor Cells *Cold Spring Harbor Perspectives in Medicine* 2
- [26] Fadini G P, Losordo D and Dimmeler S 2012 Critical reevaluation of endothelial progenitor cell phenotypes for therapeutic and diagnostic use *Circ Res* 110 624-37
- [27] Nowak G, Karrar A, Holmen C, Nava S, Uzunel M, Hulténby K and Sumitran-Holgersson S 2004 Expression of vascular endothelial growth factor receptor-2 or Tie-2 on peripheral blood cells defines functionally competent cell populations capable of reendothelialization *Circulation* 110 3699-707
- [28] Hristov M, Erl W and Weber P C 2003 Endothelial Progenitor Cells *Mobilization, Differentiation, and Homing* 23 1185-9
- [29] Xu Q, Zhang Z, Davison F and Hu Y 2003 Circulating progenitor cells regenerate endothelium of vein graft atherosclerosis, which is diminished in ApoE-deficient mice *Circulation research* 93 e76-86
- [30] Asahara T, Murohara T, Sullivan A, Silver M, van der Zee R, Li T, Witzenbichler B, Schatteman G and Isner J M 1997 Isolation of putative progenitor endothelial cells for angiogenesis *Science* 275 964-7
- [31] Zampetaki A, Kirton J P and Xu Q 2008 Vascular repair by endothelial progenitor cells *Cardiovasc Res* 78 413-21
- [32] Kalka C, Masuda H, Takahashi T, Kalka-Moll W M, Silver M, Kearney M, Li T, Isner J M and Asahara T 2000 Transplantation of ex vivo expanded endothelial progenitor cells for therapeutic neovascularization *Proceedings of the National Academy of Sciences* 97 3422-7
- [33] Foteinos G, Hu Y, Xiao Q, Metzler B and Xu Q 2008 Rapid endothelial turnover in atherosclerosis-prone areas coincides with stem cell repair in apolipoprotein E-deficient mice *Circulation* 117 1856-63

- [34] Li Z F, Fang X G, Yang P F, Huang Q H, Zhao W Y, Liang C, Zhao R and Liu J M 2013 Endothelial progenitor cells contribute to neointima formation in rabbit elastase-induced aneurysm after flow diverter treatment *CNS neuroscience & therapeutics* 19 352-7
- [35] De Maria G L, Porto I, Burzotta F, Brancati M F, Trani C, Pirozzolo G, Leone A M, Niccoli G, Prati F and Crea F 2015 Dual role of circulating endothelial progenitor cells in stent struts endothelialisation and neointimal regrowth: a substudy of the IN-PACT CORO trial *Cardiovascular revascularization medicine : including molecular interventions* 16 20-6
- [36] Hristov M and Weber C 2008 Endothelial progenitor cells in vascular repair and remodeling *Pharmacological research* 58 148-51
- [37] Tsai S, Butler J, Rafii S, Liu B and Kent K C 2009 The role of progenitor cells in the development of intimal hyperplasia *Journal of Vascular Surgery* 49 502-10
- [38] Hristov M, Zerneck A, Schober A and Weber C 2008 Adult progenitor cells in vascular remodeling during atherosclerosis *Biological chemistry* 389 837-44
- [39] Gratwohl A, Baldomero H, Aljurf M, Pasquini M C, Bouzas L F, Yoshimi A, Szer J, Lipton J, Schwendener A, Gratwohl M, Frauendorfer K, Niederwieser D, Horowitz M and Kodera Y 2010 Hematopoietic stem cell transplantation A Global Perspective *JAMA : the journal of the American Medical Association* 303 1617-24
- [40] de Winther M P and Heeringa P 2011 Bone marrow transplantations to study gene function in hematopoietic cells *Methods in molecular biology (Clifton, N.J.)* 693 309-20
- [41] Sata M 2003 Circulating vascular progenitor cells contribute to vascular repair, remodeling, and lesion formation *Trends in cardiovascular medicine* 13 249-53
- [42] Takakura N, Watanabe T, Suenobu S, Yamada Y, Noda T, Ito Y, Satake M and Suda T 2000 A Role for Hematopoietic Stem Cells in Promoting Angiogenesis *Cell* 102 199-209
- [43] Wang X, Gao M, Schouteden S, Roebroek A, Eggermont K, van Veldhoven P P, Liu G, Peters T, Scharffetter-Kochanek K, Verfaillie C M and Feng Y 2015 Hematopoietic stem/progenitor cells directly contribute to arteriosclerotic progression via integrin beta2 *Stem Cells* 33 1230-40
- [44] Sata M, Saiura A, Kunisato A, Tojo A, Okada S, Tokuhisa T, Hirai H, Makuuchi M, Hirata Y and Nagai R 2002 Hematopoietic stem cells differentiate into vascular cells that participate in the pathogenesis of atherosclerosis *Nat Med* 8 403-9
- [45] Asahara T, Masuda H, Takahashi T, Kalka C, Pastore C, Silver M, Kearne M, Magner M and Isner J M 1999 Bone marrow origin of endothelial progenitor cells responsible for postnatal vasculogenesis in physiological and pathological neovascularization *Circ Res* 85 221-8
- [46] Bailey A S, Willenbring H, Jiang S, Anderson D A, Schroeder D A, Wong M H, Grompe M and Fleming W H 2006 Myeloid lineage progenitors give rise to vascular endothelium *Proceedings of the National Academy of Sciences* 103 13156-61
- [47] Kovacic J C and Boehm M 2009 Resident vascular progenitor cells: an emerging role for non-terminally differentiated vessel-resident cells in vascular biology *Stem cell research* 2 2-15
- [48] Hirschi K K and Majesky M W 2004 Smooth muscle stem cells *The anatomical record. Part A, Discoveries in molecular, cellular, and evolutionary biology* 276 22-33
- [49] Saiura A, Sata M, Hirata Y, Nagai R and Makuuchi M 2001 Circulating smooth muscle progenitor cells contribute to atherosclerosis *Nature medicine* 7 382-3
- [50] Shimizu K, Sugiyama S, Aikawa M, Fukumoto Y, Rabkin E, Libby P and Mitchell R N 2001 Host bone-marrow cells are a source of donor intimal smooth-muscle-like cells in murine aortic transplant arteriopathy *Nature medicine* 7 738-41
- [51] Schroeter M R, Humboldt T, Schäfer K and Konstantinides S 2009 Rosuvastatin reduces atherosclerotic lesions and promotes progenitor cell mobilisation and recruitment in apolipoprotein E knockout mice *Atherosclerosis* 205 63-73
- [52] Bentzon J F and Falk E 2010 Circulating smooth muscle progenitor cells in atherosclerosis and plaque rupture: Current perspective and methods of analysis *Vascular Pharmacology* 52 11-20

- [53] Religa P, Bojakowski K, Maksymowicz M, Bojakowska M, Sirsjo A, Gaciong Z, Olszewski W, Hedin U and Thyberg J 2002 Smooth-muscle progenitor cells of bone marrow origin contribute to the development of neointimal thickenings in rat aortic allografts and injured rat carotid arteries *Transplantation* 74 1310-5
- [54] Case J, Mead L E, Bessler W K, Prater D, White H A, Saadatzaheh M R, Bhavsar J R, Yoder M C, Haneline L S and Ingram D A 2007 Human CD34+AC133+VEGFR-2+ cells are not endothelial progenitor cells but distinct, primitive hematopoietic progenitors *Experimental hematology* 35 1109-18
- [55] Timmermans F, Van Hauwermeiren F, De Smedt M, Raedt R, Plasschaert F, De Buyzere M L, Gillebert T C, Plum J and Vandekerckhove B 2007 Endothelial outgrowth cells are not derived from CD133+ cells or CD45+ hematopoietic precursors *Arteriosclerosis, thrombosis, and vascular biology* 27 1572-9
- [56] Yoder M C, Mead L E, Prater D, Krier T R, Mroueh K N, Li F, Krasich R, Temm C J, Prchal J T and Ingram D A 2007 Redefining endothelial progenitor cells via clonal analysis and hematopoietic stem/progenitor cell principals *Blood* 109 1801-9
- [57] Bentzon J F, Weile C, Sondergaard C S, Hindkjaer J, Kassem M and Falk E 2006 Smooth Muscle Cells in Atherosclerosis Originate From the Local Vessel Wall and Not Circulating Progenitor Cells in ApoE Knockout Mice *Arteriosclerosis, thrombosis, and vascular biology* 26 2696-702
- [58] Daniel J M, Bielenberg W, Stieger P, Weinert S, Tillmanns H and Sedding D G 2010 Time-course analysis on the differentiation of bone marrow-derived progenitor cells into smooth muscle cells during neointima formation *Arteriosclerosis, thrombosis, and vascular biology* 30 1890-6
- [59] Iwata H, Manabe I, Fujiu K, Yamamoto T, Takeda N, Eguchi K, Furuya A, Kuro-o M, Sata M and Nagai R 2010 Bone marrow-derived cells contribute to vascular inflammation but do not differentiate into smooth muscle cell lineages *Circulation* 122 2048-57
- [60] Hu Y, Davison F, Ludewig B, Erdel M, Mayr M, Url M, Dietrich H and Xu Q 2002 Smooth muscle cells in transplant atherosclerotic lesions are originated from recipients, but not bone marrow progenitor cells *Circulation* 106 1834-9
- [61] Groenewegen H C, Onuta G, Goris M, Zandvoort A, Zijlstra F, van Gilst W H, Rozing J, de Smet B J G L, Roks A J M and Hillebrands J L 2008 Non-Bone Marrow Origin of Neointimal Smooth Muscle Cells in Experimental In-Stent Restenosis in Rats *Journal of vascular research* 45 493-502
- [62] Campagnolo P, Wong M M and Xu Q 2011 Progenitor cells in arteriosclerosis: good or bad guys? *Antioxidants & redox signaling* 15 1013-27
- [63] Xu Q 2007 Progenitor cells in vascular repair *Current opinion in lipidology* 18 534-9
- [64] Alessandri G, Girelli M, Taccagni G, Colombo A, Nicosia R, Caruso A, Baronio M, Pagano S, Cova L and Parati E 2001 Human vasculogenesis ex vivo: embryonal aorta as a tool for isolation of endothelial cell progenitors *Laboratory investigation; a journal of technical methods and pathology* 81 875-85
- [65] Majka S M, Jackson K A, Kienstra K A, Majesky M W, Goodell M A and Hirschi K K 2003 Distinct progenitor populations in skeletal muscle are bone marrow derived and exhibit different cell fates during vascular regeneration *The Journal of Clinical Investigation* 111 71-9
- [66] Tintut Y, Alfonso Z, Saini T, Radcliff K, Watson K, Bostrom K and Demer L L 2003 Multilineage potential of cells from the artery wall *Circulation* 108 2505-10
- [67] Messina E, De Angelis L, Frati G, Morrone S, Chimenti S, Fiordaliso F, Salio M, Battaglia M, Latronico M V, Coletta M, Vivarelli E, Frati L, Cossu G and Giacomello A 2004 Isolation and expansion of adult cardiac stem cells from human and murine heart *Circ Res* 95 911-21
- [68] Ingram D A, Mead L E, Moore D B, Woodard W, Fenoglio A and Yoder M C 2005 Vessel wall-derived endothelial cells rapidly proliferate because they contain a complete hierarchy of endothelial progenitor cells *Blood* 105 2783-6

- [69] Covas D T, Piccinato C E, Orellana M D, Siufi J L C, Silva Jr W A, Proto-Siqueira R, Rizzatti E G, Neder L, Silva A R L, Rocha V and Zago M A 2005 Mesenchymal stem cells can be obtained from the human saphena vein *Experimental Cell Research* 309 340-4
- [70] Pasquinelli G, Tazzari P L, Vaselli C, Foroni L, Buzzi M, Storci G, Alviano F, Ricci F, Bonafè M, Orrico C, Bagnara G P, Stella A and Conte R 2007 Thoracic Aortas from Multiorgan Donors Are Suitable for Obtaining Resident Angiogenic Mesenchymal Stromal Cells *STEM CELLS* 25 1627-34
- [71] Sainz J, Al Haj Zen A, Caligiuri G, Demerens C, Urbain D, Lemitre M and Lafont A 2006 Isolation of "side population" progenitor cells from healthy arteries of adult mice *Arteriosclerosis, thrombosis, and vascular biology* 26 281-6
- [72] Torsney E, Mandal K, Halliday A, Jahangiri M and Xu Q 2007 Characterisation of progenitor cells in human atherosclerotic vessels *Atherosclerosis* 191 259-64
- [73] Howson K M, Aplin A C, Gelati M, Alessandri G, Parati E A and Nicosia R F 2005 The postnatal rat aorta contains pericyte progenitor cells that form spheroidal colonies in suspension culture *American journal of physiology. Cell physiology* 289 C1396-407
- [74] Chen C-W, Okada M, Proto J D, Gao X, Sekiya N, Beckman S A, Corselli M, Crisan M, Saparov A, Tobita K, Péault B and Huard J 2013 Human Pericytes for Ischemic Heart Repair *Stem Cells (Dayton, Ohio)* 31 305-16
- [75] Torsney E and Xu Q 2011 Resident vascular progenitor cells *Journal of molecular and cellular cardiology* 50 304-11
- [76] Awgulewitsch C P, Trinh L T and Hatzopoulos A K 2017 The Vascular Wall: a Plastic Hub of Activity in Cardiovascular Homeostasis and Disease *Current cardiology reports* 19 51
- [77] Psaltis P J and Simari R D 2015 Vascular Wall Progenitor Cells in Health and Disease *Circulation research* 116 1392-412
- [78] Yu B, Wong M M, Potter C M F, Simpson R M L, Karamariti E, Zhang Z, Zeng L, Warren D, Hu Y, Wang W and Xu Q 2016 Vascular Stem/Progenitor Cell Migration Induced by Smooth Muscle Cell-Derived Chemokine (C-C Motif) Ligand 2 and Chemokine (C-X-C motif) Ligand 1 Contributes to Neointima Formation *Stem Cells (Dayton, Ohio)* 34 2368-80
- [79] Who 2014 Global status report on noncommunicable diseases, 2014 *Global status report*
- [80] Libby P, Ridker P M and Hansson G K 2009 Inflammation in atherosclerosis: from pathophysiology to practice *J Am Coll Cardiol* 54 2129-38
- [81] Parks B W and Lusis A J 2013 Macrophage accumulation in atherosclerosis *The New England journal of medicine* 369 2352-3
- [82] Libby P, Ridker P M and Hansson G K 2011 Progress and challenges in translating the biology of atherosclerosis *Nature* 473 317-25
- [83] Lusis A J 2000 Atherosclerosis *Nature* 407 233-41
- [84] Falk E 2006 Pathogenesis of atherosclerosis *J Am Coll Cardiol* 47 C7-12
- [85] Hagensen M K, Raarup M K, Mortensen M B, Thim T, Nyengaard J R, Falk E and Bentzon J F 2012 Circulating endothelial progenitor cells do not contribute to regeneration of endothelium after murine arterial injury *Cardiovasc Res* 93 223-31
- [86] Channon K M 2006 The endothelium and the pathogenesis of atherosclerosis *Medicine* 34 173-7
- [87] Tabas I, García-Cardena G and Owens G K 2015 Recent insights into the cellular biology of atherosclerosis *The Journal of Cell Biology* 209 13-22
- [88] Rensen S S, Doevendans P A and van Eys G J 2007 Regulation and characteristics of vascular smooth muscle cell phenotypic diversity *Netherlands heart journal : monthly journal of the Netherlands Society of Cardiology and the Netherlands Heart Foundation* 15 100-8
- [89] Owens G K, Kumar M S and Wamhoff B R 2004 Molecular regulation of vascular smooth muscle cell differentiation in development and disease *Physiological reviews* 84 767-801

- [90] Hao H, Gabbiani G and Bochaton-Piallat M L 2003 Arterial smooth muscle cell heterogeneity: implications for atherosclerosis and restenosis development *Arteriosclerosis, thrombosis, and vascular biology* 23 1510-20
- [91] Beamish J A, He P, Kottke-Marchant K and Marchant R E 2010 Molecular regulation of contractile smooth muscle cell phenotype: implications for vascular tissue engineering *Tissue engineering. Part B, Reviews* 16 467-91
- [92] Alexander M R and Owens G K 2012 Epigenetic control of smooth muscle cell differentiation and phenotypic switching in vascular development and disease *Annual review of physiology* 74 13-40
- [93] Gomez D and Owens G K 2012 Smooth muscle cell phenotypic switching in atherosclerosis *Cardiovasc Res* 95 156-64
- [94] Bennett M R, Sinha S and Owens G K 2016 Vascular Smooth Muscle Cells in Atherosclerosis *Circ Res* 118 692-702
- [95] Shankman L S, Gomez D, Cherepanova O A, Salmon M, Alencar G F, Haskins R M, Swiatlowska P, Newman A A, Greene E S, Straub A C, Isakson B, Randolph G J and Owens G K 2015 KLF4-dependent phenotypic modulation of smooth muscle cells has a key role in atherosclerotic plaque pathogenesis *Nature medicine* 21 628-37
- [96] Hu Y, Davison F, Zhang Z and Xu Q 2003 Endothelial replacement and angiogenesis in arteriosclerotic lesions of allografts are contributed by circulating progenitor cells *Circulation* 108 3122-7
- [97] Takamiya M, Okigaki M, Jin D, Takai S, Nozawa Y, Adachi Y, Urao N, Tateishi K, Nomura T, Zen K, Ashihara E, Miyazaki M, Tatsumi T, Takahashi T and Matsubara H 2006 Granulocyte Colony-Stimulating Factor–Mobilized Circulating c-Kit+/Flk-1+ Progenitor Cells Regenerate Endothelium and Inhibit Neointimal Hyperplasia After Vascular Injury *Arteriosclerosis, thrombosis, and vascular biology* 26 751-7
- [98] Vasa M, Fichtlscherer S, Aicher A, Adler K, Urbich C, Martin H, Zeiher A M and Dimmeler S 2001 Number and migratory activity of circulating endothelial progenitor cells inversely correlate with risk factors for coronary artery disease *Circ Res* 89 E1-7
- [99] Bentzon J F, Sondergaard C S, Kassem M and Falk E 2007 Smooth muscle cells healing atherosclerotic plaque disruptions are of local, not blood, origin in apolipoprotein E knockout mice *Circulation* 116 2053-61
- [100] Passman J N, Dong X R, Wu S P, Maguire C T, Hogan K A, Bautch V L and Majesky M W 2008 A sonic hedgehog signaling domain in the arterial adventitia supports resident Sca1+ smooth muscle progenitor cells *Proceedings of the National Academy of Sciences of the United States of America* 105 9349-54
- [101] Xiao Q, Zeng L, Zhang Z, Hu Y and Xu Q 2007 Stem cell-derived Sca-1+ progenitors differentiate into smooth muscle cells, which is mediated by collagen IV-integrin alpha1/beta1/alpha5 and PDGF receptor pathways *American journal of physiology. Cell physiology* 292 C342-52
- [102] Wong M M, Winkler B, Karamariti E, Wang X, Yu B, Simpson R, Chen T, Margariti A and Xu Q 2013 Sirolimus stimulates vascular stem/progenitor cell migration and differentiation into smooth muscle cells via epidermal growth factor receptor/extracellular signal-regulated kinase/beta-catenin signaling pathway *Arteriosclerosis, thrombosis, and vascular biology* 33 2397-406
- [103] Chen Y, Wong M M, Campagnolo P, Simpson R, Winkler B, Margariti A, Hu Y and Xu Q 2013 Adventitial stem cells in vein grafts display multilineage potential that contributes to neointimal formation *Arteriosclerosis, thrombosis, and vascular biology* 33 1844-51
- [104] Toledo-Flores D, Schwarz N, Di Bartolo B, Delacroix S, Puranik A, Simari R, Nicholls S and Psaltis P Murine Adventitial Sca-1+CD45+ Progenitor Cells are Proangiogenic and Give Rise to Vasa Vasorum in Atherosclerosis *Heart, Lung and Circulation* 25 S17

- [105] Torsney E, Mandal K, Halliday A, Jahangiri M and Xu Q 2007 Characterisation of progenitor cells in human atherosclerotic vessels *Atherosclerosis* 191 259-64
- [106] Tsai T N, Kirton J P, Campagnolo P, Zhang L, Xiao Q, Zhang Z, Wang W, Hu Y and Xu Q 2012 Contribution of stem cells to neointimal formation of decellularized vessel grafts in a novel mouse model *The American Journal of Pathology* 181 362-73
- [107] Tang Z, Wang A, Yuan F, Yan Z, Liu B, Chu J S, Helms J A and Li S 2012 Differentiation of multipotent vascular stem cells contributes to vascular diseases *Nat Commun* 3 875
- [108] Rosenfeld M E 2015 Converting smooth muscle cells to macrophage-like cells with KLF4 in atherosclerotic plaques *Nature medicine* 21 549-51
- [109] George J, Herz I, Goldstein E, Abashidze S, Deutch V, Finkelstein A, Michowitz Y, Miller H and Keren G 2003 Number and adhesive properties of circulating endothelial progenitor cells in patients with in-stent restenosis *Arteriosclerosis, thrombosis, and vascular biology* 23 e57-60
- [110] Silvestre J S, Gojova A, Brun V, Potteaux S, Esposito B, Duriez M, Clergue M, Le Ricousse-Roussanne S, Barateau V, Merval R, Groux H, Tobelem G, Levy B, Tedgui A and Mallat Z 2003 Transplantation of bone marrow-derived mononuclear cells in ischemic apolipoprotein E-knockout mice accelerates atherosclerosis without altering plaque composition *Circulation* 108 2839-42
- [111] George J, Afek A, Abashidze A, Shmilovich H, Deutsch V, Kopolovich J, Miller H and Keren G 2005 Transfer of endothelial progenitor and bone marrow cells influences atherosclerotic plaque size and composition in apolipoprotein E knockout mice *Arteriosclerosis, thrombosis, and vascular biology* 25 2636-41
- [112] Jamkhande P G, Chandak P G, Dhawale S C, Barde S R, Tidke P S and Sakhare R S 2014 Therapeutic approaches to drug targets in atherosclerosis *Saudi Pharmaceutical Journal* 22 179-90
- [113] Back M and Hansson G K 2015 Anti-inflammatory therapies for atherosclerosis *Nat Rev Cardiol* 12 199-211
- [114] Panoulas V F and Colombo A 2014 Interventional cardiology: Outcomes in coronary stent trials[mdash]1 year is not enough *Nat Rev Cardiol* 11 318-20
- [115] Tomey M I, Kini A S and Sharma S K 2014 Current status of rotational atherectomy *JACC. Cardiovascular interventions* 7 345-53
- [116] Mitra A K and Agrawal D K 2006 In stent restenosis: bane of the stent era *Journal of clinical pathology* 59 232-9
- [117] Buccheri D, Piraino D, Andolina G and Cortese B 2016 Understanding and managing in-stent restenosis: a review of clinical data, from pathogenesis to treatment *Journal of Thoracic Disease* 8 E1150-62
- [118] MJ C and DJ K Cytokines, Chemokines and Their Receptors. In: Madame Curie Bioscience Database [Internet].
- [119] Ramji D P and Davies T S 2015 Cytokines in atherosclerosis: Key players in all stages of disease and promising therapeutic targets *Cytokine Growth Factor Rev* 26 673-85
- [120] Aukrust P, Halvorsen B, Yndestad A, Ueland T, Øie E, Otterdal K, Gullestad L and Damås J K 2008 Chemokines and Cardiovascular Risk *Arteriosclerosis, thrombosis, and vascular biology* 28 1909-19
- [121] Moss J W E and Ramji D P 2016 Cytokines: Roles in atherosclerosis disease progression and potential therapeutic targets *Future medicinal chemistry* 8 1317-30
- [122] Ait-Oufella H, Taleb S, Mallat Z and Tedgui A 2011 Recent advances on the role of cytokines in atherosclerosis *Arteriosclerosis, thrombosis, and vascular biology* 31 969-79
- [123] Moore K J, Sheedy F J and Fisher E A 2013 Macrophages in atherosclerosis: a dynamic balance *Nat Rev Immunol* 13 709-21
- [124] Tedgui A and Mallat Z 2006 Cytokines in Atherosclerosis: Pathogenic and Regulatory Pathways *Physiological reviews* 86 515-81

- [125] Jin T, Xu X and Hereld D 2008 Chemotaxis, chemokine receptors and human disease *Cytokine* 44 1-8
- [126] de Munnik S M, Smit M J, Leurs R and Vischer H F 2015 Modulation of cellular signaling by herpesvirus-encoded G protein-coupled receptors *Frontiers in Pharmacology* 6
- [127] Mantovani A 1999 The chemokine system: redundancy for robust outputs *Immunology today* 20 254-7
- [128] Townson D H and Liptak A R 2003 Chemokines in the corpus luteum: Implications of leukocyte chemotaxis *Reproductive biology and endocrinology : RB&E* 1 94
- [129] Nibbs R J B and Graham G J 2013 Immune regulation by atypical chemokine receptors *Nat Rev Immunol* 13 815-29
- [130] Griffith J W, Sokol C L and Luster A D 2014 Chemokines and chemokine receptors: positioning cells for host defense and immunity *Annual review of immunology* 32 659-702
- [131] Balkwill F R 2012 The chemokine system and cancer *The Journal of pathology* 226 148-57
- [132] Zlotnik A and Yoshie O 2000 Chemokines: A New Classification System and Their Role in Immunity *Immunity* 12 121-7
- [133] Lazennec G and Richmond A 2010 Chemokines and chemokine receptors: new insights into cancer-related inflammation *Trends in molecular medicine* 16 133-44
- [134] Juan M and Colobran R 2001 *eLS*: John Wiley & Sons, Ltd)
- [135] Lacalle R A, Blanco R, Carmona-Rodríguez L, Martín-Leal A, Mira E and Mañes S 2017 *International Review of Cell and Molecular Biology*, ed G Lorenzo: Academic Press) pp 181-244
- [136] Stone M, Hayward J, Huang C, E. Huma Z and Sanchez J 2017 Mechanisms of Regulation of the Chemokine-Receptor Network *International Journal of Molecular Sciences* 18 342
- [137] Patel J, Channon K M and McNeill E 2013 The downstream regulation of chemokine receptor signalling: implications for atherosclerosis *Mediators of inflammation* 2013 459520
- [138] Salanga C L, O'Hayre M and Handel T 2009 Modulation of Chemokine Receptor Activity through Dimerization and Crosstalk *Cellular and molecular life sciences : CMLS* 66 1370-86
- [139] Vacchini A, Busnelli M, Chini B, Locati M and Borroni E M 2016 *Methods in enzymology*, ed M H Tracy: Academic Press) pp 421-40
- [140] Galkina E and Ley K 2009 Immune and Inflammatory Mechanisms of Atherosclerosis *Annual review of immunology* 27 165-97
- [141] Wan W and Murphy P M 2013 Regulation of atherogenesis by chemokines and chemokine receptors *Archivum immunologiae et therapiae experimentalis* 61 1-14
- [142] van der Vorst E P, Döring Y and Weber C 2015 Chemokines and their receptors in Atherosclerosis *Journal of molecular medicine (Berlin, Germany)* 93 963-71
- [143] Teicher B A and Fricker S P 2010 CXCL12 (SDF-1)/CXCR4 Pathway in Cancer *Clinical Cancer Research* 16 2927-31
- [144] Zerneck A, Schober A, Bot I, von Hundelshausen P, Liehn E A, Mopps B, Mericskay M, Gierschik P, Biessen E A and Weber C 2005 SDF-1 α /CXCR4 axis is instrumental in neointimal hyperplasia and recruitment of smooth muscle progenitor cells *Circ Res* 96 784-91
- [145] van der Vorst E P C, Döring Y and Weber C 2015 MIF and CXCL12 in Cardiovascular Diseases: Functional Differences and Similarities *Frontiers in Immunology* 6
- [146] Chatterjee M and Gawaz M 2013 Platelet-derived CXCL12 (SDF-1 α): basic mechanisms and clinical implications *Journal of thrombosis and haemostasis : JTH* 11 1954-67
- [147] van der Vorst E P, Döring Y and Weber C 2015 Chemokines *Arteriosclerosis, thrombosis, and vascular biology* 35 e52-6
- [148] Karshovska E, Weber C and von Hundelshausen P 2013 Platelet chemokines in health and disease *Thrombosis and haemostasis* 110 894-902
- [149] Noels H, Zhou B, Tilstam P V, Theelen W, Li X, Pawig L, Schmitz C, Akhtar S, Simsekylmaz S, Shagdarsuren E, Schober A, Adams R H, Bernhagen J, Liehn E A, Döring Y and Weber C 2014

- Deficiency of endothelial CXCR4 reduces reendothelialization and enhances neointimal hyperplasia after vascular injury in atherosclerosis-prone mice *Arteriosclerosis, thrombosis, and vascular biology* 34 1209-20
- [150] Doring Y, Pawig L, Weber C and Noels H 2014 The CXCL12/CXCR4 chemokine ligand/receptor axis in cardiovascular disease *Frontiers in physiology* 5 212
- [151] Cojoc M, Peitzsch C, Trautmann F, Polishchuk L, Telegeev G D and Dubrovskaya A 2013 Emerging targets in cancer management: role of the CXCL12/CXCR4 axis *OncoTargets and therapy* 6 1347-61
- [152] Gustavsson M, Wang L, van Gils N, Stephens B S, Zhang P, Schall T J, Yang S, Abagyan R, Chance M R, Kufareva I and Handel T M 2017 Structural basis of ligand interaction with atypical chemokine receptor 3 *Nat Commun* 8 14135
- [153] Sanchez-Martin L, Sanchez-Mateos P and Cabanas C 2013 CXCR7 impact on CXCL12 biology and disease *Trends in molecular medicine* 19 12-22
- [154] Cancellieri C, Vacchini A, Locati M, Bonecchi R and Borroni Elena M 2013 Atypical chemokine receptors: from silence to sound *Biochemical Society Transactions* 41 231-6
- [155] Vacchini A, Busnelli M, Chini B, Locati M and Borroni E M 2016 Analysis of G Protein and beta-Arrestin Activation in Chemokine Receptors Signaling *Methods in enzymology* 570 421-40
- [156] Luttrell L M and Lefkowitz R J 2002 The role of β -arrestins in the termination and transduction of G-protein-coupled receptor signals *Journal of cell science* 115 455-65
- [157] Bonecchi R and Graham G J 2016 Atypical Chemokine Receptors and Their Roles in the Resolution of the Inflammatory Response *Frontiers in Immunology* 7
- [158] Chen Q, Zhang M, Li Y, Xu D, Wang Y, Song A, Zhu B, Huang Y and Zheng J C 2015 CXCR7 Mediates Neural Progenitor Cells Migration to CXCL12 Independent of CXCR4 *Stem Cells (Dayton, Ohio)* 33 2574-85
- [159] Virgintino D, Errede M, Rizzi M, Girolamo F, Strippoli M, Walchli T, Robertson D, Frei K and Roncali L 2013 The CXCL12/CXCR4/CXCR7 ligand-receptor system regulates neuro-glio-vascular interactions and vessel growth during human brain development *Journal of inherited metabolic disease* 36 455-66
- [160] Bonecchi R and Graham G J 2016 Atypical Chemokine Receptors and Their Roles in the Resolution of the Inflammatory Response *Frontiers in Immunology* 7 224
- [161] Berahovich R D, Zabel B A, Lewen S, Walters M J, Ebsworth K, Wang Y, Jaen J C and Schall T J 2014 Endothelial expression of CXCR7 and the regulation of systemic CXCL12 levels *Immunology* 141 111-22
- [162] Costello C M, McCullagh B, Howell K, Sands M, Belperio J A, Keane M P, Gaine S and McLoughlin P 2012 A role for the CXCL12 receptor, CXCR7, in the pathogenesis of human pulmonary vascular disease *European Respiratory Journal*
- [163] Wurth R, Bajetto A, Harrison J K, Barbieri F and Florio T 2014 CXCL12 modulation of CXCR4 and CXCR7 activity in human glioblastoma stem-like cells and regulation of the tumor microenvironment *Frontiers in cellular neuroscience* 8 144
- [164] Thomas M N, Kalnins A, Andrassy M, Wagner A, Klussmann S, Rentsch M, Habicht A, Pratschke S, Stangl M, Bazhin A V, Meiser B, Fischereeder M, Werner J, Guba M and Andrassy J 2015 SDF-1/CXCR4/CXCR7 is pivotal for vascular smooth muscle cell proliferation and chronic allograft vasculopathy *Transplant international : official journal of the European Society for Organ Transplantation* 28 1426-35
- [165] Chatterjee M, Rath D and Gawaz M 2015 Role of chemokine receptors CXCR4 and CXCR7 for platelet function *Biochem Soc Trans* 43 720-6
- [166] Li X, Zhu M, Penfold M E, Koenen R R, Thiemann A, Heyll K, Akhtar S, Koyadan S, Wu Z, Gremse F, Kiessling F, van Zandvoort M, Schall T J, Weber C and Schober A 2014 Activation of CXCR7 limits atherosclerosis and improves hyperlipidemia by increasing cholesterol uptake in adipose tissue *Circulation* 129 1244-53

- [167] Zerneck A and Weber C 2014 Chemokines in atherosclerosis: proceedings resumed *Arteriosclerosis, thrombosis, and vascular biology* 34 742-50
- [168] Lamallice L, Le Boeuf F and Huot J 2007 Endothelial Cell Migration During Angiogenesis *Circulation Research* 100 782-94
- [169] Mostowy S and Cossart P 2012 Septins: the fourth component of the cytoskeleton *Nat Rev Mol Cell Biol* 13 183-94
- [170] Pollitt A Y and Insall R H 2009 WASP and SCAR/WAVE proteins: the drivers of actin assembly *Journal of cell science* 122 2575-8
- [171] Krause M and Gautreau A 2014 Steering cell migration: lamellipodium dynamics and the regulation of directional persistence *Nat Rev Mol Cell Biol* 15 577-90
- [172] Mattila P K and Lappalainen P 2008 Filopodia: molecular architecture and cellular functions *Nat Rev Mol Cell Biol* 9 446-54
- [173] Le Clainche C and Carlier M-F 2008 Regulation of Actin Assembly Associated With Protrusion and Adhesion in Cell Migration *Physiological reviews* 88 489-513
- [174] Pollard T D and Borisy G G 2003 Cellular motility driven by assembly and disassembly of actin filaments *Cell* 112 453-65
- [175] Parri M and Chiarugi P 2010 Rac and Rho GTPases in cancer cell motility control *Cell Communication and Signaling* 8 23
- [176] Hanna S and El-Sibai M 2013 Signaling networks of Rho GTPases in cell motility *Cellular signalling* 25 1955-61
- [177] Ridley A 2000 Rho Gtpases: Integrating Integrin Signaling *J Cell Biol* 150 f107-9
- [178] Biname F, Pawlak G, Roux P and Hibner U 2010 What makes cells move: requirements and obstacles for spontaneous cell motility *Molecular bioSystems* 6 648-61
- [179] Spiering D and Hodgson L 2011 Dynamics of the Rho-family small GTPases in actin regulation and motility *Cell Adh Migr* 5 170-80
- [180] Chi Q, Yin T, Gregersen H, Deng X, Fan Y, Zhao J, Liao D and Wang G 2014 Rear actomyosin contractility-driven directional cell migration in three-dimensional matrices: a mechano-chemical coupling mechanism *Journal of the Royal Society Interface* 11
- [181] Dráber P, Sulimenko V and Dráberová E 2012 Cytoskeleton in Mast Cell Signaling *Frontiers in Immunology* 3
- [182] Insall R H and Jones G E 2006 Moving matters: signals and mechanisms in directed cell migration *Nat Cell Biol* 8 776-9
- [183] Kölsch V, Charest P G and Firtel R A 2008 The regulation of cell motility and chemotaxis by phospholipid signaling *Journal of cell science* 121 551-9
- [184] Cenni V, Sirri A, Riccio M, Lattanzi G, Santi S, de Pol A, Maraldi N M and Marmiroli S 2003 Targeting of the Akt/PKB kinase to the actin skeleton *Cellular and molecular life sciences : CMLS* 60 2710-20
- [185] New D C and Wong Y H 2007 Molecular mechanisms mediating the G protein-coupled receptor regulation of cell cycle progression *Journal of Molecular Signaling* 2 2
- [186] Morrison D K 2012 MAP kinase pathways *Cold Spring Harbor perspectives in biology* 4
- [187] Goldsmith Z G and Dhanasekaran D N 0000 G Protein regulation of MAPK networks *Oncogene* 26 3122-42
- [188] Huang C, Jacobson K and Schaller M D 2004 MAP kinases and cell migration *Journal of cell science* 117 4619-28
- [189] Dhillon A S, Hagan S, Rath O and Kolch W 0000 MAP kinase signalling pathways in cancer *Oncogene* 26 3279-90
- [190] Eishingdrelo H and Kongsamut S 2013 Minireview: Targeting GPCR Activated ERK Pathways for Drug Discovery *Current Chemical Genomics and Translational Medicine* 7 9-15
- [191] Ueda Y, Hirai S, Osada S, Suzuki A, Mizuno K and Ohno S 1996 Protein kinase C activates the MEK-ERK pathway in a manner independent of Ras and dependent on Raf *The Journal of biological chemistry* 271 23512-9

- [192] Bar-Sagi D and Hall A 2000 Ras and Rho GTPases: a family reunion *Cell* 103
- [193] Vial E, Sahai E and Marshall C J 2003 ERK-MAPK signaling coordinately regulates activity of Rac1 and RhoA for tumor cell motility *Cancer Cell* 4
- [194] Zohrabian V M, Forzani B, Chau Z, Murali R and Jhanwar-Uniyal M 2009 Rho/ROCK and MAPK signaling pathways are involved in glioblastoma cell migration and proliferation *Anticancer research* 29 119-23
- [195] Pullikuth A K and Catling A D 2010 Extracellular signal-regulated kinase promotes Rho-dependent focal adhesion formation by suppressing p190A RhoGAP *Mol Cell Biol* 30 3233-48
- [196] Mendoza M C, Er E E and Blenis J The Ras-ERK and PI3K-mTOR pathways: cross-talk and compensation *Trends in Biochemical Sciences* 36 320-8
- [197] Sobolik-Delmaire T, Raman D, Sai J, Fan G H and Richmond A 2013 *Encyclopedia of Biological Chemistry*, ed M D Lane (Waltham: Academic Press) pp 480-5
- [198] DeFea K A 2007 Stop that cell! Beta-arrestin-dependent chemotaxis: a tale of localized actin assembly and receptor desensitization *Annual review of physiology* 69 535-60
- [199] DeWire S M, Ahn S, Lefkowitz R J and Shenoy S K 2007 Beta-arrestins and cell signaling *Annual review of physiology* 69 483-510
- [200] Xiao K, Sun J, Kim J, Rajagopal S, Zhai B, Villén J, Haas W, Kovacs J J, Shukla A K, Hara M R, Hernandez M, Lachmann A, Zhao S, Lin Y, Cheng Y, Mizuno K, Ma'ayan A, Gygi S P and Lefkowitz R J 2010 Global phosphorylation analysis of β -arrestin-mediated signaling downstream of a seven transmembrane receptor (7TMR) *Proceedings of the National Academy of Sciences* 107 15299-304
- [201] Vicente-Manzanares M, Choi C K and Horwitz A R 2009 Integrins in cell migration – the actin connection *Journal of cell science* 122 199-206
- [202] Hood J D and Cheresch D A 2002 Role of integrins in cell invasion and migration *Nat Rev Cancer* 2 91-100
- [203] Huttenlocher A and Horwitz A R 2011 Integrins in Cell Migration *Cold Spring Harbor perspectives in biology* 3
- [204] Niehrs C 0000 Function and biological roles of the Dickkopf family of Wnt modulators *Oncogene* 25 7469-81
- [205] Glinka A, Wu W, Delius H, Monaghan A P, Blumenstock C and Niehrs C 1998 Dickkopf-1 is a member of a new family of secreted proteins and functions in head induction *Nature* 391 357-62
- [206] Krupnik V E, Sharp J D, Jiang C, Robison K, Chickering T W, Amaravadi L, Brown D E, Guyot D, Mays G, Leiby K, Chang B, Duong T, Goodearl A D, Gearing D P, Sokol S Y and McCarthy S A 1999 Functional and structural diversity of the human Dickkopf gene family *Gene* 238
- [207] Niehrs C 2006 Function and biological roles of the Dickkopf family of Wnt modulators *Oncogene* 25 7469-81
- [208] Glinka A, Wu W, Delius H, Monaghan A P, Blumenstock C and Niehrs C 1998 Dickkopf-1 is a member of a new family of secreted proteins and functions in head induction *Nature* 391
- [209] Lieven O, Knobloch J and Rütter U 2010 The regulation of Dkk1 expression during embryonic development *Developmental biology* 340 256-68
- [210] Fedon Y, Bonniou A, Gay S, Vernus B, Bacou F and Bernardi H 2012 *Skeletal Muscle - From Myogenesis to Clinical Relations*, ed J Cseri (Rijeka: InTech) p Ch. 04
- [211] Komiya Y and Habas R 2008 Wnt signal transduction pathways *Organogenesis* 4 68-75
- [212] MacDonald B T, Tamai K and He X 2009 Wnt/ β -catenin signaling: components, mechanisms, and diseases *Developmental cell* 17 9-26
- [213] Bao J, Zheng J J and Wu D 2012 The structural basis of DKK-mediated inhibition of Wnt/LRP signaling *Science signaling* 5 pe22
- [214] MacDonald B T, Tamai K and He X 2009 Wnt/ β -catenin signaling: components, mechanisms, and diseases *Developmental cell* 17 9-26

- [215] Monaghan A P, Kioschis P, Wu W, Zuniga A, Bock D, Poustka A, Delius H and Niehrs C 1999 Dickkopf genes are co-ordinately expressed in mesodermal lineages *Mech Dev* 87
- [216] Nie X 2005 Dkk1, -2, and -3 expression in mouse craniofacial development *Journal of molecular histology* 36 367-72
- [217] Federico G, Meister M, Mathow D, Heine G H, Moldenhauer G, Popovic Z V, Nordström V, Kopp-Schneider A, Hielscher T, Nelson P J, Schaefer F, Porubsky S, Fliser D, Arnold B and Gröne H J Tubular Dickkopf-3 promotes the development of renal atrophy and fibrosis *JCI Insight* 1
- [218] Diep D B, Hoen N, Backman M, Machon O and Krauss S 2004 Characterisation of the Wnt antagonists and their response to conditionally activated Wnt signalling in the developing mouse forebrain *Brain research. Developmental brain research* 153 261-70
- [219] Zhang Y, Liu Y, Zhu X H, Zhang X D, Jiang D S, Bian Z Y, Zhang X F, Chen K, Wei X, Gao L, Zhu L H, Yang Q, Fan G C, Lau W B, Ma X and Li H 2014 Dickkopf-3 attenuates pressure overload-induced cardiac remodelling *Cardiovasc Res* 102 35-45
- [220] Bao M W, Cai Z, Zhang X J, Li L, Liu X, Wan N, Hu G, Wan F, Zhang R, Zhu X, Xia H and Li H 2015 Dickkopf-3 protects against cardiac dysfunction and ventricular remodelling following myocardial infarction *Basic research in cardiology* 110 25
- [221] Lu D, Bao D, Dong W, Liu N, Zhang X, Gao S, Ge W, Gao X and Zhang L 2016 Dkk3 prevents familial dilated cardiomyopathy development through Wnt pathway *Laboratory investigation; a journal of technical methods and pathology* 96 239-48
- [222] Cheng W L, Yang Y, Zhang X J, Guo J, Gong J, Gong F H, She Z G, Huang Z, Xia H and Li H 2017 Dickkopf-3 Ablation Attenuates the Development of Atherosclerosis in ApoE-Deficient Mice *Journal of the American Heart Association* 6
- [223] Wagner W, Wein F, Seckinger A, Frankhauser M, Wirkner U, Krause U, Blake J, Schwager C, Eckstein V, Ansorge W and Ho A D 2005 Comparative characteristics of mesenchymal stem cells from human bone marrow, adipose tissue, and umbilical cord blood *Experimental hematology* 33 1402-16
- [224] Medinger M, Tzankov A, Kern J, Pircher A, Hermann M, Ott H W, Gastl G, Untergasser G and Gunsilius E 2011 Increased Dkk3 protein expression in platelets and megakaryocytes of patients with myeloproliferative neoplasms *Thrombosis and haemostasis* 105 72-80
- [225] Tsuji T, Miyazaki M, Sakaguchi M, Inoue Y and Namba M 2000 A REIC Gene Shows Down-Regulation in Human Immortalized Cells and Human Tumor-Derived Cell Lines *Biochemical and Biophysical Research Communications* 268 20-4
- [226] Edamura K, Nasu Y, Takaishi M, Kobayashi T, Abarzua F, Sakaguchi M, Kashiwakura Y, Ebara S, Saika T, Watanabe M, Huh N H and Kumon H 2007 Adenovirus-mediated REIC/Dkk-3 gene transfer inhibits tumor growth and metastasis in an orthotopic prostate cancer model *Cancer gene therapy* 14 765-72
- [227] Romero D, Al-Shareef Z, Gorrone-Etxebarria I, Atkins S, Turrell F, Chhetri J, Bengoa-Vergniory N, Zenzmaier C, Berger P, Waxman J and Kypka R 2016 Dickkopf-3 regulates prostate epithelial cell acinar morphogenesis and prostate cancer cell invasion by limiting TGF-beta-dependent activation of matrix metalloproteases *Carcinogenesis* 37 18-29
- [228] Huo J, Zhang Y, Li R, Wang Y, Wu J and Zhang D 2016 Upregulated MicroRNA-25 Mediates the Migration of Melanoma Cells by Targeting DKK3 through the WNT/ β -Catenin Pathway *International Journal of Molecular Sciences* 17 1124
- [229] Xiang T, Li L, Yin X, Zhong L, Peng W, Qiu Z, Ren G and Tao Q 2013 Epigenetic silencing of the WNT antagonist Dickkopf 3 disrupts normal Wnt/beta-catenin signalling and apoptosis regulation in breast cancer cells *Journal of Cellular and Molecular Medicine* 17 1236-46
- [230] Saeb-Parsy K, Veerakumarasivam A, Wallard M J, Thorne N, Kawano Y, Murphy G, Neal D E, Mills I G and Kelly J D 2008 MT1-MMP regulates urothelial cell invasion via transcriptional regulation of Dickkopf-3 *Br J Cancer* 99 663-9

- [231] Guo Q and Qin W 2015 DKK3 blocked translocation of beta-catenin/EMT induced by hypoxia and improved gemcitabine therapeutic effect in pancreatic cancer Bxpc-3 cell *Journal of Cellular and Molecular Medicine* 19 2832-41
- [232] Pei Y, Yao Q, Yuan S, Xie B, Liu Y, Ye C and Zhuo H 2016 GATA4 promotes hepatoblastoma cell proliferation by altering expression of miR125b and DKK3 *Oncotarget* 7 77890-901
- [233] Katase N, Lefeuvre M, Tsujigiwa H, Fujii M, Ito S, Tamamura R, Buery R R, Gunduz M and Nagatsuka H 2013 Knockdown of Dkk-3 decreases cancer cell migration and invasion independently of the Wnt pathways in oral squamous cell carcinoma-derived cells *Oncology reports* 29 1349-55
- [234] Tsujimura N, Yamada N O, Kuranaga Y, Kumazaki M, Shinohara H, Taniguchi K and Akao Y 2016 A Novel Role of Dickkopf-Related Protein 3 in Macropinocytosis in Human Bladder Cancer T24 Cells *International Journal of Molecular Sciences* 17
- [235] Wang Z, Lin L, Thomas D G, Nadal E, Chang A C, Beer D G and Lin J 2015 The role of Dickkopf-3 overexpression in esophageal adenocarcinoma *The Journal of thoracic and cardiovascular surgery* 150 377-85.e2
- [236] Untergasser G, Steurer M, Zimmermann M, Hermann M, Kern J, Amberger A, Gastl G and Gunsilius E 2008 The Dickkopf-homolog 3 is expressed in tumor endothelial cells and supports capillary formation *International journal of cancer* 122 1539-47
- [237] Zitt M, Untergasser G, Amberger A, Moser P, Stadlmann S, Zitt M, Muller H M, Muhlmann G, Perathoner A, Margreiter R, Gunsilius E and Ofner D 2008 Dickkopf-3 as a new potential marker for neoangiogenesis in colorectal cancer: expression in cancer tissue and adjacent non-cancerous tissue *Disease markers* 24 101-9
- [238] Muhlmann G, Untergasser G, Zitt M, Zitt M, Maier H, Mikuz G, Kronberger I E, Haffner M C, Gunsilius E and Ofner D 2010 Immunohistochemically detectable dickkopf-3 expression in tumor vessels predicts survival in gastric cancer *Virchows Archiv : an international journal of pathology* 456 635-46
- [239] Kim B R, Lee E J, Seo S H, Lee S H and Rho S B 2015 Dickkopf-3 (DKK-3) obstructs VEGFR-2/Akt/mTOR signaling cascade by interacting of beta2-microglobulin (beta2M) in ovarian tumorigenesis *Cellular signalling* 27 2150-9
- [240] Li Y, Ye X, Tan C, Hongo J A, Zha J, Liu J, Kallop D, Ludlam M J and Pei L 2009 Axl as a potential therapeutic target in cancer: role of Axl in tumor growth, metastasis and angiogenesis *Oncogene* 28 3442-55
- [241] Watanabe M, Kashiwakura Y, Huang P, Ochiai K, Futami J, Li S A, Takaoka M, Nasu Y, Sakaguchi M, Huh N H and Kumon H 2009 Immunological aspects of REIC/Dkk-3 in monocyte differentiation and tumor regression *International journal of oncology* 34 657-63
- [242] Kinoshita R, Watanabe M, Huang P, Li S A, Sakaguchi M, Kumon H and Futami J 2015 The cysteine-rich core domain of REIC/Dkk-3 is critical for its effect on monocyte differentiation and tumor regression *Oncology reports* 33 2908-14
- [243] Wang X, Karamariti E, Simpson R, Wang W and Xu Q 2015 Dickkopf Homolog 3 Induces Stem Cell Differentiation into Smooth Muscle Lineage via ATF6 Signalling *The Journal of biological chemistry* 290 19844-52
- [244] Karamariti E, Margariti A, Winkler B, Wang X, Hong X, Baban D, Ragoussis J, Huang Y, Han J D, Wong M M, Sag C M, Shah A M, Hu Y and Xu Q 2013 Smooth muscle cells differentiated from reprogrammed embryonic lung fibroblasts through DKK3 signaling are potent for tissue engineering of vascular grafts *Circ Res* 112 1433-43
- [245] Fukusumi Y, Meier F, Gotz S, Matheus F, Irmeler M, Beckervordersandforth R, Faus-Kessler T, Minina E, Rauser B, Zhang J, Arenas E, Andersson E, Niehrs C, Beckers J, Simeone A, Wurst W and Prakash N 2015 Dickkopf 3 Promotes the Differentiation of a Rostrolateral Midbrain Dopaminergic Neuronal Subset In Vivo and from Pluripotent Stem Cells In Vitro in the Mouse *J Neurosci* 35 13385-401

- [246] Zhou M, Li Q and Wang R 2016 Current Experimental Methods for Characterizing Protein–Protein Interactions *ChemMedChem* 11 738-56
- [247] Merlini L, Dudin O and Martin S G 2013 Mate and fuse: how yeast cells do it *Open Biology* 3
- [248] Haber J E 2012 Mating-Type Genes and MAT Switching in *Saccharomyces cerevisiae* *Genetics* 191 33-64
- [249] Klar A J S 2010 The Yeast Mating-Type Switching Mechanism: A Memoir *Genetics* 186 443-9
- [250] Osman A 2004 Yeast two-hybrid assay for studying protein-protein interactions *Methods in molecular biology (Clifton, N.J.)* 270 403-22
- [251] Brückner A, Polge C, Lentze N, Auerbach D and Schlattner U 2009 Yeast Two-Hybrid, a Powerful Tool for Systems Biology *International Journal of Molecular Sciences* 10 2763-88
- [252] Traven A, Jelacic B and Sopta M 2006 Yeast Gal4: a transcriptional paradigm revisited *EMBO Reports* 7 496-9
- [253] Van Criekinge W and Beyaert R 1999 Yeast Two-Hybrid: State of the Art *Biological Procedures Online* 2 1-38
- [254] Chien C T, Bartel P L, Sternglanz R and Fields S 1991 The two-hybrid system: a method to identify and clone genes for proteins that interact with a protein of interest *Proceedings of the National Academy of Sciences of the United States of America* 88 9578-82
- [255] Hulme E C and Trevethick M A 2010 Ligand binding assays at equilibrium: validation and interpretation *Br J Pharmacol* 161 1219-37
- [256] Pollard T D 2010 A Guide to Simple and Informative Binding Assays *Mol Biol Cell* 21 4061-7
- [257] de Wit R H, de Munnik S M, Leurs R, Vischer H F and Smit M J 2016 *Methods in enzymology*, ed M H Tracy: Academic Press) pp 457-515
- [258] Copeland R A 2002 *Enzymes: John Wiley & Sons, Inc.*) pp 76-108
- [259] Worsdorfer P, Mekala S R, Bauer J, Edenhofer F, Kuerten S and Ergun S 2017 The vascular adventitia: An endogenous, omnipresent source of stem cells in the body *Pharmacol Ther* 171 13-29
- [260] Goligorsky M S and Salven P 2013 Concise review: endothelial stem and progenitor cells and their habitats *Stem cells translational medicine* 2 499-504
- [261] Stenmark K R, Yeager M E, El Kasmi K C, Nozik-Grayck E, Gerasimovskaya E V, Li M, Riddle S R and Frid M G 2013 The adventitia: essential regulator of vascular wall structure and function *Annual review of physiology* 75 23-47
- [262] Kawabe J and Hasebe N 2014 Role of the vasa vasorum and vascular resident stem cells in atherosclerosis *BioMed research international* 2014 701571
- [263] Sakihama H, Masunaga T, Yamashita K, Hashimoto T, Inobe M, Todo S and Uede T 2004 Stromal Cell–Derived Factor-1 and CXCR4 Interaction Is Critical for Development of Transplant Arteriosclerosis *Circulation* 110 2924-30
- [264] Zernecke A, Schober A, Bot I, von Hundelshausen P, Liehn E A, Möpps B, Mericskay M, Gierschik P, Biessen E A and Weber C 2005 SDF-1 α /CXCR4 Axis Is Instrumental in Neointimal Hyperplasia and Recruitment of Smooth Muscle Progenitor Cells *Circulation Research* 96 784-91
- [265] Hellstrom M, Kalen M, Lindahl P, Abramsson A and Betsholtz C 1999 Role of PDGF-B and PDGFR-beta in recruitment of vascular smooth muscle cells and pericytes during embryonic blood vessel formation in the mouse *Development* 126 3047-55
- [266] He C, Medley S C, Hu T, Hinsdale M E, Lupu F, Virmani R and Olson L E 2015 PDGFR β signalling regulates local inflammation and synergizes with hypercholesterolaemia to promote atherosclerosis *Nature Communications* 6 7770
- [267] Tang J, Kozaki K, Farr A G, Martin P J, Lindahl P, Betsholtz C and Raines E W 2005 The Absence of Platelet-Derived Growth Factor-B in Circulating Cells Promotes Immune and Inflammatory Responses in Atherosclerosis-Prone ApoE–/– Mice *The American Journal of Pathology* 167 901-12

- [268] Kozaki K, Kaminski W E, Tang J, Hollenbach S, Lindahl P, Sullivan C, Yu J C, Abe K, Martin P J, Ross R, Betsholtz C, Giese N A and Raines E W 2002 Blockade of Platelet-Derived Growth Factor or Its Receptors Transiently Delays but Does Not Prevent Fibrous Cap Formation in ApoE Null Mice *The American Journal of Pathology* 161 1395-407
- [269] Baker M, Robinson S D, Lechertier T, Barber P R, Tavora B, D'Amico G, Jones D T, Vojnovic B and Hodivala-Dilke K 2012 Use of the mouse aortic ring assay to study angiogenesis *Nat. Protocols* 7 89-104
- [270] Raines E W 2004 PDGF and cardiovascular disease *Cytokine & Growth Factor Reviews* 15 237-54
- [271] Bornfeldt K E, Raines E W, Nakano T, Graves L M, Krebs E G and Ross R 1994 Insulin-like growth factor-I and platelet-derived growth factor-BB induce directed migration of human arterial smooth muscle cells via signaling pathways that are distinct from those of proliferation *The Journal of Clinical Investigation* 93 1266-74
- [272] Ferns G, Raines E, Sprugel K, Motani A, Reidy M and Ross R 1991 Inhibition of neointimal smooth muscle accumulation after angioplasty by an antibody to PDGF *Science* 253 1129-32
- [273] Kang H, Ahn D H, Pak J H, Seo K, Baek N and Jang S 2016 Magnobovitol inhibits smooth muscle cell migration by suppressing PDGF-R β phosphorylation and inhibiting matrix metalloproteinase-2 expression *International Journal of Molecular Medicine* 37 1239-46
- [274] Lee C-K, Lee H M, Kim H J, Park H-J, Won K-J, Roh H Y, Choi W S, Jeon B H, Park T-K and Kim B 2007 Syk contributes to PDGF-BB-mediated migration of rat aortic smooth muscle cells via MAPK pathways *Cardiovascular Research* 74 159-68
- [275] Son J E, Jeong H, Kim H, Kim Y A, Lee E, Lee H J and Lee K W 2014 Pelargonidin attenuates PDGF-BB-induced aortic smooth muscle cell proliferation and migration by direct inhibition of focal adhesion kinase *Biochemical Pharmacology* 89 236-45
- [276] Yang K and Proweller A 2011 Vascular smooth muscle Notch signals regulate endothelial cell sensitivity to angiogenic stimulation *The Journal of biological chemistry* 286 13741-53
- [277] Getz G S and Reardon C A 2012 Animal Models of Atherosclerosis *Arteriosclerosis, thrombosis, and vascular biology* 32 1104-15
- [278] Potteaux S, Ait-Oufella H and Mallat Z 2007 Mouse models of atherosclerosis *Drug Discovery Today: Disease Models* 4 165-70
- [279] Bellacen K and Lewis E C 2009 Aortic Ring Assay *Journal of Visualized Experiments : JoVE*
- [280] Nicosia R F 2009 The aortic ring model of angiogenesis: a quarter century of search and discovery *Journal of Cellular and Molecular Medicine* 13 4113-36
- [281] Schober A, Knarren S, Lietz M, Lin E A and Weber C 2003 Crucial role of stromal cell-derived factor-1 α in neointima formation after vascular injury in apolipoprotein E-deficient mice *Circulation* 108 2491-7
- [282] Hattermann K and Mentlein R 2013 An Infernal Trio: The chemokine CXCL12 and its receptors CXCR4 and CXCR7 in tumor biology *Annals of Anatomy - Anatomischer Anzeiger* 195 103-10
- [283] Puchert M and Engele J 2014 The peculiarities of the SDF-1/CXCL12 system: in some cells, CXCR4 and CXCR7 sing solos, in others, they sing duets *Cell and tissue research* 355 239-53
- [284] Thelen M and Thelen S 2008 CXCR7, CXCR4 and CXCL12: An eccentric trio? *Journal of Neuroimmunology* 198 9-13
- [285] Mao B, Wu W, Davidson G, Marhold J, Li M, Mechler B M, Delius H, Hoppe D, Stannek P, Walter C, Glinka A and Niehrs C 2002 Kremen proteins are Dickkopf receptors that regulate Wnt/ β -catenin signalling *Nature* 417
- [286] Mao B, Wu W, Li Y, Hoppe D, Stannek P, Glinka A and Niehrs C 2001 LDL-receptor-related protein 6 is a receptor for Dickkopf proteins *Nature* 411 321-5
- [287] Mao B and Niehrs C 2003 Kremen2 modulates Dickkopf2 activity during Wnt/LRP6 signaling *Gene* 302

- [288] Mao B and Niehrs C 2003 Kremen2 modulates Dickkopf2 activity during Wnt/IRP6 signaling *Gene* 302 179-83
- [289] Heesen M, Berman M A, Charest A, Housman D, Gerard C and Dorf M E 1998 Cloning and chromosomal mapping of an orphan chemokine receptor: mouse RDC1 *Immunogenetics* 47 364-70
- [290] Wu K, Cui L, Yang Y, Zhao J, Zhu D, Liu D, Zhang C, Qi Y, Li X, Li W and Zhao S 2016 Silencing of CXCR2 and CXCR7 protects against esophageal cancer *American journal of translational research* 8 3398-408
- [291] Huang Y L, Liu X L, Xu N, Xiao Y J and Gao G L 2014 Expression and function of CXCR2, CXCR7 of acute leukemic cells in rat *Asian Pacific journal of tropical medicine* 7 417-20
- [292] Nakamura R E I and Hackam A S 2010 Analysis of Dickkopf3 interactions with Wnt signaling receptors *Growth Factors* 28 232-42
- [293] Gong J, Meng H-B, Hua J I E, Song Z-S, He Z-G, Zhou B O and Qian M-P 2014 The SDF-1/CXCR4 axis regulates migration of transplanted bone marrow mesenchymal stem cells towards the pancreas in rats with acute pancreatitis *Molecular medicine reports* 9 1575-82
- [294] Shi X, Guo L- W, Seedial S, Takayama T, Wang B, Zhang M, Franco S R, Si Y, Chaudhary M A, Liu B and Kent K C 2016 Local CXCR4 Upregulation in the Injured Arterial Wall Contributes to Intimal Hyperplasia *Stem Cells (Dayton, Ohio)* 34 2744-57
- [295] Cai W-W, Fang N-Y, Sheng J, Ma S-J and Chen Z-H 2011 Effects of SDF-1 α /CXCR4 on vascular smooth muscle cells and bone marrow mesenchymal cells in a rat carotid artery balloon injury model *Journal of Applied Biomedicine* 9 129-41
- [296] Jie W, Wang X, Zhang Y, Guo J, Kuang D, Zhu P, Wang G and Ao Q 2010 SDF-1 α /CXCR4 axis is involved in glucose-potentiated proliferation and chemotaxis in rat vascular smooth muscle cells *International journal of experimental pathology* 91 436-44
- [297] Balabanian K, Lagane B, Infantino S, Chow K Y, Harriague J, Moepps B, Arenzana-Seisdedos F, Thelen M and Bachelier F 2005 The chemokine SDF-1/CXCL12 binds to and signals through the orphan receptor RDC1 in T lymphocytes *The Journal of biological chemistry* 280 35760-6
- [298] Di Salvo J, Koch G E, Johnson K E, Blake A D, Daugherty B L, DeMartino J A, Sirotna-Meisher A, Liu Y, Springer M S, Cascieri M A and Sullivan K A 2000 The CXCR4 agonist ligand stromal derived factor-1 maintains high affinity for receptors in both Galpha(i)-coupled and uncoupled states *European Journal of Pharmacology* 409 143-54
- [299] Campbell M, Allen W E, Sawyer C, Vanhaesebroeck B and Trimble E R 2004 Glucose-potentiated chemotaxis in human vascular smooth muscle is dependent on cross-talk between the PI3K and MAPK signaling pathways *Circ Res* 95 380-8
- [300] Walker E H, Pacold M E, Perisic O, Stephens L, Hawkins P T, Wymann M P and Williams R L 2000 Structural Determinants of Phosphoinositide 3-Kinase Inhibition by Wortmannin, LY294002, Quercetin, Myricetin, and Staurosporine *Molecular Cell* 6 909-19
- [301] Vlahos C J, Matter W F, Hui K Y and Brown R F 1994 A specific inhibitor of phosphatidylinositol 3-kinase, 2-(4-morpholinyl)-8-phenyl-4H-1-benzopyran-4-one (LY294002) *The Journal of biological chemistry* 269 5241-8
- [302] Chrzanowska-Wodnicka M and Burridge K 1996 Rho-stimulated contractility drives the formation of stress fibers and focal adhesions *The Journal of Cell Biology* 133 1403-15
- [303] Amano M, Nakayama M and Kaibuchi K 2010 Rho-Kinase/ROCK: A Key Regulator of the Cytoskeleton and Cell Polarity *Cytoskeleton (Hoboken, N.j.)* 67 545-54
- [304] Katoh K, Kano Y and Noda Y 2011 Rho-associated kinase-dependent contraction of stress fibres and the organization of focal adhesions *Journal of the Royal Society Interface* 8 305-11
- [305] Ai S, Kuzuya M, Koike T, Asai T, Kanda S, Maeda K, Shibata T and Iguchi A 2001 Rho-Rho kinase is involved in smooth muscle cell migration through myosin light chain phosphorylation-dependent and independent pathways *Atherosclerosis* 155 321-7

- [306] Nakamura R E, Hunter D D, Yi H, Brunken W J and Hackam A S 2007 Identification of two novel activities of the Wnt signaling regulator Dickkopf 3 and characterization of its expression in the mouse retina *BMC Cell Biol* 8 52
- [307] Caricasole A, Ferraro T, Iacovelli L, Barletta E, Caruso A, Melchiorri D, Terstappen G C and Nicoletti F 2003 Functional characterization of WNT7A signaling in PC12 cells: interaction with a FZD5 × LRP6 receptor complex and modulation by Dickkopf proteins *The Journal of biological chemistry* 278
- [308] Hoang B H, Kubo T, Healey J H, Yang R, Nathan S S, Kolb E A, Mazza B, Meyers P A and Gorlick R 2004 Dickkopf 3 inhibits invasion and motility of Saos-2 osteosarcoma cells by modulating the Wnt-beta-catenin pathway *Cancer Res* 64
- [309] Hsieh S Y, Hsieh P S, Chiu C T and Chen W Y 2004 Dickkopf-3/REIC functions as a suppressor gene of tumor growth *Oncogene* 23
- [310] Veeck J and Dahl E 2012 Targeting the Wnt pathway in cancer: The emerging role of Dickkopf-3 *Biochimica et Biophysica Acta (BBA) - Reviews on Cancer* 1825 18-28
- [311] Das D S, Wadhwa N, Kunj N, Sarda K, Pradhan B S and Majumdar S S 2013 Dickkopf Homolog 3 (DKK3) Plays a Crucial Role Upstream of WNT/ β -CATENIN Signaling for Sertoli Cell Mediated Regulation of Spermatogenesis *PLoS ONE* 8
- [312] Anastas J N and Moon R T 2013 WNT signalling pathways as therapeutic targets in cancer *Nat Rev Cancer* 13 11-26
- [313] Tamai K, Semenov M, Kato Y, Spokony R, Liu C, Katsuyama Y, Hess F, Saint-Jeannet J-P and He X 2000 LDL-receptor-related proteins in Wnt signal transduction *Nature* 407 530-5
- [314] Pinson K I, Brennan J, Monkley S, Avery B J and Skarnes W C 2000 An LDL-receptor-related protein mediates Wnt signalling in mice *Nature* 407 535-8
- [315] Le P N, McDermott J D and Jimeno A 2015 Targeting the Wnt pathway in human cancers: Therapeutic targeting with a focus on OMP-54F28 *Pharmacology & Therapeutics* 146 1-11
- [316] Wallingford J B and Habas R 2005 The developmental biology of Dishevelled: an enigmatic protein governing cell fate and cell polarity *Development* 132 4421-36
- [317] Verheyen E M and Gottardi C J 2010 Regulation of Wnt/ β -Catenin Signaling by Protein Kinases *Developmental dynamics : an official publication of the American Association of Anatomists* 239 34-44
- [318] Yamanaka H, Moriguchi T, Masuyama N, Kusakabe M, Hanafusa H, Takada R, Takada S and Nishida E 2002 JNK functions in the non-canonical Wnt pathway to regulate convergent extension movements in vertebrates *EMBO Reports* 3 69-75
- [319] Li L, Yuan H, Xie W, Mao J, Caruso A M, McMahon A, Sussman D J and Wu D 1999 Dishevelled proteins lead to two signaling pathways. Regulation of LEF-1 and c-Jun N-terminal kinase in mammalian cells *The Journal of biological chemistry* 274 129-34
- [320] Habas R, Dawid I B and He X 2003 Coactivation of Rac and Rho by Wnt/Frizzled signaling is required for vertebrate gastrulation *Genes & development* 17 295-309
- [321] Veeman M T, Axelrod J D and Moon R T 2003 A second canon. Functions and mechanisms of beta-catenin-independent Wnt signaling *Developmental cell* 5 367-77
- [322] Kim G H and Han J K 2005 JNK and ROK α function in the noncanonical Wnt/RhoA signaling pathway to regulate *Xenopus* convergent extension movements *Developmental dynamics : an official publication of the American Association of Anatomists* 232 958-68
- [323] Tahinci E and Symes K 2003 Distinct functions of Rho and Rac are required for convergent extension during *Xenopus* gastrulation *Developmental biology* 259 318-35
- [324] Rao V S, Srinivas K, Sujini G N and Kumar G N S 2014 Protein-Protein Interaction Detection: Methods and Analysis *International Journal of Proteomics* 2014 12
- [325] Serebriiskii I 2010 Yeast two-hybrid system for studying protein-protein interactions--stage 2: Transforming and characterizing the library *Cold Spring Harbor protocols* 2010 pdb.prot5430

- [326] Wagemans J and Lavigne R 2015 Identification of protein-protein interactions by standard gal4p-based yeast two-hybrid screening *Methods in molecular biology (Clifton, N.J.)* 1278 409-31
- [327] Iwabuchi K, Li B, Bartel P and Fields S 1993 Use of the two-hybrid system to identify the domain of p53 involved in oligomerization *Oncogene* 8 1693-6
- [328] Zech T, Calaminus S D, Caswell P, Spence H J, Carnell M, Insall R H, Norman J and Machesky L M 2011 The Arp2/3 activator WASH regulates alpha5beta1-integrin-mediated invasive migration *Journal of cell science* 124 3753-9
- [329] Collo G and Pepper M S 1999 Endothelial cell integrin alpha5beta1 expression is modulated by cytokines and during migration in vitro *Journal of cell science* 112 (Pt 4) 569-78
- [330] Schaffner F, Ray A M and Dontenwill M 2013 Integrin $\alpha 5\beta 1$, the Fibronectin Receptor, as a Pertinent Therapeutic Target in Solid Tumors *Cancers* 5 27-47
- [331] Takagi J, Strokovich K, Springer T A and Walz T 2003 Structure of integrin alpha5beta1 in complex with fibronectin *Embo j* 22 4607-15
- [332] Lomas Amanda C, Mellody Kieran T, Freeman Lyle J, Bax Daniel V, Shuttleworth C A and Kielty Cay M 2007 Fibulin-5 binds human smooth-muscle cells through $\alpha 5\beta 1$ and $\alpha 4\beta 1$ integrins, but does not support receptor activation *Biochemical Journal* 405 417-28
- [333] Yanagisawa H, Schluterman M K and Brekken R A 2009 Fibulin-5, an integrin-binding matricellular protein: its function in development and disease *Journal of Cell Communication and Signaling* 3 337-47
- [334] Mitchell R N and Libby P 2007 Vascular remodeling in transplant vasculopathy *Circ Res* 100 967-78
- [335] Adams B, Xiao Q and Xu Q 2007 Stem Cell Therapy for Vascular Disease *Trends in Cardiovascular Medicine* 17 246-51
- [336] Costa M A and Simon D I 2005 Molecular basis of restenosis and drug-eluting stents *Circulation* 111 2257-73
- [337] von Hundelshausen P and Weber C 2007 Platelets as immune cells: bridging inflammation and cardiovascular disease *Circ Res* 100 27-40
- [338] Tuttolomondo A, Di Raimondo D, Pecoraro R, Arnao V, Pinto A and Licata G 2012 Atherosclerosis as an inflammatory disease *Current pharmaceutical design* 18 4266-88
- [339] Hansson G K, Robertson A K and Soderberg-Naucler C 2006 Inflammation and atherosclerosis *Annual review of pathology* 1 297-329
- [340] Libby P 2002 Inflammation in atherosclerosis *Nature* 420 868-74
- [341] Hansson G K 2005 Inflammation, atherosclerosis, and coronary artery disease *The New England journal of medicine* 352 1685-95
- [342] Gleissner C A, von Hundelshausen P and Ley K 2008 Platelet chemokines in vascular disease *Arteriosclerosis, thrombosis, and vascular biology* 28 1920-7
- [343] Zerneck A, Shagdarsuren E and Weber C 2008 Chemokines in atherosclerosis: an update *Arteriosclerosis, thrombosis, and vascular biology* 28 1897-908
- [344] Kukhtina N B, Aref'eva T I, Aref'eva A M, Akchurin R S and Krasnikova T L 2008 [Expression of chemokines and cytokines in atherosclerotic plaques and internal membrane of the arteries in patients with coronary artery disease] *Terapevticheskii arkhiv* 80 63-9
- [345] Weber C, Doring Y and Noels H 2016 Potential cell-specific functions of CXCR4 in atherosclerosis *Hamostaseologie* 36 97-102
- [346] Askari A T, Unzek S, Popovic Z B, Goldman C K, Forudi F, Kiedrowski M, Rovner A, Ellis S G, Thomas J D, DiCorleto P E, Topol E J and Penn M S 2003 Effect of stromal-cell-derived factor 1 on stem-cell homing and tissue regeneration in ischaemic cardiomyopathy *The Lancet* 362 697-703
- [347] Sainz J and Sata M 2007 CXCR4, a key modulator of vascular progenitor cells *Arteriosclerosis, thrombosis, and vascular biology* 27 263-5

- [348] Stellos K and Gawaz M 2007 Platelets and stromal cell-derived factor-1 in progenitor cell recruitment *Seminars in thrombosis and hemostasis* 33 159-64
- [349] Sainz J and Sata M 2008 Open sesame! CXCR4 blockade recruits neutrophils into the plaque *Circ Res* 102 154-6
- [350] Akhtar S, Gremse F, Kiessling F, Weber C and Schober A 2013 CXCL12 promotes the stabilization of atherosclerotic lesions mediated by smooth muscle progenitor cells in Apoe-deficient mice *Arteriosclerosis, thrombosis, and vascular biology* 33 679-86
- [351] Wei D, Wang G, Tang C, Qiu J, Zhao J, Gregersen H and Deng L 2012 Upregulation of SDF-1 is associated with atherosclerosis lesions induced by LDL concentration polarization *Annals of biomedical engineering* 40 1018-27
- [352] Ma W, Liu Y, Ellison N and Shen J 2013 Induction of C-X-C chemokine receptor type 7 (CXCR7) switches stromal cell-derived factor-1 (SDF-1) signaling and phagocytic activity in macrophages linked to atherosclerosis *The Journal of biological chemistry* 288 15481-94
- [353] Luker K, Gupta M and Luker G 2009 Bioluminescent CXCL12 fusion protein for cellular studies of CXCR4 and CXCR7 *BioTechniques* 47 625-32
- [354] Burns J M, Summers B C, Wang Y, Melikian A, Berahovich R, Miao Z, Penfold M E, Sunshine M J, Littman D R, Kuo C J, Wei K, McMaster B E, Wright K, Howard M C and Schall T J 2006 A novel chemokine receptor for SDF-1 and I-TAC involved in cell survival, cell adhesion, and tumor development *The Journal of experimental medicine* 203 2201-13
- [355] Balabanian K, Lagane B, Infantino S, Chow K Y C, Harriague J, Moepps B, Arenzana-Seisdedos F, Thelen M and Bachelier F 2005 The Chemokine SDF-1/CXCL12 Binds to and Signals through the Orphan Receptor RDC1 in T Lymphocytes *Journal of Biological Chemistry* 280 35760-6
- [356] Tarnowski M, Liu R, Wysoczynski M, Ratajczak J, Kucia M and Ratajczak M Z 2010 CXCR7: a new SDF-1-binding receptor in contrast to normal CD34(+) progenitors is functional and is expressed at higher level in human malignant hematopoietic cells *European journal of haematology* 85 472-83
- [357] Zabel B A, Lewen S, Berahovich R D, Jaen J C and Schall T J 2011 The novel chemokine receptor CXCR7 regulates trans-endothelial migration of cancer cells *Molecular cancer* 10 73
- [358] Luker K E, Mihalko L A, Schmidt B T, Lewin S A, Ray P, Shcherbo D, Chudakov D M and Luker G D 2011 In vivo imaging of ligand receptor binding with Gaussia luciferase complementation *Nature medicine* 18 172-7
- [359] Liu Y, Carson-Walter E and Walter K A 2014 Chemokine receptor CXCR7 is a functional receptor for CXCL12 in brain endothelial cells *PLoS ONE* 9 e103938
- [360] Hatse S, Princen K, Bridger G, De Clercq E and Schols D 2002 Chemokine receptor inhibition by AMD3100 is strictly confined to CXCR4 *FEBS letters* 527 255-62
- [361] Cashen A, Lopez S, Gao F, Calandra G, MacFarland R, Badel K and DiPersio J 2008 A phase II study of plerixafor (AMD3100) plus G-CSF for autologous hematopoietic progenitor cell mobilization in patients with Hodgkin lymphoma *Biology of blood and marrow transplantation : journal of the American Society for Blood and Marrow Transplantation* 14 1253-61
- [362] Donahue R E, Jin P, Bonifacino A C, Metzger M E, Ren J, Wang E and Stroncek D F 2009 Plerixafor (AMD3100) and granulocyte colony-stimulating factor (G-CSF) mobilize different CD34+ cell populations based on global gene and microRNA expression signatures *Blood* 114 2530-41
- [363] Broxmeyer H E, Orschell C M, Clapp D W, Hangoc G, Cooper S, Plett P A, Liles W C, Li X, Graham-Evans B, Campbell T B, Calandra G, Bridger G, Dale D C and Srour E F 2005 Rapid mobilization of murine and human hematopoietic stem and progenitor cells with AMD3100, a CXCR4 antagonist *The Journal of experimental medicine* 201 1307-18
- [364] Jujo K, Hamada H, Iwakura A, Thorne T, Sekiguchi H, Clarke T, Ito A, Misener S, Tanaka T, Klyachko E, Kobayashi K, Tongers J, Roncalli J, Tsurumi Y, Hagiwara N and Losordo D W 2010

- CXCR4 blockade augments bone marrow progenitor cell recruitment to the neovasculature and reduces mortality after myocardial infarction *Proceedings of the National Academy of Sciences* 107 11008-13
- [365] Nishimura Y, Li M, Qin G, Hamada H, Asai J, Takenaka H, Sekiguchi H, Renault M-A, Jujo K, Katoh N, Kishimoto S, Ito A, Kamide C, Kenny J, Millay M, Misener S, Thorne T and Losordo D W 2012 CXCR4 Antagonist AMD3100 Accelerates Impaired Wound Healing in Diabetic Mice *Journal of Investigative Dermatology* 132 711-20
- [366] Hatzistergos K E, Saur D, Seidler B, Balkan W, Breton M, Valasaki K, Takeuchi L M, Landin A M, Khan A and Hare J M 2016 Stimulatory Effects of Mesenchymal Stem Cells on cKit+ Cardiac Stem Cells Are Mediated by SDF1/CXCR4 and SCF/cKit Signaling Pathways *Circ Res* 119 921-30
- [367] Blum A, Childs R W, Smith A, Patibandla S, Zalos G, Samsel L, McCoy J P, Calandra G, Csako G and Cannon R O, 3rd 2009 Targeted antagonism of CXCR4 mobilizes progenitor cells under investigation for cardiovascular disease *Cytotherapy* 11 1016-9
- [368] Kraemer B F, Borst O, Gehring E M, Schoenberger T, Urban B, Ninci E, Seizer P, Schmidt C, Bigalke B, Koch M, Martinovic I, Daub K, Merz T, Schwanitz L, Stellos K, Fiesel F, Schaller M, Lang F, Gawaz M and Lindemann S 2010 PI3 kinase-dependent stimulation of platelet migration by stromal cell-derived factor 1 (SDF-1) *Journal of molecular medicine (Berlin, Germany)* 88 1277-88
- [369] Young K C, Torres E, Hatzistergos K E, Hehre D, Suguihara C and Hare J M 2009 Inhibition of the SDF-1/CXCR4 Axis Attenuates Neonatal Hypoxia-Induced Pulmonary Hypertension *Circulation Research* 104 1293-301
- [370] Shiba Y, Takahashi M, Yoshioka T, Yajima N, Morimoto H, Izawa A, Ise H, Hatake K, Motoyoshi K and Ikeda U 2007 M-CSF Accelerates Neointimal Formation in the Early Phase After Vascular Injury in Mice *The Critical Role of the SDF-1-CXCR4 System* 27 283-9
- [371] Hristov M and Weber C 2009 Progenitor cell trafficking in the vascular wall *Journal of thrombosis and haemostasis : JTH* 7 Suppl 1 31-4
- [372] Hristov M and Weber C 2008 Ambivalence of progenitor cells in vascular repair and plaque stability *Current opinion in lipidology* 19 491-7
- [373] Xu J, Wu D, Yang Y, Ji K and Gao P 2016 Endothelial-like cells differentiated from mesenchymal stem cells attenuate neointimal hyperplasia after vascular injury *Molecular medicine reports* 14 4830-6
- [374] Chappell J, Harman J L, Narasimhan V M, Yu H, Foote K, Simons B D, Bennett M R and Jorgensen H F 2016 Extensive Proliferation of a Subset of Differentiated, yet Plastic, Medial Vascular Smooth Muscle Cells Contributes to Neointimal Formation in Mouse Injury and Atherosclerosis Models *Circ Res* 119 1313-23
- [375] Mayr M, Zampetaki A, Sidibe A, Mayr U, Yin X, De Souza A I, Chung Y L, Madhu B, Quax P H, Hu Y, Griffiths J R and Xu Q 2008 Proteomic and metabolomic analysis of smooth muscle cells derived from the arterial media and adventitial progenitors of apolipoprotein E-deficient mice *Circ Res* 102 1046-56
- [376] Majesky M W, Horita H, Ostriker A, Lu S, Regan J N, Bagchi A, Dong X R, Poczobutt J, Nemenoff R A and Weiser-Evans M C 2017 Differentiated Smooth Muscle Cells Generate a Subpopulation of Resident Vascular Progenitor Cells in the Adventitia Regulated by Klf4 *Circ Res* 120 296-311
- [377] Klein D, Hohn H P, Kleff V, Tilki D and Ergun S 2010 Vascular wall-resident stem cells *Histology and histopathology* 25 681-9
- [378] Tigges U, Komatsu M and Stallcup W B 2013 Adventitial pericyte progenitor/mesenchymal stem cells participate in the restenotic response to arterial injury *Journal of vascular research* 50 134-44
- [379] Pacilli A and Pasquinelli G 2009 Vascular wall resident progenitor cells: a review *Experimental cell research* 315 901-14

- [380] Ergun S, Tilki D, Hohn H P, Gehling U and Kilic N 2007 Potential implications of vascular wall resident endothelial progenitor cells *Thrombosis and haemostasis* 98 930-9
- [381] Basile D P and Yoder M C 2014 Circulating and tissue resident endothelial progenitor cells *Journal of cellular physiology* 229 10-6
- [382] Bobryshev Y V, Orekhov A N and Chistiakov D A 2015 Vascular stem/progenitor cells: current status of the problem *Cell and tissue research* 362 1-7
- [383] Fricker S P 2008 A novel CXCR4 antagonist for hematopoietic stem cell mobilization *Expert opinion on investigational drugs* 17 1749-60
- [384] Tomankova T, Kriegova E and Liu M 2015 Chemokine receptors and their therapeutic opportunities in diseased lung: Far beyond leukocyte trafficking *American Journal of Physiology - Lung Cellular and Molecular Physiology* 308 L603-L18
- [385] Klarenbeek A, Maussang D, Blanchetot C, Saunders M, van der Woning S, Smit M, de Haard H and Hofman E 2012 Targeting chemokines and chemokine receptors with antibodies *Drug Discovery Today: Technologies* 9 e237-e44
- [386] Xu D, Li R, Wu J, Jiang L and Zhong H A 2016 Drug Design Targeting the CXCR4/CXCR7/CXCL12 Pathway *Current topics in medicinal chemistry* 16 1441-51
- [387] Ali M T, Martin K, Kumar A H, Cavallin E, Pierrou S, Gleeson B M, McPheat W L, Turner E C, Huang C L, Khider W, Vaughan C and Caplice N M 2015 A novel CX3CR1 antagonist eluting stent reduces stenosis by targeting inflammation *Biomaterials* 69 22-9
- [388] Louis S F and Zahradka P 2010 Vascular smooth muscle cell motility: From migration to invasion *Experimental & Clinical Cardiology* 15 e75-85
- [389] Marx S O, Totary-Jain H and Marks A R 2011 Vascular Smooth Muscle Cell Proliferation in Restenosis *Circulation. Cardiovascular interventions* 4
- [390] Dzau V J, Braun-Dullaeus R C and Sedding D G 2002 Vascular proliferation and atherosclerosis: new perspectives and therapeutic strategies *Nature medicine* 8 1249-56
- [391] Surmi B K and Hasty A H 2010 The Role of Chemokines in Recruitment of Immune Cells to the Artery Wall and Adipose Tissue *Vascul Pharmacol* 52 27-36
- [392] Orlandi A 2015 The Contribution of Resident Vascular Stem Cells to Arterial Pathology *International Journal of Stem Cells* 8 9-17
- [393] Vagima Y, Lapid K, Kollet O, Goichberg P, Alon R and Lapidot T 2011 Pathways implicated in stem cell migration: the SDF-1/CXCR4 axis *Methods in molecular biology (Clifton, N.J.)* 750 277-89
- [394] Justus C R, Leffler N, Ruiz-Echevarria M and Yang L V 2014 In vitro Cell Migration and Invasion Assays *Journal of Visualized Experiments : JoVE*
- [395] Valster A, Tran N L, Nakada M, Berens M E, Chan A Y and Symons M 2005 Cell migration and invasion assays *Methods* 37 208-15
- [396] Decaestecker C, Debeir O, Van Ham P and Kiss R 2007 Can anti-migratory drugs be screened in vitro? A review of 2D and 3D assays for the quantitative analysis of cell migration *Medicinal research reviews* 27 149-76
- [397] Kramer N, Walzl A, Unger C, Rosner M, Krupitza G, Hengstschlager M and Dolznig H 2013 In vitro cell migration and invasion assays *Mutation research* 752 10-24
- [398] Xu H and Heilshorn S C 2013 Microfluidic investigation of BDNF-enhanced neural stem cell chemotaxis in CXCL12 gradients *Small (Weinheim an der Bergstrasse, Germany)* 9 585-95
- [399] Neel N F, Schutyser E, Sai J, Fan G H and Richmond A 2005 Chemokine receptor internalization and intracellular trafficking *Cytokine Growth Factor Rev* 16 637-58
- [400] Marchese A, Chen C, Kim Y-M and Benovic J L 2003 The ins and outs of G protein-coupled receptor trafficking *Trends in Biochemical Sciences* 28 369-76
- [401] Mirisola V, Zuccarino A, Bachmeier B E, Sormani M P, Falter J, Nerlich A and Pfeffer U 2009 CXCL12/SDF1 expression by breast cancers is an independent prognostic marker of disease-free and overall survival *European Journal of Cancer* 45 2579-87

- [402] Wang Y and Irvine D J 2013 Convolution of chemoattractant secretion rate, source density, and receptor desensitization direct diverse migration patterns in leukocytes() *Integrative biology : quantitative biosciences from nano to macro* 5 481-94
- [403] De Donatis A, Comito G, Buricchi F, Vinci M C, Parenti A, Caselli A, Camici G, Manao G, Ramponi G and Cirri P 2008 Proliferation versus migration in platelet-derived growth factor signaling: the key role of endocytosis *The Journal of biological chemistry* 283 19948-56
- [404] Uchida K, Sasahara M, Morigami N, Hazama F and Kinoshita M 1996 Expression of platelet-derived growth factor B-chain in neointimal smooth muscle cells of balloon injured rabbit femoral arteries *Atherosclerosis* 124 9-23
- [405] Liu Y, Sinha S, McDonald O G, Shang Y, Hoofnagle M H and Owens G K 2005 Kruppel-like factor 4 abrogates myocardin-induced activation of smooth muscle gene expression *The Journal of biological chemistry* 280 9719-27
- [406] Wyler von Ballmoos M, Yang Z, Volzmann J, Baumgartner I, Kalka C and Di Santo S 2010 Endothelial progenitor cells induce a phenotype shift in differentiated endothelial cells towards PDGF/PDGFRbeta axis-mediated angiogenesis *PLoS ONE* 5 e14107
- [407] Hao X, Silva E A, Mansson-Broberg A, Grinnemo K H, Siddiqui A J, Dellgren G, Wardell E, Brodin L A, Mooney D J and Sylven C 2007 Angiogenic effects of sequential release of VEGF-A165 and PDGF-BB with alginate hydrogels after myocardial infarction *Cardiovasc Res* 75 178-85
- [408] Lee C K, Lee H M, Kim H J, Park H J, Won K J, Roh H Y, Choi W S, Jeon B H, Park T K and Kim B 2007 Syk contributes to PDGF-BB-mediated migration of rat aortic smooth muscle cells via MAPK pathways *Cardiovasc Res* 74 159-68
- [409] Jie W, Wang X, Zhang Y, Guo J, Kuang D, Zhu P, Wang G and Ao Q 2010 SDF-1alpha/CXCR4 axis is involved in glucose-potentiated proliferation and chemotaxis in rat vascular smooth muscle cells *International journal of experimental pathology* 91 436-44
- [410] Ho T K, Shiwen X, Abraham D, Tsui J and Baker D 2012 Stromal-Cell-Derived Factor-1 (SDF-1)/CXCL12 as Potential Target of Therapeutic Angiogenesis in Critical Leg Ischaemia *Cardiology Research and Practice* 2012
- [411] Kolovou G, Anagnostopoulou K, Mikhailidis D P and Cokkinos D V 2008 Apolipoprotein E knockout models *Current pharmaceutical design* 14 338-51
- [412] Jawien J 2012 The role of an experimental model of atherosclerosis: apoE-knockout mice in developing new drugs against atherogenesis *Current pharmaceutical biotechnology* 13 2435-9
- [413] Vasquez E C, Peotta V A, Gava A L, Pereira T M and Meyrelles S S 2012 Cardiac and vascular phenotypes in the apolipoprotein E-deficient mouse *Journal of biomedical science* 19 22
- [414] Ross R, Glomset J and Harker L 1977 Response to injury and atherogenesis *The American Journal of Pathology* 86 675-84
- [415] Wang G, Jacquet L, Karamariti E and Xu Q 2015 Origin and differentiation of vascular smooth muscle cells *The Journal of physiology* 593 3013-30
- [416] Campbell J H and Campbell G R 1994 The role of smooth muscle cells in atherosclerosis *Current opinion in lipidology* 5 323-30
- [417] Hillebrands J L, Klatter F A, van den Hurk B M, Popa E R, Nieuwenhuis P and Rozing J 2001 Origin of neointimal endothelium and alpha-actin-positive smooth muscle cells in transplant arteriosclerosis *Journal of Clinical Investigation* 107 1411-22
- [418] Li J, Han X, Jiang J, Zhong R, Williams G M, Pickering J G and Chow L H 2001 Vascular smooth muscle cells of recipient origin mediate intimal expansion after aortic allotransplantation in mice *The American Journal of Pathology* 158 1943-7
- [419] Hu Y, Mayr M, Metzler B, Erdel M, Davison F and Xu Q 2002 Both donor and recipient origins of smooth muscle cells in vein graft atherosclerotic lesions *Circ Res* 91 e13-20
- [420] Chaabane C, Coen M and Bochaton-Piallat M L 2014 Smooth muscle cell phenotypic switch: implications for foam cell formation *Current opinion in lipidology* 25 374-9

- [421] Orr A W, Hastings N E, Blackman B R and Wamhoff B R 2010 Complex regulation and function of the inflammatory smooth muscle cell phenotype in atherosclerosis *Journal of vascular research* 47 168-80
- [422] Margariti A, Zeng L and Xu Q 2006 Stem cells, vascular smooth muscle cells and atherosclerosis *Histology and histopathology* 21 979-85
- [423] Manabe I and Nagai R 2003 Regulation of smooth muscle phenotype *Current atherosclerosis reports* 5 214-22
- [424] Owens G K 1995 Regulation of differentiation of vascular smooth muscle cells *Physiological reviews* 75 487-517
- [425] Cherepanova O A, Pidkovka N A, Sarmiento O F, Yoshida T, Gan Q, Adiguzel E, Bendeck M P, Berliner J, Leitinger N and Owens G K 2009 Oxidized phospholipids induce type VIII collagen expression and vascular smooth muscle cell migration *Circ Res* 104 609-18
- [426] Yoshida T, Kaestner K H and Owens G K 2008 Conditional deletion of Kruppel-like factor 4 delays downregulation of smooth muscle cell differentiation markers but accelerates neointimal formation following vascular injury *Circ Res* 102 1548-57
- [427] Hoofnagle M H, Wamhoff B R and Owens G K 2004 Lost in transdifferentiation *Journal of Clinical Investigation* 113 1249-51
- [428] Fong D, Hermann M, Untergasser G, Pirkebner D, Draxl A, Heitz M, Moser P, Margreiter R, Hengster P and Amberger A 2009 Dkk-3 expression in the tumor endothelium: a novel prognostic marker of pancreatic adenocarcinomas *Cancer science* 100 1414-20
- [429] Semenov M V, Tamai K, Brott B K, Kuhl M, Sokol S and He X 2001 Head inducer Dickkopf-1 is a ligand for Wnt coreceptor LRP6 *Current biology : CB* 11
- [430] Bafico A, Liu G, Yaniv A, Gazit A and Aaronson S A 2001 Novel mechanism of Wnt signalling inhibition mediated by Dickkopf-1 interaction with LRP6/Arrow *Nat Cell Biol* 3 683-6
- [431] Li L, Mao J, Sun L, Liu W and Wu D 2002 Second cysteine-rich domain of Dickkopf-2 activates canonical Wnt signaling pathway via LRP-6 independently of dishevelled *The Journal of biological chemistry* 277
- [432] Fujii Y, Hoshino T and Kumon H 2014 Molecular simulation analysis of the structure complex of C2 domains of DKK family members and beta-propeller domains of LRP5/6: explaining why DKK3 does not bind to LRP5/6 *Acta medica Okayama* 68 63-78
- [433] Brott B K and Sokol S Y 2002 Regulation of Wnt/LRP signaling by distinct domains of Dickkopf proteins *Mol Cell Biol* 22
- [434] Wang K 2008 Characterization of the Kremen-binding Site on Dkk1 and Elucidation of 283 23371-5
- [435] Chen L, Wang K, Shao Y, Huang J, Li X, Shan J, Wu D and Zheng J J 2008 Structural insight into the mechanisms of Wnt signaling antagonism by Dkk *The Journal of biological chemistry* 283 23364-70
- [436] Chen S, Bubeck D, MacDonald Bryan T, Liang W-X, Mao J-H, Malinauskas T, Llorca O, Aricescu A R, Siebold C, He X and Jones E Y 2011 Structural and Functional Studies of LRP6 Ectodomain Reveal a Platform for Wnt Signaling *Developmental cell* 21 848-61
- [437] Ahn V E, Chu M L, Choi H J, Tran D, Abo A and Weis W I 2011 Structural basis of Wnt signaling inhibition by Dickkopf binding to LRP5/6 *Developmental cell* 21 862-73
- [438] Cheng Z, Biechele T, Wei Z, Morrone S, Moon R T, Wang L and Xu W 2011 Crystal structures of the extracellular domain of LRP6 and its complex with DKK1 *Nature structural & molecular biology* 18 1204-10
- [439] Mohammadpour H, Pourfathollah A A, Nikougoftar Zarif M and Khalili S 2016 Key role of Dkk3 protein in inhibition of cancer cell proliferation: An in silico identification *Journal of theoretical biology* 393 98-104
- [440] Poorebrahim M, Sadeghi S, Rahimi H, Karimipoor M, Azadmanesh K, Mazlomi M A and Teimoori-Toolabi L 2017 Rational design of DKK3 structure-based small peptides as

- antagonists of Wnt signaling pathway and in silico evaluation of their efficiency *PLoS ONE* 12 e0172217
- [441] Ma W, Liu Y, Wang C, Zhang L, Crocker L and Shen J 2014 Atorvastatin inhibits CXCR7 induction to reduce macrophage migration *Biochem Pharmacol* 89 99-108
- [442] Law N M and Rosenzweig S A 1994 Characterization of the G-protein linked orphan receptor GPRN1/RDC1 *Biochem Biophys Res Commun* 201 458-65
- [443] Klein K R, Karpinich N O, Espenschied S T, Willcockson H H, Dunworth W P, Hoopes S L, Kushner E J, Bautch V L and Caron K M 2014 Decoy receptor CXCR7 modulates adrenomedullin-mediated cardiac and lymphatic vascular development *Developmental cell* 30 528-40
- [444] Mahabaleshwar H, Tarbashevich K, Nowak M, Brand M and Raz E 2012 beta-arrestin control of late endosomal sorting facilitates decoy receptor function and chemokine gradient formation *Development* 139 2897-902
- [445] Boldajipour B, Mahabaleshwar H, Kardash E, Reichman-Fried M, Blaser H, Minina S, Wilson D, Xu Q and Raz E 2008 Control of chemokine-guided cell migration by ligand sequestration *Cell* 132 463-73
- [446] Inaguma S, Riku M, Ito H, Tsunoda T, Ikeda H and Kasai K 2015 GLI1 orchestrates CXCR4/CXCR7 signaling to enhance migration and metastasis of breast cancer cells *Oncotarget* 6 33648-57
- [447] Chen N, Jiang X, Wang J, Wu T, Cheng B and Xia J 2016 CXCL12-CXCR4/CXCR7 axis contributes to cell motilities of oral squamous cell carcinoma *Tumor Biology* 37 567-75
- [448] Wang H, Beaty N, Chen S, Qi C F, Masiuk M, Shin D M and Morse H C, 3rd 2012 The CXCR7 chemokine receptor promotes B-cell retention in the splenic marginal zone and serves as a sink for CXCL12 *Blood* 119 465-8
- [449] Naumann U, Cameroni E, Pruenster M, Mahabaleshwar H, Raz E, Zerwes H G, Rot A and Thelen M 2010 CXCR7 functions as a scavenger for CXCL12 and CXCL11 *PLoS ONE* 5 e9175
- [450] Van Rechem C, Rood B R, Touka M, Pinte S, Jenal M, Guerardel C, Ramsey K, Monte D, Begue A, Tschan M P, Stephan D A and LePrince D 2009 Scavenger chemokine (CXC motif) receptor 7 (CXCR7) is a direct target gene of HIC1 (hypermethylated in cancer 1) *The Journal of biological chemistry* 284 20927-35
- [451] Heesen M, Berman M A, Charest A, Housman D, Gerard C and Dorf M E 1998 Cloning and chromosomal mapping of an orphan chemokine receptor: mouse RDC1 *Immunogenetics* 47 364-70
- [452] Jones S W, Brockbank S M V, Mobbs M L, Le Good N J, Soma-Haddrick S, Heuze A J, Langham C J, Timms D, Newham P and Needham M R C 2006 The orphan G-protein coupled receptor RDC1: evidence for a role in chondrocyte hypertrophy and articular cartilage matrix turnover *Osteoarthritis and Cartilage* 14 597-608
- [453] Shimizu N, Soda Y, Kanbe K, Liu H Y, Mukai R, Kitamura T and Hoshino H 2000 A putative G protein-coupled receptor, RDC1, is a novel coreceptor for human and simian immunodeficiency viruses *Journal of virology* 74 619-26
- [454] Nagasawa T, Nakajima T, Tachibana K, Iizasa H, Bleul C C, Yoshie O, Matsushima K, Yoshida N, Springer T A and Kishimoto T 1996 Molecular cloning and characterization of a murine pre-B-cell growth-stimulating factor/stromal cell-derived factor 1 receptor, a murine homolog of the human immunodeficiency virus 1 entry coreceptor fusin *Proceedings of the National Academy of Sciences* 93 14726-9
- [455] Jo D Y, Rafii S, Hamada T and Moore M A 2000 Chemotaxis of primitive hematopoietic cells in response to stromal cell-derived factor-1 *Journal of Clinical Investigation* 105 101-11
- [456] Kim C H and Broxmeyer H E 1998 In Vitro Behavior of Hematopoietic Progenitor Cells Under the Influence of Chemoattractants: Stromal Cell-Derived Factor-1, Steel Factor, and the Bone Marrow Environment *Blood* 91 100-10

- [457] Watt S M and Forde S P 2008 The central role of the chemokine receptor, CXCR4, in haemopoietic stem cell transplantation: will CXCR4 antagonists contribute to the treatment of blood disorders? *Vox sanguinis* 94 18-32
- [458] Grymula K, Tarnowski M, Wysoczynski M, Drukala J, Barr F G, Ratajczak J, Kucia M and Ratajczak M Z 2010 Overlapping and distinct role of CXCR7-SDF-1/ITAC and CXCR4-SDF-1 axes in regulating metastatic behavior of human rhabdomyosarcomas *International journal of cancer* 127 2554-68
- [459] Kalatskaya I, Berchiche Y A, Gravel S, Limberg B J, Rosenbaum J S and Heveker N 2009 AMD3100 Is a CXCR7 Ligand with Allosteric Agonist Properties *Molecular Pharmacology* 75 1240-7
- [460] Gravel S, Malouf C, Boulais P E, Berchiche Y A, Oishi S, Fujii N, Leduc R, Sinnett D and Heveker N 2010 The peptidomimetic CXCR4 antagonist TC14012 recruits beta-arrestin to CXCR7: roles of receptor domains *The Journal of biological chemistry* 285 37939-43
- [461] Pawig L, Klasen C, Weber C, Bernhagen J and Noels H 2015 Diversity and Inter-Connections in the CXCR4 Chemokine Receptor/Ligand Family: Molecular Perspectives *Frontiers in Immunology* 6
- [462] Schwartz V, Lue H, Kraemer S, Korbiel J, Krohn R, Ohl K, Bucala R, Weber C and Bernhagen J 2009 A functional heteromeric MIF receptor formed by CD74 and CXCR4 *FEBS letters* 583 2749-57
- [463] Tillmann S, Bernhagen J and Noels H 2013 Arrest Functions of the MIF Ligand/Receptor Axes in Atherogenesis *Frontiers in Immunology* 4
- [464] Crump M P, Gong J H, Loetscher P, Rajarathnam K, Amara A, Arenzana-Seisdedos F, Virelizier J L, Baggiolini M, Sykes B D and Clark-Lewis I 1997 Solution structure and basis for functional activity of stromal cell-derived factor-1; dissociation of CXCR4 activation from binding and inhibition of HIV-1 *The EMBO Journal* 16 6996-7007
- [465] Subramanian P, Karshovska E, Reinhard P, Megens R T A, Zhou Z, Akhtar S, Schumann U, Li X, van Zandvoort M, Ludin C, Weber C and Schober A 2010 Lysophosphatidic Acid Receptors LPA₁ and LPA₃ Promote CXCL12-Mediated Smooth Muscle Progenitor Cell Recruitment in Neointima Formation *Circulation Research* 107 96-105
- [466] Subramanian P, Karshovska E, Reinhard P, Megens R T, Zhou Z, Akhtar S, Schumann U, Li X, van Zandvoort M, Ludin C, Weber C and Schober A 2010 Lysophosphatidic acid receptors LPA₁ and LPA₃ promote CXCL12-mediated smooth muscle progenitor cell recruitment in neointima formation *Circ Res* 107 96-105
- [467] Zerneck A, Bot I, Djalali-Talab Y, Shagdarsuren E, Bidzhekov K, Meiler S, Krohn R, Schober A, Sperandio M, Soehnlein O, Bornemann J, Tacke F, Biessen E A and Weber C 2008 Protective role of CXC receptor 4/CXC ligand 12 unveils the importance of neutrophils in atherosclerosis *Circ Res* 102 209-17
- [468] Gerrits H, van Ingen Schenau D S, Bakker N E, van Disseldorp A J, Strik A, Hermens L S, Koenen T B, Krajnc-Franken M A and Gossen J A 2008 Early postnatal lethality and cardiovascular defects in CXCR7-deficient mice *Genesis (New York, N.Y. : 2000)* 46 235-45
- [469] Sierro F, Biben C, Martinez-Munoz L, Mellado M, Ransohoff R M, Li M, Woehl B, Leung H, Groom J, Batten M, Harvey R P, Martinez A C, Mackay C R and Mackay F 2007 Disrupted cardiac development but normal hematopoiesis in mice deficient in the second CXCL12/SDF-1 receptor, CXCR7 *Proceedings of the National Academy of Sciences of the United States of America* 104 14759-64
- [470] Yu S, Crawford D, Tsuchihashi T, Behrens T W and Srivastava D 2011 The chemokine receptor CXCR7 functions to regulate cardiac valve remodeling *Developmental dynamics : an official publication of the American Association of Anatomists* 240 384-93
- [471] Hao H, Hu S, Chen H, Bu D, Zhu L, Xu C, Chu F, Huo X, Tang Y, Sun X, Ding B S, Liu D P, Hu S and Wang M 2017 Loss of Endothelial CXCR7 Impairs Vascular Homeostasis and Cardiac

- Remodeling After Myocardial Infarction: Implications for Cardiovascular Drug Discovery *Circulation* 135 1253-64
- [472] Zhang X Y, Su C, Cao Z, Xu S Y, Xia W H, Xie W L, Chen L, Yu B B, Zhang B, Wang Y and Tao J 2014 CXCR7 upregulation is required for early endothelial progenitor cell-mediated endothelial repair in patients with hypertension *Hypertension (Dallas, Tex. : 1979)* 63 383-9
- [473] Dai X, Tan Y, Cai S, Xiong X, Wang L, Ye Q, Yan X, Ma K and Cai L 2011 The role of CXCR7 on the adhesion, proliferation and angiogenesis of endothelial progenitor cells *Journal of Cellular and Molecular Medicine* 15 1299-309
- [474] Dai X, Yan X, Zeng J, Chen J, Wang Y, Chen J, Li Y, Barati M T, Wintergerst K A, Pan K, Nystoriak M A, Conklin D J, Rokosh G, Epstein P N, Li X and Tan Y 2017 Elevating CXCR7 Improves Angiogenic Function of EPCs via Akt/GSK-3beta/Fyn-Mediated Nrf2 Activation in Diabetic Limb Ischemia *Circ Res* 120 e7-e23
- [475] Cao Z, Tong X, Xia W, Chen L, Zhang X, Yu B, Yang Z and Tao J 2016 CXCR7/p-ERK-Signaling Is a Novel Target for Therapeutic Vasculogenesis in Patients with Coronary Artery Disease *PLoS ONE* 11 e0161255
- [476] Yamada K, Maishi N, Akiyama K, Towfik Alam M, Ohga N, Kawamoto T, Shindoh M, Takahashi N, Kamiyama T, Hida Y, Taketomi A and Hida K 2015 CXCL12-CXCR7 axis is important for tumor endothelial cell angiogenic property *International journal of cancer* 137 2825-36
- [477] Feng Y F, Guo H, Yuan F and Shen M Q 2015 Lipopolysaccharide Promotes Choroidal Neovascularization by Up-Regulation of CXCR4 and CXCR7 Expression in Choroid Endothelial Cell *PLoS ONE* 10 e0136175
- [478] Feng Y F, Yuan F, Guo H and Wu W Z 2014 TGF-beta1 enhances SDF-1-induced migration and tube formation of choroid-retinal endothelial cells by up-regulating CXCR4 and CXCR7 expression *Molecular and cellular biochemistry* 397 131-8
- [479] Jin J, Zhao W C and Yuan F 2013 CXCR7/CXCR4/CXCL12 axis regulates the proliferation, migration, survival and tube formation of choroid-retinal endothelial cells *Ophthalmic research* 50 6-12
- [480] Yan X, Cai S, Xiong X, Sun W, Dai X, Chen S, Ye Q, Song Z, Jiang Q and Xu Z 2012 Chemokine receptor CXCR7 mediates human endothelial progenitor cells survival, angiogenesis, but not proliferation *J Cell Biochem* 113 1437-46
- [481] Yin D T, Wu W, Li M, Wang Q E, Li H, Wang Y, Tang Y and Xing M 2013 DKK3 is a potential tumor suppressor gene in papillary thyroid carcinoma *Endocrine-related cancer* 20 507-14
- [482] Gu Y M, Ma Y H, Zhao W G and Chen J 2011 Dickkopf3 overexpression inhibits pancreatic cancer cell growth in vitro *World Journal of Gastroenterology : WJG* 17 3810-7
- [483] Lorsy E, Topuz A S, Geisler C, Stahl S, Garczyk S, von Stillfried S, Hoss M, Gluz O, Hartmann A, Knuchel R and Dahl E 2016 Loss of Dickkopf 3 Promotes the Tumorigenesis of Basal Breast Cancer *PLoS ONE* 11 e0160077
- [484] Zhou S, Zhu Y, Mashrah M, Zhang X, He Z, Yao Z, Zhang C, Guo F, Hu Y and Zhang C 2017 Expression pattern of DKK3, dickkopf WNT signaling pathway inhibitor 3, in the malignant progression of oral submucous fibrosis *Oncology reports* 37 979-85
- [485] Cargnello M and Roux P P 2011 Activation and Function of the MAPKs and Their Substrates, the MAPK-Activated Protein Kinases *Microbiology and Molecular Biology Reviews : MMBR* 75 50-83
- [486] Wang X Y, Yin Y, Yuan H, Sakamaki T, Okano H and Glazer R I 2008 Musashi1 modulates mammary progenitor cell expansion through proliferin-mediated activation of the Wnt and Notch pathways *Mol Cell Biol* 28 3589-99
- [487] Xia P and Xu X Y 2017 DKK3 attenuates the cytotoxic effect of natural killer cells on CD133+ gastric cancer cells *Molecular carcinogenesis*

- [488] Mazharian A, Watson S P and Severin S 2009 Critical role for ERK1/2 in bone marrow and fetal liver-derived primary megakaryocyte differentiation, motility, and proplatelet formation *Experimental hematology* 37 1238-49.e5
- [489] Chen D, Xia Y, Zuo K, Wang Y, Zhang S, Kuang D, Duan Y, Zhao X and Wang G 2015 Crosstalk between SDF-1/CXCR4 and SDF-1/CXCR7 in cardiac stem cell migration *Scientific reports* 5 16813
- [490] Ryu C H, Park S A, Kim S M, Lim J Y, Jeong C H, Jun J A, Oh J H, Park S H, Oh W-i and Jeun S-S 2010 Migration of human umbilical cord blood mesenchymal stem cells mediated by stromal cell-derived factor-1/CXCR4 axis via Akt, ERK, and p38 signal transduction pathways *Biochemical and Biophysical Research Communications* 398 105-10
- [491] Ngo H T, Leleu X, Lee J, Jia X, Melhem M, Runnels J, Moreau A-S, Burwick N, Azab A K, Roccaro A, Azab F, Sacco A, Farag M, Sackstein R and Ghobrial I M 2008 SDF-1/CXCR4 and VLA-4 interaction regulates homing in Waldenstrom macroglobulinemia *Blood* 112 150-8
- [492] Alsayed Y, Ngo H, Runnels J, Leleu X, Singha U K, Pitsillides C M, Spencer J A, Kimlinger T, Ghobrial J M, Jia X, Lu G, Timm M, Kumar A, Cote D, Veilleux I, Hedin K E, Roodman G D, Witzig T E, Kung A L, Hideshima T, Anderson K C, Lin C P and Ghobrial I M 2007 Mechanisms of regulation of CXCR4/SDF-1 (CXCL12)-dependent migration and homing in multiple myeloma *Blood* 109 2708-17
- [493] Lee E, Han J, Kim K, Choi H, Cho E G and Lee T R 2013 CXCR7 mediates SDF1-induced melanocyte migration *Pigment cell & melanoma research* 26 58-66
- [494] Zheng H, Fu G, Dai T and Huang H 2007 Migration of endothelial progenitor cells mediated by stromal cell-derived factor-1alpha/CXCR4 via PI3K/Akt/eNOS signal transduction pathway *Journal of cardiovascular pharmacology* 50 274-80
- [495] Yu J, Li M, Qu Z, Yan D, Li D and Ruan Q 2010 SDF-1/CXCR4-mediated migration of transplanted bone marrow stromal cells toward areas of heart myocardial infarction through activation of PI3K/Akt *Journal of cardiovascular pharmacology* 55 496-505
- [496] Ryu C H, Park S A, Kim S M, Lim J Y, Jeong C H, Jun J A, Oh J H, Park S H, Oh W I and Jeun S S 2010 Migration of human umbilical cord blood mesenchymal stem cells mediated by stromal cell-derived factor-1/CXCR4 axis via Akt, ERK, and p38 signal transduction pathways *Biochem Biophys Res Commun* 398 105-10
- [497] Zhou H, Yang J, Xin T, Zhang T, Hu S, Zhou S, Chen G and Chen Y 2015 Exendin-4 enhances the migration of adipose-derived stem cells to neonatal rat ventricular cardiomyocyte-derived conditioned medium via the phosphoinositide 3-kinase/Akt-stromal cell-derived factor-1alpha/CXC chemokine receptor 4 pathway *Molecular medicine reports* 11 4063-72
- [498] Li S, Deng L, Gong L, Bian H, Dai Y and Wang Y 2010 Upregulation of CXCR4 favoring neural-like cells migration via AKT activation *Neuroscience research* 67 293-9
- [499] Zhao M, Mueller B M, DiScipio R G and Schraufstatter I U 2008 Akt plays an important role in breast cancer cell chemotaxis to CXCL12 *Breast cancer research and treatment* 110 211-22
- [500] Li J, Liu S, Li W, Hu S, Xiong J, Shu X, Hu Q, Zheng Q and Song Z 2012 Vascular smooth muscle cell apoptosis promotes transplant arteriosclerosis through inducing the production of SDF-1alpha *American journal of transplantation : official journal of the American Society of Transplantation and the American Society of Transplant Surgeons* 12 2029-43
- [501] Conley-LaComb M K, Saliganan A, Kandagatla P, Chen Y Q, Cher M L and Chinni S R 2013 PTEN loss mediated Akt activation promotes prostate tumor growth and metastasis via CXCL12/CXCR4 signaling *Molecular cancer* 12 85
- [502] Barbero S, Bonavia R, Bajetto A, Porcile C, Pirani P, Ravetti J L, Zona G L, Spaziante R, Florio T and Schettini G 2003 Stromal cell-derived factor 1alpha stimulates human glioblastoma cell growth through the activation of both extracellular signal-regulated kinases 1/2 and Akt *Cancer Res* 63 1969-74

- [503] Majka M, Janowska-Wieczorek A, Ratajczak J, Kowalska M A, Vilaire G, Pan Z K, Honczarenko M, Marquez L A, Poncz M and Ratajczak M Z 2000 Stromal-derived factor 1 and thrombopoietin regulate distinct aspects of human megakaryopoiesis *Blood* 96 4142-51
- [504] Lataillade J J, Clay D, Bourin P, Herodin F, Dupuy C, Jasmin C and Le Bousse-Kerdiles M C 2002 Stromal cell-derived factor 1 regulates primitive hematopoiesis by suppressing apoptosis and by promoting G(0)/G(1) transition in CD34(+) cells: evidence for an autocrine/paracrine mechanism *Blood* 99 1117-29
- [505] Lee Y, Gotoh A, Kwon H J, You M, Kohli L, Mantel C, Cooper S, Hangoc G, Miyazawa K, Ohyashiki K and Broxmeyer H E 2002 Enhancement of intracellular signaling associated with hematopoietic progenitor cell survival in response to SDF-1/CXCL12 in synergy with other cytokines *Blood* 99 4307-17
- [506] Zenzmaier C, Sampson N, Plas E and Berger P 2013 Dickkopf-related protein 3 promotes pathogenic stromal remodeling in benign prostatic hyperplasia and prostate cancer *The Prostate* 73 1441-52
- [507] Xu X Y, Xia P, Yu M, Nie X C, Yang X, Xing Y N, Liu Y P, Takano Y and Zheng H C 2012 The roles of REIC gene and its encoding product in gastric carcinoma *Cell cycle (Georgetown, Tex.)* 11 1414-31
- [508] Lin C H, Guo Y, Ghaffar S, McQueen P, Pourmorady J, Christ A, Rooney K, Ji T, Eskander R, Zi X and Hoang B H 2013 Dkk-3, a Secreted Wnt Antagonist, Suppresses Tumorigenic Potential and Pulmonary Metastasis in Osteosarcoma *Sarcoma* 2013 11
- [509] Aznar S, Fernandez-Valeron P, Espina C and Lacal J C 2004 Rho GTPases: potential candidates for anticancer therapy *Cancer Lett* 206
- [510] Boettner B and Van A L 2002 The role of Rho GTPases in disease development *Gene* 286
- [511] Etienne-Manneville S and Hall A 2002 Rho GTPases in cell biology *Nature* 420 629-35
- [512] Azab A K, Azab F, Blotta S, Pitsillides C M, Thompson B, Runnels J M, Roccaro A M, Ngo H T, Melhem M R, Sacco A, Jia X, Anderson K C, Lin C P, Rollins B J and Ghobrial I M 2009 RhoA and Rac1 GTPases play major and differential roles in stromal cell-derived factor-1-induced cell adhesion and chemotaxis in multiple myeloma *Blood* 114 619-29
- [513] Nishita M, Aizawa H and Mizuno K 2002 Stromal Cell-Derived Factor 1 α Activates LIM Kinase 1 and Induces Cofilin Phosphorylation for T-Cell Chemotaxis *Mol Cell Biol* 22 774-83
- [514] Yang F-C, Atkinson S J, Gu Y, Borneo J B, Roberts A W, Zheng Y, Pennington J and Williams D A 2001 Rac and Cdc42 GTPases control hematopoietic stem cell shape, adhesion, migration, and mobilization *Proceedings of the National Academy of Sciences* 98 5614-8
- [515] Sahin A O and Buitenhuis M 2012 Molecular mechanisms underlying adhesion and migration of hematopoietic stem cells *Cell Adh Migr* 6 39-48
- [516] Cancelas J 2011 On how Rac controls hematopoietic stem cell activity *Transfusion* 51 153s-9s
- [517] Suwa T, Chen M, Hawks C L and Hornsby P J 2003 Zonal expression of dickkopf-3 and components of the Wnt signalling pathways in the human adrenal cortex *The Journal of endocrinology* 178 149-58
- [518] Nakamura R E, Hunter D D, Yi H, Brunken W J and Hackam A S 2007 Identification of two novel activities of the Wnt signaling regulator Dickkopf 3 and characterization of its expression in the mouse retina *BMC Cell Biology* 8 52
- [519] Yue W, Sun Q, Dacic S, Landreneau R J, Siegfried J M, Yu J and Zhang L 2008 Downregulation of Dkk3 activates beta-catenin/TCF-4 signaling in lung cancer *Carcinogenesis* 29 84-92
- [520] Clevers H 2006 Wnt/beta-catenin signaling in development and disease *Cell* 127
- [521] Schlessinger K, Hall A and Tolwinski N 2009 Wnt signaling pathways meet Rho GTPases *Genes & development* 23 265-77
- [522] Veeck J, Bektas N, Hartmann A, Kristiansen G, Heindrichs U, Knüchel R and Dahl E 2008 Wnt signalling in human breast cancer: expression of the putative Wnt inhibitor Dickkopf-3 (DKK3) is frequently suppressed by promoter hypermethylation in mammary tumours *Breast cancer research : BCR* 10 R82

- [523] Ray R M, Vaidya R J and Johnson L R 2007 MEK/ERK regulates adherens junctions and migration through Rac1 *Cell motility and the cytoskeleton* 64 143-56
- [524] Hampsch R A, Shee K, Bates D, Lewis L D, Desire L, Leblond B, Demidenko E, Stefan K, Huang Y H and Miller T W 2017 Therapeutic sensitivity to Rac GTPase inhibition requires consequential suppression of mTORC1, AKT, and MEK signaling in breast cancer *Oncotarget* 8 21806-17
- [525] Bamburg J R and Bernstein B W 2010 Roles of ADF/cofilin in actin polymerization and beyond *F1000 Biology Reports* 2
- [526] Dos Remedios C G, Chhabra D, Kekic M, Dedova I V, Tsubakihara M, Berry D A and Nosworthy N J 2003 Actin Binding Proteins: Regulation of Cytoskeletal Microfilaments *Physiological reviews* 83 433-73
- [527] Krause U, Ryan D M, Clough B H and Gregory C A 2014 An unexpected role for a Wnt-inhibitor: Dickkopf-1 triggers a novel cancer survival mechanism through modulation of aldehyde-dehydrogenase-1 activity *Cell death & disease* 5 e1093
- [528] Rachner T D, Gobel A, Thiele S, Rauner M, Benad-Mehner P, Hadji P, Bauer T, Muders M H, Baretton G B, Jakob F, Ebert R, Bornhauser M, Schem C and Hofbauer L C 2014 Dickkopf-1 is regulated by the mevalonate pathway in breast cancer *Breast cancer research : BCR* 16 R20
- [529] Shusterman K, Gibson C W, Li Y, Healey M and Peng L 2014 Wnt-RhoA signaling pathways in fluoride-treated ameloblast-lineage cells *Cells, tissues, organs* 199 159-68
- [530] Ridley A J 2015 Rho GTPase signalling in cell migration *Current opinion in cell biology* 36 103-12
- [531] Ricker E, Chowdhury L, Yi W and Pernis A 2016 *The RhoA-ROCK pathway in the regulation of T and B cell responses [version 1; referees: 3 approved]* vol 5
- [532] Struckhoff A P, Vitko J R, Rana M K, Davis C T, Foderingham K E, Liu C-H, Vanhoy-Rhodes L, Elliot S, Zhu Y, Burow M and Worthylake R A 2010 Dynamic regulation of ROCK in tumor cells controls CXCR4-driven adhesion events *Journal of cell science* 123 401-12
- [533] Xu Z, Zheng X, Yang L, Liu F, Zhang E, Duan W, Bai S, Safdar J, Li Z and Sun C 2015 Chemokine receptor 7 promotes tumor migration and invasiveness via the RhoA/ROCK pathway in metastatic squamous cell carcinoma of the head and neck *Oncology reports* 33 849-55
- [534] Tauriello D V F, Jordens I, Kirchner K, Slootstra J W, Kruitwagen T, Bouwman B A M, Noutsou M, Rüdiger S G D, Schwamborn K, Schambony A and Maurice M M 2012 Wnt/ β -catenin signaling requires interaction of the Dishevelled DEP domain and C terminus with a discontinuous motif in Frizzled *Proceedings of the National Academy of Sciences* 109 E812–E20
- [535] Kumar R, Tripathi V, Ahmad M, Nath N, Mir R A, Chauhan S S and Luthra K 2012 CXCR7 mediated Gialpha independent activation of ERK and Akt promotes cell survival and chemotaxis in T cells *Cellular immunology* 272 230-41
- [536] Odemis V, Boosmann K, Heinen A, Kury P and Engele J 2010 CXCR7 is an active component of SDF-1 signalling in astrocytes and Schwann cells *Journal of cell science* 123 1081-8
- [537] Guo J C, Li J, Zhou L, Yang J Y, Zhang Z G, Liang Z Y, Zhou W X, You L, Zhang T P and Zhao Y P 2016 CXCL12-CXCR7 axis contributes to the invasive phenotype of pancreatic cancer *Oncotarget* 7 62006-18
- [538] Kim B-R, Lee E-J, Seo S H, Lee S-H and Rho S B 2015 Dickkopf-3 (DKK-3) obstructs VEGFR-2/Akt/mTOR signaling cascade by interacting of β 2-microglobulin (β 2M) in ovarian tumorigenesis *Cellular signalling* 27 2150-9
- [539] Ochiai K, Morimatsu M, Kato Y, Ishiguro-Oonuma T, Udagawa C, Rungsuriyawiboon O, Azakami D, Michishita M, Ariyoshi Y, Ueki H, Nasu Y, Kumon H, Watanabe M and Omi T 2016 Tumor suppressor REIC/DKK-3 and co-chaperone SGTA: Their interaction and roles in the androgen sensitivity *Oncotarget* 7 3283-96
- [540] Rocchi S, Tartare-Deckert S, Sawka-Verhelle D, Gamha A and van Obberghen E 1996 Interaction of SH2-containing protein tyrosine phosphatase 2 with the insulin receptor and

- the insulin-like growth factor-I receptor: studies of the domains involved using the yeast two-hybrid system *Endocrinology* 137 4944-52
- [541] Oakley R H, Busillo J M and Cidlowski J A 2017 Cross-talk between the glucocorticoid receptor and MyoD family inhibitor domain-containing protein provides a new mechanism for generating tissue-specific responses to glucocorticoids *The Journal of biological chemistry* 292 5825-44
- [542] Nakamura T, Lozano P R, Ikeda Y, Iwanaga Y, Hinek A, Minamisawa S, Cheng C-F, Kobuke K, Dalton N, Takada Y, Tashiro K, Ross Jr J, Honjo T and Chien K R 2002 Fibulin-5/DANCE is essential for elastogenesis in vivo *Nature* 415 171-5
- [543] Williamson M R, Shuttleworth A, Canfield A E, Black R A and Kielty C M 2007 The role of endothelial cell attachment to elastic fibre molecules in the enhancement of monolayer formation and retention, and the inhibition of smooth muscle cell recruitment *Biomaterials* 28 5307-18
- [544] Cox E A and Huttenlocher A 1998 Regulation of integrin-mediated adhesion during cell migration *Microsc Res Tech* 43
- [545] Marchetti G, Escuin S, Van Der Flier A, De Arcangelis A, Hynes R O and Georges-Labouesse E 2010 Integrin $\alpha 5 \beta 1$ is necessary for regulation of radial migration of cortical neurons during mouse brain development *The European Journal of Neuroscience* 31 399-409
- [546] Veevers-Lowe J, Ball S G, Shuttleworth A and Kielty C M 2011 Mesenchymal stem cell migration is regulated by fibronectin through $\alpha 5 \beta 1$ -integrin-mediated activation of PDGFR- β and potentiation of growth factor signals *Journal of cell science* 124 1288-300
- [547] Caswell P T, Spence H J, Parsons M, White D P, Clark K, Cheng K W, Mills G B, Humphries M J, Messent A J, Anderson K I, McCaffrey M W, Ozanne B W and Norman J C 2007 Rab25 Associates with $\alpha 5 \beta 1$ Integrin to Promote Invasive Migration in 3D Microenvironments *Developmental cell* 13 496-510
- [548] White D P, Caswell P T and Norman J C 2007 $\alpha v \beta 3$ and $\alpha 5 \beta 1$ integrin recycling pathways dictate downstream Rho kinase signaling to regulate persistent cell migration *The Journal of Cell Biology* 177 515-25
- [549] Kabir-Salmani M, Shiokawa S, Akimoto Y, Sakai K and Iwashita M 2004 The role of alpha(5)beta(1)-integrin in the IGF-I-induced migration of extravillous trophoblast cells during the process of implantation *Molecular human reproduction* 10 91-7
- [550] Davenpeck K L, Marcinkiewicz C, Wang D, Niculescu R, Shi Y, Martin J L and Zalewski A 2001 Regional differences in integrin expression: role of alpha(5)beta(1) in regulating smooth muscle cell functions *Circ Res* 88 352-8
- [551] Wijelath E S, Rahman S, Murray J, Patel Y, Savidge G and Sobel M 2004 Fibronectin promotes VEGF-induced CD34+ cell differentiation into endothelial cells *Journal of Vascular Surgery* 39 655-60
- [552] Cascone I, Napione L, Maniero F, Serini G and Bussolino F 2005 Stable interaction between $\alpha 5 \beta 1$ integrin and Tie2 tyrosine kinase receptor regulates endothelial cell response to Ang-1 *J Cell Biol* 170 993-1004
- [553] Yurdagul A, Jr., Green J, Albert P, McInnis M C, Mazar A P and Orr A W 2014 alpha5beta1 integrin signaling mediates oxidized low-density lipoprotein-induced inflammation and early atherosclerosis *Arteriosclerosis, thrombosis, and vascular biology* 34 1362-73
- [554] Landry J P, Fei Y and Zhu X 2012 Simultaneous measurement of 10,000 protein-ligand affinity constants using microarray-based kinetic constant assays *Assay and drug development technologies* 10 250-9
- [555] Sun Y S, Landry J P, Fei Y Y, Zhu X D, Luo J T, Wang X B and Lam K S 2008 Effect of fluorescently labeling protein probes on kinetics of protein-ligand reactions *Langmuir : the ACS journal of surfaces and colloids* 24 13399-405

- [556] Kastritis P L, Moal I H, Hwang H, Weng Z, Bates P A, Bonvin A M and Janin J 2011 A structure-based benchmark for protein-protein binding affinity *Protein science : a publication of the Protein Society* 20 482-91
- [557] Zhang H, Williams P S, Zborowski M and Chalmers J J 2006 Binding affinities/avidities of antibody-antigen interactions: quantification and scale-up implications *Biotechnology and bioengineering* 95 812-29
- [558] Fu C Y, Su Y F, Lee M H, Chang G D and Tsai H J 2012 Zebrafish Dkk3a Protein Regulates the Activity of myf5 Promoter through Interaction with Membrane Receptor Integrin α 6b *The Journal of biological chemistry* 287 40031-42
- [559] Genecards
- [560] Shimazu Y, Kurozumi K, Ichikawa T, Fujii K, Onishi M, Ishida J, Oka T, Watanabe M, Nasu Y, Kumon H and Date I 2015 Integrin antagonist augments the therapeutic effect of adenovirus-mediated REIC/Dkk-3 gene therapy for malignant glioma *Gene therapy* 22 146-54
- [561] Plow E F, Haas T A, Zhang L, Loftus J and Smith J W 2000 Ligand binding to integrins *The Journal of biological chemistry* 275 21785-8
- [562] Sung C C, O'Toole E A, Lannutti B J, Hunt J, O'Gorman M, Woodley D T and Paller A S 1998 Integrin alpha 5 beta 1 expression is required for inhibition of keratinocyte migration by ganglioside GT1b *Experimental cell research* 239 311-9
- [563] Raftopoulou M and Hall A 2004 Cell migration: Rho GTPases lead the way *Developmental biology* 265 23-32
- [564] Chernyavsky A I, Arredondo J, Karlsson E, Wessler I and Grando S A 2005 The Ras/Raf-1/MEK1/ERK signaling pathway coupled to integrin expression mediates cholinergic regulation of keratinocyte directional migration *The Journal of biological chemistry* 280 39220-8
- [565] Teoh C M, Tam J K C and Tran T 2012 Integrin and GPCR Crosstalk in the Regulation of ASM Contraction Signaling in Asthma *Journal of Allergy* 2012 9
- [566] Soung Y H, Clifford J L and Chung J 2010 Crosstalk between integrin and receptor tyrosine kinase signaling in breast carcinoma progression *BMB reports* 43 311-8
- [567] Short S M, Boyer J L and Juliano R L 2000 Integrins regulate the linkage between upstream and downstream events in G protein-coupled receptor signaling to mitogen-activated protein kinase *The Journal of biological chemistry* 275 12970-7
- [568] Yu B, Chen Q, Le Bras A, Zhang L and Xu Q 2017 Vascular Stem/Progenitor Cell Migration and Differentiation in Atherosclerosis *Antioxidants & redox signaling*
- [569] Shan T, Liu W and Kuang S 2013 Fatty acid binding protein 4 expression marks a population of adipocyte progenitors in white and brown adipose tissues *FASEB journal : official publication of the Federation of American Societies for Experimental Biology* 27 277-87
- [570] Furuhashi M and Hotamisligil G S 2008 Fatty acid-binding proteins: role in metabolic diseases and potential as drug targets *Nat Rev Drug Discov* 7 489-503
- [571] Boord J B, Fazio S and Linton M F 2002 Cytoplasmic fatty acid-binding proteins: emerging roles in metabolism and atherosclerosis *Current opinion in lipidology* 13 141-7
- [572] Xie L, Wang P X, Zhang P, Zhang X J, Zhao G N, Wang A, Guo J, Zhu X, Zhang Q and Li H 2016 DKK3 expression in hepatocytes defines susceptibility to liver steatosis and obesity *Journal of hepatology* 65 113-24
- [573] Garin-Shkolnik T, Rudich A, Hotamisligil G S and Rubinstein M 2014 FABP4 Attenuates PPAR γ and Adipogenesis and Is Inversely Correlated With PPAR γ in Adipose Tissues *Diabetes* 63 900-11
- [574] Tso A W, Xu A, Sham P C, Wat N M, Wang Y, Fong C H, Cheung B M, Janus E D and Lam K S 2007 Serum adipocyte fatty acid binding protein as a new biomarker predicting the development of type 2 diabetes: a 10-year prospective study in a Chinese cohort *Diabetes care* 30 2667-72

- [575] Xu A, Wang Y, Xu J Y, Stejskal D, Tam S, Zhang J, Wat N M, Wong W K and Lam K S 2006 Adipocyte fatty acid-binding protein is a plasma biomarker closely associated with obesity and metabolic syndrome *Clinical chemistry* 52 405-13
- [576] Engl T, Relja B, Marian D, Blumenberg C, Muller I, Beecken W D, Jones J, Ringel E M, Bereiter-Hahn J, Jonas D and Blaheta R A 2006 CXCR4 chemokine receptor mediates prostate tumor cell adhesion through alpha5 and beta3 integrins *Neoplasia (New York, N.Y.)* 8 290-301
- [577] Sun Y X, Fang M, Wang J, Cooper C R, Pienta K J and Taichman R S 2007 Expression and activation of alpha v beta 3 integrins by SDF-1/CXC12 increases the aggressiveness of prostate cancer cells *The Prostate* 67 61-73
- [578] Yamada K M and Even-Ram S 2002 Integrin regulation of growth factor receptors *Nat Cell Biol* 4 E75-E6
- [579] Schluterman M K, Chapman S L, Korpanty G, Ozumi K, Fukai T, Yanagisawa H and Brekken R A 2010 Loss of fibulin-5 binding to beta1 integrins inhibits tumor growth by increasing the level of ROS *Disease models & mechanisms* 3 333-42
- [580] Wang M, Topalovski M, Toombs J E, Wright C M, Moore Z R, Boothman D A, Yanagisawa H, Wang H, Witkiewicz A, Castrillon D H and Brekken R A 2015 Fibulin-5 Blocks Microenvironmental ROS in Pancreatic Cancer *Cancer Res* 75 5058-69
- [581] Nakamura T, Ruiz-Lozano P, Lindner V, Yabe D, Taniwaki M, Furukawa Y, Kobuke K, Tashiro K, Lu Z, Andon N L, Schaub R, Matsumori A, Sasayama S, Chien K R and Honjo T 1999 DANCE, a novel secreted RGD protein expressed in developing, atherosclerotic, and balloon-injured arteries *The Journal of biological chemistry* 274 22476-83
- [582] Spencer J A, Hacker S L, Davis E C, Mecham R P, Knutsen R H, Li D Y, Gerard R D, Richardson J A, Olson E N and Yanagisawa H 2005 Altered vascular remodeling in fibulin-5-deficient mice reveals a role of fibulin-5 in smooth muscle cell proliferation and migration *Proceedings of the National Academy of Sciences of the United States of America* 102 2946-51